Andrew Gaya
Anand Mahadevan *Editors*

Stereotactic Body Radiotherapy

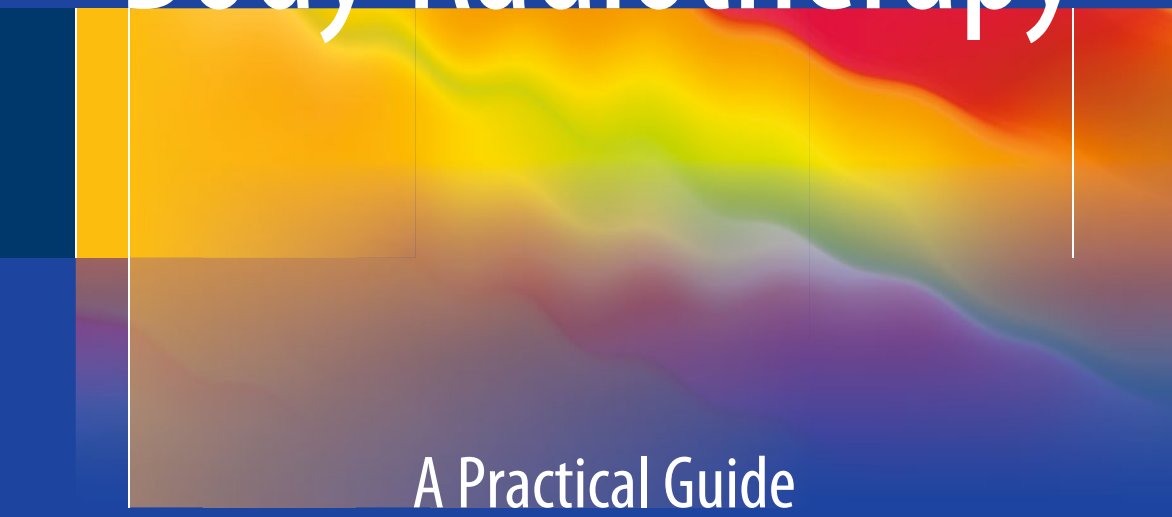

A Practical Guide

Springer

Stereotactic Body Radiotherapy

Andrew Gaya • Anand Mahadevan
Editors

Stereotactic Body Radiotherapy

A Practical Guide

Springer

Editors
Andrew Gaya
Guy's Hospital
London
UK

Anand Mahadevan
Department of Radiation Oncology
Harvard Medical School
Beth Israel Deaconess Medical Center
Boston, MA
USA

ISBN 978-0-85729-596-5 ISBN 978-0-85729-597-2 (eBook)
DOI 10.1007/978-0-85729-597-2
Springer London Heidelberg New York Dordrecht

Library of Congress Control Number: 2015931082

Printed on acid-free paper

Springer is part of Springer Science+Business Media (www.springer.com)

Contents

1 Introduction to Stereotactic Body Radiotherapy 1
Andrew M. Gaya and Anand Mahadevan

2 History and the Technological Evolution of Stereotactic Body Radiotherapy 19
Dharanipathy Rangaraj and Lech S. Papiez

3 Stereotactic Body Radiation Therapy Systems 27
Xing-Qi Lu

4 Physics of Stereotactic Body Radiotherapy—Commissioning, Quality Assurance, and Treatment Planning 45
Cynthia F. Chuang, Maximian F. D'Souza, and John A. Rossman

5 Radiobiology of High Dose Fractions 67
Bleddyn Jones and Roger G. Dale

6 Planning and Dosimetry for Stereotactic Body Radiotherapy 87
Sonja Dieterich

7 Spinal Radiosurgery 109
Iris C. Gibbs, Banu Atalar, and Lei Wang

8 Stereotactic Radiotherapy for Lung Tumors 127
Joost J. Nuyttens

9 Stereotactic Body Radiation Therapy to Liver 149
Andrew M. Gaya

10 Stereotactic Body Radiotherapy (SBRT) for Pancreatic Cancer 183
Anand Mahadevan and Andrew M. Gaya

11 Prostate Stereotactic Body Radiotherapy—Methods, Rationale, Outcomes, and Future Directions 195
Donald B. Fuller

12 Stereotactic Body Radiotherapy for Renal Cancer 225
Irving D. Kaplan, Anand Mahadevan, and Andrew A. Wagner

13 Stereotactic Body Radiotherapy for Oligometastasis 233
Nergiz R. Dagoglu and Anand Mahadevan

14 Stereotactic Body Radiotherapy in Head and Neck Cancer 253
David N. Teguh, Peter C. Levendag, Abrahim Al-Mamgani, and Anand Mahadevan

15 Radiosurgery for Uveal Melanoma 283
Alexander Muacevic, Kirsten H. Eibl-Lindner, Christoph Fürweger, Martin M. Nentwich, Paul Foerster, Berndt Wowra, and Ulrich C. Schaller

16 Stereotactic Body Radiotherapy: A Practical Guide for the Delivery of Accelerated Partial Breast Irradiation 293
Sandra S. Vermeulen, Huan B. Giap, Cristian Cotrutz, Robert M. Douglas, and Astrid Morris

17 Stereotactic Body Radiotherapy for Bone and Soft Tissue Sarcoma 315
Mary Ann Stevenson, Anand Mahadevan, Megan E. Anderson, and Anna Cassoni

Index 325

Contributors

Abrahim Al-Mamgani, MD, PhD Department of Radiation Oncology, Erasmus MC – Daniel den Hoed Cancer Center, Rotterdam, The Netherlands

Megan E. Anderson, MD Department of Orthopedic Surgery, Beth Israel Deaconess Medical Center, Harvard Medical School, Boston, MA, USA

Banu Atalar, MD Department of Radiation Oncology, Acibadem University, Istanbul, Turkey

Anna Cassoni , FRCR Department of Clinical Oncology, University College London Hospitals, London, UK

Cynthia F. Chuang, PhD Department of Radiation Oncology, University of California, San Francisco, San Francisco, CA, USA

Cristian Cotrutz, PhD Department of Radiation Oncology, Swedish Cancer Institute, Radiosurgery Center, Seattle, WA, USA

Maximian F. D'Souza, PhD Department of Radiation Oncology, Frank C. Love Cancer Institute at St. Anthony Hospital, Oklahoma City, OK, USA

Nergiz R. Dagoglu, MD Department of Radiation Oncology, Istanbul Medical Faculty, Istanbul, Turkey

Roger G. Dale, PhD Department of Surgery and Cancer, Faculty of Medicine, Imperial College, London, UK

Sonja Dieterich, PhD Department of Radiation Oncology, Stanford University Hospital, Stanford, CA, USA

Robert M. Douglas, MD Department of Radiation Oncology, Valley Medical Center, Renton, WA, USA

Kirsten H. Eibl-Lindner, MD Department of Ophthalmology, Ludwig-Maximilians-University of Munich, Munich, Germany

Paul Foerster, MD Department of Ophthalmology, Ludwig-Maximilians-University of Munich, Munich, Germany

Donald B. Fuller, MD CyberKnife Centers of San Diego, Genesis Healthcare Partners, San Diego, CA, USA

Christoph Fürweger, Dr. tchn European CyberKnife Center Munich, Munich, Germany

Andrew M. Gaya, MD Department of Clinical Oncology, Guy's & St. Thomas' NHS Foundation Trust, London, UK

Huan B. Giap, MD, PhD Clinical Research, GI, Lung, and Breast Services, University of California of San Diego, Scripps Proton Therapy Center, San Diego, CA, USA

Iris C. Gibbs, MD Department of Radiation Oncology, Stanford University, Stanford, CA, USA

Bleddyn Jones, MA, MSc, MB, BChir, MD, FRCP CRUK-MRC Oxford Institute, ORCRB Building, University of Oxford, OX37DQ, Oxford, Oxfordshire, UK

Irving D. Kaplan, MD Department of Radiation Oncology, Beth Israel Deaconess Medical Center, Harvard Medical School, Boston, MA, USA

Peter C. Levendag, MD, PhD Department of Radiation Oncology, Erasmus MC – Daniel den Hoed Cancer Center, Rotterdam, The Netherlands

Xing-Qi Lu, PhD Department of Radiation Oncology, Beth Israel Deaconess Medical Center, Harvard Medical School, Boston, MA, USA

Anand Mahadevan, MD, FRCS, FRCR Department of Radiation Oncology, Beth Israel Deaconess Medical Center, Harvard Medical School, Boston, MA, USA

Astrid Morris, MD Department of Radiation Oncology, Tumor Institute Radiation Onc., Seattle, WA, USA

Alexander Muacevic, MD European CyberKnife Center Munich, Munich, Germany

Martin M. Nentwich, MD Department of Ophthalmology, Ludwig-Maximilians-University of Munich, Munich, Germany

Joost J. Nuyttens, MD, PhD Department of Radiation Oncology, Erasmus MC Cancer Institute, Rotterdam, Zuid-Holland, The Netherlands

Lech S. Papiez, PhD Adjunct Associate Professor, Purdue University School of Health Sciences, West Lafayette, IN, USA

Dharanipathy Rangaraj, PhD Department of Radiation Oncology, Baylor Scott & White Health, Temple, TX, USA

John A. Rossman, MS Department of Radiation Oncology, Beth Israel Deaconess Medical Center, Boston, MA, USA

Ulrich C. Schaller, MD Herzog Carl-Theodor Eye Clinic, Munich, Germany

Mary Ann Stevenson, MD, PhD Department of Radiation Oncology, Beth Israel Deaconess Medical Center, Harvard Medical School, Boston, MA, USA

David N. Teguh, MD, PhD Department of Radiation Oncology, Erasmus MC – Daniel den Hoed Cancer Center, Rotterdam, The Netherlands

Sandra S. Vermeulen, MD Swedish Radiosurgery Department, Swedish Medical Center, Swedish Radiosurgery Center, Seattle, WA, USA

Andrew A. Wagner, MD Department of Urology, Beth Israel Deaconess Medical Center, Harvard Medical School, Boston, MA, USA

Lei Wang, PhD Radiation Oncology Department, Stanford University Medical School, Palo Alto, CA, USA

Berndt Wowra, MD European CyberKnife Center Munich, Munich, Germany

Chapter 1
Introduction to Stereotactic Body Radiotherapy

Andrew M. Gaya and Anand Mahadevan

Abstract Indications for Stereotactic Radiotherapy have expanded in recent years from intracranial treatment to extracranial, leading to the development of a thriving subspecialty within radiation oncology. The evidence base is growing exponentially. However there is still a lack of good quality prospective randomized clinical trial data. This chapter provides an introduction to the subject and a broad review of the major indications, which are then covered in more depth within individual chapters.

Keywords Stereotactic Body Radiotherapy • SBRT • SABR • Ablation • Cyberknife

Stereotactic body radiotherapy (SBRT) refers to the precise irradiation of an image-defined extracranial target using a small number (usually 1–5) of high-dose fractions. It has developed as an extension of intracranial stereotactic radiosurgery (SRS), and is conceptually different from conventionally fractionated external beam radiotherapy (CFR).

In CFR the tumour volume is irradiated together with a margin to account for tumour and organ motion, and the inaccuracies of planning, setup and delivery. The total dose is limited by the tolerance of normal tissue within, or close to, the planning target volume (PTV). Conventional fractionation (typically 1.8–2 Gy per fraction) optimises the therapeutic ratio.

In SBRT, the PTV contains the target lesion together with a much smaller margin of normal tissue. The intention is to deliver an ablative radiation dose to all tissue within the PTV, exploiting the potent radiobiological effect of large fraction sizes (see Chap. 5).

The safe delivery of ablative doses of radiation requires effective patient immobilisation, precise target localisation (which may involve fusion of different imaging modalities), sophisticated planning software, accurate treatment delivery, and the

A.M. Gaya, MD, MRCP, FRCR (✉)
Department of Clinical Oncology, Guy's Hospital,
Guy's & St. Thomas' NHS Foundation Trust, London, UK
e-mail: agaya@theloc.com

A. Mahadevan, MD, FRCS, FRCR
Department of Radiation Oncology, Beth Israel Deaconess Medical Center,
Harvard Medical School, Boston, MA, USA

A. Gaya, A. Mahadevan (eds.), *Stereotactic Body Radiotherapy: A Practical Guide*,
DOI 10.1007/978-0-85729-597-2_1

ability to produce a steep isodose gradient outside the target volume. In addition, extracranial lesions pose further challenges to treatment delivery due to inter- and intra-fraction tumour and critical organ motion. Until recently this has limited our ability to deliver stereotactic radiotherapy to targets outside the brain. However, advances in image guidance have allowed treatment systems to account for such motion, and consequently the use of SBRT is increasing.

1.1 History of SBRT

Stereotactic surgery was first described by Horsley and Clarke in 1906. They developed a method of locating deep-seated brain lesions by assigning coordinates in three planes to neuroanatomical structures, based on cranial landmarks [1]. In 1947 Spiegel and Wycis introduced frame-based stereotaxy using a plaster head cap known as a stereoencephalatome, and a 3-D coordinate system relative to this [2].

Lars Leksell, a Swedish Neurosurgeon, was the first person to marry the two developing fields of stereotaxy and radiation therapy, and introduced the term "Radiosurgery" in 1951. He used a rigid metal stereotactic head frame fixed to the skull. Small intracranial targets were localised relative to the frame, and radiation was delivered in a single high-dose fraction [3]. The technique initially employed 250 KV x-rays, but in 1967 the first Gamma Knife prototype was developed, using 179 Cobalt-60 sources focused on the target. Since then, Gamma Knife has become widely used for intracranial stereotactic radiosurgery, with sub-millimetre total system accuracy [4].

The 1980s saw the adaptation of linear accelerators for intracranial stereotactic delivery, again using rigid stereotactic head frames, and specialist dosimetry software e.g. X-Knife (Radionics, Boston, MA).

In 1995, Hamilton et al. proposed a method of delivering linac-based stereotactic radiotherapy to spinal lesions using a prototype rigid "extracranial stereotactic frame" and associated 3-D coordinate system. Immobilisation was achieved by transcutaneous frame fixation to spinous processes superior and inferior to the target. They reported an overall treatment accuracy of 2 mm, but the technique was time-consuming, cumbersome, and limited to the delivery of single fractions [5].

Around the same time, Lax et al. developed a stereotactic body frame which, together with a vacuum bag, immobilised the patient from head to mid-thigh. They found the setup reproducibility for liver and lung lesions to be within 5–8 mm for 90 % of the patients. Diaphragmatic movements were reduced to 5–10 mm by applying pressure on the abdomen [6]. Many stereotactic radiotherapy systems today use a similar setup of body frame immobilisation, and some centres use corsets to limit diaphragmatic movement.

However for most extracranial sites the position of the tumour does not enjoy a fixed relationship relative to the external body contour, and can move both between and during each fraction of radiotherapy. An external body frame alone is therefore not sufficient to ensure accurate delivery of radiation to the target. Safe delivery of large fractions of radiotherapy requires sophisticated image guidance.

Image guidance in radiotherapy became a realistic concept with the development of the electronic portal imaging device (EPID) and software to aid quantitative evaluation of patient setup, thus allowing correction of translational errors. The next step was moving from "off-line" to "on-line" image guidance (ie adjusting patient position on the basis of imaging, before each fraction). Accurate identification of tumour position has improved with the use of inserted metal fiducial markers with planar images, or alternatively with the development of volumetric image guidance (eg cone beam CT, or in-room CT on rails). More recently, improved software, together with more sophisticated treatment couches, have meant that correcting for rotational setup errors is now possible. Finally, intra-fractional image guidance is now available, and is a key component of some of the stereotactic treatment systems described below.

Stereotactic systems which use planar imaging have great flexibility with respect to taking multiple intra-fraction images, but largely rely on implanted fiducials. Percutaneous fiducial insertion can be technically difficult, especially in the upper abdomen where it may be necessary to pass through other organs to reach the target lesion. See also Chap. 2.

1.2 Fractionation and Radiobiology

The therapeutic benefit achieved with dose fractionation has been recognised for over 100 years [7]. Conventional fractionation has emerged from such early observations, with subsequent refinement as our knowledge of radiobiology has developed. The linear quadratic model [8] and its ability to describe cellular response to radiation, together with Withers' "4 Rs" of radiotherapy—DNA ***R***epair, ***R***eoxygenation of the tumor, ***R***edistribution within the cell cycle, and ***R***epopulation of cells [9], have had a big influence on modern CFR regimes.

In contrast, intracranial radiosurgery exploits the ablative power of large single doses of radiation, which transcends the considerations proposed by Withers. Considerable dose inhomogeneity within the target volume is standard practice, due to the internal dose gradient achieved by using a low prescription isodose (commonly 40–60 % with gamma knife radiosurgery). There is some evidence to suggest that, rather than being a problem, target dose inhomogeneity may enhance the tumoricidal effect [10].

SBRT sits somewhere between the extremes of CFR and radiosurgery. Large doses per fraction are used, and a moderate internal dose gradient achieved, with a typical prescription isodose of around 60–80 %. However, unlike intracranial radiosurgery, inter- and intra-fraction target movement is a significant problem, increasing the risk of irradiating normal tissue, or missing the tumor, during treatment. Also we are treating at sites where the overwhelming clinical experience and evidence is with conventional fractionation. Conceptually, moving to a single large fraction is big step. The linear quadratic model and its derivatives can help clinicians to predict tissue response to altered fractionation regimes. However, there has been concern that it does not accurately predict tumor cell response at the higher doses per fraction (>10 Gy) seen with stereotactic treatment [11]. At these doses it

is not clear to what extent modest fractionation (2–5 fractions) differs from a single fraction with respect to tumour response and normal tissue effects.

Unsurprisingly, therefore, there has been a large variation in dose and fractionation across SBRT series published to date. Whilst some SBRT centres adopt a "single large fraction" strategy for many patients, other centres would prefer to fractionate in similar cases. Current regimes have in many cases been derived empirically, often the result of cautious dose escalation.

See also Chap. 5.

1.3 Overview of SBRT Systems

A number of modern linacs with on-board imaging capabilities meet the basic image guidance requirements for delivering SBRT (e.g. Varian TruBeam, Elekta Synergy). A micro-multi leaf collimator can be added to produce the required degree of conformality for stereotactic plans.

More recently we have seen the introduction of linacs fully adapted as integrated stereotactic delivery systems. Novalis TX has a Varian Trilogy linac base with micro (2.5 mm) MLC, together with Brainlab ExacTrac image guidance and 6D Robotic Treatment Couch, and associated software. Elekta Axesse is a similar integrated system.

The TomoTherapy System (Accuray Inc, Sunnyvale, CA) has a ring gantry as used in diagnostic CT scanners, and delivers helical IMRT via thousands of small beamlets. Couch movement is continuous during radiation delivery. The system has on-board image guidance with megavoltage CT.

The Cyberknife (Accuray, Sunnyvale, CA) is an image-guided robotic radiosurgery system. A compact 6 MV x-band linac is mounted on a six joint robotic arm. This provides huge flexibility in beam pattern generation, allowing the system to produce very conformal, non-isocentric plans with a steep dose gradient around the target. Near real-time imaging is achieved using two diagnostic x-ray sources positioned orthogonally in the treatment room. Targets that move with breathing can be tracked using the Synchrony respiratory tracking system. Thus the system can correct for both inter- and intra-fraction target movement, which obviates the need for a stereotactic frame. Total system accuracy has been found to be less than 1 mm [12, 13].

See also Chap. 3.

1.4 Respiratory Motion

With thoracic or upper abdominal SBRT we face the additional challenge of accounting for intra-fraction target movement with breathing. The majority of the published data come from centres using gantry-based linacs with vacuum and/or frame body immobilisation, and diaphragmatic pressure to reduce breathing

movement. Respiratory gating methods such as Active Breathing Control (used in some series) have sought to reduce the volume of tissue irradiated by requiring a smaller GTV-PTV margin. The latest gantry-based stereotactic systems (eg Novalis TX) allow respiratory gating using infra-red chest wall tracking and intra-fraction x-ray imaging. 4-D CT planning allows the construction of an internal target volume which takes into account the tumour position at all phases of the respiratory cycle. It has been shown to increase the accuracy of, and reduce the volume of normal tissue irradiated in conformal radiotherapy, and is now being used in some lung SBRT centres.

For Cyberknife, the Synchrony Respiratory Tracking System monitors chest wall movement continuously via an infra-red camera and LEDs placed on the patient's chest. Regular static KV images of the tumour are taken during setup and treatment, and correlated with chest wall movement. A regularly updated predictive model is generated which anticipates future tumour movement with breathing, and the robotic arm moves the radiation beam accordingly. The total accuracy for moving targets has been reported as 1.5 mm. "Xsight Lung" is a further software development for Cyberknife, which allows the tracking of certain peripheral lung lesions (within strict parameters) without the need for implanted fiducials.

1.5 Summary of Major SBRT Indications

1.5.1 Primary Non-Small Cell Lung Cancer (NSCLC)

There are several important published series of lung SBRT. The largest is a Japanese retrospective review of 257 patients from 14 institutions [14]. Patients had resectable stage I disease, but were either medically inoperable or declined surgery. There was considerable variation in immobilisation and respiratory motion management protocols, and also heterogeneity of dose and fractionation (30–84 Gy in 1–14 fractions). Five year actuarial local control rates were 84 % for patients receiving a BED of 100 Gy or more (based on assumed tumour α/β of 10) and 37 % for those receiving less than 100 Gy. Five year overall survival for medically operable patients receiving the higher dose range was 71 %. This was achieved with relatively low rates of radiation toxicity.

There have also been a number of published series of linac-based lung SBRT from European centres [15–19], reporting 88 % local control at around 3 years.

A phase 2 study enrolled 70 inoperable Stage I patients with peripheral or central (within 2 cm of the proximal bronchial tree) tumours, giving 60–66 Gy in 3 fractions. Two year LC and OS were estimated at 95 and 54 % respectively. However, eight patients developed grade 3–4 pulmonary or skin toxicity, and there were six possible cases of grade 5 pulmonary toxicity. The risk of severe pulmonary toxicity was 11 times higher for central, compared to peripheral, tumours [20]. On the basis of these results, centrally located tumours, as defined above, were excluded from two subsequent phase II trials.

For central tumours, the maximum tolerated dose is still under investigation. Chang et al. treated a series of 27 centrally or superiorly located lesions with a slightly more modest dose of 40–50 Gy in 4 fractions. At a median of 17 months, there was no local recurrence seen in the 20 patients receiving 50 Gy (BED 112.5 Gy). There were three cases of grade 2–3 skin/chest wall toxicity and one brachial plexopathy, related to a large volume of plexus receiving 40 Gy. However there was no observed grade ≥3 pulmonary or oesophageal toxicity [21]. RTOG 0813, a phase I/II dose escalation trial, is underway for central stage I tumours in medically inoperable patients.

There have been a number of published series of primary lung SBRT using Cyberknife [22, 23]. Brown et al. treated 59 stage I patients with peripheral tumours. Doses ranged from 15 to 67.5 Gy in 1–5 fractions. With follow up ranging from 1 to 33 months, only 10 % patients had persistent or recurrent disease, and OS was 86 % [23].

SBRT appears to be a safe and effective treatment for early stage NSCLC. With respect to LC, achieving a BED of >100 appears to be very important. Unfortunately there are still no published randomised data comparing SBRT and surgery for operable patients with early stage disease. However, these trials are now underway. ROSEL is a Dutch multi-centre phase III randomised study of linac-based SBRT vs surgery for peripheral Stage 1A NSCLC. The Lung Cancer STARS Trial is an international phase III trial of SBRT with Cyberknife vs Surgery for Stage IA or IB patients (maximum diameter <4 cm). Peripheral tumors receive 60 Gy in 3 fractions, and central tumors 60 Gy in 4 fractions. It will be some time before these trials produce mature data, and in the meantime surgery remains the standard of care. For the large number of medically inoperable patients, SBRT has emerged as the best treatment option.

See also Chap. 8.

1.5.2 Lung Oligometastases

The term “oligometastases” refers to a finite small number of metastases (usually ≤6) confined to a single or limited number of organs. Long term follow up of patients following surgical resection of lung and liver metastases has shown that some of these patients are effectively cured following surgery [24, 25]. For example, in an analysis of over 5,000 patients with lung metastases, the survival following complete surgical resection was 36 % at 5 years and 22 % at 15 years [24]. Thus in some cancers, there appears to be a stable tumor state somewhere between purely localised and widely metastatic. This, together with the results of administering ablative doses of radiation to primary lung tumors, has led to increasing interest in the use of SBRT for oligometastases.

The early data on SBRT for pulmonary metastases emerged as heterogenous published series including both primary and metastatic lung lesions. Wulf et al. [15] demonstrated that with 9 months median follow up, local recurrence/progression was

seen in 5 of 51 metastatic lesions. Once again there was evidence of a dose-response relationship, as four of these five lesions had received the lowest dose (3 × 10 Gy). In a subsequent publication from the same centre, at 18 months median follow up they reported recurrence in 6 of 48 metastatic lesions, giving a crude LC rate of 88 %. Symptomatic pneumonitis was seen in 10 % of patients, with one case of grade 3 pneumonitis [26]. Similar results have been seen in other such series [27, 28].

More recently, several series of purely metastatic lung cases have been reported [29–31] with similar results.

As with primary NSCLC, there are as yet no published randomised data comparing surgery and SBRT for oligometastatic lung disease, but the results seen are encouraging, and the non-invasive approach with low risk of toxicity makes it an attractive option for these patients.

See also Chaps. 8 and 13.

1.5.3 Liver Metastases

As with lung metastases, surgical series of metastectomy for liver metastases have shown a proportion of long term survivors. In a series of 1,000 patients from Memorial Sloan-Kettering Cancer Center with resectable liver-only metastases from colorectal cancer, survival was 37 % at 5 years and 22 % at 10 years [25]. Surgery remains the gold standard for resectable disease, but many patients are unresectable, either due to the extent of metastatic disease, insufficient functional liver reserve or general medical condition. There has therefore been interest in potentially curative, non-surgical options for unresectable patients with oligometastatic disease. Radiofrequency ablation (RFA) is widely practiced with local control rates comparable to surgery for lesions less than 3 cm [32], but lesions close to large vessels or the diaphragm are contraindicated for this technique. Transarterial embolisation, chemoembolisation, irreversible electroporation and radioembolisation are further options.

Whilst whole liver radiation has been used in the past for palliation [33], the radiosensitivity of normal liver tissue has limited the ability to deliver a radical dose to oligometastases in the liver using conventional radiotherapy techniques. Radiation induced liver disease (RILD) is now well documented as a potentially life-threatening condition. SBRT offers the opportunity to deliver ablative doses, whilst staying within acceptable liver DVH constraints.

Patients with liver metastases formed part of Blomgren et al's early series of SBRT using the Elekta stereotactic body frame [34]. Since then there have been a number of published series and early phase trials in this area [35]. Stanford University has published single fraction Cyberknife experience in liver mets [36].

Other centres have adopted a 3-fraction approach to treating liver metastases. In a phase I study by Schefter et al. for 18 patients with 1–3 metastases, the dose was escalated from 36 to 60 Gy without causing any dose-limiting toxicity. In fact, no toxicity >grade 1 was recorded. Patients were treated with linac-based SBRT, using

a body frame and either abdominal compression or Active Breathing Control to account for respiratory motion. Final results of a subsequent multi-institutional phase II study from the same group have recently been published [30]. All patients received 60 Gy in 3 fractions. Thirty six of the 47 patients were assessable for LC, which was estimated to be 92 % at 2 years (100 % for lesions <3 cm diameter). OS was 30 % at 2 years, although 45 % patients had active extrahepatic disease at the time of treatment. Other series also show promising results [37, 38].

See also Chap. 9.

1.5.4 Primary Liver Tumours

Wherever possible, surgery is the treatment of choice for primary hepatocellular carcinoma (HCC), but a significant number of patients are not suitable for either resection or liver transplantation. Studies have shown RFA and Transarterial Chemoembolisation (TACE) to be effective treatments, but again not all patients are suitable. In primary liver disease, SBRT has been used predominantly in patients in whom other local treatments are not suitable, or who have recurred following previous local treatment. There have also been exclusive published SBRT series of primary liver tumors [39, 40].

Princess Margaret Hospital published a parallel phase I study of 41 patients with unresectable HCC or intrahepatic cholangiocarcinoma (IHC). Patients were required to have Child-Pugh A liver function, and >800 cc of uninvolved liver, but tumor sizes were large. One year LC was 65 %, with 51 % 1 year OS. There was no RILD or DLT, but a high incidence of grade 3 liver dysfunction [39]. Choi et al. reported results of SBRT for 20 patients with HCC. 80 % patients had at least partial response and 2 year OS was 43 %, with no toxicity ≥grade 3 [40].

Mirabel has reported the Lille experience of treating HCC and liver metastases with Cyberknife. Twenty one patients with HCC received 45 Gy in 3 fractions. One year progression free survival was 94 % and median survival estimated at 18 months. There was one case of grade 3 duodenal stenosis [41]. There have also been published series of both Cyberknife and linac-based SBRT used in combination with TACE for HCC, showing that these two modalities can be safely used together where appropriate [42, 43].

See also Chap. 9.

1.5.5 Pancreas

Surgery is the standard of care for pancreatic cancer, but unfortunately only 10–20 % of patients are diagnosed with resectable disease. Patients with metastatic disease at diagnosis proceed directly to systemic therapy. For locally advanced non-metastatic or medically inoperable patients, the optimum treatment is less clear. Trials have

shown chemoradiotherapy to improve survival compared to radiotherapy alone [44, 45], but there is conflicting evidence as to whether chemoradiotherapy is superior to chemotherapy alone, both in comparisons with 5 FU-based chemotherapy [46, 47], and with newer gemcitabine-based regimes [48, 49].

Local failure is still a problem in patients treated with CFR. The radiotherapy dose prescribed is limited by small bowel and, especially, duodenal toxicity, although the latter becomes less important following palliative gastrojejunal bypass surgery, which is performed in some centres. The development of conformal radiotherapy has led to interest in the possibility of safe dose escalation to achieve better LC. A Dutch phase II study treated patients with a dose of 70–72 Gy in 2 Gy fractions, but LC with median 9 months follow up was only 56 % [50]. There were also unacceptable normal tissue effects, with 9 % grade 3 acute toxicity and 18 % grade 3–5 late toxicity, including three deaths due to GI bleeding.

There has been hope that SBRT may succeed where CFR has failed in safe and effective dose escalation. Hoyer et al. treated 22 patients with locally advanced pancreatic cancer, with a dose of 45 Gy in 3 fractions. LC at 6 months was again disappointing at 57 %, and median survival only 5.4 months, with 95 % developing metastatic disease at the time of recurrence. Furthermore, 64 % patients experienced ≥grade 2 toxicity, including one case of non-fatal gastric ulcer perforation [51].

Other published results have, however, been more promising. Koong et al. used single fraction Cyberknife radiosurgery for patients with locally advanced disease. Two of the 15 patients had received prior chemoradiotherapy to 50 Gy. The dose started at 15 Gy and was increased to 25 Gy in 5 Gy increments. No toxicity ≥grade 3 was reported, although median follow up was only 5 months. In the group receiving 25 Gy, LC was achieved until death or end of follow up. However, median survival was only 11 months for the whole study group [52].

More recently, an updated series of 77 patients treated with a 25 Gy single fraction has been published by the same institution, with 6 months median follow up [52]. Whilst this is the largest series of SBRT for pancreatic cancer to date, it is heterogenous. Nineteen percent patients had metastatic disease and 10 % had recurrent local disease. Also 27 % were resectable, with surgery not possible due to either medical reasons or metastatic disease. Nevertheless, the results confirm that this regime provides good LC, with estimated 84 % freedom from local progression at 12 months. Unfortunately median survival was still only 6.7 months from time of radiosurgery treatment, although only 9 % of patients had received chemotherapy. Ten percent patients developed ≥grade 3 acute or late GI toxicity.

Whilst SBRT can significantly reduce local recurrence, and may improve quality of life as a result, there is no evidence yet that it improves overall survival. It should be stressed that systemic therapy is central to the management of locally advanced patients, as most will still die of metastatic disease. With this in mind, a short course of stereotactic radiotherapy is much less likely to interfere with a patient's systemic therapy regime, than 5–7 weeks of CFR. Patients with at least stable disease after initial chemotherapy and a PET scan negative for distant disease at that time are the ones most likely to benefit from stereotactic radiotherapy to the primary tumour.

See also Chap. 10.

1.5.6 Kidney

Renal cell carcinoma (RCC) has traditionally been viewed as a radioresistant tumour, as results of CFR on primary and metastatic lesions have been disappointing. However, published series of radiosurgery for metastatic RCC in the brain have shown that the tumour is sensitive to hypofractionated treatment [53, 54]. This has led to interest in the use of SBRT for primary RCC [55], and for extracranial oligometastatic RCC [56].

Wersall et al. published the Karolinska Institute 5 year experience of linac-based SBRT in RCC (primary and metastatic tumors). They treated 162 lesions in 58 patients, including eight inoperable primary tumors and 117 lung metastases. Dose was heterogenous, varying between 25 and 45 Gy in 2–5 fractions according to the size and location of the lesions. Overall LC was impressive at 90 % with median 37 months follow up. However, 40 % patients experienced side effects, and half of the registered side effects were grade 3 in severity [57]. The authors published prospective phase II results the following year, which confirmed the impressive LC seen with their technique (98 % in the 82 treated RCC lesions) [58]. Seventy-three percent of patients with metastatic disease at the time of treatment developed new metastases during follow up.

Given the unpredictable natural history of renal cell metastases, we need randomised data to determine whether an aggressive management strategy, involving SBRT, significantly improves survival in oligometastatic RCC.

See also Chap. 12.

1.5.7 Prostate

There is randomised evidence showing that dose escalation in CFR for localised prostate cancer results in improved biochemical progression free survival, at the expense of an increased risk of late rectal toxicity [59, 60]. There is also increasing evidence to suggest that the α/β ratio of prostate cancer is considerably lower than many other cancers, and indeed lower than that of the surrounding organs at risk [61]. The precise value is still uncertain, although has been estimated to be as low as 1.2 [62]. If this is true, and if we assume that the linear quadratic model holds sufficiently at moderate doses per fraction (2.5–8 Gy), then hypofractionation should improve the therapeutic ratio of prostate radiotherapy. A number of randomised trials of hypofractionation are underway.

SBRT has been shown to produce favourable rectal DVHs when compared to IMRT and conformal 3-D CFRT [63]. This, together with the extreme hypofractionation of stereotactic treatment, would suggest that a stereotactic approach could significantly improve the therapeutic ratio of prostate radiotherapy, in addition to the obvious convenience to patients and radiotherapy departments of shorter courses of treatment. Published series have looked at predominantly low risk localised prostate carcinoma, as the risk of microscopic disease outside the gland is very low.

There is also early interest in using SBRT as a boost following CFR for intermediate and high risk patients.

Madsen et al. published a series of forty low risk patients treated with SBRT using a conventional linac with stereotactic cones. Patients were treated in a "flex-prone" position with inserted fiducial markers for on-line image guidance, and six stationary noncoplanar fields. A dose of 33.5 Gy in 5 fractions was used, as this is equivalent to 78 in 2 Gy fractions to the tumour, assuming a α/β of 1.5. With a 41 month median follow up, the actuarial 4 year biochemical progression free survival was 90 %. One case of acute grade 3 urinary toxicity was reported, and there was no late toxicity $\geq$grade 3 [64].

King et al. have reported preliminary results of a phase II clinical trial of prostate SBRT using Cyberknife [65]. Forty-one low risk patients were treated with 36.25 Gy in 5 fractions either daily or on alternate days. Seventy-eight percent of the 32 patients with minimum 12 months follow up achieved a PSA nadir $\leq$0.4, and the results show that the nadir continues to fall up to and beyond 3 years. There were no cases of PSA failure with median 33 months follow up. There were two cases of grade 3 late urinary toxicity, but no $\geq$grade 3 rectal toxicity.

The planning method described by King et al. aims for a relatively homogenous dose distribution within the PTV. This differs from HDR brachytherapy, a technique with proven efficacy [66, 67], where there is substantial heterogeneity of dose within the target, often with high dose in the peripheral zone of the gland. Fuller et al. have adopted a different approach to Cyberknife prostate radiotherapy, aiming to mimic the dosimetry achieved with HDR brachytherapy [68]. They have published early results of ten low and intermediate risk patients treated in this way, using a dose of 38 Gy in 4 fractions—a standard HDR brachytherapy dose. For each plan, a corresponding simulated HDR brachytherapy plan was produced. Qualitatively, Cyberknife achieved a similar PTV coverage, but lower urethral dose and sharper rectal dose falloff. Follow up is currently too short to assess efficacy. Both Cyberknife dosimetric approaches are under further evaluation in the US, in multicentre phase II trials.

See also Chap. 11.

1.5.8 Vertebral Metastases

Conventional radiotherapy is widely used in the management of spinal metastases, for local control, palliation of pain and treatment of spinal cord compression. However, the prescribed dose is limited by spinal cord and cauda equina radiation tolerance. The steep dose fall off seen with SBRT allows for delivery of a higher dose to the tumor, whilst staying within cord tolerance. Spinal SBRT has, in many ways, developed from intracranial radiosurgery, with heavy neurosurgical involvement. It is unsurprising, therefore, that many of the published series of spine SBRT have used single fraction treatments.

Chang et al. have reported on a Phase I/II trial of linac-based, intensity-modulated SBRT (IMSBRT) for spinal metastases, using a body frame and "near simultaneous"

CT image-guided treatment. Forty-six percent patients had had previous spinal surgery. Using a dose of 30 Gy in 5 fractions or 27 Gy in 3 fractions, 1 year LC was 84 % for the 74 treated lesions, and mean pain scores were significantly reduced. There were three cases of acute grade 3 toxicity, but no significant late toxicity [69]. There have been other reports of IMSBRT for spinal metastases [70–73], including series using the Brainlab Novalis system [71, 72] and Tomotherapy [73].

There have been a number of publications of Cyberknife SBRT in this setting [74–79]. Gerszten et al. published a series of 500 metastatic spinal lesions in 393 patients [74]. Sixty-nine percent lesions had received previous radiotherapy, such that any further meaningful conventional irradiation was not possible. Cervical lesions were tracked relative to skull bony landmarks; lesions at other levels required intraosseus gold fiducial insertion for system tracking. Patients received a single fraction of 12.5–25 Gy, depending on previous radiation dose and proximity to cord/cauda, and median follow up was 21 months. LC was 90 % in patients with no prior radiotherapy, and 88 % overall. Long term pain improvement was seen in 86 % of patients in whom the indication for treatment was pain. There were no cases of radiation myelopathy observed in the follow up period. Smaller, more specific series of patients with spinal metastases from primary melanoma [75], breast [76], lung [77] and renal cell carcinoma [78] have also been published by the same authors.

Since the above patients were treated, Accuray have introduced "Xsight Spine" software for Cyberknife, which verifies tumour position relative to bony landmarks throughout the spine, thus allowing fiducial-free tracking of spinal lesions. The total system error of the Xsight targeting technology has been reported as 0.61 mm.

Wowra et al. reported the Munich experience of single fraction Cyberknife radiosurgery. With a prescribed dose of 15–24 Gy, 348 lesions were treated in 287 patients. Forty-nine of these patients had benign spinal tumours. With median 9.6 months follow up, LC was 94 % for malignant and 100 % for benign lesions. There have been seven cases of late toxicity: one patient with myelopathy, two with spinal instability, and three with tumour haemorrhage [79].

See also Chap. 7.

1.5.9 Primary Spinal Tumors

Microsurgical resection is a safe and effective treatment for benign spinal tumours [80]. However, surgery may not always be possible, for example with post-surgical recurrence or medical comorbidity. SBRT is a useful treatment in these situations.

Several series of Cyberknife SBRT for benign intradural tumours have been published [81–84]. From Stanford University, Dodd et al. [81] treated 55 tumors in 51 patients in whom surgery was contraindicated. Doses ranged from 16 to 30 Gy in 1–5 fractions, although 80 % of patients were treated with 1 or 2 fractions. Median follow up was 23 months. There was evidence of tumour growth post treatment in one patient, but LC was 100 % in those followed up for more than 2 years.

Similarly, Gerszten et al. have reported on 73 intradural lesions treated with Cyberknife, using a single fraction of 12–20 Gy. With 37 months median follow up, LC was once again 100 %, and there was long term improvement in pain scores in 73 % patients [82].

There have been smaller, more specific published series of SBRT for nerve sheath tumours [85], chordomas [86] and sarcomas [87]. Stanford University have also published a series of spinal AVMs treated with Cyberknife [88], although further work is needed here to establish efficacy and optimum radiation dose.

Late spinal cord toxicity is one of the major concerns when planning radiotherapy to spinal lesions. In the largest published retrospective review, 1,075 patients with primary or metastatic tumours were treated with Cyberknife at Stanford or Pittsburgh Universities between 1996 and 2005. Six patients developed radiation-induced late myelopathy at 2–9 months after treatment. In three of these patients, symptoms improved with intervention, and one patient progressed to paraplegia. Specific dosimetric factors associated with development of myelopathy could not be identified [89].

The data presented for both primary and metastatic lesions show SBRT can safely administer higher doses to spinal tumours than is possible with conventional radiotherapy. It is also a non-invasive alternative to surgery for spine metastases, both as primary treatment in unirradiated patients, and as a salvage technique for progressive disease in previously irradiated patients. It has been shown to improve disease-related pain and neurological symptoms. However, once again there are no randomised data comparing SBRT and surgery. Surgery remains the optimum strategy for intradural primary tumours, and, where possible, would be the favoured option in metastatic cases where spinal stabilisation or significant neural decompression is required [90, 91].

See also Chap. 7.

1.6 Conclusion

Advances in image guidance and radiotherapy planning software, together with improved accuracy of treatment delivery, have led to the successful use of stereotactic radiotherapy for extracranial targets. Careful patient selection is especially important. As the volume of normal tissue at the target periphery is related to the cube of the radius, smaller lesions are preferable. The steep dose falloff outside the target volume means that lesions with unclear, infiltrative margins should be avoided. In patients with active disease distant to the treatment site(s), SBRT is unlikely to improve survival, although may achieve good palliation through local control. Similarly, in radical treatment, the risk of distant micrometastatic disease must be carefully considered before proceeding. These qualifications aside, Phase I/II data appear very promising, with excellent local control rates at a number of treatment sites. The results of phase III comparisons with surgery are eagerly awaited.

References

1. Horsley VA, Clarke RH. The structure and functions of the cerebellum examined by a new method. Brain. 1908;31:45–124.
2. Spiegel EA, Wycis HT, Marks M, et al. Stereotactic apparatus for operations on the human brain. Science. 1947;106:349–50.
3. Leksell L. The stereotactic method and radiosurgery of the brain. Acta Chir Scand. 1951;102:316–9.
4. Heck B, Jess-Hempen A, Kreiner HJ, et al. Accuracy and stability of positioning in radiosurgery: long-term results of the gamma knife system. Med Phys. 2007;34(4):1487–95.
5. Hamilton AJ, Lulu BA, Fosmire H, et al. Preliminary clinical experience with linear accelerator-based spinal stereotactic radiosurgery. Neurosurgery. 1995;36:311–9.
6. Lax I, Blomgren H, Naslund I, et al. Stereotactic radiotherapy of malignancies in the abdomen: methodological aspects. Acta Oncol. 1994;33:677–83.
7. Freund L. Elements of general radiotherapy for practitioners. New York: Rebman; 1904.
8. Fowler JF. The linear quadratic formula and progress in fractionated radiotherapy. Br J Radiol. 1989;62:679–94.
9. Withers HR. The four R's of radiotherapy. Adv Radiat Biol. 1975;5:241–7.
10. Tome WA, Fowler JF. Selective boosting of tumor subvolumes. Int J Radiat Oncol Biol Phys. 2000;48:593–9.
11. Guerrero M, Li XA. Extending the linear-quadratic model for large fraction doses pertinent to stereotactic radiotherapy. Phys Med Biol. 2004;49:4825–35.
12. Yu C, Main W, Taylor D, Kuduvalli G, Apuzzo ML, Adler Jr JR. An anthropomorphic phantom study of the accuracy of Cyberknife spinal radiosurgery. Neurosurgery. 2004;55(5):1138–49.
13. Ho AK, Fu D, Cotrutz C, Hancock SL, Chang SD, Gibbs IC, Maurer Jr CR, Adler Jr JR. A study of the accuracy of Cyberknife spinal radiosurgery using skeletal structure tracking. Neurosurgery. 2007;60(2 Suppl 1):147–56.
14. Onishi H, Shirato H, Nagata Y, et al. Hypofractionated stereotactic radiotherapy (HypoFXSRT) for stage I non-small cell lung cancer: updated results of 257 patients in a Japanese multi-institutional study. J Thorac Oncol. 2007;2(7 Suppl 3):S94–100.
15. Wulf J, Haedinger U, Oppitz U, et al. Stereotactic radiotherapy for primary lung cancer and pulmonary metastases: a noninvasive treatment approach in medically inoperable patients. Int J Radiat Oncol Biol Phys. 2004;60(1):186–96.
16. Baumann P, Nyman J, Lax I, et al. Factors important for efficacy of stereotactic body radiotherapy of medically inoperable stage I lung cancer. A retrospective analysis of patients treated in the Nordic countries. Acta Oncol. 2006;45(7):787–95.
17. Zimmerman FB, Geinitz H, Schill S, et al. Stereotactic hypofractionated radiotherapy in stage I (T1–2 N0 M0) non-small-cell lung cancer (NSCLC). Acta Oncol. 2006;45(7):796–801.
18. Hof H, Muenter M, Oetzel D, et al. Stereotactic single-dose radiotherapy (radiosurgery) of early stage nonsmall-cell lung cancer (NSCLC). Cancer. 2007;110(1):148–55.
19. Baumann P, Nyman J, Hoyer M, et al. Outcome in a prospective phase II trial of medically inoperable stage I non-small-cell lung cancer patients treated with stereotactic body radiotherapy. J Clin Oncol. 2009;27(20):3290–6.
20. Timmerman R, McGarry R, Yiannoutsos C, et al. Excessive toxicity when treating central tumors in a phase II study of stereotactic body radiation therapy for medically inoperable early-stage lung cancer. J Clin Oncol. 2006;24(30):4833–9.
21. Chang JY, Balter PA, Dong L, et al. Stereotactic body radiation therapy in centrally and superiorly located stage I or isolated recurrent non-small-cell lung cancer. Int J Radiat Oncol Biol Phys. 2008;72(4):967–71.
22. Le QT, Loo BW, Ho A, et al. Results of phase I dose escalation study using single fraction stereotactic radiotherapy for lung tumors. J Thorac Oncol. 2006;1(8):802–9.
23. Brown WT, Wu X, Fayad F, et al. Cyberknife radiosurgery for stage I lung cancer: results at 36 months. Clin Lung Cancer. 2007;8(8):488–92.

24. Pastorino UB, Buyse M, Friedel G, et al. Long-term results of lung metastasectomy: prognostic analyses based on 5206 cases: the International Registry of Lung Metastases. J Thorac Cardiovasc Surg. 1997;113:37–49.
25. Fong Y, Fortner J, Sun RL, et al. Clinical score for predicting recurrence after hepatic resection for metastatic colorectal cancer: analysis of 1001 consecutive cases. Ann Surg. 1999;230:309–21.
26. Guckenberger M, Heilman K, Wulf J, et al. Pulmonary injury and tumor response after stereotactic body radiotherapy (SBRT): results of a serial follow-up CT study. Radiother Oncol. 2007;85(3):435–42.
27. Lee SW, Choi EK, Park HJ, et al. Stereotactic body frame based fractionated radiosurgery on consecutive days for primary or metastatic tumours in the lung. Lung Cancer. 2003;40(3):309–15.
28. Fritz P, Kraus HJ, Muhlnickel W, et al. Stereotactic, singledose irradiation of stage I non-small cell lung cancer and lung metastases. Radiat Oncol. 2006;1:30.
29. Norihisa Y, Nagata Y, Takayama K, et al. Stereotactic body radiotherapy for oligometastatic lung tumors. Int J Radiat Oncol Biol Phys. 2008;72(2):398–403.
30. Rusthoven KE, Kavanagh BD, Cardenes H, et al. Multi-institutional phase I/II trial of stereotactic body radiation therapy for lung metastases. J Clin Oncol. 2009;27:1572–8.
31. Brown WT, Wu X, Fowler JF, et al. Lung metastases treated by Cyberknife image-guided robotic stereotactic radiosurgery at 41 months. South Med J. 2008;101(4):376–82.
32. Mulier S, Ruers T, Jamart J, et al. Radiofrequency ablation versus resection for resectable colorectal liver metastases: time for a randomized trial? An update. Dig Surg. 2008;25(6):445–60.
33. Leibel SA, Pajak TF, Massullo V, et al. A comparison of misonidazole sensitized radiation therapy to radiation therapy alone for the palliation of hepatic metastases: results of a Radiation Therapy Oncology Group randomized prospective trial. Int J Radiat Oncol Biol Phys. 1987;13:1057–64.
34. Blomgren H, Lax I, Naslund I, et al. Stereotactic high dose fraction radiation therapy of extracranial tumors using an accelerator. Clinical experience of the first thirty-one patients. Acta Oncol. 1995;34(6):861–70.
35. Herfarth KK, Debus J, Lohr F, et al. Stereotactic single-dose radiation therapy of liver tumors: results of a phase I/II trial. J Clin Oncol. 2001;19:164–70.
36. Anderson EM, Koong A, Yang G, et al. Phase I dose escalation study of stereotactic radiosurgery for liver malignancies (poster presentation). In: Proceedings of the ASCO 2007 gastrointestinal cancers symposium, Orlando, 19–21 Jan 2007.
37. Katz AW, Carey-Sampson M, Muhs AG, et al. Hypofractionated stereotactic body radiation therapy (SBRT) for limited hepatic metastases. Int J Radiat Oncol Biol Phys. 2007;67:793–8.
38. Lee MT, Kim JJ, Dinniwell R, et al. Phase I study of individualized stereotactic body radiotherapy for liver metastases. J Clin Oncol. 2009;27:1585–91.
39. Tse RV, Hawkins M, Lockwood G, et al. Phase I study of individualized stereotactic body radiotherapy for hepatocellular carcinoma and intrahepatic cholangiocarcinoma. J Clin Oncol. 2008;26(4):657–64.
40. Choi BO, Jang HS, Kang KM, et al. Fractionated stereotactic radiotherapy in patients with primary hepatocellular carcinoma. Jpn J Clin Oncol. 2006;36:154–8.
41. Louis C, Dewas S, Mirabel X, Lartigau E, et al. Stereotactic radiotherapy of hepatocellular carcinoma: preliminary results. Technol Cancer Res Treat. 2010;9(5):479–87.
42. Takeda A, Takahashi M, Kunieda E, et al. Hypofractionated stereotactic radiotherapy with and without transarterial chemoembolization for small hepatocellular carcinoma not eligible for other ablation therapies: preliminary results for efficacy and toxicity. Hepatol Res. 2008;38(1):60–9.
43. Choi BO, Choi IB, Jang HS, et al. Stereotactic body radiation therapy with or without transarterial chemoembolization for patients with primary hepatocellular carcinoma: preliminary analysis. BMC Cancer. 2008;8:351.
44. Moertel CG, Childs DS, Reitmeier RJ, et al. Combined 5-fluorouracil and supervoltage radiation therapy of locally unresectable gastrointestinal cancer. Lancet. 1969;2:865–7.

45. Moertel C, Frytak S, Hahn R, et al. Therapy of locally unresectable pancreatic carcinoma: a randomized comparison of high dose (6000 rads) radiation alone, moderate dose radiation (4000 rads 5-fluorouracil), and high dose radiation 5-fluorouracil: the Gastrointestinal Tumor Study Group. Cancer. 1981;48:1705–10.
46. Gastrointestinal Tumor Study Group. Treatment of locally unresectable carcinoma of the pancreas: comparison of combined-modality therapy (chemotherapy plus radiotherapy) to chemotherapy alone. J Natl Cancer Inst. 1988;80:751–5.
47. Klaassen DJ, MacIntyre JM, Catton GE, et al. Treatment of locally unresectable cancer of the stomach and pancreas: a randomized comparison of 5-fluorouracil alone with radiation plus concurrent and maintenance 5-fluorouracil—an Eastern Cooperative Oncology Group study. J Clin Oncol. 1985;3:373–8.
48. Chauffert B, Mornex F, Bonnetain F, et al. Phase III trial comparing initial chemoradiotherapy (intermittent cisplatin and infusional 5-FU) followed by gemcitabine vs. gemcitabine alone in patients with locally advanced non metastatic pancreatic cancer: a FFCD-SFRO study. J Clin Oncol. 2006;24(18S, Part I):4008.
49. Loehrer PJ, Powell ME, Cardenes HR, et al. A randomized phase III study of gemcitabine in combination with radiation therapy versus gemcitabine alone in patients with localized, unresectable pancreatic cancer: E4201. abstract 4506. J Clin Oncol. 2008;26(Suppl):214s.
50. Ceha HM, van Tienhoven G, Gouma DJ, et al. Feasibility and efficacy of high dose conformal radiotherapy for patients with locally advanced pancreatic carcinoma. Cancer. 2000;89:2222–9.
51. Hoyer M, Roed H, Sengelov L, et al. Phase-II study on stereotactic radiotherapy of locally advanced pancreatic carcinoma. Radiother Oncol. 2005;76:48–53.
52. Koong AC, Christofferson E, Le QT, et al. Phase II study to assess the efficacy of conventionally fractionated radiotherapy followed by a stereotactic radiosurgery boost in patients with locally advanced pancreatic cancer. Int J Radiat Oncol Biol Phys. 2005;63:320–3.
53. Sheehan JP, Sun MH, Kondziolka D, et al. Radiosurgery in patients with renal cell carcinoma metastasis to the brain: long-term outcomes and prognostic factors influencing survival and local tumor control. J Neurosurg. 2003;98(2):342–9.
54. Muacevic A, Kreth FW, Mack A, et al. Stereotactic radiosurgery without radiation therapy providing high local tumor control of multiple brain metastases from renal cell carcinoma. Minim Invasive Neurosurg. 2004;47(4):203–8.
55. Beitler JJ, Makara D, Silverman P, et al. Definitive, high dose per fraction, conformal, stereotactic external radiation for renal cell carcinoma. Am J Clin Oncol. 2004;27:646–8.
56. Svedman C, Karlsson K, Rutlowska E, et al. Stereotactic body radiotherapy of primary and metastatic renal lesions for patients with only one functioning kidney. Acta Oncol. 2008;47(8):1578–83.
57. Wersall PJ, Blomgren H, Lax I, et al. Extracranial stereotactic radiotherapy for primary and metastatic renal cell carcinoma. Radiother Oncol. 2005;77(1):88–95.
58. Svedman C, Sandstrom P, Pisa P, et al. A prospective phase II trial of using extracranial stereotactic radiotherapy in primary and metastatic renal cell carcinoma. Acta Oncol. 2006;45(7):870–5.
59. Dearnaley DP, Sydes MR, Graham JD, et al. Escalated-dose versus standard-dose conformal radiotherapy in prostate cancer: first results from the MRC RT01 randomised controlled trial. Lancet Oncol. 2007;8:475–87.
60. Pollack A, Zagars GK, Starkschall G, et al. Prostate cancer radiation dose response: results of the MD Anderson phase III randomized trial. Int J Radiat Oncol Biol Phys. 2002;53:1097–105.
61. Dasu A. Is the alpha/beta value for prostate tumours low enough to be safely used in clinical trials? Clin Oncol. 2007;19:289–301.
62. Brenner DJ, Martinez AA, Edmundson GK, et al. Direct evidence that prostate tumors show high sensitivity to fractionation (low alpha/beta ratio), similar to late responding normal tissue. Int J Radiat Oncol Biol Phys. 2002;52:6–13.
63. Madsen BL, Pham HT, Hsi RA, et al. Comparison of rectal dose volume histograms for definitive prostate radiotherapy among stereotactic radiotherapy, IMRT, and 3D-CRT techniques [abstract]. Int J Radiat Oncol Biol Phys. 2004;60:S633.

64. Madsen BL, Hsi RA, Pham HT, et al. Stereotactic hypofractionated accurate radiotherapy of the prostate (SHARP), 33.5 Gy in five fractions for localized disease: first clinical trial results. Int J Radiat Oncol Biol Phys. 2007;67(4):1099–105.
65. King CR, Brooks JD, Gill H, et al. Stereotactic body radiotherapy for localized prostate cancer: interim results of a prospective phase II clinical trial. Int J Radiat Oncol Biol Phys. 2009;73(4):1043–8.
66. Grills IS, Martinez AA, Hollander M, et al. High dose rate brachytherapy as prostate cancer monotherapy reduces toxicity compared to low dose rate palladium seeds. J Urol. 2004;171:1098–104.
67. Demanes DJ, Rodriguez RR, Schour L, et al. High-dose-rate intensity-modulated brachytherapy with external beam radiotherapy for prostate cancer: California endocurietherapy's 10-year results. Int J Radiat Oncol Biol Phys. 2005;61:1306–16.
68. Fuller DB, Naitoh J, Lee C, et al. Virtual HDRSM CyberKnife treatment for localized prostatic carcinoma: dosimetry comparison with HDR brachytherapy and preliminary clinical observations. Int J Radiat Oncol Biol Phys. 2008;70(5):1588–97.
69. Chang EL, Shiu AS, Mendel E, et al. Phase I/II study of stereotactic body radiotherapy for spinal metastasis and its pattern of failure. J Neurosurg Spine. 2007;7(2):151–60.
70. Nelson JW, Yoo DS, Sampson JH, et al. Stereotactic body radiotherapy for lesions of the spine and paraspinal regions. Int J Radiat Oncol Biol Phys. 2009;73(5):1369–75.
71. De Salles AA, Pedroso AG, Medin P, et al. Spinal lesions treated with Novalis shaped beam intensity-modulated radiosurgery and stereotactic radiotherapy. J Neurosurg. 2004;101 Suppl 3:435–40.
72. Ryu S, Jian-Yue J, Jin R, et al. Partial volume tolerance of the spinal cord and complications of single-dose radiosurgery. Cancer. 2007;109(3):628–36.
73. Kim B, Soisson ET, Duma C, et al. Image-guided helical tomotherapy for treatment of spine tumors. Clin Neurol Neurosurg. 2008;110(4):357–62.
74. Gerszten PC, Burton SA, Ozhasoglu C, et al. Radiosurgery for spinal metastases: clinical experience in 500 cases from a single institution. Spine. 2007;32(2):193–9.
75. Gerszten PC, Burton SA, Quinn AE, et al. Radiosurgery for the treatment of spinal melanoma metastases. Stereotact Funct Neurosurg. 2005;83(5–6):213–21.
76. Gerszten PC, Burton SA, Welch WC, et al. Single-fraction radiosurgery for the treatment of spinal breast metastases. Cancer. 2005;104(10):2244–54.
77. Gerszten PC, Burton SA, Belani CP, et al. Radiosurgery for the treatment of spinal lung metastases. Cancer. 2006;107(11):2653–61.
78. Gerszten PC, Burton SA, Ozhasoglu C, et al. Stereotactic radiosurgery for spinal metastases from renal cell carcinoma. J Neurosurg Spine. 2005;3(4):288–95.
79. Wowra B, Zausinger S, Drexler C, et al. CyberKnife radiosurgery for malignant spinal tumors: characterization of well-suited patients. Spine. 2008;33(26):2929–34.
80. Parsa A, Lee J, Parney I, et al. Spinal cord and intradural extraparenchymal spinal tumors: current best care practices and strategies. J Neurooncol. 2004;69:291–318.
81. Dodd RL, Ryu MR, Kammerdsupaphon P, et al. CyberKnife radiosurgery for benign intradural extramedullary spinal tumors. Neurosurgery. 2006;58:674–85.
82. Gerszten PC, Burton SA, Ozhasoglu C, et al. Radiosurgery for benign intradural spinal tumors. Neurosurgery. 2008;62(4):887–96.
83. Bhatnagar AK, Gerszten PC, Ozhasaglu C, et al. CyberKnife frameless radiosurgery for the treatment of extracranial benign tumors. Technol Cancer Res Treat. 2005;4(5):571–6.
84. Sahgal A, Chou D, Ames C, et al. Image-guided robotic stereotactic body radiotherapy for benign spinal tumors: the University of California San Francisco preliminary experience. Technol Cancer Res Treat. 2007;6(6):595–603.
85. Murovic JA, Gibbs IC, Chang SD, et al. Foraminal nerve sheath tumors: intermediate follow up after cyberknife radiosurgery. Neurosurgery. 2009;64(2 Suppl):A33–43.
86. Henderson FC, McCool K, Seigle J, et al. Treatment of chordomas with CyberKnife: Georgetown University experience and treatment recommendations. Neurosurgery. 2009;64(2 Suppl):A44–53.

87. Levine AM, Coleman C, Horasek S, et al. Stereotactic radiosurgery for the treatment of primary sarcomas and sarcoma metastases of the spine. Neurosurgery. 2009;64(2 Suppl):A54–9.
88. Sinclair J, Chang SD, Gibbs IC, et al. Multisession CyberKnife radiosurgery for intramedullary spinal cord arteriovenous malformations. Neurosurgery. 2006;58(6):1081–9.
89. Gibbs IC, Patil C, Gerszten PC, et al. Delayed radiation induced myelopathy after spinal radiosurgery. Neurosurgery. 2009;64(2 Suppl):A67–72.
90. Klimo P, Kestle JR, Schmidt MH. Treatment of metastatic spinal epidural disease: a review of the literature. Neurosurg Focus. 2003;15(5):E1.
91. Patchell RA, Tibbs PA, Regine WF, et al. Direct decompressive surgical resection in the treatment of spinal cord compression caused by metastatic cancer: a randomised trial. Lancet. 2005;366:643–8.

Chapter 2
History and the Technological Evolution of Stereotactic Body Radiotherapy

Dharanipathy Rangaraj and Lech S. Papiez

Abstract After the discovery of use of therapeutic radiation, tremendous advances have been made towards targeted radiation. 3D conformal and intensity modulation have led to conformal therapy minimizing normal tissue toxicity. Improvements in diagnostic technology in delineating tumors, complex planning algorithms, robotic tracking devices, and megavoltage and particle beams have led to use of ablative radiation in the body with minimal side effects.

Keywords Stereotactic radiosurgery • Extracranial • Hypofractionation

2.1 Introduction

Traditional radical radiation therapy delivery requires multiple fractions of 1.5–3 Gy administered daily over a period of 3–7 weeks. These regimens have been derived and calculated from widely accepted models of the radiobiological effect of X rays on human tissue. However, hypo-fractionated, or even single large dose fraction treatments, were practiced in early days of application of X-rays in the treatment of cancer. It has been observed that large doses per fraction were tumorcidal, especially for epithelial tumors, but early clinical experience provided also lessons regarding the balance between tumor control and normal tissue toxicities. Early evaluations of radiation therapy showed that the delivery of large dose per fraction treatments was leading to unacceptably high acute and consequential late normal tissue toxicities. Therefore, quite early in the development of radiation therapy these schedules were abandoned because of complications such as fibrosis, stenosis, and vascular injury. Data collected at the initial stages of the development of radiation therapy supported the understanding that large dose single fractions lead to unacceptable treatment complications.

D. Rangaraj, PhD (✉)
Department of Radiation Oncology, Baylor Scott & White Health, Temple, TX, USA
e-mail: drangaraj@sw.org

L.S. Papiez, PhD
Adjunct Associate Professor, Purdue University School of Health Sciences,
550 Stadium Mall Drive, West Lafayette, IN 47907, USA

A. Gaya, A. Mahadevan (eds.), *Stereotactic Body Radiotherapy: A Practical Guide*,
DOI 10.1007/978-0-85729-597-2_2

The ability to manage the parameters underlying the unfavorable results for large dose per fraction therapy was severely limited in the early days of radiation therapy by the immature technologies of dose delivery. Particularly unfavorable were the relatively low energies of external beams used in the therapy. They were responsible for delivering large doses to normal tissues that were situated between skin and the target. These early experiences and their impact on the acceptance of particular fractionation schemes have been largely forgotten by later practitioners of radiation therapy, even when the megavoltage energies started to become available in radiation therapy. The paradigm of delivering a dose in small daily fractions has been taken for granted, and disconnected from the reflection that early treatments suffered multiple dosimetric limitations resulting from inadequate physical parameters of beams and unsophisticated therapy delivery technology. The exception to this was the treatment proposed by neurosurgeons in the Karolinska Institute; Dr. Leksell, inspired by the availability of high energy, megavoltage Cobalt beams, designed the radiosurgical treatment technique for brain known as Gamma Knife. The technique was not only utilizing the ability to move highly energetic photons to the targeted tissue in brain without depositing excessive energy to cells located between beam entrance at the skull surface and the target, but also relying on the relatively small separation distance between target tissue and the skull surface, and on limiting dose to healthy tissue by moving photons concentrically on the target from many directions (using 201 Cobalt sources).

Characteristic of this technique was that volumes exposed to high dose were relatively small in comparison to the total mass of brain tissue and delivered with high geometrical precision to targets (brain structures have fixed position relative to the skull). These properties of permanent localization of brain structures relative to the skull were helping to achieve the high accuracy of dose delivery when assisted by precise fixation of the skull relative to the Gamma Knife focus through a frame attached surgically to the patient's skull. The precision achieved by the attachment of the frame to the skull made it very inconvenient to irradiate brain in multiple fractions; therefore the regime of single fraction treatment was established for this radiosurgical procedure. The single fraction treatment made radiation oncologists who were practicing multi-fraction radiotherapy delivery skeptical about the radiosurgical treatment mode. Nevertheless, positive outcomes of these treatments accumulating over many years of clinical use of the technique (high success in target ablation and relatively small treatment toxicity with limited and manageable complications) gave enough evidence to reconsider the paradigm of multi-fraction treatments in radiotherapy.

Attempts to transfer the Gamma Knife experience to extracranial treatments were tried in Karolinska. However, initial attempts to transfer Gamma Knife experience to extracranial sites exposed differences in both therapies that pose technical difficulties [1].

First of all most extracranial structures are not fixed in position relative to the skin and so having information about location of the body surface relative to accelerator focus (isocenter) does not guarantee that the target is precisely positioned

relative to irradiating beams. Moreover, extracranial organs are moving both interfraction and intrafraction, and so their location at treatment may be different from their location at simulation and planning, even if we were able to reproduce the position of the target relative to machine focus with perfect precision before treatment was initiated. Therefore therapy practitioners who wanted to transfer cranial radiosurgery experience to extra cranial targets faced considerable technical challenges. The precise positioning of the target in the isocenter of the machine required setting a target by coordinate system derived from imaging of the body, together with verification that body geometry during treatment was close to identical to body geometry at the time of simulation and planning. Finally, there was a clear indication of the need for elimination, or significant suppression at least, of the body structures motion during treatment.

These conditions were to a large degree achieved by the body frame designed for this treatment in Karolinska by Drs. Henrik Blomgren and Ingmar Lax [1]. A treatment technique for extracranial radiosurgery was thus proposed by these researchers. The body frame allowed comfortable repositioning of the patient's body relative to the frame, equipped with metallic fiducial markers determining the system of coordinates relative to the frame geometry that was easily and accurately localizable relative to the room coordinate system of the simulator and the treatment accelerator.

The abdominal compression attached to the body frame allowed for minimization of respiratory motion of the organs within the chest and abdomen. Reproducible positioning of the patient's body with respect to frame assured, after accurate placement of the frame within the room system of coordinates, close correlation between treatment room system of coordinates of the target and organs at risk relative to accelerator isocenter and relative to spatial geometry of treatment beams.

Rescanning patients before each treatment fraction assured moreover the geometry of the body at treatment conformed to the body geometry at simulation and planning as referred to the body frame. Application of abdominal compression made the breathing motion small enough to keep margins around the target from 5 to 10 mm guaranteeing the volume of high dose exposure to be small. To keep the volume of normal tissues exposed to high dose per fraction in extracranial radiosurgery small, the original recommendation for hypofractionated treatment was to not treat targets exceeding 7 cm diameter. The final recommendation of Karolinska clinicians was that multiple beams converging on the target are used to concentrate high dose volume only in the target and its close vicinity. Following these recommendations assured that the dose distribution in extracranial radiosurgery was similar with standards of dose distribution utilized by Gamma Knife intracranial radiosurgery. These properties of extracranial dose characteristics gave them the confidence of recommending hypofractionated treatment, following the experience of Gamma Knife cranial radiosurgery. Generally three to five fractions (ranging between 8 and 20 Gy. per fraction) were used for extracranial radiosurgery with these characteristics. To obviate radiobiological uncertainties, these treatments were recommended initially for targets situated in parallel organs such as lung and liver.

2.2 Clinical Evolution of SBRT

The early extra cranial radiosurgery (now called – stereotactic body radiation therapy – SBRT) that followed guidance from the Karolinska group required considerable effort from radiation oncologist, radiotherapy physicist, dosimetrist and radiotherapist to ensure the treatment conformed to all requirements considered necessary for successful therapy. To ensure success of the treatment it was necessary to (with CT or MRI) simulate the patient carefully within the stereotactic frame when the patient was immobilized with abdominal compression applied, and spatial parameters recorded that located the patient relative to the frame and estimated the motion of the target subsequent to abdominal compression. Treatment planning demanded the identification of target relative to internal fiducial markers determining the position of the target within the body frame coordinate system, and then application of multiple beams (including non-coplanar beams for minimization of volume exposed to over the threshold dose) as well as careful analysis of DVH, and limiting of dose to sensitive structures in the vicinity of the target.

Before each treatment the patient had to be placed cautiously in the frame to reproduce the position of the body relative to the frame as performed during simulation. Nevertheless, even perfect reproduction of the surface and body bony landmarks with respect to the stereotactic frame was not a guarantee of the same relation of the soft tissue target relative to the frame. Therefore, there was a need to verify position of the target location within soft tissue before treatment initiation, by rescanning the patient in the frame. The comparison of body images prepared for treatment with images at simulation had to be evaluated by the radiation oncologist who would then decide if the treatment with parameters derived at planning could proceed, or required correction in placement of the frame relative to treatment room coordinate system. The whole process of patient setup for treatment, excluding time of rescan lasted 30–40 min and when time of treatment was added (with many beams and the large number of monitor units characteristic for hypo-fractionated therapy), the entire process of one fraction of treatment took around 1 hour.

This relative inefficiency of treatment in SBRT has made many physicians sceptical about the potential of this technique to become mainstream. However, it is worth bearing in mind that typical SBRT therapy needs only 1–5 fractions for the completion of the full therapy, making it still efficient when comparison of the total time of therapy is performed between SBRT and traditional fractionation.

In the USA the first center that regularly applied SBRT technique in the treatment of patients was Indiana University Department of Radiation Oncology, where Dr. R. Timmerman who had abundant experience in cranial radiosurgical therapy endorsed with enthusiasm the idea of extracranial radiosurgery [2–4]. The technique was routinely used originally for lung cancer patients who volunteered for this irradiation when faced with the choice of being untreated (inoperable lung cancer) or risking the potential futility of traditional fractionation radiation therapy. When the results from the internal Indiana University protocol were positive (high local control with limited toxicities observed) the natural next step was to test the technique in multi-institutional protocols.

Therefore, being encouraged by results of internal protocol Dr. Timmerman's group decided to design a national protocol for lung cancer treatment with extracranial radiosurgery technique. The primary goal of the national protocol was initially a phase 1 dose escalation trial to establish the appropriate dose in three equal fractions to be delivered to tumor in the lung with the goal of target ablation, whilst preventing significant toxicity [5]. The trial results have shown that dose can be escalated to 18–20 Gy. per fraction (with total of three fractions) resulting in local tumor control exceeding 90 %. These results were difficult to ignore and interest in the SBRT technique caught the attention of radiotherapy practitioners in the USA. Similar advances were also being made in other countries [6].

2.3 Devices, Delivery System and Localization: Early Techniques and Technology

Fortunately these developments coincided with advances in radiotherapy image guidance that enabled SBRT treatment set up to be less complex than was initially required. The important development in treatment delivery was the routine use of cone beam CT installed on new generation linear accelerators.

Cone beam CT made it possible to verify soft tissue anatomy of the patient when located on the treatment couch, removing the need for moving the patient being prepared for treatment to CT or MRI simulator. This resulted in substantial time savings during patient setup for treatment, and eradicated potential errors in target shifts relative to frame when transporting the patient in the frame from CT to treatment room. On the other hand tissue motion management techniques and tools permitted physicians to have more confidence that the dose prescribed to the target would actually be delivered even if the motion of the target exceeded margins assumed at planning.

Another major hurdle which needed to be managed was addressing random and respiratory motion management. Tissue motion management tools most regularly used in radiation oncology and applied to SBRT are dampening respiration, as described above, respiratory gating, and live respiratory motion tracking as performed by CyberKnife. These techniques are not perfect and so abolishing completely the margin for the target when these tools are applied is risky. Breathing motion is not perfectly stable and reproducible in spatial domain. The gating window will therefore always carry a residual error margin; prediction of the position of the target on which tracking properties of the CyberKnife are based may slightly differ from the model derived by CyberKnife Synchrony software if respiratory motion exhibits irregularity. Nevertheless, if combined with abdominal compression these techniques give a better chance of delivering the dose to the target as prescribed for the treatment plan. They may also be applied in cases, with relevant margins defined, when abdominal compression is not applicable.

Thus existing motion management tools can give the physician more confidence that prescribed dose is delivered to the target and that body organs at risk will not

exceed radiation exposure beyond tolerance. However, one also has to keep in mind that gating increases the treatment time still further. Nevertheless, the inconvenience for patient and decrease in efficiency of this factor may also lead to diminished comfort, that in turn may contribute to body dislocation relative to frame resulting in decreased accuracy of treatment delivery. The other aspect that needs to be taken into account when treatments lengthen is the potential radiobiological consequence of the decreased average dose ratio of the treatment. These concerns have to be appropriately taken into account when gating techniques are included as standard in SBRT practice. Modern gating techniques employ dynamic collimation, fiducial based gating including radiofrequency beacons, and active breathing control.

The other aspect of technological progress in radiotherapy delivery in SBRT is the ability to modulate the dose delivery by IMRT. Here we note that this may not be an essential development for SBRT as it has been practiced originally. In the case of SBRT the primary concern was to concentrate dose on the target and minimize the volume of high dose exposure to normal tissue. Achieving this dose distribution has more to do with appropriate directing of radiation beams in space than with modulating beam intensity, when beam directions are fixed in space. Nevertheless, the advance of SBRT to target locations such as liver or pancreas, that are in extreme proximity to sensitive organs, may require shaping of dose clouds that minimize dose in organs at risk.

2.4 Radiobiological Rationale and Its Impact on SBRT Techniques

The crucial question that arises in SBRT is the rationale for its effectiveness. Taking into account that radiobiology is not an exact science, we cannot answer these questions with absolute certainty. However, convincing heuristic advice is possible and should address speculative doubts about the technique. First it is easy to convince radiation oncologists that 54 Gy in three fractions should be a potentially ablative dose. This statement is sustained by radiobiological modeling. More surprising is the result that delivering this extremely high dose to the target in just a small number of fractions allows avoidance of excessive toxicity.

At this point, we should mention that with targets irradiated in parallel tissue, it seems reasonable to expect that cells incapacitated by radiation are not necessarily debilitating the functioning of the whole organ [7, 8]. Cells removed or inactive in lung and liver can be replaced in their functions by other cells within these organs. The important concern is that the inactive or ablated cells do not constitute too large a portion of the organ. However, this concern is explicitly addressed by the conditions of SBRT therapy delivery.

The other aspect of radiobiology that seems unclear from the point of view of SBRT results is the similar effectiveness of the treatment for extensively different fractionation schemes. For example SBRT methods in Japan where fractionation differed from the US RTOG 0236 produced comparable clinical results [6]. The possible explanation of this is that the LQ model routinely applied for deriving

equivalent dose is not directly applicable to hypofractionated regimes. A more detailed analysis of these aspects has been provided in [9] where some evidence suggests that Japanese dose schemes were actually similar to fractionation schemes employed in RTOG 0236.

2.5 Evolution to Treat Other Sites

The critical question for the SBRT technique is its applicability to organs and sites that have not been systematically investigated so far. These questions are justified, as the rationale for SBRT was to a large extent based on the assumption that parallel organs can tolerate limited volume radiation damage without grave consequences for their function, and the overall health of the patient. The existing results indicate that SBRT should be a treatment of choice for lung (excluding targets located in close vicinity of the bronchial tree) and liver and spine.

The success in treatment of prostate cancer with SBRT depends clearly on different factors than the success of treatment of lung cancer with SBRT. The prostate has to be irradiated in SBRT to a large dose in small number of fractions, however, as it is not contained in a parallel functioning organ, the primary concern will be to avoid dose to sensitive organs rather than minimizing the volume of the dose cloud overall. It seems rather convincing that doses of 50–60 Gy in 3–5 fractions delivered to prostate should have a huge potential of controlling the disease, and the fundamental question is then if current delivery techniques allow limiting of dose to rectum and bladder to avoid unmanageable toxicities in these organs. It is somewhat unclear at this time to decide if the combination of optimal beam spatial directions, modulation of beam intensities with the goal of shaping the dose cloud to envelop prostate whilst properly avoiding rectum and bladder, and management of prostate motion, at the time of treatment can result in suitable avoidance of toxicity with adequate irradiation of prostate itself. There are at the present time further trials (such as PACER) that try to answer these questions. Currently SBRT experiences have been reported in almost all body sites in both primary and metastatic cancer.

2.6 Conclusion

SBRT is at the present time a proven technique of radiotherapy delivery for lung and liver and spine. It has definitive radiobiological and convenience advantages relative to traditional fractionation. Clinically it shows unprecedented success in local control (comparable to surgery). It effectively uses new advances in technology of radiotherapy delivery. It applies these tools only as frequently as the fractionation regime requires. This encourages them to be used at each fraction for enhancement of the precision of therapy delivery. The small number of fractions makes also very efficient use of equipment and human resources in radiotherapy departments, to provide more courses of radiation treatment to more patients within the same

amount of time. The shortened course of irradiation can make also easier planning of comprehensive cancer therapy involving, surgery, chemotherapy and radiotherapy. More clinical trial data and longer patient follow up is required to justify the use of this technique in the treatment of other organs (such as pancreas, breast and prostate) and a better understanding of underlying radiobiological principles.

References

1. Lax I, Blomgren H, Näslund I, Svanström R. Stereotactic radiotherapy of malignancies in the abdomen. Methodological aspects. Acta Oncol. 1994;33(6):677–83.
2. Papiez L, Timmerman R, DesRosiers C, Randall M. Extracranial stereotactic radioablation: physical principles. Acta Oncol. 2003;42(8):882–94.
3. Papiez L, Moskvin V, Timmerman R. The physics and dosimetry of SBRT: treatment planning. In: Stereotactic body radiotherapy. Lippincott Williams & Wilkins: Philadelphia; 2004. p. 160.
4. Timmerman R, Papiez L, Suntharalingam M. Extracranial stereotactic radiation delivery: expansion of technology beyond the brain. Technol Cancer Res Treat. 2003;2(2):153–60.
5. Timmerman R, Galvin J, Michalski J, Straube W, Ibbott G, Martin E, et al. Accreditation and quality assurance for Radiation Therapy Oncology Group: multicenter clinical trials using stereotactic body radiation therapy in lung cancer. Acta Oncol. 2006;45(7):779–86.
6. Hiraoka M, Nagata Y. Stereotactic body radiation therapy for early-stage non-small-cell lung cancer: the Japanese experience. Int J Clin Oncol. 2004;9(5):352–5.
7. Wolbrast B, Chin L, Svenson G. Optimization of radiation therapy: integral response of a model biological system. Int J Radiat Oncol Biol Phys. 1983;8:1761–82.
8. Yaes RJ, Kalend A. Local stem cell depletion model for radiation myelitis. Int J Radiat Oncol Biol Phys. 1988;14(6):1247–59.
9. Park C, Papiez L, Zhang S, Story M, Timmerman RD. Universal survival curve and single fraction equivalent dose: useful tools in understanding potency of ablative radiotherapy. Int J Radiat Oncol Biol Phys. 2008;70(3):847–52.

Chapter 3
Stereotactic Body Radiation Therapy Systems

Xing-Qi Lu

Abstract With the development of extracranial stereotactic radiation, there has been an evolution of hardware and software technology to cope with the challenges of SBRT. Advances in immobilization, beam characteristics, image guidance and on-line tracking including continuous respiratory motion management have led to the ability to successfully deliver SBRT with confidence. This chapter explores the capabilities of various SBRT systems.

Keywords Stereotactic Body Radiotherapy (SBRT) • Systems • Immobilization • Tracking • Image Guidance • Quality Control

3.1 Introduction

As an emerging radiotherapy procedure, SBRT (Stereotactic Body Radiation Therapy) is in rapid development. In the previous decade, various radiotherapy techniques and systems for SBRT have been developed and SBRT has become an increasingly common practice.

SBRT's two major features define the requirements for the systems. First, SBRT aims to reproduce physical and biologic aspects of the successful SRS and SRT (intracranial stereotactic radiosurgery and radiotherapy) experience. Since it delivers large doses in a few fractions, it is critical that the high doses to the target are precise and conformal; meanwhile there must be rapid dose fall off away from target to minimize toxicity to normal tissues and critical organs at risk. This is of paramount importance since the increased dose intensification also increases the risk of consequential normal tissue toxicities. Secondly, a feature that distinguishes SBRT from SRT/SRS is that it deals with the area outside the skull base. The target may thus undergo intra- and inter-fraction motion and deformation, and in many cases there is an absence of a reliable surrounding rigid body structure for reference. All these impose stringent requirements in targeting and beam delivery. The system

X.-Q. Lu, PhD
Department of Radiation Oncology, Beth Israel Deaconess Medical Center,
Harvard Medical School, Boston, MA, USA
e-mail: xlu@bidmc.harvard.edu

A. Gaya, A. Mahadevan (eds.), *Stereotactic Body Radiotherapy: A Practical Guide*,
DOI 10.1007/978-0-85729-597-2_3

should be able to either reduce or compensate for this movement during beam delivery.

To satisfy these requirements, various new image guidance techniques have been developed and used along with the other matured techniques. Integration of these techniques in different ways has led to the successful development of several commercially available SBRT systems. In this chapter we first discuss these individual techniques grouped into several sub-systems (Sect. 3.2) and then introduce the commercially available systems (Sect. 3.3). It is our intention to deal with them in a non-biased way.

3.2 System Components and Requirements

The various components that are important for SBRT systems are discussed here. They are grouped into the following sub-systems: (1) Patient immobilization, (2) Target localization and tracking, (3) Simulation imaging and other imaging modalities, (4) Beam characteristics, (5) Planning, and (6) Quality Assurance.

3.2.1 Patient Immobilization

In conventionally fractionated treatment the goal is to reproduce the patient setup during CT simulation for each treatment fraction. In this approach, patient positioning is usually accomplished by using laser alignment to skin marks. Due to the skin mark movements, and patient weight loss during treatment, this method is at best within 2.0–2.5 mm for a perfectly immobilized phantom, and inadequate patient immobilization contributes approximately 1–4 mm of additional error, depending on the site treated [1].

This level of setup accuracy is not adequate for SBRT. An accurate system that accounts for both patient immobilization and intra- and interfraction motion compensation is especially important for the successful delivery of SBRT. Even with highly sophisticated image-guided systems, immobilization is still useful, serving both to physically immobilize the patient and to provide initial approximate target localization.

There are various commercially available stereotactic body frames (Bionix Radiation Therapy, Toledo, OH; CDR system, Calgary, Canada; Body Fix® of Elekta, Stockholm, Sweden). With these devices, vacuum cushions are frequently used. A localizer arch, affixed to the body frame or to the linac couch top, can define the reference coordinate system for body frame fiducials. Some body frame systems include equipment for abdominal compression that can minimize respiratory motion. An immobilization system with such abdominal compression by the CDR system is shown in Fig. 3.1.

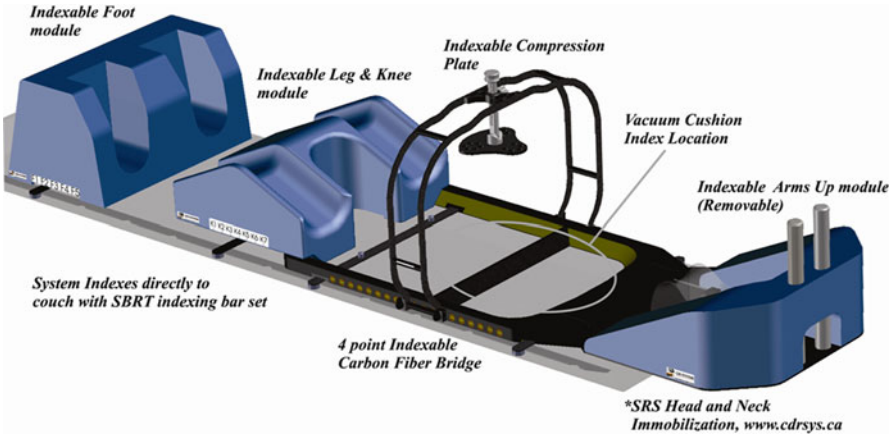

Fig. 3.1 LB-SBRT immobilization system with abdominal compression by CDR Systems

3.2.2 Image-Guided Localization and Tracking

Immobilization devices can reduce body and organ movement to a certain degree, whilst image-guided localization and tracking, with or without immobilization systems, may reduce the targeting spatial uncertainty to a minimum.

We first discuss the imaging techniques used for locating the tumor in 3D. A variety of technologies are used—some of which involve imaging before the treatment, while others allow monitoring of target during treatment, either continuously or intermittently. These techniques include:

1. 2D MV electronic portal imaging (EPID) [2]. Images are created with the megavoltage beam that is used to treat the patient. Although the imaging quality may be limited, it offers real-time, direct monitoring of the areas being irradiated.
2. Dual or multiple KV image systems, either room-mounted [3, 4] or built into the treatment machine. The real-time images can be compared with DRRs, which represent the ideal patient position, and be adjusted accordingly. It has a high imaging quality, but the imaging frequency is limited due to the potentially excessive radiation exposure.
3. CT systems in various forms, including in-the-vault conventional CT [5], MV or KV cone beam CT [6, 7], and the onboard MV fan beam CT in TomoTherapy [8]. CT images are taken right before the treatment and the target position can then be adjusted. KV CT has better image quality, but the MV CT has its advantages. With MV CT it is less susceptible to the artifacts of metal objects such as the fiducials; there is no need for an additional KV source, and its CT values are reliable for accurate calculation of dose distribution.

4. When the 2D radiography and CT localization systems (items 1–3) are used, implanted metal (gold or stainless steel) markers can be very helpful for improved visualization and localization of soft tissue target. The markers are usually implanted into the target area a few weeks before simulation, allowing time for the stabilization of the markers position. During treatment, the markers' on-line position can be precisely compared with those in the simulated image. With this information the body can be repositioned or the beam targeting can be adjusted accordingly.
5. There are several inventions for 3D real-time fiducial localization during treatment with sub-millimeter accuracy. A radiofrequency-based tracking system has been developed by Varian—Calypso Technology (San Francisco, CA) [9, 10]. Small (1.8×8.6 mm) electromagnetic transponders (beacons) implanted into the tumor emit a unique resonant frequency signal when excited by an external electromagnetic field. The magnetic array, which is the source of the electromagnetic field, also receives the frequency signal and determines the transponders' relative positions. A somewhat similar system, the PayPilot® by Micropos Medical (Gorthenburg, Sweden), uses an active radiofrequency emitter, which has a cable connected to outside radiofrequency source. It is suitable for prostate treatment.

   Another device, RealTrack™ technology by Navotek (Yokneam, Israel), uses radioactive sources emitting photons that are detected by an array of detectors located outside the patient's body.

   The advantage of these inventions is that they allow a continuous localization without the KV or MV ionization exposure. A potential disadvantage is that it may not be easily identifiable if the fiducials shifted between CT simulation and treatment, thus resulting in mistreatment.
6. Ultrasound devices are used for localizing soft tissue structures. With these devices the probe's position can be tracked, for instance, by an infrared camera system, thus the soft tissue found by the probe can be located in reference to the isocenter [11]. Accordingly, the couch position can be adjusted before treatment. Currently, there are several US vendors marketing products for assistance with SBRT: SonArray (Zmed, Ashland, MA), ExacTrac Ultrasound Localization (BrainLAB, Heimstetten, Germany), and the BAT® (B-mode Acquisition and Targeting) ultrasound system (Nomos, Sewickley, PA).
7. Low-field open Magnetic Resonance Imaging (MRI) -based systems were first developed for real-time monitoring during surgery. Since MRI provides superior soft-tissue contrast without ionizing radiation, it is ideal for real-time volumetric monitoring of soft-tissue targets in SBRT. Prototype of integration of MRI and linac has been developed [12, 13]. In these systems it is necessary to avoid the interference of the MR magnetic field with the trajectory of the electrons in the linac waveguide, and to avoid the interference of the radiofrequency (RF) signals from each system with the operation of others. From that point of view, it seems advantageous in integration of MRI with a cobalt device. The Renaissance System is based on the technique and is currently being developed by ViewRay, Inc. (Oakwood Village, OH).

8. Optical systems use two or more cameras to relay positional information. Various wavelengths are used, including ultraviolet, visible, and infrared light. Light reflectors or emitters attached to the body may be used, supplying continuous external body information. A laser-based optical surface scanning system, C-RAD Sentinel™ (Uppsala, Sweden), is able to monitor the patient motion during treatment and assist in repositioning.

With the target's 3D position determined, either the patient position or the beam position/direction can be adjusted as desired if the target is well-immobilized. For moving targets, such as targets with respiratory motion (lung and upper-abdominal tumors), the next step, image-guided tracking, becomes necessary. Significant effort has been devoted to solving the problem [14]. Various techniques have been developed in the past, including:

- Gating techniques using either respiratory gating during free-breathing or breath holding [15–19]. With these techniques, the treatment beam is fixed in space and gated to turn on only when the target, fiducial marker, or other surrogate signal (such as an optical system) moves into the preplanned area. Gating is required in both CT simulation and treatment with either external respiratory signals, such as the Varian Real-time Position Management ™ (RPM) system, or using internal fiducial markers tracked by a pair of stereotactic KV X-ray imaging systems [20]. In this approach the treatment beam follows the breath phase but not the absolute position of the target during treatment. As a result of this inherent inaccuracy these techniques still need a substantial safety margin.
- Targeting based on four-dimensional (4D) respiration-correlated CT. Ten or more sets of CT data are reconstructed at each respiratory phase. The patient-specific treatment volumes are determined using extreme tumor positions based on the 4D CT. Treatment planning margins from the gross tumor volume to the planning target volume (PTV) can be reduced substantially on a composite gross tumor volume derived from 4D-CT (known as internal target volume—ITV) [21, 22]. This 4D CT method may also combine with the gating technique, thus leading to a smaller margin. The drawback of this method is that the patient may receive substantial dose from the CT and the number of CT slices generated may well above 1,000.

The above two techniques, however, may not be good enough for SBRT in certain locations. Real-time dynamic tumor-tracking methods or respiratory-synchronized techniques offer a much improved solution. Currently this technique has only been realized by Synchrony™ Respiratory Tracking system (Accuray, Sunnyvale, CA). In this system, the treatment plan is based on a static CT scan, usually in the end-expiration phase. The accelerator is robotically controlled, which allows for non-isocentric beam delivery within a solid angle of over 2π. In order to compensate for the time delay between data acquisition and accelerator repositioning, the tumor's real-time position is predicted by the correlation model of an optical monitor system (with three optical light-emitting markers fitted on a

tight vest worn by the patient) and a pair of orthogonal X-ray images which locate the internal gold fiducials implanted inside the tumor. The external marker position is continuously measured using the optical system and the X-ray images are taken every 3–5 beams (or in newer systems according to how much time has elapsed since the last image, a flexible user-defined variable). The patient can breathe freely; the beam is delivered by a linear accelerator mounted on a robotic arm which follows the corresponding model. This model is checked and updated by acquisition of new pairs of X-ray images. With this tracking system, the tumor's translational movement can be largely compensated, but not for the tumor rotation and body deformation. As a result, a margin of up to 5 mm may be required in selected cases [23]. An improved tracking mode, X-sight Lung by Accuray, allows the dynamic tracking to be achieved based on the lung tumor radiograph images without using fiducials for certain lung cases (about 30 % patients in some centers).

Besides using the robotic controlled linac, the dynamic tumor-tracking can be achieved by a technique currently being developed by Vero, in which a linac is mounted on gimbals that allows tilting of the linac following a moving target. Conceptually, this tracking may also be achieved by dynamic moving MLCs in a conventional linac [24–31] based on the MV EPID or KV imaging. This approach, however, is still in a development stage.

3.2.3 Simulation and Other Imaging Modalities

CT is a primary imaging modality for SBRT. Since CT provides geometric information with minimal spatial distortion (less than 1 mm in 20 cm as the general QA requirement) and provides the tissue density needed for dose calculation, it is the basis for treatment planning. CT images are helpful in identifying pulmonary nodules, parenchymal diseases, and chest wall involvement for superior sulcus tumors and lung diseases [32, 33]. Contrast-enhanced CT is the most sensitive study for the hepatic system [34]. A typical scan length should extend at least 5–10 cm superior and inferior beyond the treatment area; for non-coplanar systems this length should be extended to 15 cm. Tomographic slice thicknesses of 1–3 mm are required.

MR and ^{18}F-fluorodeocyglucose (^{18}FDG) PET are frequently used. As the gold standard for visualization of brain neoplasms, MR also found increasing applications in prostate, spinal tumors, and chest and solid abdominal tumors. PET (Positron Emission Tomography) is valuable in staging, planning and evaluating treatment response and might predict long-term outcome [35]. PET-CT is now popular for reduced image registration uncertainties and widely used for lung cancer, head-and-neck tumors, colon cancer, etc. Whenever possible, the initial patient setup (along with any immobilization device) during CT simulation should be reproduced during other imaging modalities, which helps to significantly reduce the uncertainty when it is fused with the CT imaging.

3.2.4 Beam Characteristics

Among the photon beam characteristics, the beam penetration power and the beam penumbra are important factors to achieve the following dosimetry goals:

- For small narrow beams used in SBRT, the higher the beam energy, the larger the beam penumbra due to lateral electron transport in medium. In a low-density medium, such as lung tissue, this effect becomes more significant. For SBRT lung application a 6 MV photon beam provides a reasonable compromise between beam penetration and penumbra characteristics [36].
- A sharp penumbra is required for a rapid dose fall-off. Inherited from SRS, the cone collimators are naturally a good choice (e.g., they are used in CyberKnife). The Iris™ Collimator in CyberKnife, is adjustable (cone size from 5 to 60 mm) with sub-millimeter accuracy. It has a similar beam profile as the fixed cone and increases the dose delivery efficiency. Another alternative is the multi-leaf collimator (MLC). A study compared a 3 mm micro MLC (Brianlab), a 5 mm MLC, and a 10 mm MLC (Varian Millennium) using the Eclipse treatment-planning system. It was found that the narrower leaf-width MLC provided slightly better results than the wider leaf-width MLCs in an overall dosimetric comparison. This advantage decreases as the target volume increases [37]. In practice, the 3 mm MLCs are more demanding in maintenance. Thus, the 5 mm MLC seems favorable in many SBRT applications.

A new development is the photon beam generated without usage of the flattening filter (Varian TrueBeam™, Varian Medical System, Palo Alto, CA) [38, 39]. When flattening filter-free (FFF) beams are used, out-of-field doses can be reduced significantly. This is mainly due to reduced head scatter and residual electron contamination. FFF beams should therefore lead to reduced peripheral doses and patients may benefit from decreased exposure of normal tissue to scattered doses outside the field. Removal of the flattening filter implies also the possibility to deliver treatments with higher dose rates, up to a factor of 4 at 10 MV, and with a much higher dose per pulse. Besides further improving time efficiency for delivery, this might have subsequent potential radiobiology implications. Whilst interest for FFF beams is increasing in the medical physics field, there are few instances where FFF beams are applied in clinical practice, particularly in SBRT treatments. Initial clinical outcomes for local control are promising. However, aspects related to standardization, dosimetry, treatment planning, and optimization need to be addressed in more detail in order to facilitate the clinical implementation [38, 39].

Tomotherapy is a new concept for beam delivery [8]. A small megavoltage X-ray source was mounted on a ring gantry in a similar fashion to a CT x-ray source, the patient moves through the bore of the gantry simultaneously with gantry rotation. The beam intensity is modulated by temporally modulating multiple independent leaves that open and close across the slit opening. The geometry provided the opportunity to provide CT images of the body in the treatment setup position. The

incident electron beam with 6 and 3.5 MeV in the treatment and imaging modes, respectively.

Cobalt-60 with MLC is also a suitable beam source. It has been shown that the common assumption that the cobalt penumbra is inferior to linac penumbra for MLC-based IMRT is not supported by comparative analysis [40]. Nearly identical plans can be achieved using cobalt source when compared to 6 MV IMRT.

Proton beams are being investigated for SBRT in certain sites. Dosimeric studies for using proton beam in SBRT have been performed by comparison between photon and proton-based SBRT for liver and lung treatment [41, 42]. It indicates that protons resulted in lower doses to critical organs at risk and a smaller volume of non-targeted normal lung exposed to radiation. However, the clinical significance and relevance of these dosimetric improvements remain unknown at the moment.

3.2.5 Planning

The terminology defined for conventional radiation therapy by ICRU 50 and ICRU 62 [43, 44], such as GTV, CTV, PTV, and ITV, is still used in SBRT. In many cases, especially for the metastatic lung, liver, and paraspinal cases, the GTV and CTV are often identical [45–47].

Due to the inevitable movement in most of the extracranial targets, SBRT is inherently imprecise compared to SRS and SRT, unless adequate immobilization or compensation for the target motions, both inter- and intra-fractional, is achieved. Thus dosimetric benefits of targeting essentially rely on the appropriate utilization of immobilization devices and/or on the techniques for precise organ motion compensation [23, 48–50]. The uncertainty in the CTV is generally accounted for by an internal margin added to the CTV, resulting in the internal target volume (ITV) [44]. The PTV then addresses all other possible geometrical variations, including setup uncertainties, machine tolerances, and intra-treatment variations, by adding all these margins to the CTV. This margin should be determined based on the particular SBRT system, the target site, and other clinical conditions.

The main objectives for high-dose-per-fraction SBRT are the precise and conformal targeting and rapid dose fall off to normal surrounding tissues. These objectives can be spelled out in the following dosimetric considerations during treatment planning:

1. The shape of the iso-surface defined by the prescribed dose should conform to the outline of the target. Planning systems providing iso-lines in each CT image, and the DVH (dose-volume histogram) are good tools for evaluating the quality of proposed treatment planning. The Conformity Index is a complementary indicator, which attributes a score to a treatment plan. It can be used to compare several treatment plans for the same patient [51].

2. Rapid fall off of dose from the tumor volume to healthy tissue in all directions, provided the OARs (organs at risk, i.e. serially functioning organs such as the spinal cord or sensitive mucosa) are sufficiently spaced from the target [52]. Otherwise, particular attention has to be paid to the direction of the adjacent critical organs.

   These first two objectives can be achieved primarily by using a large number of preferably non-coplanar beams from as many directions as possible in the treatment.
3. Dose heterogeneity: distribution throughout the volume of the tumor, with the highest dose delivered to the central portion of the tumor, or to a site-specifically defined area. Unlike in conventional radiation therapy where the goal is to deliver uniformly distributed doses to the whole target, in SBRT hot spots (e.g., 130 % of the prescribed dose) within the target volumes are common and generally viewed to be clinically desirable, as long as there is no spillage into normal tissue. It has been hypothesized that hot spots within the central region offer a special advantage in eradicating radio-resistant hypoxic cells that are more likely to be located therein [53].
4. The number of total monitor units used in SBRT in order to achieve the required dosimetry criteria is usually much higher than in conventional and IMRT cases. It has been noticed that the move from 3D-CRT to intensity-modulated radiation therapy (IMRT) involves more fields and a larger volume of normal tissue is exposed to lower doses. In addition, since the number of monitor units is increased by a factor of 2–3, the total body exposure is increased due to the leakage radiation. Both factors tend to increase the risk of secondary cancers. Altogether, IMRT is likely to almost double the incidence of secondary malignancies compared with conventional radiotherapy from about 1–1.75 % for patients surviving 10 years [54]. For certain SBRT treatments the number of monitor units could be increased by another factor of 2 or more. It is advisable to control the ratio of the total monitor units and the prescribed dose, especially for younger patients.

3.2.6 Quality Assurance in SBRT

The QA process is a critical part in conventional radiation therapy, but it assumes an even more important role in SBRT. Because large fraction sizes and small planning target volume (PTV) margins are used, any small setup error risks not only missing the target, but also adding significant toxicity to adjacent normal tissue. The fact that SBRT is administered in a single, or a few, individual treatments does not allow for compensatory random error-driven averaging of the target dose coverage. Therefore, the QA, in particular for targeting and tracking, is such a critical part of the treatment, thus imposing stringent requirements to the QA process.

The AAPM task group has provided guidance on the best practices for performing radiation therapy QA [55]. The supplement of the publication [56] suggests a set

of annual, monthly, and daily QA activities and tolerances which allow the verification of the overall accuracy of the various aspects in SBRT treatment process. In addition, each manufacturer has its own QA recommendations. Based on these published reports and recommendations, an institution should establish a QA plan according to its own individual situation.

3.3 Commercially Available Systems

By integrating different techniques described in the last section, various systems that can treat both SBRT and SRS/SRT have been developed. Here we briefly list the main systems currently available commercially or currently being developed.

1. Major manufactures of conventional radiation therapy linacs have developed their new products, aiming for a seamless transition from conventional therapy to SBRT:

   Varian's latest product for SBRT is the TrueBeam STx. In addition to X-ray imaging, CBCT (cone beam CT) imaging and RPM (Real-Time Position Management TM) gating for respiratory treatment, its new IMR (intra-fraction motion review), or "triggered imaging" system, triggers the low-dose X-ray imager at a specific point in the patient's respiratory cycle, which enables visual verification that a tumor is being properly targeted (refer to Sect. 3.2.2). It also implemented the FFF (flattening filter-free) mode, which has been discussed in Sect. 3.2.4. Treatment deliveries include static and dynamic conformal arcs, conformal beams, and beam or arc intensity-modulated radiosurgery and radiotherapy.

   A combination of Varian's SBRT product with the immobilization and image-guidance system developed by BrainLab AG (Feldkirchen, Germany) is the TrueBeam STx with Novalis Radiosurgery (shown in Fig. 3.2). ExacTrac® Robotic 6D Couch provides automated patient positioning. Room-based X-ray imaging offers fast and accurate patient setup and intra-fraction verification. It is a noninvasive frameless system and allows image-guided spine radiosurgery, gated liver and lung SBRT, and image-guided prostate radiotherapy.

   Elekta Axesse™, developed by Elekta AB (Stockholm, Sweden) includes patient positioning (Hexapod) with 6 degrees of freedom, CBCT and KV images, realized 4D treatment, and HDR-like prostate SBRT. Its XVI Symmetry captures image data during the breathing phase and provides 4D data. This data helps to visualize the tumor position in each respiratory phase, thus warrantees an accurate treatment.

   Siemens Primatom™ developed by Siemens AG (Munich, Germany) is a hybrid system that integrates a linac and a CT with two pairs of high-precision rails. The CT gantry moves on one pair of rails, enabling a rapid diagnostic-quality image of the patient on the treatment table. After the CT scan, the tabletop is moved into position for treatment.

Fig. 3.2 Varian's TrueBeam STx system with Novalis Radiosurgery, including ExacTrac® Robotic 6D Couch, Room-based X-ray imaging

2. The CyberKnife® system by Accuray (Sunnyvale, CA) has emerged from the concept of frameless stereotactic radiosurgery and image guidance with robotic surgical technologies (shown in Fig. 3.3). The imagine system consists of an orthogonal pair of kV x-ray imaging devices and an optical system that monitors the light emitter on the patient surface. It allows non-isocentric, frameless treatment. There are several tracking modalities including that based on bony structure or implanted fiducials, and a real-time dynamic tumor-tracking (Synchorony™ Respiratory Tracking system), which has been discussed in Sect. 3.2.2.
3. Tomotherapy, another product by Accuray, is based on helical tomotherapy processes for image-guided intensity-modulated radiotherapy (refer to Sect. 3.2.4). The image-guidance system includes megavoltage CT acquisition, automated segmentation of CT images, dose reconstruction using the CT image set, deformable registration of CT images, and re-optimization [8]. A Tomotherapy Hi Art system is shown in Fig. 3.4.

Fig. 3.3 A CyberKnife M6 system, where a robotic controlled linac, two X-ray sources, an optical monitor (on the *left side*) and a couch are shown

Fig. 3.4 Tomotherapy HDA, where the linac is mounted on the CT-like gantry and rotates through a full circle

Fig. 3.5 The Vero SBRT System's exterior view. The O-ring (labeled as "1") is skewed in the counterclockwise direction. The ring can rotate over ±60°. Label "2" indicates dynamic MLC, in both sides are two X-ray source. Label "3" indicates the gumbal for iso-center calibration and tumor chasing. Label "4" indicates the integrated real-time patient monitor

4. The Vero SBRT System (known as "TM2000" in Japan), is a joint product of Mitsubishi Heavy Industries Ltd. and BrainLab (shown in Fig. 3.5), utilizing a rotating, rigid ring structure to integrate a beam delivery platform and image guidance systems. The system includes an electronic MV portal imaging device (EPID) and dual KV fluoroscopy, and cone beam CT imaging for image guided setup and real-time fluoroscopic monitoring for pursuit irradiation. An inline 6 MV C-band linac with MLC is mounted on orthogonal gimbals built into the ring structure. The gimbaled irradiation head with tilt functions allows isocentric or non-isocentric treatment and dynamic tracking (refer to Sect. 3.2.2).
5. The Gamma Knife has evolved in treatment for extra-cranial diseases. Several manufacturers have emerged; promising clinical outcome for patients with inoperable stage I/II non-small-cell lung cancer has been reported [57]. Shown in Fig. 3.6 is a stereotactic gamma-ray body therapeutic system, GyroKnife developed by γ[gamma]-Star (Shanghai, China). It uses a source, which is comprised by 154 self-focusing micro-cobalt sources. The combination of "triple focusing" and a body frame can result in sharp dose gradients and high-precision localization.
6. ViewRay is another Body Gamma Knife system, currently being developed by Renaissance Systems (Oakwood Village, OH). Three cobalt beams are modulated

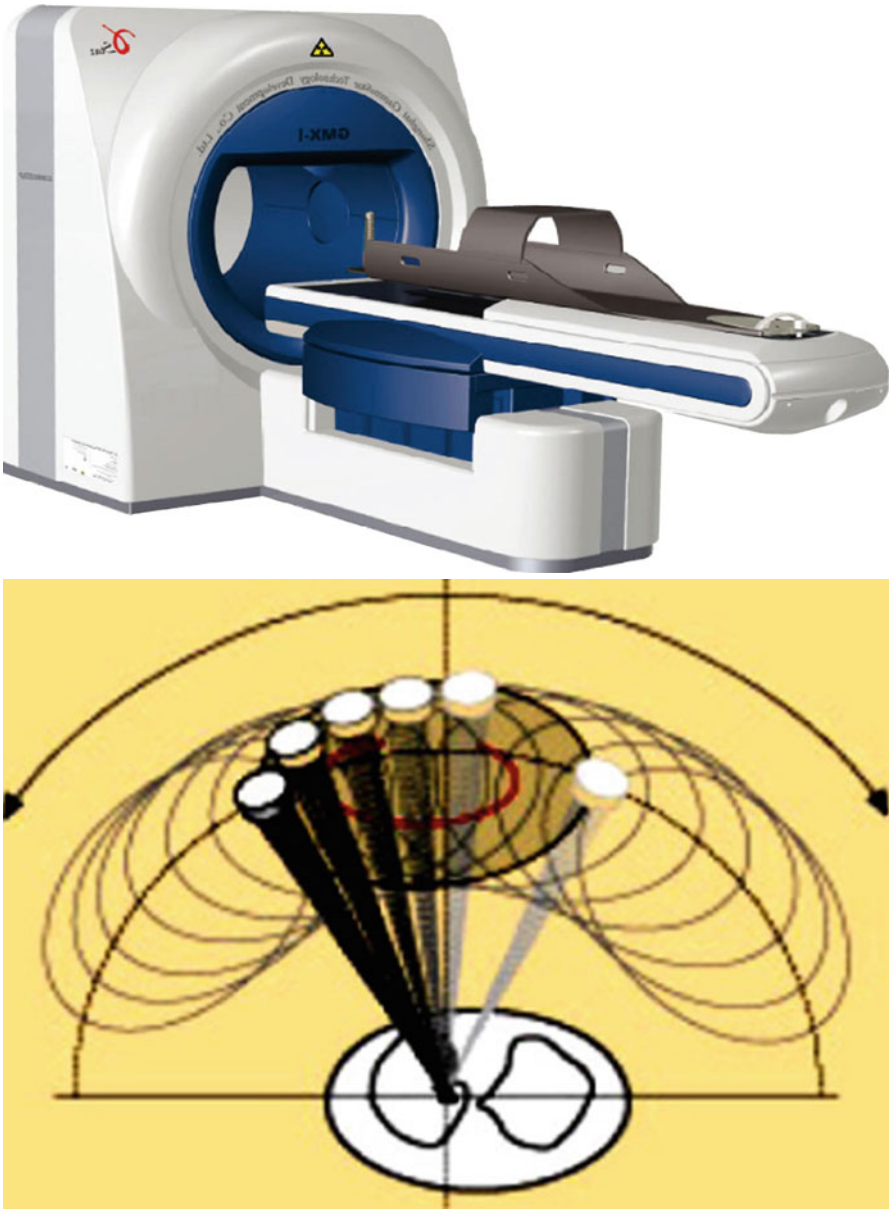

Fig. 3.6 The GyroKnife system. The "triple focusing" is illustrated in the small picture

with MLCs. This system is equipped with low-field open magnetic resonance imaging (refer to Sect. 3.2.2). Dynamic MR images are acquired to track patients in real-time. The ability to see soft tissue clearly in motion with MR is of great benefit in delivering high dose in a single fraction.

References

1. Verhey LJ. Immobilizing and positioning patients for radiotherapy. Semin Radiat Oncol. 1995;5:100–14.
2. Lovelock DM, Hua C, Wng P, et al. Accurate setup of paraspinal patients using a noninvasive patient immobilization cradle and portal imaging. Med Phys. 2005;32:2606–14.
3. Chang SD, Main W, Martin DP, et al. An analysis of the accuracy of the CyberKnife: a robotic frameless stereotactic radiosurgical system. Neurosurgery. 2003;52:140–7.
4. Shirato H, Shimizu S, Kunieda K, et al. Physical aspects of a real-time tumor-tracking system for gated radiotherapy. Int J Radiat Biol. 2000;48:1187–95.
5. Yenice KM, Lovelock DM, Hunt MA, et al. CT image-guided intensity-modulated therapy for paraspinal tumors using stereotactic immobilization. Int J Radiat Biol. 2003;55:583–93.
6. Pouliot J, Bani-Hashemi A, Chen J, et al. Low-dose megavoltage cone-beam CT for radiation therapy. Int J Radiat Biol. 2005;61:552–60.
7. Jaffray DA, Siewerdsen JH, Wong JW, et al. Flat-panel cone-beam computed tomography for image-guided radiation therapy. Int J Radiat Biol. 2002;53:1337–49.
8. Mackie TR, Kapatoes J, Ruchala K, et al. Image guidance for precise conformal radiotherapy. Int J Radiat Oncol Biol Phys. 2003;56:89–105.
9. Balter JM, Wright JN, Newell LJ, et al. Accuracy of a wireless localization system for radiotherapy. Int J Radiat Oncol Biol Phys. 2005;61:933–7.
10. Willoughby TR, Kupelian PA, Pouliot J, et al. Target localization and real-time tracking using the Calypso 4D localization system with localized prostate cancer. Int J Radiat Oncol Biol Phys. 2006;65:528–34.
11. Meeks SL, Buatti JM, Bouchet LG, et al. Ultrasound-guided extracranial radiosurgery: technique and application. Int J Radiat Oncol Biol Phys. 2003;55:1092–101.
12. Lagendjijk J, Raaymakers B, Raaijmakers A, et al. MRI/linac integration. Radiother Oncol. 2008;86:25–9.
13. Fallone B, Murray B, Rathee S, et al. First MR images obtained during megavoltage photon irradiation from a prototype integrated linac-MR system. Med Phys. 2009;36:2009.
14. AAPM T. AAPM Report No. 91, The management of respiratory motion in radiation oncology. 2006.
15. Harada T, Shirato H, Ogura S. Real-time tumor-tracking radiation therapy for lung carcinoma by the aid of insertion of a gold maker using bronchofibroscopy. Cancer. 2002;95:1720–7.
16. Zhang T, Keller H, O'Brien M, et al. Application of the spirometer in respiratory gated radiotherapy. Med Phys. 2003;30:3165–71.
17. Berson AM, Emery R, Rodriguez L, et al. Clinical experience using respiratory gated radiation therapy: comparison of free-breathing and breath-hold techniques. Int J Radiat Oncol Biol Phys. 2004;60:419–26.
18. Berbeco RI, Nishioka S, Shirato H, et al. Residual motion of lung tumors in end-of-inhale respiratory gated radiotherapy based on external surrogates. Med Phys. 2006;33:4149–56.
19. Wong J. Methods to manage respiratory motion in radiation treatment. In: Palta J, Rockwell M, editors. Intensity-modulated radiation therapy. Madison: Medical Physics; 2003. p. 663–702.
20. Kitamura K, Shirato H, Seppenwoolde Y, et al. Three-dimensional intrafractional movement of prostate measure during real-time tumor-tracking radiotherapy in supine and prone treatment position. Int J Radiat Oncol Biol Phys. 2002;53:1117–23.
21. Rietzel E, Liu A, Doppke K, et al. Design of 4D treatment planning target volumes. Int J Radiat Oncol Biol Phys. 2006;66:287–95.
22. Coolens C, Evans PM, Seco J, et al. The susceptibility of IMRT dose distributions to intrafraction organ motion: an investigation into smoothing filters derived from four dimensional computed tomography data. Med Phys. 2006;33:2809–18.
23. Lu X-Q, Shanmugham LN, Mahadevan A, et al. Organ deformation and dose coverage in robotic respiratory-tracking radiotherapy. Int J Radiat Oncol Biol Phys. 2008;71:281–9.

24. Keall PJ, Chen G, Joshi S. Time-the fourth dimension in radiotherapy (ASTRO panel discussion). Int J Radiat Oncol Biol Phys. 2003;57:88–9.
25. McQuaid D, Webb S. MRT delivery to a moving target by dynamic MLC tracking: delivery for targets moving in two dimensions in the beam's-eye view. Med Phys. 2006;33:2296.
26. Papiez L, Rangaraj D, Keall PJ. Real-time DMLC IMRT delivery for mobile and deforming targets. Med Phys. 2005;32:3037–48.
27. Webb S. Limitations of a simple technique for movement compensation via movement-modified fluence profiles. Phys Med Biol. 2005;50:N155–61.
28. Neicu T, Berbeco R, Wolfgang J, et al. Synchronized moving aperture radiation therapy (SMART): improvement of breathing pattern reproducibility using respiratory coaching. Phys Med Biol. 2006;61:617–36.
29. Ahn S, Yi B, Suh Y, et al. A feasibility study on the prediction of tumor location in the lung from skin motion. Br J Radiol. 2004;77:588–96.
30. Gierga D, Chen G, Kung JH, et al. Quantification of respiration-induced abdominal tumor motion and its impact on IMRT dose distributions. Int J Radiat Oncol Biol Phys. 2004;58:1584–95.
31. Poulsen P, Cho B, Sawant A, et al. Dynamic MLC tracking of moving targets with a single kV imager for 3D conformal and IMRT treatments. Acta Oncol. 2010;49:1092–100.
32. Kauczor HU, Heussel CP, Thelen M. Radiodiagnosis of the lung. Radiologe. 2000;40:870–7.
33. Komaki R, Putnam JB, Walsh G, et al. The management of superior sulcus tumors. Semin Surg Oncol. 2000;18:152–64.
34. Kamel IR, Fishman EK. Recent advances in CT imaging of liver metastases. Cancer J. 2004;10:104–20.
35. Coon D, Gokhale AS, Burton SA, et al. Fractionated stereotactic body radiation therapy in the treatment of primary, recurrent, and metastatic lung tumors: the role of position emission tomography/computed tomography-based treatment planning. Clin Lung Cancer. 2008;9:217–21.
36. Benedict SH, Yenice KM, Followill D, et al. Stereotactic body radiation therapy: the report of AAPM Task Group 101. Med Phys. 2010;37:4078–101.
37. Jin JY, Yin FF, Ryu S. Dosimetric study using different leaf-width MLCs for treatment planning of dynamic conformal arcs and intensity-modulated radiosurgery. Med Phys. 2005;32:405–11.
38. Vassiliev O, Kry S, Kuban D, et al. Treatment planning study of prostate cancer intensity modulated radiotherapy with a Varian clinac operated without a flattening filter. Int J Radiat Oncol Biol Phys. 2007;68:1567–71.
39. Georg D, Knoos T, McClean B. Current status and future perspective of flattening filter free photon beams. Med Phys. 2011;38:1280–93.
40. Fox C, Romeijn H, Lynch B, et al. Comparative analysis of $_{6}0$ Co intensity-modulated radiation therapy. Phys Med Biol. 2008;53:3175–88.
41. Petersen J, Lassen Y, Hansen A, et al. Normal liver tissue sparing by intensity-modulated proton stereotactic body radiotherapy for solitary liver tumors. Acta Oncol. 2011;50:823–8.
42. Register S, Zhang X, Mohan R, et al. Proton stereotactic body radiation therapy for clinically challenging cases of centrally and superiorly located stage I non-small-cell lung cancer. Int J Radiat Oncol Biol Phys. 2011;80:1015–22.
43. ICRU50. Prescribing, recording, and reporting photon beam therapy. ICRU Report 50. Bethesda: International Commission on Radiation Units and Measurements; 1993.
44. ICRU62. Prescribing, recording and reporting photon beam therapy (supplement to ICRU Report 50). ICRU Report 62. Bethesda: International Commission on Radiation Units and Measurements; 1999.
45. Herfarth K, Debus J, Lohr F, et al. Stereotactic single-dose radiation therapy of liver tumors: results of a phase I/II trial 19. J Clin Oncol. 2001;19:164–70.
46. Bilsky Y, Yamada KM, Yenice K, et al. Intensity-modulated stereotactic radiotherapy of paraspinal tumors: a preliminary report. Neurosurgery. 2004;54:823–30.

47. Takayama K, Nagata Y, Negoro Y, et al. Treatment planning of stereotactic radiotherapy for solitary lung tumor. Int J Radiat Oncol Biol Phys. 2005;61:1565–71.
48. Hadinger U, Thiele W, Wulf J. Extracranial stereotactic radiotherapy: evaluation of PTV coverage and dose conformity. Z Med Phys. 2002;12:221–9.
49. Hara R, Itami J, Kondo T, et al. Stereotactic single high dose irradiation of lung tumors under respiratory gating. Radiother Oncol. 2002;63:159–63.
50. Onishi H, Kuriyama K, Komiyama T, et al. A new irradiation system for lung cancer combining linear accelerator, computed tomography, patient self-breath-holding, and patient-directed beam-control without respiratory monitoring devices. Int J Radiat Oncol Biol Phys. 2003;56:14–20.
51. Feuvret L, Noel G, Mazeron JJ, et al. Conformity index: a review. Int J Radiat Oncol Biol Phys. 2006;64:333–42.
52. Papiez L, Timmerman R, DesRosiers C, et al. Extracranial stereotactic radioablation: physical principles. Acta Oncol. 2003;42:882–94.
53. Fowler JF, Tome WA, Fenwich JD, et al. A challenge to traditional radiation oncology. Int J Radiat Oncol Biol Phys. 2004;60:1241–56.
54. Hall EJ, Wuu C-S. Radiation-induced second cancers: the impact of 3D-CRT and IMRT. Int J Radiat Oncol Biol Phys. 2003;56:83–8.
55. Kutcher GJ, et al. Comprehensive QA for radiation oncology: report of AAPM Radiation Therapy Committee Task Group 40. Med Phys. 1994;21:581–618.
56. Klein EE, Hanley J, Bayouth J, et al. AAPM Task Group 142 report: quality assurance of medical accelerators. Med Phys. 2009;36:4197–211.
57. Xia T, Li H, Sun Q, et al. Promising clinical outcome of stereotactic body radiation therapy for patients with inoperable stage I/II non-small-cell lung cancer. Int J Radiat Oncol Biol Phys. 2006;66:117–25.

Chapter 4
Physics of Stereotactic Body Radiotherapy—Commissioning, Quality Assurance, and Treatment Planning

Cynthia F. Chuang, Maximian F. D'Souza, and John A. Rossman

Abstract Stereotactic radiosurgery (SRS) and Stereotactic body radiotherapy (SBRT) have gained wide spread use as a modality of treatment in Radiation Oncology during the last decade. In this chapter, we describe various devices that are capable of delivering SBRT. These systems are complex combinations of treatment and imaging capabilities. Therefore, they require substantial efforts in commissioning and clinical validation before being used for patient treatment. We present a broad overview of commissioning whilst emphasizing the complexity of small field dosimetry. In addition, Treatment Planning System (TPS) commissioning is also discussed. Clinical validation of TPS, SBRT and Imaging systems must be validated both by performing end-to-end measurements and also by using third party (for example, Radiological Physics Center (RPC) phantoms and systems) before using the system clinically. Routine quality assurance (QA) and quality control (QC) is an important aspect of this treatment modality and must be strictly maintained to ensure stringent quality requirements. In addition, some systems provide patient specific QA options which further assists in ensuring high quality treatment delivery. Finally we review a variety of scenarios where SBRT may be used, demonstrating the ability to deliver high doses to the tumor whilst significantly sparing surrounding organs at risk.

Keywords Stereotactic body radiotherapy • Radiosurgery • Quality assurance • Commissioning • Treatment planning

C.F. Chuang, PhD
Department of Radiation Oncology, University of California, San Francisco, San Francisco, CA, USA
e-mail: cchuang@radonc.ucsf.edu

M.F. D'Souza, PhD
Department of Radiation Oncology, Frank C. Love Cancer Institute at St. Anthony Hospital, Oklahoma City, OK, USA
e-mail: mdsouza007@gmail.com

J.A. Rossman, MS (✉)
Department of Radiation Oncology, Beth Israel Deaconess Medical Center, Boston, MS, USA
e-mail: jrossman@bidmc.harvard.edu

A. Gaya, A. Mahadevan (eds.), *Stereotactic Body Radiotherapy: A Practical Guide*,
DOI 10.1007/978-0-85729-597-2_4

4.1 Introduction

Stereotactic radiosurgery (SRS) is a technique of precisely delivering a large dose of radiation to small intracranial targets. SRS has been commonly used by neurosurgeons since the advent of the Gamma Knife (Elekta Inc., Atlanta, GA) in the early 1960s. With the advancement of linear accelerator technology with micro multi leaf collimators (mMLC) and devices like the Novalis system (Brain Lab AB, Heimstetten, Germany), Cyberknife (Accuray Inc., Sunnyvale, CA) and Varian True Beam system (Varian, Palo Alto, CA) it has been possible to deliver radiosurgical doses to extracranial targets with the requisite precision. These devices combine imaging equipment to the radiation delivery system to allow accurate localization of the target just prior to radiation. This advancement is especially important for treating moving targets such as in lung, liver, pancreas, and prostate.

Steretactic body radiotherapy (SBRT) is a term commonly used for hypofractionated treatment (1–5 fractions) of extra cranial lesions. SBRT offers a high biologically effective dose (BED) dose to the tumor with a sharp decline in dose to surrounding normal tissues and critical structures [1]. The dose delivery accuracy requirements are similar for SRS and SBRT. Utilization of a large number of small fields for delivering very high dose in comparison with traditional radiotherapy places significant importance on the accuracy of small field dosimetry. Typical end-to-end targeting error for SBRT is of the order of 1–1.5 mm which includes tumor imaging, beam data, system targeting and patient positioning accuracy. This demands greater dosimetry accuracy than that required for radiotherapy, in addition to system mechanical stability and accuracy which includes the imaging sub-system that is used for patient positioning.

4.2 SBRT System Commissioning

Acceptance testing involves verification of a subset of machine parameters based on manufacturer's specifications for the entire treatment delivery system. This includes both the mechanical and the radiation component of the entire system. In addition, the imaging sub-system used for patient positioning guidance is also tested for both mechanical accuracy and stability and radiation characteristics whenever applicable. The commissioning process, typically is a more extensive process predominantly focused on radiation beam characteristics. A full set of data is acquired that is input into the planning system to be used for patient treatment. This data set also provides a baseline characteristic of the treatment delivery system for future comparison.

4.2.1 Beam Data

There are many common beam data requirements between various SBRT delivery systems, however, some treatment planning systems (TPS) require additional specific data that may be needed for full commissioning of a system. Typically there is only a single energy that is used for SBRT treatments. Hence the time commitment required for the commissioning process is less than that required for the typical linear accelerator used for radiotherapy, which generally has at least two photon energies and 5–6 electron energies. SBRT systems require careful measurement of complete beam data on site. Although, some manufacturers may provide golden beam data sets, which contain most or all of the commissioning beam data required by the TPS. Use of this data with validation of subset of data may be acceptable for radiotherapy treatments. However, this is strongly discouraged for SBRT treatments. The accuracy of beam data measured should be independent of data scanning equipment and/or individuals performing the measurement. As per AAPM TG-106 report [2], this variation among individuals and/or scanning systems should be less than 1 %.

Typical beam data requirements characterize beam energy, beam flatness and symmetry and beam output. The following parameters are typically required for all SBRT systems currently on the market; percentage depth dose (PDD) and/or tissue phantom ratio (TPR), beam profiles at various depths to determine off-axis ratio (OAR), output factors relative to a normalization field size. In SBRT systems that use micro multi-leaf collimators (mMLC), the mMLC system needs to be further characterized for leaf transmission, inter-leaf leakage, penumbra, tongue and groove effect. The data obtained during the commissioning process is used as the standard data for clinical use and should be verified periodically as described by TG-142 [1]. The data measured also depends on the TPS requirements. Hence any changes to the TPS or the delivery system that may affect the measured data may require additional data collection for verification [3, 4]. Additional data that is not required for the TPS commissioning but may assist in annual QA may also be acquired at this time. For example, for Cyberknife systems direct TPR's are measured for the commissioning requirements, however for annual QA, PDD's could be used for comparison providing significant time saving.

4.2.2 Data Acquisition

There are several water scanners on the market (example; PTW-Freiburg, IBA dosimetry (formerly Scanditronix Wellhoffer), ARM Inc., SunNuclear Corp, etc.) that are capable of meeting the beam data acquisition requirements of an SBRT system. Scanned beam data measurements require water scanners to provide full

scatter conditions and measurement depth of at least 30 cm with at least 5 cm of backscatter depth. Smaller water tanks may be used after ensuring the lateral dimensions are at least twice that of the largest field size measured to allow for lateral buildup and extra scanning range [3]. Non-scanned data may be acquired in water phantoms or solid phantoms using an ion chamber, diode detectors, TLD or film.

The choice of detector(s) to be used presents a significant challenge since improper choice of detector can severely affect the accuracy of the data collected [5]. Small field dosimetry presents unique challenges due to availability of detectors with widths approaching field sizes used in SBRT. There is a large selection of stereotactic detectors available that claim to have the needed accuracy for small field measurements; ionization chambers, semi-conductor diode detectors, edge detectors or liquid filled chambers. Figure 4.1 shows wide variability in PDD for small and large field measurements [3]. Detectors with spatial resolution of 1 mm or better are needed [2]. Standard Farmer type chamber with average active volume of 0.6 cm^3 may only be used for the absolute dose measurement in the reference field that is greater than the dimensions of the chamber. The reference field size in SBRT is typically greater than 5 cm^2 or 5 cm diameter. For scanning purposes, microchambers with an active volume on average of less than 0.01 cm^3 are ideally suited for small field dosimetry as applicable in SBRT [3, 6–8]. However, these small volume chambers have a very low signal-to-noise ratio (SNR), hence the data sampling time should be increased correspondingly to provide adequate SNR. Solid state diode detectors typically have an active area of 1 mm^2 with a thickness of the order of 2.5 microns. Small volume detectors that have minimum energy, dose and dose rate dependency should not be used. Table 4.1 provides a comparison of some of the small field dosimeters used in SBRT commissioning.

Accurate detector-water scanner configuration with respect to the beam central axis and center of detector is critical. Li et al. [9] have demonstrated large errors can be caused due to small measurement displacement from beam central axis. Even with accurate detector-water scanner configuration, there can still be greater than 10 % discrepancies among measurement of small fields [2]. See Figs. 4.2 and 4.3 explaining the effect of scanning arm tilt and gantry angle tilt on the measured beam data. It is imperative that a thorough check is performed on the robustness of the data scanning equipment and setup prior to commencing the final beam data collection process.

Examples of data scanning: SBRT systems use either circular collimator and/or mMLC for beam shaping. Cyberknife uses both circular cones and an IRIS collimator (variable aperture MLC) whereas Novalis uses both circular cones and mMLC. Cyberknife systems are commonly commissioned with solid state diode detectors (PTW 60012, 60018- PTW Freiburg) for all relative measurements as recommended by the vendor. This provides excellent opportunity for data comparison among large numbers of users. This can assist an individual site to ensure their data is not outside of the expected tolerance and prevent potentially large dosimetric errors. The mMLC type systems have been commissioned with a range of detectors including mini-ion chamber, diode detectors and film [10].

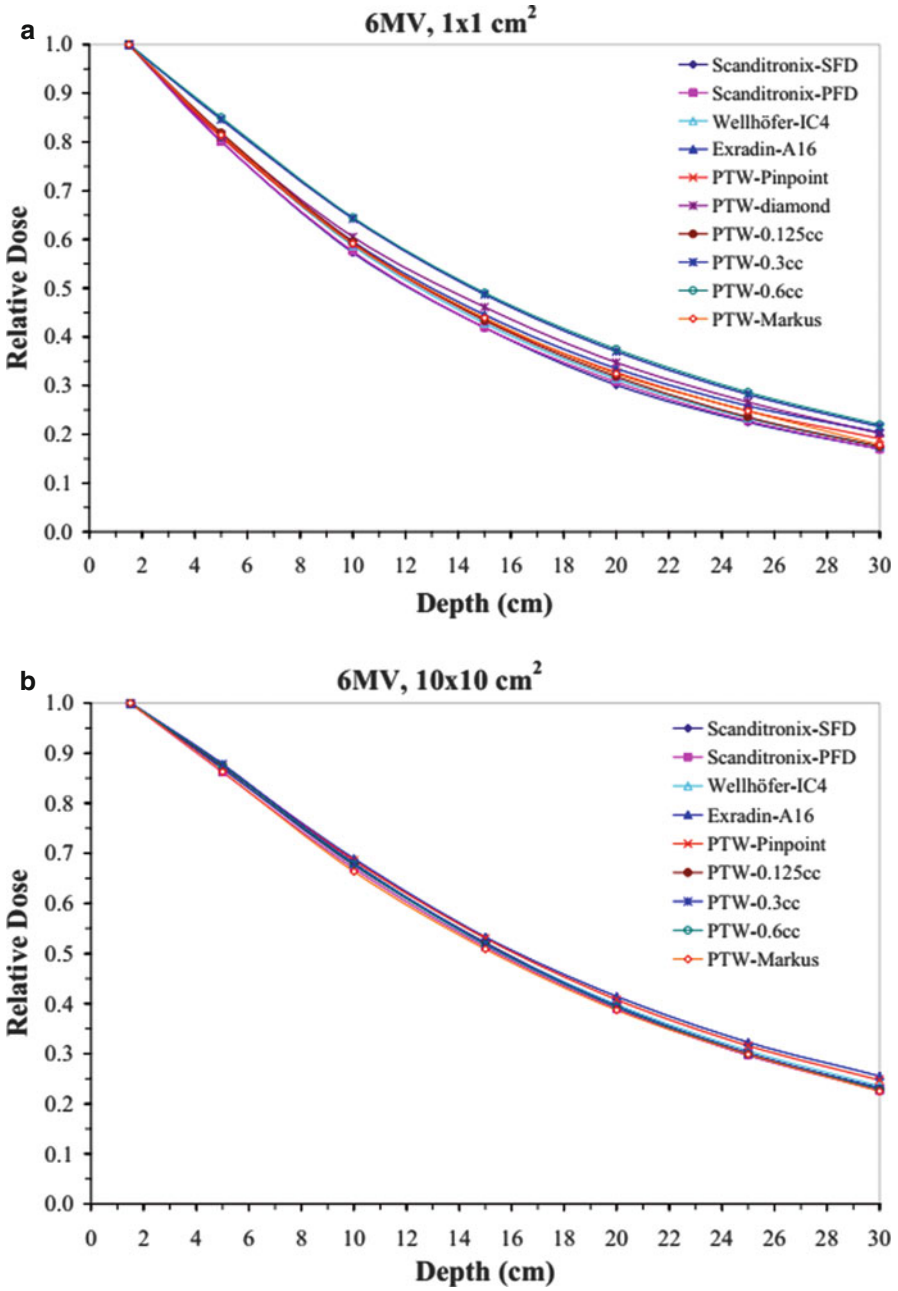

Fig. 4.1 Depth dose data for a 6 MV beam for (**a**) 1×1 cm^2, (**b**) 10×10 cm^2, and (**c**) 40×40 cm^2 fields using different detectors (From Klein et al. [1]; used with permission)

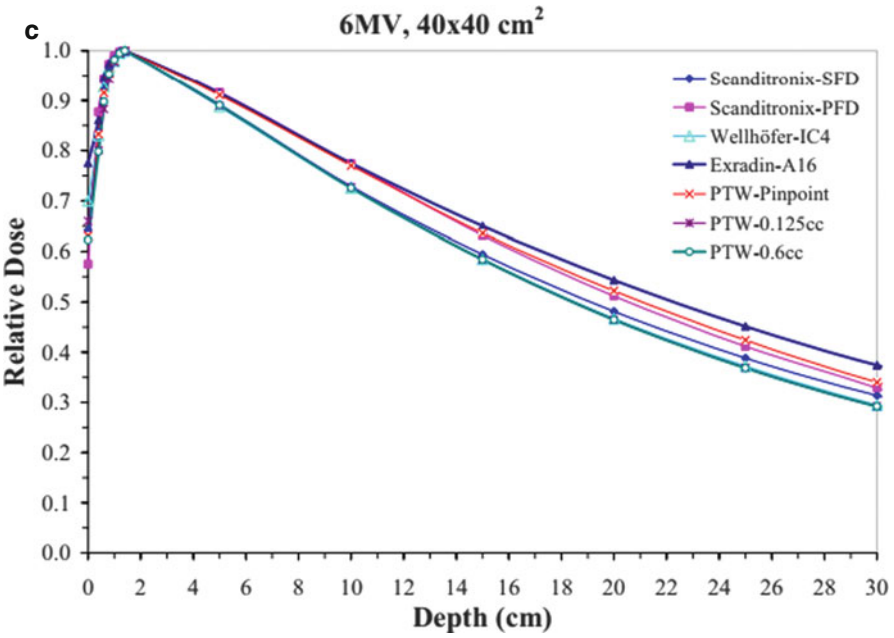

Fig. 4.1 (continued)

Table 4.1 Output factors; the agreement between different dosimeters is good down to a 2×2 cm² field

Field (cm)	Diamond IC15	Wellhofer A14SL	Exradin pinpoint	PTW A16	Exradin
1	0.639	0.512	0.541	0.561	0.643
2	0.788	0.786	0.769	0.777	0.786
3	0.831	0.832	0.827	0.829	0.829
4	0.866	0.866	0.866	0.867	0.864
5	0.898	0.898	0.896	0.898	0.895
10	1	1	1	1.014	1
15	1.062	1.058	1.062	1.089	1.07
20	1.098	1.096	1.098	1.146	1.117

From Stasi et al. [15]

Non scanned beam data, such as the total scatter (output) factors must be measured under full scatter conditions in the water phantom. Typically they are measured at the SSD or SAD setting as used for absolute dose calibration. In air output factors for SBRT field sizes must be measured at an extended distance so as to ensure adequate coverage of the field size in relation to the detector size. They should be measured with a build-up cap or mini phantom sufficiently large enough to provide electronic equilibrium and not be affected by electron contamination in the beam which can produce erroneous results. The minimum field size is determined by the requirement that there is sufficient "flash" of at least 1 cm around the mini-phantom [3].

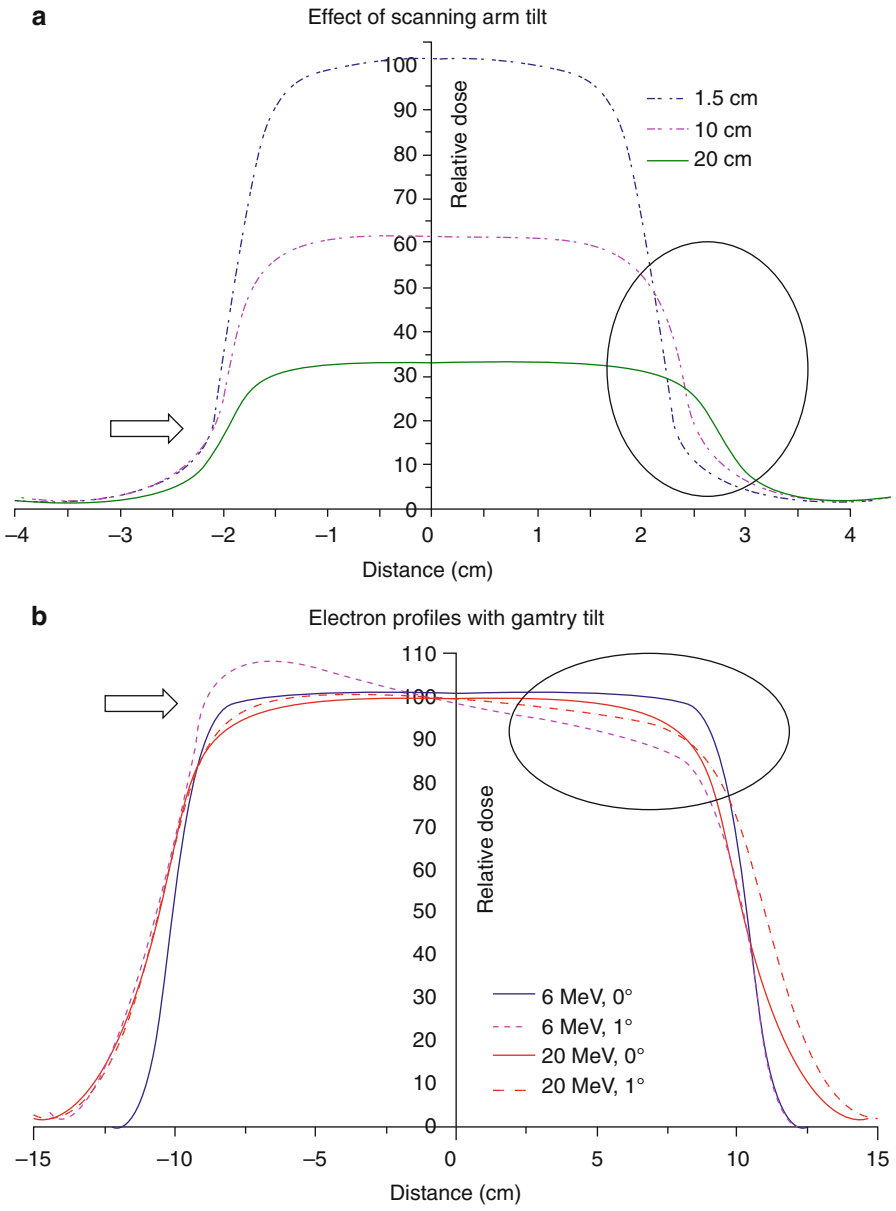

Fig. 4.2 (**a**) Beam profiles of a 6 MV beam at different depths with scanning arm tilt for a 4×4 cm^2 field, (**b**) Electron beam profiles at depth of 80 % depth dose for 20×20 cm^2 cone with gantry tilt. *Arrows* and *circle* shown to represent the impact of arm and gantry tilt (From Klein et al. [1]; used with permission)

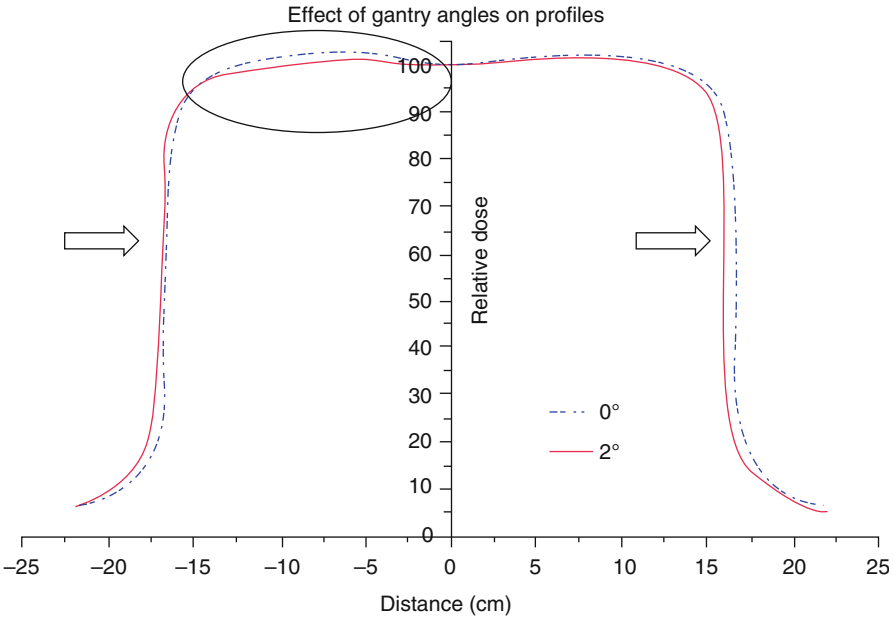

Fig. 4.3 Effect of gantry angle tilt on the profiles of a 6 MV beam for 30×30 cm^2 field at 10 cm depth (From Klein et al. [1]; used with permission)

4.2.3 TPS Commissioning

TPS commissioning must be performed [4] to ensure the planned dose matches the delivered dose prior to start of a clinical SBRT program. This must include not only spot check validation with simple beam geometry in a uniform water phantom but also complex field setups that include heterogeneity to simulate patient setup. Anthropomorphic phantoms provide a useful way to determine the overall accuracy of the acquired data and TPS dose calculation algorithm accuracy. The Radiological Physics Center (RPC) provides such phantoms for various body sections, for sites participating in Radiation Therapy Oncology Group (RTOG). Alternatively, they may be obtained from Radiation Doimetry Services (RDS) at MD Anderson Cancer Center, Houston, TX. Additionally, end-to-end analysis with phantoms imbedded with known objects with film provide overall system imaging, mechanical and dosimetry accuracy.

4.3 Quality Assurance

For any system that is used for SBRT or SRS, which delivers a very high dose to a region in a single or a very small number of fractions, a systematic evaluation of the treatment accuracy is required. This would include CT/MR imaging, fusion

uncertainties, planning calculation, target localization and then dose delivery. AAPM Task Group 101 report on "Stereotactic Body Radiation Therapy" Section VII.B states that "Specific tests should be developed to look at all aspects of the system both individually and in an integrated fashion" [2].

In this section, we are assuming that routine quality assurance has been conducted for the accuracy of CT/MR imaging, fusion and the treatment planning system, and will concentrate on the quality assurance procedures needed for target localization and dosimetry.

Ensuring target localization accuracy is a top priority for SBRT/SRS treatments. Because of the high dose delivered per fraction, any slight deviation in targeting accuracy could result in potentially damaging dose to the normal tissue, and it may be impossible to correct for any such errors in radiation delivery by modifying subsequent fractions. The standard for determining this targeting accuracy is the "Winston-Lutz" test or similar procedures for frameless SRS/SBRT procedures [11].

Since most of the currently available SBRT systems utilize either stereoscopic localization x-rays or CBCT for target localization and patient set up, in addition to the basic check on treatment beam and imaging isocenter, microMLC positioning, quality assurance on the imaging system and couch shift positioning accuracy is also needed. For any IGRT procedures that are used to ensure target localization accuracy, quality assurance of the imaging system is essential, following the test and frequency as shown in Table 4.2.

4.3.1 Imaging System Quality Assurance

Since the primary goal of an IGRT system is to localize target and organs at risk in the treatment room and derive correction strategies to minimize geometric uncertainties, any significant deviation from baseline could impact the accuracy of the IGRT system. Therefore, it is essential that the imaging system performance is kept at an optimal level with the highest accuracy possible. Both the kV-CBCT and MV-CBCT systems necessitate calibration procedures to properly register the treatment beam isocenter and correct for accelerator and imaging component sags and flexes, to certify the geometric accuracy of the imaged guided procedures.

In addition, image quality, scale and distance accuracy, contrast resolution, spatial and contrast resolution, noise, image registration accuracy and the accuracy of remote controlled couch are also important aspects of quality assurance for these systems. These aspects and patient safety all need to be part of a regularly scheduled QA program designed and managed by medical physicists.

The importance of quality assurance for on-line imaging systems has been recognized by the community and by AAPM (Task Group 142: QA of Medical Accelerators – this report has a section on imager QA). Tables 4.2 and 4.3 specify the frequency and tolerance of certain tasks that is recommended for both planar

Table 4.2 Summary of relevant imaging tolerances for SRS/SBRT

Daily	
Procedure	Tolerance
Planar kV and MV (EPID) imaging	SRS/SBRT
Collision interlocks	Functional
Positioning/repositioning	≦1 mm
Imaging and treatment coordinate coincidence (single gantry angle)	≦1 mm
Cone-beam CT (kV and MV)	
Collision interlocks	Functional
Imaging and treatment coordinate coincidence	≦1 mm
Positioning/repositioning	≦1 mm
Monthly	
Contrast	Baseline
Imaging and treatment coordinate coincidence (four cardinal angles)	≦1 mm
Scaling	≦2 mm
Spatial resolution	Baseline
Contrast	Baseline
Uniformity and noise	Baseline
Planar kV imaging	
Imaging and treatment coordinate coincidence (four cardinal angles)	≦1 mm
Scaling	≦1 mm
Spatial resolution	Baseline
Contrast	Baseline
Uniformity and noise	Baseline
Cone-beam CT (kV and MV)	
Geometric distortion	≦1 mm
Spatial resolution	Baseline
HU constancy	Baseline
Uniformity and noise	Baseline
Annual	
Planar MV imaging (EPID)	
Full range of travel SDD	≦5 mm
Imaging dose	Baseline
Planar kV imaging	
Beam quality/energy	Baseline
Imaging dose	Baseline
Cone-beam CT (kV and MV)	
Imaging dose	Baseline

Modified from Klein et al. [1]; used with permission

and cone beam images. The tasks include (1) safety and functionality; (2) geometrical accuracy: Imager isocenter accuracy, 2D2D match and couch shift accuracy, Image magnification accuracy, Imager isocenter accuracy with gantry rotation; (3) image quality: Contrast and spatial resolution, Hounsefield Units linearity and uniformity, In-slice spatial linearity and slice thickness [1].

Table 4.3 Summary of relevant tolerances for SRS/SBRT

Daily	
Procedure	Tolerance
Laser localization	1 mm
Distance indicator (ODI) @ iso	2 mm
Collimator size indicator	1 mm
Monthly	
Typical dose rate output constancy	2 % (@ stereo dose rate)
Treatment couch position indicators	1 mm/0.5°
Localizing lasers	<±1 mm
Annual	
Typical dose rate output constancy	2 %
Treatment couch position indicators	1 mm/0.5°
Localizing lasers	<±1 mm
SRS arc rotation mode (range: 0.5–10 MU/deg)	Monitor units set vs. delivered: 1.0 MU or 2 %
	Gantry arc set vs delivered: 1° or 2 %
X-ray monitor unit linearity (output constancy)	±5 % (2–4 MU), ±2 % ≥5 MU
Coincidence of radiation and mechanical isocenter	±1 mm from baseline
Stereotactic accessories, lockouts, etc…	Functional

In addition, a special task group has been formed, TG-179, to come up with recommendations for quality assurance for Image-Guided Radiation Therapy Utilizing CT-based Technologies. Even though the task group recommendation itself has not been published, a white paper has been created and submitted to specifically advise users on the frequency and types of quality assurance needed for the various types of imaging modalities [12].

As a result of the critical importance of the imaging system in SBRT patient positioning, daily quality checks on geometric accuracy are necessary. TG-179 recommends that daily QC tests for CT-based IGRT systems be performed. For example, a phantom with multiple markers at known positions would provide information on volumetric image orientation, confirm source-to-imager distance, assess image sharpness, and even assess dose. Currently, these phantoms are aligned to the accelerator isocenter using the room lasers, even though this would speed up the execution of the daily test, however, the test accuracy would be lower.

By using the "residual correction error" method, the physicist can verify the accuracy of the robotic couch, ensure proper operation of the IGRT device and to assess communication between the image registration software and the remote-controlled couch is working correctly. The residual correction error can be determined by placing a phantom at isocenter, apply a known displacement from isocenter, acquire a localization image dataset to assess the couch motions required to align the phantom with a reference CT dataset, and target the phantom as in the image-guided treatment. A verification image dataset is acquired

and registered again to the reference CT dataset after the suggested couch correction is applied, using the linac console. The displacement indicated from registering the verification dataset to the reference CT defines the residual error of the couch correction. This value should be near 0 ± 2 mm, according to TG-179.

This simple approach would help to determine not only the imaging localization accuracy, but also potential problems with the fusion/deviation calculation part of the IGRT procedure.

After the IGRT system localization accuracy is assured, quality assurance on the dosimetry would need to be conducted. The IGRT system accuracy should be assessed routinely, daily imaging isocenter check and simple localization check should be done daily when there is SBRT treatments.

Similarly, image quality issues such as spatial integrity, uniformity of the panel signal, contrast detectability and resolution, CT number accuracy and stability and imaging dose all need to undergo a quality check on a monthly basis, according to the recommendation of TG-179.

4.3.2 Dosimetric Quality Assurance

4.3.2.1 Validation Measurement Vs. Treatment Planning Output

After commissioning of the treatment planning system, and before the start of SBRT programs, validation measurements should be conducted.

Simple square field or circular cone field size outputs and PDD/energy should be independently verified based on new measurements and compared with treatment planning calculations. For absolute dosimetry, pin point chamber or diode should be used for small field sizes. However, energy dependence of the diode response should be taken into consideration when conducting the energy check, and some cross calibration might be warranted.

Once the output and energy of the calculation is verified to be accurate for square fields and circular fields, simple 3D plans such as the 4 field box, opposed fields, and some IMRT plans should be planned and delivered, and verified at least using single ion chamber measurements to verify the dose calculation and delivery accuracy.

Then typical SBRT sites and plans (spine, brain, lung, prostate, pancreas, etc..) should be verified with different collimator/field sizes to cover the whole range of possible field size, and different tracking methods (i.e. kV imaging, cone beam, for CK, different track algorithms). If multiple metastasis will be treated in the SRS/SBRT program, double or multiple isocenters plans would needed to be verified as well.

These measurements are the end-to-end tests that need to be conducted to ensure that the TPS is calculating the correct dose, and that the IGRT imaging system and the tracking/delivery system is delivering accurately. The process should start with CT scanning of phantom with hidden target suited for the sites under testing. For example, if one is to test the spine tracking delivery module on the Cyberknife, it is

essential to use a phantom that has features that is suitable to test the spine tracking algorithm. Same thing if the site under testing is for respiratory gating or Synchrony tracking, a motion phantom should be used.

Small field sizes should be emphasized during these End-to-End tests, since this particular area is most prone to commissioning inaccuracy and also dose planning uncertainty. Film would give the highest resolution for the isodose distribution verification, but care must be taken to ensure that the films are calibrated so the dose uncertainty is within 2 or 3 %.

4.3.2.2 Routine Quality Assurance Program

Once the validation measurements are completed, and the End-to-End tests shown dose targeting accuracy within 1 mm, SBRT treatments could be initiated.

However, there are many routine quality assurance measurements needed to ensure the continuing dosimetry accuracy for these treatments.

Beam Stability Test

The output and energy of the beam should be checked daily. Special equipment for SBRT could be used to check more beam characteristics daily, such as the SRS profiler, daily QA 3, etc. For example, using the SRS profiler could check that the beam flatness and symmetry are constant.

Based on TG 142's recommendation on QA of Medical Accelerators [1], the highlights pertaining specifically to SRS/SBRT are listed in Table 4.3.

For SBRT/SRS treatments delivered using micro-MLC or high definition MLC (such as Novalis and Varian TrueBeam), it is recommended that physicists consult with TG-142 Table V for MLC quality assurance, but bear in mind that tighter tolerance (constancy and accuracy to the sub mm) would be needed for these high definition MLCs.

For Cyberknife robotic radiosurgery, TG 135 recommends individual component QA and overall system QA, with specific daily, monthly and annual frequency and tolerance.

End-to-End Test: Including Motion Tracking/Gating End-to-End Test

Based on TG101, the individual components of the SBRT process (imaging, localization, treatment delivery, etc.) each have associated error [2]. The cumulative system accuracy for the procedure could be significant even if each of these individual errors is small by themselves. Therefore, the cumulative system accuracy needs to be characterized through an end-to end test using phantoms with measurement detectors and imaging on a routine basis, probably on a monthly or twice a month basis.

Therefore, End-to-end tests have to be done during validation measurements before the SBRT program begins, routine End-to-end test should be conducted to ensure continuing whole procedure accuracy. Depending on the treatment types, End-to-End tests could be done on the physicists' discretion. For example, if the SBRT program primarily treats spine lesions, then respiratory gating/tracking End-to-end tests might not have to be done as frequently, but should be done before such patient is to be treated.

4.3.3 Patient Specific QA

According to TG101, treatment-specific and patient-specific QA procedures should be established to govern both the treatment planning and delivery process as a whole as well as to provide sanity check of the setup.

For a new SBRT program, more frequent patient specific QA should be conducted until the physicist in charge is confident of the delivery accuracy of the modality.

For small fields, patient specific QA should be done to ensure that the dosimetry is accurate. For example, if the physicist feels that the output factor measured for an extremely small field carries an uncertainty, he/she might want to conduct patient specific QA for any plans that involve the extremely small field. Patient specific QA should also be done if the physicist is concerned about the microMLC or the IRIS positioning accuracy for a small field. For example, a Cyberknife physicist might want to conduct patient specific QA for all patients treated with the 5 or 7.5 mm collimators since these fields involve both potential measurement uncertainty and positioning uncertainty.

These small field size patient specific QA measurements should be conducted using equipment that has the correct resolution, using film to obtain isodose distribution, and using either pin point chamber or diode for absolute measurement to avoid any volume averaging issues. Therefore, the popular MapCheck or Matrix might not be suitable for the really small fields due to low density and larger spacing of the detectors, and film should be used.

4.4 Treatment Planning

4.4.1 Introduction

Delivering ablative or near ablative doses using stereotactic body radiation therapy (SBRT) requires treatment planning to be of the highest quality to minimize the potential for severe toxicities. In conventional radiation therapy the goal of the planner is to cover the target to a uniform or homogenous prescribed dose. The requirement of delivering a very high dose with an extremely sharp fall off is the fundamental difference between SBRT and conventional radiation therapy (CRT). To accomplish this, the

beam arrangement will include a multitude of non-coplanar beams or arcs to keep the entrance dose low and the dose gradient high. As a result, homogeneity is lost and the targets have hot spots, sometimes above 20 % and even as high as 50 % depending on the modality. Rather than being a problem, this is seen as a clinical advantage [2].

Stereotactic refers to locating, targeting and planning with known 3-D coordinate systems which creates another fundamental difference between CRT. CRT traditionally relies on the anatomical or clinical patient set up while SBRT relies on image guidance to monitor the target or a surrogate for the target. Treatment planning starts at simulation with additional requirements for SBRT and does not end with beam delivery but with a continued group effort of quality assurance throughout all steps of the process. The following will describe briefly the fundamentals of treatment planning found in SBRT.

4.4.2 Simulation, Motion Management and Target Delineation

In addition to providing effective immobilization, Simulation must assess the targets' motion. There are many ways to accomplish this. Commonly used techniques include slow CT, breath hold inspiration/expiration scans and 4D reconstructed CTs. All of these methods are discussed at length in TG-91 and TG-101 [2]. Depending on the system employed, abdominal compression can also be utilized to reduce motion due to respiration, thereby also reducing the margins needed to cover the target. Another strategy is to employ respiratory gating. Lastly, assessing whether or not a patient can tolerate longer treatment times, some exceeding an hour, is of critical importance as well. For example, in a lung case it may be of dosimetric advantage to treat a patient prone but if the patient cannot reliably hold that position then it could compromise treatment delivery.

The SBRT requirements of assessing motion of well-defined targets and organs at risk require multiple imaging sets to be fused. Additional image sets can be fused for target and critical structure delineation. For example, MRIs can be used for delineation of brain lesions and critical structures nearby such as optical chiasm and brain stem. PET scans can further help localized targets and distinguish between disease and normal tissue (Fig. 4.4).

Once the fusion is complete and the motion is assessed, the Radiation Oncologist can create an Internal Target Volume (ITV) which is a volume that encompasses the CTV and any motion due to respiration, rotations or organ deformations. It is important to note that the CTV will often equal the GTV due to the need to keep the target volume minimized. Target delineation is not a straight forward task and often the exact motion cannot be determined due to deformations and rotations. Assessing the motion of the target determines the margins and therefore the greater uncertainly in motion, the greater margins must be used. In the case of fiducial or electromagnetic tracking, fusions also determines whether or not the target moves with the fiducial. This relationship between the fiducial and the target must be well known for planning and delivery [13]. With multiple targets, the tracking can be complicated if it is determined they are moving synchronously.

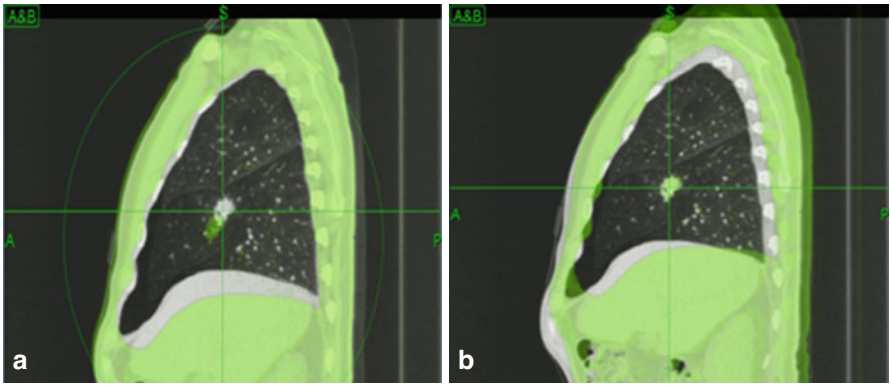

Fig. 4.4 Expiration and inhalation CTs on a lung window are fused and displayed in a color overlay. (**a**) Image on the left is fused to the spine and the lung motion is apparent. (**b**) On the right is fused to the fiducial or in other words, comparing movement relative to the fiducial. It can be seen that the lesion is moving with the fiducial and is therefore a good surrogate for the lesion's motion

4.4.3 Dose Heterogeneity and Prescription Normalization

Delivering large does with an extremely sharp dose gradient is achieved by using several non-coplanar beams. This technique also lowers the entrance dose and consequently prevents acute skin toxicities. As discussed previously, these beam arrangements create large dose heterogeneities which can be used a clinical tool by shaping the dose distribution, or dose painting. Hot spots can then be encouraged to populate contrast enhancing, FDG avid, and suspected hypoxic areas. The idea of dose painting in SBRT is to ensure the target receives as high a dose as possible while keeping critical structures as low as reasonably achievable; sometimes leading to a compromise of target coverage while meeting critical structure tolerances. The homogeneity index is a metric that is used to capture this information. There are many different proposed methods to calculate HI but in general it can be thought to be proportional to: HI = Maximum dose/Prescription dose (Fig. 4.5).

Similar to conventional radiotherapy, there are many ways to normalize a prescription, such as prescribing either to the isocenter or to the PTV. A common convention in SBRT is prescribing to an isodose line as a percentage of the maximum dose point and not the prescription dose. In Fig. 4.6 the isodose lines are percentages of the maximum dose, for example, the orange line is 76 % of the maximum dose which is the prescription divided by the normalization or 24 Gy/0.76 = 31.58 Gy. As a result, it is often more useful to display the isodose lines as the actual absorbed dose values rather than percentages. This can translate the isodose lines into conventional fractionation. With the previously example of 24 Gy in 3 fractions, the 20 % line or 6.3 Gy line is approximately 2 Gy per fraction.

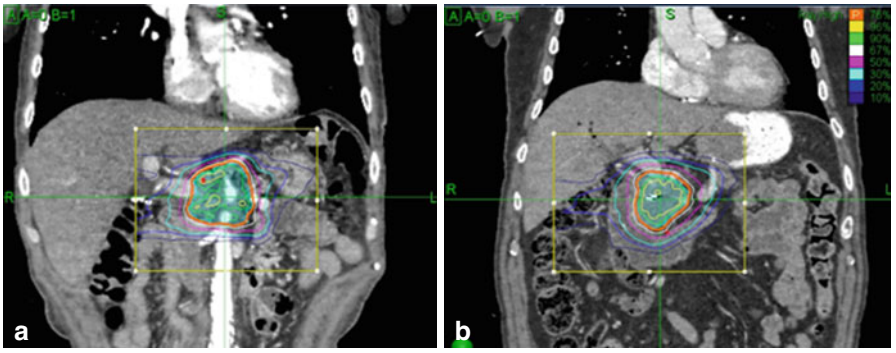

Fig. 4.5 Two pancreas SBRT plans with identical prescriptions (24 Gy in three fractions, normalized to 76 %). By looking at the 96 % isodose line (*yellow*) and the 90 % isodose lines (*green*), it is clear that these metrics alone do not completely describe the dose distributions

4.4.4 Practical Considerations

When creating a beam arrangement, a common approach is to avoid critical structures when possible. Mechanical limits and the potential for patient collision are also considered. Because of this, SBRT beam angles are more constrained than for cranial targets and larger patients add to the constraints. It is therefore important for the treatment planner to be aware of these restrictions and determine if there is a potential problem [14]. In some clinics, a dry run of the final plan is performed to conclude there will be no collisions. Furthermore, a Radiation Therapist may set up the patient and rotate the gantry to all positions just prior to treatment delivery.

While the goal is to create a conformal plan with a sharp dose gradient, is it sometimes necessary to accept a clinical compromise between conformality and creating a sharp dose gradient. This is seen with strict dose tolerances, such as the spinal cord, or when the planner can encourage exit and entrances doses to a specific area. The conformality index is a metric used to describe how closely the prescription isodose line circumscribes the target volume. It is defined as CI = Prescription Isodose Volume / PTV Volume with the goal of 1 in an ideal plan (Fig. 4.6).

SBRT normal tissue tolerances are not generally well known and/or validated due to the dramatic differences in fractionation schemes. Because dose tolerances cannot be extrapolated, treatment planners rely on in-house or RTOG protocols or institutional experience for observed toxicities. However, there are resources available in the AAPM TG-101 and in RTOG protocols. Moreover, SBRT late effects as well as retreatment tolerances are still not known [2]. Table 4.4 is from AAPM Task Group Report 101 displaying tolerances compared to fractionation schemes which can be useful to change fractionation to meet dose tolerances.

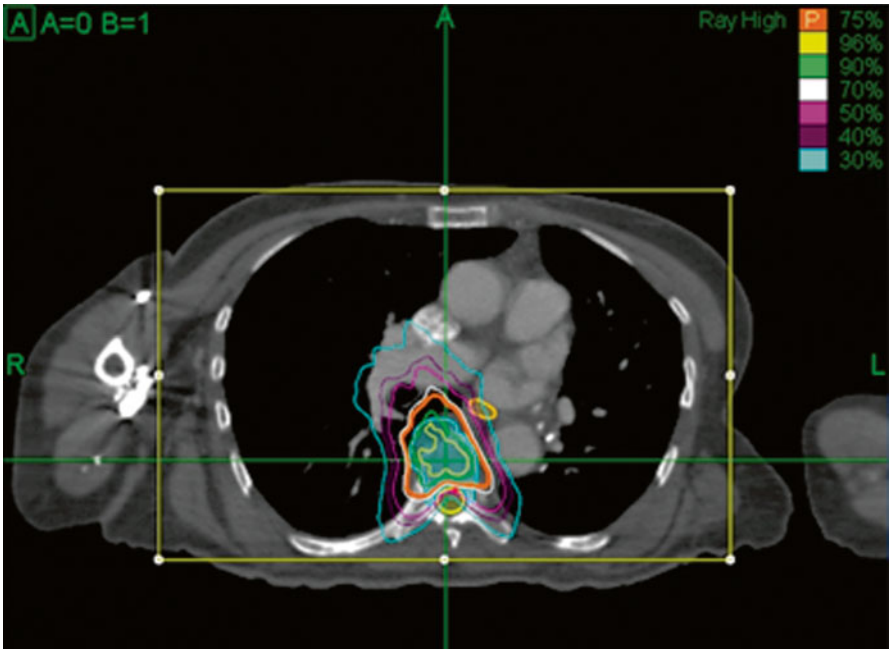

Fig. 4.6 SBRT spine plan demonstrating a compromise of anterior coverage for a steep posterior gradient protecting the spinal cord

Table 4.4 The AAPM task report 101 compilation of normal tissue dose tolerance from the University of Texas Southwestern and the University of Virginia

		One fraction		Three fractions		Five fractions		
Serial fraction	Max critical volume above threshold (cc)	Threshold dose (Gy)	Max point dose (Gy)	Threshold dose (Gy)	Max point dose (Gy)	Threshold dose (Gy)	Max point dose (Gy)	End point
Spinal cord	<0.35	10	14	18 (6 Gy/fx)	21.9 (7.3 Gy/fx)	23 (4.6 Gy/fx)	30 (6 Gy/fx)	Myelitis
Cauda equina	<5	14	16	21.9 (7.3 Gy/fx)	24 (8 Gy/fx)	30 (6 Gy/fx)	32 (6.4 Gy/fx)	Neuritis
Sacral plexus	<5	14.4	16	22.5 (7.5 Gy/fx)	24 (8 Gy/fx)	30 (6 Gy/fx)	32 (6.4 Gy/fx)	Neuropathy
Esophagus	<5	11.9	15.4	17.7 (5.9 Gy/fx)	25.2 (8.4 Gy/fx)	19.5 (3.9 Gy/fx)	35 (7 Gy/fx)	Stenosis/fistula
Brachial plexus	<3	14	17.5	20.4 (6.8 Gy/fx)	24 (8 Gy/fx)	27 (5.4 Gy/fx)	30.5 (6.1 Gy/fx)	Neuropathy

From Benedict et al. [2]; used with permission

References

1. Klein EE, Harley J, Yin F, Simon W, Dresser S, Serago C, Aguirre F, Ma L, Ajomandy B, Liu C, Sandin C, Holmes T. Task Group 142 report: quality assurance of medical accelerators. Med Phys. 2009;36:4192–212.
2. Benedict SH, Yenice KM, Followill D, Galvin JM, Hinson W, Kavanagh B, Keall P, Lovelock M, Meeks S, Papiez L, Purdie T, Sadagopan R, Schell MC, Salter B, Schlesinger DJ, Shiu AS, Song DY, Stieber V, Timmerman R, Tome WA, Verellen D, Wang L, Yin F. Stereotactic body radiation therapy: the report of AAPM Task Group 101. Med Phys. 2010;37(8):4078–101.
3. Das IJ, Cheng C, Watts R, Ahnesjo A, Gibbons J, Li XA, Lowenstein J, Mitra R, Simon W, Zhu TC. Accelerator beam data commissioning equipment and procedures: report of the TG-106 of the Therapy Physics Committee of the AAPM. Med Phys. 2008;35:4186–215.
4. Fraass B, Doppke K, Hunt M, Kutcher G, Starkschall G, Stern R, Van Dyke J. AAPM Radiation Therapy Committee Task Group 53: quality assurance for clinical radiotherapy treatment planning. Med Phys. 1998;25:1773–829.
5. Sharma SC, Ott JT, Williams JB, Dickow D. Commissioning and acceptance testing of a Cyberknife linear accelerator. J Appl Clin Med Phys. 2007;8:119–25.
6. Sauer O, Wilbert J. Measurement of output factors for small photon beams. Med Phys. 2007;34:1983–8.
7. Zhu XR, Allen JJ, Shi J, Simon WE. Total scatter factors and tissue maximum ratios for small radiosurgery fields: comparison of diode detectors, a parallel-plate ion chamber, and radiographic film. Med Phys. 2000;27:472–7.
8. Francescon P, Cora S, Cavedon C. Total scatter factors of small beams: a multidetector and Monte Carlo Study. Med Phys. 2008;35:504–13.
9. Li S, Rashid A, He S, Dajajaputra D. A new approach in dose measurement and error analysis for narrow photon beams (beamlets) shaped by different multileaf collimators using a small detector. Med Phys. 2004;31:2020–32.
10. Yin F, Zhu J, Yan H, Gaun H, Hammoud R, Ryu S, Kim JH. Dosimetric characteristics of Novalis shaped beam surgery unit. Med Phys. 2002;29:1729–38.
11. Solberg TD, Medin PM, Mullins J, Li S. Quality assurance of immobilization and target localization systems for frameless stereotactic cranial and extracranial hypofractionated radiotherapy. Int J Radiat Oncol Biol Phys. 2008;71:S131–5.
12. Bissonnette JP, Balter PA, Dong L, Langen KM, Lovelock DM, Miften M, Moseley DJ, Pouliot J, Ramsey CR, Sonke JJ, Yoo S. Quality assurance for image-guided radiation therapy utilizing CT-based technologies: general principles report of the AAPM TG-179 (in press).
13. Shah AP, Kupelian PA, Willoughby TW, Meeks SL. Expanding the use of real-time electromagnetic tracking in radiation oncology. J Appl Clin Med Phys. 2011;12(4):3590.
14. Becker S. Collision indicator charts for gantry-couch position combinations for Varian linacs. J Appl Clin Med Phys. 2011;12(3):3405.
15. Stasi M, Baiotta B, Barboni G, Scielzo G. The behavior of several microionization chambers in small intensity modulated radiotherapy fields. Med Phys. 2004;31:2792–5.

Further Reading: Quality Assurance

16. Balter JM, Antonuk LE. Quality assurance for kilo- and megavoltage in-room imaging and localization for off and online setup error correction. Int J Radiat Oncol Biol Phys. 2008;71:S48–52.
17. Bissonnette JP. Quality assurance of image-guidance technologies. Semin Radiat Oncol. 2007;17:278–86.

18. Bissonnette JP, Moseley D, White E, Sharpe M, Purdie T, Jaffray DA. Quality assurance for the geometric accuracy of cone-beam CT guidance in radiation therapy. Int J Radiat Oncol Biol Phys. 2008;71:S57–61.
19. Bissonnette JP, Moseley DJ, Jaffray DA. A quality assurance program for image quality of cone-beam CT guidance in radiation therapy. Med Phys. 2008;35:1807–15.
20. Dieterich S, Sherouse GW. Experimental comparison of seven commercial dosimetry diodes for measurement of stereotactic radiosurgery cone factors. Med Phys. 2011;38:4166–73.
21. Dieterich S, et al. Report of AAPM TG 135: quality assurance for robotic radiosurgery. Med Phys. 2011;38:2914–36.
22. Galvin JM, Bednarz G. Quality assurance procedures for stereotactic body radiation therapy. Int J Radiat Oncol Biol Phys. 2008;71:S122–5.
23. Goetsch SJ. Linear accelerator and gamma knife-based stereotactic cranial radiosurgery: challenges and successes of existing quality assurance guidelines and paradigms. Int J Radiat Oncol Biol Phys. 2008;71:S118–21.
24. Langen KM, Meeks SL, Pouliot J. Quality assurance of onboard megavoltage computed tomography imaging and target localization systems for on- and off-line image-guided radiotherapy. Int J Radiat Oncol Biol Phys. 2008;71:S62–5.
25. Medin PM, Verellen D. Novalis. In: Slotman BJ, Solberg TD, Verellen D, editors. Extracranial stereotactic radiotherapy and radiosurgery. CRC Press, New York; 2010.
26. Saw CB, Yang Y, Li F, Yue NJ, Ding C, Komanduri K, Huq S, Heron DE. Performance characteristics and quality assurance aspects of kilovoltage cone-beam CT on medical linear accelerator. Med Dosim. 2007;32:80–5.
27. Sharpe MB, Moseley DJ, Purdie TG, Islam M, Siewerdsen JH, Jaffray DA. The stability of mechanical calibration for a kV cone beam computed tomography system integrated with linear accelerator. Med Phys. 2006;33:136–44.
28. Yoo S, Kim GY, Hammoud R, Elder E, Pawlicki T, Guan H, Fox T, Luxton G, Yin FF, Munro P. A quality assurance program for the on-board imagers. Med Phys. 2006;33:4431–47.

Further Reading List: Treatment Planning

29. Keall P, Mageras GS, Balter JM, Emery RS, Forster KM, Jiang SB, Kapatoes JM, Kubo HD, Low DA, Murphy MJ, Murray BR, Ramsey CR, Van Herk MB, Vedam SS, Wong JW, Yorke E. The management of respiratory motion in radiation oncology: report of AAPM Task Group 76. Med Phys. 2006;33(10):3874–900.

Chapter 5
Radiobiology of High Dose Fractions

Bleddyn Jones and Roger G. Dale

Abstract Advances in the technology of radiotherapy delivery have resulted in deliberate radiation fluence and dose displacement away from designated normal tissues, and with improved conformity of tumour dose. This applies to normal tissues outside the planning target volume (PTV) in most cases. The prospects for hypofractionation improve in these circumstances provided that loss of function of the normal tissue included in the PTV is not considered harmful or deleterious to the subsequent health and well-being of the patient.

The radiobiology of large fractions is considered in the context of the linear quadratic (LQ) model of radiation effect and the concept of the biological effective dose (BED). One feature of the model is that it might overestimate high fractional dose effects especially in tumours or tissues which have low α/β ratios. For normal tissues, this is probably advantageous since the model provides a 'worst case scenario', and protects against overdosage. Substantial benefits in the therapeutic ratio with increasing fractionation only apply where there is a marked difference between the α/β ratios of the tumour and relevant normal tissues. Thus slow growing tumours with low α/β ratios are preferred candidates for hypofractionation. Where high dose fractions are employed it is vital to ensure that the prescribed dose is not exceeded in relevant normal tissue where overdosage can be harmful.

Some worked examples are given to illustrate these principles, using BED calculations, with examples of how to include straightening out of the dose response curve.

Keywords Fractionation • Radiotherapy • Linear quadratic model • Biological effective dose (BED)

B. Jones, MA, MSc, MB, BChir, MD, FRCP (✉)
CRUK-MRC Oxford Institute, ORCRB Building,
University of Oxford, OX37DQ, Oxford, Oxfordshire, UK
e-mail: Bleddyn.Jones@oncology.ox.ac.uk

R.G. Dale, PhD
Department of Surgery and Cancer, Faculty of Medicine, Imperial College, London, UK

A. Gaya, A. Mahadevan (eds.), *Stereotactic Body Radiotherapy: A Practical Guide*,
DOI 10.1007/978-0-85729-597-2_5

5.1 Introduction

Quantitative radiobiological analysis of conventional radiotherapy schedules is usually performed by means of the well-established linear-quadratic (LQ) model of radiation effect [1–3]. The model, which is based on assessments of surviving fraction following radiation inherently includes all known modes of cell death due to radiation exposure, such as apoptosis, autophagy and bystander effects. At high fraction doses it should be noted that most cell death will occur due to intra-mitotic death, since the other forms of cell death become saturated at relatively low dose, usually below 2Gy. As well as the direct effect of cell killing, there will also be secondary or 'indirect' components which effect tumour and normal tissue responses, mostly due to associated vascular injury resulting in an 'avalanche' effect. Such effects can also be expected to be a function of dose and tumour cell kill.

In the most common applications the LQ model uses tissue-specific parameters, primarily the so-called α[alpha]/β[beta] ratios (which relate to dose fraction sensitivity), together with other parameters, such as those which adjust for dose rate effects, inter-fraction intervals or overall treatment time. These parameters are used in conjunction with the medically controllable treatment dose prescription details (dose per fraction, total dose and overall treatment time), in order to assess the biological effect of schedules on both tumour and normal tissue. The LQ model is also extensively used in the assessment of other types of radiation treatment delivery, such as those involving continuous low dose-rate irradiation, permanent radioactive implants and treatments which make use of more exotic types of radiation, such as brachytherapy, protons or ions [4–8].

The ability to quantify the differential response between different tumours and normal tissues is a major feature of all LQ methodology and allows comparison of the relative merits of different schedules. It also opens the way to the design of alternative dose-time schedules as well as in the use of new radiation treatments which may offer better therapeutic effects, such as improved or maintained tumour control in association with the same or reduced normal tissue complications.

In fractionated radiotherapy applications, the LQ model is essentially reliable provided the individual fraction sizes are around 6Gy or less. Beyond 6Gy the predictive reliability of the model is seen to deteriorate in some cell assay systems, marginally at first but more significantly when fraction size is >10Gy. This is a consequence of the quadratic cell-kill component inherent in the model and which predicts that cell survival curves should continue to bend downwards indefinitely with increasing fraction dose (Fig. 5.1). In measured survival curves the continuous "downward curvature effect" is seen in some cases to moderate at higher doses, with cell survival curves appearing to become straight (or almost straight) at very high dose. This may be due to overkill processes or saturation of intracellular repair mechanisms. As a result, and irrespective of the exact mechanisms involved, LQ predictions based on parameters determined from treatments using conventional dose fraction sizes are likely to over-estimate the biological impact (cell kill) of treatments utilising very high doses per fraction.

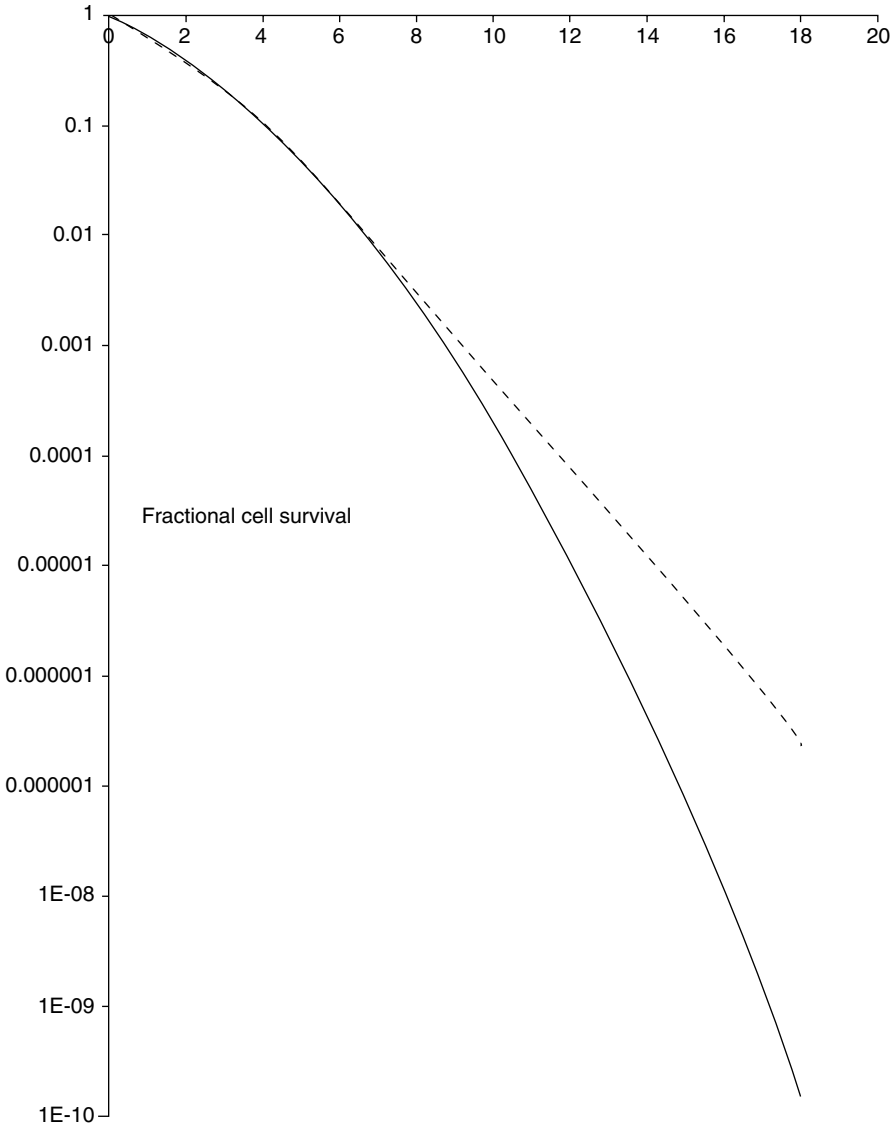

Fig. 5.1 The solid line shows the typical variation of cell survival with fraction size as predicted by the standard linear-quadratic (LQ) model [Eq. 5.2]. The curve is characterised by a finite initial slope at zero dose and an ever-increasing slope as dose increases. In practice however, most human cell lines do not bend downwards indefinitely but tend to a finite limiting slope (*dotted line*). In the case illustrated here the deviation in response from the standard LQ prediction begins at around 6–7 Gy and thereafter becomes increasingly significant, with the LQ model over-estimating the effect actually achieved. Radiobiological assessments of treatments which utilise high dose fractions (typically >10 Gy) must therefore make allowance for this potential weakness in the basic LQ model

Although the LQ model remains the method of choice for quantitative evaluation of radiotherapy treatments, it should be noted that the earlier multi-target (MT) model does predict the observed "straightening out" of cell survival curves at higher doses. In practice the MT model is much less amenable to clinical application than the LQ model (especially over the conventional range of dose/fraction) but, as discussed below, attempts have been made to empirically combine the main features of the two models in order to provide better predictions over a wider dose range.

5.2 The Basic LQ Model

The LQ model was originally used to provide an empirical fit to observations on radiation chromosome damage by Lea & Catcheside [9] and also to fit radiation induced suppression of broad bean growth and development by Gray and Scholes [10]. However, LQ-type formulations can also be developed from more rigorous bio-physical considerations by considering how radiation damage accrues from immediately lethal radiation events and from the complementary interaction of sub-lethal events irrespective of their precise molecular basis [1, 11, 12]. The propensity for lethal damage to be created through these two alternative processes is reflected in the two radiosensitivity coefficients (α[alpha] and β[beta]) which are principal features of the model.

The essential mathematics behind the LQ model is as follows:

For a single acute fractional dose of magnitude d, the total number of lethal lesions produced is L, where:

$$L = \alpha[\text{alpha}]\,d + \beta[\text{beta}]\,d^2 \tag{5.1}$$

The surviving fraction of cells (S) is expressed as the probability of no lethal hits as deduced from Poisson statistics and is written simply as:

$$S = \exp(-L)$$

$$\text{i.e.: } S = \exp\left[-\alpha[\text{alpha}]\,d - \beta[\text{beta}]\,d^2\right] \tag{5.2}$$

Equation 5.2 describes the shape of the LQ cell-survival curve for a specific cell line or tissue type in terms of the relevant α[alpha] and β[beta] values which characterise them and, as noted above, is characterised by a continuous downward curvature (ie increasing steepness) with increasing d. When plotting cell-survival curves it is the universal practice to use a linear scale for d (on the x-axis) and a logarithmic scale for S (on the y-axis). The adoption of this convention allows easy visualisation of the characteristics of cell survival curves and of any differences that may exist between alternative cell lines.

In Eq. 5.2 the magnitude of α relative to β[beta] determines the increment of effect with increasing dose per fraction, the trend becoming more particularly pronounced at higher fraction doses. This is because the β[beta]-component of cell kill

is related to the square of the dose (d^2) and it thus follows that the downward curvature of the cell survival curve will be more pronounced in tissues for which β is relatively large compared with α[alpha], i.e. in tissues with lower α[alpha]/β[beta] ratios. Since late-responding normal tissues (LRNTs) are usually associated with smaller α[alpha]/β[beta] values than are many fast- growing tumours (typically 2–5 Gy cf 7–20 Gy), it follows that the LQ cell-survival curves of the former will exhibit more pronounced curvature than the latter.

In practice the cell surviving fraction is a cumbersome measure of treatment efficacy and a more useful parameter to use is the so-called Biologically Effective Dose (BED). BED is a measure of the overall "biological impact" of a schedule and takes account of the specific radiation response characteristics of the irradiated tissue by means of the inclusion of the relevant α[alpha]/β[beta] value in its calculation. Thus, even though two adjacent tissues might each receive the same radiotherapy fractionation schedule, their BEDs can be different because of the different tissue specific α/β[beta] values. The usefulness of the BED concept lies in the fact that it allows the design of new schedules (which may involve different fractionation) to be iso-effective to existing, well-tried, schedules. Since there are two ways of matching iso-effectiveness (for the tumour and LRNT responses) then there is the possibility of designing a new schedule which is radiobiologically superior, i.e. in terms of increased tumour BED and/or reduced LRNT BED.

In words, BED is defined to be the negative of the logarithm of surviving fraction, divided by the linear radiosensitivity coefficient (α[alpha]). More usefully, BED may be thought of as the dose required if given in ultra-small fractions and represents the 'ceiling' dose capable of causing the observed effect. Derivation of the BED from Eq. 5.2 is thus effected by taking natural logarithms of both sides of the equation and dividing throughout by α[alpha]:

$$BED = -\frac{\ln S}{\alpha} = d + \frac{d^2}{(\alpha / \beta)} \tag{5.3}$$

Equation 5.3 provides the BED value for a single fraction. For a complete treatment involving N well-spaced fractions the resultant BED (BED_N) is simply N times larger than the single fraction BED, i.e.:

$$BED_N = N\left(d + \frac{d^2}{(\alpha / \beta)}\right) \tag{5.4}$$

Equation 5.4 is usually written in the more familiar form:

$$BED_N = Nd\left(1 + \frac{d}{(\alpha / \beta)}\right) \tag{5.5}$$

Since Nd is the total physical dose delivered in a treatment, it follows that the BED is the product of the physical dose and a factor [the bracketed term in Eq. 5.5] which

is dependent of the dose/fraction and the α[alpha]/β[beta] value characteristic of the tissue under consideration. As noted earlier, LRNTs are generally characterised by smaller values of α[alpha]/β[beta] and therefore, for a given N and d, are associated with a higher BED than tumours. Once calculated, BED acts as a reference value for iso-effect so that it is possible to estimate the dose per fraction and number of fractions required to achieve the same BED using different schedules.

5.3 Example of Simple LQ Modelling

Suppose it is required to emulate the biological effects of a conventional (60 Gy in 2 Gy-fractions) treatment with a single fraction treatment involving highly-focussed beams. What single fraction dose should be delivered?

Firstly, we consider the tumour (assumed α[alpha]/β[beta] = 10 Gy for a rapidly growing tumour). From Eq. 5.5, the BED (BED30) delivered in the conventional 30-fraction treatment is:

$$BED30 = 30 \times 2 \times \left(1 + \frac{2}{10}\right) = 72 Gy_{10} \tag{5.6}$$

(The Gy suffix of 10 is simply a reminder of the α[alpha]/β[beta] value used in the calculation).

If X is the total dose required in the single-fraction treatment to deliver this same BED then, from re-application of Eq. 5.5 it follows that:

$$1 \times X \times \left(1 + \frac{X}{10}\right) = 72 Gy_{10} \tag{5.7}$$

Equation 5.7 is a quadratic equation for which the solution is X = 22.3 Gy. Thus for equal tumour effect, the "standard" LQ model predicts that a single fraction physical dose of 22.3 Gy is equivalent to 60 Gy delivered in 30 fractions. However, if the tumour were to be slower growing and had an α[alpha]/β[beta] of, say, 4 Gy (representative of some breast cancers), the associated BED would be:

$$30 \times 2 \times \left(1 + \frac{2}{4}\right) = 90 Gy_{4} \tag{5.8}$$

Such a tumour would have enhanced fractionation sensitivity and, in such case, the equivalent single dose is given by the solution for X in:

$$1 \times X \times \left(1 + \frac{X}{4}\right) = 90 Gy_{4} \tag{5.9}$$

which is 17.1 Gy.

For a LRNT with α[alpha]/β[beta] = 3 Gy (and assuming the tissue is subjected to the same fractionation pattern as the tumour) the BED30 is:

$$BED30 = 30 \times 2 \times \left(1 + \frac{2}{3}\right) = 100 Gy_3 \tag{5.10}$$

In this case, the single fraction dose (X) required for equivalent effect is the solution of:

$$1 \times X \times \left(1 + \frac{X}{3}\right) = 100 Gy_3 \tag{5.11}$$

i.e. X = 15.9 Gy.

In practice, because the dose-response curves may straighten out (compared with the increasing curvature predicted by the standard LQ model), the iso-effect doses calculated using the above methodology will be under-estimates of the true doses required to achieve iso-effect with the original treatment. To that extent such calculations tend to "fail-safe"; both the required tumour and normal tissue doses will be under-estimated, but the degree of under-estimation is probably greater in the latter case. This is because the LRNT dose-response curve has greater curvature (and lower α[alpha]/β[beta] ratio) than has the tumour. In the case of slow growing tumours with α[alpha]/β[beta] ratios that are close to that of the LRNT, there should be less difference. However the LQ model will probably continue to underestimate the effect and will fail-safe with respect to normal tissue late reacting effects.

5.3.1 *Allowance for "Straightening-Out" of the Dose-Response Curve*

Some authors [13] have suggested methods which emulate the gradual transition of the dose-response from purely-LQ to one which is increasingly linear at higher doses and which mirrors the predictions of the MT model discussed earlier. It is claimed that such approaches may be better suited for assessing high-dose-fraction radiotherapy, but others [14] consider that the consequential introduction of a new layer of complexity requires more caution to be exercised in the application of the model. Indeed, Fowler [14] suggests that reasonable accurate prediction of response at high fractions is more easily possible by the simple expedient of selecting a higher α[alpha]/β[beta] value for the BED calculations, e.g., in the case of a typical tumours, selecting a value of 20 Gy instead of 10 Gy.

As a further alternative we present here an essentially simplistic model which assumes that the transition from pure LQ cell kill to purely logarithmic (i.e. straight-line) cell kill is abrupt rather than gradual and occurs at a specific fraction size (c). In this model the log cell kill at lower doses will be given by the LQ expression and,

beyond a certain dose (c), the slope of the dose-response curve will remain constant. In terms of the number (L) of lethal lesions created:

$$\begin{aligned}&\text{At low fraction doses}\left(\text{less than c}\right)\text{Eq.}\left(5.1\right)\text{holds, i.e.: L} = \alpha\left[\text{alpha}\right]\text{d} + \beta\left[\text{beta}\right]\text{d}^2\\&\text{At dose greater than c: L} = \alpha\left[\text{alpha}\right]\text{c} + \beta\left[\text{beta}\right]\text{c}^2 + \left(\alpha\left[\text{alpha}\right] + 2\beta\left[\text{beta}\right]\text{c}\right)\left(\text{d} - \text{c}\right)\end{aligned} \tag{5.12}$$

Equation 5.12 is derived by considering that the slope of the dose-response curve beyond dose c is linear and therefore has a constant slope given by the value of the first differential coefficient of the linear quadratic equation at dose c, represented by the term $\alpha + 2\beta c$.

Following exactly the same sequence of steps as were applied in Eqs. 5.1, 5.2, 5.3, 5.4, and 5.5, the BED (BED_N) for N fraction treatments involving fraction doses greater than c is given by:

$$BED_N = N\left(c + \frac{c^2}{(\alpha/\beta)} + \left(1 + \frac{2c}{(\alpha/\beta)}\right)(d - c)\right) \tag{5.13}$$

Equation 5.13 simplifies to:

$$BED_N = Nd\left(1 + \frac{c}{(\alpha/\beta)}\left(2 - \frac{c}{d}\right)\right) \tag{5.14}$$

For purposes of illustration, we assume that the cross-over from LQ cell kill to linear (logarithmic) cell kill occurs at 10 Gy, i.e. c = 10 in Eq. 5.14. Then, again following the steps used earlier, for a single fraction treatment to be iso-effective to a conventional 30 × 2 Gy treatment:

$$\text{For a tumour}\left(\alpha\left[\text{alpha}\right]/\beta\left[\text{beta}\right] = 10\ \text{Gy}\right): 1 \times d \times \left(1 + \frac{10}{10}\left(2 - \frac{10}{d}\right)\right) = 72\ \text{Gy}_{10} \tag{5.15}$$

i.e., the single fraction iso-effective tumour dose (d) is 27.3 Gy (cf 22.3 Gy derived above for the "pure-LQ" case).

$$\text{In the case of a LRNT}\left(\alpha\left[\text{alpha}\right]/\beta\left[\text{beta}\right] = 3\ \text{Gy}\right): 1 \times d \times \left(1 + \frac{10}{3}\left(2 - \frac{10}{d}\right)\right) = 100\ \text{Gy}_3 \tag{5.16}$$

i.e., the single fraction iso-effective LRNT dose (d) is 17.4 Gy (cf 15.9 Gy derived above for the "pure-LQ" case).

These examples show how standard BED equations (those assuming that the LQ model holds for indefinitely large fraction doses) will always underestimate the

iso- effective doses required for treatments involving high fraction doses. However, caution must be advocated in applying this alternative and un-tested BED approach, but it might be useful for those who wish to analyse their data and attempt to isolate what is the best dose in particular situations for c.

5.3.2 Normal Tissue "Hot-Spots"

The assessment of any treatment must include careful consideration of areas of normal tissues which receive doses in excess of the prescription dose [15]. Within the LQ model and BED formulation these can be accounted for by a term x where, for example, x = 1.05 represents a 5 % increment in dose, x = 1.07 a 7 % increment etc. Thus, any dose per fraction (d) is increased to dx and the BED [Eq. 5.5] is modified to become:

$$BED_N = Ndx\left(1+\frac{dx}{(\alpha/\beta)}\right) \tag{5.17}$$

Since the dose increment (x) is experienced by both, the total dose (Ndx) and the fractional dose (dx) in the bracketed term of Eq. 5.10, it is clear that the resultant increment in BED is supra-linear. Thus, additional dose can produce higher increments in bioeffect than would be expected from the dose increment itself. In the case of normal tissue 'hot-spots' when 2 Gy fractions are prescribed, the incremental effect in the higher dose areas, usually normal tissues included within the clinical target volume (CTV) and planning target volume (PTV), has been termed "double trouble" and may be significant. A further supra-linear increment in BED occurs in the hot-spots when the prescription dose per fraction is increased beyond 2 Gy; this has been called "treble (or triple) trouble" [15].

Thus greater care is required when considering allowable degrees of dose inhomogeneity in normal tissues within PTVs and the dose variation limits accepted for 2 Gy per fraction may be too great at much higher fraction doses such as 3, 6, 12 Gy etc. In each case, separate calculations should be performed. This is especially important in the case of very large fraction sizes, particularly as, in some SBRT treatments, doses may be prescribed to lower-than-usual isodoses (typically 50–80 %), meaning that tumour "hot-spots" of around 140–160 % may not be uncommon. In principle such a degree of tumour overdosing should be an advantage, but nonetheless great care is still required to ensure that normal structures are not being taken beyond their radiation tolerance. The alternative is to accept functional loss in these tissues, which will vary in importance according to the anatomical site being treated. Such a decision requires clinical judgment and is sometimes assisted by Dose Volume Histograms, although these have their own limitations.

By way of example, consider the effect of a 6 % normal tissue hot-spot in the two cases considered above i.e., conventional treatment (30 × 2 Gy) versus the LQ-equivalent single dose treatment (1 × 15.9 Gy). Both these schedules were

shown to be nominally iso-effective since each deliver a normal tissue BED of 100 Gy_3.

For the conventional treatment the increased BED in the normal tissue hot-spot is [by extension of Eq. 5.8]:

$$30\times 2\times 1.06\times\left(1+\frac{2\times 1.06}{3}\right)=108.5Gy_3 \tag{5.18}$$

i.e., an 8.5 % increase.

For the equivalent single-dose treatment, the increased BED is even higher:

$$1\times 15.9\times 1.06\times\left(1+\frac{15.9\times 1.06}{3}\right)=111.5Gy_3 \tag{5.19}$$

This represents an 11.5 % increase in BED accruing from a 6 % increase in physical dose to the hot-spot and could have important clinical significance.

Although normal tissue radiobiology is complex and should take account of the integrated effects across the whole tissue or organ, point-BED assessments of the type outlined here are nonetheless helpful since they are an easy way of highlighting the potential severity of double- or triple-trouble effects. It is, however, important to note that a single value of BED cannot provide a summary of an entire treatment volume in terms of risk, although integrated values and a mean BED can be useful in some applications.

Of particular relevance is Niemerko's concept of Equivalent Uniform Dose (EUD) which effectively uses the concepts discussed above to derive the magnitude of the physical dose which, if uniformly applied, would be expected to deliver the same biological effect as a given non-uniform distribution [16]. The usefulness of EUD mainly lies in the fact that it allows comparison of newer (and possibly non-uniform) treatments with those conventional schedules which, over many years, have contributed to the pool of existing clinical experience. EUDs may, for example, be very easily converted to equivalent 2 Gy per fraction schedules.

The limitation with the EUD concept is essentially the same as that noted with BED. The methodology inherently assumes that biological effect is governed only by the surviving fraction of cells. This is probably not unreasonable when considering tumours (although it ignores the possibility of, for example, Bystander Effects) but the assumption may fall down badly when considering gross normal tissue effects, for which the observed response is governed as much by their physiology and complex structural hierarchy as by cell surviving fraction. EUD methods are therefore probably more reliable in the assessment of TCP, rather than in assessing NTCP.

5.4 Other Radiobiological Factors

At the high fractional doses used with SBRT the observed in-vivo response may depend in part on radiation-induced changes to the microvasculature [17]. Further support for the role of vascular/stromal damage has been provided by radiosurgery

studies on arteriovenous malformations [18]. Such considerations add support to the idea that, in addition to the DNA damage observed at all doses, there is a further radiation effect, related to membrane, vascular and stromal damage, which is only observed at higher fractional doses. Furthermore, at higher doses delivered in small fraction numbers, any radioresistant subpopulations of cells may respond less favourably. In practice these and other mechanisms may act synergistically in ways which could explain the "straightening-out" effect on the basic LQ response curve (as discussed above) or, as has been suggested by some authors, could even lead to a response which is greater than that predicted by LQ [19]. Clearly the results of well-planned and well-conducted SBRT will play an important role in helping to clarify such matters.

Other significant radiobiological influences which may impact on treatment outcome include tumour repopulation effects, the possibility of incomplete-repair between dose fractions, durations of individual treatments in excess of about 15 min, cell-reassortment and re-oxygenation effects and (especially in relation to normal tissues), volume effects. It is possible to allow for the first two of these influences within LQ methodology but allowance for volume effects is more problematic since additional assumptions need to be made in relation to the hierarchical structure and physiology of the normal tissue in question. Since the mathematics is in all cases quite complex the discussion here will be limited to qualitative explanation of the issues involved.

5.4.1 Tumour Repopulation

Conventional treatment schedules (extending over several weeks) allow the possibility of increased tumour repopulation as treatment progresses, meaning that any cells which remain un-sterilised by radiation may progress through their cell cycle and continue to divide. A significant feature of the repopulation effect is that it is a radiation-stimulated phenomenon and therefore becomes a more sizeable influence towards the end of treatment, when most of the prescribed dose has been delivered.

Repopulation is particularly significant in SCC-type tumours and the amount of dose "wasted" in combating such repopulation (once it has got under way) may be very high [20, 21]. For such tumours the BEDs are therefore less than would be calculated by the simpler formulations [e.g. Eq. 5.5] and a subtractive term should be included to allow for the repopulation influence [22].

For radiotherapy involving high-dose fractions the fraction number may be small, or may involve just one fraction. In general, therefore, the overall duration of such treatments will be less than that of a conventional schedule and the loss of biological effect on the tumour, due to any concurrent repopulation, will be much reduced (or absent in the case of single fractions) and will confer a further therapeutic advantage on high-dose treatment.

As an example of this, consider the standard 30×2 Gy schedule discussed earlier. Using Eq. 5.6 this schedule was shown to be associated with a BED of 72 Gy_{10}. However, if substantial concurrent repopulation occurs, the effective BED (and

hence, cell kill) may be significantly smaller. In the case of head and neck squamous cell cancers, repopulation towards the end of treatment may correspond to a high BED-equivalent loss of around 0.9 Gy day^{-1} [23]. Such a high rate of repopulation is believed to begin at around 28 days after initiation of treatment so, for a conventional 30-fraction schedule lasting approximately 39 days, the BED loss due to repopulation is $(39—28) \times 0.9 = 9.9$ Gy_{10}, i.e. the effective BED is reduced to 72.0—9.9 = 62.1 Gy_{10}. Thus, the repopulation "wastage" in the conventional treatment amounts to around 14 % of the prescribed BED in this particular case. For the single-dose equivalent schedule of 27.3 Gy [discussed after Eq. 5.15 above], no repopulation can occur and hence there is zero dose wastage to this effect. This therefore is one of the potential advantages of using high dose-fractions for tumours with fast repopulation kinetics, and may apply to all SBRT treatments involving small fraction numbers in short overall times.

5.4.2 Problems with Incomplete-Repair Following Large Dose Fractions

Conventional fractionation typically involves inter-fraction intervals of 24 h or longer and a prime radiobiological reason for wanting to retain reasonable time spacing between fractions is to allow sub-lethal damage (usually associated with DNA breaks γ which are not immediately lethal) to repair itself. In the absence of such repair some of the sub-lethal damage is compounded to additional lethal damage in subsequent treatment fractions. In terms of LQ methodology the resultant BED will be greater than that calculated via Eq. 5.5, which assumes complete repair between fractions. Corrections to the model can be made to take account of this effect [24, 25] but in some instances they involve fairly complex mathematics, as discussed below.

The parameters which govern how much additional damage will be created by too-close spacing of fractions are the sub-lethal damage repair half-times. For tumours the half-times are generally quite short (often 30 min or less), meaning that most sub-lethal damage will repair itself in 24 h fraction intervals and there is effectively no accumulation of compounded damage as treatment progresses. However, for some LRNTs, there may be repair components present with repair half-times of the order of several hours [26–28], meaning that a significant amount of un-repaired sub-lethal damage will remain at the end of each dose fraction and which is available to be compounded (by subsequent fractions) into excess lethal damage. Thus, uncorrected BED calculations may significantly under-estimate the potency to normal tissues of treatments involving close fraction spacing.

When small numbers of large dose fractions are involved (as may happen with stereotactic guided therapy *etc.*) the issue of un-repaired damage may be significant even if 24 h inter-fraction gaps are maintained, simply because the large fraction sizes create proportionately more sub-lethal damage than do conventional fraction sizes and there is thus more to be repaired in each interval. For this reason large-dose radiotherapy of any kind should be delivered with inter-fraction spacing of

(where possible) >24 h or longer. Furthermore, when large-fraction boosts are added to conventional radiotherapy schedules, it is better to deliver the large-fractions at times when there will be longer-than-usual time gaps before treatment resumes, e.g., deliver the boost on the Friday before a weekend break.

5.4.3 *Effect of Extended Fraction Times*

In conventional radiotherapy the overall fraction time (i.e. the time taken to deliver the one, two, three etc. applied radiation fields in each daily treatment and including the time involved in re-positioning the patient and treatment unit between fields) is usually quite short and rarely exceeds 15 min. Even so, for a tumour with a fairly short repair half-time (say, 30 min) there will be some sub-lethal damage repair (and hence, loss of biological effect during the fraction delivery period). Although this is probably a real effect it is not normally necessary to be taken into account since clinically-evolved conventional treatment schedules will use dose prescriptions which inherently allow for any inter-fraction tumour repair.

However, with more complex (e.g. stereotactic) radiation delivery patterns, the overall fraction times may be further prolonged (to as much as 1 h or more) and it may be necessary to consider the possible significance of the reduced radiation impact on the tumour resulting from increased repair. One way of assessing this is by means of BED equations which have been derived for use with extended radiotherapy schedules [29]. For an N-fraction treatment involving fraction dose (d) being delivered in overall fraction time (T), the relevant equation may be written in the form:

$$BED_N = N \times d \times \left(1 + \frac{2 \times d}{\mu T \left(\alpha / \beta \right)} \times \left\{ 1 - \frac{1 - \exp\left(-\mu T \right)}{\mu T} \right\} \right) \tag{5.20}$$

In Eq. 5.13 the parameter μ[mu] is the time constant associated with sub-lethal repair and is related to the repair half-time ($T_{1/2}$) by:

$$\mu = \frac{0.693}{T_{1/2}} \tag{5.21}$$

Returning to the case of a single fraction of 15.9 Gy we calculate, by way of example, the BED when fraction duration is extended to 40 min. The tumour repair half-time is taken as 30 min (0.5 h). In this case the numerical values to use in Eq. 5.14 are: N = 1, d = 15.9 Gy, T = 40/60 = 0.67 h, μ[mu] = 0.693/0.5 = 1.39 h^{-1} and α[alpha]/β[beta] = 10 Gy.

The resultant BED in this case is 79.1 Gy_3, 21 % lower than the BED value of 100 Gy_3 obtained using the conventional equation which assumes instantaneous delivery, i.e. Eq. 5.5. This calculation thus illustrates that extending fraction times

to a point where they become comparable with, or greater than, the tumour repair half-times can lead to significant underestimation of the tumour bio-effect and may require physical dose adjustments to compensate. (A similar effect occurs in normal tissues. However, the loss in biological effectiveness would be less since the normal tissue repair times are generally longer and, in any case, any increase in repair occurring in normal tissues would be considered beneficial). Further clinical assessments of so called single fraction treatments given over relatively long durations have been published by Hopewell and colleagues [30], using a more sophisticated approach with two half times of repair.

5.4.4 Effect of Cell Cycle Re-Assortment and Re-Oxygenation

Since there are radioresistant phases of the cell cycle, irradiation using multiple treatment fractions will overcome the potential inefficiency of a single fraction in this respect, but it is not known what optimum fraction number is required to overcome this effect in individual tumours.

A further issue with low fraction numbers, or treatments given in very short durations, is that reoxygenation of hypoxic tumours may be incomplete. This problem can in principle be partly overcome by use of hypoxic cell sensitising drugs (HCS). It is not often acknowledged that HCS were tested along with large single fractions in animal experiments, but were later found to be of little or no benefit in human tumours treated by protracted fractionation schedules [31, 32]. HCS also caused considerable toxicity due to cumulative effects in tissues such as the nervous system when given with conventionally fractionated therapy, but such effects would not be expected with single doses. Early experiments in mice indicated that the optimum tumour control could be achieved either with a moderate number of fractions or with only a few used with HCS, without affecting the normal tissue response, although only acute skin effects were assessed [31]. There is scope for reconsidering the issue of HCS within modern hypofractionated radiotherapy as long as normal tissues are not adversely sensitised. Further research is indicated.

5.4.5 Normal Tissue Volume Effects

Volume effects are probably the most important radiobiological factor for normal tissues (both acute and late reacting) but are also the least well understood. Although there is much on-going development work in this area [33–38], none of the associated models are yet perfected and there are concerns about their validity amongst practical radiobiologists with experience of assessing tissue effects [39]. However, several commercially-available treatment planning systems make use of algorithms that estimate NTCP and which can be of use in the development of new treatment techniques or in the assessment of especially difficult treatment situations. These estimated complication probabilities should not automatically be assumed to reflect

the absolute clinical risks which will ultimately be deduced from retrospective review of the subsequent clinical results, but they may be useful in terms of ranking treatment options or in eliminating extremely dangerous treatments.

5.4.6 Tumour Volume Effects (and Volume Changes with Time)

An advantage of hypofractionated treatment is that the treatment geometry remains more predictable. Conventionally prolonged treatment courses can be accompanied by patient weight loss, changes in dose distribution and tumour shrinkage with shifts in normal tissue position relative to the radiation beams. Even in hypofractionated treatments the tumour can enlarge (due to oedema) after the first few fractions and the treatment volume might need to be enlarged. Such effects are often overlooked but use of image guided systems and adaptive radiotherapy should detect such an effect, although usually the tumour volume is not routinely estimated during such procedures.

5.5 Other Relevant Clinical Factors

5.5.1 Co-Morbidity from Other Sources

Consideration of co-morbidity is a complex issue and may arise when radiotherapy is given in conjunction with other treatment modalities (e.g. chemotherapy or hyperthermia) or in cases where patients have received an earlier course of radiotherapy. Patient age, or previous surgery, may also be factors which can affect response to radiation. In the case of chemotherapy or hyperthermia it is possible to assign an approximate BED-equivalent of such treatments and from which the maximum tolerable radiation dose which can be estimated [40–44], but the methodology involved, although better than making no allowance at all, remains speculative. For treatments involving high-fraction doses these uncertainties need to be viewed alongside the other confounding factors discussed in this Chapter.

5.5.2 High-Let and RBE Issues for Hypofractionation

There is increasing World-wide use of charged particle beams using protons and heavier ions where the radiation quality, expressed in terms of the linear energy transfer (LET), is higher than that for conventional megavoltage x-rays [45–50]. The relative biological effect (RBE) between the two forms of radiation being compared (usually standard megavoltage x-rays and a higher LET radiation) is the ratio of the doses required for the same bio-effect. For proton beams the RBE is of the

order of 1.1 (i.e. such beams are, dose for dose, about 10 % more effective) but for more complex ion species (e.g. carbon ions) the RBE may be much higher and in the range 3–5.

RBE effects may be incorporated within the BED concept [5, 6, 8, 51, 52] and the general expression for calculating the BED of an N fraction high-RBE treatment is:

$$BED_N = Nd_H\left(RBE_{\max} + \frac{RBE_{\min}^2 d_H}{(\alpha/\beta)_L}\right) \tag{5.22}$$

where d_H is the high-RBE dose per fraction and $(\alpha[\text{alpha}]/\beta[\text{beta}])_L$ is the low-RBE fractionation factor (i.e. as would be used in the earlier equations relating to conventional photon treatments). RBE_{max} is the maximum RBE at very low fraction sizes and RBE_{min} is the asymptotic minimum RBE which occurs at very high fraction sizes. RBE_{min} is conventionally assumed to be unity, but there is gathering evidence that it may have a non-unity value for some ion species and Eq. 5.22 allows this to be taken into account. A further major advantage of using Eq. 5.17 is that there is no requirement to know the RBE value relating to the dose per fraction (d_H) in question, since the inclusion of the $(\alpha[\text{alpha}]/\beta[\text{beta}])_L$ parameter, in conjunction with RBE_{max} and RBE_{min}, inherently allows for the variation of RBE with fraction size. Finally, in the case of high-RBE radiations such as carbon ions, the straightening-out of the underlying dose-response curve is much less significant than for photons, meaning that BEDs calculated via Eq. 5.22 are likely to be reliable even for large fraction sizes. There may also be an advantage for extreme hypofractionation if RBE_{min} is significantly lower for late reacting normal tissues than in most tumours [52].

5.6 Conclusions and Future Implications

Although the mechanisms governing radiotherapy response to conventional fractionation are now well-understood, some doubt remains over the precise nature of radiation response characteristics when high dose fractions are involved. Indeed there may even be a role for mitochondrial damage rather than nuclear effects at very high dose [53]. There may be deviation from the standard LQ predictions at higher doses, but it remains unclear whether radiation response becomes completely exponential (i.e. cell survival curves eventually becoming straight) or whether some reduced degree of downward curvature continues indefinitely. Whatever the exact nature of this deviation from the LQ predictions, the uncertainties will increase as fraction size is increased (especially for LRNTs) and this is a point to be borne in mind when considering new schedules involving particularly large dose fractions. Past clinical experience may be a poor guide (again, especially for tissue tolerance) since the dose distributions associated with modern techniques are so different and will involve steep dose gradients and changed volume effects.

In general, however, design of high-dose schedules using LQ methodology will tend to over-estimate the biological effect associated with high-dose fractions and will therefore tend naturally to err on the safe side. Since the fractionation sensitivity of LRNTs at higher dose/fractions is much more marked than that of tumours, the prudent approach always is to first use the LRNT parameters to design schedules and then to consider the likely effect on tumour. Calculus-based methods also may be used may be used to optimise the dose per fraction. Here it is possible to take account of the degree of sparing of normal tissues and of tumour repopulation rates to estimate the optimal dose per fraction required in hypofractionated treatments [6, 54, 55]. The equations suggest that increasing the dose per fraction when progressively improved LRNT sparing is achieved will produce better results in terms of the yield of tumour cell kill relative to a maintained LRNT isoeffect. Again, this advantage will not apply to normal tissues inside the PTV.

For any type of radiotherapy, accurate recording of the details of treatment schedules is essential in order to allow the subsequent treatment outcomes to properly inform future practice. Such observation is especially relevant in the case of radiotherapy involving high dose fractions and it is recommended that records of the following should be kept: overall treatment time, number of fields used for each fraction and the fraction duration, precise details of the dose/time pattern received by the critical organ a risk (including those at any hotspots within the PTV) and DVHs for tumour and all critical normal structures. Such records are essential since, in the longer term, statistical analysis of large DVH atlases, compiled from individual DVHs of previously treated patients, could be an excellent way of using prescription and DVH information, not merely to prospectively improve treatment design, but also to develop better normal tissue complication models [56–58]. Additionally, if the treatment has been designed using radiobiological considerations then full details of the methodology should be recorded, along with all the assumed parameter values.

Since it is always the responsibility of clinicians to prescribe dose and fractionation, they should maintain an interest in the radiobiological issues discussed in this Chapter. In particular, the need to assess the volume and likely tolerance of irradiated normal tissue is essential since (as demonstrated above) the volume of normal tissue exposed to doses per fraction that exceed that of the prescription in especially important. Although dose volume histograms display the summated volume which receives a particular dose they cannot account for separate areas of high dose. Individual clinicians, according to their treatment site of interest, should therefore carefully observe dose distributions in 3-D displays and note the volumes which exceed certain dose limits. In some instances 1 cm^3 volumes of high dose can be important. But it is even more relevant to search for special anatomical regions which may incur such a penalty; in the CNS for example, the spinal cord, brainstem and the optic chiasm are obvious areas. It may also be useful undertake BED calculations over distinct areas of interest, such as bowel wall adjacent to a tumour.

Some clinicians, especially those unfamiliar with the BED approach, may prefer to have their potential treatments expressed in terms of equivalent doses in 2 Gy fractions. This appears reasonable but must be tempered with the knowledge that

some known tolerance doses may be associated with treatments using 1.8 Gy fractions and which are delivered in overall treatment times which are longer than usual. Extended treatment times can adversely influence tumour control and, in some instances, normal tissue repopulation and late side effects also.

Those performing radiobiological calculations must also be aware of the sensitivity of the models described. If it is required to choose a dose to be given in (say) 1–4 fractions, what reference dose in (say) 2 Gy fractions should be used as the basis for the iso-effectiveness calculations? If a rapidly repopulating tumour is being treated then a 70 Gy schedule involves much wasted dose due to tumour repopulation, to an extent that a 56 Gy dose given in a much shorter time might lead to the same outcome. It should therefore be necessary to take account of time and repopulation effects in the conventional (reference) schedule when assessing the equivalent SBRT dose [25].

References

1. Barendsen GW. Dose fractionation, dose-rate and iso-effect relationships for normal tissue responses. Int J Radiat Oncol Biol Phys. 1982;8:1981–97.
2. Fowler JF. The linear-quadratic formula and progress in fractionated radiotherapy. Br J Radiol. 1989;62:679–94.
3. Fowler JF. 21 years of biologically effective dose. Br J Radiol. 2010;83:554–68.
4. Dale RG, Jones B. The clinical radiobiology of brachytherapy. Br J Radiol. 1998;71:465–83.
5. Dale RG, Jones B. The assessment of RBE effects using the concept of biologically effective dose. Int J Radiat Oncol Biol Phys. 1999;43:639–45.
6. Jones B, Dale RG. The clinical radiobiology of high-LET radiotherapy with particular reference to proton radiotherapy. Clin Oncol. 2003;15:S16–22.
7. Armpilia CI, Dale RG, Coles IP, Jones B, Antipas V. The determination of radiobiologically optimized half-lives for radionuclides used in permanent brachytherapy implants. Int J Radiat Oncol Biol Phys. 2003;55:378–85.
8. Carabe-Fernandez A, Dale RG, Jones B. The incorporation of the concept of minimum RBE (RBE_{min}) into the linear-quadratic model and the potential for improved radiobiological analysis of high-LET treatments. Int J Radiat Biol. 2007;83:27–39.
9. Lea DE, Catcheside DG. The mechanism of the induction by radiation of chromosome aberrations in Tradescantia. J Genet. 1942;44:216–45.
10. Gray LH, Scholes MF. The effect of ionising radiation on the broad bean root. Br J Radiol. 1951;24:285–91.
11. Kellerer AM, Rossi HH. The theory of dual radiation action. Curr Top Radiat Res Q. 1972;8:85–158.
12. Chadwick KH, Leenhouts HP. A molecular theory of cell survival. Phys Med Biol. 1973;18:78–87.
13. Park C, Papiez L, Zhang S, Story M, Timmerman RD. Universal survival curve and single fraction equivalent dose: useful tools in understanding potency of ablative radiotherapy. Int J Radiat Oncol Biol Phys. 2008;70:847–52.
14. Fowler JF. Linear quadratics is alive and well: in response to Park et al. (IJROBP 2008: 70: 847–852). Int J Radiat Oncol Biol Phys. 2008;72:957.
15. Jones B, Dale RG, Khaksar SJ. Biological equivalent dose assessment of the consequences of hypofractionated radiotherapy. Int J Radiat Oncol Biol Phys. 2000;47:1379–84.
16. Niemierko A. Reporting and analyzing dose distributions: a concept of equivalent uniform dose. Med Phys. 1997;24:103–10.

17. Fuks Z, Kolesnick R. Engaging the vascular component of the tumor response. Cancer Cell. 2005;8(2):89–91.
18. Park HJ, Griffin RJ, Hui S, Levitt SH, Song CW. Radiation-induced vascular damage in tumors: implications of vascular damage in ablative hypofractionated radiotherapy (SBRT and SRS). Radiat Res. 2012;177(3):311–27.
19. Kirkpatrick JP, Meyer JJ, Marks LB. The linear-quadratic model is inappropriate to model high dose per fraction effects in radiosurgery. Semin Radiat Oncol. 2008;18:240–3.
20. Hendry JH, Roberts SA, Slevin NJ, Keane TJ, Barton MB, Agren-Conqvst A. Influence of radiotherapy treatment time on control of laryngeal cancer: comparisons between centres in Manchester, UK and Toronto, Canada. Radiother Oncol. 1994;31:14–22.
21. Roberts SA, Hendry JH, Brewster AE, Slevin NJ. The influence of radiotherapy treatment time on the control of laryngeal cancer: a direct analysis of data from two British Institute of Radiology trials to calculate the lag period and the time factor. Br J Radiol. 1994;67:790–4.
22. Dale RG. Time-dependent tumour repopulation factors in linear-quadratic equations—implications for treatment strategies. Radiother Oncol. 1989;15:371–82.
23. Dale RG, Hendry JH, Jones B, Robertson G, Deehan C, Sinclair JA. Practical methods for compensating for missed treatment days in radiotherapy, with particular reference to head and neck schedules. Clin Oncol. 2002;14:382–93.
24. Thames HD, Hendry JH, editors. Fractionation in radiotherapy. London/Philadelphia: Taylor and Francis; 1987. ISBN 0–85066–374–1.
25. Jones B, Dale RG, Deehan C, Hopkins KI, Morgan DA. The role of biologically effective dose (BED) in clinical oncology. Clin Oncol. 2001;13:71–81.
26. Pop LA, van der Plas M, Ruifrok AC, Schalkwijk LJ, Hanssen AE, van der Kogel AJ. Tolerance of rat spinal cord to continuous interstitial irradiation. Int J Radiat Oncol Biol Phys. 1998;40(3):681–9.
27. Van den Aardweg GJMJ, Hopewell JW. The kinetics of repair of sublethal radiation—induced damage in the pig epidermis: an interpretation based on a fast and a slow component of repair. Radiother Oncol. 1992;23:94–104.
28. Ruifrok ACC, Kleiber BJ, van der Kogel AJ. Repair kinetics of radiation damage in the developing rat cervical spinal cord. Int J Radiat Biol. 1993;63:501–8.
29. Dale RG. The application of the linear-quadratic dose-effect equation to fractionated and protracted radiotherapy. Br J Radiol. 1985;55:515–28.
30. Hopewell JW, Millar WT, Lindquist C, Nordström H, Lidberg P, Gårding J. Application of the concept of biologically effective dose (BED) to patients with Vestibular Schwannomas treated by radiosurgery. J Radiosurg SBRT. 2013;2:259–71.
31. Fowler JF, Sheldon PW, Denekamp J, Field SB. Optimum fractionation of the C_3H mouse mammary carcinoma using x-rays, the hypoxic-cell radiosensitizer Ro-07–0582, or fast neutrons. Int J Radiat Oncol Biol Phys. 1976;1(7–8):579–92.
32. Fowler JF, Denekamp J. A review of cell radiosensitisation in experimental tumours. Pharmacol Ther. 1979;7:413–44.
33. Niemierko A, Goitein M. Dose-volume effects in the spinal cord. Radiother Oncol. 1994;31:265–7.
34. Sanchez-Nieto B, Nahum AE, Dearnaley DP. Individualisation of dose prescription based on normal-tissue-dose-volume and radiosensitivity data. Int J Radiat Oncol Biol Phys. 2001;49:487–99.
35. Seppenwoolde Y, Lebesque JV, de Jaeger K, Belderbos JS, Boersma LJ, Schilstra C, Henning GT, Hayman JA, Martel MK, Ten Haken RK. Comparing different NTCP models that predict the incidence of radiation pneumonitis. Normal tissue complication probability. Int J Radiat Oncol Biol Phys. 2003;55:724–35.
36. Werner-Wasik M, Yorke E, Deasy J, Nam J, Marks LB. Radiation dose-volume effects in the esophagus. Int J Radiat Oncol Biol Phys. 2010;76:S86–93.
37. Marks LB, Bentzen SM, Deasy JO, Kong FM, Bradley JD, Vogelius IS, El Naga I, Hubbs JL, Lebesque JV, Timmerman RD, Martel MK, Jackson A. Int J Radiat Oncol Biol Phys. 2010;76:S70–6.

38. Rutkowska ES, Syndikus I, Baker CR, Nahum AE. Mechanistic modelling of radiotherapy-induced lung toxicity. Br J Radiol. 2012;85:1242–8.
39. Schultheiss TE. The controversies and pitfalls in modelling normal tissue radiation injury/damage. Semin Radiat Oncol. 2001;11:210–4.
40. Jones B, Dale RG, Gaya A. Linear quadratic modelling of increased late normal tissue effects in special clinical situations. Int J Radiat Oncol Biol Phys. 2006;64:948–53.
41. Jones B, Dale RG. The potential for mathematical modelling in the assessment of the radiation dose equivalent of cytotoxic chemotherapy given concomitantly with radiotherapy. Br J Radiol. 2005;78:939–44.
42. Plataniotis GA, Dale RG. Biologically effective dose-response relationships for breast cancer treated by conservative surgery and postoperative radiotherapy. Int J Radiat Oncol Biol Phys. 2009;75:512–7.
43. Cattaneo GM, Passoni P, Longobardi B, Slim N, Reni M, Cereda S, di Muzio N, Calandrino R. Dosimetric and clinical predictors of toxicity following combined chemotherapy and moderately hypofractionated rotational radiotherapy of locally advanced pancreatic adenocarcinoma. Radiother Oncol. 2013. doi:10.1016/j.radonc.2013.05.011. pii S0167–8140(13)00224–7.
44. Meade S, Sanghera P, McConkey C, Fowler J, Fountzilas G, Glaholm J, Hartley A. Revising the radiobiological model of synchronous chemotherapy in head-and—neck cancer: a new analysis examining reduced weighting of accelerated repopulation. Int J Radiat Oncol Biol Phys. 2013;86:157–63.
45. Schultz-Ertner D, Tsujii H. Particle radiation therapy using proton and heavier ion beams. J Clin Oncol. 2007;25:953–64.
46. Jones B. The case for particle therapy. Br J Radiol. 2006;79:24–31.
47. Jones B. Modelling carcinogenesis after radiotherapy using Poisson statistics: implications for IMRT, protons and ions. J Radiol Prot. 2009;29:A143–57.
48. Weber U, Kraft G. Comparison of carbon ions versus protons. Cancer J. 2009;15:325–32.
49. Jiang GL. Particle therapy for cancers: a new weapon in radiation therapy. Front Med. 2012;6:165–72.
50. Loeffler JS, Durante M. Charged particle therapy—optimisation, challenges and future directions. Nat Rev Clin Oncol. 2013;10:411–24.
51. Jones B, Dale RG, Carabe-Fernandez A. High LET radiotherapy: chapter 15. In: Dale RG, Jones B, editors. Radiobiological modelling in radiation oncology. London: Brit Inst Radiol; 2007. p. 265–75.
52. Jones B, Underwood TC, Carabe-Fernandez A, Dale RG. Further analysis of fast neutron relative biological effects and implications for charged particle therapy. Br J Radiol. 2011;84:S11–8.
53. Zhang B, Davidson MM, Zhou H, Wang C, Walker WF, Hei TK. Cytoplasmic irradiation results in mitochondrial dysfunction and DRP1-dependent mitochondrial fission. Cancer Res. 2013;73(22):6700–10. doi:10.1158/0008–5472.CAN-13–1411. Epub 2013 Sep 30.
54. Jones B, Tan LT, Dale RG. Derivation of the optimum dose per fraction from the linear quadratic model. Br J Radiol. 1995;68:894–902.
55. Armpilia CI, Dale RG, Jones B. Determination of the optimum doe per fraction in fractionated radiotherapy when there is delayed onset of tumour repopulation during treatment. Br J Radiol. 2004;77:765–7.
56. Jackson A, Yorke ED, Rosenzweig KE. The atlas of complication incidence: a proposal for a new standard for reporting the results of radiotherapy protocols. Semin Radiat Oncol. 2006;16:260–8.
57. Bentzen SM, Constine LS, Deasy JO, Fisbruch A, Jackson A, Marks LB, Ten Haken RK, Yorke ED. Quantitative analysis of normal tissue effects in the clinic (QUANTEC): an introduction to the scientific issues. Int J Radiat Oncol Biol Phys. 2010;76(3 Supp):S3–9.
58. Deasy JO, Bentzen SM, Jackson A, Ten Haken RK, Yorke ED, Constine LS, et al. Improving normal tissues complications probability models: the need to adopt a “data pooling” culture. Int J Radiat Oncol Biol Phys. 2010;73(3 Supp):S151–4.

Chapter 6
Planning and Dosimetry for Stereotactic Body Radiotherapy

Sonja Dieterich

Abstract Planning for SBRT is characterized by the need to create high dose gradients from target to critical structures in the vicinity. Since SBRT is a relatively new field, appropriate DVH constraints are still under development in clinical trials and single-center studies.

The effect of residual motion such as deformation, rotation and residual respiratory motion has to be considered to determine appropriate ITV and PTV margins. SBRT targets such as lung are located in areas of the body with large tissue inhomogeneities. Treatment algorithms must be capable of modeling these inhomogeneities appropriately to generate a dose calculation which is close to the delivered dose. Planner skill has traditionally played a large role in designing high quality treatment plans with optimum target coverage and tissue sparing. Data mining of existing plans and the use of plan libraries is being explored to aid the treatment planner in standardizing planning approaches to more consistently find the optimum dose distribution. To ensure a close match between plan dose calculations and delivered dose calculations, the dosimetry of small fields must be well understood and modelled in the treatment planning system. The small fields and sharp dose gradients pose more stringent challenges for patient-specific SBRT QA.

Keywords Stereotactic radiosurgery • Treatment planning • Stereotactic dose constraints • Tissue heterogeneity • Small field dosimetry

6.1 Introduction

Treatment planning for stereotactic radiosurgery is very diverse in that it can range from using the same planning techniques as conventional IMRT (Intensity Modulated Radiation Therapy) with the only difference being in the dose-fractionation scheme and the technical constraints of delivery, to

S. Dieterich, PhD
Department of Radiation Oncology, Stanford University Hospital, Stanford, CA, USA

UC Davis, Davis, CA, USA
e-mail: sonja.dieterich@stanford.edu

A. Gaya, A. Mahadevan (eds.), *Stereotactic Body Radiotherapy: A Practical Guide*,
DOI 10.1007/978-0-85729-597-2_6

device-specific planning such as for a Gamma Knife treatment. As SBRT delivery devices, planning systems and clinical evidence have developed over the years, basic principles of SBRT planning emerged that span across technologies, with minor variations accounting for device-specific differences. This chapter focuses on the basic principles of SBRT planning, mentioning device-specific differences as appropriate.

Single-fraction stereotactic radiosurgery in the brain and spine will be referred to as SRS (Stereotactic Radiosurgery). Stereotactic radiosurgery in the body (except spine) delivered in 1–5 fractions, will be referred to as SBRT (Stereotactic Body Radiotherapy).

6.2 Basic Principles of SBRT Planning: Homogeneous Vs. Heterogeneous Planning

One notable aspect of SBRT planning is the differing schools of thought on homogeneous plans vs. heterogeneous plans. Unlike many IMRT planning conventions, most SBRT planning techniques will normalize the maximum dose to 100 %, with the prescription isodose line between 50 and 85 % of the maximum dose.

In Gamma Knife planning, which is the oldest SRS planning technique, the prescription isodose line is typically set to 50–60 % of maximum dose. The reason is that in a single-isocenter Gamma Knife plan, the steepest dose falloff is near the 50 % isodose line, therefore affording the most OAR (Organ at Risk) sparing. For traditional linacs with flattened beams, single-isocenter plans typically have their steepest dose falloff near the 80 % isodose line, whereas in multi-isocentric plans, the steepest falloff may be closer to 70 %. In CyberKnife planning, the tendency is to plan with dose homogeneity, that is, with a prescription line between 75 and 80 % of maximum dose following in the tradition of linac-based planning. The sequential optimization algorithm [1] and the IRIS collimator[2] have allowed for the creation of even more homogeneous plans with prescription isodose lines of 85–90 % of maximum dose. The CyberKnife treatment planning software also allows for single isocentric and multi isocentric treatment delivery. These features have been explored to create hypofractionated prostate plans which emulate HDR dose distributions, as well as to design SRS plans similar to Gamma Knife plans.

There are no published studies on the advantage of one planning technique over the other. One theoretical consideration would be the potential advantage of higher doses in the center of the tumor to offset the effects of hypoxia [2].

6.3 General Concepts for SRS/SBRT Planning

SBRT plans are characterized by high dose to the target, small fields, and often significant intensity modulation, which all result in a high MU-to-dose ratio. This, in turn, means that the entrance skin dose per beam can also be very high,

potentially leading to significant toxicities [3]. Non-isocentric treatment techniques can lead to hot spots away from the axial plane of treatment, which requires special attention during the planning and plan evaluation phase. The high prescription dose also means that OAR sparing is essential. Two parameters are generally used to define stereotactic OAR sparing. High CI (Conformality Index), i.e. close agreement of the 3D prescription isodose line with the target shape, describes how well the planned dose conforms to the target. Mathematically, the inverse of the conformity index described by Knoos et al. [4] is used to evaluate the plan conformality. In addition to plan conformality, critical structures in close proximity to the target will need to be spared to a greater extent than soft tissue such as fat and/or muscle. Therefore, any planning approach used for SBRT must be able to create steep dose gradients and concave dose distributions. Typically, dose gradients of Gy/cm around the PTV (Planning Target Volume) can be achieved, with gradients becoming as steep as Gy/mm for targets abutting OARs. In summary, we can define the following criteria for SRS/SBRT planning as follows:

- At least seven treatment field angles, or rotational arcs should be used
- High conformality index
- Steep dose gradients on the order of Gy/cm around the PTV, approaching the Gy/mm scale for OARs such as spinal cord

6.4 Treatment Delivery Time

Frameless, image-guided delivery of SRS/SBRT treatments is rapidly becoming the standard of care. Even though the patient is still immobilized and set up with image guidance, there is always the risk for residual motion [5–8] unless real-time imaging techniques are employed. It is beyond the scope of this chapter to discuss motion compensation, but in summary, the risk of residual patient motion can be minimized by shortening the treatment time. As part of the planning process, the treatment time needs to be considered as one criterion for plan quality evaluation.

In cone-based SBRT on a linac, the two variables which control treatment time are the collimator size and the number of shots used. The collimator size largely depends on the size of the target. Complex targets will require a combination of large collimators to fill in the bulk of the tumor with dose, and smaller collimators to infuse the intricate, smaller aspects of the structure [9]. For SBRT in which IMRT based delivery techniques are used, minimizing the number of beams and the number of control points per beam will lead to faster delivery times. Sliding window techniques are also faster in delivering dose than step-and-shoot IMRT.

Respiratory motion compensation techniques also have an impact on delivery time. The treatment is delivered continuously when either compression or real-time tracking delivery techniques [10, 11] are used. Breath-hold does significantly increase treatment time for IMRT-based SBRT; however, with fast VMAT (Volume Modulated Arc Therapy) deliveries, the increase in delivery time is less significant.

Gating techniques can increase delivery time depending on the length of the gating window. Using a hybrid of breath-hold and gating, i.e. delivering a breath-hold treatment running the accelerator in gating mode, is the most efficient way of minimizing respiratory motion while optimizing the delivery speed.

The longer the delivery time, the more likely it is for a patient to move during treatment delivery. Residual motion errors for image-guided treatments also tend to increase, because patients tend to move more often if they are immobilized for a longer time [7]. This in turn increases the uncertainty of treatment delivery, which needs to be considered in the design of the PTV treatment margin. Treatment margins will be discussed in more detail in Sect. 5.4.

6.5 Dose Calculation Algorithms and Heterogeneities

In SRS treatments, much emphasis is placed on spatial treatment delivery accuracy. However, physicists need to be aware that inaccuracies in the dose calculation algorithm can shift isodose lines on the same order of magnitude (>1 mm or more) than inaccuracies in treatment delivery. It is therefore essential, especially when delivering SBRT treatments in highly heterogeneous areas of the body such as lung, to use a dose calculation algorithm that has been verified to be accurate in such an environment. Figure 6.1 shows an example of a T-spine SRS treatment. The left panel shows the dose calculation with a ray-tracing algorithm using a simplistic path-length correction. The right panel shows the same beam configuration, but calculated with a Monte Carlo algorithm to a 2 % uncertainty at the maximum dose point. The prescription isodose line (green) in the anatomical, anterior right quadrant of the lesion is shifted by about 1 mm. These changes in isodose are much more significant for lung lesions and are further pronounced with smaller tumors and greater density differences between the tumor and surrounding tissues.

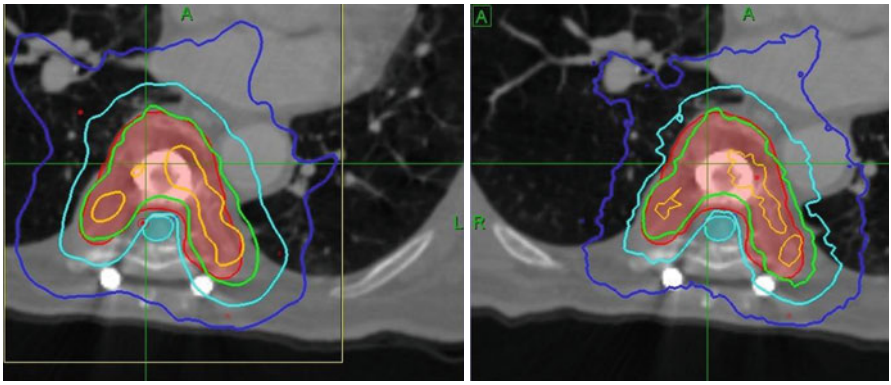

Fig. 6.1 Shift of 1 mm in prescription isodose line (*green*) in the anatomical, anterior right quadrant comparing ray-tracing plan (*left*) with Monte Carlo calculation (*right*)

The need for an algorithm that can accurately account for heterogeneities highly depends on the area of the body being treated. An additional factor to consider is the presence of inorganic materials from ancillary treatments. Examples are metal spine hardware or bone cement used to stabilize vertebral bodies.

6.6 Lung

The greatest heterogeneities occur with lesions in the lung. In the early clinical trials for lung cancer, algorithms for heterogeneity corrections were in their infancy; therefore, clinical trials such as RTOG-0236 required all internal tissues to be treated as though they possessed the same density as water. As the quality of dose calculation algorithms improved, the RTOG created a hybrid approach in which the treatment plan was based on the original homogeneous planning philosophy, while the actual delivered plan, based on a dose inhomogeneity calculation, was tracked. Currently, the clinical treatment planning practice varies from the traditional, homogeneous planning approach to hybrid models to the exclusive use of heterogeneity dose calculation algorithms.

The contrast in doses between the homogeneous planning approach and heterogeneity calculations can be substantial in lung. Wilcox et al. [12] have demonstrated a 20 % difference in maximum tumor dose between a pathway density correction algorithm and photon Monte Carlo [13, 14]. Davidson et al. [15] evaluated five treatment planning systems for the performance of their respective dose calculation algorithms in lung. The most widely used algorithm is the anisotropic analytic algorithm [16] (AAA). Increased processor speeds and better phase-space reduction methods have made it feasible to use photon Monte Carlo dose calculation algorithms clinically [13, 14]. A more recent development is the use of an algorithm belonging to the class of Linear Boltzman Equation Transport solvers. Early studies demonstrate accuracy comparable to AAA [17].

6.7 Other Materials

Treatment planning systems are currently not able to accurately calculate dose in the vicinity of metal, especially for smaller metallic structures such as stents and dental fillings. CT artifacts complicate the situation, although secondary reconstruction algorithms are being developed which, once implemented in the clinic, will significantly reduce the metal artifacts in simulation CT scans.

Strategies to minimize the effects of metal artifacts include density overwrites of the planning CT volume including the metal object and the imaging artifacts caused by it. The HU number is commonly set to water. For small implants such as aneurysm clips, stents, or dental fillings, a density overwrite is also recommended unless the planning system has been demonstrated to correctly compensate for the heterogeneity.

In the evaluation of the plan, potential changes to the actual delivered dose compared to the dose displayed by the treatment planning system should be estimated and discussed based on published literature. In rare situations, e.g. with dental fillings, it is possible to evaluate the dose using in-vivo dosimeters and making adjustments to the treatment plan for subsequent SBRT fractions.

AVMs are most common in the brain, but can also occur, albeit rarely, in the spine. Commonly used therapeutic approaches are endovascular embolization with coils, glue or particles [18]. These treatments introduce high electron density material into the AVM. If the patient is then treated with SBRT for a recurrence, the difference in densities has to be considered during treatment planning [19].

Ethiodol, which is radiopaque poppy seed oil, is used as a contrast agent in TACE (Transarterial Chemoembolization) for liver tumors. As with embolization materials for AVMs, the higher electron density of these materials need to be considered in treatment planning.

Metallic stents are commonly used in the esophagus, pancreas and liver. Experimental measurements of dose in the vicinity of esophageal stents [20] have shown patterns of hot and cold spots depending on the construction material of the stent. Dose in the vicinity of an platinum aneurysm clip used in the brain has shown to be elevated by 10–20 %, while no changes in dose could be measured for other metals [21].

6.8 Plan Evaluation

Plans are evaluated based on whether the dose constraint goals are met. Some clinical case presentations do not allow for satisfying all goals simultaneously; therefore compromises have to be made on an individual patient assessment. To account for this variability, the RTOG has defined the concept of “minor” and “major” protocol violations, which the author highly recommends to adopt into clinical treatment planning for SBRT. For example, a planning target goal may be to limit the conformality index (CI) to <1.2. A minor violation, which would still allow the patient to be included in the protocol, would be a conformality index $1.2<CI<1.4$, while a CI >1.5 would prevent a patient from being included in the protocol or render the plan unacceptable.

6.8.1 Skin Dose

Acute skin toxicity has been reported for early-stage NSCLC SBRT treatments [3]. The authors reported that “Distance from the tumor to the skin on the patient’s back <5 cm ($p=0.006$), treatment with three beams ($p=0.0007$), and a maximum back skin dose >50 % of prescribed dose on the planning scan ($p=0.02$) were all

significantly associated with those patients that developed Grade 2 or higher skin reaction." It is also important to carefully assess dose in skin folds, especially posterior skin folds which may not be as immediately obvious as anterior skin folds. For beams passing through the treatment couch and any setup devices, it is important to verify these to be accurately modeled by the treatment planning systems. Several couch models have been shown to change the dose delivered by oblique posterior beams by up to 6 %. Carbon fiber couches used in conjunction with electromagnetic tracking systems have been measured to be at the upper limit, or even exceeding, this level of dosimetric impact. The upcoming AAPM Task Group 176 "Dosimetric Effect of Immobilization Devices" will summarize a clinical review of the dosimetric effect of setup devices, including recommendations for clinical dosimetry.

6.8.2 Peripheral Dose

While the main focus of plan evaluation is naturally on the high-dose regions, the distribution of peripheral dose has significant impact both on short-term as well as long-term complication rates.

Many delivery devices, such as Gamma Knife, CyberKnife and Tomotherapy, are limited to one beam energy. When planning highly modulated beams from many directions, and especially when using non-coplanar or non-isocentric planning techniques, the planner must pay close attention to dose delivered in the periphery of the targeted treatment area. These "hot spots" can be more pronounced for obese patients, where the path-length from skin to target exceeds ~15 cm. In planning systems which use a calculation grid to define the body volume in which the dose is calculated and displayed for planning purposes, it is important for the planner to open up the calculation grid and evaluate the plan for peripheral hot spots. Effective ways to minimize the potential for peripheral hot spots include the use of a higher number of beams, limiting the number of MUs per beam direction, and using soft tissue constraints or phantom structures to control the peripheral dose.

Another consideration must be the peripheral dose distribution into peripheral OARs. With increasing cancer survival rates, considering low-dose regions to radiation sensitive organs may affect secondary cancer rates in the decades to follow. One of many examples of increased secondary malignancy caused by low peripheral doses to an OAR was published by Kleinerman et al. [22]. There are four sources for this dose: (1) Low-dose regions of the treatment plan itself, (2) Imaging dose, (3) Leakage, and (4) internal scatter. Leakage and internal scatter are machine-dependent. Imaging dose management is part of simulation and treatment delivery design. During the planning process, low-dose regions is the only peripheral dose parameter which can be influences by the planner under physician guidance.

6.9 Plan Standardization and Evaluation

The goal of designing optimum tumor coverage with the best organ sparing is a multi-criteria optimization problem. Until very recently, treatment planning systems (TPS) relied on a combination of planner skill and hardcoded optimization algorithm to try and find the best possible solution for each patient. Plan evaluation relied on physician and planner experience of what might be possible clinically; there was no scientific method to assess plan quality. More recently, improvements in informatics, specifically class-based database analysis and automation, have opened the door toward more quantitative plan quality analysis methods. In turn, these methods can be used as a tool to aid treatment planners in the analysis of plan quality and increase planning efficiency. For example, Moore et al. [23, 24] developed an experimental fit on the achievable lower limit for mean OAR dose based on OAR/PTV overlap. By making the lower OAR dose limit prediction available to planners, successive treatment plans showed lower variability and smaller deviation from the predicted minimum possible OAR dose without compromising PTV coverage.

Interactive multi-criteria IMRT planning [25], made possible by increased computing power and faster optimization algorithms, integrates plan optimization even earlier in the treatment planning process. Instead of calculating one or a few plans which are then selected and optimized, the treatment planning system will create a "plan bundle" based on the planner selected parameter space, i.e. lower and upper limits of dose constraints for all OARs. From amongst this plan bundle, the planner can then further restrict the Pareto surface by restricting multiple criteria through a user interface. Real-time update of the dose distribution provides the planner with an efficient method to assess and modulate DVH parameter restrictions for all structures involved in the treatment plan.

Another method for treatment planning standardization pulls treatment planning parameters such as beam angle, energy, DVH limits etc. from the existing library of clinically accepted plans to automatically create input parameters for a new treatment plan. This method allow the treatment planner to more efficiently set up the baseline treatment parameters from which to further optimize the treatment plan quality.

While these plan standardization and evaluation methods are in the early stages of clinical implementation, current treatment planning software development is rapidly moving towards integrating these tools into standard clinical practice. Minimizing the variability of treatment plans for the same treatment target is expected to lead to better treatment quality for patients by minimizing the influence of human factors on plan quality variance.

6.10 Tumor Dose and OAR Constraints

SBRT is a relatively new treatment concept, which means dose-fractionation schemes are still evolving. Biological effects studies are slowly becoming available as clinical trial results provide more information about complication rates. RTOG

study protocols, AAPM TG-101 [26], QUANTEC [27–30] and an increasing number of peer-reviewed papers are available as clinical guidance to develop dose-fractionation schemes for SRS and SBRT.

In general, dose fractionation schemes for SBRT are adapted based on the position of the tumor relative to OARs. For targets which are isolated deep within a larger organ far away from other OARs, e.g. deep-seated liver lesions or peripheral lung lesions, maximizing the dose gradient to the healthy tissue of the affected organ becomes the planning priority. For targets abutting OARs, e.g. medial lung lesions or most pancreatic tumors, the OAR becomes the dose-limiting constraint in the treatment planning process.

6.10.1 Brain

Dose prescriptions schemes for brain tumors are based on several decades of experience with the Gamma Knife. Dose prescriptions are based on published complication rates based on lesion diameter [31]. The largest lesion diameter considered for SRS is typically 3 cm.

The development of frameless SRS has enabled physicians to develop fractionated treatment courses to alleviate the risk of necrosis associated with high doses in the brain. A special consideration to make when planning SRS to the brain is the fact that many cases are metastatic and therefore have a high probability of returning for further treatment, either to the same lesion or to new lesions. It is therefore advantageous to plan each case with consideration of dose to critical structures such as the lenses of the eyes, the optic chiasm and the brain stem regardless of their proximity, as well as to "normal" brain tissue.

6.10.2 Spine

The utilization of SRS for spine has increased with the implementation of frameless, image-guided SRS techniques [32]. The predominant fractionation scheme is still a single fraction of 10–18 Gy [33–36] although radiobiological considerations of cord tolerance for tumors in close proximity to the spinal cord or invading into the epidural space have led to fractionated treatments of 10 Gy × 3 or 80 Gy × 3. The tumor contour is typically standardized to include the complete vertebral body and the peduncles. The most significant OAR is of course the spinal cord. Contouring, and in consequence DVH constraints, vary between contouring the spinal canal (thecal sac) or the visible cord. Several authors have published retrospective studies on spinal cord tolerance [33, 37–39]; Choi et al. [40] published a study on cord tolerance for SRS in recurrent spinal malignancies.

The Canadian Association of Radiation Oncology (CARO) Stereotactic Body Radiotherapy task force has published guidance recommendations [41] for spine SRS which are listed in Table 6.1.

Table 6.1 CARO recommendations for SRS

Previously irradiated spine mets	35 Gy/5 Fx
Spine mets with no prior radiation	30 Gy/4 fx
Post-op patients (±prior radiation)	24–26 Gy/3 Fx
Selected primary spine tumors	24–26 Gy/2 Fx
No more than three consecutive vertebrae	16–24 Gy/1 Fx

Table 6.2 Dose-fractionation recommendation from selected society recommendations and clinical trials

Target		Source	Dose Rx
Lung	Medically inoperable T1/T2 N0M0 non-small cell	CARO	60 Gy/8 Fx
	Lung mets		50 Gy/5 Fx
	Tumors <5 cm		48 Gy/4 Fx
			54–60 Gy/3 Fx
			34 Gy/1 Fx
	Inoperable stage I/II NSCLC, peripheral lesions	RTOG-0236 (phase II)	60 Gy/3 Fx over 1.5–2 weeks
		RTOG-0618 (phase II)	
	Inoperable stage I/II NSCLC, peripheral lesions	RTOG-0915 (phase II)	34 Gy/1 FX
			Or
			48 Gy/4 Fx (consecutive days)

6.10.3 Lung

The most widely used dose-fractionation scheme of 60 Gy in 3 fractions is based on the RTOG-0236 and RTOG-0618 protocols. These protocols used dose calculation algorithms based on homogeneous tissue models and have been shown to overestimate the dose by approximately 10 % [42]. As a result of these studies, some physicians have advocated using 54 Gy × 3 if inhomogeneity-correcting dose calculation algorithms are used. Other publications have studied outcomes as a function of tumor size, concluding a volume-adaptive dosing for lung SBRT could improve local control [43]. Table 6.2 summarizes selected society and clinical trial recommendations for lung SBRT dose-fractionation.

Pneumonitis is the predominant reported toxicity for lung treatments. Because lung cancer patients are often elderly and have limited lung function, a V20 dose limit of 20 Gy is often used as a hard OAR constraint. Research efforts are underway to distinguish high-functioning from low-functioning lung regions with the goal to steer the OAR dose towards the low-functioning lung regions [44].

An added consideration is the dose delivered to the chest wall. Woody et al. [45] developed a predictive model for different dose-fractionation schemes based on a retrospective data analysis of 102 SBRT patients using a modified EUD model.

6.10.4 Pancreas

SBRT for Pancreas is warranted for resections, locally advanced cases, local recurrences and Oligometastatic Pancreas Cancers. The doses are designed by applying a tolerance-based approach, meaning that the proximity of the lesion within the Pancreases to critical structures, i.e., the stomach and duodenum, governs the total dose (Fig. 6.2) [46].

The liver, kidneys, spinal cord and bowel are among the other dose constraints to consider when planning SBRT to the pancreas.

6.10.5 Liver

SBRT for liver cancer is one of many possible therapeutic options to treat liver malignancies. Therefore, it is not utilized as often as e.g. SBRT for lung lesions. Early dose escalation studies [47–49] confirmed the safety of liver SBRT as non-surgical treatment option. Table 6.3 lists a selection of current society recommendations and clinical trials related to liver SBRT.

6.10.6 Prostate

Prostate SBRT is the most recent development in SBRT targets. The biological characteristics of early-stage prostate cancer require long-term follow-up studies to provide data on local control, late effects, and biochemically disease-free intervals. Because

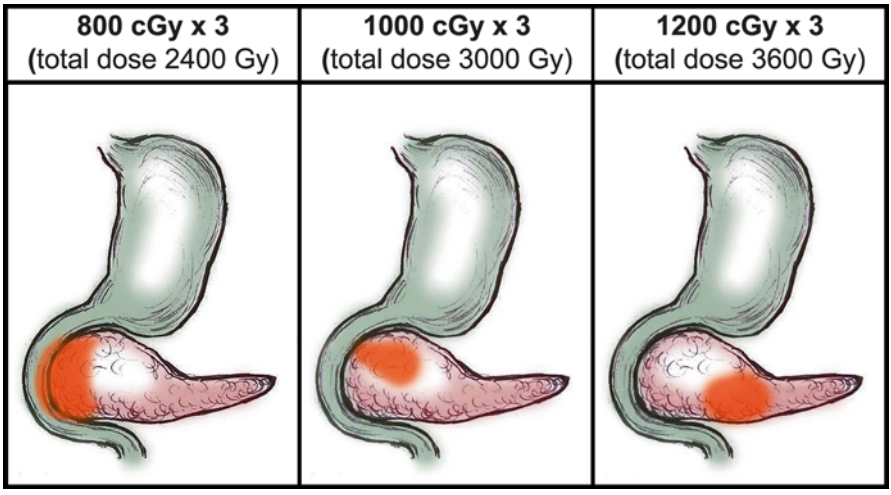

Fig. 6.2 The stomach and duodenum are the contiguous dose-limiting structures and the location of the lesion within the Pancreas dictates which dose scheme to assign (From Mahadevan et al. [46])

Table 6.3 Selected dose/fractionation recommendations for liver based on clinical trials and society recommendations

Hepatocellular CA <8 cm	CARO	42–60 Gy/5 Fx
Liver mets <6 cm and/or ≤5 lesions		50 Gy/5 Fx
		48 Gy/5 fx
		45 Gy/3 Fx
Hepatocellular CA	RTOG-1112 (phase III)	27.5–50 Gy/5 Fx, 24–72 h between Fx

Table 6.4 Typical dose fractionation and dose constraints for early stage low risk prostate cancer

Prostate	7.25 Gy × 5, 3 × per week
	95 % coverage
	5 mm margin (3 mm posterior)
	10 % dose heterogeneity
Rectum	V50 < 50 %
	V20 < 80 %
	V10 < 90 %
	V5 < 100 %

prostate SBRT trails at this point have only relatively short clinical follow-up, it is highly recommended limit the clinical use of this technique on a clinical trial basis. Until results are published, caution is advised in applying dose constraints for prostate SBRT.

There are currently two trials on hypo-fractionated prostate treatments. The major difference between them is that one aims for dose distributions with heterogeneities modeling prostate brachytherapy [50], while the other chooses a homogeneous dose approach [51]. The latter published their early prospective Phase II study results [52] which includes the treatment planning constraints found in Table 6.4.

6.11 Planning in the Presence of Respiratory Motion and Deformation

Three common sites treated with SBRT are lung, liver and pancreas. In all three cases, respiratory motion can be significant. Larger tumors in the lung and liver also undergo deformation throughout the respiratory cycle. Accounting for respiratory motion and deformation in treatment planning strongly depends on the availability of 4D imaging studies, the respiratory motion compensation method chosen for treatment delivery, and individual patient considerations.

6.11.1 Imaging and Image Fusion for Planning

4D CT in planning is most commonly used to determine a gating window, and create an ITV (Internal Target Volume) based on the width of the gating window chosen for a particular patient. If compression is used to manage respiratory motion, the

4D CT can be used to generate a MIP image which determines the residual motion to be covered by the ITV.

If the treatment delivery system is capable of tumor and/or fiducial tracking instead of compression, breath-hold or gating, there are several additional issues to assess in the planning phase: deformation, rotation, and the relative position of the tumor to the OARs. Deformation and rotation margins can be determined by fusing the tumor center of mass in different respiratory phases and determining the ITV. The relative position of tumor to critical organs is much more difficult to assess with current technology. Deformable image registration algorithms have very limited suitability for this task, because relative voxel motion is not based on anatomically correct modeling of tissue motion.

6.11.2 Relative Motion of Tumor to OAR

Relative motion of tumor and OAR is a concern for pancreas and liver targets because of the proximity to critical structures such as the stomach, esophagus and duodenum. Prostate motion is driven by bladder filling and bowel gas. While the bladder filling may cause a baseline shift, fast delivery techniques have lessened these concerns. Bowel gas, on the other hand, causes a transient shift of organs relative to each other and should be considered during treatment planning. Relative motion of tumor to OARs caused by periodic motion such as respiratory motion may, in the future, be modeled by a combination of 4D imaging and deformable image registration. 4D planning could be a tool to optimize the treatment plan toward robustness in the presence of respiratory motions. It must be emphasized that at this time, research on this topic is not ready for clinical implementation. On the contrary, data has shown [53, 54] that 4DCT motion patterns determined at simulation may deviate significantly from 4D motion patterns observed during treatment.

6.11.3 Margin Determination

ICRU Report 62 defines an ITV and IM (Internal Margin) to account for physiologic variations in the position and shape of the CTV (Clinical Tumor Volume.) The SM (Setup Margin) is added to account for uncertainties in patient positioning.

An concept that is very helpful for SBRT planning, especially when steep dose gradients near OARs are present, is the PRV (Planning Organ at Risk) volume. The PRV is designed based on how much the organ at risk may move relative to the setup and systematic uncertainties at isocenter. Figure 6.3 shows an example of a head & neck treatment plan in which a PRV (yellow) is added to the spinal cord (dark blue) contour. The isocenter for this large treatment area, which includes three PTVs, is more than 10 cm away from the cord at this location.

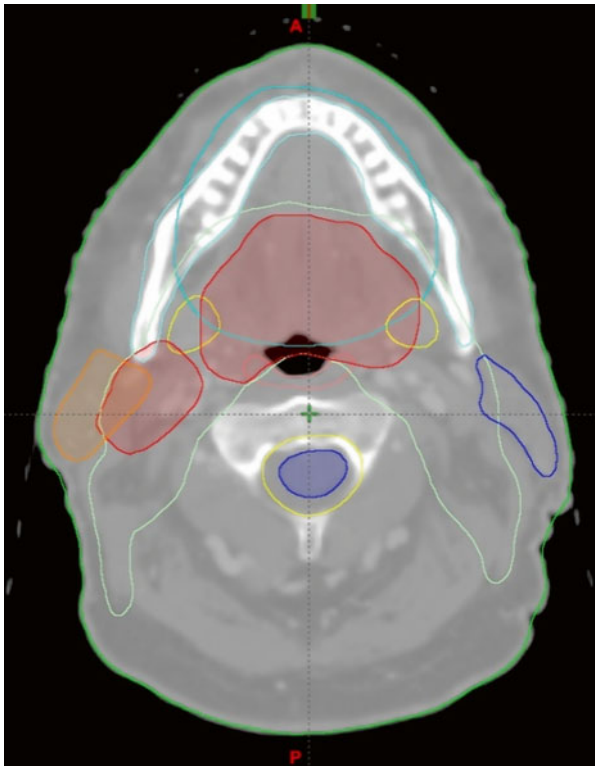

Fig. 6.3 Cord PRV (*yellow*) around the spinal cord (*dark blue*) to account for setup variations

ICRU report 83 updated ICRU report 62 on how to create nomenclature for adaptive treatment planning. Instead of including physiological changes in tumor shape or contouring uncertainties in the ITV, the recommendation is to account for those in the PTV. For clarity, the use of an ITV is optional, being most useful to define positional changes due to internal motion such as respiration. The report emphasizes that the PTV margin *should not be compromised* when overlapping with, or being close to, an OAR.

Margin determination is dependent on the clinical process specific to an individual clinic. This includes the types of image guidance and setup devices employed, and the technical skill of the staff. Ideally, each clinic should carefully analyze their uncertainties to define appropriate margins. The assumption in the development of margin recipes is that the data distribution is Gaussian, and uncertainties will accumulate over a large number of fractions. This assumption does not hold for the hypo-fractionated regimens used in SBRT. Until margins specific to for SBRT are studied, the implicit assumption is that high-level image guidance will offset the potential failure for uncertainties. Herschtal et al. [55] published a Monte Carlo study simulating patient motion during SBRT based on sets of systematic and random uncertainties, using existing margin recipes as boundary conditions. The paper demonstrates that larger PTV margins are needed for hypofractionation vs. regular fractionation given the same uncertainties.

6.12 Dosimetry

Stereotactic Radiosurgery is characterized by the use of very small fields and a high number of monitor units. Detectors that are appropriate for dosimetry in larger fields are generally not appropriate for performing dosimetry under stereotactic conditions. Therefore, familiarity with the appropriate use of small detectors, small-field measurement techniques and reference dosimetry protocols are all essential to ensure safe treatments. The accuracy of dose calculation algorithms in the presence of inhomogeneities for SBRT is becoming equally important as the spatial dose delivery accuracy. For accelerator-based SRS/SBRT, dose from scatter and leakage as well as imaging needs to be taken into consideration.

6.12.1 Reference and Relative Dosimetry

The reference dosimetry method of choice depends on the method of treatment delivery. Alfonso et al. [56] have developed a framework for reference dosimetry depending on the availability of a 10×10 cm reference field, or a machine specific reference field.

If a 10×10 cm reference field is available, i.e. for all linac-based SRS treatments, AAPM TG-51 [57] or IAEA Report TRS- 398 [58] should be used for reference dosimetry. For CyberKnife and Tomotherapy, AAPM TG-135 [59] and AAPM TG-148 [60] provide guidance on the currently accepted methods using the machine-specific reference field method for either device. More recently, data on k_Q detector correction factors for non-standard beams are becoming available. E.g. for Tomotherapy, Gago-Arias et al. [61] have calculated a 2 % correction for the A1SL chamber, which agrees with an observed 2 % systematic deviation of absolute dose in beam data measurements taken by the IROC QA Center Houston.

It cannot be over-emphasized that the reference dosimetry must be verified by an independent means of measurement *before* any patient is treated on the machine. The optimum solution is to use an external calibration program, e.g. the IAEA TLD program or, in the United States, the services provided by the ADCL laboratories. A peer-review process in which an outside qualified medical physicist verifies the reference dosimetry is acceptable in situations where independent dosimetry labs are not available.

For relative dosimetry, the output factor measurements for small fields need to be corrected based on the detector used. Ideally, two independent, peer-reviewed publications would be available for each detector/beam combination to determine an average correction factor. In the absence of two independent calculation, the recommended approach is to measure output factors with two different detectors using their respective correction factors, and average the result.

Beams used for SRS/SBRT treatments are small, and therefore dominated by the penumbra region. An accurate measurement of the beam penumbra is therefore necessary to correctly model the dose gradient from tumor to OAR. If a detector

with dimensions too large relative to the penumbra is used, the volume-averaging effect would lead to a flattening of the penumbra [62]. Therefore, the recommended maximum beam diameter to detector size ratio is 3:1.

6.12.2 Scatter, Leakage and Imaging Dose

Scatter, leakage and imaging dose are highly device-specific [63] and usually not accounted for in the treatment planning process. While not the highest priority, a good planner will use techniques to minimize additional whole-body dose to the patient, following the ALARA approach to radiation safety. Scatter and leakage dose are dependent on the ratio of MU to delivered dose. A skilled planner will be able to limit the number of MU used to achieve the planning constraints without affecting plan quality. Selected treatment planning software has built-in tools to optimize (minimize) the MU after initial planning optimization.

Several modern delivery systems are capable of intra-fraction imaging while other techniques allow treatment interruption and re-imaging if the patient has moved significantly from the original setup position. Imaging dose from either technique can be minimized by keeping treatment times as short as possible [5, 7, 8, 26], and adjusting imaging techniques to lower dose. Non-ionizing imaging techniques have been implemented for cranial SRS and demonstrated to be safe [64, 65].

6.12.3 Patient-Specific Dosimetry Measurements

The challenges of reference dosimetry, beam data commissioning, accurate dose calculation and complex technologies make it essential to develop a quality assurance program for patient-specific delivery QA (DQA). Whenever a new technology or a new procedure is implemented into clinical use, DQA measurements should be performed to verify the accuracy and quality of the treatment process using an end-to-end QA method [66].

Considering the high dose gradients present in SRS/SBRT, it is not advised to simply apply DQA methods used in IMRT. For example, Fig. 6.4 shows a typical SRS plan for a previously irradiated spine lesion in which the PTV is treated to 16 Gy while the cord is limited to 12 Gy. In this particular case, a dose gradient of 1 Gy/mm is achieved between the PTV and cord. If typical IMRT QA criteria of 3 %/3 mm for Gamma, or 3 mm criteria for distance to agreement (DTA) were to be used, a shift of the dose distribution of 2.9 mm in the posterior direction would pass QA. This shift would then deliver 15 Gy to the cord, significantly increasing the risk of serious complications for the patient. Therefore, any patient-specific QA measurement method used to measure delivery accuracy for this plan will need to be much more accurate than 3 mm DTA or 3 %/3 mm Gamma; ideally, the measurement method should be able to measure DTA to better than 1.5 mm.

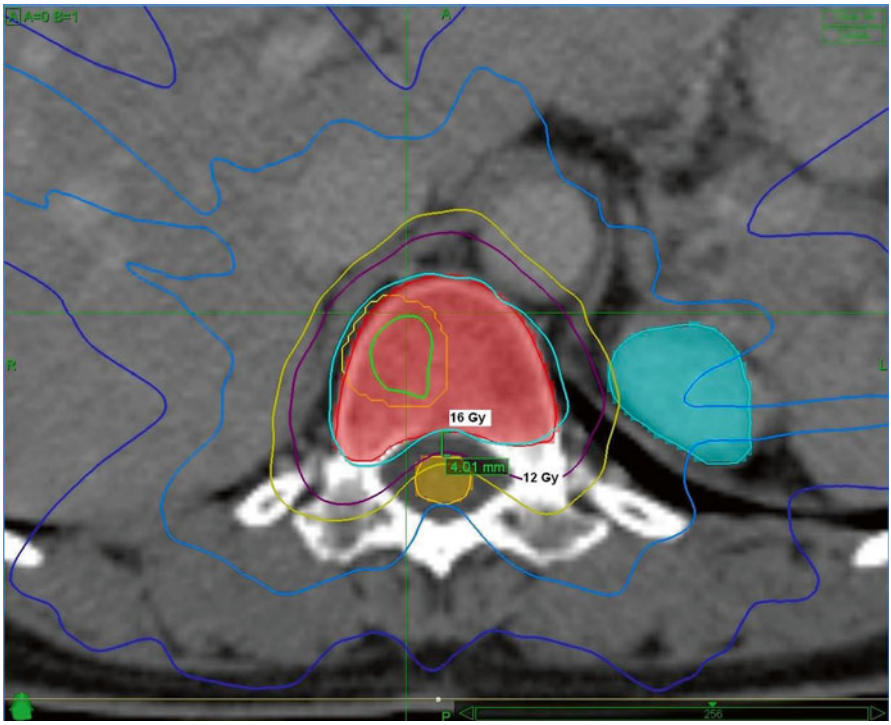

Fig. 6.4 Dose gradient for a typical spine SRS plan. (CyberKnife G4 treatment unit and MultiPlan 3.5 planning system)

Meaningful patient-specific QA measurements get even more challenging for treatment plans used in functional diseases such as trigeminal neuralgia. Figure 6.5 shows a treatment plan used in trigeminal neuralgia with a dose gradient of 16 Gy/mm from the nerve root toward the brainstem. The accuracy required to do appropriate DQA for these plans meets or exceeds the current technical capabilities of high spatial resolution DQA methods such as film or gels. Therefore, very stringent technical machine and planning system QA must be integrated with the currently most accurate available DQA method to ensure patient safety.

6.13 Summary

At first impression, treatment planning for SBRT might not seem to be significantly different than treatment planning for conventionally fractionated treatments; however, the combination of high dose per fraction and steep dose gradients require high performance standards for dosimetry, planning system accuracy and plan robustness. The high impact of planning errors which might pass quality control

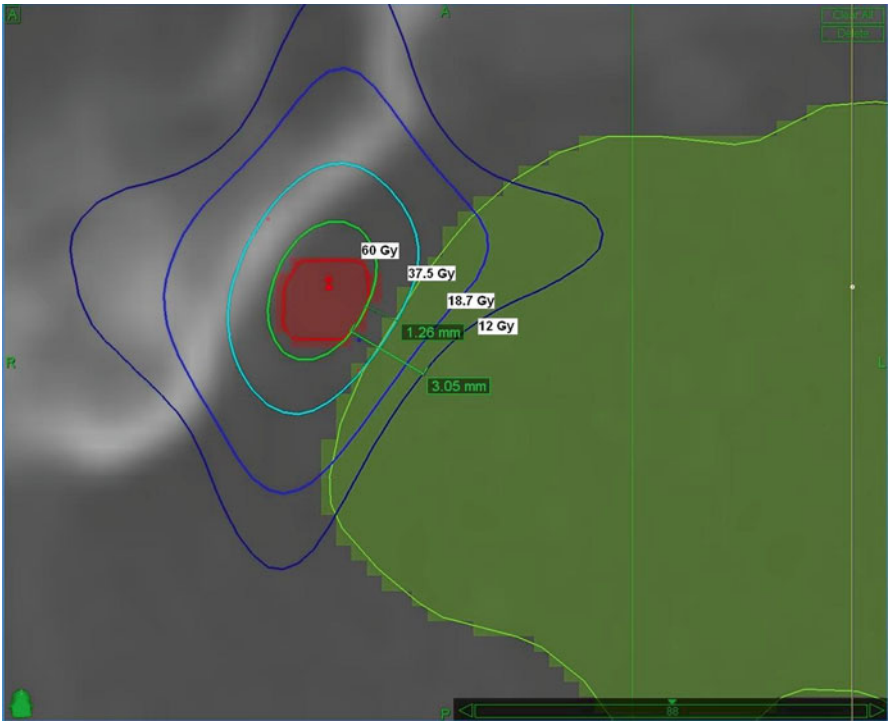

Fig. 6.5 Treatment plan for trigeminal neuralgia

undetected necessitates achieving the highest possible standard in error prevention. The treatment planner should therefore be able to identify potential errors, deviations from standard or high-risk situations quickly. SBRT is a relatively new treatment modality for which dose/fractionation schemes and OAR dose limits are still evolving. Treatment planning systems are also still evolving toward implementing tools for standardization of workflow and implementation of class solutions. As technological standards evolve, the treatment planning team must participate in continuing education to achieve the optimum plan quality for patients.

References

1. Schlaefer A, Schweikard A. Stepwise multi-criteria optimization for robotic radiosurgery. Med Phys. 2008;35(5):2094–103. PubMed PMID: 18561685. Epub 2008/06/20. eng.
2. Lax I. Target dose versus extratarget dose in stereotactic radiosurgery. Acta Oncol. 1993;32(4):453–7. PubMed PMID: 8369134. Epub 1993/01/01. eng.
3. Hoppe BS, Laser B, Kowalski AV, Fontenla SC, Pena-Greenberg E, Yorke ED, et al. Acute skin toxicity following stereotactic body radiation therapy for stage I non-small-cell lung cancer: who's at risk? Int J Radiat Oncol Biol Phys. 2008;72(5):1283–6.

4. Knöös T, Kristensen I, Nilsson P. Volumetric and dosimetric evaluation of radiation treatment plans: radiation conformity index. Int J Radiat Oncol Biol Phys. 1998;42(5):1169–76.
5. Fürweger C, Drexler C, Kufeld M, Muacevic A, Wowra B, Schlaefer A. Patient motion and targeting accuracy in robotic spinal radiosurgery: 260 single-fraction fiducial-free cases. Int J Radiat Oncol Biol Phys. 2010;78(3):937–45.
6. Murphy MJ. Intrafraction geometric uncertainties in frameless image-guided radiosurgery. Int J Radiat Oncol Biol Phys. 2009;73(5):1364–8.
7. Murphy MJ, Chang SD, Gibbs IC, Le QT, Hai J, Kim D, et al. Patterns of patient movement during frameless image-guided radiosurgery. Int J Radiat Oncol Biol Phys. 2003;55(5):1400–8. PubMed PMID: 12654453.
8. Willoughby TR, Kupelian PA, Pouliot J, Shinohara K, Aubin M, Roach 3rd M, et al. Target localization and real-time tracking using the Calypso 4D localization system in patients with localized prostate cancer. Int J Radiat Oncol Biol Phys. 2006;65(2):528–34. PubMed PMID: 16690435. Epub 2006/05/13. eng.
9. Wagner TH, Yi T, Meeks SL, Bova FJ, Brechner BL, Chen Y, et al. A geometrically based method for automated radiosurgery planning. Int J Radiat Oncol Biol Phys. 2000;48(5):1599–611.
10. Keall PJ, Colvill E, O'Brien R, Ng JA, Poulsen PR, Eade T, et al. The first clinical implementation of electromagnetic transponder-guided MLC tracking. Med Phys. 2014;41(2):020702.
11. Schweikard A, Shiomi H, Adler J. Respiration tracking in radiosurgery. Med Phys. 2004;31(10):2738–41. PubMed PMID: 15543778.
12. Wilcox EE, Daskalov GM, Lincoln H, Shumway RC, Kaplan BM, Colasanto JM. Comparison of planned dose distributions calculated by Monte Carlo and Ray-Trace algorithms for the treatment of lung tumors with CyberKnife: a preliminary study in 33 patients. Int J Radiat Oncol Biol Phys. 2009;77:277–84. PubMed PMID: 20004530. Epub 2009/12/17. Eng.
13. Deng J, Guerrero T, Ma CM, Nath R. Modelling 6 MV photon beams of a stereotactic radiosurgery system for Monte Carlo treatment planning. Phys Med Biol. 2004;49(9):1689–704. PubMed PMID: 15152924. Epub 2004/05/22. eng.
14. Deng J, Ma CM, Hai J, Nath R. Commissioning 6 MV photon beams of a stereotactic radiosurgery system for Monte Carlo treatment planning. Med Phys. 2003;30(12):3124–34. PubMed PMID: 14713079. Epub 2004/01/10. eng.
15. Davidson SE, Popple RA, Ibbott GS, Followill DS. Technical note: heterogeneity dose calculation accuracy in IMRT: study of five commercial treatment planning systems using an anthropomorphic thorax phantom. Med Phys. 2008;35(12):5434–9. PubMed PMID: 19175103. Pubmed Central PMCID: 2736720. Epub 2009/01/30. eng.
16. Van Esch A, Tillikainen L, Pyykkonen J, Tenhunen M, Helminen H, Siljamaki S, et al. Testing of the analytical anisotropic algorithm for photon dose calculation. Med Phys. 2006;33(11):4130–48. PubMed PMID: 17153392.
17. Fogliata A, Nicolini G, Clivio A, Vanetti E, Cozzi L. Accuracy of Acuros XB and AAA dose calculation for small fields with reference to RapidArc((R)) stereotactic treatments. Med Phys. 2011;38(11):6228–37. PubMed PMID: 22047388.
18. Krings T, Mull M, Gilsbach JM, Thron A. Spinal vascular malformations. Eur Radiol. 2005;15(2):267–78. PubMed PMID: 15538580. Epub 2004/11/13. eng.
19. Galván de la Cruz OO, Lárraga-Gutiérrez JM, Moreno-Jiménez S, García-Garduño OA, Celis MA. Effect of the embolization material in the dose calculation for stereotactic radiosurgery of arteriovenous malformations. Med Dosim. 2013;38(2):110–4.
20. Atwood TF, Hsu A, Ogara MM, Luba DG, Tamler BJ, DiSario JA, et al. Radiotherapy dose perturbation of esophageal stents examined in an experimental model. Int J Radiat Oncol Biol Phys. 2011;82:1659–64.
21. Cheung JY, Yu KN, Chan JF, Ho RT, Yu CP. Dose distribution close to metal implants in Gamma Knife Radiosurgery: a Monte Carlo study. Med Phys. 2003;30(7):1812–5. PubMed PMID: 12906199. Epub 2003/08/09. eng.
22. Kleinerman RA, Smith SA, Holowaty E, Hall P, Pukkala E, Vaalavirta L, et al. Radiation dose and subsequent risk for stomach cancer in long-term survivors of cervical cancer. Int J Radiat

Oncol Biol Phys. 2013;86(5):922–9. PubMed PMID: 23707149. Pubmed Central PMCID: PMC3831516. eng.
23. Moore KL, Brame RS, Low DA, Mutic S. Experience-based quality control of clinical intensity-modulated radiotherapy planning. Int J Radiat Oncol Biol Phys. 2011;81(2):545–51. PubMed PMID: 21277097.
24. Moore KL, Brame RS, Low DA, Mutic S. Quantitative metrics for assessing plan quality. Semin Radiat Oncol. 2012;22(1):62–9.
25. Monz M, Küfer K, Bortfeld T, Thieke C. Pareto navigation—algorithmic foundation of interactive multi-criteria IMRT planning. Phys Med Biol. 2008;53(4):985.
26. Benedict SH, Yenice KM, Followill D, Galvin JM, Hinson W, Kavanagh B, et al. Stereotactic body radiation therapy: the report of AAPM Task Group 101. Med Phys. 2010;37(8):4078–101. PubMed PMID: 20879569. Epub 2010/10/01. eng.
27. Kavanagh BD, Pan CC, Dawson LA, Das SK, Li XA, Ten Haken RK, et al. Radiation dose–volume effects in the stomach and small bowel. Int J Radiat Oncol Biol Phys. 2010;76(3):S101–7.
28. Kirkpatrick JP, van der Kogel AJ, Schultheiss TE. Radiation dose–volume effects in the spinal cord. Int J Radiat Oncol Biol Phys. 2010;76(3):S42–9.
29. Marks LB, Bentzen SM, Deasy JO, Kong F-MS, Bradley JD, Vogelius IS, et al. Radiation dose–volume effects in the lung. Int J Radiat Oncol Biol Phys. 2010;76(3):S70–6.
30. Marks LB, Yorke ED, Jackson A, Ten Haken RK, Constine LS, Eisbruch A, et al. Use of normal tissue complication probability models in the clinic. Int J Radiat Oncol Biol Phys. 2010;76(3):S10–9.
31. Flickinger JC, Schell MC, Larson DA. Estimation of complications for linear accelerator radiosurgery with the integrated logistic formula. Int J Radiat Oncol Biol Phys. 1990;19(1):143–8.
32. Hsu W, Nguyen T, Kleinberg L, Ford EC, Rigamonti D, Gokaslan ZL, et al. Stereotactic radiosurgery for spine tumors: review of current literature. Stereotact Funct Neurosurg. 2010;88(5):315–21. PubMed PMID: 20714211. Epub 2010/08/18. Eng.
33. Schipani S, Wen W, Jin J-Y, Kim JK, Ryu S. Spine radiosurgery: a dosimetric analysis in 124 patients who received 18 Gy. Int J Radiat Oncol Biol Phys. 2012;84(5):e571–6.
34. Shin DA, Huh R, Chung SS, Rock J, Ryu S. Stereotactic spine radiosurgery for intradural and intramedullary metastasis. Neurosurg Focus. 2009;27(6):E10. PubMed PMID: 19951053.
35. Ryu S, Jin R, Jin J-Y, Chen Q, Rock J, Anderson J, et al. Pain control by image-guided radiosurgery for solitary spinal metastasis. J Pain Symptom Manage. 2008;35(3):292–8. PubMed PMID: 18215498.
36. Gerszten PC, Burton SA, Ozhasoglu C, Welch WC. Radiosurgery for spinal metastases: clinical experience in 500 cases from a single institution. Spine. 2007;32(2):193–9. PubMed PMID: 17224814.
37. Daly ME, Choi CYH, Gibbs IC, Adler Jr JR, Chang SD, Lieberson RE, et al. Tolerance of the spinal cord to stereotactic radiosurgery: insights from hemangioblastomas. Int J Radiat Oncol Biol Phys. 2011;80(1):213–20.
38. Medin PM, Boike TP. Spinal cord tolerance in the age of spinal radiosurgery: lessons from preclinical studies. Int J Radiat Oncol Biol Phys. 2011;79(5):1302–9.
39. Sahgal A, Ma L, Gibbs I, Gerszten PC, Ryu S, Soltys S, et al. Spinal cord tolerance for stereotactic body radiotherapy. Int J Radiat Oncol Biol Phys. 2010;77(2):548–53.
40. Choi CYH, Adler JR, Gibbs IC, Chang SD, Jackson PS, Minn AY, et al. Stereotactic radiosurgery for treatment of spinal metastases recurring in close proximity to previously irradiated spinal cord. Int J Radiat Oncol Biol Phys. 2010;78(2):499–506. PubMed PMID: 20133079.
41. Sahgal A, Roberge D, Schellenberg D, Purdie TG, Swaminath A, Pantarotto J, et al. The Canadian Association of Radiation Oncology scope of practice guidelines for lung, liver and spine stereotactic body radiotherapy. Clin Oncol. 2012;24(9):629–39. PubMed PMID: 22633542.
42. Trakul N, Harris JP, Le Q-T, Hara WY, Maxim PG, Loo Jr BW, et al. Stereotactic ablative radiotherapy for reirradiation of locally recurrent lung tumors. J Thorac Oncol. 2012;7(9):1462–5.
43. Trakul N, Chang CN, Harris J, Chapman C, Rao A, Shen J, et al. Tumor volume-adapted dosing in stereotactic ablative radiotherapy of lung tumors. Int J Radiat Oncol Biol Phys. 2012;84(1):231–7. PubMed PMID: 22381907.

44. Yamamoto T, Kabus S, Von Berg J, Lorenz C, Keall PJ. Impact of four-dimensional computed tomography pulmonary ventilation imaging-based functional avoidance for lung cancer radiotherapy. Int J Radiat Oncol Biol Phys. 2011;79(1):279–88.
45. Woody NM, Videtic GM, Stephans KL, Djemil T, Kim Y, Xia P. Predicting chest wall pain from lung stereotactic body radiotherapy for different fractionation schemes. Int J Radiat Oncol Biol Phys. 2011;83:427–34. PubMed PMID: 22197087. Epub 2011/12/27. Eng.
46. Mahadevan A, Jain S, Goldstein M, Miksad R, Pleskow D, Sawhney M, et al. Stereotactic body radiotherapy and gemcitabine for locally advanced pancreatic cancer. Int J Radiat Oncol Biol Phys. 2010;78(3):735–42.
47. Goodman KA, Wiegner EA, Maturen KE, Zhang Z, Mo Q, Yang G, et al. Dose-escalation study of single-fraction stereotactic body radiotherapy for liver malignancies. Int J Radiat Oncol Biol Phys. 2010;78(2):486–93. PubMed PMID: 20350791.
48. Schefter TE, Kavanagh BD, Timmerman RD, Cardenes HR, Baron A, Gaspar LE. A phase I trial of stereotactic body radiation therapy (SBRT) for liver metastases. Int J Radiat Oncol Biol Phys. 2005;62(5):1371–8.
49. Rusthoven KE, Kavanagh BD, Cardenes H, Stieber VW, Burri SH, Feigenberg SJ, et al. Multi-institutional phase I/II trial of stereotactic body radiation therapy for liver metastases. J Clin Oncol. 2009;27(10):1572–8.
50. Fuller DB, Naitoh J, Lee C, Hardy S, Jin H. Virtual HDR ^{SM} CyberKnife treatment for localized prostatic carcinoma: dosimetry comparison with HDR brachytherapy and preliminary clinical observations. Int J Radiat Oncol Biol Phys. 2008;70(5):1588–97.
51. King CR, Brooks JD, Gill H, Pawlicki T, Cotrutz C, Presti Jr JC. Stereotactic body radiotherapy for localized prostate cancer: interim results of a prospective phase II clinical trial. Int J Radiat Oncol Biol Phys. 2009;73(4):1043–8.
52. Wiegner EA, King CR. Sexual function after stereotactic body radiotherapy for prostate cancer: results of a prospective clinical trial. Int J Radiat Oncol Biol Phys. 2010;78(2):442–8.
53. Minn AY, Schellenberg D, Maxim P, Suh Y, McKenna S, Cox B, et al. Pancreatic tumor motion on a single planning 4D-CT does not correlate with intrafraction tumor motion during treatment. Am J Clin Oncol. 2009;32:364–8. PubMed PMID: 19398901. Epub 2009/04/29. Eng.
54. Velec M, Moseley JL, Eccles CL, Craig T, Sharpe MB, Dawson LA, et al. Effect of breathing motion on radiotherapy dose accumulation in the abdomen using deformable registration. Int J Radiat Oncol Biol Phys. 2011;80(1):265–72.
55. Herschtal A, Foroudi F, Silva L, Gill S, Kron T. Calculating geometrical margins for hypofractionated radiotherapy. Phys Med Biol. 2013;58(2):319–33. PubMed PMID: 23257319.
56. Alfonso R, Andreo P, Capote R, Huq MS, Kilby W, Kjall P, et al. A new formalism for reference dosimetry of small and nonstandard fields. Med Phys. 2008;35(11):5179–86. PubMed PMID: 19070252. Epub 2008/12/17. eng.
57. Almond PR, Biggs PJ, Coursey BM, Hanson WF, Huq MS, Nath R, et al. AAPM's TG-51 protocol for clinical reference dosimetry of high-energy photon and electron beams. Med Phys. 1999;26(9):1847–70. PubMed PMID: 10505874.
58. Pedro Andreo DTB, Klaus H, Saiful Huq M, Tatsuaki K, Fedele L, Vere S, Stefaan V. Absorbed dose determination in external beam radiotherapy: an international code of practice for dosimetry based on standards of absorbed dose to water. Vienna: IAEA; 2000. TRS-398.
59. Dieterich S, Cavedon C, Chuang CF, Cohen AB, Garrett JA, Lee CL, et al. Report of AAPM TG 135: quality assurance for robotic radiosurgery. Med Phys. 2011;38(6):2914–36. PubMed PMID: 21815366. Epub 2011/08/06. eng.
60. Langen KM, Papanikolaou N, Balog J, Crilly R, Followill D, Goddu SM, et al. QA for helical tomotherapy: report of the AAPM Task Group 148. Med Phys. 2010;37(9):4817–53. PubMed PMID: 20964201. Epub 2010/10/23. eng.
61. Gago-Arias A, Rodríguez-Romero R, Sánchez-Rubio P, González-Castaño DM, Gómez F, Núñez L, et al. Correction factors for A1SL ionization chamber dosimetry in TomoTherapy: machine-specific, plan-class, and clinical fields. Med Phys. 2012;39(4):1964–70.

62. Bassinet C, Huet C, Derreumaux S, Brunet G, Chéa M, Baumann M, et al. Small fields output factors measurements and correction factors determination for several detectors for a CyberKnife® and linear accelerators equipped with microMLC and circular cones. Med Phys. 2013;40(7).
63. Di Betta E, Fariselli L, Bergantin A, Locatelli F, Del Vecchio A, Broggi S, et al. Evaluation of peripheral dose in stereotactic radiotherapy and radiosurgery treatments. Med Phys. 2010;37(7):3587–94. PubMed PMID: 20831066. Pubmed Central PMCID: 2902541.
64. Cerviño LI, Detorie N, Taylor M, Lawson JD, Harry T, Murphy KT, et al. Initial clinical experience with a frameless and maskless stereotactic radiosurgery treatment. Pract Radiat Oncol. 2012;2(1):54–62.
65. Pan H, Cerviño LI, Pawlicki T, Jiang SB, Alksne J, Detorie N, et al. Frameless, real-time, surface imaging-guided radiosurgery: clinical outcomes for brain metastases. Neurosurgery. 2012;71(4):844–52.
66. Wang L, Kielar KN, Mok E, Hsu A, Dieterich S, Xing L. An end-to-end examination of geometric accuracy of IGRT using a new digital accelerator equipped with onboard imaging system. Phys Med Biol. 2012;57(3):757–69. PubMed PMID: 22252134.

Chapter 7
Spinal Radiosurgery

Iris C. Gibbs, Banu Atalar, and Lei Wang

Abstract Spinal radiosurgery has proven to be not only technically feasible, but efficacious for local control and pain relief of spinal metastases and benign spinal lesions. Due to the proximity of the target tumors in relation to the spinal cord and the high stakes associated with radiation injury of the spinal cord, spinal radiosurgery requires even more accuracy than other applications of stereotactic body radiation. Exquisite care must be taken to ensure appropriate target delineation and avoidance of normal tissue damage. Fortunately, guidelines for normal tissue constraints have been useful to keep the risk of myelopathy low. Recent studies have also explored predictive factors for the complication of vertebral compression fracture.

Keywords Spinal radiosurgery • Spinal metastasis • Vertebral metastasis • Spinal meningioma • Spinal schwannoma • Spinal arteriovenous malformations • Vertebral compression fracture • Myelopathy • Spinal cord injury

7.1 Introduction

In 1995, Hamilton and Lulu at the University of Arizona published the first studies of spinal radiosurgery. Using a rigid skeletal fixation device applied intraoperatively, conformal radiation treatment was delivered stereotactically on a linear accelerator after the patient was transported to the radiotherapy department under anesthesia [1]. Though this technique proved to be impractical and was ultimately supplanted by other minimally invasive approaches for routine stereotactic radiation, it established the foundations for spinal radiosurgery. In 1996 at Stanford

I.C. Gibbs, MD (✉)
Department of Radiation Oncology, Stanford University, Stanford, CA, USA
e-mail: iris.gibbs@stanford.edu

B. Atalar, MD
Department of Radiation Oncology, Acibadem University, Istanbul, Turkey

L. Wang, PhD
Radiation Oncology Department, Stanford University Medical School, Palo Alto, CA, USA

A. Gaya, A. Mahadevan (eds.), *Stereotactic Body Radiotherapy: A Practical Guide*,
DOI 10.1007/978-0-85729-597-2_7

University, the first spinal lesion was treated using a robotic image-guided radiosurgery system prototype of what later became commercialized as the Cyberknife (Accuray, Inc., Sunnyvale, CA) radiosurgical system [2]. Since that time, the feasibility, safety, and efficacy of radiosurgery (also referred to as stereotactic body radiotherapy or SBRT) for spinal lesions using a variety of modified LINAC systems has been established [3–8] while the most common indication for spinal radiosurgery is spinal metastases, other spinal conditions including benign extramedullary tumors, paraspinal tumors, spinal arteriovenous malformations, and intramedullary tumors have been successfully treated with stereotactic techniques. Over nearly the past two decades, investigators have worked to establish improved understanding of the tolerance of the human spinal cord to the relatively large doses per fraction used for stereotactic radiosurgery.

7.2 Case Histories

7.2.1 Case 1

An 81-year-old man with painful spinal metastases at T6 and T7 of metastatic melanoma with known pulmonary, bony, and brain metastases at diagnosis. Both the T6 and T7 lesions were treated with radiosurgery to 20 Gy in 1 fraction to the 75 % isodose line; target volumes were 3.043 and 3.091 cubic cm, respectively. As the lesions were in adjacent levels, and involved a portion of the vertebral body without extending into the pedicle or paraspinal soft tissues, the lesion only was treated. Alternatively, the entire vertebral body or the lesion plus the ipsilateral pedicle with margin up to 2–3 mm would be acceptable. During the treatment planning process, critical structures including the esophagus and spinal cord were identified and contoured. Both organs were satisfactorily protected with dose constraints well within current guidelines; the maximum esophageal dose was 10 Gy and the maximum spinal cord dose 12.2 Gy. As the target lesion involves the thoracic spine where there are interfaces between air in the lung, soft tissue, and bone, dose calculation using a more sophisticated algorithm such as convolution/superposition or Monte Carlo should be considered. In this particular, case, however, there was not a significant dosimetric effect (Fig. 7.1).

7.2.2 Case 2

A 50-year-old man with metastatic malignant peripheral nerve sheath tumor who developed two separate areas of vertebral column tumor spread; T5–6 and T12. Multi-modality treatment was employed in this case. As the patient presented with symptomatic spinal cord compression resulting from the T5–6 lesion, he underwent laminectomy and resection at this site with spinal instrumentation. The unresected

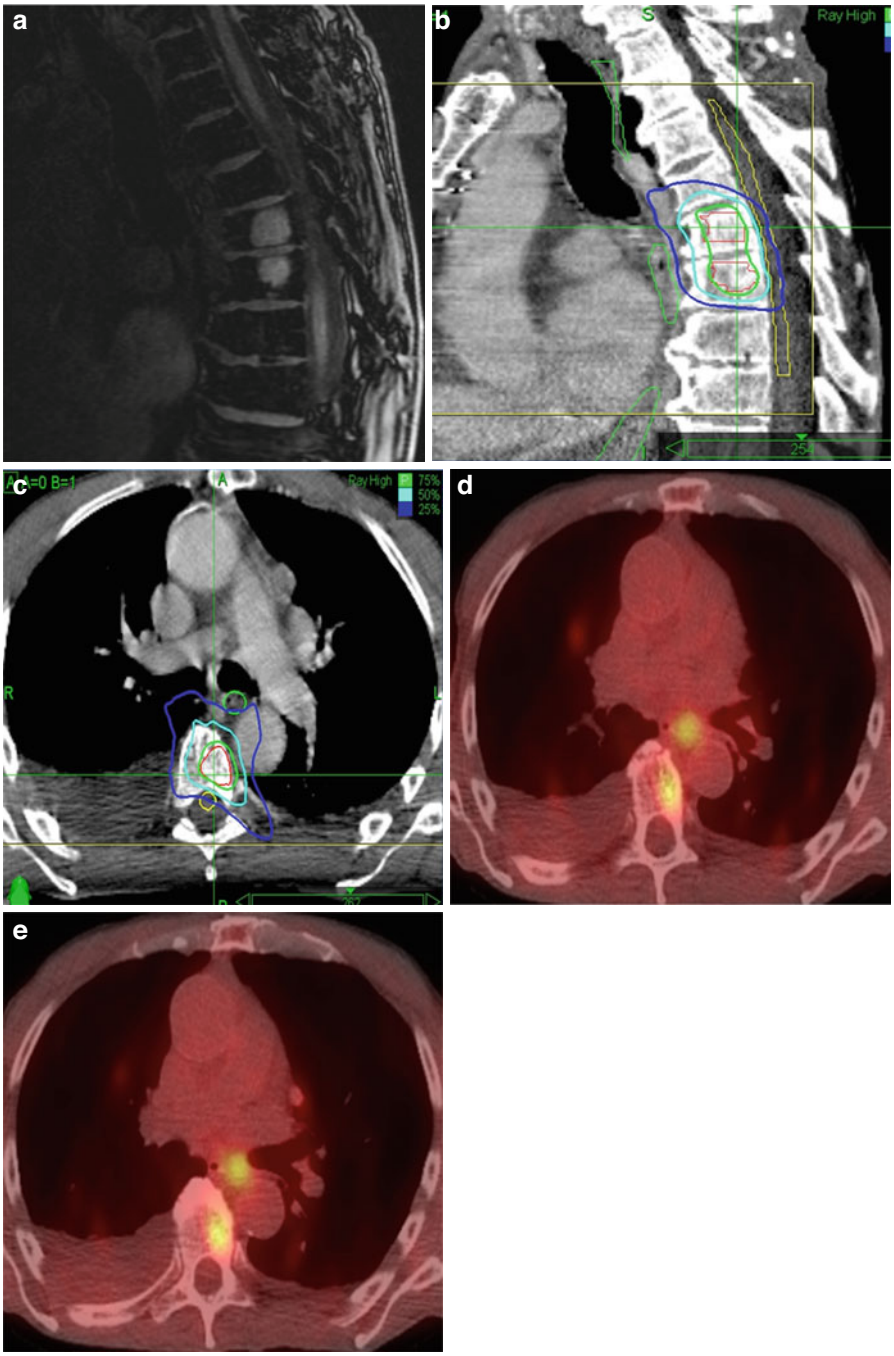

Fig. 7.1 A 81 year old man with painful spine metastases at T6 and T7 of metastatic melanoma as demonstrated on sagittal MRI (**a**) and sagittal CT treatment plan (**b**). Axial treatment plan for T6 (**c**) outlined in *red* with each target treated to 20 Gy in 1 fraction the 75 % isodose line (ISL) shown in *green* with 50 % ISL in cyan and 25 % ISL in *blue*. Target volumes: 3.043 and 3.091 cm^3. Maximum spinal cord dose 12.2 Gy. Maximum esophagus dose 10 Gy. Axial PET/CT images for each lesion (**d**, **e**)

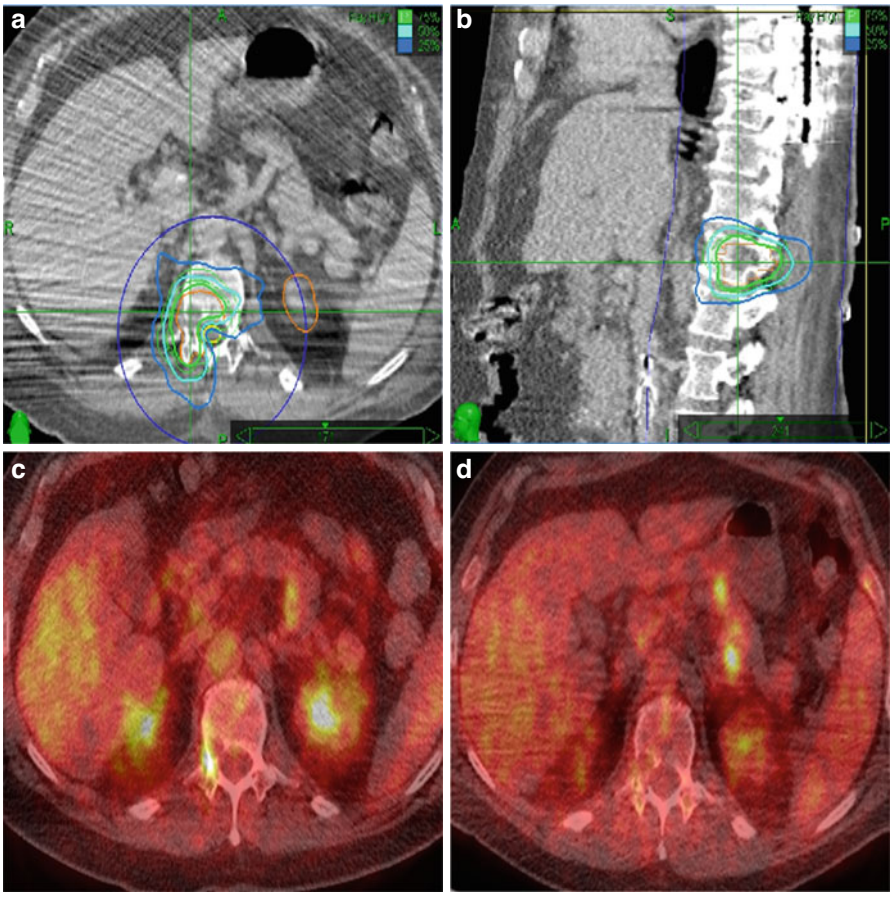

Fig. 7.2 A 50-year old man with right T12 spinal metastasis of malignant peripheral nerve sheath tumor who had previously undergone laminectomy and resection of T5-T6 tumor due to spinal cord compression. Panel **a** (Axial), **b** (sagittal). The unresected tumor involving the right T12 pedicle (contoured in orange; note the contralateral kidney also contoured in *orange*) was treated to 20 Gy in a single fraction to the 75 % isodose line (ISL). Prescription dose illustrated by the *green line* with the 50 % ISL (cyan) and 25 % ISL (*medium blue*) 90.66 % coverage of target volume. The spinal cord maximum dose was 11.10 Gy. Panel **c**-Pretreatment PETCT scan demonstrating FDG-avidity at the right T12 pedicle. Panel **d**: Follow-up PETCT at 4 months: T12 lesion demonstrates near complete resolution of the hypermetabolic activity

tumor involving the right T12 pedicle was treated by radiosurgery to 20 Gy in a single fraction to the 75 % isodose line with 90.66 % coverage of target volume. The spinal cord maximum dose was 11.10 Gy. A follow up PET/CT at 4 months demonstrated no hypermetabolic uptake at either site. This case illustrates general principle that surgery remains the standard management option for patients presenting with progressive, symptomatic spinal cord compression (Fig. 7.2).

7.3 Literature Review

As evidenced by the dramatic increase in publications on the topic in the past 5 years, review of the literature shows that spinal radiosurgery is increasingly being utilized. Most reports are single institutions studies of <100 patients with a heterogeneous mix of patients with spinal and paraspinal lesions of various primary histologies. Despite these limitations, these studies collectively have demonstrated the effectiveness of spinal radiosurgery with most series reporting nearly 85 % or higher local control and pain improvement [4, 5, 9–14]. Table 7.1 [4, 5, 9–15] summarizes the results of selected series containing >25 patients. In the largest single study of patients with spinal metastases treated by radiosurgery, investigators at the University of Pittsburgh reported long term overall pain improvement in 86 % of the 336 patients with pain as a presenting symptom at up to 53 months follow-up [9]. Although most series have not rigorously used quality of life assessments, a few have attempted to quantify the effectiveness of spinal radiosurgery on quality of life [4, 15, 16]. For example, in a report by Gagnon et al. who prospectively evaluated pain control and quality of life in 200 patients with benign or malignant tumors treated by Cyberknife spinal radiosurgery, there was statistically significant improved pain levels which was durable over 48 months of follow-up [15]. Using the SF-12 validated instrument to evaluate QoL, they also found statistically significant improvements particularly in the mental component of the measurements. Sheehan et al., evaluated the outcomes of 40 previously un-irradiated patients treated by spinal radiosurgery using a helical tomotherapy technique [16]. There was significant improvement of pain relief as assessed by a 10-point visual analog scale (VAS) with a mean score of 3.2 post-treatment compared to a mean pre-treatment level of 6.2. Additionally, function as assessed by Oswestry Disability Index was also improved with the mean pre-treatment score of 43 decreasing to 25 following radiosurgical intervention.

In general, epidural spinal cord compression is considered a relative contraindication to spinal radiosurgery. However, investigators at Henry Ford Health System reported a study of 62 patients with 85 metastatic spinal lesions causing epidural spinal cord compression treated with spinal radiosurgery [17]. With 80 % overall response in the epidural tumor (27 % complete response), significant improvement of the thecal sac patency (from 55 to 76 %), and only 16 % exhibiting neurological progression following treatment, the authors conclude that radiosurgery may be a viable option.

Based on the effectiveness of radiosurgery for benign intracranial tumors such as nerve sheath tumors and meningiomas, spinal radiosurgery has been evaluated in similar tumors occurring in the spine [18–21]. The two largest series of radiosurgery for benign intradural spinal tumors were reported by Sachdev et al. of Stanford and Gerszten et al. [20] of University of Pittsburgh. Using a single fraction regimen, Gertszten et al. [20] treated 73 lesions (13 meningiomas, 35 schwannomas, 25 neurofibromas) to a mean dose of 17.3 Gy to the 80 % isodose line. At median follow-up of 37 months, they reported 100 % radiographic control rate and 73 % of patients

Table 7.1 Selected series of spinal SRS/SBRT

Author and year	Number of patients/ lesions	Age (years)	Method	Prior treatment %		Total dose (Gy)/ fractions/ isodose	Spinal cord dose limit	Follow up months	PI, %	LC, %	Major non-neurologic toxicity
				Surgery	Radiation						
Degen et al. [4]	51/72	Mean 53	CyberKnife	0	53	10–37.5/1–5/100 %	2.2–27.1 Gy	Mean 12	97	100	0
Gibbs et al. [5]	74/102	Mean 59	CyberKnife	3	49	16–25/1–5/80 %	10 Gy in single fraction		84		
Gerszten et al. [9]	393/500	Mean 56	CyberKnife	2	69	12.5–25/1/80 %	<8 Gy to mean 0.6 cm^3	Median 21	86	88	0
Jin et al. [10]	196/270	n.r.	Novalis	n.r.	n.r.	10–18/1/90 %	<10 Gy to 10 % volume	n.r.	85	n.r.	0
Yamada et al. [11]	93/103	Median 62	Linac/ IMRT	0	0	18–24/1/100 %	12–14 Gy point dose	2–45	n.r.	90	1
Ryu et al. [12]	177/230	Median 61	Novalis	0	0	8–18/1/90 %	<10 Gy to 10 % volume	Median 6.4	n.r	n.r	n.r.
Chang et al. [13]	63/74	Median 59	Exact varian	38	55.6	30/5 or 27/3/n.r.	<10 Gy	Median 21.3	Decreased narcotic usage	84	5
Nelson et al. [14]	32/33	Median 60	Linac/ IMRT	n.r.	69	5.1–16/1–4/n.r.	Varied	Median 7	97	87	0
Gagnon et al. [15]	200/274	Median 56	CyberKnife	7	46	21–26/3/75	n.r.	Median 12	n.r.	44-significant improvement in pain score average	3

had pain improvement. The investigators at Stanford used both single fraction and multi-fraction schedules to treat 103 tumors (32 meningiomas, 47 schwannomas, 24 neurofibromas) with mean dose of 19.4 Gy over an average of 2 fractions. In this series, at mean follow-up of 33 months there was radiographic control in all but 1 tumor, with 40 % of tumors demonstrating decrease in size while the remaining 59 % were stable. Reporting the results of patients whose pain was improved or stable, the best clinical results were observed in patients with meningiomas (100 %) or schwannomas (89 %) while poorer symptomatic outcomes (67 %) were seen with neurofibromas. Radiation myelopathy as a result of treatment developed in a single patient in the Stanford series and 3 patients in the Pittsburgh series.

7.4 Treatment Techniques

Stereotactic body RT has emerged as a new treatment option and is increasingly being applied to treat spinal disease with high biologic equivalent dose (BED) and a steep dose gradient. Stereotactic radiosurgery of spinal lesions requires exquisite body immobilization, sophisticated contouring, complex treatment planning, and near-real-time image-guidance to ensure accurate dose delivery due to the proximity of the spinal cord. Since even modest positioning errors can result in significantly higher dose to the spinal cord [22], stereotactic radiosurgery of spinal lesions is preferably delivered using systems that allow for intra-fractional target imaging and repositioning during treatment. The CyberKnife (CK) (Accuray, Inc., Sunnyvale), Novalis (Brainlab, Ammerthalstrabe, Germany), and other LINAC-based systems using cone-beam CT are the current SRS systems equipped with in-room real time imaging and capable of adjustments during the delivery of treatment. The CK uses intrafractional stereoscopic X-ray imaging, every 30–60 s, and automatically adjusts positional errors with an accuracy of <0.5 mm whereas Novalis has intrafractional positioning adjustments based on the infrared markers placed on the patient's surface with an accuracy of 1.36 + 0.11 mm [23]. Although tomotherapy (Accuray, Inc., Madison, WI, USA) is a promising technique with a reported phantom accuracy of 0.6–1.2 mm [24], patient studies of accuracy, however, describe greater errors of approximately 4 mm since the megavoltage CT scan is used only for initial set-up and not for re-positioning. Table 7.2 [8, 22–28] summarizes the accuracy data for the most common radiosurgical systems currently in use.

7.5 Patient Selection Criteria

Although there is considerable variability among clinicians regarding patient selection for spinal SRS, the current clinical practice is mainly based on retrospective data and phase I-II trials [5, 7, 9, 11, 13, 14, 22, 29–32]. ASTRO has published very conservative suggestions strongly encouraging that these patients be treated within

Table 7.2 The accuracy data for the most common radiosurgical systems currently in use

System	Immobilization	Image-guidance	Error analysis
Cyberknife [23] (Accuray, Inc)	Head mask, cradle, vacuum bag	Xsight skeletal tracking or fiducial tracking	Phantom- 0.61 ± 0.27 mm
			Patient- 0.49 ± 0.22 mm
Novalis [25] (BrainLAb, Inc.)	Head mask, cradle, vacuum bag	Orthogonal images to set-up	Measure iso dose 2–4 %
		Optical tracking	Patient- 1.36 ± 0.11 mm
TomoTherapy [24] (Accuray, Inc.)	Head mask, vacuum bag	CT	Phantom- ± 0.6–1.2 mm
			Patient- ± 4–4.3 mm
Synergy S [26] (Elekta, Inc.)	BodyFix (Elekta)	Conebeam CT	Patient (w/o image guidance)- 5.2 ± 2.2 mm
		HexaPOD robotic couch	Patient (with image guidance)- 0.9–1.8 mm (translational) 0.8–1.6° (rotational)
In-house systems [8, 22, 27, 28]	Stereotactic body frame or body cast	CT	Patient- varies from 1 to 3.6 mm

Table 7.3 Recommendations for indications and contraindications for spinal SRS

Indications	Contraindications
Progressive but minimal neurologic deficit	Severe neurologic deficit with significant cord compression
Post resection local irradiation	Neurologic deficit caused by bony compression
Disease progression despite surgery and/or irradiation	Spinal instability
Medically inoperable	Lesion not responsive to radiation
Inoperable	Maximal tolerable radiation doses delivered to adjacent spinal cord

the confines of clinical trials or at centers who are highly experienced at spinal radiosurgery [33]. The following recommendations (Table 7.3) are generated based upon the range of indications as described in the previous studies [4, 5, 7–9, 11, 13, 14, 19, 20, 32–37] and our clinical experiences at Stanford.

Recommended indications for spinal SRS of metastatic tumors include; (1) proven spinal disease on MRI or biopsy, (2) single or multiple spinal metastases ($\leq$2 consecutive vertebral levels or up to 3 noncontiguous spinal sites) without symptomatic spinal cord compression or pathologic fracture requiring surgical stabilization (3) previously irradiated ($\geq$6 months interval between courses), (4) residual tumor after surgery, (5) recurrent tumor after prior surgical resection, or radiosurgical boost for radioresistant (e.g., renal cell, melanoma, sarcoma) tumors. In addition, candidates for spinal SRS should have a good performance status (KPS > 60) and be able to lie supine in comfort on the treatment table for the duration of treatment. Benign intradural extramedullary tumors may benefit from spinal SRS where complete resection is not feasible or for recurrent tumors after surgery [18, 20]. While

spinal radiosurgery for intramedullary conditions such as spinal arteriovenous malformations (AVMs) and intramedullary hemangioblastomas have been reported by our institution, radiosurgery should be performed in circumstances when surgery is not an option and only by the most skilled interdisciplinary teams [38].

Contraindications for spinal SRS include; symptomatic spinal cord compression, previous SBRT to the same level, unstable spine, inability to assume a position suitable for accurate treatment, and life expectancy <3 months. Based on limited reports of potential spinal cord toxicity, care may be needed when targeted angiogenic therapy is planned within 2 months of spinal radiosurgery. Although ASTRO guidelines suggests an interval of at least 90 days between EBRT and when reirradiation by radiosurgery is being considered, our clinical experience showed that those most benefit from SRS was seen with patients with at least 12 months interval [39].

7.6 Diagnostic Images

Spinal magnetic resonance imaging (MRI) is the imaging modality of choice. However, additional information may be gained from, PET/CT scan, or CT myelography. MRI of the entire spine is recommended in order to exclude multi-level disease. MRI of the involved spine within 4 weeks prior to SRS is crucial both for defining the extent of disease and delineation purposes.

MRI may be acquired using either 1.5-Tesla (T) or 3-T. While 3 T may improve anatomic visualization in the spine and more precisely differentiate tumor infiltration versus normal bone marrow based on its increased signal-to-noise ratio, shorter scan times, and improved resolution, compared to 1.5, 3 T MRI may also be more challenging. For example, 3 T may be associated with increased susceptibility to metal, degradation of bone interfaces (related to chemical shift), reduced contrast on some T1 images (related to longer relaxation times), and higher likelihood of tissue heating (related to higher specific absorption rate). The most useful MRI sequences include T1- and T2-weighted sagittal and axial images as well as short tau inversion recovery (STIR) images [40]. Fat suppression imaging can help to distinguish tumor from normal bone marrow on T2 STIR images. Typically, pathological lesions are hypointense on T1-weighted images with respect to bone marrow, hyperintense on T2-weighted images, and may have variable levels of enhancement with gadolinium. Gadolinium-enhanced, fat-suppressed T1 imaging is particularly useful for imaging of paravertebral or epidural disease. CT myelography is an invasive procedure requiring injection of contrast into the subarachnoidal space and may be used as an alternative to MRI for the purposes of visualizing the spinal cord. While CT myelography, is used less frequently, it can be particularly helpful in circumstances where MRI is not feasible (e.g. claustrophobia or metal implants). Some groups have also investigated the use of 3D Fast Imaging Employing Steady-state Acquisition (FIESTA) MRI for the purpose of spinal cord delineation [41].

7.7 Simulation Studies

Immobilization is a key factor in the accurate delivery of spinal SRS. Patients should be positioned in a stable, comfortable, and reproducible position using vacuum bag, alpha cradle or stereotactic frame. Considering the long treatment duration, supine positioning is preferred over prone. Rigid plastic head and neck mask are preferred for immobilization, for lesions involving the cervical or upper thoracic spine areas. CT scan is the primary imaging for simulation and is used for target delineation and treatment planning. Preferably, high resolution thin slice CT with slice thickness of <2 mm should be used with images extending 5–10 cm above and below the region of interest. For non-coplanar beam arrangements, it is suggested that imaging extend ±15 cm. Co-registration of the CT images with the MRI (gadolinium contrast T1-weighted and T2-weighted images) and/or CT myelogram is highly recommended to delineate the spinal cord properly [7, 8]. Computed tomography (CT) myelography can be used for contouring spinal cord when MRI is not available [7, 41–43]. The CT-myelogram may also play an important role especially for patients with metal implants or claustrophobic. If both MRI and myelogram are not available, the thecal sac or spinal canal should be delineated rather than spinal cord itself.

7.8 Planning and Treatment Delivery

There is considerable variability in target delineation; the main goal for spinal SRS is to identify areas of tumor involvement and anatomic areas of potential tumor contiguity [7]. In general, gross tumor volume (GTV) and clinical target volume (CTV) are outlined without adding a planning target volume (PTV) margin. The CTV includes the GTV and the potential microscopic disease areas, PTV is identical to CTV. Contouring of CTV is primarily based on simulation CT imaging with MRI fusion. At Stanford, the SRS target volume includes the involved gross tumor seen on MRI and/or planning CT, vertebral body and involved pedicle(s). When there is no involvement of pedicles or posterior elements and the majority of the vertebral body is uninvolved by tumor, the GTV alone may be targeted for treatment. Table 7.4 shows the target volume definitions for individual clinical situations. In all cases, the epidural or paraspinal component should be included in the target volume if present. Recently "International Spine Radiosurgery Consortium Consensus Guidelines for Volume Definition in Spinal radiosurgery" have summarized consensus target delineation of common scenarios metastatic spine SRS [44].

The most critical normal organ to contour and to incorporate radiation dose restrictions during treatment planning is the spinal cord. The spinal cord is usually outlined on the simulation CT based on co-registration with thin slice high-resolution MRI images through the region of interest. CT myelograms may also be very helpful when available. Our approach is to delineate the cord at least 5 cm above and below the superior and inferior margins of target volume, particularly in cases where non-coplanar beams are used. Acceptable radiation dose constraints for the spinal

Table 7.4 Spinal radiosurgery target definitions

Involved field	Metastases involving only vertebral body	Metastases extending through pedicles, not the posterior elements	Metastases involving only the posterior elements	Multiple lesions in a single vertebra	Postoperative volume
Clinical target volume (CTV)	GTV + vertebral body ± both pedicles	GTV + vertebral body + involved pedicle(s)	Spinous process and laminae	Whole vertebra	Residual tumor, operative tumor bed
	GTV + up to 2 mm margin	Whole vertebra including posterior elements			

cord are typically a maximum dose of 12–14 Gy in single fraction [11, 13, 45]. Other volumetric constraints may also be useful. It is sometimes helpful to outline the cauda equine as a separate critical organ because of its higher tolerance dose, up to 14 Gy [12]. Another alternative contouring method for the spinal cord when using strictly coplanar beam arrangements is applying a relative or partial volume dose constraint. Accordingly, the spinal cord is contoured 6 mm above or below SRS target volume, and constraints are set such that no more than 10 % of the contoured cord is treated above 10 Gy as described by Ryu et al. The AAPM Task report 101 has summarized both single fraction and multi-fraction suggested dose constraints for spinal cord and other critical structures [45]. Our current dose constraints as well as published alternative constraints for spinal cord and other critical organs are detailed in Table 7.5 [9–12, 45]. Dose constraints are occasionally relaxed for previously un-irradiated spinal cord as designated by the asterisk (*) in Table 7.5.

Depending on the vertebral level of the spinal lesion, other critical organs such as the pharynx, lung, and bowel may need to be considered. In the upper thoracic spine, the esophagus is an important organ to consider due to the risk of fistula or rupture. The mediastinal window is used for contouring esophagus, starting usually 5–10 cm above and below target volume. In the lower thoracic and upper lumbar spine kidneys become an important critical structure, especially in patients who have undergone nephrectomy.

In radiation treatment planning, it is important to adhere to the quality assurance guidelines as described by the AAPM Task Group 101 (TG101). Some important issues to consider for treatment planning include (1) imaging parameters, (2) calculation algorithms, (3) beam orientation. CT slice thickness of 1–3 mm and calculation grid of 2 mm or finer are generally recommended (TG101). Due to the variation of tissue interfaces encountered with spinal radiosurgery it is also recommended that more sophisticated dose calculation algorithms be used, e.g. convolution/superposition technique or Monte Carlo (MC) technique (TG101). Pencil beam algorithm was found to be inadequate for volumes with lung/tissue interface. Since the Cyberknife Multi-plan ray tracing

Table 7.5 Various dose-volume constraints for selected normal organs

Study	Spinal cord	Esophagus	Kidney (right and left)
Benedict et al. (2010) [45]			
Single fraction	V10 < 0.35	V 11.9 < 5 cc	V10.6 < 2/3 volume
3 fractions	V7 < 1.2 cc	Dmax 15.4 Gy	Dmax 18.6 Gy
5 fractions	Dmax 15 Gy	V17.7 < 5 cc	V23 < 2/3 volume
	V18 < 0.35 cc	Dmax 25.2 Gy	
	V12.3 < 1.2 cc	V19.5 < 5 cc	
	Dmax 21.9 Gy	Dmax 35 Gy	
	V23 < 0.35		
	V14.5 < 1.2 cc		
	Dmax 30 Gy		
RTOG 0631			
Single fraction	V10 < 0.35 cc	V16 < 0.03 cc	V8.4 < 200 cc
	V10 < 10 % of the partial spinal cord	V11.9 < 5 cc	
	V14 < 0.03		
Yamada et al. (2008) [11]			
Single fraction	12–14 Gy point dose	n.r.	n.r
Ryu et al. [12]			
Single fraction	<10 Gy to 10 % volume	n.r	n.r.
Jin et al. (2007) [10]			
Single fraction	<10 Gy to 10 % volume	n.r.	n.r.
Gerszten et al. (2007) [9]			
Single fraction	<8 Gy to mean 0.6 cm	n.r.	n.r.
Our constraints	V8 < 1 cm^3	D5cc < 12 Gy	V10.6 < 2/3 volume
Single fraction	V10 < 0.35 cm^3	Dmax 14 Gy	Dmax 18.6 Gy
3 fractions	*V8 < 1.5 cm^3	D5cc < 18 Gy	
	*V10 < 0.5 cm^3	Dmax 25 Gy	
	Dmax 14 Gy		
	V15 < 1 cm^3		
	V18 < 0.5 cm^3		
	Dmax 21 Gy		

algorithm is based on pencil beam algorithm, it is best to use the option of MC calculation for thoracic spine with the target volumes adjacent to lung tissue. Depending on the treatment technique employed, aspects of beam orientation may be an important determinant of the achievement of optimal dose distributions. Linac-based stereotactic systems use co-planar or non-coplanar beams (5–10 beams) well spread out to spare the normal tissues. Recently, volumetric modulated arc therapy is widely adapted to deliver conformal SBRT doses while substantially shortening delivery time. The Cyberknife robotic system is capable of

non-isocentric beams delivery and typically uses 50–200 beams per plan. Because of the limitation of the robot workspace, however, most beams are oriented in an anterior, lateral, or anterior oblique fashion with little access to posterior beams. The lack of posterior beams has the potential to give more doses to anterior normal structures, such as heart and thus, may be clinically important for large patients or where the target is located at significant depth. Efforts to overcome this limitation have been recently introduced by allowing prone positioning of the patient and incorporating motion tracking to maintain sub-millimeter accuracy.

7.9 Dose and Fractionation

Dose fractionation preferences have been largely derived from retrospective data rather than formal dose escalation studies. Therefore there is wide variability in dose schedules currently in clinical practice. In general, single fraction dose equivalent for spinal metastasis are in the range of 18–24 Gy for spinal metastases (Table 7.1). Investigators from Memorial Sloan-Kettering report that prescription doses of 24 Gy and minimum doses >15 Gy may be necessary for durable local control [46]. Table 7.5 summarizes dose schemes at select institutions.

7.10 Toxicity

Similar to other modalities of radiation, non-neurologic complications such as fatigue and nausea may occur after spinal SRS. The most serious late complications are radiation myelopathy, vertebral compression fracture (VCF) and esophageal complications such as tracheoesophageal fistula or esophageal perforation.

Spinal cord tolerance dose guidelines that limit toxicity to <5 % have been described to help guide practice [31, 47, 48]. Although the risk is low, spinal cord injury may cause paralysis or death. Therefore, in SRS treatment planning special care must be taken during contouring, planning, and treatment delivery. The largest series reported radiation myelopathy in nine patients and compared dosimetric and clinical factors with a cohort of 66 spine SRS patients without radiation myelopathy [48]. The authors recommend limiting thecal sac maximum point doses to 12.4 Gy in 1 fraction [48]. Similarly, Gibbs et al. have reported radiation myelopathy in six patients and one half of these patients have received spinal cord biologic equivalent doses exceeding 8 Gy, consequently their recommendation was to limit the volume of treated spinal cord above 8 Gy [49].

Vertebral compression fracture (VCF) is a complication of spinal SRS that has been reported crude rates of up to nearly 40 % [50–52]. Osteolytic or osteoblastic metastatic disease may induce change the architecture and mineralization of bone that can decrease bone quality that may result in VCF [53]. The reported rates of VCF appear to be significantly higher with spinal SRS compared to the <5 % rate

after conventional palliative radiotherapy [54]. A recent multi-institutional review of VCF in a cohort of 252 patients with 410 spinal segments treated by spinal radiosurgery, showed the cumulative incidence of VCF at 1 and 2 years of 12.3 and 13.5 %, respectively [55]. Radiation dose per fraction >20 Gy was associated with a significantly higher risk of VCF. Additionally, this study confirmed baseline VCF, lytic tumor, and spinal misalignment as predictive factors for VCF. While most patients who developed VCF in the published series were asymptomatic, approximately 22 % of patients required intervention for pain relief and mechanical stabilization. Minimally-invasive percutaneous cement augmentation procedures such as vertebroplasty and kyphoplasty may be used when feasible [53].

Limited data exist to predict esophageal toxicity from spinal SRS. Grade 3 or higher late esophageal toxicity risk was reported to be low in recent series [56, 57]. Patients treated with prior or concurrent chemotherapy have higher risk of esophageal toxicity [56, 57] and iatrogenic manipulation of the esophagus such as dilatation, biopsy and stent placement may increase esophageal toxicity [57].

7.11 Follow Up

Physical and neurological examinations for the first 1–2 weeks after spinal SRS is recommended to evaluate any unusual symptoms or side effects. An MRI of the treated spine at 1–3 monthly after SRS is performed for follow-up of spinal metastases. For benign lesions, 6–12 monthly intervals are typically recommended.

7.12 Future Directions

While SRS of spinal tumors is an emerging trend, there is a need for further investigation and research to refine the optimal treatment parameters, to confirm long-term durability of tumor control, and to better understand the limits of spinal cord tolerance. Even in the absence of randomized prospective studies, current data strongly supports the efficacy of this treatment in terms of local control, pain management, and toxicity for metastatic and benign intradural spinal tumors. To some degree the availability of 3 T spinal imaging has improved the delineation of tumor in the bone marrow. In the future, assessments of response and tumor control will likely be aided by improvements in imaging. For example, specialized MRI sequences that correlate tumor vascular effects of radiation may be helpful in determining tumor control. With careful patient selection and planning, SRS has the potential to be applied beyond spinal tumors. In our own experience, it has been used to manage spinal arteriovenous malformations and functional indications such as facetogenic back pain.

References

1. Hamilton AJ, Lulu BA, Fosmire H, Stea B, Cassady JR. Preliminary clinical experience with linear accelerator-based spinal stereotactic radiosurgery. Neurosurgery. 1995;36(2):311–9.
2. Adler Jr JR, Murphy MJ, Chang SD, Hancock SL. Image-guided robotic radiosurgery. Neurosurgery. 1999;44(6):1299–306; discussion 306–7.
3. Bilsky MH, Yenice K, Lovelock M, Yamada J. Stereotactic intensity-modulation radiation therapy for vertebral body and paraspinal tumors. Neurosurg Focus. 2001;11(6):e7.
4. Degen JW, Gagnon GJ, Voyadzis JM, McRae DA, Lunsden M, Dieterich S, et al. CyberKnife stereotactic radiosurgical treatment of spinal tumors for pain control and quality of life. J Neurosurg Spine. 2005;2(5):540–9.
5. Gibbs IC, Kamnerdsupaphon P, Ryu MR, Dodd R, Kiernan M, Chang SD, et al. Image-guided robotic radiosurgery for spinal metastases. Radiother Oncol. 2007;82(2):185–90.
6. Ryu S, Fang Yin F, Rock J, Zhu J, Chu A, Kagan E, et al. Image-guided and intensity-modulated radiosurgery for patients with spinal metastasis. Cancer. 2003;97(8):2013–8.
7. Sahgal A, Larson DA, Chang EL. Stereotactic body radiosurgery for spinal metastases: a critical review. Int J Radiat Oncol Biol Phys. 2008;71(3):652–65.
8. Yamada Y, Lovelock DM, Yenice KM, Bilsky MH, Hunt MA, Zatcky J, et al. Multifractionated image-guided and stereotactic intensity-modulated radiotherapy of paraspinal tumors: a preliminary report. Int J Radiat Oncol Biol Phys. 2005;62(1):53–61.
9. Gerszten PC, Burton SA, Ozhasoglu C, Welch WC. Radiosurgery for spinal metastases: clinical experience in 500 cases from a single institution. Spine. 2007;32(2):193–9.
10. Jin JY, Chen Q, Jin R, Rock J, Anderson J, Li S, et al. Technical and clinical experience with spine radiosurgery: a new technology for management of localized spine metastases. Technol Cancer Res Treat. 2007;6(2):127–33.
11. Yamada Y, Bilsky MH, Lovelock DM, Venkatraman ES, Toner S, Johnson J, et al. High-dose, single-fraction image-guided intensity-modulated radiotherapy for metastatic spinal lesions. Int J Radiat Oncol Biol Phys. 2008;71(2):484–90.
12. Ryu S, Jin JY, Jin R, Rock J, Ajlouni M, Movsas B, et al. Partial volume tolerance of the spinal cord and complications of single-dose radiosurgery. Cancer. 2007;109(3):628–36.
13. Chang EL, Shiu AS, Mendel E, Mathews LA, Mahajan A, Allen PK, et al. Phase I/II study of stereotactic body radiotherapy for spinal metastasis and its pattern of failure. J Neurosurg Spine. 2007;7(2):151–60.
14. Nelson JW, Yoo DS, Sampson JH, Isaacs RE, Larrier NA, Marks LB, et al. Stereotactic body radiotherapy for lesions of the spine and paraspinal regions. Int J Radiat Oncol Biol Phys. 2009;73(5):1369–75.
15. Gagnon GJ, Nasr NM, Liao JJ, Molzahn I, Marsh D, McRae D, et al. Treatment of spinal tumors using cyberknife fractionated stereotactic radiosurgery: pain and quality-of-life assessment after treatment in 200 patients. Neurosurgery. 2009;64(2):297–306; discussion –7.
16. Sheehan JP, Shaffrey CI, Schlesinger D, Williams BJ, Arlet V, Larner J. Radiosurgery in the treatment of spinal metastases: tumor control, survival, and quality of life after helical tomotherapy. Neurosurgery. 2009;65(6):1052–61; discussion 61–2.
17. Ryu S, Rock J, Jain R, Lu M, Anderson J, Jin JY, et al. Radiosurgical decompression of metastatic epidural compression. Cancer. 2010;116(9):2250–7.
18. Dodd RL, Ryu MR, Kamnerdsupaphon P, Gibbs IC, Chang Jr SD, Adler Jr JR. CyberKnife radiosurgery for benign intradural extramedullary spinal tumors. Neurosurgery. 2006;58(4):674–85; discussion –85.
19. Gerszten PC, Ozhasoglu C, Burton SA, Vogel WJ, Atkins BA, Kalnicki S, et al. CyberKnife frameless single-fraction stereotactic radiosurgery for benign tumors of the spine. Neurosurg Focus. 2003;14(5):e16.
20. Gerszten PC, Burton SA, Ozhasoglu C, McCue KJ, Quinn AE. Radiosurgery for benign intradural spinal tumors. Neurosurgery. 2008;62(4):887–95; discussion 95–6.

21. Sachdev S, Dodd RL, Chang SD, Soltys SG, Adler JR, Luxton G, et al. Stereotactic radiosurgery yields long-term control for benign intradural, extramedullary spinal tumors. Neurosurgery. 2011;69(3):533–9; discussion 9.
22. Chang EL, Shiu AS, Lii MF, Rhines LD, Mendel E, Mahajan A, et al. Phase I clinical evaluation of near-simultaneous computed tomographic image-guided stereotactic body radiotherapy for spinal metastases. Int J Radiat Oncol Biol Phys. 2004;59(5):1288–94.
23. Ho AK, Fu D, Cotrutz C, Hancock SL, Chang SD, Gibbs IC, et al. A study of the accuracy of cyberknife spinal radiosurgery using skeletal structure tracking. Neurosurgery. 2007;60(2 Suppl 1):ONS147–56; discussion ONS56.
24. Mahan SL, Ramsey CR, Scaperoth DD, Chase DJ, Byrne TE. Evaluation of image-guided helical tomotherapy for the retreatment of spinal metastasis. Int J Radiat Oncol Biol Phys. 2005;63(5):1576–83.
25. Yin FF, Ryu S, Ajlouni M, Zhu J, Yan H, Guan H, et al. A technique of intensity-modulated radiosurgery (IMRS) for spinal tumors. Med Phys. 2002;29(12):2815–22.
26. Guckenberger M, Meyer J, Wilbert J, Baier K, Bratengeier K, Vordermark D, et al. Precision required for dose-escalated treatment of spinal metastases and implications for image-guided radiation therapy (IGRT). Radiother Oncol. 2007;84(1):56–63.
27. Lohr F, Debus J, Frank C, Herfarth K, Pastyr O, Rhein B, et al. Noninvasive patient fixation for extracranial stereotactic radiotherapy. Int J Radiat Oncol Biol Phys. 1999;45(2):521–7.
28. Shiu AS, Chang EL, Ye JS, Lii M, Rhines LD, Mendel E, et al. Near simultaneous computed tomography image-guided stereotactic spinal radiotherapy: an emerging paradigm for achieving true stereotaxy. Int J Radiat Oncol Biol Phys. 2003;57(3):605–13.
29. Rock JP, Ryu S, Yin FF, Schreiber F, Abdulhak M. The evolving role of stereotactic radiosurgery and stereotactic radiation therapy for patients with spine tumors. J Neurooncol. 2004;69(1–3):319–34.
30. Ryu S, Rock J, Rosenblum M, Kim JH. Patterns of failure after single-dose radiosurgery for spinal metastasis. J Neurosurg. 2004;101 Suppl 3:402–5.
31. Sahgal A, Ma L, Gibbs I, Gerszten PC, Ryu S, Soltys S, et al. Spinal cord tolerance for stereotactic body radiotherapy. Int J Radiat Oncol Biol Phys. 2010;77(2):548–53.
32. Sahgal A, Ames C, Chou D, Ma L, Huang K, Xu W, et al. Stereotactic body radiotherapy is effective salvage therapy for patients with prior radiation of spinal metastases. Int J Radiat Oncol Biol Phys. 2009;74(3):723–31.
33. Lutz S, Berk L, Chang E, Chow E, Hahn C, Hoskin P, et al. Palliative radiotherapy for bone metastases: an ASTRO evidence-based guideline. Int J Radiat Oncol Biol Phys. 2011;79(4):965–76.
34. Gerszten PC, Burton SA, Belani CP, Ramalingam S, Friedland DM, Ozhasoglu C, et al. Radiosurgery for the treatment of spinal lung metastases. Cancer. 2006;107(11):2653–61.
35. Gerszten PC, Burton SA, Ozhasoglu C. CyberKnife radiosurgery for spinal neoplasms. Prog Neurol Surg. 2007;20:340–58.
36. Gerszten PC, Burton SA, Ozhasoglu C, Vogel WJ, Welch WC, Baar J, et al. Stereotactic radiosurgery for spinal metastases from renal cell carcinoma. J Neurosurg Spine. 2005;3(4):288–95.
37. Gerszten PC, Welch WC. Cyberknife radiosurgery for metastatic spine tumors. Neurosurg Clin N Am. 2004;15(4):491–501.
38. Sinclair J, Chang SD, Gibbs IC, Adler Jr JR. Multisession CyberKnife radiosurgery for intramedullary spinal cord arteriovenous malformations. Neurosurgery. 2006;58(6):1081–9; discussion –9.
39. Choi CY, Adler JR, Gibbs IC, Chang SD, Jackson PS, Minn AY, et al. Stereotactic radiosurgery for treatment of spinal metastases recurring in close proximity to previously irradiated spinal cord. Int J Radiat Oncol Biol Phys. 2010;78(2):499–506.
40. Dahele M, Zindler JD, Sanchez E, Verbakel WF, Kuijer JP, Slotman BJ, et al. Imaging for stereotactic spine radiotherapy: clinical considerations. Int J Radiat Oncol Biol Phys. 2011;81(2):321–30.

41. Thariat J, Castelli J, Chanalet S, Marcie S, Mammar H, Bondiau PY. CyberKnife stereotactic radiotherapy for spinal tumors: value of computed tomographic myelography in spinal cord delineation. Neurosurgery. 2009;64(2 Suppl):A60–6.
42. Uhl M, Sterzing F, Habl G, Schubert K, Sroka-Perez G, Debus J, et al. CT-myelography for high-dose irradiation of spinal and paraspinal tumors with helical tomotherapy: revival of an old tool. Strahlenther Onkol. 2011;187(7):416–20.
43. Plathow C, Thilmann C, Delorme S, Stippich C, Wannenmacher M, Debus J. Radiotherapy planning for paraspinal tumors with CT-myelography. Strahlenther Onkol. 2001;177(6):307–12.
44. Cox BW, Spratt DE, Lovelock M, Bilsky MH, Lis E, Ryu S, et al. International Spine Radiosurgery Consortium consensus guidelines for target volume definition in spinal stereotactic radiosurgery. Int J Radiat Oncol Biol Phys. 2012;83(5):e597–605.
45. Benedict SH, Yenice KM, Followill D, Galvin JM, Hinson W, Kavanagh B, et al. Stereotactic body radiation therapy: the report of AAPM Task Group 101. Med Phys. 2010;37(8):4078–101.
46. Lovelock DM, Zhang Z, Jackson A, Keam J, Bekelman J, Bilsky M, et al. Correlation of local failure with measures of dose insufficiency in the high-dose single-fraction treatment of bony metastases. Int J Radiat Oncol Biol Phys. 2010;77(4):1282–7.
47. Lo SS, Sahgal A, Chang EL, Mayr NA, Teh BS, Huang Z, et al. Serious complications associated with stereotactic ablative radiotherapy and strategies to mitigate the risk. Clin Oncol (R Coll Radiol). 2013;25(6):378–87.
48. Sahgal A, Weinberg V, Ma L, Chang E, Chao S, Muacevic A, et al. Probabilities of radiation myelopathy specific to stereotactic body radiation therapy to guide safe practice. Int J Radiat Oncol Biol Phys. 2013;85(2):341–7.
49. Gibbs IC, Patil C, Gerszten PC, Adler Jr JR, Burton SA. Delayed radiation-induced myelopathy after spinal radiosurgery. Neurosurgery. 2009;64(2 Suppl):A67–72.
50. Rose PS, Laufer I, Boland PJ, Hanover A, Bilsky MH, Yamada J, et al. Risk of fracture after single fraction image-guided intensity-modulated radiation therapy to spinal metastases. J Clin Oncol. 2009;27:5075–9.
51. Cunha MV, Al-Omair A, Atenafu EG, Masucci GL, Letourneau D, Korol R, et al. Vertebral compression fracture (VCF) after spine stereotactic body radiation therapy (SBRT): analysis of predictive factors. Int J Radiat Oncol Biol Phys. 2012;84(3):e343–9.
52. Boehling NS, Grosshans DR, Allen PK, McAleer MF, Burton AW, Azeem S, et al. Vertebral compression fracture risk after stereotactic body radiotherapy for spinal metastases. J Neurosurg Spine. 2012;16(4):379–86.
53. Sahgal A, Whyne CM, Ma L, Larson DA, Fehlings MG. Vertebral compression fracture after stereotactic body radiotherapy for spinal metastases. Lancet Oncol. 2013;14(8):e310–20.
54. Chow E, Harris K, Fan G, Tsao M, Sze WM. Palliative radiotherapy trials for bone metastases: a systematic review. J Clin Oncol. 2007;25(11):1423–36.
55. Sahgal A, Atenafu EG, Chao S, Al-Omair A, Boehling N, Balagamwala EH, et al. Vertebral compression fracture after spine stereotactic body radiotherapy: a multi-institutional analysis with a focus on radiation dose and the spinal instability neoplastic score. J Clin Oncol. 2013;31(27):3426–31.
56. Abelson JA, Murphy JD, Loo Jr BW, Chang DT, Daly ME, Wiegner EA, et al. Esophageal tolerance to high-dose stereotactic ablative radiotherapy. Dis Esophagus. 2012;25(7):623–9.
57. Cox BW, Jackson A, Hunt M, Bilsky M, Yamada Y. Esophageal toxicity from high-dose, single-fraction paraspinal stereotactic radiosurgery. Int J Radiat Oncol Biol Phys. 2012;83(5):e661–7.

Chapter 8
Stereotactic Radiotherapy for Lung Tumors

Joost J. Nuyttens

Abstract Early stage lung cancer may often be not amenable for surgery due to poor underlying lung function. While conventional radiation therapy may be utilized, respiratory motion often implies inclusion of large volumes of normal lung, to cover the planning target volume with the attending morbidity. This poses a significant challenge for utilising SBRT, where sharp gradients and short treatment schedules benefit these patients. Different techniques have been utilized to address this, and SBRT has been a useful treatment option for peripheral lung tumors with excellent local control. Central lung tumors still pose challenges due to anatomical location and proximity of critical structures, emphasizing the need for careful patient selection.

This chapter outlines the role of SBRT in Lung cancer, serves as practical guide addressing the technical challenges and provides an overview of the available literature

In stereotactic radiotherapy, many different techniques have been developed to control for motion of tumors in the lung. The following methods have been applied to reduce the impact of respiratory tumor motion on dose distribution: (1) patient-specific treatment volumes based on tumor motion observed during planning CT scans (CT-based ITV), (2) forced shallow breathing with abdominal compression, (3) breath-hold methods, (4) respiratory gating methods, and (5) real-time tumor tracking. These different techniques will be reviewed in this chapter. The simulation and target definition depend on the technique.

The local control is excellent for peripheral tumors. However, the local control for central tumors varies depending on the total dose administered. The reported overall survival is excellent but depends on patient selection. The acute and late the toxicity of treatment of peripheral tumors is low. When treating central tumors, caution must be taken because the organs at risk are in close proximity and fatal toxicity has been reported by some authors.

Keywords Real-time tumor tracking • ITV • Breath hold • Forced shallow breathing • Respiratory gating • Local control • Outcome • Toxicity

J.J. Nuyttens, MD, PhD
Department of Radiation Oncology, Erasmus MC Cancer Institute,
Rotterdam, Zuid-Holland, The Netherlands
e-mail: j.nuyttens@erasmusmc.nl

A. Gaya, A. Mahadevan (eds.), *Stereotactic Body Radiotherapy: A Practical Guide*,
DOI 10.1007/978-0-85729-597-2_8

8.1 Introduction

Lung cancer is the most common cause of cancer related death. Seventy-five percent of patients with bronchogenic carcinoma will be diagnosed with non-small cell lung cancer (NSCLC). Approximately 15–20 % of NSCLC patients present with early or localized disease [1]. Surgical resection of stage I (T1–2, N0) NSCLC results in 5-year survival rates of approximately 60–70 % and remains the treatment of choice for this population [2–4]. Unfortunately, some patients with early-stage NSCLC are unable to tolerate the rigors of surgery or the postoperative recovery period due to severe comorbidity. Patients deemed medically inoperable or who refuse surgery have been treated with non surgical therapies, such as conventionally fractionated radiotherapy, or have been simply observed without any anti-tumor therapy. While some patients succumb to their comorbid illnesses, many of these patients will die of progressive lung carcinoma. Mc Garry et al. reviewed the outcome in 75 medically inoperable patients who received no specific cancer therapy at time of diagnosis for stage I NSCLC, and the cause of death was cancer in 53 % of cases [5].

To control the tumor in these patients, the dose must be increased without correspondingly increasing normal tissue toxicity. Therefore, not only is a precise dose delivery required but also a respiratory tracking method must be used to reduce the planning target volume. In a planning study, Prevost et al. compared stereotactic radiotherapy with real-time tumor tracking and three-dimensional conformal radiotherapy (3D CRT). They were able to deliver a 75 % higher mean dose with stereotactic radiotherapy and real-time tumor tracking compared to 3D CRT without increasing the dose to the lungs or other organs at risk [6]. This precise dose delivery is now achieved with the image-guided linear accelerators like the cone beam linear accelerator. Tomotherapy (Accuray Inc, Sunnyvale, CA) linear accelerators with X-ray tubes mounted on the ceiling or floor, and the CyberKnife.

Due to the precise delivery of image-guided radiotherapy, a reduction of safety margins surrounding the gross tumor volume is allowed. Sometimes GTV and CTV can be combined. Consequently, treatment volumes are reduced and treatment doses can be escalated. However, tumors can move considerably during the breathing cycle. These tumors can often move by more than 1 cm and sometimes as much as 3 cm during deep inspiration or expiration [7]. The following methods have been applied to reduce the impact of respiratory tumor motion on dose distribution: (1) patient-specific treatment volumes based on tumor motion observed during planning CT scans (CT-based ITV), (2) forced shallow breathing with abdominal compression, (3) breath-hold methods, (4) respiratory gating methods, and (5) real-time tumor tracking [8]. So, due to the combination of a precise delivery and a reduction in the impact of the motion of the tumor, the target volume can be reduced and the dose can thus be safely escalated. Due to this dose escalation, high local control rates exceeding 90 % have been reported for early-stage NSCLC patients treated with stereotactic radiotherapy (SRT) [9–11]. In this chapter, different methods to reduce the impact of tumor motion, the clinical results of the treatment of primary lung tumors, including central tumors, and lung metastases will be reviewed.

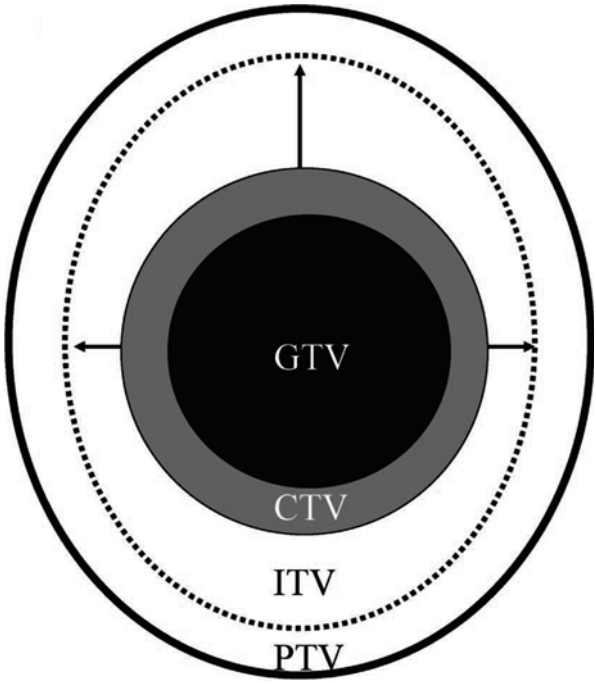

Fig. 8.1 The definition of GTV, CTV, ITV, and PTV. *GTV* gross tumor volume, *CTV* clinical target volume, *ITV* internal target volume, *PTV* planning target volume

8.2 Methods to Reduce the Impact of the Tumor Motion

8.2.1 Introduction

The ultimate goal of methods to reduce the impact of tumor motion is reducing the planning target volume margin from GTV or CTV. Reducing the target volume will reduce the radiation dose to organs at risk. However, by reducing the PTV margin, the tumor could be missed (a geographical miss). An extra margin around CTV is necessary because the tumor moves internally with respiratory motion. The ICRU reports define the margins that are necessary: the tumor as seen on a CT scan or on other examination is called the gross tumor volume (GTV) (Fig. 8.1). The GTV plus a margin to take into account microscopic extension of the tumor is the clinical tumor volume (CTV). The CTV plus a margin for the internal motion of the CTV is called the internal target volume (ITV). The ITV represents the movements of the clinical target volume (CTV) referenced to the patient coordinate system and is specified in relation to internal and external reference points, which preferably should be rigidly related to each other through bony structures. Finally a margin for positioning and motion of the patient on the table is added to the ITV and results in a planning target volume or the volume that must be used to get the correct dose within the tumor [12]. Most methods reduce all margins except the margin from GTV to CTV.

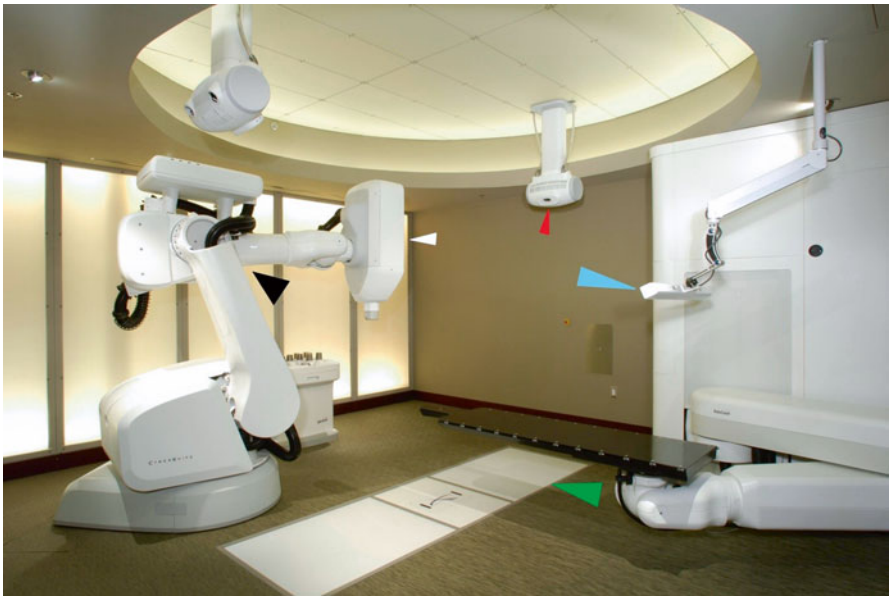

Fig. 8.2 The CyberKnife. *White arrow*, linear accelerator; *black arrow*, robot; *red arrow*, one of the 2 X-ray tubes; *green arrow*, one of the 2 flat panels; *blue arrow*, Synchrony camera

8.2.2 Real-Time Tumor Tracking

The most commonly used method of real-time online tumor tracking is the CyberKnife Synchrony system. With real-time tumor tracking, the GTV is expanded to a CTV and then to a PTV and results usually in a total margin from the GTV to PTV of 5–8 mm. An ITV is not required. The CyberKnife (Fig. 8.2) is a frameless image-guided radiotherapy system involving a 6 MV x-band linear accelerator mounted on a robotic arm, which possesses six degrees of freedom of motion. The imaging system consists of 2 diagnostic X-ray sources mounted to the ceiling paired with amorphous silicon detectors to acquire live digital radiographic images of the tumor, or tumor localizing surrogates such as the skull, spine, or fiducial markers. The Synchrony system enables 4-dimensional real-time tracking of tumors that move with respiration. An advantage of the Synchrony subsystem is that the patients can breathe normally. Synchrony combines non continuous X-ray imaging of internal fiducial markers as surrogates for the tumor position, with a continuously updated external breathing signal. In more recent system versions, it is possible to track the tumor directly in the X-ray images (in certain very specific circumstances) using the contrast between tumor and surrounding lung tissue, thereby removing the need to implant fiducial markers. A correlation model that relates the external breathing signal with the motion of the tumor provides a real-time update of the beam position that is fed to the robotic arm on which the linear accelerator is mounted. In the treatment room, the patient is placed in a supine position on the couch in the vacuum mattress. Three light-emitting diodes (LEDs) are placed on the patient's chest or abdomen to provide the external breathing signal. The

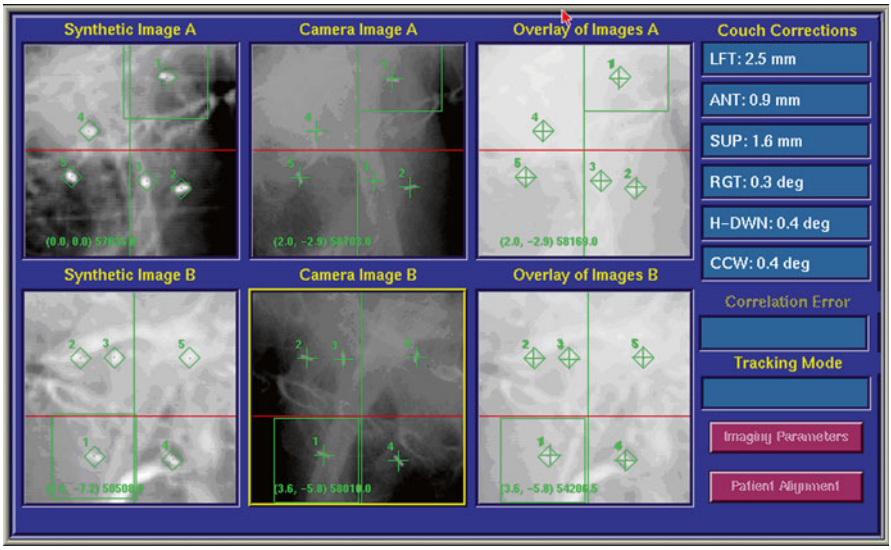

Fig. 8.3 Alignment of the tumor with the use of implanted fiducial markers. A screen dump of the digital display at the CyberKnife treatment console taken before treatment in order to align the tumor. In the *first column*, the DRR is shown. In the *green* cubes, the markers on the DRRs are shown. In the *second column*, 2 orthogonal images of the patient are shown. The *green* crosses indicate the marker positions detected automatically by the tracking software. The offsets between the target centroid position in the treatment plan and that calculated from the live X-ray images are shown under the heading "Couch Corrections." Initially this information is used to automatically adjust the couch position. Once treatment starts, the couch remains static and all tracking is performed using the robotic arm and LINAC. The *third column* shows an overlay of the DRRs and the X-ray images after the calculated offsets are applied

motion of these LEDs due to respiration is registered by a digital camera array (the Synchrony camera) (Fig. 8.2). Initial patient alignment is conducted by the X-ray image-guidance system and the remotely controlled treatment couch, such that the extent of the respiratory motion is within the translational limits of the robot. The tumor is localized by reconstructing the 3D position of the tumor or the fiducial markers, which are automatically segmented in the X-ray images. The reconstructed position is compared with the position in the planning CT scan (Fig. 8.3). Just prior to the start of the irradiation, the correlation model is built by acquiring approximately 8 X-ray image pairs at different phases of the breathing cycle (Fig. 8.4). The Synchrony system makes a correlation model that relates the movement of the tumor or the fiducial markers and the LEDs. Non linear models are used to account for hysteresis in the tumor trajectory. Using this model, the linear accelerator can continuously track the motion of the tumor via the motion of the LEDs. The correlation model is intermittently validated and updated throughout treatment by acquiring new X-ray image pairs (typically every 1–6 min at our site). After each image-pair acquisition, the correlation model error is displayed on the system console. This measures the distance between the tumor position detected from the new images and the expected position based on the current correlation model. If the correlation model error is larger than 5 mm, a system interruption is generated and the operator has to build a new model.

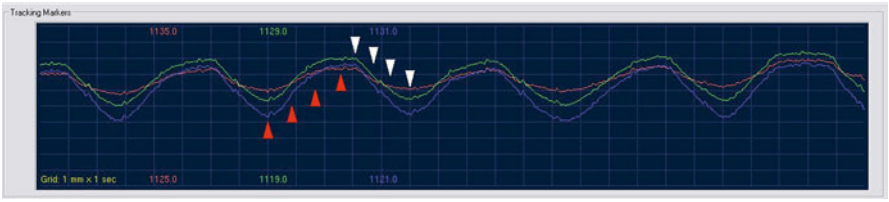

Fig. 8.4 The timing of imaging to calculate tumor trajectory in three dimensions. *Green*, *blue*, and *purple lines*: breathing cycle as recorded with the Synchrony camera; *red arrows*, imaging during expiration; *white arrows*, imaging during inspiration. In reality the image acquisitions are spaced over multiple breathing cycles and can be timed automatically by the Synchrony system to ensure that the entire respiratory cycle is evenly sampled

Otherwise, the new tumor position and corresponding LED positions are added as a new data point into the existing set of correlation model data points, and the model is regenerated such that the model adapts during each treatment fraction to changes in the internal external motion correlation [13–18]. Tumor tracking during respiration can be done in two ways using the CyberKnife system: one way is with the use of digital radiographic images of the tumor with the Xsight lung system and the other way is with the use of fiducial markers. The Xsight lung system was commercially released in 2006 and has been updated twice since then by the vendor. Clinical experience with the latest algorithms is currently limited. On the other hand, several CyberKnife users did report on the technique to place fiducials based on extensive clinical experience. In total, five different techniques are available to place markers: (1) bronchoscopic, (2) percutaneous intrapulmonary, (3) percutaneous extrapulmonary, (4) intravascular, and (5) bronchoscopic with electromagnetic navigation.

8.2.3 CT-Based Internal Gross Tumor Volume (ITV)

The movement of tumors in the lung depends on their location within the lung. These tumors often move by more than 1 cm and sometimes as much as 3 cm during deep inspiration or expiration. The reduction of margins with a CT-based ITV is based on the individual movement of the tumor. A tumor that is moving less than one centimeter will thus get a smaller margin than a tumor that is moving more than 1 cm. A CT-based ITV is preferably outlined on the expiratory phase of the 4 D images and registered with the outline on other respiratory phases to create a union of target contours enclosing all possible positions of the target (an ITV). Another method is to create an image of maximum intensity projection by combining data from the multiple CT data sets with data from the whole-breath cycle and modify tumor volume by visual verification of the target volume throughout the breathing phases. In this case, the ITV should consist of the GTV plus a margin to account for microscopic disease (8 mm). Even with 4D-CT, the free-breathing simulation is only a snapshot and a single stochastic sampling of the patient's respiratory cycle. Attention should be paid to irregular breathing and variations in the patient's breathing pattern over

the course of each treatment session and the entire treatment course and to the effects of these irregularities on the ITV margin [19]. If 4 D CT is not available, an ITV can be developed based on breath-hold spiral CT images that require the patient to hold his/her breath once during the simulation at the end of expiration and once at the end of inspiration, but not during treatment delivery. In this procedure, images are acquired through the use of a standard extended temporal thoracic CT protocol. In this protocol, patients are asked to breathe normally, and the extended temporal CT images are acquired at the beginning of the simulation; the isocenter is then set. Subsequently, images are obtained by using a fast CT simulation protocol while at the end of inspiration and expiration. Separate GTVs and CTVs should be delineated by a physician both on the end of expiration CT image set and on the end of inspiration image set. An ITV is then generated by combining the two CTVs on the extended temporal CT scan to form an ITV that includes the entire path of the CTV as it moves from inspiration to expiration. Normal tissues should be contoured in the extended temporal CT images as well. The ITV will be superimposed on the slow CT images, which will serve as the basis for treatment planning [20].

8.2.4 Forced Shallow Breathing with Abdominal Compression

The patient is immobilized in a stereotactic body frame (Fig. 8.5). This usually consists of a vacuum pillow and a rigid frame with a laser system attached for positioning and a diaphragm control device. Several small tattoos are placed on the patient's chest for repeated positioning. A pressure can be applied to the upper abdomen using the diaphragm control device. This device consists of an abdominal plate and a screw that is attached to the body frame (Fig. 8.6). The pressure on the upper abdomen is regulated by adjusting the height of the plate with the screw (Fig. 8.7). The patient is now only able to have shallow breathing. Margin reduction from CTV to PTV is possible because on one hand the tumor will move less than 1 cm due to the shallow breathing and on the other hand due to the exact immobilization with the whole body frame and the abdominal compression [21–24].

8.2.5 Breath-Hold Methods

With the breath-hold methods, the CTV to PTV margin is reduced because radiation is only delivered when the tumor is not moving during the breath hold. This method is also called the deep inspiration breath-hold technique (DIBH). Barnes et al. found that, on average, self-gated DIBH decreased the percent of lung volume receiving 20 Gy (V20) from 12.8 to 8.8 % with GTV-to-PTV margin reduction [25].

In the DIBH technique, the patient is initially maintained at quiet tidal breathing, followed by a deep inspiration, a deep expiration, a second deep inspiration, and breath hold. At this point the patient is at approximately 100 % vital capacity, and simulation, verification, and treatment take place during this phase of breath-holding.

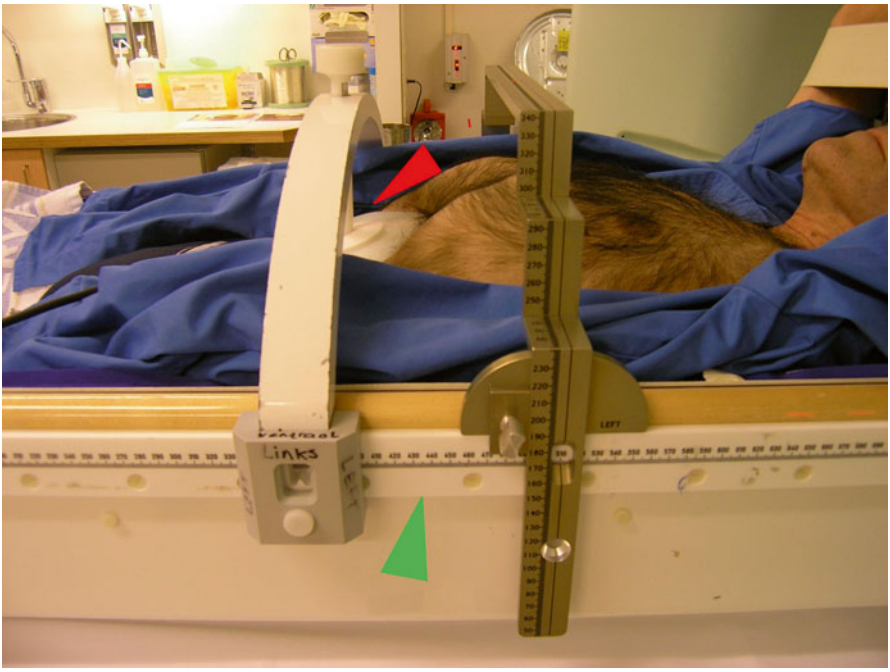

Fig. 8.5 The whole body frame with abdominal immobilization. *Green arrow*, the whole body frame; *red arrow*, the abdominal compression plate

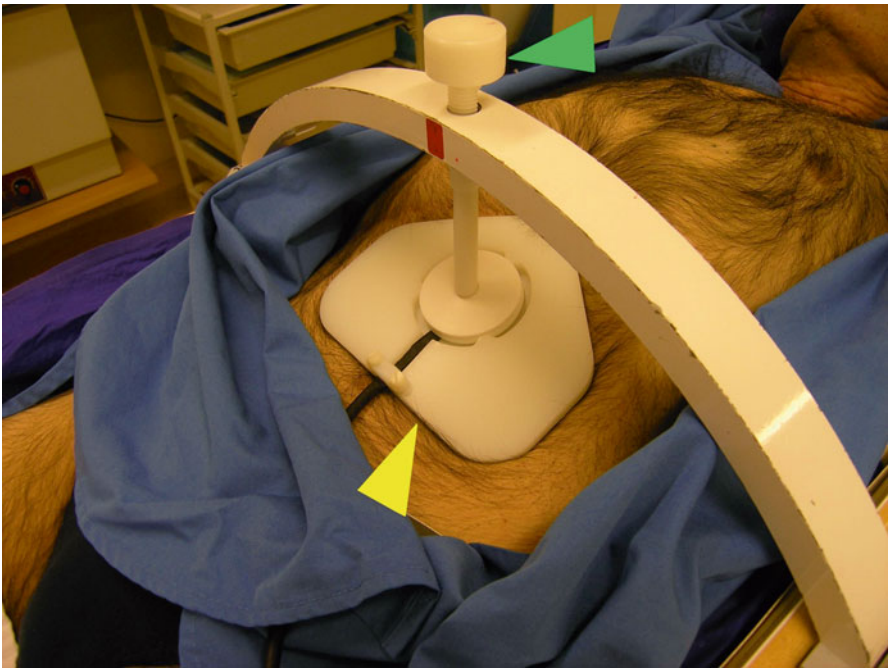

Fig. 8.6 A detailed picture of the whole body frame with abdominal immobilization. *Yellow arrow*, abdominal plate; *green arrow*, screw to regulate the degree of abdominal compression

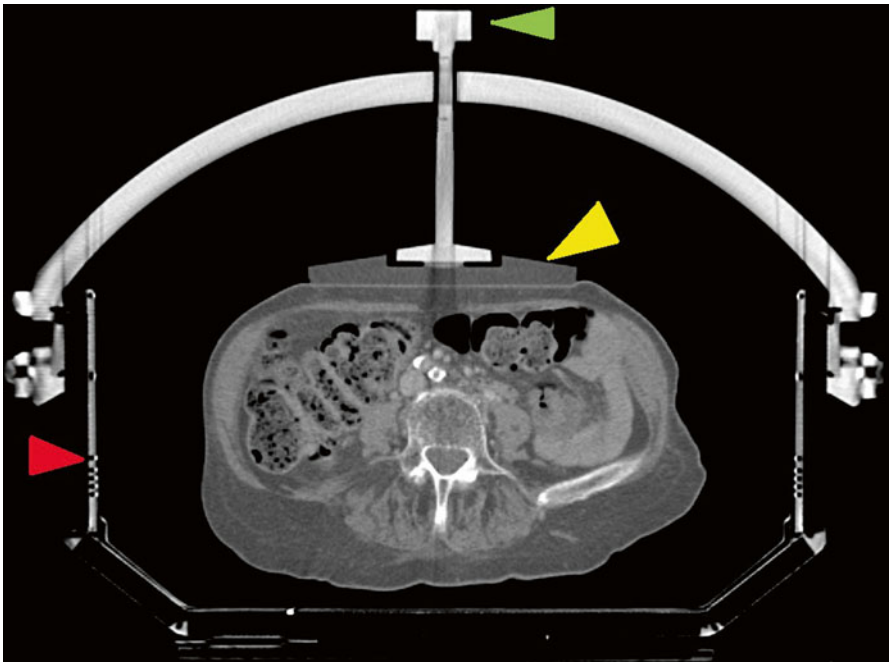

Fig. 8.7 A CT scan slice through the whole body frame. *Red arrow*, the whole body frame; *yellow arrow*, abdominal plate; *green arrow*, screw to regulate the degree of abdominal compression

Different methods have been implemented based on this principle. To monitor lung inflation levels, the patient breaths through a mouthpiece connected to a differential pressure pneumotachograph spirometer or modified ventilator interfaced to a laptop computer to monitor the air flow. A nose clip is used to prevent nasal breathing [26–28]. If the patient is at the right inspiration level, the therapist can turn on the beam. With another method, the patient controls an interlock of a modified linear accelerator if he/she reaches the right inspiration level. The therapist turns on the beam when the patient judges that he/she has attained the correct breath-hold level (=self-gated DIBH). To familiarize the patient with the procedure, a training session is given a few days before the planned simulation. Breath-holding techniques may be poorly tolerated by patients with mediocre lung function, and active patient and therapist participation is often required [29].

8.2.6 Respiratory Gating Methods

The ITV is smaller because irradiation of the tumor only occurs during a certain phase in the breathing cycle. A device monitors patient breathing and allows delivery of radiation only during certain respiratory phases, synchronous with the patient's respiratory cycle. Several devices have been developed; however, the real-time position management respiratory gating system (RPM) is most commonly used [30–32]. This system uses two passive reflective markers that are placed on the patient's chest

or abdomen. An illuminator sends infrared light to the reflective markers and the markers send the light back to a video camera. The respiratory movement is tracked by the upper marker; the lower marker calibrates the system. A computer processes the video signals and sends on-off control signals to the linear accelerator. The patient has to breathe regularly and stably during simulation and treatment. At the start of the simulation and the irradiation, the minimum and maximum position of the upper marker is determined by recording a few breathing cycles [33]. The planning CT scan must be acquired in the same phase of the breathing cycle as the treatment.

8.3 Simulation, Treatment Planning, Constraints, and Prescription

The simulation depends on the radiation therapy technique as is explained in Chap. 6. Usually, the patient is simulated and treated in the prone position with or without a vacuum mattress to minimize motion of the patient. The treatment planning CT scan is performed with intravenous contrast, usually with a wide-bore multi-slice computed tomography (CT) simulator. The use of 4D CT scans, exhale or inhale CT scan combined or not combined with a contrast enhanced planning CT scan, depends on the radiation technique (see Chap. 6). The patient is scanned from his/her teeth to the middle of his/her abdomen, and the trans axial imaging has a slice thickness of 1.5–3 mm.

The planning CT is transferred to the treatment planning system (TPS). The tumor and organs at risk (OAR) are then contoured. The gross tumor volume (GTV) is contoured using the lung window. Margins to the GTV are added depending on the radiation technique (see Chap. 6). The OAR consist of both lungs, esophagus, the heart, and the spinal cord.

Usually, inverse treatment planning is used; however, the treatment plan can also be calculated using forward planning, and depending on the radiation technique, the number of beams varies between 7 and 15 using conventional IG-IMRT techniques or up to 150 beams using stereotactic radiotherapy with the CyberKnife. The total dose is prescribed to the isodose surface that covers 95 % of the volume of the PTV. The total dose depends on the fractionation scheme (see Chap. 5 and 6). The dose to normal tissues (lungs, heart, spinal cord, etc.) should be within the constraints. An example of dose constraints to the OAR using different treatment schedules is shown in Table 8.1. Two opposite (90°) digitally reconstructed radiographs (DRRs) are generated to align the patient correctly; however, also this depends on the radiation technique.

8.4 Clinical Outcome of Primary Lung Tumors

8.4.1 Introduction

Stereotactic body radiotherapy (SBRT) targets and delivers high ablative doses of radiation to sites within the body while applying methods to reduce the effects of tumor motion to help assure accuracy and precision, as described in Chap. 6.

Table 8.1 Dose constraints

Dose constraints for		1 fraction	3 fractions	5 fractions	7 fractions
Organ	Volume	Dose (Gy/fr)	Dose (Gy/fr)	Dose (Gy/fr)	Dose (Gy/fr)
Spinal cord	Any point	12.5	6	5.5	4.5
Esophagus	Any point	13	7	7	6
Heart	Any point	15	12	10	8
Trachea and main bronchus	Any point	16	10	10	8
Plexus brachialis	Any point	14	8	6	5
Liver	Any point	30	20	12	8
Lung	V_{20} (EQD2)	<31 %	<31 %	<31 %	<31 %

V_{20} (EQD2): the volume (in %) receiving ≥20 Gy, expressed in equivalent dose of 2 Gy

However, caution must be taken if the tumor is close to organs at risk such as the trachea, mainstem bronchus, esophagus, or heart. Serious complications, including death following bacterial pneumonia, pericardial effusion, radiation pneumonitis, or massive hemoptysis, have been reported [34, 35]. Therefore, the tumors are classified into two groups: the peripheral tumors and the central tumors. Although there are several definitions, central tumors are tumors located <2 cm from the trachea, mainstem bronchus, main bronchus, or esophagus, as well as tumors located close to the heart and tumors located in the mediastinum.

SBRT to peripheral tumors has resulted in high local tumor control rates [9–11]. An example of an excellent local control in one patient is shown in Fig. 8.8. Less experience exists in SBRT for central lung tumors because they are relatively rare and because common SBRT dosing schedules, such 3 fractions of 20 Gy, cannot be safely used due to the proximity of the trachea, mainstem bronchus, esophagus, or heart. By increasing the number of fractions to 5, 8 or even 10 and reducing the fractional dose, some groups have reported successful treatment of central lung tumors with minimal complications [36]. However, some authors did report grade 5 toxicity related to the treatment [34, 37–39].

8.4.2 Peripheral Tumors

Although many articles did report the outcome of stereotactic radiotherapy of peripheral tumors, a randomized trial comparing surgery or different methods of radiation delivery has not been done. Treatment schedules with single fractions were mainly used in the beginning but are still used by some radiation centers. Whyte was one of the first to report his/her results with a single fraction of 15 Gy in a phase I clinical trial [40]. Later on, dose escalation studies were done [30, 34]. Hara et al. reported a 2-year local control rate for patients receiving a single fraction of 30 Gy or more of 83 % compared to 52 % in those treated with a single fraction less than 30 Gy [30]. However, Hof et al. concluded that single fraction SRT was a safe and effective treatment option for patients with small tumors but that the application to larger tumors was unclear [41]. While these articles did appear, other

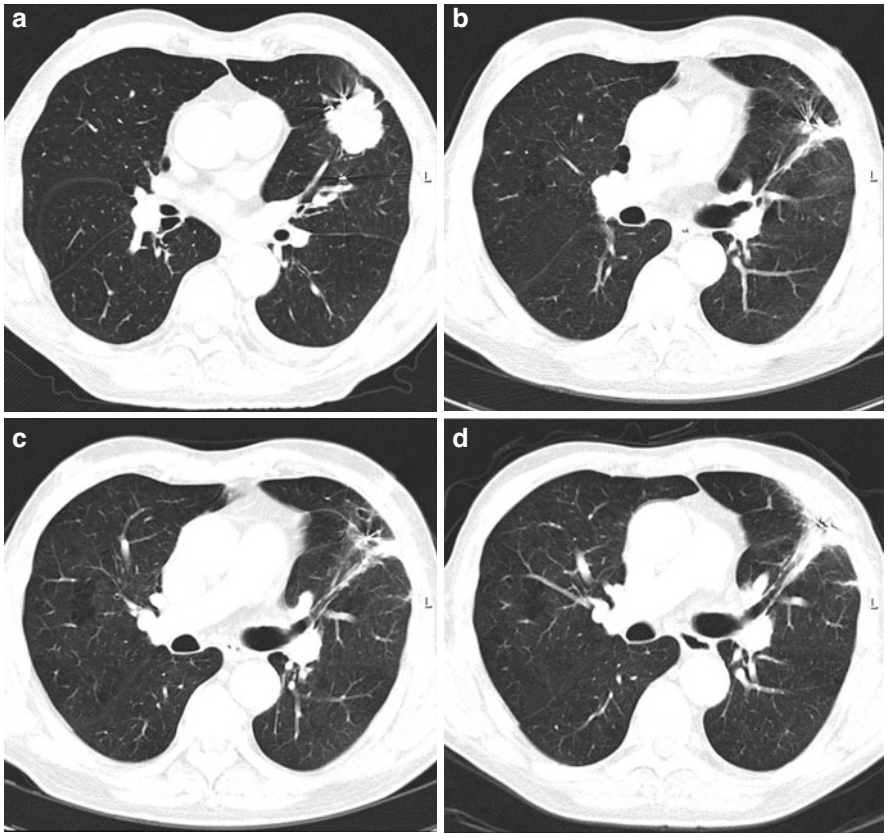

Fig. 8.8 T2 N0 NSCLC before the treatment (**a**) and the clinical result after 1 year (**b**), 2 years (**c**), and 3 years (**d**). Note pulmonary fibrotic change

articles did report the outcome of multiple fractions. The most commonly used schedule for peripheral tumors is one with 3 fractions of 18-20Gy, but schedules with 4 or more fractions also exist.

The first three most important articles are from Timmerman et al., Onishi et al., and Wulf et al. [9, 42, 43]. Timmerman et al. performed a dose escalation study with inoperable early-stage lung cancer patients. He started with 24 Gy in 3 fractions and escalated the dose at 2 Gy per fraction [42]. Patients with T1 vs T2 tumors underwent separate independent dose escalations. Thirty-seven patients were enrolled and both T-stage groups ultimately reached and tolerated 60 Gy in 3 fractions. The maximum tolerated dose for this therapy in either T-stage group was not reached. Tumors responded to treatment in 87 % of patients (complete response, 27 %). After a median follow-up period of 15 months, 6 patients experienced local failure, all of whom had received doses of <18 Gy per fraction since February 2000. One patient experienced grade 3 pneumonitis and another patient had grade 3 hypoxia. Onishi et al. reported in 2004 the clinical outcome of a Japanese multicenter

Table 8.2 Local control after treatment for early-stage lung cancer, peripherally located

Technique	Number of patients	Total dose	Number of fractions	Local control at 2 years (%)	Author
Real-time tumor tracking	70	60	3	96	Van der Voort et al. [10]
Real-time tumor tracking	20	42–60	3	95	Vahdat et al. [44]
CT-based ITV	591	60	3–5-8	93	Verstegen et al. [45]
Real-time tumor tracking	43	50	10	95	Xia et al. [46]
Whole body frame	45	48	4	100	Nagata et al. [47]
Breath hold or respiratory gating	20	45–54	3–4	94	Ng et al. [48]

study [9]. Two hundred forty-five patients with stage I NSCLC (T1N0M0, n = 155; T2N0M0, n = 90) were treated with hypofractionated high-dose stereotactic radiotherapy in 13 institutions. Stereotactic three-dimensional treatment was performed using non-coplanar dynamic arcs or multiple static ports. A total dose of 18–75 gray (Gy) at the isocenter was administered in 1–22 fractions. The median calculated biologic effective dose (BED) was 108 Gy (range, 57–180 Gy). Local progression after a median follow-up of 24 months occurred in 14.5 %, and the local recurrence rate was 8.1 % for BED ≥100 Gy compared with 26.4 % for <100 Gy ($p < 0.05$). The 3-year overall survival rate of medically operable patients was 88.4 % for BED ≥100 Gy compared with 69.4 % for <100 Gy ($P < 0.05$).

Wulf et al. compiled the results of several studies. They included both lung metastases (n = 56) and primary lung tumors (n = 36) [43]. Twenty-four patients receiving 3 × 10 Gy, 22 patients receiving 3 × 12.5 Gy, and thirty-one patients receiving 1 × 26 Gy had 2-year local control rates of 71, 92, and 100 % respectively. After a median follow-up of 14 months (2–85 months), 11 local recurrences were observed with significant advantage for higher doses. These 3 studies did show the efficacy of a biologically effective dose (BED) of 100 Gy or more, and therefore, these are the most used schedules with 3 fractions of 17–20 Gy. With the current techniques as described in Chap. 6, the 2-year local control is 93 % or more (see Table 8.2). The 2-year overall survival varies between 58 and 91 %, but depends on patient selection as most treated patients are not candidates for surgery due to their comorbidities as cardiovascular and pulmonary diseases (see Table 8.3).

8.4.3 Central Lung Tumors

The tumor-ablative effects of high-dose SBRT for lung cancer can be safely extended to lesions in the central chest if treatment is adapted to reduce the risk of OAR injury. Several studies have now shown that delivering lower doses over 4–10 fractions can considerably reduce toxicity of SBRT in the central chest [11, 39, 44,

Table 8.3 Survival after treatment for early-stage lung cancer, peripherally located

Technique	Number of patients	Total dose	Number of fractions	Survival at 2 years	Author
Real-time tumor tracking	70	60	3	63 %	Van der Voort et al. [10]
Real-time tumor tracking	20	42–60	3	90	Vahdat et al. [46]
CT-based ITV	591	60	3–5-8	65	Verstegen et al. [45]
CT-based ITV	43	50	10	91	Xia et al. [44]
Whole body frame	45	45	3	71	Nyman et al. [49]
Whole body frame	45	48	4	90 (T1N0M0)	Nagata et al. [47]
				72 (T2N0M0)	
Breath hold or respiratory gating	35	60	10	58	Onishi et al. [50]

51–54], although doses that are often used in treating peripheral lung lesions can result in serious toxicity and death when delivered to central lesions [24, 34, 35, 37] or can result in at least a higher rate of toxicity than for peripheral lesions [38]. The published studies to date have typically consisted of a mixed population of peripheral and central tumors and included a relatively small number of patients (8–27 patients) with central tumors. However, 2 studies reported on a larger group: Haasbeek et al. reported on 63 patients who were treated with eight fractions of 7.5 Gy [55]. Of these 63, 37 patients had a tumor at a central hilar location, whereas 26 patients had tumors abutting the pericardium or mediastinal structures. The median follow-up was 35 months. Three-year local control rate was 92.6 %, and the 3-year overall survival rate was 64.3 %. Nuyttens et al. reported on 58 central lesions in 56 patients (39 with primary, 17 with metastatic tumors) [56]. Fifteen tumors located near the esophagus were treated with 6 fractions of 8 Gy. Other tumors were treated according to the following dose escalation scheme: 5 fractions of 9 Gy (n = 6), then 5 fractions of 10 Gy (n = 15), and finally 5 fractions of 12 Gy (n = 22). In 21 patients, the coverage of the PTV was reduced below 95 % to protect adjacent organs at risk. At a median follow-up of 23 months, the actuarial 2-year local tumor control was 85 % for tumors treated with a BED >100 Gy compared to 60 % for tumors treated with a BED ≤100 Gy. The median volume of the main bronchus irradiated to an EQD2 of 130 Gy or a BED of 216 Gy in 29 patients was 0.4 cm^3 (range, 0.001–4.9 cm^3). The median Dmax to the esophagus was 88 Gy_3 EQD2 of 143 Gy BED.

In some studies in which lower doses per fraction were delivered, reduced toxicity seemed to come at the expense of local control. For example, Taremi et al. delivered 50 or 60 Gy in 8 fractions to 20 patients with central lesions (out of 108 patients treated overall) and observed no severe toxicity related to tumor location [54]. However, seven of the ten local recurrences were central lesions, five of which were treated with 50 Gy. Chang et al. observed low toxicity but a high recurrence rate (43 %) in seven patients treated with 40 Gy in 4 fractions [52]. A similar combination of low dose (BED < 100 Gy) with relatively low toxicity and relatively low local

control was obtained by Onimaru et al. [39] and Guckenberger et al. [57]. We treated several of our patients with doses lower than 50 Gy and found a statistical trend toward poorer tumor control in these patients, a finding that is consistent with these reports.

Other authors, however, have reported the ability to deliver doses equal to or above BED = 100 Gy, resulting in the combination of good tumor control (>85 % at 1.5–2 years) and low toxicity [11, 44, 53]. Stephans et al., for example, were able to treat central lung lesions without serious toxicity using 50 Gy delivered in 5 fractions [53]. Patients were immobilized in a stereotactic frame and abdominal compression was applied to reduce tumor motion. Tumor control at a median follow-up of 18.4 months was 98 %.

A risk-adapted treatment of central lesions requires both a consideration of the maximum overall and fraction doses and care to optimize the dose distribution to meet strict dose constraints for sensitive central structures, because several authors did report grade 4 and 5 toxicity (see Chap. 6). The fact that even doses as low as 40 Gy can cause significant complications points to the critical importance of careful treatment planning, accurate patient setup, and precise radiation delivery throughout a treatment fraction [24].

8.5 Clinical Outcome in the Treatment of Lung Metastases

Patients with metastatic disease to the lung who are referred for radiotherapy are, for a number of reasons, a very different group: they often have centrally located lesions, may have one or more lesions in each lung, have previously undergone a lobectomy or pneumonectomy, or are bad surgical candidates due to their medical condition. The presumed state of oligometastasis, as described by Hellman et al., is one in which lesions are detected prior to the widespread distribution of malignant cells [58]. In such a state, an effective local therapy such as SRT should, in theory, arrest the disease progression and extend life. If a local therapy is non invasive and associated with low toxicity, then life-extending treatment can be delivered without seriously impacting a patient's quality of life during or after treatment [59, 60]. Combined with surgical and chemotherapeutic approaches as necessary, as well as aggressive use of modern imaging to detect smaller, tumours, the potential to control disease progression over the long term with stereotactic radiotherapy makes it a powerful tool in the oligometastatic state. Stereotactic radiotherapy may also be applied in patients who cannot endure surgery, or patients who have undergone repeated systemic treatments, thus extending the potential of local treatment of oligometastases to patients who might otherwise have been treated palliatively.

Published reports of SRT for lung oligometastases reveal a wide variety of dose/fractionation schemes, approaches to image guidance and motion management, and related margins to account for microscopic disease extension and radiation delivery error. These reports typically show good long-term tumor control, but overall survival can be disappointing. For example, Milano et al. treated 121 patients with 5 or fewer

metastases in 10 fractions of 5 Gy; 41 % of patients had tumors in the lung. Overall survival was promising at the 2-year time point (50 %), but at 6 years, although local control was maintained at relatively high levels, overall survival fell to 20 % [61]. Similar outcomes have been reported frequently, with local control at 2–3 years ranging from 70 to 100 % but overall survival generally being much lower, typically due to progression outside the treated region, [62, 63] for example, in a phase I/II study in which 48–60 Gy was delivered in 3 fractions, obtained local control of 96 % at 2 years whilst median survival was only 19 months [62]. We can conclude from this and other studies that the identification of "oligometastatic" patients, who can benefit from long-term disease control, requires additional investigation.

8.6 Toxicity and Quality of Life

8.6.1 Toxicity of Treatment of Peripheral Lesions

The difficulty in distinguishing between treatment-related symptoms and the natural course of COPD may cause variation in the incidence of reported toxicity. The 2-year overall late toxicity is reported in 2–10 % of patients [9, 10]. Onishi et al. treated 245 patients and reported pneumonitis grade 3 and 4 of 2.4 %, esophagitis grade 2 and 3 of 2 %, and rib fractures in 0.8 % [9]. Grade 1 pulmonary symptoms resolved in most patients with or without steroid therapy, but continuous oxygen supply was required in three patients who displayed poor respiratory function before irradiation. Chronic segmental bronchitis and wall thickening causing atelectasis on the peripheral lung were observed in one patient. Grade 3 or 4 dermatitis was observed in two patients with tumors adjacent to the chest wall. Verstegen et al. reported the outcome of 592 patients [45]. Severe (CTCAE v3) late toxicity was uncommon. A total of 18 patients (3 %) developed grade 3 radiation pneumonitis, 10 patients showed rib fractures on follow-up scans (2 %), and three patients experienced grade 3 chest wall pain (1 %). Van der Voort et al. reported the results of 70 patients and reported no grade 4 or 5 toxicity [10]. Acute grade 1–2 toxicity occurred in 32 patients, consisting mostly of fatigue, dyspnea, and cough. One patient had acute grade 3 toxicity, requiring morphine for severe thoracic pain. Late grade 3 toxicity was observed in seven patients (10 %). Three patients had radiation pneumonitis treated with antibiotics and corticosteroids. Four patients had thoracic pain requiring morphine. They all had a tumor near the chest wall. A rib fracture was found in one of these patients. Although most authors report a low incidence of rib fractures, Nambu et al. reported that rib fractures were seen in 41 of the 177 patients (23 %) [64]. Rib fractures appeared at a mean of 21.2 months after the completion of SRT (range, 4–58 months). Chest wall edema, thinning of the cortex, and osteosclerosis were findings frequently associated with and tending to precede rib fractures. No patients with rib fracture had tumors >16 mm from the adjacent chest wall. Chest wall pain was seen in 18 of 177 patients (10 %), of whom 14 patients

developed rib fracture. Bongers et al. found on multivariate analysis that patients with chest wall pain had larger treatment volumes and shorter tumor-chest wall distances, whereas patients with rib fractures had larger tumor diameters and treatment volumes [65]. Grade 3 chest wall pain and rib fractures were associated with larger volumes of chest wall receiving doses of 30–50 Gy and rib fractures specifically with a higher maximum dose in the chest wall. Stephans et al. reported that on multivariate analysis of 134 patients, the tumor volume was no longer correlated with symptomatic chest wall toxicity and only V30 through V60 remained statistically significant [53].

8.6.2 Toxicity of Treatment of Central Lesions

The toxicity following treatment of central lesions is quite similar with the toxicity after the treatment of peripheral lesions. However, 5 publications did report death due to pulmonary complications and two due to esophageal complications. Two authors reported the death of one patient secondary to bronchial stenosis and subsequent bleeding from the bronchus [24, 38]. In one patient, the dose to the tumor was 48 Gy in 4 fractions, and in the other patient the dose was not specified (but was probably 60 Gy in 4 fractions, based on other details in the report). Milano et al. reported one death due to fatal hemoptysis after treatment of a mediastinal mass abutting the bronchus. The cumulative dose to the bronchus was 98 Gy [66]. Le et al. reported 2 deaths due to pulmonary complications [34]. Both patients were treated previously with radiotherapy to the chest. Fakiris et al. reported five grade 5 toxicities, all possibly related to the stereotactic treatment of 22 patients and three of them due to pneumonia, one to hemoptysis, and one to respiratory failure [37]. Le et al. reported the death of one patient due to esophageal fistula followed by a fatal hemoptysis from a tracheovascular fistula [34]. Brachial plexopathy has been reported in two patients: one patient developed a brachial plexopathy that was managed medically; however, the dose to the plexus was not reported [51]. The other one developed brachial plexus neuropathy and partial arm paralysis after receiving a dose of 40 Gy (in 4 fractions) to a significant volume of the plexus [52].

8.6.3 Quality of Life

Two groups of authors studied patient quality of life after treatment. Van der Voort et al. reported the quality of life of 39 patients with pathologically confirmed T1 to T2N0M0 NSCLC [59]. The European Organization for Research and Treatment of Cancer Quality of Life Questionnaire (EORTC QLQ) C30 and the QLQ LC13 lung cancer-specific questionnaire were used to investigate changes in quality of life.

Assessments were done before treatment, at 3 weeks, and at 2, 4, 6, 9, and 12 months after treatment, until death or progressive disease. Toxicity was evaluated using common terminology criteria for adverse events version 3.0. The emotional functioning improved significantly after treatment. Other function scores and QLQ-C30 and QLQ-LC13 lung symptoms (such as dyspnea and coughing) showed no significant changes. Widder et al. investigated changes of health-related quality of life parameters after stereotactic radiotherapy (202 patients) and 3 D treatment (27 patients) [67]. Two prospective cohorts of inoperable patients with T1–2N0M0 primary lung tumors were analyzed. Patients received 70 Gy in 35 fractions with 3D CRT or 60 Gy in three to eight fractions with stereotactic radiotherapy. The EORTC QLQ-C30 and the QLQ-LC13 lung cancer-specific questionnaire were also used. Global quality of Life and physical functioning were stable after stereotactic radiotherapy ($p=0.21$ and $p=0.62$, respectively). Dyspnea increased after stereotactic radiotherapy by 3.2 out of 100 points ($p<0.01$), which is clinically insignificant. At 1 year, physical performance status decreased by an excess of 8.7 out of 100 points ($p<0.01$) after 3D CRT compared with stereotactic radiotherapy.

8.7 Conclusion

Stereotactic radiation can minimize lung toxicity in the treatment of early stage lung cancer. However, respiratory motion of the tumors may often lead to inclusion of surrounding normal lung in the target volume. In stereotactic radiotherapy, many different techniques have been developed to control for motion of tumors in the lung. The local control is excellent for peripheral tumors. The local control for central tumors depends on the total dose administered. The reported overall survival varies but depends on the patient selection. The toxicity in the treatment of peripheral tumors is low. When treating central tumors, caution must be taken because the organs at risk are close and high toxicity has been reported by some authors.

References

1. Shields TW. Surgical therapy for carcinoma of the lung. Clin Chest Med. 1993;14(1):121–47.
2. Naruke T, Goya T, Tsuchiya R, Suemasu K. Prognosis and survival in resected lung carcinoma based on the new international staging system. J Thorac Cardiovasc Surg. 1988;96(3):440–7.
3. Mountain CF. Revisions in the international system for staging lung cancer. Chest. 1997;111(6):1710–7.
4. Adebonojo SA, Bowser AN, Moritz DM, Corcoran PC. Impact of revised stage classification of lung cancer on survival: a military experience. Chest. 1999;115(6):1507–13.
5. McGarry RC, Song G, des Rosiers P, Timmerman R. Observation-only management of early stage, medically inoperable lung cancer: poor outcome. Chest. 2002;121(4):1155–8.
6. Prevost JB, Voet P, Hoogeman M, Praag J, Levendag P, Nuyttens JJ. Four-dimensional stereotactic radiotherapy for early stage non-small cell lung cancer: a comparative planning study. Technol Cancer Res Treat. 2008;7(1):27–34.

7. Seppenwoolde Y, Shirato H, Kitamura K, Shimizu S, van Herk M, Lebesque JV, et al. Precise and real-time measurement of 3D tumor motion in lung due to breathing and heartbeat, measured during radiotherapy. Int J Radiat Oncol Biol Phys. 2002;53(4):822–34.
8. Keall PJ, Mageras GS, Balter JM, Emery RS, Forster KM, Jiang SB, et al. The management of respiratory motion in radiation oncology report of AAPM Task Group 76. Med Phys. 2006;33(10):3874–900.
9. Onishi H, Araki T, Shirato H, Nagata Y, Hiraoka M, Gomi K, et al. Stereotactic hypofractionated high-dose irradiation for stage I nonsmall cell lung carcinoma: clinical outcomes in 245 subjects in a Japanese multiinstitutional study. Cancer. 2004;101(7):1623–31.
10. van der Voort van Zyp NC, Prevost JB, Hoogeman MS, Praag J, van der Holt B, Levendag PC, et al. Stereotactic radiotherapy with real-time tumor tracking for non-small cell lung cancer: clinical outcome. Radiother Oncol. 2009;91(3):296–300.
11. Lagerwaard FJ, Haasbeek CJ, Smit EF, Slotman BJ, Senan S. Outcomes of risk-adapted fractionated stereotactic radiotherapy for stage I non-small-cell lung cancer. Int J Radiat Oncol Biol Phys. 2008;70(3):685–92.
12. Purdy JA. Current ICRU definitions of volumes: limitations and future directions. Semin Radiat Oncol. 2004;14(1):27–40.
13. Schweikard A, Glosser G, Bodduluri M, Murphy MJ, Adler JR. Robotic motion compensation for respiratory movement during radiosurgery. Comput Aided Surg. 2000;5(4):263–77.
14. Murphy MJ. Tracking moving organs in real time. Semin Radiat Oncol. 2004;14(1):91–100.
15. Chang SD, Adler JR. Robotics and radiosurgery—the cyberknife. Stereotact Funct Neurosurg. 2001;76(3–4):204–8.
16. Adler Jr JR, Chang SD, Murphy MJ, Doty J, Geis P, Hancock SL. The Cyberknife: a frameless robotic system for radiosurgery. Stereotact Funct Neurosurg. 1997;69(1–4 Pt 2):124–8.
17. Nuyttens JJ, van de Pol M. The CyberKnife radiosurgery system for lung cancer. Expert Rev Med Devices. 2012;9(5):465–75.
18. Sayeh S, Wang J, Main WT, Kilby W, Maurer Jr CR. Respiratory motion tracking for robotic radiosurgery. In: Urschel Jr HC, Kresl JJ, Luketich JD, Papiez L, Timmerman RD, editors. Robotic Radiosurgery: Treating Tumors that Move with Respiration. Berlin: Springer; 2007. p. 15–29.
19. Britton KR, Starkschall G, Tucker SL, Pan T, Nelson C, Chang JY, et al. Assessment of gross tumor volume regression and motion changes during radiotherapy for non-small-cell lung cancer as measured by four-dimensional computed tomography. Int J Radiat Oncol Biol Phys. 2007;68(4):1036–46.
20. Fukumoto S, Shirato H, Shimzu S, Ogura S, Onimaru R, Kitamura K, et al. Small-volume image-guided radiotherapy using hypofractionated, coplanar, and noncoplanar multiple fields for patients with inoperable Stage I nonsmall cell lung carcinomas. Cancer. 2002;95(7):1546–53.
21. Guckenberger M, Wilbert J, Meyer J, Baier K, Richter A, Flentje M. Is a single respiratory correlated 4D-CT study sufficient for evaluation of breathing motion? Int J Radiat Oncol Biol Phys. 2007;67(5):1352–9.
22. Jensen HR, Hansen O, Hjelm-Hansen M, Brink C. Inter- and intrafractional movement of the tumour in extracranial stereotactic radiotherapy of NSCLC. Acta Oncol. 2008;47(7):1432–7.
23. Hansen AT, Petersen JB, Hoyer M. Internal movement, set-up accuracy and margins for stereotactic body radiotherapy using a stereotactic body frame. Acta Oncol. 2006;45(7):948–52.
24. Song SY, Choi W, Shin SS, Lee SW, Ahn SD, Kim JH, et al. Fractionated stereotactic body radiation therapy for medically inoperable stage I lung cancer adjacent to central large bronchus. Lung Cancer. 2009;66(1):89–93.
25. Barnes EA, Murray BR, Robinson DM, Underwood LJ, Hanson J, Roa WH. Dosimetric evaluation of lung tumor immobilization using breath hold at deep inspiration. Int J Radiat Oncol Biol Phys. 2001;50(4):1091–8.
26. Wong JW, Sharpe MB, Jaffray DA, Kini VR, Robertson JM, Stromberg JS, et al. The use of active breathing control (ABC) to reduce margin for breathing motion. Int J Radiat Oncol Biol Phys. 1999;44(4):911–9.

27. Rosenzweig KE, Hanley J, Mah D, Mageras G, Hunt M, Toner S, et al. The deep inspiration breath-hold technique in the treatment of inoperable non-small-cell lung cancer. Int J Radiat Oncol Biol Phys. 2000;48(1):81–7.
28. Mah D, Hanley J, Rosenzweig KE, Yorke E, Braban L, Ling CC, et al. Technical aspects of the deep inspiration breath-hold technique in the treatment of thoracic cancer. Int J Radiat Oncol Biol Phys. 2000;48(4):1175–85.
29. Jiang SB. Radiotherapy of mobile tumors. Semin Radiat Oncol. 2006;16(4):239–48.
30. Hara R, Itami J, Kondo T, Aruga T, Abe Y, Ito M, et al. Stereotactic single high dose irradiation of lung tumors under respiratory gating. Radiother Oncol. 2002;63(2):159–63.
31. Shirato H, Shimizu S, Kitamura K, Nishioka T, Kagei K, Hashimoto S, et al. Four-dimensional treatment planning and fluoroscopic real-time tumor tracking radiotherapy for moving tumor. Int J Radiat Oncol Biol Phys. 2000;48(2):435–42.
32. Shirato H, Shimizu S, Kunieda T, Kitamura K, van Herk M, Kagei K, et al. Physical aspects of a real-time tumor-tracking system for gated radiotherapy. Int J Radiat Oncol Biol Phys. 2000;48(4):1187–95.
33. Giraud P, Yorke E, Ford EC, Wagman R, Mageras GS, Amols H, et al. Reduction of organ motion in lung tumors with respiratory gating. Lung Cancer. 2006;51(1):41–51.
34. Le QT, Loo BW, Ho A, Cotrutz C, Koong AC, Wakelee H, et al. Results of a phase I dose-escalation study using single-fraction stereotactic radiotherapy for lung tumors. J Thorac Oncol. 2006;1(8):802–9.
35. Timmerman R, McGarry R, Yiannoutsos C, Papiez L, Tudor K, DeLuca J, et al. Excessive toxicity when treating central tumors in a phase II study of stereotactic body radiation therapy for medically inoperable early-stage lung cancer. J Clin Oncol. 2006;24(30):4833–9.
36. Chi A, Liao Z, Nguyen NP, Xu J, Stea B, Komaki R. Systemic review of the patterns of failure following stereotactic body radiation therapy in early-stage non-small-cell lung cancer: clinical implications. Radiother Oncol. 2010;94(1):1–11.
37. Fakiris AJ, McGarry RC, Yiannoutsos CT, Papiez L, Williams M, Henderson MA, et al. Stereotactic body radiation therapy for early-stage non-small-cell lung carcinoma: four-year results of a prospective phase II study. Int J Radiat Oncol Biol Phys. 2009;75(3):677–82.
38. Bral S, Gevaert T, Linthout N, Versmessen H, Collen C, Engels B, et al. Prospective, risk-adapted strategy of stereotactic body radiotherapy for early-stage non-small-cell lung cancer: results of a phase II trial. Int J Radiat Oncol Biol Phys. 2010;12.
39. Onimaru R, Shirato H, Shimizu S, Kitamura K, Xu B, Fukumoto S, et al. Tolerance of organs at risk in small-volume, hypofractionated, image-guided radiotherapy for primary and metastatic lung cancers. Int J Radiat Oncol Biol Phys. 2003;56(1):126–35.
40. Whyte RI, Crownover R, Murphy MJ, Martin DP, Rice TW, DeCamp Jr MM, et al. Stereotactic radiosurgery for lung tumors: preliminary report of a phase I trial. Ann Thorac Surg. 2003;75(4):1097–101.
41. Hof H, Muenter M, Oetzel D, Hoess A, Debus J, Herfarth K. Stereotactic single-dose radiotherapy (radiosurgery) of early stage nonsmall-cell lung cancer (NSCLC). Cancer. 2007;110(1):148–55.
42. Timmerman R, Papiez L, McGarry R, Likes L, DesRosiers C, Frost S, et al. Extracranial stereotactic radioablation: results of a phase I study in medically inoperable stage I non-small cell lung cancer. Chest. 2003;124(5):1946–55.
43. Wulf J, Baier K, Mueller G, Flentje MP. Dose-response in stereotactic irradiation of lung tumors. Radiother Oncol. 2005;77(1):83–7.
44. Vahdat S, Oermann EK, Collins SP, Yu X, Abedalthagafi M, Debrito P, et al. CyberKnife radiosurgery for inoperable stage IA non-small cell lung cancer: 18 F-fluorodeoxyglucose positron emission tomography/computed tomography serial tumor response assessment. J Hematol Oncol. 2010;3:6.
45. Verstegen NE, Lagerwaard FJ, Haasbeek CJ, Slotman BJ, Senan S. Outcomes of stereotactic ablative radiotherapy following a clinical diagnosis of stage I NSCLC: comparison with a contemporaneous cohort with pathologically proven disease. Radiother Oncol. 2011;101(2):250–4.

46. Xia T, Li H, Sun Q, Wang Y, Fan N, Yu Y, et al. Promising clinical outcome of stereotactic body radiation therapy for patients with inoperable Stage I/II non-small-cell lung cancer. Int J Radiat Oncol Biol Phys. 2006;66(1):117–25.
47. Nagata Y, Takayama K, Matsuo Y, Norihisa Y, Mizowaki T, Sakamoto T, et al. Clinical outcomes of a phase I/II study of 48 Gy of stereotactic body radiotherapy in 4 fractions for primary lung cancer using a stereotactic body frame. Int J Radiat Oncol Biol Phys. 2005;63(5):1427–31.
48. Ng AW, Tung SY, Wong VY. Hypofractionated stereotactic radiotherapy for medically inoperable stage I non-small cell lung cancer—report on clinical outcome and dose to critical organs. Radiother Oncol. 2008;87(1):24–8.
49. Nyman J, Johansson KA, Hulten U. Stereotactic hypofractionated radiotherapy for stage I non-small cell lung cancer—mature results for medically inoperable patients. Lung Cancer. 2006;51(1):97–103.
50. Onishi H, Kuriyama K, Komiyama T, Tanaka S, Sano N, Marino K, et al. Clinical outcomes of stereotactic radiotherapy for stage I non-small cell lung cancer using a novel irradiation technique: patient self-controlled breath-hold and beam switching using a combination of linear accelerator and CT scanner. Lung Cancer. 2004;45(1):45–55.
51. Bradley JD, El Naqa I, Drzymala RE, Trovo M, Jones G, Denning MD. Stereotactic body radiation therapy for early-stage non-small-cell lung cancer: the pattern of failure is distant. Int J Radiat Oncol Biol Phys. 2010;77(4):1146–50.
52. Chang JY, Balter PA, Dong L, Yang Q, Liao Z, Jeter M, et al. Stereotactic body radiation therapy in centrally and superiorly located stage I or isolated recurrent non-small-cell lung cancer. Int J Radiat Oncol Biol Phys. 2008;72(4):967–71.
53. Stephans KL, Djemil T, Reddy CA, Gajdos SM, Kolar M, Machuzak M, et al. Comprehensive analysis of pulmonary function test (PFT) changes after stereotactic body radiotherapy (SBRT) for stage I lung cancer in medically inoperable patients. J Thorac Oncol. 2009;4(7):838–44.
54. Taremi M, Hope A, Dahele M, Pearson S, Fung S, Purdie T, et al. Stereotactic body radiotherapy for medically inoperable lung cancer: prospective, single-center study of 108 consecutive patients. Int J Radiat Oncol Biol Phys. 2011;4.
55. Haasbeek CJ, Lagerwaard FJ, Slotman BJ, Senan S. Outcomes of stereotactic ablative radiotherapy for centrally located early-stage lung cancer. J Thorac Oncol. 2011;6(12):2036–43.
56. Nuyttens JJ, van der Voort van Zyp NC, Praag J, Aluwini S, van Klaveren RJ, Verhoef C, et al. Outcome of four-dimensional stereotactic radiotherapy for centrally located lung tumors. Radiother Oncology. 2012;102(3):383–7.
57. Guckenberger M, Krieger T, Richter A, Baier K, Wilbert J, Sweeney RA, et al. Potential of image-guidance, gating and real-time tracking to improve accuracy in pulmonary stereotactic body radiotherapy. Radiother Oncol. 2009;91(3):288–95.
58. Hellman S, Weichselbaum RR. Oligometastases. J Clin Oncol. 1995;13(1):8–10 [Editorial].
59. van der VoortvanZyp NC, Prevost JB, van der Holt B, Braat C, van Klaveren RJ, Pattynama PM, et al. Quality of life after stereotactic radiotherapy for stage I non-small-cell lung cancer. Int J Radiat Oncol Biol Phys. 2010;77(1):31–7.
60. Tree AC, Khoo VS, Eeles RA, Ahmed M, Dearnaley DP, Hawkins MA, et al. Stereotactic body radiotherapy for oligometastases. Lancet Oncol. 2013;14(1):e28–37.
61. Milano MT, Katz AW, Zhang H, Okunieff P. Oligometastases treated with stereotactic body radiotherapy: long-term follow-up of prospective study. Int J Radiat Oncol Biol Phys. 2012;83(3):878–86.
62. Rusthoven KE, Kavanagh BD, Burri SH, Chen C, Cardenes H, Chidel MA, et al. Multi-institutional phase I/II trial of stereotactic body radiation therapy for lung metastases. J Clin Oncol. 2009;27(10):1579–84.
63. Alongi F, Arcangeli S, Filippi AR, Ricardi U, Scorsetti M. Review and uses of stereotactic body radiation therapy for oligometastases. Oncologist. 2012;17(8):1100–7.
64. Nambu A, Onishi H, Aoki S, Koshiishi T, Kuriyama K, Komiyama T, et al. Rib fracture after stereotactic radiotherapy on follow-up thin-section computed tomography in 177 primary lung cancer patients. Radiat Oncol. 2011;6:137.

65. Bongers EM, Haasbeek CJ, Lagerwaard FJ, Slotman BJ, Senan S. Incidence and risk factors for chest wall toxicity after risk-adapted stereotactic radiotherapy for early-stage lung cancer. J Thorac Oncol. 2011;6(12):2052–7.
66. Milano MT, Chen Y, Katz AW, Philip A, Schell MC, Okunieff P. Central thoracic lesions treated with hypofractionated stereotactic body radiotherapy. Radiother Oncol. 2009;91(3):301–6.
67. Widder J, Postmus D, Ubbels JF, Wiegman EM, Langendijk JA. Survival and quality of life after stereotactic or 3D-conformal radiotherapy for inoperable early-stage lung cancer. Int J Radiat Oncol Biol Phys. 2011;81(4):e291–7.

Chapter 9
Stereotactic Body Radiation Therapy to Liver

Andrew M. Gaya

Abstract Stereotactic body radiotherapy (SBRT) to liver has an increasingly important role as a locally ablative therapy in the management of colorectal and other oligometastatic disease, in combination or as an alternative to other treatment modalities such as radiofrequency ablation, radioembolisation, irreversible electroporation (NanoKnife), chemoembolisation or surgery. In primary hepatocellular carcinoma SBRT can be used as an ablative therapy in its own right, but also importantly as a bridge to liver transplantation for select patient groups. It is increasingly being used in combination or when other liver directed therapies, like radio frequency ablation or trans arterial chemoembolisation, have failed. In this chapter the evidence for SBRT in these indications is presented, and the complexities of radiotherapy planning and management of patients is discussed.

Keywords Stereotactic radiotherapy (SBRT) • Liver • Cyberknife • Liver metastases • Hepatocellular carcinoma (HCC) • SABR • Ablation

9.1 Introduction and Literature Review

Primary malignancies of the liver include hepatocellular carcinoma (HCC), which is the third most common cause of cancer death in the world [1], and intra-hepatic cholangiocarcinoma (IHC). The liver is a common site for metastases, especially from carcinomas of the lung, breast and colon [2]. For up to 40 % of patients with metastatic colorectal cancer, the liver will be the only site of metastases. This is due to venous drainage from the colon and rectum via the portal vein, and its major vascular inflow to the liver. Fifteen to twenty-five per cent of patients will have liver metastases at the time of diagnosis (synchronous—worse prognosis), and a further 50 % develop liver metastases during the course of their illness [3].

A.M. Gaya, MD
Department of Clinical Oncology, Guy's and St Thomas' NHS Foundation Trust, London, UK
e-mail: agaya@theloc.com

A. Gaya, A. Mahadevan (eds.), *Stereotactic Body Radiotherapy: A Practical Guide*,
DOI 10.1007/978-0-85729-597-2_9

9.2 HCC/IHC

HCC is the third most common cancer in the world, responsible for over 19,000 deaths annually in the United States alone. HCC accounts for 90 % of primary liver cancers. The disease often presents in patients with advanced cirrhosis (chronic hepatitis B/C, chronic alcohol use, haemochromatosis etc.), and orthotopic liver transplant provides the greatest chance for both cure and long-term survival. Resection is also performed for more limited disease in patients with reasonable liver function. Results give variable 5-year survival rates from 30 to 82 %, but surgery is feasible in only 20–30 % of patients [1, 4, 5]. Liver function is important in treatment decision making. The best survival outcomes are for HCC fulfilling the Milan transplant criteria (single HCC <5 cm or ≤3HCC <3 cm).

Surgical resection and percutaneous ablation can provide comparable rates of long-term overall survival, but pre-existing hepatic dysfunction and lesion size can significantly limit both the use and efficacy of these techniques [6].

Non-surgical treatment options for HCC and IHC include Radiofrequency Ablation (RFA), Transarterial chemoembolisation (TACE), percutaneous ethanol injection (PEI), systemic chemotherapy, and radiotherapy. The small molecule tyrosine kinase inhibitors show promise for the treatment of HCC, but currently results appear disappointing for IHC.

Many HCC staging systems have been developed which incorporate the number and extent of tumors, and the degree of vascular involvement. The Barcelona Clinic Liver Cancer (BCLC) system is amongst the most widely used (Fig. 9.1) [7].

RFA achieves excellent control rates of >90 % for HCC and IHC if lesions are less than 3–3.4 cm in diameter, but local recurrences are more common if tumours are adjacent to large vessels which exert a cooling effect, or are larger than 4 cm diameter [8, 9]. In addition tumours close to the biliary tract or near the diaphragm can be technically demanding to ablate, making the procedure highly operator dependent.

Palliative TACE offers only a modest gain in overall survival compared with best supportive care in advanced HCC and IHC, but can also be used as a bridge to transplant in conjunction with other local ablative options [10, 11].

Systemic chemotherapy with agents such as doxorubicin, cisplatin, gemcitabine, and oxaliplatin for HCC has disappointing response rates (5–20 %), and does not prolong survival [12–14]. Newer targeted agents such as Sorafenib (SHARP trial), Sunitinib and Erlotinib are showing promise [15, 16], but are unlikely to be associated with cure in the absence of local ablative therapies. A phase 3 trial comparing sorafenib with sunitinib was stopped early due to safety concerns over sunitinib [17].

Systemic chemotherapy for IHC with Gemcitabine & Cisplatin has a response rate of 30 % [18]. Sorafenib had a response rate of 0 % in a SWOG study [19]. Studies of newer Tyrosine Kinase Inhibitors are ongoing.

Historically, the role of radiotherapy for liver tumours has been limited by the risk of radiation-induced liver disease (RILD). RILD is characterised by anicteric hepatomegaly, ascites, and elevated alkaline phosphatase occurring within 3 months of liver irradiation [20]. Recently, however, advances in radiotherapy technique (including radiotherapy planning, motion management strategies, and image guidance) have made it possible for radiation to be delivered conformally to partial liver volumes. Dawson et al. analysed over 180 patients and demonstrated that the liver exhibits a large volume effect with a low volume threshold for RILD [21]. Emami et al. have

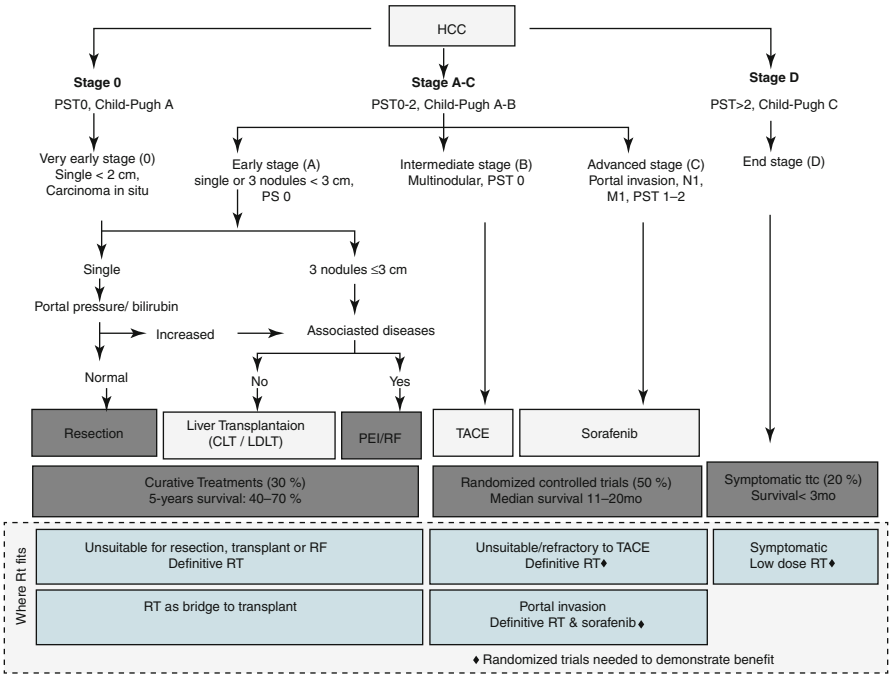

Fig. 9.1 Barcelona Clinic Liver Cancer Staging System (From Klein et al. [7] based on Dawson [102]) This figure describes potential treatment options, and suggestions for the incorporation of radiotherapy treatment, and trials. *CLT* cadaver liver transplant, *LDLT* live donor liver transplant, *PST* performance status (ECOG), *RT* radiotherapy, *RF* radiofrequency ablation

shown that when two-thirds of the liver is irradiated, doses up to 35 Gy are permissible and when only one-third is irradiated, permissible dose increases to 50 Gy [22].

Awareness of this important dose-volume effect, in conjunction with advances in radiotherapy technique, has allowed the development of SBRT techniques for hepatic malignancy.

Radiation therapy has a particularly important role for HCC unsuitable for, or resistant to other locoregional liver directed therapies. Radiotherapy does not feature in many consensus guidelines or documents largely due to a relative lack of Level 1 randomised trial data. However it is also clear that non radiation oncologists currently have a poor understanding of the potential of this rapidly advancing field.

SBRT is a form of high-precision radiotherapy characterised by: reproducible immobilisation; measures to account for tumour motion during treatment planning and delivery; dose distributions tightly covering the tumour, with rapid dose fall off in surrounding normal tissues; and most importantly, the use of relatively few, high dose fractions of radiation (extreme hypofractionation), usually delivered in 1–8 treatments [23].

9.2.1 Summary of Evidence for SBRT in Inoperable HCC

The evidence for SBRT for HCC is largely confined to retrospective series, and prospective phase 1 trials (Table 9.1). SBRT has comparable efficacy with other

Table 9.1 Trials of SBRT in unresectable HCC

Author [ref]	Year	Number of patients	Dose (Gy), no. fractions	Median volume (cm^3)	Median follow up (months)	LC 1 year (%)	LC 2 years (%)	OS 1 year (%)	OS 2 years (%)	Comments
Blomgren et al. [24]	1998	11	15–45 in 1 or 3			100				
Choi et al. [25]	2006	20	50 Gy in 5 or 10	25	23			81	43	Retrospective
Mendez Romero et al. [26]	2006	11	25 in 5, 30 in 3 or 37.5 in 3	22	12.9	94	82	75	40	Phase I/II
Tse et al. [27]	2008	41	24–54 in 6	173	17.6	65		48		Phase 1
Choi et al. [28]	2008	32	30–39 in 3	25	17.3	72		81		Retrospective +/– TACE
Seong et al. [29]	2009	37							28	Survey
Cardenes et al. [30]	2010	17	36–48 in 3, 40 in 5 (CP B)	34	24	100		75	60	Phase 1
Loius et al. [31]	2010	25	45 in 3	73	15	91	90	79	52	Retrospective
Seo et al. [32]	2010	38	33–57 in 3 or 4	40					61	Retrospective, prior TACE
Kwon et al. [33]	2010	42	30–39 in 3	15.4	28.7	72		93	58 (3 years)	
Chan et al. [34]	2011	16	45 in 10	134	24	91		62	28 (3 years)	
Andolino et al. [6]	2011	60	40 in 5 (CP-B), 42 in 3 (CP-A)		27		90		67	Retrospective
Bujold et al. [35]	2011	102	24–54 in 6		15	79				
Ibarra et al. [36]	2012	21	21–45 in 3	334	7.8	63 %		87	55	Retrospective
Huang et al. [37]	2012	36	25–48 in 4 or 5		14	88	75		64	Retrospective
Katz et al. [38]	2012	18	50 in 10	63	19.6			100		Bridging
Sanuki et al. [39]	2013	185	35–40 in 5		24		91 (3 years)		70 (3 years)	Retrospective
Takeda et al. [40]	2013	63	35–40 in 5		31	100	95	100	87	

Bujold et al. [41]	2013	102	24–54 in 6	283 (PTV)	17	87				
Kang et al. [42]	2012	47	42–60 in 3 (median 57 Gy)				95		69	Prospective salvage therapy following TACE
Ibarra et al. [36]	2012	32 (21 HCC)	21–45 in 3		13			87	55	Retrospective

LC local control, *OS* overall survival, *CP* Child Pugh score

local therapies and should be considered for early stage HCC unsuitable or refractory to, other liver directed therapies. Use of SBRT to slow progression of HCC whilst awaiting transplantation is growing in popularity although generally has been investigated in patients not suitable or refractory to, other bridging therapies [38, 43]. Pathological complete responses seen after SBRT bridging to transplant demonstrate that SBRT is an effective treatment however Level 1 evidence is urgently required. SBRT can also be considered for Child Pugh B patients unsuitable for standard locoregional therapy, however the risk of radiation induced liver disease (RILD) is higher.

9.3 Liver Metastases

The annual incidence of colorectal cancer (CRC) in the US is over 150,000 cases. There are over 50,000 annual deaths. Approximately 80 % of patients with stage IV CRC have liver disease considered unresectable at presentation [44].

Autopsy studies show that 40 % of colorectal cancer patients relapse with liver only metastases [45–47]. Oligometastatic liver disease (that is up to 5 metastases) may be amenable to aggressive local therapy with the potential for long term disease control [48, 49], or even cure [50, 51]. The evidence to support the local ablation of oligometastases is largely single institution retrospective case series, and some small prospective phase 2 trials. There are currently no prospective trials comparing aggressive local therapy with best supportive care.

Surgery has been the gold standard treatment for colorectal liver metastases, with retrospective series reporting 5 year survivals of 25–47 %, [50–54]. However, up to 80 % of patients are not suitable for resection due to the location, size and distribution of metastases, or poor patient performance status, or significant medical comorbidities. Chemotherapy can downstage inoperable to operable disease in only around 10–20 % of cases [55]. Newer chemotherapy combinations such as FOLFOXIRI, or FOLFOX/FOLFIRI in combination with the biological agents Bevacizumab or Cetuximab can downstage a significantly higher proportion, but at the cost of considerable toxicity. Response rates can be as high as 70 % with triplet combinations. These chemotherapy combinations have also extended median survival in metastatic CRC to 24 months [56].

Thermal destruction by radiofrequency ablation (RFA) or microwave for CRC liver metastases gives 3 year survival rates of 30–46 % [57–60]. There are data to suggest that local control of CRC liver metastases is related to survival—Aloia et report a sevenfold increase in the risk of local failure and a threefold increase in the risk of death, in patients treated with RFA rather than surgical resection, despite similar rates of distant intrahepatic and extrahepatic failure in both groups [61]. Chang et al. report also a strong correlation between local control and survival in patients treated with SBRT for liver metastases [62].

Surgical data for resection of non-CRC liver metastases are more limited. However, a large (n = 1,452) retrospective, multi-institutional series has reported

a 5 year survival of 36 % and 10 year survival of 23 % for carefully selected non-CRC, with metastases from breast cancer having the best and melanoma and squamous cell cancers the poorest survival [63]. There are some reports of non-CRC having better local control and survival than CRC when treated with SBRT [64, 65].

9.3.1 Evidence Supporting SBRT to Liver Metastases

Currently, the evidence for SBRT for liver metastases is predominantly retrospective case series (Table 9.2), with some prospective phase 1 and 2 trials (Table 9.3). Within the studies there is significant heterogeneity in patient selection, size and number of lesions treated, dose-fractionation, prescription points and dosimetric criteria.

Patients were often heavily pre-treated with chemotherapy, surgery, or other local ablative therapies [70, 75]. SBRT has historically been used when the liver metastases were no longer amenable to other treatments (i.e. last resort, until recently).

Local control rates are 70–100 % at 1 year, and 60–90 % at 2 years [2] Several factors predicting local control (LC) may be identified, which may help in patient selection for treatment. The most consistently observed correlation with local control is baseline tumour volume [81–85]. Rusthoven et al. report a superior LC rate for tumours less than 3 cm (100 % vs 77 % at 2 years, $p = 0.015$) [76]. Number of tumours <3 and size <6 cm predicts for better outcome. Also, delivered BED >117 Gy_{10} is associated with improved local control at 1 year [62]. Metachronous CRC liver metastases has a better prognosis than synchronous [75] Median overall survival is 10–34 months, and 2 year survival ranges from 30 to 83 % [2]. For CRC specifically, Hoyer et al. report a median survival of 1.6 years from SBRT [75]. Out-of-field progression of disease occurs in a substantial proportion of patients, although this is also reported after hepatic resection [48].

There are a number of predictors of overall survival, and long term survival is seen after treatment. Factors associated with increased survival are:

- The absence of extra-hepatic disease (35.8 months vs 11.3 months [64, 75]).
- Primary histology. Favourable primary histology includes breast, CRC, renal, carcinoid and GIST. Unfavourable primary sites include lung, ovary and non-CRC gastro-intestinal. Rusthoven et al. report median survival for favourable primary sites as 32 months vs 12 months for unfavourable primaries ($p < 0.001$) [76]. Lee et al. report superior 1 year survival for CRC (63 %) and breast cancers (79 %) compared to other primary sites (38 %) [65].
- Tumours <3 cm diameter are associated with improved overall survival [65, 70].

Liver SBRT is very well tolerated, both in terms of acute and late toxicity, and may be used safely after other liver directed therapy (surgery or RFA). The means

Table 9.2 Retrospective studies of SBRT for liver metastases

Study	n	Vol/number of mets	Histology	Immobilisation/ resp motion	Dose	Prescription point	Toxicity	Outcome
Blomgren et al. (1995) [66]	14	3–260 mL	CRC (11); anal canal (1); kidney (1); ovarian (1)	SBF/AC	7.7–45 Gy (1–4 frx)	Periphery of PTV	2 cases of haemorrhagic gastritis	50 % response rate
Wada et al. (2004) [67]	5	NR	NR	VM/AC	45 Gy (3 frx)	90–100 % isodose	No serious toxicity	2 year LC 71.2 %
							No RILD	
Wulf et al. (2006) [68]	44	9–355 mL	CRC (23); breast (11); ovarian (4); other (13)	SBF/AC	30–37.5 Gy (3 frx)	30 Gy: 65 % isodose; others—80 % isodose (covering 95 % of PTV)	No grade 2–4 toxicity	1 year LC 92 %;2 year LC 66 %
					26 Gy 1 frx			1 year OS 72 %;2 year OS 32 % (LC for 37.5 Gy: 1 year 100 %; 2 year: 82 %)
Katz et al. (2007) [69]	69	0.6–12.5 cm; (median 2.7 cm)	CRC (20); breast (16); pancreas (9)	VM/Resp. gating	30–55 Gy (5–15 frx)	100 % isodose with 80 % covering PTV	No grade 3–4 toxicity	10 months LC 76 %
			Lung (5); other (19)		50 Gy/5frx preferred			20 month LC 57 %
								Median OS 14.5 months
Van der Pool et al. (2010) [70]	20	0.7–6.2 cm (median 2.3 cm)	CRC (20)	SBF/AC	37.5–45 Gy (3 frx)	95 % of PTV received prescribed dose	2 grade 3 late liver enzyme changes; 1 grade 2 rib fracture	1 year LC 100 %
								2 year LC 74 %
								Median survival 34 months

Habermehl et al. (2013) [71]	90	62 (11–333)	50 % colorectal	VM, AC	17–30 Gy median 24 Gy single		Grade 1 fatigue, fever, loss appetite, raised transaminases	Median OS 24 months
								1 year PFS 70 %
Berber et al. (2013) [72]	153	363 mets, GTV of 138.5 ± 126.8 cm^3	50 % GI		37.5 ± 8.2 Gy in 5 ± 3 fractions			1 year LC = 62 %
								1 year OS = 51 %
Fumagalli et al. (2012) [73]	90	113 liver mets	70 % GI	Cyberknife	45 Gy in 3	80 %	G1–3	LC 1 year 84 %, 2 years 66 %
								2 years OS = 70 %
Lanciano et al. (2012) [74]	30	41 lesions.	23 mets, 7 HCC	Cyberknife	Varying		G1/2 toxicities	Median FU 22 months
								2 years LC 75 % (if BED > 100)

Abbreviations: *SBRT* stereotactic body radiotherapy, *Mets* metastases, *RT* radiotherapy, *CRC* colorectal cancer, *SBF* stereotactic body frame, *VM* vacuum mould, *AC* abdominal compression, *ABC* active breath control, *NR* not reported, *LC* local control, *OS* overall survival, frx fractions

Table 9.3 Prospective studies of SBRT for liver metastases

Study	Design	n	Volume/ number of mets	Histology	Immobilisation/ resp motion	Dose	Prescript. point	Toxicity	Outcome
Herfath et al. (2004) [64]	Ph 1–2	35	1–132 mL (median 10 ml)	CRC (18); breast (10); other (7)	SBF and VM/ AC	Dose escalation: 14–26 Gy (1 frx)	Isocentre, with 80 % covering PTV	No significant toxicity reported	1 year LC 71 %; 18 month LC 67 % (18 month LC 81 % for Ph2)
									1 year OS 72 %; Med 25 months
Mendez Romero et al. (2006) [26]	Ph 1–2	25 (17 liver mets)	1.1–322 mL (median 22.2 mL)	CRC (14); lung (1); breast (1); carcinoid (1);	SBF/AC	37.5 Gy (3 frx)	65 % Isodose	2 grade 3 gammaGT elevations;	2 year LC 86 %
						30 Gy (3 frx) in 3 patients to spare OAR		1 grade 3 asthenia	2 year OS 62 %
								1 late portal hypertension	
Hoyer et al. (2006) [75]	Ph 2	64 (44 liver)	1–8.8 cm (median 3.5 cm)	CRC only	SBF or VM/AC	45 Gy (3 frx)	ICRU ref-95 % to CTV and 67 % PTV	1 liver failure; 2 severe late GI toxicities	2 year LC 79 % (by tumour)
									2 year LC 64 % (by patient)
Rusthoven et al. (2009) [76]	Ph 1–2	47	0.75–98 mL (median 14.93 mL)	CRC (15); lung (10); breast (4); ovarian (3); Oes (3); HCC (2); other (10):	VM/ABC or AC	Dose escalation: 36–60 Gy (3 frx) Ph2 60 Gy (3 frx)—36 pts	Isodose covering PTV (80–90 %)	No RILD	1 year LC 95 %; 2 year LC 92 %; median survival 20.5 months (32 months for breast and CRC $p<0.001$). 2 year OS 30 %
								Late grade 3/4 < 2 %	

Lee et al. (2009) [65]	Ph 1–2	68	1.2—3,090 ml (med. 75.9 mL)	CRC (40); breast (12); gallbladder (4); lung (2); anal (2); melanoma (2); other (6)	VM/ABC or AC (AC if resp excursion >5 mm)	Individualised Dose 27.7–60 Gy (6 frx)	Isodose covering PTV (max 140 % in PTV)	No RILD 10 % grade 3/4 acute toxicity No grade 3/4 late toxicity	1 year LC 71 % Median survival 17.6 months
Ambrosino et al. (2009) [77]	Prospect cohort	27	20–165 mL (median 69 mL)	CRC (11); pancreas (10); breast (2); 1 each of gallbladder, gastric, ovary, lung	Cyberknife™ (with synchrony™ to track US-placed gold fiducials)	25–60 Gy (3 frx)	80 % of prescribed dose covered PTV	No serious toxicity 36.2 % CRC cases—mild-moderate transient hepatic dysfunction. 3.7 % GI bleed; 3.7 % portal vein thrombosis	Crude LC rate 74 %
Goodman et al. (2010) [78]	Ph 1 (HCC and liver mets)	26 (19 liver mets)	0.8–146.6 mL (median 32.6 mL)	CRC (6); pancreas (3); gastric (2); ovarian (2); other (6)	Alpha-cradle. Cyberknife™ (with synchrony™ to track US-placed gold fiducials)	18–30 Gy (1 frx)	Isodose that covered PTV (65–90 %)	4 cases grade 2 late toxicity (2 GI, 2 soft tissue/rib)	1 year local failure 23 % Median survival 28.6 months 2 year survival 49 % (mets only)
Rule et al. (2011) [79]	Ph 1 Liver mets	27	0.75–135	Colorectal (12)		30 Gy (3 F) 50 Gy (5 F) 60 Gy (5 F)			24-month LC rates for the 30-, 50-, and 60-Gy cohorts were 56, 89, and 100 %

(continued)

Table 9.3 (continued)

Study	Design	n	Volume/ number of mets	Histology	Immobilisation/ resp motion	Dose	Prescript. point	Toxicity	Outcome
Scorsetti et al. (2013) [80]	Ph 2	61	76 mets	Colorectal 48 %	Rapidarc VMAT, VM	60–75 Gy (3 F)		65 % fatigue	Median FU 12 months (2–26)
	Liver mets		7.7–209	Breast 18 %				26 % transaminase rise (settle in 3 months)	CR + PR + SD = 95 %
				Gynae 12 %					LC at 6, 12, 22 months = 100, 94, 91 %
				Other 22 %					1 year OS = 84 %, median OS = 19 months

Abbreviations: *SBRT* stereotactic body radiotherapy, *Mets* metastases, *RT* radiotherapy, *CRC* colorectal cancer, *SBF* stereotactic body frame, *VM* vacuum mould, *AC* abdominal compression, *ABC* active breath control, *NR* not reported, *LC* local control, *OS* overall survival, *frx* fractions

by which liver SBRT has been delivered in published series is variable, but with generally good outcomes. No particular SBRT technique has superior outcomes in terms of tumor control or toxicity.

Patient Selection Criteria

- For HCC, enhancement typically in the arterial phase on two imaging modalities and α-fetoprotein (AFP) increased on a background of liver disease
- Biopsy-confirmed IHC
- Unresectable tumour or inappropriate for other treatment modalities, or as a bridge to transplant for HCC
- Patients should be discussed in Multi-Disciplinary Tumour Board meetings
- Karnofsky Performance Status (KPS) ≥60
- Life expectancy >3 months
- Child-Pugh score: A, or B7/8 (Table 9.4)
- >700 cc of uninvolved liver
- No chemotherapy within 2 weeks prior, and 4 weeks after, SABR
- No, or limited and potentially treatable, extra-hepatic disease.
- Recovered from any previous therapy (such as surgery, chemotherapy or radiotherapy to other areas) with a minimum of 2 weeks break (for HCC, anthracycline based chemotherapy should be completed 4 weeks before SBRT)
- Up to three metastases, with no limitation on actual size of a given tumour provided functional residual volume, and organ at risk (OAR) dose constraints can be met
- Adequate organ function, defined as: Hemoglobin 90 g/L, absolute neutrophil count 1.5, platelets 80, bilirubin <3.0 times upper limit of normal, INR <1.3 or correctable with vitamin K and unless the patient is taking warfarin/coumarin, AST or ALT <5.0 times upper limit of normal. Creatinine less than 200 umol/L (if creatinine is above the normal range consideration should be given to dynamic renal scintigraphy (renography)) if there is anticipated to be any appreciable renal dose from the delivery of treatment.

Table 9.4 Child-Pugh liver score

Measure	1 point	2 points	3 points
Total bilirubin (μmol/l) (mg/dl)	<34 (<2)	34–50 (2–3)	>50 (>3)
Serum albumin (g/l)	>35	28–35	<28
INR	<1.7	1.71–2.20	<2.20
Ascites	None	Mild	Severe
Hepatic encephalopathy	None	Grade 1–2 (or suppressed with medication)	Grade 3 or 4

Points	Class	One year survival (%)	Two year survival (%)
5–6	A	100	85
7–9	B	81	57
10–15	C	45	35

9.3.2 Exclusion Criteria

- Active hepatitis or clinically significant liver failure (encephalopathy, portal hypertension, varices)
- Clinically apparent ascites
- Prior radiotherapy to the right upper abdomen (unless 700 cc normal unirradiated liver <17 Gy)
- If patient is for fiducial placement: Gold allergy, Coagulopathy preventing safe fiducial placement
- Any previous radiotherapy where the mean dose to the liver was 15 Gy (conventional fractionation), or where beams would be likely to overlap with those used to deliver SBRT, or where previous doses to other critical normal structures would make re-irradiation unsafe.
- Any other severe comorbidity such as unstable angina, congestive cardiac failure or transmural MI requiring hospitalisation in the preceding 6 months, or acute bacterial/fungal infection requiring intravenous antibiotics
- CNS metastases

9.3.3 Patient Assessment

- Clinical assessment. Assess general performance status, and for signs of hepatic decompensation.
- Baseline blood profile. Complete blood count, coagulation screen, renal function, liver function, calcium, αFP (HCC), CEA (colorectal mets)
- Diagnostic Imaging.
  - Liver MRI, ideally with liver specific contrast agent to aid tumour definition and delineation
  - Contrast-enhanced CT—ideally triple phase
  - PET may be useful if MRI not available or further clarification required on defining treatment target volume.
  - DMSA or MAG3 scan to assess differential renal function may be required if the kidney(s) are close to the target volume.

9.4 Planning for Radiotherapy

See Table 9.5 for a comparison between various SBRT delivery systems.

Table 9.5 Comparison of liver SBRT delivery systems

Device	Manufacturer	Image guidance system	Gating capability	Tracking capability	Collimation	Fiducials essential	Arc delivery	Isocentric Rx	6D positioning
Axesse	Elekta	Cone beam CT	No	No	Fixed cones/ dynamic MLC	No	Yes (VMAT)	Yes	Yes
CyberKnife	Accuray	Dual-diagnostic kV X-rays	No[a]	Yes	Fixed cones. MLC on M6 model	Yes[b]	No	No	Yes
Novalis TX	Brainlab	Cone beam CT & dual-diagnostic kV X-rays	Yes	No	Dynamic MLC	No	Yes	Yes	Yes
Synergy	Elekta	Cone beam CT & dual-diagnostic kV X-rays	No	No	Dynamic MLC: micro-MLC add on	No	Yes (VMAT)	Yes	Yes
TomoTherapy	Accuray	MV- CT	No	No	Dynamic micro-MLC	No	Helical	Yes	Yes
Trilogy	Varian	Cone beam CT & dual-diagnostic kV X-rays	Yes	No	Dynamic micro-MLC	No	Yes (rapid Arc)	Yes	Yes
TrueBeam	Varian	Cone beam CT & dual-diagnostic kV X-rays	Yes	No	Dynamic micro-MLC	No	Yes	Yes	Yes
Vero	MHI/ Brainlab	Cone beam CT & dual-diagnostic kV X-rays & fluoroscopy	No	No	Dynamic micro-MLC	No	Yes	Yes	Yes

[a]Synchrony system allows dynamic tracking of target throughout the respiratory cycle, without gating in any particular respiratory phase
[b]Unless alternative tracking method i.e. 6D-skull tracking, X-Sight Spine, or X-Sight Lung can be utilized

9.4.1 Fiducial Placement

Patients receiving SBRT with the CyberKnife system (Accuray, Sunnyvale, CA, USA) will require the insertion of gold fiducial markers to guide treatment. Fiducial placement is usually performed under CT or ultrasound (percutaneous) guidance. Appropriate spacing of multiple fiducials is important if the Cyberknife system is to accurately track rotational setup errors [86].

- Ideally, 4–6 fiducials are placed in or in close proximity to the tumour
- Minimum of 2 cm spacing between fiducials
- Fiducials should be placed as close as possible to target lesion, and no further than 5 cm from the target.
- There must be at least a 15^0 angle between any grouping of 3 fiducials i.e. they must be non collinear
- Approved fiducial type
- Allow sufficient time between fiducial insertion and Planning CT—normally 7 days

A minimum of three fiducials is required to track rotations at the time of treatment delivery.

The reasons for siting fiducials as close as possible to the target lesion (and no more than 5 cm from target) are twofold. First, the closer the distance between fiducial and tumour target, the greater the probability that the fiducial will move in the same plane as target. Second, it is important that all fiducials can be captured on the live image field of view (FOV), which measures 20×20 cm.

It is important that fiducials are non-collinear in order that the treatment system can image and interpret individual fiducial position accurately on the kV live images at the time of treatment.

Despite optimum fiducial insertion technique, there is potential for fiducial migration, post-insertion, and for haemorrhage or oedema at the fiducial site. It is important, therefore, to allow sufficient time between fiducial placement and planning scans. One week is generally considered to be reasonable. The fiducial tracking procedure assumes that the geometry in the planning CT scan (which establishes the relative position of the fiducials to the target), is precisely reproduced on the day(s) of treatment i.e. there is Rigid Body Geometry [87].

9.4.2 Pre-treatment

9.4.2.1 Patient Positioning

Reproducible repositioning is essential for delivering SBRT accurately—use of body immobilisation devices, such as stereotactic frames or individualised vacuum moulds have been utilised in most published studies. Patients can be scanned with arms above the head (can be uncomfortable with long delivery time), or arms by side, and every effort should be made to optimise comfort and thus reduce the potential for intra-fraction motion.

9.4.2.2 Pre-treatment Imaging

Contrast-enhanced CT underestimates tumour volume in colorectal metastases [81] and other primary sites (ideal would be a dynamic contrast CT in end expiratory breath hold, capturing the portal venous phase of contrast enhancement) [88]. MRI provides higher contrast ratios and allows superior lesion detection and characterisation [89].

Use of MRI (plain T1W or T2W sequences) fused with CT to delineate tumour increases accuracy of definition, but also increases the volume of CTV [81, 88]. FDG-PET has also been shown to increase the CTV volume when merged with CT, and also MRI, in treating colorectal liver metastases [90]. PET is particularly useful in target delineation in previously treated liver tumors, where it is able to more accurately distinguish active tumor from fibrosis [82]. Radiologist assistance in outlining targets and organs at risk is strongly encouraged.

9.4.3 Tumour Motion

A major challenge in SBRT for liver tumors is the management of intra fraction motion, which can potentially result in a geographical miss of the PTV, and hence reduced local control, as well as excess dose to nearby organs at risk. The amplitude of respiratory motion may be assessed by kV fluoroscopy [83], 4D-CT or cine-MRI [91]. The data indicates that whilst the amplitude of breathing may be significant, the variability of respiratory amplitude is small [92].

There are several possible means of controlling for respiratory motion:

9.4.3.1 Restrict Respiratory Motion

Abdominal Compression

Abdominal compression reduces liver motion, resulting in far smaller superior-inferior movement (less than 10 mm and in many cases less than 5 mm) that are reproducible between cycles [93]. It is the most commonly used means of respiratory motion control in published series. AC also reduces inter- and intra-fractional changes in liver position relative to bony anatomy [83].

Active Breathing Control (ABC)

This technique is a means of active respiratory gating and in effect produces a forced breath hold during radiation delivery. A disadvantage is that it requires a breath-hold of 20–35 s, and the experience of some centres has shown that 30–50 % of patients are unable to manage this technique adequately [85]. However, set-up errors can be reduced to less than 5 mm (cranio-caudal) using ABC with image guidance [84, 94].

Passive Respiratory Gating

This technique allows patients to free breathe, and delivers the radiation dose to target during a predefined phase of the respiratory cycle, when the target will lie within the treatment beam. Most commonly, end expiration is used. It has the advantage of being better tolerated, but requires additional hardware and software. However, its use has been shown to allow significant margin reduction and escalation of tumour dose for the same level of normal tissue toxicity [85]. Reproducibility can be problematic with breath-holding approaches in some patients. Gating requires the user to set the percentage of session time during which the beam is turned on, i.e. the gating window. Setting a larger 'gating window' allows the fraction to be delivered faster; however, it leads to an increase in the volume of normal tissue irradiated. In practice, gating windows of 25–40 % are common.

9.4.3.2 Tracking and Compensating for Tumor Motion

Real time tracking of implanted fiducial markers is extremely accurate, but has the disadvantage of being invasive [87, 95]. This approach (on the Cyberknife system) adjusts for changes in tumor motion in real time, throughout treatment, whilst the patient breathes normally without any restriction. Motion tracking is driven by the correlation between the location of the fiducials, as detected by orthogonal X-Ray films, and the location of external LED markers on the patient's chest. The predictive correlation algorithm is constructed just after patient set up and is continually updated throughout treatment each time new x-rays are obtained (every 30–90 s).

9.4.3.3 Planning with No Respiratory Tracking or Restriction

A further means of managing respiratory motion is to plan radiotherapy simply allowing for the motion within margins. This may be appropriate if other means of motion management can not be applied or the tumour moves less than 5 mm. A 4D CT data set can be acquired allowing the creation of an internal target volume (ITV) with relative certainty of tumour respiratory motion.

9.4.4 Delineation and Treatment Planning

9.4.4.1 Treatment Planning

Patient Postioning and Immobilisation

The most appropriate supine immobilisation depends partly on the SBRT delivery system being utilised. Also consider the image guidance system (i.e. real-time tracking vs. Cone-beam CT pre-treatment).

Immobilisation for SBRT treatment to the liver is often achieved with the use of a vacuum-formed personalised immobilisation device. A treatment position must be chosen that the patient can comfortably maintain. Consideration should also be given to arm position to allow the optimum range of beam angles. Patients' arms should be by their side, with hands tucked posteriorly behind the body, and shoulders as posterior and inferior as possible. The Vacbag is then applied so that it encompasses the shoulders and arms, and wraps as far around the body as possible. As an alternative, patients may have their arms above the head on a chest board as long as this position can be maintained in a stable way for the duration of treatment. Knee and ankle supports are used as needed. Patients are generally scanned in the supine position.

Linac-based SBRT systems will allow treatment beams to pass through the couch. In contrast, the CyberKnife system does not allow beams to enter through the treatment couch. A comparison of the features of the commercially available SBRT systems can be seen in Table 9.5.

Planning Scans

All SBRT systems utilise a non-contrast CT scan as their primary scan, so a non-contrast CT with the patient positioned and immobilised as described above will always be required. This CT should be obtained at end expiration breathold with 1–2 mm slices for DRR reconstruction. Typical scan levels would be 20 cm above and below the liver. Patients would normally be asked to fast for 2 hours prior to their CT. Contrast protocols may vary according to Center, but a typical protocol would be 100 ml administered via peripheral cannula at 3 ml/s. Scan after a 30–35 s delay for arterial phase, 45–60s for venous.

MRI

MRI should ideally be performed on the same day as the CT with the patient immobilised in the treatment position. Liver-specific Contrast can be used to highlight tumour position. Close liaison with Radiologists is recommended to select the most appropriate MRI sequence to show the target. Consideration should also be given to any fiducials used as to the sequence that will show the markers optimally, as fusion of scans by fiducial position is often performed.

Volume Definition

Gross tumour volume (GTV) is outlined on the images that best display the tumor target. This will often be the MRI or contrast CT. GTV should always be reviewed on the Primary (Non-contrast) CT scan.

The Clinical target volume (CTV) is sometimes defined on the basis of the GTV expanded by 3–5 mm. Many studies add no margin between GTV and CTV.

The Planning Target Volume (PTV) is defined as the CTV with an expansion to account for internal organ motion and daily set up process. Margins will therefore

depend on the Immobilisation being used, and whether the SBRT system is capable of motion tracking (see Table 9.1). Typically, much smaller margins (1.5–3 mm) can be used on SBRT devices that track respiratory motion.

If no Breathing control/Tracking methods are employed, the CTV is often expanded 5 mm radially, and 10 mm in cranio-caudal direction. If 4D CT is used CTV-PTV margins may be reduced to 3–5 mm.

9.4.4.2 Organs at Risk (OAR)

Any organ that is traversed by part or all of a beam should be contoured so that the dose it receives can be assessed. Organs should be outlined by the treating oncologist. The whole liver should be contoured, and for dose calculation this volume minus PTV is used. Cord should be outlined using the bony limits of the spinal canal, including that section of the spinal cord 2 cm above and below the extent of the PTV.

Table 9.6 indicates suggested constraints for use in planning SBRT liver patients in single, 3 or 5 fraction regimes. These are not absolute and values do vary between

Table 9.6 SBRT liver suggested constraints

OAR	Single fraction constraints	Three fraction constraints	Five fraction constraints	Dose limiting toxicity
Liver	700 cc <9 Gy	700 cc <17 Gy	700 cc <21 Gy	RILD
		V15 <50 %		
		V21 <30 %		
Spinal cord	V10 <0.35 cc	V18 <0.35 cc	V23 <0.35 cc	Myelopathy
	V7 <1.2 cc	V12 <1.2 cc	V14.5 <1.2 cc	
	14 Gy point dose	22 Gy point dose	30 Gy point dose	
Esophagus	V12 <5 cc	V18 <5 cc	V20 <5 cc	Stenosis/fistula/ perforation
	15 Gy point dose	25 Gy point dose	35 Gy point dose	
Heart/ pericardium	V16 <15 cc	V24 <15 cc	V32 <15 cc	Pericarditis
	22 Gy point dose	30 Gy point dose	38 Gy point dose	
Rib	V22 <1 cc	V29 <1 cc	V35 <1 cc	Chronic pain or fracture
	30 Gy point dose	37 Gy point dose	43 Gy point dose	
Skin	V23 <10 cc	V30 <10 cc	V37 <10 cc	Chronic ulceration
	26 Gy point dose	33 Gy point dose	39.5 Gy point dose	
Stomach	V11 <10 cc	V16.5 <10 cc	V18 <10 cc	Chronic ulcer/fistula/ perforation
	12 Gy point dose	22 Gy point dose	32 Gy point dose	
Duodenum	V11 <5 cc	V16.5 <5 cc	V18 <5 cc	Chronic ulcer/fistula/ perforation
	V9 <10 cc	V11.5 <10 cc	V12.5 <10 cc	
	12 Gy point dose	22 Gy point dose	32 Gy point dose	
Jejunum/ ileum	V12 <5 cc	V18 <5 cc	V19.5 <5 cc	Enteritis/obstruction/ perforation
	15 Gy point dose	25 Gy point dose	35 Gy point dose	

(continued)

Table 9.6 (continued)

OAR	Single fraction constraints	Three fraction constraints	Five fraction constraints	Dose limiting toxicity
Colon/ rectum	V14 <20 cc	V24 <20 cc	V25 <20 cc	Colitis/fistula/ perforation
	18 Gy point dose	28 Gy point dose	38 Gy point dose	
Renal hilum/ vascular trunk	10.6 Gy to 67 %	18.6 Gy to 67 %	23 Gy to 67 %	Malignant hypertension
Kidney	200 cc <8.5 Gy	200 cc <16 Gy	200 cc <17.5 Gy	Renal dysfunction
Lung (R & L)	1,500 cc <7 Gy	1,500 cc <11.5 Gy	1,500 cc <12.5 Gy	Pneumonitis

Note—Point dose <0.035 cc

published studies. These have been adapted from AAPM Task Group 101 [96] and adapted with use of other published liver SBRT studies.

9.4.4.3 Treatment Planning

Increasing beam number improves the conformality of dose to the target and the dose gradient. However, increasing the number of beams also increases the integral dose of normal tissue treated, the theoretical risk of toxicity, as well as increasing treatment time. Liu et al. have shown that in treating liver and lung lesions with SABR, the dose gradient is improved as the number of beams increases from 5 to 15, for both coplanar and non-coplanar treatments, and that the normal tissue complication probability (NTCP) decreases from 5 to 9 beams, but does not increase significantly when more than 9 beams are used, irrespective of the size of the target. They conclude that the optimal number of beams is 9 [97]. Published studies have used up to 10 beams in generating plans, but use of 6–8 beams is most common. Increasingly, however, VMAT (volumetric modulated arc therapy) is used. See Fig. 9.2 for illustration. Figure 9.3 illustrates a plan where OAR constraints could not be met.

9.5 Fractionation

To date, there are no randomised, controlled trials comparing dose-fractionation regimens for SBRT in liver metastases. A large number of different fractionation regimens have been employed. There is clear evidence of a dose response relationship, and a BED >100 Gy_{10} equivalent appears important for tumour control.

Two year local control rates of 90 % are achievable for lesions receiving 54–60 Gy in 3 fractions, compared to 59 % (36–53.9 Gy/3 fractions), and 8.1 % (less than 36 Gy) [98].

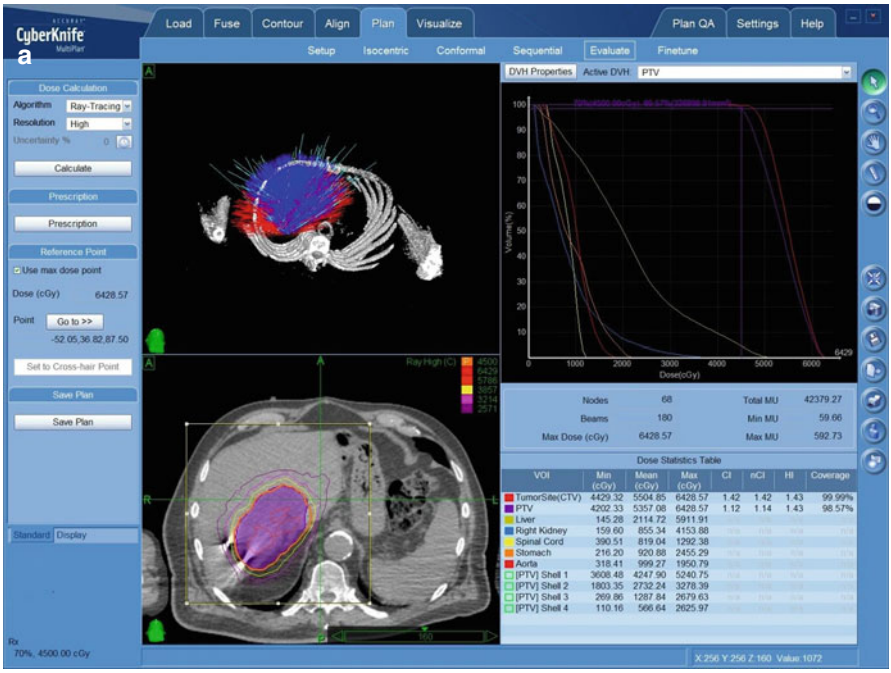

Fig. 9.2 (**a**) Solitary 9 cm hilar liver metastasis spanning multiple segments, and inoperable. Target volume delineated in *purple*, and covered by 70 % isodose line (*orange*). Note steep dose gradient away from target. Patient received 45 Gy in 3 fractions over 3 days. Total dose was reduced from 54 Gy in order to meet liver constraints. Planned using accuray multiplan. (**b**) Axial, sagittal and coronal plane visualisations of target volume. (**c**) Illustration showing position of fiducial markers at set up—Note the tumour target surrounded by three implanted fiducials. (**d**) Axial CT slice pre treatment, showing hypodense hilar metastasis. (**e**) Seven months post SABR, note change in density of target volume—PET scan confirmed no evidence of FDG uptake at this time. (**f**) Four-year followup CT scan. (**g**) Four-year followup CT scan

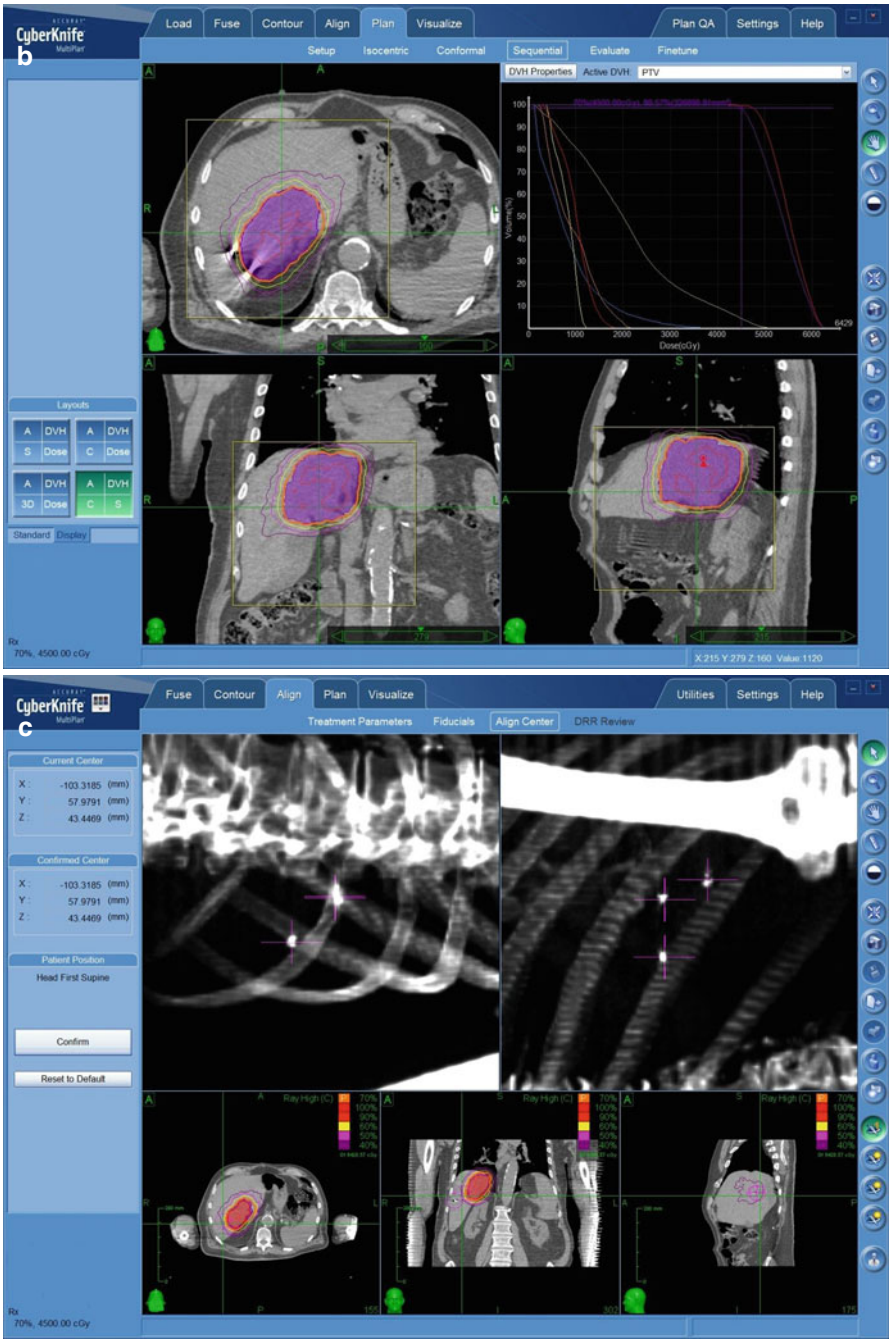

Fig. 9.2 (continued)

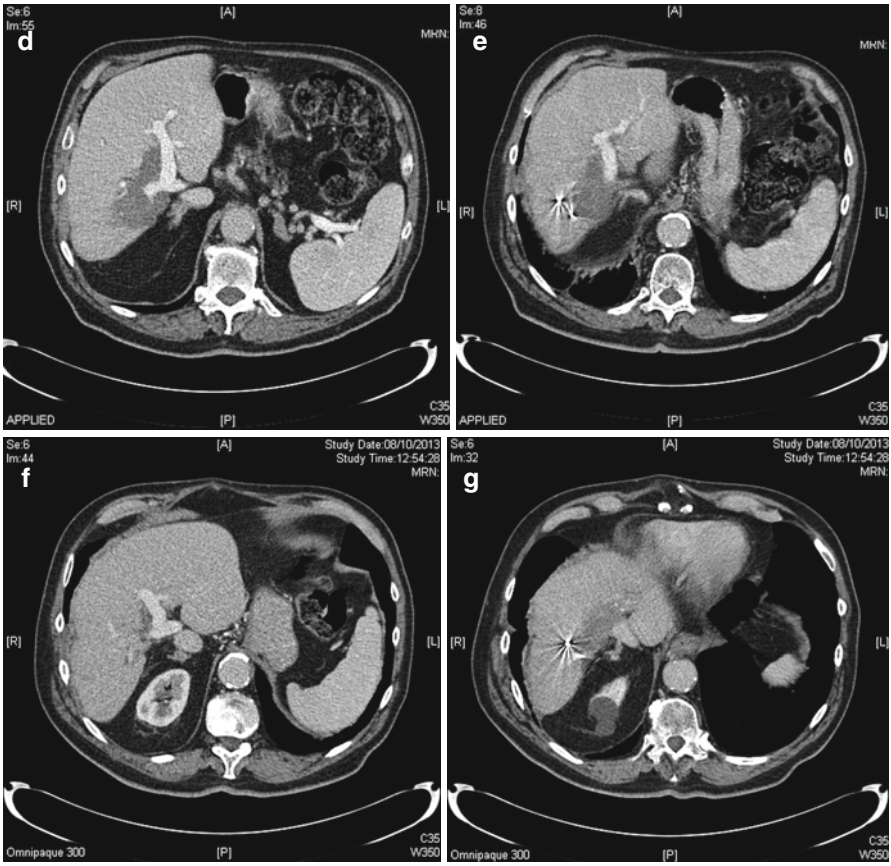

Fig. 9.2 (continued)

9.5.1 Suggested Fractionation Schemes

- 18–30 Gy in a single fraction
- 45–60 Gy in 3 fractions over 3–10 days
- 50–60 Gy in 5 fractions over 5–12 days
- 60 Gy in 8 fractions over 10 days
- 50–60 Gy in 10 fractions over 12 days

A tolerance based dose prescription using the normal tissue complication probability (NTCP) model is another approach, and is commonly used in Canadian centres (Lock M, personal communication, 2013).

The dose would conventionally be prescribed at the 70–80 % isodose. If OAR constraints are not met, then the 95 % isodose can be relaxed or total dose can be reduced according to clinical discretion. The target coverage goal is that a minimum

of 95 % prescribed dose will cover 99 % of the PTV. Any hot spots should be within PTV, no greater than 1 cc, and the maximum dose should be <120 %. GTV should be covered by the 100 % of the prescribed dose.

9.5.2 Minimum Standard for Reporting

- Prescription dose
- Prescription ICRU reference point or dose/volume e.g.% isodose covering PTV
- Number of treatment fractions
- Total treatment delivery period
- Target coverage
- Plan conformity, e.g. Ratio of prescription isodose volume to PTV or a conformity index

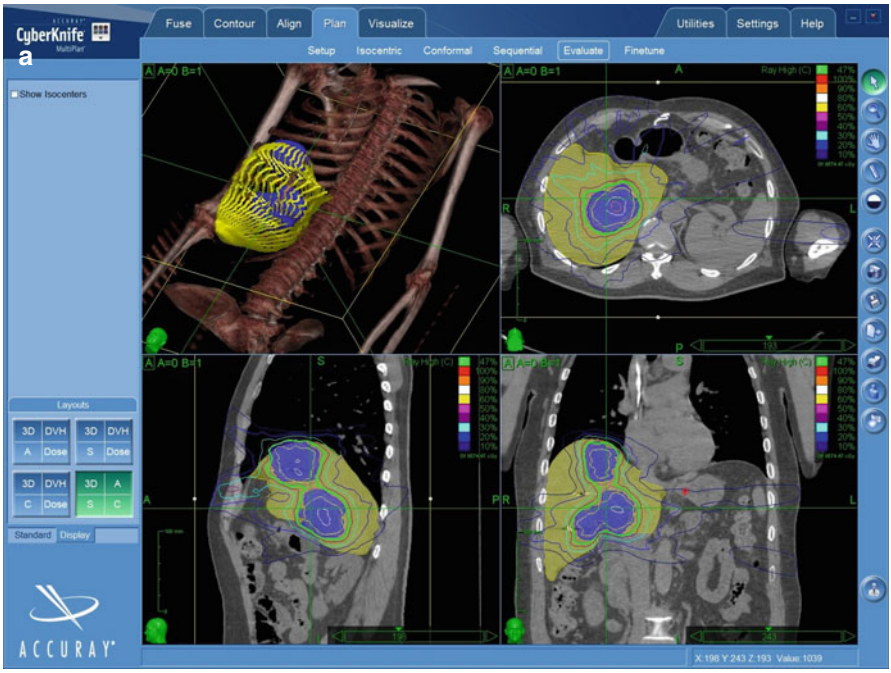

Fig. 9.3 (**a**) Axial, sagittal and coronal sections illustrating difficulty of planning SABR to patients with previous hepatic resection. This patient had undergone a left hepatectomy 12 months prior to SABR. The combined size and location of these metastases within the central portion of the remaining right lobe meant that an acceptable treatment plan could not be achieved that would deliver a meaningful potentially ablative dose. Further chemotherapy was necessary. (**b**) Dosimetric analysis confirmed that the dose required (45 Gy in 3 fractions) could not be achieved in this case within acceptable liver constraints—see box, *bottom right*. The patient was referred back to medical oncologists for further chemotherapy

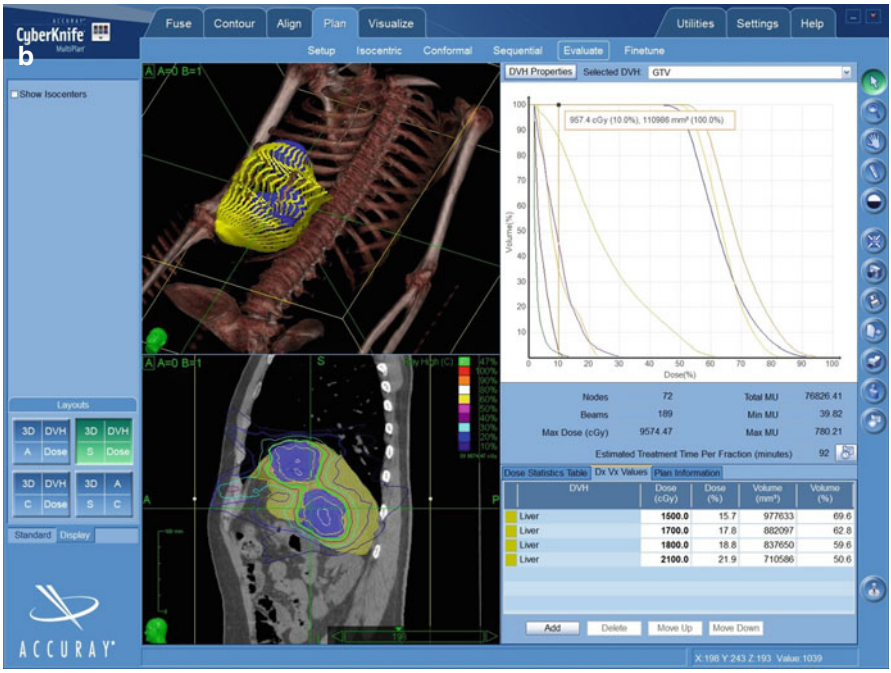

Fig. 9.3 (continued)

- Dose fall off outside the target e.g. ratio of the volume of the 50 % isodose curve to PTV
- Heterogeneity index e.g. the ratio of highest dose received by 5 % of PTV to lowest dose received by 95 % of PTV
- Notable areas of high or low dose outside of the PTV
- Dose to organs at risk—dose to 1 and 5 % volumes and mean doses.

9.6 Treatment Delivery and Clinical Follow-Up

Daily Image-guidance is mandatory in delivering liver SBRT safely, in order to reduce interfraction variability. Cone beam kV-CT (CBCT) is superior to most other means of achieving this. The Cyberknife system also enables on line intrafraction variability correction using the Synchrony real time tracking system. The ideal is matching to the soft tissues of the liver, but matching to vertebral bodies is a commonly used surrogate, although it is recognised that the liver can move between fractions relative to the vertebrae. Fiducials provide a useful alternative in matching, and are mandatory for the Cyberknife system. Errors of 3 mm or more should be corrected. When using CBCT, a post-treatment scan is advised as well, to assess intra-fraction variation.

9.7 Treatment Assessment and Follow-Up

9.7.1 Acute Toxicity

Overall, rates of G1–2 toxicity are reported to range from 0 to 27 % and grade 3–4 toxicities are observed in around 5 % [69] The rate of morbidity for liver radiotherapy is reported to be independent of dose-fractionation schedule [99], and the toxicity rates are consistently low despite the heterogeneity of dose/fractionation schedules, and delivery systems. The likely explanation is the limited dose delivered to uninvolved liver and the parallel functioning of liver parenchyma. The most commonly reported toxicities are fatigue, right upper quadrant pain, low grade pyrexia, transaminase rise (normally settles by 3 months post treatment), nausea, and loss of appetite.

A syndrome of minor pain, fever and chills is observed in some patients—Grade 1 (requiring no treatment) in 14 %, and grade 2 (requiring treatment with analgesics/steroids) in 13 %, usually occurring within 1–3 weeks of treatment [64, 66, 68]. Rates of gastric ulceration and esophagitis are low (G2 7 %, G3 in 3 %) and most centres advise the use of prophylactic proton-pump inhibitors [65]. The rates of RILD are notably very low in all published series. Child Pugh B and Hepatitis B carriage are associated with greater risk of RILD [26].

Rates of transaminase derangement are also low. For example, Grade 1/2 elevation of liver function tests were observed in 28 % patients treated with 30–55 Gy (median 48 Gy) by Katz et al. [69] and transient elevation of liver enzymes described as mild-moderate is noted in 31–36 % of patients receiving 25–60 Gy in 3 fractions [77].

Several studies have reported the use of liver SBRT in patients who have previously undergone surgical resection and/or RFA, and reported low levels of toxicity, suggesting SBRT is safe to use in this context [70, 75].

9.7.2 Late Toxicity

Only one study to date has reasonable follow up of 4.3 years [75]. Most others have follow up of around 16–18 months and, therefore, the extent of late radiation effects may be underestimated. However, the rates of high grade toxicity (G3 or worse) are generally reported as being extremely low at around 2–5 % [76, 78]. Late gastrointestinal toxicity (grade 2 or less—ulceration/bleeding) is reported in 8 % patients, and is far less likely in peripheral liver targets [78]. Other late effects include rib fractures.

In the early work of Blomgren et al. [24, 66] one patient experienced hemorrhagic gastritis following irradiation of less than one third of the stomach to more than 7 Gy during each of two treatment sessions, and another patient developed a duodenal ulcer after part of the distal stomach and proximal duodenum received 5 Gy in each of 4 fractions. Hoyer et al. [75] also observed colonic ulceration and duodenal ulceration when part of the intestine received more than 30 Gy. These

experiences have partially guided the tolerances suggested in Table 9.6, and illustrate the need for careful treatment planning and delivery.

9.7.3 Assessment of Response

Following SBRT, a local inflammatory and microvascular reaction develops in the liver which can sometimes be difficult to differentiate from residual disease [2]. Biphasic CT is reported to differentiate focal radiotherapy fibrotic reaction from active disease [100]. Distinct patterns of enhancement, shrinkage of hypodense areas, and displacement of vessels are indicative of local response [101]. Some reports suggest MRI may be superior in differentiating residual disease from normal tissue reaction [26]. CT-PET imaging a minimum of 3 months post SBRT can be useful in confirming response to treatment.

9.7.4 Follow-Up

The purpose of follow up is to detect any signs of further disease progression, and to accurately document toxicity. A suggested follow up schedule would be clinical review at 4–6 weeks post SBRT with a restaging CT, then 3 monthly to 2 years and 6 monthly thereafter. Follow up should include CT and/or MRI assessment (especially if there is the potential of further treatment), blood profile and clinical review.

References

1. Parkin DM, Bray F, Ferlay J, et al. Global cancer statistics, 2002. CA Cancer J Clin. 2005;55:74–108.
2. Hoyer M, Swaminath A, Bydder S. Radiotherapy for liver metastases: a review of the evidence. Int J Radiat Oncol Biol Phys. 2012;82(3):1047–57.
3. Dawood O, Mahadaven A, Goodman KA. SBRT for liver metastases. Eur J Cancer. 2009;45:2947–59.
4. Chou FF, Sheen-Chen SM, Chen YS, et al. Surgical treatment of cholangiocarcinoma. Hepatogastroenterology. 1997;44:760–5.
5. Aljiffry M, Walsh M, Molinari M. Advances in diagnosis, treatment and palliation of cholangiocarcinoma: 1990–2009. World J Gastroenterol. 2009;15(34):4240–61.
6. Andolino DL, Johnson CS, Mallucio M. SBRT for primary HCC. Int J Radiat Oncol Biol Phys. 2011;81(4):e447–53.
7. Klein J, Dawson LA. Hepatocellular carcinoma radiation therapy: review of evidence and future opportunities. Int J Radiat Oncol Biol Phys. 2013;87(1):22–32.
8. Kuvshinoff BW, Ota DM. Radiofrequency ablation of liver tumours. Influence of technique and tumour size. Surgery. 2002;132:605–11.

9. Giorgio A, Calisti G, Stefano DE, et al. Radiofrequency ablation for intrahepatic cholangiocarcinoma: retrospective analysis of a single centre experience. Anticancer Res. 2011;12:4575–80.
10. Camma C, Schepis F, Orlando A, et al. Transarterial chemoembolisation for unresectable hepatocellular carcinoma: meta-analysis of randomised controlled trials. Radiology. 2002;224:47–54.
11. Burger I, Hong K, Schulick R, et al. Transcatheter arterial chemoembolisation in unresectable cholangiocarcinoma: initial experience in a single institution. J Vasc Interv Radiol. 2005;16:353–61.
12. Yeo W, Mok TS, Zee B, et al. A randomised phase III study of doxorubicin versus cisplatin/interferon alpha-2b/doxorubicin/fluorouracil (PIAF) combination chemotherapy for unresectable hepatocellular carcinoma. J Natl Cancer Inst. 2005;97:1532–8.
13. Lopez PM, Villanueva A, Llovet JM. Systematic review: evidence-based management of hepatocellular carcinoma- an updated analysis of randomised controlled trials. Aliment Pharmacol Ther. 2006;23:1535–47.
14. Zhu AX. Systemic therapy of advanced HCC—how hopeful should We Be? Oncologist. 2006;11:790–800.
15. Lang L. FDA approves sorafenib for patients with inoperable liver cancer. Gastroenterology. 2008;134:379.
16. Philip PA, Mahoney MR, Allmer C, et al. Phase II study of Erlotinib (OSI-774) in patients with advanced hepatocellular cancer. J Clin Oncol. 2005;23:6657–63.
17. Cheng A, Kang Y, Lin D, et al. Phase 3 trial of sunitinib vs sorafenib in advanced HCC. Abstract. 2011. ASCO Annual Meeting, Chicago, IL, USA.
18. Knox JJ, Hedley D, Oza A, et al. Combining gemcitabine and capecitabine in patients with advanced biliary cancer: a phase II trial. J Clin Oncol. 2005;23:2332–8.
19. El-Khoueiry AB, Rankin CJ, Ben-Josef E, et al. SWOG 0514: a phase II study of Sorafenib in patients with unresectable or metastatic gall bladder carcinoma and cholangiocarcinoma. Invest New Drugs. 2012;30(4):1646–51.
20. Lawrence TS, Robertson JM, Ancher MS, et al. Hepatic toxicity resulting from cancer treatment. Int J Radiat Oncol Biol Phys. 1995;31:1237–48.
21. Dawson LA, Ten Haken RK, Lawrence TS. Partial irradiation of the liver. Semin Radiat Oncol. 2001;11(3):240–6.
22. Emami B, Lyman J, Brown A, et al. Tolerance of normal tissue to therapeutic radiation. Int J Radiat Oncol Biol Phys. 1991;21(1):109–22.
23. Kavanagh BD, et al. Extracranial radiosurgery (stereotactic body radiation therapy) for oligometastases. Semin Radiat Oncol. 2006;16:77–84.
24. Blomgren H, Lax I, Goranson H, et al. Radiosurgery for tumors in the body: clinical experience using a new method. J Radiosurg. 1998;1:63–74.
25. Choi BO, Jang HS, Kang KM, et al. Fractionated stereotactic radiotherapy in patients with primary HCC. Jpn J Clin Oncol. 2006;36(3):154–8.
26. Mendez Romero A, Wunderink W, Hussain SM, et al. SBRT for primary and metastatic liver tumors: a single institution phase I—II study. Acta Oncol. 2006;45(7):831–7.
27. Tse RV, Hawkins M, Lockwood G, et al. Phase I study of individualised SBRT for HCC and IHC. J Clin Oncol. 2008;26(4):657–64.
28. Choi BO, Choi IB, Jang HS, et al. SBRT with or without TACE for patients with HCC: preliminary analysis. BMC Cancer. 2008;8:351.
29. Seong J, Lee IJ, Shim SJ, et al. A multicenter retrospective cohort study of practice patterns and clinical outcome on radiotherapy for HCC in Korea. Liver Int. 2009;29(2):147–52.
30. Cardenes HR, Price TR, Perkins SM, et al. Phase I feasibility trial of SBRT for primary HCC. Clin Transl Oncol. 2010;12(3):218–25.
31. Louis C, Dewas S, Mirabel X, Lartigau E, et al. SBRT of HCC. Preliminary results. Technol Cancer Res Treat. 2010;9(5):479–87.
32. Seo YS, Kim MS, Yoo SY, et al. Preliminary result of SBRT as a local salvage treatment for inoperable HCC. J Surg Oncol. 2010;102(3):209–14.

33. Kwon JH, Bae SH, Kim JY, et al. Long term effect of SBRT for primary HCC ineligible for local ablation therapy or surgical resection: stereotactic radiotherapy for liver cancer. BMC Cancer. 2010;10:475.
34. Chan LC, Chiu SK, Chan SL. SBRT for HCC: report of a local single centre experience. Hong Kong Med J. 2011;17(2):112–8.
35. Bujold A, Massey C, Kim JJ, et al. Outcomes of SBRT for HCC. Int J Radiat Oncol Biol Phys. 2011;81(2):S70–1. ASTRO Abstract 138.
36. Ibarra RA, Rojas D, Snyder L, et al. Multicenter results of stereotactic body radiotherapy (SBRT) for non-resectable primary liver tumors. Acta Oncol. 2012;51(5):575–83.
37. Huang WY, Jen YM, Lee MS, et al. SBRT in recurrent HCC. Int J Radiat Oncol Biol Phys. 2012;84(2):355–61.
38. Katz AW, Chawla S, Qu Z, et al. Stereotactic hypofractionated radiation therapy as a bridge to transplantation for HCC. Clinical outcome and pathological correlation. Int J Radiat Oncol Biol Phys. 2012;83:895–900.
39. Sanuki N, Takeda A, Oku Y, et al. Stereotactic body radiotherapy for small hepatocellular carcinoma: a retrospective outcome analysis in 185 patients. Acta Oncol. 2014;53(3):399–404.
40. Takeda A, Sanuki N, Eriguchi T, et al. Stereotactic ablative body radiotherapy for previously untreated solitary hepatocellular carcinoma. J Gastroenterol Hepatol. 2014;29(2):372–9. doi:10.1111/jgh.12350.
41. Bujold A, Massey CA, Kim JJ, et al. Sequential phase I and II trials of stereotactic body radiotherapy for locally advanced hepatocellular carcinoma. J Clin Oncol. 2013;31(13):1631–9.
42. Kang JK, Kim MS, Cho CK, et al. Stereotactic body radiation therapy for inoperable hepatocellular carcinoma as a local salvage treatment after incomplete transarterial chemoembolization. Cancer. 2012;118(21):5424–31.
43. Al Hamad AA, Hassanain M, Michel RP, et al. Stereotactic radiotherapy of the liver. A bridge to transplantation. Technol Cancer Res Treat. 2009;8:401–5.
44. Nordlinger B, Van Cutsem E, Rougier P, et al. Does chemotherapy prior to liver resection increase the potential for cure in patients with metastatic colorectal cancer? A report from the European Colorectal Metastases Treatment Group. Eur J Cancer. 2007;43:2037–45.
45. Weiss L, Grundmann E, Torhorst J, et al. Haematogenous metastatic patterns in colonic carcinoma: an analysis of 1541 necropsies. J Pathol. 1986;150:195–203.
46. Sherman DM, Weischselbaum R, Order SE, et al. Palliation of hepatic metastatic. Cancer. 1978;41:2013–7.
47. Scheele J, Stangl R, Altendorf-Hoffman A. Hepatic metastases from colorectal carcinoma: impact of surgical resection on natural history. Br J Surg. 1990;77:1241–6.
48. Fong Y, Blumgart LH, Cohen AM. Surgical treatment of colorectal metastases to the liver. CA Cancer J Clin. 1995;45:50–62.
49. Bozzetti F, Cozzaglio L, Baracchi P, et al. Comparing surgical resection of limited hepatic metastases from colorectal cancer to non-operative treatment. Eur J Surg Oncol. 1993;19:162–7.
50. Nordlinger B, Guiguet M, Vaillant JC, et al. Surgical resection of colorectal carcinoma metastases to the liver. A prognostic system to improve case selection based on 1568 patients. Association Francaise de Chirurgie. Cancer. 1996;77:1254–62.
51. Fong Y, Fortner J, Sun RL, et al. Clinical score for predicting recurrence after hepatic resection for metastatic colorectal cancer: analysis of 1001 consecutive cases. Ann Surg. 1999;230:309–18.
52. House MG, Ito H, Gonen M, et al. Survival after hepatic resection for metastatic colorectal cancer. : Trends in outcome for 1,600 patients during two decades at a single institution. J Am Coll Surg. 2010;210:744–5.
53. Wei AC, Greig PD, Grant D, et al. Survival after hepatic resection for colorectal metastases: a 10 year experience. Ann Surg Oncol. 2006;13:668–76.

54. Robertson DJ, Stukel TA, Gottlieb DJ, et al. Survival after hepatic resection of colorectal cancer metastases: a national experience. Cancer. 2009;115:752–9.
55. Adam R, Avisar E, Ariche A, et al. Five year survival following hepatic resection after neoadjuvant therapy for non-resectable colorectal liver metastases. Ann Surg Oncol. 2001;8:347–53.
56. Glimelius B, Cavalli-Björkman N. Metastatic colorectal cancer: current treatment and future options for improved survival. Medical approach—present status. Scand J Gastroenterol. 2012;47(3):296–314.
57. Abdala EK, Vauthey JN, Ellis V. Recurrence and outcomes following hepatic resection, radiofrequency ablation, and combined resection/ablation for colorectal liver metastases. Ann Surg. 2004;239:818–25.
58. Solbiati L, Livraghi T, Goldberg SN. Percutaneous radio-frequency ablation of hepatic metastases from colorectal cancer: long term results in 117 patients. Radiology. 2001;221:159–66.
59. Berber E, Pelley R, Siperstien AE. Predictors of survival after radiofrequency thermal ablation of colorectal cancer metastases to the liver: a prospective study. J Clin Oncol. 2005;23:1358–64.
60. De Meijer VE, Verhoef C, Kuiper JW. Radiofrequency ablation in patients with primary and secondary hepatic malignancies. J Gastrointest Surg. 2006;10:960–73.
61. Aloia TA, Vauthey JN, Loyer EM. Solitary colorectal liver metastasis: resection determines outcome. Arch Surg. 2006;141:460–6.
62. Chang D, Swaminath A, Kozak M, et al. Stereotactic body radiotherapy for colorectal liver metastases. Cancer. 2011;117:4060–9.
63. Adam R, Chiche L, Aloia T, et al. Hepatic Resection for non-colorectal, non-neuroendocrine liver metastases: analysis of 1452 patients and development of a prognostic model. Ann Surg. 2006;244:524–53.
64. Herfarth KK, Debus J, Wannenmacher M. Stereotactic radiation therapy of liver metastases: update of the initial phase 1/2 trial. Front Radiat Ther Oncol. 2004;38:100–5.
65. Lee MT, Kim JJ, Dinniwell R. Phase I study of individualized stereotactic body radiotherapy of liver metastases. J Clin Oncol. 2009;27:1585–91.
66. Blomgren H, Lax I, Naslund I, et al. Stereotactic high dose fraction radiation therapy of extracranial tumours using an accelerator. Acta Oncol. 1995;34:861–70.
67. Wada H, Takai Y, Nemoto K. Univariate analysis of factors correlated with tumour control probability of three-dimensional conformal hypofractionated radiotherapy for small pulmonary or hepatic tumours. Int J Radiat Oncol Biol Phys. 2004;58:114–1120.
68. Wulf J, Guckenberger M, Haedinger U. Stereotactic radiotherapy of primary liver cancer and hepatic metastases. Acta Oncol. 2006;45:838–47.
69. Katz AW, Carey-Simpson M, Muhs AG, et al. Hypofractionated stereotactic body radiation therapy (SBRT) for limited hepatic metastases. Int J Radiat Oncol Biol Phys. 2007;67:793–8.
70. Van der Pool AEM, Mendez-Romero A, Wunderink W, et al. Sterotactic body radiation therapy for colorectal liver metastases. Br J Surg. 2010;97:377–82.
71. Habermehl D, Herfarth KK, Bermejo JL, et al. Single-dose radiosurgical treatment for hepatic metastases—therapeutic outcome of 138 treated lesions from a single institution. Radiat Oncol. 2013;8(1):175.
72. Berber B, Ibarra R, Snyder L, et al. Multicentre results of stereotactic body radiotherapy for secondary liver tumours. HPB (Oxford). 2013;15(11):851–7. doi:10.1111/hpb.12044.
73. Fumagalli I, Bibault JE, Dewas S, et al. A single-institution study of stereotactic body radiotherapy for patients with unresectable visceral pulmonary or hepatic oligometastases. Radiat Oncol. 2012;7:164.
74. Lanciano R, Lamond J, Yang J, et al. Stereotactic body radiation therapy for patients with heavily pretreated liver metastases and liver tumors. Front Oncol. 2012;2:23.
75. Hoyer M, Roed H, Anders T, et al. Phase 2 study on stereotactic body radiotherapy of colorectal metastases. Acta Oncol. 2006;45:823–30.

76. Rusthoven KE, Kavanagh BD, Cardenes H, et al. Multi-institutional Phase 1–2 Trial of stereotactic body radiation therapy for liver metastases. J Clin Oncol. 2009;27:1572–8.
77. Ambrosino G, Polistina F, Costantin G. Image-guided robotic stereotactic radiosurgery for unresectable liver metastases: preliminary results. Anticancer Res. 2009;29:3381–4.
78. Goodman K, Wiegner EA, Maturen KE. Dose-escalation study of single fraction stereotactic body radiotherapy for liver malignancies. Int J Radiat Oncol Biol Phys. 2012;78:486–93.
79. Rule W, Timmerman R, Tong L, Abdulrahman R, Meyer J, Boike T, Schwarz RE, Weatherall P, Chinsoo Cho L. Phase I dose-escalation study of stereotactic body radiotherapy in patients with hepatic metastases. Ann Surg Oncol. 2011;18(4):1081–7.
80. Scorsetti M, Arcangeli S, Tozzi A, et al. Is SBRT an attractive option for unresectable liver metastases? A preliminary report from a phase 2 trial. Int J Radiat Oncol Biol Phys. 2013;86:336–42.
81. Pech M, Mohnike K, Wieners G, et al. Radiotherapy of liver metastases. Comparison of target volumes and dose volume histograms employing CT and MRI based treatment planning. Strahlenther Onkol. 2008;184:256–61.
82. Bundschuh RA, Andratschke N, Dinges J, et al. Respiratory gated [18f] FDG PET/CT for target definition in stereotactic radiation therapy of liver metastases. Strahlenther Onkol. 2012;188:592–8.
83. Case RB, Sonke JJ, Moseley DJ, et al. Inter- and intrafraction variability in liver position in non-breath hold stereotactic body radiotherapy. Int J Radiat Oncol Biol Phys. 2009;75:302–8.
84. Dawson LA, Eccles C, Bissonnette JP, et al. Accuracy of daily image guidance for hypofractionated liver radiotherapy with active breathing control. Int J Radiat Oncol Biol Phys. 2005;62:1247–52.
85. Wagman R, Yorke E, Ford E, et al. Respiratory gating for liver tumours: use in dose escalation. Int J Radiat Oncol Biol Phys. 2003;55(3):659–68.
86. CyberKnifeTM University training manual, vol. 2. Accuray Inc, Sunnyvale, CA, USA; 2009.
87. Wunderink W, Romero A, Seppenwolde Y, et al. Potentials and limitations of guiding liver stereotactic body radiation therapy set-up on liver-implanted fiducial markers. Int J Radiat Oncol Biol Phys. 2010;77(5):1573–83.
88. Voroney JP, Brock KK, Eccles C, et al. Prospective comparison of computed tomography and magnetic resonance imaging for liver cancer delineation using deformable image registration. Int J Radiat Oncol Phys. 2006;66:780–91.
89. Sahani D, Kalva S. Imaging the liver. Oncologist. 2004;9:385–97.
90. Steffen I, Wust P, Ruhl R, et al. Value of combined PET/CT for radiation planning in CT-guided percutaneous interstitial high dose rate single fraction brachytherapy for colorectal liver metastases. Int J Radiat Oncol Biol Phys. 2010;77:1178–85.
91. Kirilova A, Lockwood G, Math M, et al. Three dimensional motion of liver tumours using cine-magnetic resonance imaging. Int J Radiat Oncol Biol Phys. 2008;71:1189–95.
92. Case RB, Moseley DJ, Bissonnette JP, et al. Variability in liver motion amplitude in patients undergoing free-breathing stereotactic body radiotherapy. Radiother Oncol. 2007;84 Suppl 2:S38.
93. Wunderink W, Mendez-Romero A, Krujif W, et al. Reduction of respiratory liver tumour motion by abdominal compression in stereotactic body frame, analysed by tracking fiducial markers implanted in liver. Int J Radiat Oncol Biol Phys. 2008;71:097–915.
94. Balter JM, Brock KK, Litzenberg DW, et al. Daily targeting of intrahepatic tumours for radiotherapy. Int J Radiat Oncol Biol Phys. 2002;52:266–71.
95. Shirato H, Shimizu S, Kitamura K, et al. Four dimensional treatment planning and fluoroscopic real-time tumour tracking radiotherapy for moving tumour. In J Radiat Oncol Biol Phys. 2000;48:435–42.
96. Benedict S, et al. SBRT—the report of AAPM Task Group 101. Med Phys. 2010;37(8):4078–101.
97. Liu R, Buatti JM, Howes TL, et al. Optimal number of beams for stereotactic body radiotherapy of lung and liver lesions. Int J Radiat Oncol Biol Phys. 2006;66:906–12.

98. McCammon R, Schefter TE, Gaspar LE. Observation of a dose-control relationship for lung and liver tumours after stereotactic body radiation therapy. Int J Radiat Oncol Biol Phys. 2009;73:112–8.
99. Carey-Simpson M, Katz A, Constine LS. Stereotactic body radiation therapy for extra-cranial oligometastases: does the sword have a double edge? Semin Radiat Oncol. 2006;16:67–76.
100. Herfarth KK, Hof F, Bahner ML, et al. Assessment of focal liver reaction by multiphasic CT after stereotactic single-dose radiotherapy of liver tumours. Int J Radiat Oncol Biol Phys. 2003;57:444–51.
101. Lo SS, The BS, Wang JZ, et al. Imaging changes after stereotactic body radiation therapy for lung and liver tumours. Expert Rev Anticancer Ther. 2011;11:613–21.
102. Dawson LA. The evolving role of radiation therapy in hepatocellular carcinoma. Cancer Radiother. 2008;12:96—101.

Chapter 10
Stereotactic Body Radiotherapy (SBRT) for Pancreatic Cancer

Anand Mahadevan and Andrew M. Gaya

Abstract Pancreatic cancer is the tenth most common cancer and is the fourth leading cause of cancer mortality. While surgery remains the current potentially curative treatment of choice, few cancers are resectable at presentation. Chemotherapy and radiation play a vital role in locally advanced non-metastatic pancreatic cancer. Systemic therapy is vital in these patients and often, when they remain non-metastatic after induction therapy radiation improves local control. Conventional chemoradiation is delivered in 5–6 weeks. Stereotactic body radiotherapy (SBRT) has been used in patients with locally advanced pancreas cancer, in fewer treatments, without significantly affecting systemic therapy, thereby maximizing systemic and local control. SBRT has also been used to boost positive margins, local recurrences after prior radiation, and in oligometastatic pancreatic cancer.

Keywords Locally advanced pancreatic cancer • Induction chemotherapy • Gemcitabine

10.1 Introduction

With an estimated 45,220 new cases, resulting in 38,460 deaths, in the United States in 2013, pancreatic cancer is the fourth-leading cause of cancer-related deaths [1]. Despite many new treatment approaches, pancreatic cancer survival has not improved in the past 25 years [2]. Surgical resection remains the only treatment approach with the potential for providing long-term survival for patients without metastatic disease at presentation, but between 40 and 50 % of patients have locally advanced

A. Mahadevan, MD, FRCS, FRCR (✉)
Department of Radiation Oncology, Beth Israel Deaconess Medical Center, Harvard Medical School, Boston, MA, USA
e-mail: amahadev@bidmc.harvard.edu

A.M. Gaya, MD
Department of Clinical Oncology, Guy's and St. Thomas' NHS Foundation Trust, London, UK
e-mail: agaya@theloc.com

A. Gaya, A. Mahadevan (eds.), *Stereotactic Body Radiotherapy: A Practical Guide*,
DOI 10.1007/978-0-85729-597-2_10

inoperable cancer at presentation or at surgical exploration [3]. The 5-year overall survival rate for patients with inoperable pancreatic cancer is less than 5 % [4–6].

Radiation therapy and chemotherapy, used either alone or in combination, are the only treatment options available for patients with locally advanced unresectable disease [6, 7]. However these treatments only marginally improve the median survival time to between 8 and 14 months [8–15]. Conventional radiation therapy requires approximately 6 weeks of daily treatments, which thus may take a significant fraction of the patient's limited life expectancy. In addition, side effects from radiation therapy can be substantial. Studies using chemotherapy alone have suggested outcomes equivalent to those of chemoradiation, raising further doubts about the value of a long course of conventional radiation therapy given the additional toxicity [16–23].

Stereotactic body radiotherapy (SBRT) is a minimally invasive treatment option that has been shown in prospective Phase I and Phase II studies and single institution studies to be a safe, quick and feasible approach for the treatment of locally advanced pancreatic cancer [24–36].

10.2 Patient Selection

Patients with biopsy proven non-metastatic locally advanced unresectable pancreatic cancer who are referred for conventional chemoradiation are also ideal potential candidates for SBRT. Patients with gastric or duodenal obstruction are generally excluded. Patients with borderline resectable disease can also be considered for this hypofractionated approach. A radiologist and experienced pancreatic surgeon should review a pancreas-specific multiphasic CT angiogram, to determine inoperability using standard CT criteria [37]. Patients who appear potentially resectable by axial imaging and considered for surgery and those found unresectable at the time of surgery would also be candidates. EUS (Endoscopic Ultrasound) has further increased diagnostic yield to identify patients with unresectable pancreas cancer and use the opportunity to obtain histological diagnosis and placement of fiducials [38].

Most patients eventually succumb to metastatic disease. This fact and randomized trials which did not show the benefit of addition of radiation therapy to systemic treatment [9] emphasizes the role of systemic therapy. As with conventional chemoradiation [12], it is now acceptable practice to use systemic therapy as induction therapy prior to SBRT for pancreas cancer. Single institution prospective studies have indeed validated tis approach [31].

10.3 Patient Work-Up

In addition to the history and clinical examination, Carbohydrate antigen 19–9 (CA19–9] measurements, complete blood counts, and a biochemistry panel including liver function tests are performed in all patients prior to treatment and at

follow-up. As mentioned above a multiphasic CT scan of the abdomen with oral and IV contrast is mandatory in the evaluation of these patients.

10.4 Treatment Planning

For image guidance, three to five fiducial seeds are commonly placed in and around the tumor percutaneously using CT guidance, at laparotomy, or (more commonly) under endoscopic ultrasound guidance. CT planning images with oral and IV contrast are obtained at least 1 week after fiducial placement, to allow for potential fiducial migration. Patients were imaged and treated in the supine position, with their arms down, lying in memory foam placed over a customized Vac-Lok™ (CIVCO Medical Solutions, Orange City, IA) immobilization cradle to ensure a comfortable and reproducible position. The CT images are transferred to a SBRT planning workstation and the target volume (visible gross disease) and critical structures, including the stomach, duodenum, kidneys, liver and spinal cord, are contoured. The clinical target volume is generally defined as the gross disease. No expansion margin is used where the tumor was in contact with the bowel (stomach or duodenum); otherwise, a 5 mm or smaller expansion margin (extending up to the outer bowel wall) is usually included to determine the planning target volume (PTV) [31].

10.5 Stereotactic Body Radiotherapy Dose Prescription

The SBRT dose is commonly prescribed to a conformal isodose line generally covering at least 95 % of the target volume (usually 70—80 %). While some institutions use a single fixed dose prescription [25–27, 29, 30, 34, 39], others use a radiation dose based on the relationship between the tumor location and the gastroduodenal loop, in order to limit toxicity (Fig. 10.1) [32]. However, when patients have had a palliative gastro-duodenal bypass, such duodenal constraints may have a lesser significance. The suggested maximal point tolerance dose of the duodenum is three fractions of 10 Gy each [40, 41]. In one institutional scheme [32], if the tumor approximated one-third or more of the circumference of the duodenum or stomach, then a dose of 24 Gy (three fractions of 8 Gy each) is used. If the tumor abutted the bowel in only one area and/or the space between the tumor and the bowel wall was less than 3 mm, then a dose of 30 Gy (three fractions of 10 Gy each) is prescribed. Finally, if the gap between the tumor and the duodenum was 3 mm or wider, a dose of 36 Gy (three fractions of 12 Gy each) is used. A representative treatment plan is shown in Fig. 10.2.

Normal tissue constraints are respected during treatment planning. When treating in three fractions, the volumes of liver receiving 21 Gy (V_{21}) or more and 15 Gy (V_{15}) or more are kept below 30 and 50 %, respectively. The corresponding doses to these volumes in single fraction would be V_{12} and V_{7} [42]. The volume of each

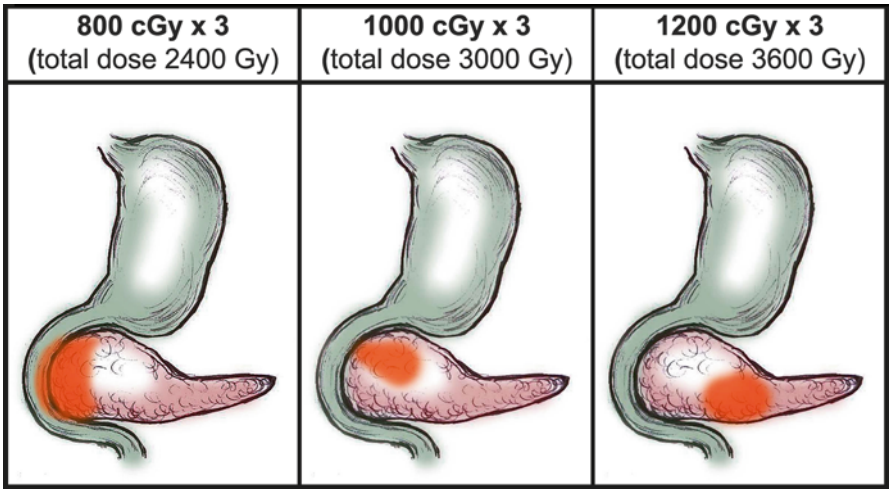

Fig. 10.1 Adaptive tolerance based stereotactic body radiotherapy dose prescription, showing a graphical depiction of the relationship between the duodenum and pancreatic tumor (*red*) that is used to determine each of the three prescribed doses

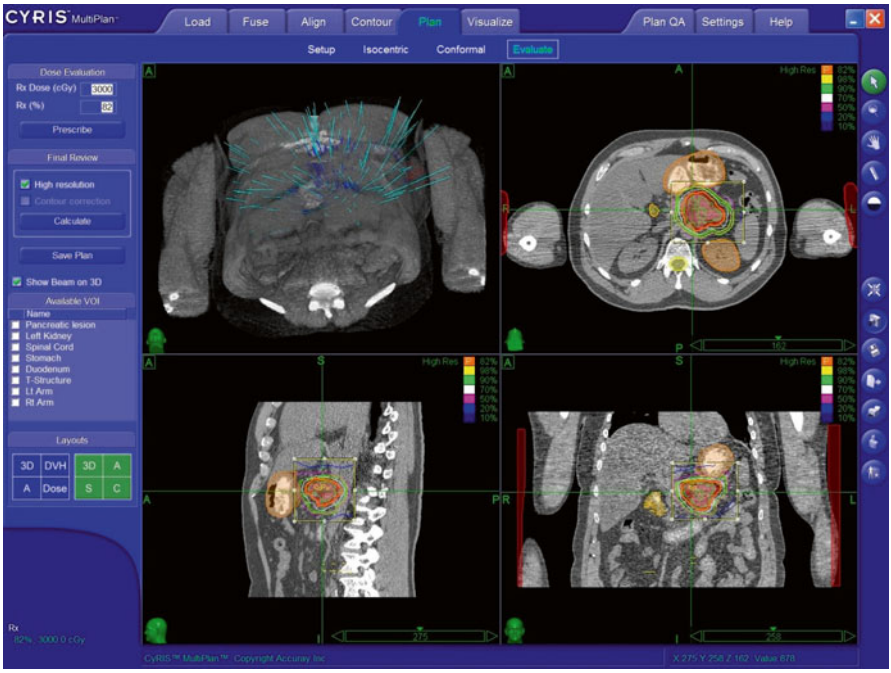

Fig. 10.2 Representative treatment plan

kidney receiving 12 Gy or more will be maintained below 25 %. The total maximal spinal cord limit is usually 12 Gy and the maximum point dose to the bowel is less 10 Gy per fraction.

10.6 Treatment Delivery

The CyberKnife Robotic Radiosurgery system (Accuray Incorporated, Sunnyvale, CA) with Synchrony motion tracking has been commonly used as a SBRT system to treat locally advanced pancreas cancer. Other SBRT modalities with image guidance and respiratory gating or dampening (E.g. Novalis, TrueBeam) can be equally applicable to treat these patients. Patients are generally premedicated with H_2 receptor blockers or proton pump inhibitors, and antiemetics.

10.7 Systemic Chemotherapy

Patients with unresectable, locally advanced pancreatic cancer often progress with metastatic disease as they harbor micrometastasis at presentation. Hence systemic therapy plays a vital role in the management of these patients. By utilizing a strategy of delivering upfront systemic chemotherapy it is possible to select those patients who are more likely to benefit from local therapy [12, 31]. Intensified chemotherapy regimens with proven improved response rates in the metastatic setting, like FOLFIRINOX, or Gemcitabine and nab-Paclitaxel is now being routinely used in patients with locally advanced pancreas cancer.

The use of single- and multiple-fraction SBRT has been shown to be feasible and safe for patients with locally advanced pancreatic cancer. The results of published data on the use of SBRT in locally advanced pancreas cancer is presented in Table 10.1 [25–27, 29–36, 39, 43]. In contrast to 5–6 weeks of conventional chemoradiation, SBRT can be performed in only 1–3 days, resulting in only a minimal delay in initiating systemic therapy. When SBRT is selectively used for patients who have been treated with systemic therapy, it appears to benefit them most without immediate overt development of metastasis when used upfront [31, 44].

Initial experience with single fraction SBRT with or without external beam radiation has been fraught with acute and chronic toxicity [25, 27, 29, 30]. Similarly high fixed doses of SBRT without accounting for respiratory motion has be associated with significant toxicity [27]. More recently tolerance based moderate doses of hypo fractionated radiation, with respiratory motion tracking and in the setting of systemic therapy has proven to be an acceptable regime [31]. Assuming an α/β ratio of 10 for pancreatic tumor response, Chang et al. calculated their scheme to be equivalent to 74 Gy delivered in 1.8-Gy fractions of conventional radiation. The Hoyer et al. study gave a dose equivalent to 95 Gy. In the study from Mahadevan et al., the equivalent dose was 51–76 Gy, comparable to a conventional radiation

Table 10.1 Clinical outcomes in published literature for SBRT for locally advanced pancreas cancer

Study (author)	Treatment	Number of patients	Progression-free survival (months)	Overall survival (months)
Koong et al. Phase I [29]	SRS 15–25 Gy	15	2	11[a]
Koong et al. Phase II [30]	RT 45 Gy + SRS 25 Gy	19	4.5	8[a]
Schellenberg et al. [26]	GEM + SRS 25 Gy + GEM	16	9	11.4[a]
Chang et al. (includes all of above patients) [25]	SRS 25 Gy ± GEM EBRT	77	–	11.4[a]
Hoyer et al. [27]	SBRT 45 Gy	22	4.8	5.7[a]
Mahadevan et al. [32]	SBRT 24–36 Gy + GEM	36	CA 19–9: 7.9 CT: 9.6	14.3[b]
Polistina et al. [33]	GEM + SBRT 30 Gy	33	NR	10.6[a]
Didolkar et al. [43]	SBRT 15–30 Gy + GEM	85[c]	NR	18.6[a] 8.6[b]
Rwigema et al. [34]	SRS 18–25 Gy	71[d]	NR	10.3[b]
Mahadevan et al. [31]	GEM- SBRT-GEM	39	15	20[a]
Goyal et al. [39]	SRS 20–25, SBRT 24–30 (3#) ± Chemo	20	NR	14.4
Chuong et al. [36]	GEM/GTX (borderline)-SBRT 35/25 Gy (5#)	64 (57 borderline)	9.7	15 (16.4 borderline)
Tozzi et al. [35]	SBRT 36 Gy (6#)	30 (9 Recc.)	8	11

Abbreviations: *EBRT* external beam radiation therapy, *GEM* gemcitabine, *GTX* gemcitabine, taxotere, xeloda, *NR* not reported, *RT* radiation therapy, *SBRT* stereotactic body radiation therapy, *SRS* stereotactic radiosurgery, *Recc* recurrent cancer

[a]From diagnosis

[b]From start of treatment

[c]Includes recurrent patients

[d]Includes recurrent and positive margin patients some of which received post-SRS chemotherapy

dose. While this may potentially appear to decrease the likelihood of local control it likely provides a better therapeutic ratio. The RBE (Relative Biological Effectiveness) and the equivalent doses for tumor control, acute and late toxicity in these series are presented in Table 10.2 [25, 27, 32].

10.8 Toxicity

Most patients experience fatigue and some nausea and temporary loss of appetite. Flare pain at the tumour site can also sometime occur and is usually self-limiting. Given the high doses of radiation per fraction, and the close association of the gasw-Phase I and Phase II SBRT toxicity data for liver tumors suggest that the maximum

Table 10.2 Relative radiation dose, local control and toxicity in three commonly used prescriptions for stereotactic radiosurgery or stereotactic body radiotherapy

Study	Fractionation	Conventional radiation equivalent dose (Gy) $Eq_{1.8}$	Tumor control biological equivalent dose (Gy) BED_{10}	Long term toxicity equivalent dose (Gy) BED_3	Median follow-up (months)	Local control (%)	Grade 3 or higher toxicity	
							Acute (%)	Long term (%)
Hoyer et al. [27]	15 Gy × 3	95	112.5	270	6	57	78	33
Chang et al. [25]	25 Gy × 1	74	87.4	233	12	84	1	9
Mahadevan et al. [32]	8–12 Gy × 3	51–76	43–54	88–180	24	78	8	6

Abbreviations: $Eq_{1.8}$ equivalent dose to conventional radiation in 1.8 Gy per daily fraction, BED_{10} biologically equivalent dose assuming α/β of 10 for tumor control and acute toxicity, BED_3 biologically equivalent dose assuming α/β of 3 for long term toxicity

point dose to the duodenum should be kept below the equivalent of three fractions each of 10 Gy (equivalent to 130 Gy in 1.8-Gy fractions, assuming an α/β ratio of 3) [40]. Other Dose Volume constraints have been proposed [45, 46]. The acute and long-term toxicity of the Hoyer study was higher than either the Stanford or the Boston groups. Assuming an α/β ratio of 3, the Chang et al., Hoyer et al. and Mahadevan et al. treatment schemes are equivalent to 233 Gy, 270 Gy, and 88–180 Gy in 1.8-Gy fractions, respectively. While this may explain the toxicity, a tolerance based (gastroduodenal tolerance) approach could decrease toxicity. This strategy has been used to reduce toxicity in other cancers treated with SBRT [47, 48].

10.9 Review of Literature

The treatment of patients with non-metastatic locally advanced pancreatic cancer continues to evolve. While the data is conflicting, the general standard of care appears to be concurrent chemoradiation in addition to systemic chemotherapy [49]. However, the effectiveness of the addition of chemoradiation to a chemotherapy treatment plan has been questioned. In addition there are significant side effects associated with 5–6 weeks of upper abdominal radiation, which are particularly problematic for these patients with short life expectancies. Nevertheless, randomized trials have shown a survival benefit to giving radiation therapy to such patients, as in other gastrointestinal cancers, and radiotherapy may be particularly helpful in local control and palliating local symptoms [50–52].

The use of single- and multiple-fraction SBRT has been shown to be feasible and safe for patients with locally advanced pancreatic cancer in several series. In contrast to 5–6 weeks of conventional chemoradiation, SBRT can be performed in only 1–3 days, resulting in only a minimal delay in initiating systemic therapy. Table 10.1 summarizes the outcomes for published studies of SRS and SBRT. Initial experience with single fraction SBRT with or without external beam radiation has been fraught with acute and chronic toxicity. Similarly high fixed doses of SBRT without accounting for respiratory motion has been associated with significant toxicity. More recently tolerance based moderate doses of hypo fractionated radiation, with respiratory motion tracking and in the setting of systemic therapy has proven to be an acceptable regime. While fractionation may decrease the likelihood of local control it potentially provides a better therapeutic ratio. The RBE (Relative Biological Effectiveness) and the equivalent doses for tumor control, acute and late toxicity in these series are presented in Table 10.2. Assuming an α/β ratio of 10 for pancreatic tumor response, 25 Gy single fraction is equivalent to 74 Gy delivered in 1.8-Gy fractions of conventional radiation. Similarly 45 Gy in three fractions delivers a dose equivalent to 95 Gy and the 24–36 Gy equivalent doses are 51–76 Gy, comparable to a conventional radiation dose. This along with consideration of equivalent doses for long-term toxicity as described above may explain the differences in outcomes.

10.10 Other Potential Roles of SBRT in Pancreas Cancer

Local failure is a significant problem in resected cancers even after an R0 resection. It is particularly relevant in patients with positive margins. A stereotactic boost to areas of known positive margins in addition to standard adjuvant therapy may provide additional local control and even a survival benefit [53]. In Boston fiducial seeds are routinely placed during pancreaticoduodenectomy at the uncinate, retroperitoneal, superior mesenteric and pancreatic margins, and pathology guided stereotactic boost of 10 Gy is delivered in addition to standard 50 Gy of postoperative chemoradiation for R1 resections.

Young patients with good performance status and isolated oligo metastasis (e.g. liver metastasis) presenting synchronously or metachronously, may also benefit from local control with SBRT in addition to systemic therapy. Yet another rare indication would include re-irradiation for local failure after prior radiation therapy in the absence of controlled metastatic disease.

10.11 Conclusion

SBRT can be delivered safely and quickly to potentially benefit patients with locally advanced unresectable pancreatic cancer. The toxicity and outcomes appear comparable or more favorable than those of conventional chemoradiation. A randomized trial will be required to answer whether SBRT plus chemotherapy will improve progression-free survival, overall survival, and patients' quality of life compared to chemotherapy with or without conventional chemoradiation. SBRT may have a role in patients with positive margins, oligometastasis and local recurrence after prior radiation.

References

1. Siegel R, Naishadham D, Jemal A. Cancer statistics, 2013. CA Cancer J Clin. 2013;63(1):11–30. PubMed PMID: 23335087.
2. Vincent A, Herman J, Schulick R, Hruban RH, Goggins M. Pancreatic cancer. Lancet. 2011;378(9791):607–20. PubMed PMID: 21620466.
3. Staley CA, Cleary KR, Abbruzzese JL, Lee JE, Ames FC, Fenoglio CJ, et al. The need for standardized pathologic staging of pancreaticoduodenectomy specimens. Pancreas. 1996;12(4):373–80. PubMed PMID: 8740405.
4. Cardenes HR, Chiorean EG, Dewitt J, Schmidt M, Loehrer P. Locally advanced pancreatic cancer: current therapeutic approach. Oncologist. 2006;11(6):612–23. PubMed PMID: 16794240.
5. Ducreux M, Boige V, Goere D, Deutsch E, Ezra P, Elias D, et al. The multidisciplinary management of gastrointestinal cancer. Pancreatic cancer: from pathogenesis to cure. Best Pract Res Clin Gastroenterol. 2007;21(6):997–1014. PubMed PMID: 18070700.
6. Yip D, Karapetis C, Strickland A, Steer CB, Goldstein D. Chemotherapy and radiotherapy for inoperable advanced pancreatic cancer. Cochrane Database Syst Rev. 2006;3, CD002093. PubMed PMID: 16855985.

7. Morganti AG, Massaccesi M, La Torre G, Caravatta L, Piscopo A, Tambaro R, et al. A systematic review of resectability and survival after concurrent chemoradiation in primarily unresectable pancreatic cancer. Ann Surg Oncol. 2010;17(1):194–205. PubMed PMID: 19856029.
8. Blackstock AW, Tepper JE, Niedwiecki D, Hollis DR, Mayer RJ, Tempero MA. Cancer and leukemia group B (CALGB) 89805: phase II chemoradiation trial using gemcitabine in patients with locoregional adenocarcinoma of the pancreas. Int J Gastrointest Cancer. 2003;34(2–3):107–16. PubMed PMID: 15361643.
9. Chauffert B, Mornex F, Bonnetain F, Rougier P, Mariette C, Bouche O, et al. Phase III trial comparing intensive induction chemoradiotherapy (60 Gy, infusional 5-FU and intermittent cisplatin) followed by maintenance gemcitabine with gemcitabine alone for locally advanced unresectable pancreatic cancer. Definitive results of the 2000–01 FFCD/SFRO study. Ann Oncol. 2008;19(9):1592–9.
10. Crane CH, Varadhachary G, Pisters PW, Evans DB, Wolff RA. Future chemoradiation strategies in pancreatic cancer. Semin Oncol. 2007;34(4):335–46. PubMed PMID: 17674962.
11. Crane CH, Winter K, Regine WF, Safran H, Rich TA, Curran W, et al. Phase II study of bevacizumab with concurrent capecitabine and radiation followed by maintenance gemcitabine and bevacizumab for locally advanced pancreatic cancer: Radiation Therapy Oncology Group RTOG 0411. J Clin Oncol. 2009;27(25):4096–102. PubMed PMID: 19636002. Pubmed Central PMCID: 2734421.
12. Huguet F, Andre T, Hammel P, Artru P, Balosso J, Selle F, et al. Impact of chemoradiotherapy after disease control with chemotherapy in locally advanced pancreatic adenocarcinoma in GERCOR phase II and III studies. J Clin Oncol. 2007;25(3):326–31. PubMed PMID: 17235048.
13. Magnino A, Gatti M, Massucco P, Sperti E, Faggiuolo R, Regge D, et al. Phase II trial of primary radiation therapy and concurrent chemotherapy for patients with locally advanced pancreatic cancer. Oncology. 2005;68(4–6):493–9. PubMed PMID: 16020980.
14. Okusaka T, Furuse J, Funakoshi A, Ioka T, Yamao K, Ohkawa S, et al. Phase II study of erlotinib plus gemcitabine in Japanese patients with unresectable pancreatic cancer. Cancer Sci. 2011;102(2):425–31. PubMed PMID: 21175992.
15. Okusaka T, Ito Y, Ueno H, Ikeda M, Takezako Y, Morizane C, et al. Phase II study of radiotherapy combined with gemcitabine for locally advanced pancreatic cancer. Br J Cancer. 2004;91(4):673–7. PubMed PMID: 15226765. Pubmed Central PMCID: 2364779.
16. Andre T, Noirclerc M, Hammel P, Meckenstock R, Landi B, Cattan S, et al. Phase II study of leucovorin, 5-fluorouracil and gemcitabine for locally advanced and metastatic pancreatic cancer (FOLFUGEM 2). Gastroenterol Clin Biol. 2004;28(8–9):645–50. PubMed PMID: 15646530.
17. El-Rayes BF, Zalupski MM, Shields AF, Vaishampayan U, Heilbrun LK, Jain V, et al. Phase II study of gemcitabine, cisplatin, and infusional fluorouracil in advanced pancreatic cancer. J Clin Oncol. 2003;21(15):2920–5. PubMed PMID: 12885810.
18. Heinemann V, Quietzsch D, Gieseler F, Gonnermann M, Schonekas H, Rost A, et al. Randomized phase III trial of gemcitabine plus cisplatin compared with gemcitabine alone in advanced pancreatic cancer. J Clin Oncol. 2006;24(24):3946–52. PubMed PMID: 16921047.
19. Louvet C, Andre T, Lledo G, Hammel P, Bleiberg H, Bouleuc C, et al. Gemcitabine combined with oxaliplatin in advanced pancreatic adenocarcinoma: final results of a GERCOR multicenter phase II study. J Clin Oncol. 2002;20(6):1512–8. PubMed PMID: 11896099.
20. Louvet C, Labianca R, Hammel P, Lledo G, Zampino MG, Andre T, et al. Gemcitabine in combination with oxaliplatin compared with gemcitabine alone in locally advanced or metastatic pancreatic cancer: results of a GERCOR and GISCAD phase III trial. J Clin Oncol. 2005;23(15):3509–16. PubMed PMID: 15908661.
21. O'Reilly EM, Abou-Alfa GK. Cytotoxic therapy for advanced pancreatic adenocarcinoma. Semin Oncol. 2007;34(4):347–53. PubMed PMID: 17674963.
22. Reni M, Passoni P, Panucci MG, Nicoletti R, Galli L, Balzano G, et al. Definitive results of a phase II trial of cisplatin, epirubicin, continuous-infusion fluorouracil, and gemcitabine in stage IV pancreatic adenocarcinoma. J Clin Oncol. 2001;19(10):2679–86. PubMed PMID: 11352960.

23. Stathopoulos GP, Syrigos K, Aravantinos G, Polyzos A, Papakotoulas P, Fountzilas G, et al. A multicenter phase III trial comparing irinotecan-gemcitabine (IG) with gemcitabine (G) monotherapy as first-line treatment in patients with locally advanced or metastatic pancreatic cancer. Br J Cancer. 2006;95(5):587–92. PubMed PMID: 16909140. Pubmed Central PMCID: 2360678.
24. Chang BW, Saif MW. Stereotactic body radiation therapy (SBRT) in pancreatic cancer: is it ready for prime time? JOP. 2008;9(6):676–82. PubMed PMID: 18981547.
25. Chang DT, Schellenberg D, Shen J, Kim J, Goodman KA, Fisher GA, et al. Stereotactic radiotherapy for unresectable adenocarcinoma of the pancreas. Cancer. 2009;115(3):665–72. PubMed PMID: 19117351.
26. Schellenberg D, Kim J, Christman-Skieller C, Chun CL, Columbo LA, Ford JM, et al. Single-fraction stereotactic body radiation therapy and sequential gemcitabine for the treatment of locally advanced pancreatic cancer. Int J Radiat Oncol Biol Phys. 2011;81(1):181–8. PubMed PMID: 21549517.
27. Hoyer M, Roed H, Sengelov L, Traberg A, Ohlhuis L, Pedersen J, et al. Phase-II study on stereotactic radiotherapy of locally advanced pancreatic carcinoma. Radiother Oncol. 2005;76(1):48–53. PubMed PMID: 15990186.
28. Schellenberg D, Goodman KA, Lee F, Chang S, Kuo T, Ford JM, et al. Gemcitabine chemotherapy and single-fraction stereotactic body radiotherapy for locally advanced pancreatic cancer. Int J Radiat Oncol Biol Phys. 2008;72(3):678–86. PubMed PMID: 18395362.
29. Koong AC, Le QT, Ho A, Fong B, Fisher G, Cho C, et al. Phase I study of stereotactic radiosurgery in patients with locally advanced pancreatic cancer. Int J Radiat Oncol Biol Phys. 2004;58(4):1017–21. PubMed PMID: 15001240.
30. Koong AC, Christofferson E, Le QT, Goodman KA, Ho A, Kuo T, et al. Phase II study to assess the efficacy of conventionally fractionated radiotherapy followed by a stereotactic radiosurgery boost in patients with locally advanced pancreatic cancer. Int J Radiat Oncol Biol Phys. 2005;63(2):320–3. PubMed PMID: 16168826.
31. Mahadevan A, Miksad R, Goldstein M, Sullivan R, Bullock A, Buchbinder E, et al. Induction gemcitabine and stereotactic body radiotherapy for locally advanced nonmetastatic pancreas cancer. Int J Radiat Oncol Biol Phys. 2011;81(4):e615–22. PubMed PMID: 21658854.
32. Mahadevan A, Jain S, Goldstein M, Miksad R, Pleskow D, Sawhney M, et al. Stereotactic body radiotherapy and gemcitabine for locally advanced pancreatic cancer. Int J Radiat Oncol Biol Phys. 2010;78(3):735–42. PubMed PMID: 20171803.
33. Polistina F, Costantin G, Casamassima F, Francescon P, Guglielmi R, Panizzoni G, et al. Unresectable locally advanced pancreatic cancer: a multimodal treatment using neoadjuvant chemoradiotherapy (gemcitabine plus stereotactic radiosurgery) and subsequent surgical exploration. Ann Surg Oncol. 2010;17(8):2092–101. PubMed PMID: 20224860.
34. Rwigema JC, Parikh SD, Heron DE, Howell M, Zeh H, Moser AJ, et al. Stereotactic body radiotherapy in the treatment of advanced adenocarcinoma of the pancreas. Am J Clin Oncol. 2011;34(1):63–9. PubMed PMID: 20308870.
35. Tozzi A, Comito T, Alongi F, Navarria P, Iftode C, Mancosu P, et al. SBRT in unresectable advanced pancreatic cancer: preliminary results of a mono-institutional experience. Radiat Oncol. 2013;8(1):148. PubMed PMID: 23799996. Pubmed Central PMCID: 3707803.
36. Chuong MD, Springett GM, Freilich JM, Park CK, Weber JM, Mellon EA, et al. Stereotactic body radiation therapy for locally advanced and borderline resectable pancreatic cancer is effective and well tolerated. Int J Radiat Oncol Biol Phys. 2013;86(3):516–22. PubMed PMID: 23562768.
37. Raptopoulos V, Steer ML, Sheiman RG, Vrachliotis TG, Gougoutas CA, Movson JS. The use of helical CT and CT angiography to predict vascular involvement from pancreatic cancer: correlation with findings at surgery. AJR Am J Roentgenol. 1997;168(4):971–7. PubMed PMID: 9124153.
38. Morris-Stiff G, Escofet X, Barry JD, Lewis WG, Puntis MC, Roberts SA. Selective use of endoscopic ultrasound in the evaluation of carcinomas of the pancreatic head. Dig Surg. 2011;28(5–6):373–8. PubMed PMID: 22134196.

39. Goyal K, Einstein D, Ibarra RA, Yao M, Kunos C, Ellis R, et al. Stereotactic body radiation therapy for nonresectable tumors of the pancreas. J Surg Res. 2012;174(2):319–25. PubMed PMID: 21937061.
40. Rusthoven KE, Kavanagh BD, Cardenes H, Stieber VW, Burri SH, Feigenberg SJ, et al. Multi-institutional phase I/II trial of stereotactic body radiation therapy for liver metastases. J Clin Oncol. 2009;27(10):1572–8. PubMed PMID: 19255321.
41. Schefter TE, Kavanagh BD, Timmerman RD, Cardenes HR, Baron A, Gaspar LE. A phase I trial of stereotactic body radiation therapy (SBRT) for liver metastases. Int J Radiat Oncol Biol Phys. 2005;62(5):1371–8. PubMed PMID: 16029795.
42. Pan CC, Kavanagh BD, Dawson LA, Li XA, Das SK, Miften M, et al. Radiation-associated liver injury. Int J Radiat Oncol Biol Phys. 2010;76(3 Suppl):S94–100. PubMed PMID: 20171524.
43. Didolkar MS, Coleman CW, Brenner MJ, Chu KU, Olexa N, Stanwyck E, et al. Image-guided stereotactic radiosurgery for locally advanced pancreatic adenocarcinoma results of first 85 patients. J Gastrointest Surg. 2010;14(10):1547–59. PubMed PMID: 20839073.
44. Gurka MK, Collins SP, Slack R, Tse G, Charabaty A, Ley L, et al. Stereotactic body radiation therapy with concurrent full-dose gemcitabine for locally advanced pancreatic cancer: a pilot trial demonstrating safety. Radiat Oncol. 2013;8:44. PubMed PMID: 23452509. Pubmed Central PMCID: 3607991.
45. Taniguchi CM, Murphy JD, Eclov N, Atwood TF, Kielar KN, Christman-Skieller C, et al. Dosimetric analysis of organs at risk during expiratory gating in stereotactic body radiation therapy for pancreatic cancer. Int J Radiat Oncol Biol Phys. 2013;85(4):1090–5. PubMed PMID: 23273994.
46. Murphy JD, Christman-Skieller C, Kim J, Dieterich S, Chang DT, Koong AC. A dosimetric model of duodenal toxicity after stereotactic body radiotherapy for pancreatic cancer. Int J Radiat Oncol Biol Phys. 2010;78(5):1420–6. PubMed PMID: 20399033.
47. Lee MT, Kim JJ, Dinniwell R, Brierley J, Lockwood G, Wong R, et al. Phase I study of individualized stereotactic body radiotherapy of liver metastases. J Clin Oncol. 2009;27(10):1585–91. PubMed PMID: 19255313.
48. Tse RV, Hawkins M, Lockwood G, Kim JJ, Cummings B, Knox J, et al. Phase I study of individualized stereotactic body radiotherapy for hepatocellular carcinoma and intrahepatic cholangiocarcinoma. J Clin Oncol. 2008;26(4):657–64. PubMed PMID: 18172187.
49. Richter J, Saif MW. Locally advanced pancreatic adenocarcinoma: where are we and where are we going? Highlights from the "2010 ASCO Gastrointestinal Cancers Symposium". Orlando, FL, USA. January 22–24, 2010. JOP. 2010;11(2):139–43.
50. Ko AH, Crane CH. Radiation therapy in operable and locally advanced pancreatic cancer. J Natl Compr Canc Netw. 2010;8(9):1022–31. PubMed PMID: 20876542.
51. Minn AY, Koong AC, Chang DT. Stereotactic body radiation therapy for gastrointestinal malignancies. Front Radiat Ther Oncol. 2011;43:412–27. PubMed PMID: 21625166.
52. Savir G, Huber KE, Saif MW. Locally advanced pancreatic cancer. Looking beyond traditional chemotherapy and radiation. JOP. 2013;14(4):337–9. PubMed PMID: 23846922.
53. Rwigema JC, Heron DE, Parikh SD, Zeh 3rd HJ, Moser JA, Bahary N, et al. Adjuvant stereotactic body radiotherapy for resected pancreatic adenocarcinoma with close or positive margins. J Gastrointest Cancer. 2012;43(1):70–6. PubMed PMID: 20809393.

Chapter 11
Prostate Stereotactic Body Radiotherapy—Methods, Rationale, Outcomes, and Future Directions

Donald B. Fuller

Abstract Stereotactic Body Radiotherapy (SBRT) describes a contemporary external beam radiotherapy method that utilizes hypofractionation, delivering a small number of large doses per fraction, potentially exploiting a radiobiologic advantage unique to prostate cancer, whose cells are thought to have a high sensitivity to fraction size. Although prostate cancer may have a greater sensitivity to fraction size than surrounding normal tissues such as rectum and bladder, translating to a theoretical therapeutic ratio improvement by SBRT hypofractionation, these surrounding normal tissues *also* have a relatively high sensitivity to fraction size, meaning they too are potentially damaged by large dose per fraction radiotherapy treatment. As such, tight margins and extreme accuracy are also a necessary prerequisite when delivering hypofractionated radiation treatment. Several very precise radiotherapy delivery technologies have emerged that satisfy this technical requirement, including both image-guided noncoplanar and image-guided or electromagnetic-guided gantry based systems. Considering the relatively narrow margins and high purported central biologic potency of SBRT, there are three different potential uses of this modality against prostate cancer:

- SBRT used as monotherapy for clinically localized lesions that have a minimal risk of tumor extension beyond the immediate peri-prostatic region
- SBRT used as a prostate boost, in conjunction with wider field "conventional" pelvic radiotherapy, against high-risk lesions that have a substantially greater risk of tumor extension beyond the immediate peri-prostatic region (i.e.—significant risk of positive seminal vesicles, lymph nodes)
- SBRT used as a narrow margin salvage method used against recurrent prostate cancer—either following failed prior prostate radiotherapy (local retreatment) or against limited metastatic foci.

This chapter critically examines the use of SBRT applied to all three of the above-described prostate cancer scenarios.

Keywords Prostate • SBRT • Hypofractionation • HDR • Brachytherapy • Radiosurgery • Stereotactic • Radiotherapy • Prostate Cancer

D.B. Fuller, MD
CyberKnife Centers of San Diego, Genesis Healthcare Partners, San Diego, CA, USA
e-mail: dfuller@genhp.com

A. Gaya, A. Mahadevan (eds.), *Stereotactic Body Radiotherapy: A Practical Guide*,
DOI 10.1007/978-0-85729-597-2_11

11.1 Background and Rationale for Prostate SBRT

Prostate cancer is the most common visceral malignancy of men in the United States, accounting for 33 % of non-skin cases, with a total incidence greater than 200,000 cases/year [1]. The most important risk factor is age, with a median onset at age 68 years and a sharply rising incidence with increasing age beyond that [2]. There is significant heterogeneity in the incidence of this disease amongst different nations worldwide, with the greatest incidence of prostate cancer in Scandinavia and the lowest incidence occurring in Asia [1]. Dietary and perhaps other environmental factors likely play a role in the development of this disease, with the strongest evidence being the observation that over time, Asian men that reside in the United States develop a higher incidence of prostate cancer than their counterparts who remain in Japan or China [3]. Another important risk factor is family history, with greater than double the incidence of prostate cancer seen in men with a positive first degree relative family history of the disease [4]. Although prostate cancer remains the second leading cause of cancer-specific mortality among American males on an absolute basis, the prostate cancer death rates in the United States have been steadily decreasing since the advent of the "PSA era" in the early 1990s, likely due to a combination of earlier diagnosis by PSA screening as well as the widespread use of more effective surgical and radiotherapeutic local treatments.

11.2 Hypofractionation

Stereotactic Body Radiotherapy (SBRT) describes a contemporary external beam radiotherapy approach that utilizes hypofractionation, delivering a small number of large doses per fraction, potentially exploiting a radiobiologic advantage unique to prostate cancer, whose cells are thought to have a very low alpha-beta ratio (<2 Gy) that indicates a high sensitivity to fraction size [5–8]. The concept of hypofractionation is not a new idea at all, and such regimens were employed at the Christie Hospital (Manchester, UK) in the treatment of localized prostate cancer decades ago; this was most famously illustrated by the case of Sir Lawrence Olivier, who was successfully treated by a 36 Gy in 6 fraction regimen over 3 weeks (given as a 10×10 cm four field brick arrangement) in the late 1960s at St Thomas' Hospital, London, surviving apparently disease-free and complication-free for greater than 20 years thereafter [9].

Brenner and Hall evaluated the published efficacy outcomes of external beam and interstitial prostate brachytherapy in 1999 to derive an estimated α/β [alpha/beta] ratio of 1.5 Gy [5]. This is probably lower than the α/β [alpha/beta] ratio of the surrounding normal tissue such as the rectum, which is commonly thought to possess an α/β [alpha/beta] ratio of approximately 3 Gy [10]. This creates a scenario in which a greater differential tumor cell versus normal tissue sensitivity is created through the use of large dose per fraction radiotherapy treatment, potentially leading

to higher cure rates or decreased normal tissue complication rates versus "conventional" fractionation radiotherapy regimens. Brenner and Hall conclude that in particular, this prostate cancer radiobiologic trait supports the use of high dose rate (HDR) brachytherapy, which inherently delivers large doses per fraction, or appropriately designed large dose per fraction external beam radiotherapy schedules [5].

The main imperfection in this theory is that not all investigators have concluded the α/β [alpha/beta] ratio of prostate cancer to be so low, with some deriving or postulating considerably higher values α/β [alpha/beta] ratio values of 3.7–5 Gy or more, leading to continued uncertainty [11–13]. Among other problems, there has been a relative paucity of >3 Gy/fraction data with requisite long-term follow-up in the literature to provide a full data base from which to derive a robust and accurate α/β [alpha/beta] ratio calculation for prostate cancer.

Assuming the low α/β [alpha/beta] rationale to be correct though, the SBRT modality is very well suited to deliver hypofractionated regimens, due to the inherent large dose per fraction provided by this approach. Although the α/β [alpha/beta] ratio of prostate cancer may well be lower than surrounding normal tissues, those normal tissues *also* have a relatively low α/β [alpha/beta] ratio, meaning they too are potentially damaged by large dose per fraction radiotherapy treatment. As such, tight margins and extreme accuracy are a necessary prerequisite when delivering hypofractionated radiation treatment. SBRT nicely fulfills this requirement, due to the very high spatial accuracy of a number of SBRT approaches [14–21].

Preceding modern SBRT, a different approach to hypofractionation has been utilized—high dose rate (HDR) prostate brachytherapy. This method has very high reported disease-free survival rates utilizing a variety of hypofractionation regimens, ranging from 3,800 cGy/4 fractions to 5,400 cGy/9 fractions as monotherapy, primarily (but not exclusively) against low-intermediate-risk lesions [22–25]. The HDR brachytherapy modality has also been used successfully as a prostate boost method, in conjunction with wide field pelvic radiotherapy, against a wider range of low-risk to high-risk prostate cancer cases, in which instance HDR brachytherapy is used to maximize radiobiologic potency against the primary lesion itself, with the wider coverage of conventional external beam radiotherapy applied to cover potential subclinical disease extension pathways beyond the prostate [26, 27]. There is some evidence that this combined modality approach has superior efficacy versus external beam monotherapy, even versus "dose escalated" external beam radiotherapy monotherapy [28, 29].

The emergence of SBRT represents a contemporary approach that potentially combines the better features of external beam radiotherapy *and* HDR brachytherapy; in that the SBRT modality maintains the noninvasive trait of external beam radiotherapy, yet with the capability to deliver "HDR-like" dose fractionation, dosimetry morphology and accuracy [30, 31].

The initial contemporary prostate SBRT regimen was described by King et al., using a hypofractionated schedule of 36.25 Gy/5 fractions, using the CyberKnife device as the delivery mechanism, against low- and low-intermediate risk cases, the first so treated in 2003. This dose regimen was selected to provide biologic equivalence to a conventionally fractionated external beam radiotherapy regimen of

74 Gy/37 fractions, assuming a prostate cancer α/β [alpha/beta] ratio of 3 Gy [14]. If the true α/β [alpha/beta] ratio of prostate cancer is lower, as is now fairly widely believed (but still not universally agreed), the biologic potency of this regimen may significantly exceed 74 Gy/ 37 fractions, and could in fact, exceed 90 Gy/45 fractions.

Considering the relatively narrow margins and high purported central biologic potency of SBRT, there are three different potential uses of this modality against prostate cancer:

- SBRT used as monotherapy for clinically localized lesions that have a minimal risk of tumor extension beyond the immediate peri-prostatic region
- SBRT used as a prostate boost, in conjunction with wider field "conventional" pelvic radiotherapy, against high-risk lesions that have a substantially greater risk of tumor extension beyond the immediate peri-prostatic region (i.e.—significant risk of positive seminal vesicles, lymph nodes)
- SBRT used as a narrow margin salvage method used against recurrent prostate cancer—either following failed prior prostate radiotherapy (local retreatment) or against limited metastatic foci.

11.2.1 Case History

A 59 year old otherwise healthy gentleman presented in 2007 with a prostate-specific antigen (PSA) level of 5.4 ng/mL (elevated versus prior levels). Prostate biopsy dated 7/27/2007 revealed Gleason score 3 + 4 = 7 adenocarcinoma from 10 % of the left lobe and Gleason score 3 + 3 = 6 adenocarcinoma from 10 % of the right lobe ("overall" Gleason score 3 + 4 = 7). His prostate was palpably normal (Clinical stage T1c). His I-PSS score was 11/35 (c/w mild preexisting voiding symptoms) and his presenting Sexual Health Inventory Matrix (SHIM) score was 25/25, indicating full potency. He was very concerned about loss of potency with treatment. After careful consideration of a number of potentially curative surgical and radiotherapeutic treatment methods, he selected CyberKnife SBRT monotherapy as his treatment of choice. Due to relatively limited efficacy data in 2007, he agreed to receive his prostate SBRT treatment as a participant in an IRB-approved clinical trial [32].

On September 7, 2007, he received 4 transperineally implanted intraprostatic gold fiducials to serve as his SBRT image guidance reference structure (Fig. 11.1). His prostate measured 59.6 cc on ultrasound imaging, with no other specific abnormally visualized. Fiducial-to-fiducial coregistered CT and MRI-based treatment planning was accomplished 1 week later, with a Foley catheter in place for both studies to identify the location of the urethra. The prostate and seminal vesicle bases were defined primarily from the MRI image set and contoured contiguously, with all contours also reconciled with the reference CT image set, to form the Gross Target Volume (GTV).

An asymmetric margin expansion was then applied to form a Clinical Target Volume (CTV) that covered the entire prostate and potential extracapsular extension

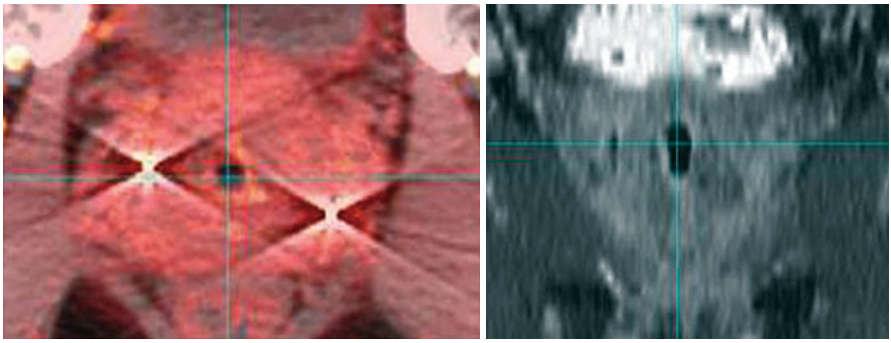

Fig. 11.1 Prostate fiducials as seen on CT-based (*L panel*) and MRI-based (*R panel*) images: Note fiducial prominence and streak artifact on the CT image, with comparatively less prominence and no artifact on the MRI image

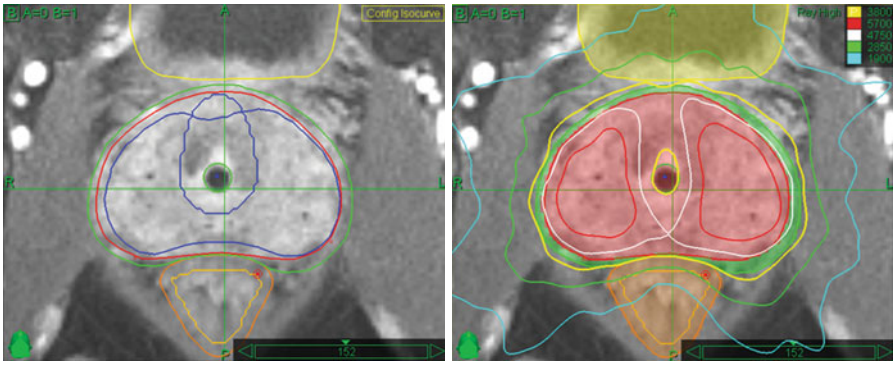

Fig. 11.2 Prostate CyberKnife SBRT contours and composite treatment plan: Note asymmetric peripheral margin expansion, with a larger left-sided margin expansion to accommodate the higher probability and potential magnitude of extracapsular tumor extension due to left-sided Gleason 7 disease. Note also the "shaving" of the PTV margin to zero at the prostate-rectal interface in the *midline*. Finally, note "HDR-brachytherapy-like" dose escalation in the extraurethral prostate, with central sparing and sharp posterior fall-off to limit urethral and rectal dose, respectively. The 100 % isodose line (*yellow*) follows the outer rectal wall while the 75 % isodose line (*green*) follows the rectal mucosa, which is defined as a 3 mm contraction from the rectal wall. The 125 and 150 % internal dose escalation isodose lines are displayed in *white* and *red*, respectively

contiguously. Specifically, this consisted of GTV + 2 mm on the right, GTV + 5 mm on the left (the side that harbored Gleason 7 disease and MRI-abnormality; felt to be at higher risk of extracapsular extension), contiguously also surrounding the seminal vesicle bases by 2 mm, and shaved to zero mm against the rectum. There was no further CTV to PTV expansion (CTV = PTV) (Fig. 11.2).

Although it could be argued that at least a mm or two of extra CTV to PTV margin expansion could also be applied to account for issues such as image interpretation/registration uncertainty and potential interfraction/intrafraction prostate

distortion, the 2 Gy/fraction radiobiological dose equivalent of the Virtual HDR protocol is 9,400 cGy for an α/β [alpha/beta] ratio of 3 Gy (a commonly assumed rectal α/β [alpha/beta] ratio value). As such, *any* added margin expansion is potentially injurious to adjacent tissue, and we thus choose to err on the side of "tight" margins on this protocol. The published sub-millimeter tracking accuracy of the CyberKnife delivery device and its ability to correct beam aiming in the translational and rotational dimensions ("6D") further support the reasonability of "tight" margins when using this technology [14, 15].

He subsequently received protocol SBRT treatment on consecutive days, from 10/15/2007—10/18/2007, using the CyberKnife device as the SBRT delivery mechanism. The prescribed dose was 3,800 cGy/4 fractions, prescribed to the 49 % isodose line, creating an intraprostatic maximum dose ("Dmax") of 7,755 cGy within the left lobe ("HDR-like" intraprostatic dose escalation) to a PTV that measured 148.2 cc,. Adjacent tissues (bladder, urethra, rectal wall and rectal mucosa) were also subject to "HDR-like" dose limitations per protocol (120, 120, 100 and 75 % of prescribed dose, respectively). Minor protocol deviations were accepted on the bladder, rectal wall and rectal mucosa Dmax levels to assure full PTV coverage, while the urethra dose level was fully protocol compliant.

Acutely, he had grade I GU and GI toxicity, including an I-PSS symptom score increase of 6 points and some rectal discomfort at the 2 week follow-up visit, fully resolved to baseline by the 1 month follow-up visit. There was no chronic GU or GI toxicity. His sexual potency was fully maintained, with a SHIM score of 25/25 at all short-term and long-term follow-up visits, out to 5 years.

The PSA level steadily decreased from 5.4 ng/mL pre-treatment to 1.0 ng/mL by 6 months post-treatment, increasing to 2.3 ng/mL at the 1 year follow-up ("PSA bounce"), thereafter decreased to 0.4 ng/mL by the 2-year follow-up visit, followed by a second minor "PSA bounce" to 0.5 ng/mL at the 30 month follow-up, steadily decreasing after that to a final PSA nadir level of 0.1 ng/mL by the 4 year and 5-year follow-up visits. The PSA response curve for this case is illustrated in Fig. 11.3.

The SBRT planning MRI had shown a 61 cc prostate with diminished left lobe T2-weighted signal intensity and gadolinium hyperperfusion, c/w stage T2b disease. Follow-up MRI at 2 years revealed resolution of abnormalities and a prostate volume shrinkage to 35 cc (reduction of 43 %). He remains free of complications, with fully maintained potency function and improved voiding function (baseline I-PSS score of 11/35 pre-SBRT decreased to 2/35 at the 5 year follow-up visit). He will continue to have annual PSA-based follow-up visits.

11.3 Review of Literature (Review of the Evidence)

11.3.1 SBRT Monotherapy for Previously Untreated Cases

The predominance of published literature to date describes SBRT monotherapy against low- and intermediate-risk prostate cancer cases [33–35]. The initial cohort was recently updated by King et al. [33] In that study 67 low and

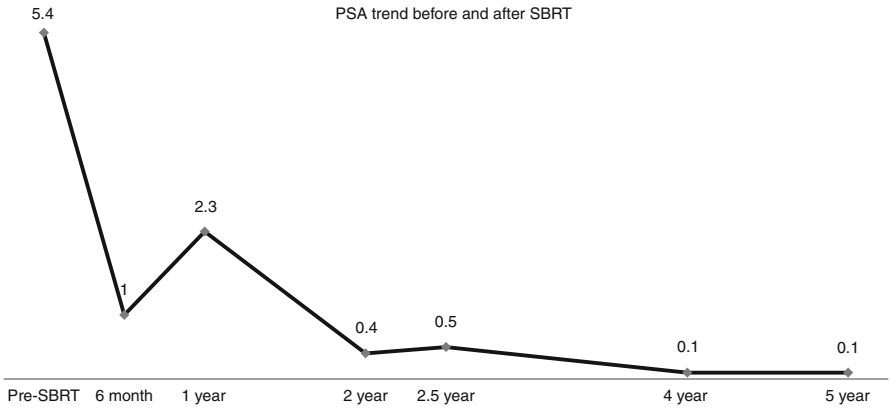

Fig. 11.3 Pre-treatment and follow-up PSA values, demonstrating common post-SBRT response kinetics: There is a rapid, early drop to 6 months, followed by a self-limited "PSA bounce" at a year, presumably reflecting post-SBRT delayed prostate inflammation, followed by resumption of a declining pattern with a second minor "PSA bounce" at 2.5 years, taking 4 years to achieve the final nadir PSA value

low-intermediate-risk patients were treated with SBRT to a dose of 36.25 Gy/5 fractions, to a planning target volume (PTV) created by an anisotropic margin expansion of the prostate, by 3 mm posteriorly and 5 mm elsewhere, prescribed to cover >95 % of the PTV with the prescription dose, using the CyberKnife as the delivery device.

The 4-year actuarial biochemical disease-free survival was 94 % (median follow-up 2.7 years), with 2 biopsy proven local failures, and a reassuringly low rate of grade 3 or higher toxicity (3 % GU, 0 % GI). The few observed cases of grade 3 GU toxicity were preceded by urologic instrumentation. Grade 1–2 GU and GI toxicity was seen in 28 and 12.5 % of patients, respectively, with a statistically significantly lower incidence of low grade toxicity in patients that were treated every other day (q.o.d.) as opposed to daily (q.d.) ($p=0.001$ for gastrointestinal and $p=0.007$ for genitourinary). It was concluded that SBRT efficacy compared well with other treatments and that the incidence of severe toxicity was low, causing the authors to suggest that "current evidence supports consideration of stereotactic body radiotherapy among the therapeutic options for localized prostate cancer."

A pooled dual institutional study by Freeman and King, restricted to a smaller cohort of 41 CyberKnife SBRT patients treated to 35–36.25 Gy/5 fractions with a significantly longer 5-year median follow-up was also reported. They reported similar findings—93 % 5-year biochemical disease-free survival and only a single case of grade 3 GU toxicity, with no Grade 3 or higher GI toxicity [34].

A different study reported by Katz et al., evaluated the efficacy of two different CyberKnife SBRT dose-fractionation regimens (35 Gy/5 fractions versus 36.25 Gy/5 fractions) in two groups of patients with predominantly low-risk prostate cases—41 consecutive patients treated to 35 Gy/5 fractions versus 41 matched subsequent cases treated to 36.25 Gy/5 fractions, with 54 and 48 months median follow-up in each group, respectively [35]. The crude biochemical disease-free survival rate

measured 97.5 % with each dose regimen, with no significant difference in PSA nadir (0.1 ng/mL at 4 years) or toxicity rates. The incidence of late grade 2 urinary toxicity was 5 and 10 % in the 35 Gy versus 36.25 Gy, groups, respectively (p = NS), with an identical 5 % rate of grade 2 GI toxicity in each group. The authors concluded that "overall, the highly favorable PSA response, limited biochemical failures, limited toxicity, and limited impact on quality of life in these low- to low-intermediate-risk patients are supportive of excellent long-term results for CyberKnife delivered SBRT" and their work suggested that there is no efficacy loss with the lower dose level. It should be pointed out though, that "local relapse" may be a very late event, meaning their conclusion of equivalence is at best "hypothesis generating," and requires longer-term confirmation before the efficacy of the lower dose arm may be considered truly identical to the more commonly used dose level of 36.25 Gy/5 fractions.

Based on ample successful brachytherapy precedent, a different and more aggressive prostate CyberKnife SBRT method and fractionation scheme, known as "Virtual HDR" SBRT, was described in an IRB-approved protocol in 2006, with comparative dosimetry analysis versus actual HDR brachytherapy published in 2008 along with very preliminary clinical results [30, 32]. Using this approach, prostate CyberKnife SBRT treatment plans are deliberately designed to mimic HDR brachytherapy as closely as possible; using an actual HDR brachytherapy schedule of 3,800 cGy/4 fractions, previously described by Grills et al. [22].

Beyond simply mimicking the dose-fractionation aspect of HDR brachytherapy, this method also applies substantially identical intraprostatic and periprostatic isodose morphology, including "HDR-like" urethra, bladder and rectal maximum "D_{max}" dose limitation constraints. Additionally, to qualify as "Virtual HDR" a prostate SBRT treatment plan is required to produce significant intraprostatic dose heterogeneity, just as is seen with actual HDR brachytherapy, with intraprostatic D_{max} dose escalation greater than 150 % of the prescribed dose, requiring prescription to an isodose line less than 67 %, and with the majority of such treatment plans prescribed to an isodose line of 50–55 %. This translates to a typical intraprostatic maximum dose level approaching twice the prescription dose level. This dose escalation region is designed to superimpose primarily over the peripheral zone of the prostate—the region that most frequently harbors the largest volume of intraprostatic cancer cell burden [33]. As imaging techniques such as multi-parametric MRI or evolving PET/CT methods more accurately define the "dominant intraprostatic lesion" ("DIL"), this technique may also be modified to restrict the intraprostatic dose escalation to the actual DIL, though the preponderance of "Virtual HDR" experience gained to date has been with the use of dose escalation to essentially the entire peripheral zone [36–39].

The Virtual HDR series was most recently updated in abstract form in 2012, reporting 51 patients (63 % low-risk; 37 % intermediate-risk), with a median follow-up of 3.5 years (range 6—60 months) [40]. Actuarial 4-year biochemical disease-free survival in this series is 98 % (both definitions), with a 100 % local control rate and a median 4-year PSA nadir of 0.1 ng/mL. There is no acute toxicity in this series greater than grade 2 in either the GU or GI domain. Late toxicity is

primarily observed in the GU domain; with 18 and 6 % rates of late grade 2 and 3 GU toxicity, respectively. All observed cases of grade 3 GU toxicity are comprised of urethral strictures requiring surgical correction—a comparable incidence versus the predicate actual prostate HDR brachytherapy series upon which this series was based [41]. There is a statistically significant correlation of increased baseline I-PSS score with an increased rate of grade 2 or higher late GU toxicity, suggesting that caution is warranted in the use of this specific technique and dose-fractionation in patients that have significant preexisting obstructive uropathy ($p = 0.0039$; I-PSS score as continuous variable versus maximum grade GU toxicity—previously unpublished data). Corresponding rates of late grade 2 and 3 GI toxicity in this series are 2 and 0 %. Patient accrual is scheduled to continue in this series for the foreseeable future, and a larger multi-institutional series that began in 2007, evaluating the same technique, has also completed accrual [42].

The UCSF group has similarly described a "HDR-like" prostate CyberKnife SBRT approach, albeit with less extreme intraprostatic dose escalation versus the Virtual HDR method (UCSF series prescribes to the 60–80 % isodose line, equating to moderately less intraprostatic dose heterogeneity), using the same 3,800 cGy/4 fraction monotherapy fractionation scheme as described above, as well as a 1,900 cGy/2 fraction prostate boost in conjunction with wider field "conventional" pelvic radiotherapy to 45–50 Gy for patients felt to be at higher risk of extraprostatic disease [31]. This series describes 38 patients (20 SBRT monotherapy and 18 SBRT boost).

With a maximum follow-up of 43.5 months, the median observed PSA nadir in this series is 0.35 ng/mL, likely not the true nadir, as their median follow-up is only 18 months. Their late grade 2 and 3 GU toxicity rates measure 8 and 5 %, respectively, with a 3 and 0 % incidence of late grade 2 and 3 GI toxicity, respectively—extremely similar to the levels observed in the San Diego Virtual HDR series described above. The extra toxicity nuance added by the UCSF series is the finding of no apparent difference in the incidence of grade 2 or higher GU or GI toxicity whether this SBRT method is used as monotherapy or as a boost in conjunction with large volume "conventional" pelvic radiotherapy, though absolute numbers of patients in this series remains small, with less than mature follow-up, such that this has to be regarded as a "preliminary" finding of toxicity equivalence between methods.

Experience with gantry-based SBRT regimens as monotherapy for low- to intermediate-risk prostate cancer has also emerged, though the efficacy result seems less established with this approach, due to greater variability of reported outcomes. The initial gantry-based SBRT approach described in contemporary literature has been the so called "SHARP" (Stereotactic hypofractionated accurate radiotherapy of the prostate) regimen described by Madsen et al., in 2007 [43]. This method applied a dose of 33.5 Gy/5 fractions prescribed at the isocenter, using a fixed beam non-coplanar IGRT approach, treating the prostate with a 4–5 mm expansion margin from the prostate to the block edge (which equates to a far smaller margin between the prostate and "quasi full dose" 90 % isodose line). The authors assumed a prostate cancer α/β [alpha/beta] ratio of 1.5, equating to a 2 Gy/fx radiobiological

dose equivalent of 78 Gy at the isocenter (author note—This decreases to a total "conventional" fractionation dose equivalent 64 Gy at the 90 % isodose line, which is at or barely beyond the margin of the prostate; lower still if the α/β [alpha/beta] ratio actually exceeds 1.5 Gy). Forty low risk patients were prospectively enrolled and evaluated in this study.

The biochemical disease-free survival rate of the "SHARP" study is unclear, as the result is substantially different depending on which specific definition of biochemical relapse is applied—70 % disease-free survival at 4 years using the ASTRO biochemical relapse-free definition versus 90 % using the Phoenix definition, with the higher biochemical relapse rate implied by the ASTRO definition potentially explained by "delayed PSA bounces" according to the authors. The most common PSA nadir level observed in this study was 0.6–1.0 ng/mL, with 74 and 32 % of all patients achieving a nadir level below 1.0 and 0.5 ng/mL, respectively. Comparison of the PSA nadir values in this series versus those reported in external beam radiotherapy literature caused the authors to conclude that this regimen likely has a biologic potency in the range of 73–78 Gy of "conventionally" fractionated radiotherapy.

Toxicity was reasonably low in this study for both the GU and GI domains. There was a single acute GU grade 3 toxicity and no delayed toxicity in either domain higher than grade 2, with 20 and 7.5 % delayed grade 2 GU and GI toxicities, respectively. The authors concluded that there is probably room for dose escalation. An update of this series with 5-year median follow-up was provided in abstract form in 2010, reporting 71 and 93 % 5-year biochemical relapse-free survival using the ASTRO and Phoenix definitions, respectively, with a median PSA nadir value of 0.65 ng/mL, implying no further degradation in efficacy to 5 years [44].

The substantial uncertainty in biochemical relapse-free survival with the SHARP regimen depending on relapse definition and the low DFS rate imputed by the ASTRO definition suggests the possibility that this regimen may not have an acceptable rate of efficacy. This concern is amplified by the fact that the suboptimal result in this series occurred in spite of restricting the treatment to low-risk patients. At best, the long-term efficacy of this specific SBRT regimen remains uncertain. Acknowledging this concern, the SHARP study authors have suggested consideration of dose escalation in both their initial and follow-up reports [43, 44].

A subsequent gantry-based prostate SBRT series described by the UT Southwestern group has employed a substantially more aggressive approach, sequentially evaluating dose levels of 45 Gy/ 5 fractions, 47.5 Gy/5 fractions and 50 Gy/5 fractions in cohorts of 15 low-risk and intermediate-risk patients, with escalation to the each succeeding dose level contingent upon the demonstration of reasonable acute safety of the previous dose level [45]. A total of 45 patients were described in their report. The treatment was delivered to a volume that included the prostate + 3 mm uniform margin expansion to form the PTV, with the dose prescribed to cover >95 % of the PTV, delivered using an axial plane IMRT method with daily image guidance, either by a helical Tomotherapy device or by a step and shoot MLC-based linear accelerator device.

At 12–30 months of follow-up, PSA control by the Phoenix definition (nadir + 2 ng/mL) is 100 %. The maximum grade 2 GU and GI toxicity incidence

rates of 31 and 18 %, respectively, and maximum grade >3 GU and GI toxicity rates of 4 and 2 %, respectively; overlap the toxicity incidence of other contemporary radiotherapy series. This suggests a non-excessive severe toxicity rate in spite of aggressive SBRT dosing, with the caveat that a maximum follow-up of 30 months is inadequate to fully define the late toxicity incidence. As such, the late toxicity result of this approach must still be regarded as preliminary. The authors postulate that the relatively low toxicity incidence observed to date in spite of aggressive dosing, is due to tight margins, strict dose limitation of all adjacent normal tissues (bladder, rectum and urethra) and the use of an endorectal balloon to stabilize the rectum and displace its lateral and posterior walls out of the high dose volume. The study has now expanded to multiple centers and is ongoing.

Another gantry-based prostate SBRT series of 65 low-risk patients has been described in abstract form by Mantz et al., using a Varian Trilogy cone beam CT (CBCT) volumetric-guided IMRT approach, with Calypso electromagnetic tracking to provide 4D localization, with an action level of 2 mm [46]. They deliver a dose of 40 Gy/5 fractions (q.o.d. schedule) to the PTV (exact expansion from the prostate not described in the abstract). With 36 months of median follow-up, the PSA response is excellent (median PSA nadir 0.3 ng/mL at 3 years) and there is a zero incidence of reported grade 3 or higher toxicity in the GU or GI domains. As with other gantry-based reports, this series seems encouraging, with further follow-up and more complete reporting necessary to fully validate the results.

11.3.2 SBRT Radiobiology Potency Considerations

11.3.2.1 Intraprostatic Dose Considerations

When contemplating a specific dose fractionation regimen, it is useful to consider the "conventional fractionation" dose equivalent under various schedules and α/β [alpha/beta] ratio scenarios, outlined in Table 11.1. As revealed by this table, all SBRT dose fractionation scenarios are likely adequately powered if the α/β [alpha/beta] ratio of this disease is less than 2 Gy, whereas greatly differing degrees of efficacy loss are predicted under higher α/β [alpha/beta] ratio scenarios (e.g. if the α/β [alpha/beta] ratio of a lesion is actually 5 Gy instead of 1.5 Gy, the higher dose regimens are still likely efficacious, whereas the lower dose regimens are likely underpowered).

11.3.2.2 Periprostatic Dose Considerations

In addition to considering the conventional fractionation dose equivalent required *within* the planning target volume, it is also useful to recall that although prostate SBRT coverage margins may be relatively sharper versus "conventional" radiotherapy approaches, there is still a non-trivial a dose gradient *beyond* the PTV, lending various degrees of effective "subclinical disease extension" coverage to the

Table 11.1 RBE table comparing four popular prostate SBRT dose fractionation regimens, converted to 2 Gy/fx dose equivalent, with differing α/β [alpha/beta] ratio scenarios

Regimen	3,500 cGy/5 fx	3,625 cGy/5 fx	4,000 cGy/5 fx	3,800 cGy/4 fx
α/β [alpha/beta] 1.5 Gy; 2 Gy/fx eq.	8,400 cGy	9,000 cGy	10,800 cGy	12,000 cGy
α/β [alpha/beta] 3 Gy—2 Gy/fx eq.	7,000 cGy	7,400 cGy	8,800 cGy	9,400 cGy
α/β [alpha/beta] 5 Gy—2 Gy/fx eq.	6,000 cGy	6,400 cGy	7,400 cGy	7,800 cGy

Table 11.2 RBE table comparing the 75 % isodose line potency of four popular prostate SBRT dose fractionation regimens converted to 2 Gy/fx dose equivalent, with differing α/β [alpha/beta] ratio scenarios.

Regimen	3,500 cGy/5 fx	3,625 cGy/5 fx	4,000 cGy/5 fx	3,800 cGy/4 fx
75 % Value	2,625 cGy/5 fx	2,720 cGy/5 fx	3,000 cGy/5 fx	2,850 cGy/4 fx
α/β [alpha/beta] 1.5 Gy; 2 Gy/fx eq.	5,000 cGy	5,400 cGy	6,400 cGy	7,000 cGy
α/β [alpha/beta] 3 Gy—2 Gy/fx eq.	4,200 cGy	4,600 cGy	5,700 cGy	5,800 cGy

Typically, a 75 % isodose line will extend another 5–10 mm beyond the PTV, more thoroughly covering the "periprostatic" region. This table clearly demonstrates that more potent *intra*prostatic regimens are also more potent *extra*prostatic disease coverage regimens

periprostatic region, such that there could be efficacy differences in various regimens based on the radiobiologic strength of lower isodose lines that extend *beyond* the prostate (e.g.—75 % of the prescription dose), with 75 % IDL conventional fractionation equivalents illustrated in Table 11.2. This table demonstrates that a regimen barely powered to control intraprostatic disease also loses efficacy beyond the prostate more rapidly versus more radiobiologically potent SBRT regimens. This implies that more conservatively dosed prostate SBRT regimens should be restricted to only those patients with the lowest risk of extraprostatic disease extension, while more potent SBRT regimens are more likely effective against a wider range of higher-risk periprostatic disease extension scenarios. An example of the extra periprostatic volume contained within the 75 % isodose line is illustrated in Fig. 11.4.

11.3.3 Conclusion

SBRT monotherapy has emerged as a potent radiotherapy option for most newly diagnosed early prostate cancer patients, as the majority of them present with disease of low- to intermediate-risk status, typically translating to "disease confined within the periprostatic region"—a region well encompassed within a typical SBRT planning target volume. Too, the "low α/β [alpha/beta]" radiobiology of prostate cancer appears ideally matched with the typical SBRT large dose per fraction hypofractionation schedule.

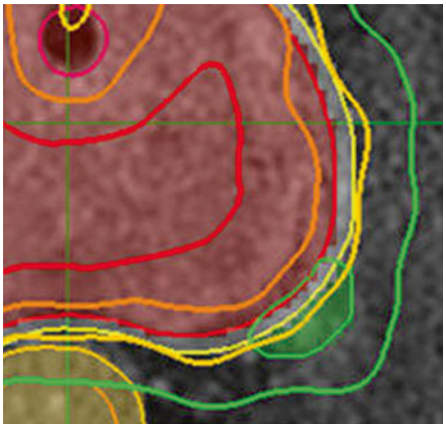

Fig. 11.4 This figure illustrates peri-prostatic SBRT dose coverage. The prescription isodose line (3,800 cGy/4 fx) is displayed in *yellow*, while the 75 % isodose line (2,850 cGy/4 fx) is displayed in *green*. If the alpha-beta ratio of prostate cancer measures 1.5 Gy, these lines reflect a "conventional" 2 Gy/fraction radiotherapy dose equivalent gradient of 12,000 cGy at the prescription isovolume surface just beyond the prostate capsule, progressively transitioning to 7,000 cGy well beyond the neurovascular bundle and potential contiguous extracapsular disease extension, illustrating robust intraprostatic ("gross disease") and peri-prostatic ("subclinical") disease coverage with this technique. If the alpha beta ratio is 3 Gy, the corresponding conventional dose equivalents decrease commensurately to 9,400 and 5,800 cGy, respectively—still likely sufficient to control "gross" and "subclinical" disease, respectively

There are enough PSA-based efficacy data and toxicity data to regard prostate SBRT as a reasonable and customary option in the armamentarium to manage properly selected clinically localized prostate cancer cases. The efficacy and morbidity of this modality clearly compare well with other contemporary radiotherapy modalities, and with some SBRT series reporting a PSA nadir so low (0.1 ng/mL) as to indicate potential superiority versus "conventional fractionation" treatment, with long-term confirmation of that hypothesis still required [35, 41].

There are caveats. Although efficacy and toxicity outcomes reported to date appear excellent with a number of different SBRT platforms and approaches, caution seems warranted before one makes a blanket assumption that "SBRT is SBRT." There is a degree of heterogeneity in the reported outcomes, with possible inferiority to some of the lower dosed prostate SBRT series (<35 Gy total dose being potentially less efficacious, particularly in the absence of "HDR-like" or other intraprostatic dose escalation measures). Too, insufficient PTV margins paired with insufficient target localization and tracking could lead to an inferior disease control outcome, regardless of prescribed dose, while excessive PTV margins and/or excessive dosing could lead to an excessive complication rate. As such, the highest and best use of SBRT as a weapon against prostate cancer requires great attention to dose fractionation, isodose line morphology, PTV margin design, target localization and target tracking methodology, to fully optimize the therapeutic ratio of this still relatively novel therapy modality.

11.4 SBRT as a Boost

There exists a subset of prostate cancer patients that present with more advanced disease, such that a narrow margin monotherapy approach will not reliably address their entire cancer burden. These patients are known as "high-risk" patients, identifiable by disease features such as a pathology Gleason score >8, tumor stage T2c or higher, PSA value >20 ng/mL, or the presence of multiple "non-favorable" prognostic factors. There has been ample precedent for using a combined modality radiotherapy approach for such patients, most typically using a combination of wide field "conventional" pelvic radiotherapy in conjunction with a LDR or HDR brachytherapy prostate boost. This approach simultaneously maximizes the central radiobiologic power against the known and invariably largest cancer cell burden within the prostate itself, while also applying "subclinical disease" radiotherapy dose coverage to known pathways of extraprostatic spread, including seminal vesicles and first echelon pelvic lymph nodes. There evidence that such an approach is more efficacious than "non-escalated" approaches such as external beam radiotherapy monotherapy [28, 29].

As prostate SBRT naturally delivers comparable fractionation and isodose volumes compared with HDR brachytherapy, it makes perfect sense to apply a SBRT prostate boost in exactly the same manner and circumstance as one would apply a HDR brachytherapy boost. In fact this method has been described by the UCSF group [31]. In this report, CyberKnife SBRT was used in "HDR-like manner" either as monotherapy for low-risk lesions (38 Gy/4 fractions) or as a boost combined with whole pelvis IMRT (WP IMRT) for intermediate to high-risk lesions, typically in combination with androgen suppressive therapy (19 Gy/2 fractions SBRT boost + 45–50 Gy WP IMRT). The patient numbers in each group remain relatively small and the median follow-up short, but some observations are still reportable. First of all, the PSA nadir in the combined SBRT boost + WP IMRT group is essentially identical with their reference group treated with HDR boost + WP IMRT—0.1 ng/mL vs. 0.09 ng/mL, respectively. Second, the toxicity incidence of the combined regimen does not appear to be significantly different than the toxicity rates seen in their SBRT monotherapy or their HDR + WP IMRT populations. The authors rightly caution that the efficacy and toxicity results with this approach must still be regarded as preliminary, with longer-term follow-up and larger patient numbers required for confirmation.

11.5 SBRT for Relapsed and/or Metastatic Cases

Unlike newly diagnosed prostate cancer cases, which are typically highly curable with a reasonably low risk of severe complications, the scenario of relapsed local disease after a prior course of definitive radiotherapy treatment presents a far more challenging and dire situation. There is no universally agreed safe and successful

salvage option for this scenario, and such patients are often consigned to "watchful waiting" or palliative androgen suppression treatments, neither of which presents any further curative potential, even though their disease has not metastasized.

A variety of "curative intent" salvage strategies have been used in this situation, but all have shortcomings. Salvage radical prostatectomy is efficacious in selected local relapse patients, but with an elevated complication rate versus "de novo" radical prostatectomy [47]. Salvage cryosurgery has also been applied in this setting but the efficacy rates are still not well established, due to a lack of a consensus definition of therapeutic success in this setting among other reasons, and the complications are significant [48]. Permanent source brachytherapy has been used with reasonable success in selected local relapse patients, but again, with a potentially elevated incidence of >grade 3 local toxicity [49–52]. A limited body of HDR brachytherapy experience suggests the possibly of a low toxicity rate and encouraging short-term efficacy [53, 54].

Due to the previously-described prostate SBRT capability to accomplish a substantial degree of HDR dosimetry replicating, SBRT also emerges as an intriguing potential salvage method for post-radiotherapy local relapse patients. Such an approach has been employed under an IRB-approved clinical trial initiated at our own center, using a fractionation scheme of 34 Gy/5 fractions, with HDR-like intraprostatic dose escalation, such that the estimated uniform dose (EUD) within the prostate is approximately 42 Gy/5 fractions [55].

The result of this trial is still preliminary, currently limited to 17 patients with a median follow-up of 12 months (range 3–36), yet the result is encouraging. The PSA nadir has not been reached, with a median 1 year PSA level of 0.65 ng/mL (from a median pre-salvage PSA level of 3.1 ng/mL) and 88 % of patients display a stable or decreasing PSA level at their last follow-up. Toxicity greater than grade 1 (CTCAE v 3.0) has been limited to the GU domain, with 2/17 patients having chronic grade 2 GU toxicity and 1/17 patients having acute and chronic grade 3 GU toxicity. The data suggest that the risk of >grade 2 GU toxicity may be higher in patients with preexisting toxicity from their initial radiotherapy course, such that it seems prudent to exercise particular caution in this patient population when contemplating "salvage" prostate SBRT [56].

Another series of salvage SBRT for relapsed prostate cancer was reported by a group from Milan [57]. This series describes a mixture of patients treated with SBRT salvage for post-radiotherapy local prostate relapse, for post-radical prostatectomy prostate bed local relapse, isolated lymph node relapse and solitary distant metastatic foci. Over half of the patients in this series received concomitant androgen suppressive therapy, making the specific SBRT contribution more difficult to ascertain. Nonetheless, some findings are noteworthy: Of 15 patients treated for post-RT prostate recurrence to a salvage SBRT dose of 30 Gy/5 fractions, 10 remained controlled at a median 30 months of follow-up, while 11 of 16 isolated lymph node recurrence SBRT salvage patients remained controlled at last follow-up. The majority of subsequent clinical relapses occurred at new sites, with relapse in SBRT target volume sites comprising only a minority of them. As observed in our own series, the incidence of grade 2 or higher toxicity was low and more prevalent

in the GU domain. They concluded that stereotactic radiotherapy is a feasible approach for isolated recurrent primary, lymph node, or metastatic prostate cancer, offering excellent in-field tumor control and a low toxicity profile.

A study from Belgium also described the use of SBRT in patients with oligometastatic prostate cancer, treating patients with <3 PET-detected lymph node and/or bone metastases, to a SBRT dose of 50 Gy/5 fractions, reporting a 2-year 100 % local control rate and a 42 % overall disease-free survival rate. Almost half of the patients in this series received a second or third SBRT course for additional limited metastatic foci, and hormonal therapy was deferred by an average of 38 months [58]. Although it remains to be seen whether any subset of patients with prostate cancer oligometastases will actually be cured by focal SBRT to their metastatic foci, judicious use of SBRT for such patients does appear to produce a substantial deferment in the need for additional systemic therapy for a many of them.

In summary, the short to intermediate-term PSA response and toxicity profile of salvage SBRT for post-RT prostate recurrence or limited extra-prostatic recurrence appears encouraging, with the local relapse salvage efficacy preliminarily resembling HDR brachytherapy salvage efficacy [53, 56]. The use of prostate SBRT as a definitive salvage measure for biopsy-confirmed post-RT prostate local relapse appears promising enough to warrant continued study under properly designed clinical trials, at least one of which is currently ongoing, but should be done with great caution outside of a clinical trial setting, until the risk of normal tissue complications is more thoroughly defined in a larger population of studied patients. The practice of SBRT for limited metastatic prostate cancer beyond the prostate (e.g. limited lymph node and/or blood borne metastases) is more likely appropriate for routine clinical use, as the efficacy appears reasonable and the toxicity rate appears suitably low [57, 58]. The use of salvage SBRT in either the prostate local recurrence setting or the limited metastatic burden setting may well allow a significant deferment in the use of androgen suppressive therapy, and may be potentially curative for some, particularly those with local recurrence.

11.6 Treatment Techniques and Strategies

11.6.1 Case Selection: SBRT Monotherapy Versus Combined Modality Therapy

Assuming the absence of demonstrated metastatic foci, there is no absolute cut-off of eligibility for the use of SBRT monotherapy against clinically localized prostate cancer, though the majority of cases so treated have had low-risk (<T2a, PSA <10 ng/mL and Gleason <6) or intermediate-risk (selected combinations of T2b and/or Gleason 7 and/or PSA 10.1–20 ng/mL) lesions [32–35]. Rather than constructing a "laundry list" of eligibility requirements for such treatment though, a practitioner should primarily consider the probability that all of the patient's disease is likely to be contained within that practitioner's typical SBRT planning target

volume (PTV). For an extremely conservative dose/narrow margin SBRT approach (e.g.—the "SHARP" protocol), it would most likely be appropriate to limit such an approach to low-risk or extremely low-risk cases in the absence of further dose escalation. On the other hand, if more aggressive SBRT methodology is used (e.g.—higher dose CyberKnife or gantry-based SBRT, HDR-like SBRT), it is certainly reasonable to apply this method as monotherapy to more advanced localized presentations.

A decision-tree starting point might be to review one's typical SBRT planning target volume (PTV) against a pathologic risk assessment tool such as the Partin Table [59], and consider designing their protocol to limit the use of SBRT monotherapy to patients with <10 % probability of disease extension beyond the SBRT PTV. For patients that present an elevated risk of seminal vesicle extension and/or lymph node metastases, combined modality approaches such as whole pelvis IMRT + LDR or HDR brachytherapy have frequently been used, albeit with little to no proof of superiority versus high quality LDR or HDR brachytherapy monotherapy. It is theoretically quite reasonable to apply SBRT as a boost in lieu of a brachytherapy boost, though literature description of this specific combination remains relatively sparse to date [31]. If SBRT is used as a boost, in conjunction with wide field external beam pelvic radiotherapy, it would seem most prudent to use a published HDR brachytherapy boost regimen as a starting point, due to the typically similar dose-volume characteristics of these two radiotherapy modalities [30, 31].

11.6.2 Treatment Planning: Diagnostic Imaging and Planning Steps

As with all contemporary external beam radiotherapy treatment, CT-based treatment planning is the foundation for prostate/ SBRT target volume and normal tissue definition. CT-based planning is a prerequisite for the accurate definition of tissue heterogeneity, to maximize the correctness of typical radiotherapy computerized treatment planning algorhythms. That said, relative to "conventional fractionation" radiotherapy techniques, the SBRT modality is characterized by potentially larger radiobiologic dose equivalents within the planning target volume (PTV) and a more rapid drop off of dose beyond the PTV, such that a greater degree of precision is required, both for treatment planning and for treatment delivery. This means that it is also desirable that more exact anatomic imaging methods such as magnetic resonance imaging (MRI) also be incorporated into the treatment planning process. MRI maximizes the spatial resolution of prostate capsule definition relative to CT-based imaging, with CT plagued by a greater tendency to "volume average" adjacent tissues such as the bladder neck, dorsal venous plexus, puborectalis musculature and external urinary sphincter into the volume interpreted as "prostate," typically leading to overestimation versus its actual anatomic volume. A comparison of CT-based versus MRI-based treatment planning images is illustrated in Fig. 11.5.

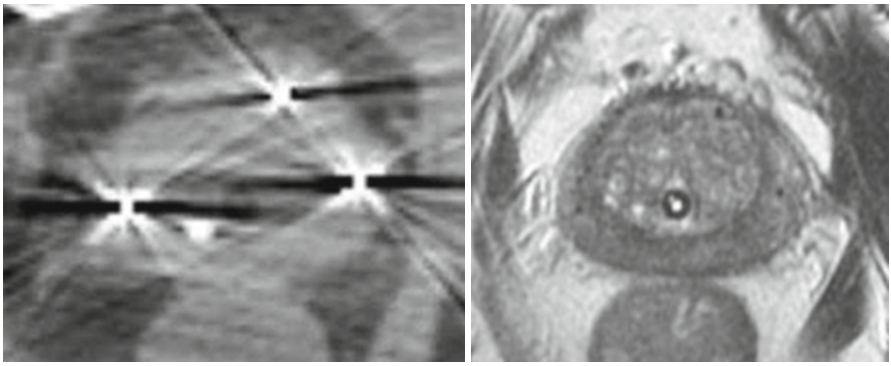

Fig. 11.5 CT-based (*left panel*) versus MRI-based (*R panel*) planning images: Note "fuzzier" anatomic boundaries with surrounding tissue volume averaging, along with significant streak artifact about the fiducials on the CT-based image, with comparatively sharper anatomic prostate definition and far less prominent fiducials with no artifact on the MRI image set. Ultimately the image sets are complimentary, as CT defines tissue density most accurately for the purpose of computerized radiotherapy dose calculation, while MRI typically defines the anatomy itself most sharply for the purpose of target volume and adjacent tissues delineation

In addition to defining the anatomic boundaries of the prostate more accurately than CT, MRI may also be used to map the dominant intraprostatic lesion ("DIL") location and boundaries with up to 80 % specificity and sensitivity [39]. The accurate localization of the DIL also more accurately identifies areas at highest risk of extracapsular extension, which typically occurs in immediate proximity to the DIL [22]. This means that the incorporation of MRI into the treatment planning process potentially leads to a more conformal and more customized SBRT treatment plan through the more accurate definition of the anatomic boundaries of the prostate, and also potentially identifies disease foci within the prostate that may be targeted by differential dose escalation within the larger prostate planning target volume, as well as allowing the design of wider margins around the DIL(s) to more completely encompass potential contiguous extracapsular extension (All of these principles may be well applied to "conventional fractionation" IGRT/IMRT, incidentally). An example of multiparametric MRI planning to demonstrate the location of the dominant intraprostatic lesion ("DIL"), with resultant more customized DIL boost escalation and margin coverage is illustrated in Fig. 11.6. Our own treatment planning goals and normal tissue dose limitation constraints for "HDR-like" prostate SBRT are illustrated in Table 11.3.

11.6.3 SBRT Image-Guidance Methodology

Prostate SBRT regimens typically make use of fiducial-based or electromagnetic image-guidance and/or tracking, to maximize the precision of this inherently small margin strategy. Our own SBRT planning process makes use of fiducial-to-fiducial

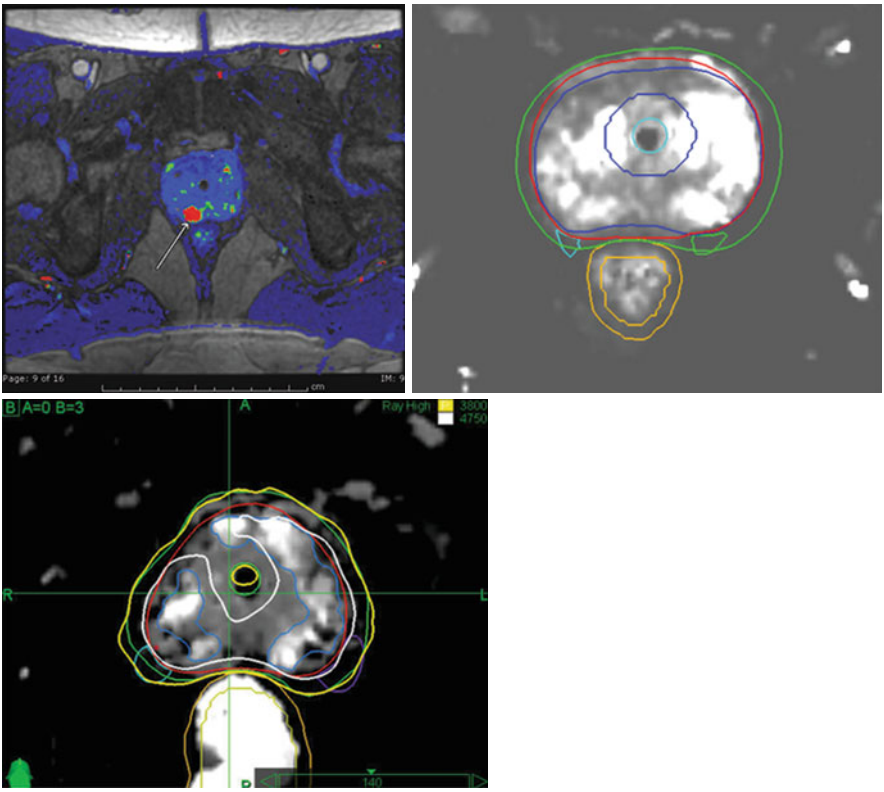

Fig. 11.6 Dynamic contrast enhanced (DCE) MRI images incorporated into the treatment planning process: The colorized image (*L panel*) illustrates a typical peripheral zone "Dominant Intraprostatic Lesion" ("DIL") that could be differentially boosted. The central panel shows a more advanced DCE lesion uptake pattern with bilateral tumor involvement and left-sided predominance, leading to differential GTV to CTV margin expansion on the more heavily involved left side, to more thoroughly cover potential extracapsular extension on that side. The *right panel* illustrates a completed SBRT dosimetry plan, with differential dose escalation covering abnormal DCE foci to a higher dose within the larger prostate PTV

CT-MRI co-registration, to enable the direct transfer of the typically more accurately defined MRI-based contours to the requisite CT-based planning image set.

Gold seed fiducials create a moderate degree of streak artifact on the CT images. This is usually manageable by adjusting CT window and level settings, and/or contouring immediately above and below the slices with the greatest degree of streak artifact and interpolating the contours through these problematic regions. There is little to no disruption of the companion MRI images by gold seed fiducials. In fact, special MRI imaging tricks (e.g. "gradient echo" image sequence; gadolinium contrast) may be required to see gold seed fiducials *at all* on MRI images, though ultimate MRI seed visualization success is virtually always achieved. Gold seed fiducials on SBRT treatment planning images are illustrated in Fig. 11.5.

Table 11.3 Dose specifications and constraints for "HDR-like" prostate SBRT—CyberKnife Centers of San Diego SBRT protocols [32, 42, 55]

	High dose regimen (original)	Moderate dose regimen (added in 2012)	Post-radiotherapy local recurrence SBRT regimen
Prescription	3,800 cGy/4 fx	3,400 cGy/5 fx	3,400 cGy/5 fx
PTV	CTV + 2–5 mm; (manually shave PTV expansion to 0 mm against the rectum)	CTV + 2–5 mm; (including a 2 mm PTV expansion against the rectum)	CTV + 0 mm (everywhere)
Heterogeneity	Intraprostatic Dmax >150 % of Rx (required)	Intraprostatic Dmax >150 % of Rx (required)	Intraprostatic Dmax >150 % of Rx (required)
Urethra	Dmax: 120 %	Dmax: 120 %	Dmax: 120 %
	D50—105 %	D50—105 %	D50—105 %
Bladder wall	Dmax 110 %	Dmax 110 %	Dmax 100 %
Rectal wall	Dmax 3,800 cGy	Dmax 3,800 cGy	Dmax 3,400 cGy
Rectal mucosa (defined as a 3 mm rectal wall contraction)	D1 %—2,850 cGy	D1 %—3,300 cGy	D1 %—2,550 cGy
Neurovascular bundles (NVB)	Contour and carry Dmax and D50 for analysis, but no specific constraint	Contour and carry Dmax and D50 for analysis, but no specific constraint	Contour and carry Dmax and D50 for analysis, but no specific constraint
Penile bulb	Contour and carry Dmax and D50 for analysis, but no specific constraint	Contour and carry Dmax and D50 for analysis, but no specific constraint	Contour and carry Dmax and D50 for analysis, but no specific constraint

SBRT techniques that pair electromagnetic transponders and planning MRI have a different challenge. CT characteristics of electromagnetic transponders are not so different versus gold seeds, but the MRI characteristics of electromagnetic transponders are vastly different, due to the fact that they contain a small amount of iron, which is extremely disruptive to MRI imaging. There is a large zone of "obliterated MRI image" around each electromagnetic transponder, making Transponder-to-Transponder MRI to CT image co-registration virtually impossible, illustrated in Fig. 11.7. As such, if electromagnetic transponder based SBRT technique is to be used, either CT-only planning is done, or MRI-based imaging is done *before* the placement of transponders, with image co-registration then based on anatomy-to-anatomy co-registration rather than fiducial-based co-registration—a process that may be somewhat less accurate due to the increased subjectivity of anatomy-based image interpretation. Such added uncertainty needs to then be considered in the final prostate to PTV margin design process, potentially leading to a minimally increased PTV expansion to account for this added image co-registration uncertainty issue.

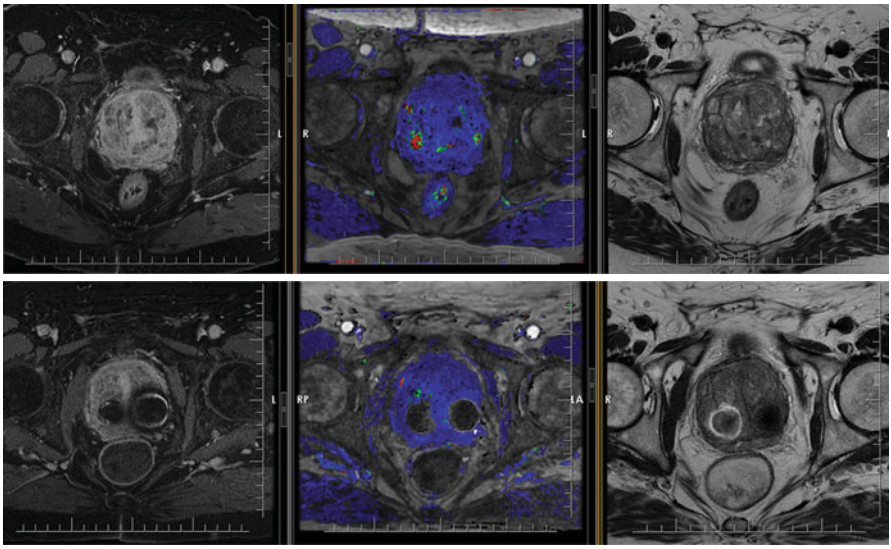

Fig. 11.7 Effect of electromagnetic transponders on MRI imaging: The *top panel* illustrates a multiparametric prostate MRI planning sequence before implantation of electromagnetic transponders, while the *bottom panel* illustrates the same MRI planning sequence and level following electromagnetic transponder implantation. Note substantial "bloom artifacts" around each transponder, with the respective *middle panels* showing complete obliteration of a Dominant Intraprostatic Lesion by this artifact (*red lesion* at *top panel*—completely obscured by artifact on *bottom panel*)

11.6.4 SBRT Treatment

The prostate may continue to move after even the most meticulous patient set-up and immobilization procedure (intrafraction motion), creating additional challenges to the successful application of SBRT treatment beyond simply defining the PTV accurately at the planning step. The magnitude of this motion problem is typically proportional to the amount of time to deliver the treatment, such that it becomes more problematic for methods that take a longer time to deliver a fraction of SBRT. Too, in addition to moving in the "X-Y-Z" plane (translational motion), the prostate may also rotate (e.g.—pivoting in the sagittal plane about the relatively "more fixed" apex). The narrower the prostate to PTV margin expansion, the more potentially problematic intrafraction translational and rotational motion becomes. A variety of simple strategies may be applied to limit intrafraction PTV motion and distortion.

11.6.4.1 Biologic Factors

To deal with organ motion, our own SBRT patient preparation protocol includes the following components [1]: Low residue/low gas diet starting 24 h before treatment planning and before the actual course of treatment, continuing until treatment is

concluded [2]; Bladder completely emptied and then re-filled with 100 cc of sterile fluid via Foley catheter at the simulation step (but *not* during the SBRT treatment itself) [3]; P.O. fluids limited for 4 h pre-treatment and bladder emptied 60–90 min pre-treatment, theoretically creating an "average" intrafraction bladder volume matching the simulated bladder volume [4] Fleets enema to empty the rectum of its contents pre-simulation and pre-treatment each day. Different SBRT practices may adopt their own "biologic" protocols, but this factor should definitely be defined in all SBRT protocols, to minimize intrafraction target volume variability.

11.6.4.2 Technical Factors

Three basic SBRT technical strategies are currently used to overcome the issue of intrafraction targeting accuracy degradation [1]: Continuous fiducial-based target tracking and automated beam aiming adjustment (Prototypical platform: CyberKnife) [2]; Continuous electromagnetic-based target tracking with manual or semi-automated compensatory isocenter adjustment (Prototypical platform: Calypso+Gantry-based linear accelerator) [3]; Initial fiducial-based or CT-based IGRT with no further intrafraction adjustment—ideally paired with a "fast" linear accelerator to minimize the treatment time, to overcome target volume motion through "sheer speed" of the SBRT application, plus or minus the use of endorectal balloon for additional intrafraction prostate motion stabilization.

All of the above strategies have been described as prostate SBRT methods, with the greatest volume of prostate SBRT experience to date currently reported with the CyberKnife platform. The continuously updated target tracking and beam aiming adjustment feature inherent to the CyberKnife device represents an "integrated end-to-end" target tracking solution with published sub-millimeter accuracy, subject to an average intrafraction tracking of <40 seconds, with occasional cases requiring more frequent tracking to maintain that degree of accuracy [15]. The CyberKnife device also automatically compensates beam aiming for rotational as well as translational prostate motion, thus representing a "complete" prostate SBRT tracking and automated aiming solution.

As the "Virtual HDR" method applies a zero mm prostate to PTV margin expansion posteriorly against the outer wall of the rectum, as well as the highest intraprostatic radiobiologic dose equivalent and the extreme intraprostatic dose heterogeneity, the CyberKnife device seems currently the best suited to deliver this specific "voxel-by-voxel" treatment method [30, 31]. The more "uniformly dosed" SBRT approaches that apply use a 3–5 mm prostate to PTV margin expansion are probably equally well treated on a variety of SBRT platforms, as millimeter by millimeter tracking and compensation, while still desirable, is relatively less critical. A variety of solutions to interfraction and intrafraction target tracking are illustrated in Figs. 11.8, 11.9, and 11.10.

Review of current prostate SBRT literature discloses no clear difference in efficacy or toxicity by therapy platform, with the exception of potential efficacy inferiority of the originally published "SHARP" treatment regimen, which perhaps

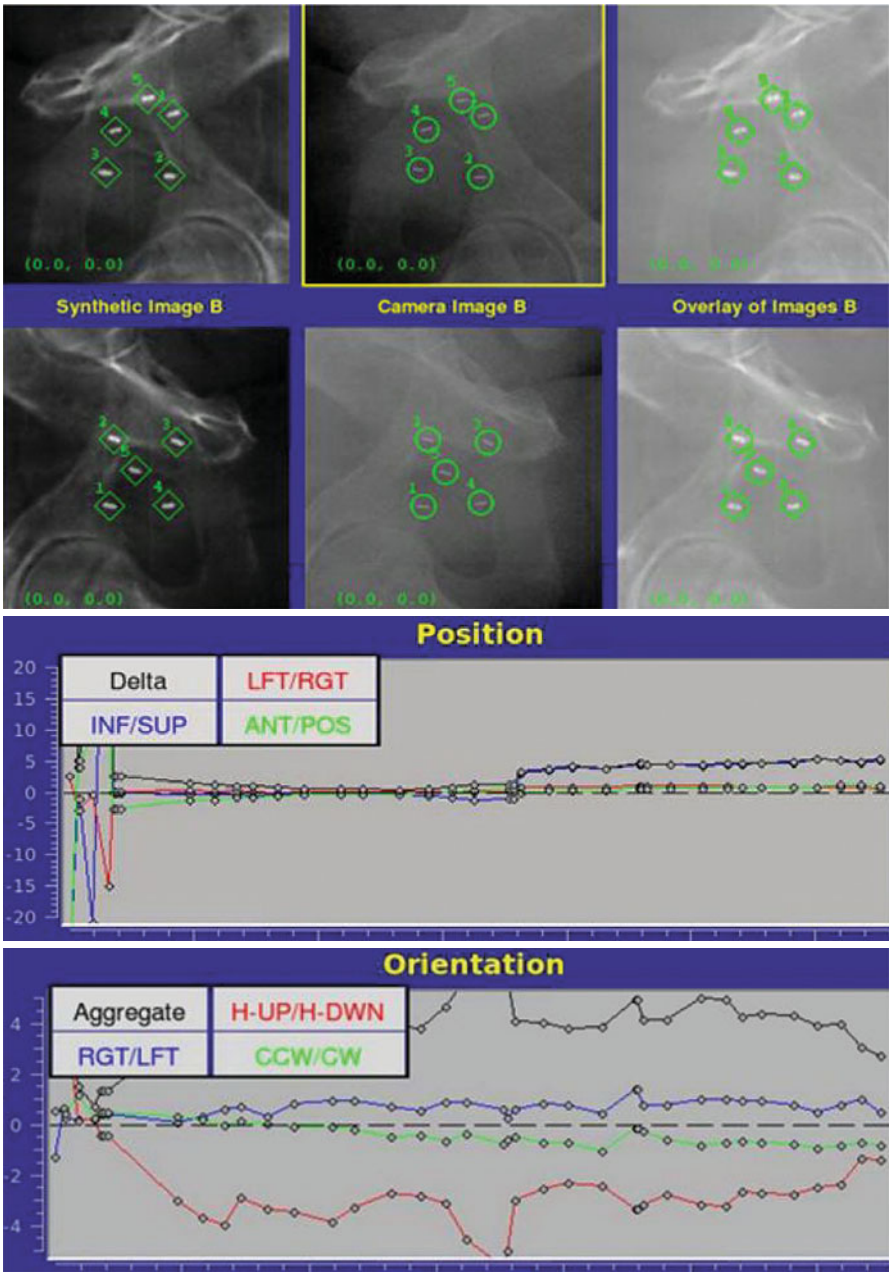

Fig. 11.8 CyberKnife Prostate SBRT Tracking methodology: In this example, 5 transperineally implanted prostate fiducials are three-dimensionally localized by orthogonal images, which are then compared with their computerized digital reconstruction radiograph (DRR) position derived from the CT-based treatment planning images. This overlay process provides full 6-dimensional (translational and rotational) tracking capability. The unique 6-dimensional robotic arm aiming functionality of the CyberKnife device allows automatic correction of tracking error, to fully compensate for all translational and rotational target motion, which makes this a prototypical prostate SBRT device, with end-to-end sub-millimeter targeting accuracy

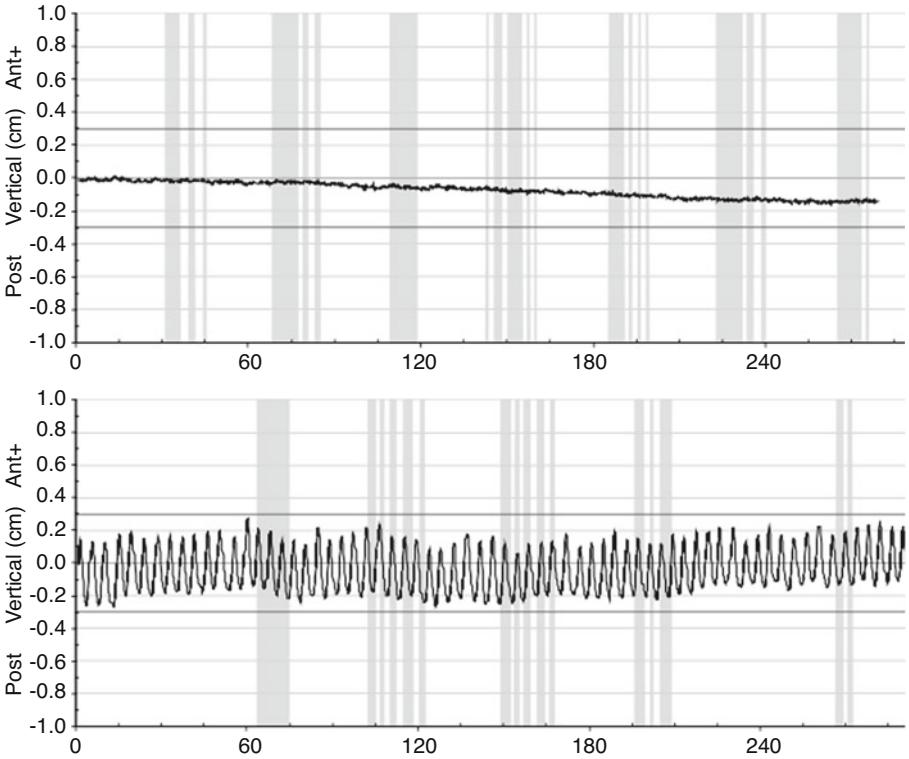

Fig. 11.9 Electromagnetic (Calypso Beacon®) transponder prostate motion tracing over the course of an individual radiation treatment in two different prostate cancer patients, demonstrating two completely different sources of prostate motion: The *top panel* reveals a "slow drift" in the vertical (A-P) dimension over time, potentially caused by gradual relaxation of pelvic musculature and/or gradual bladder filling. The *bottom panel* illustrates a 4 mm amplitude respiratory sine wave, with a frequency of approximately 14 cycles per second. This patient was treated in the prone position, which potentially exaggerates respiratory motion by compressing A-P diaphragm motion. In contrast, there is no respiratory motion component in the *top panel* case, which was treated in the supine position. The ability to continuously track translational prostate motion over time with sub-millimeter accuracy makes this a viable SBRT guidance system, with user programmable motion tolerance boundaries (set to ± 3 mm in both of these examples)

represents more of a "low dose paired with tight margin" issue than a "treatment platform" issue [43, 44].

11.7 Conclusion/Future Directions

The use of SBRT is rapidly emerging as a mainstream application in the armamentarium of radiotherapy options against prostate cancer. Although the greatest experience in the use of this modality thus far been gained with SBRT monotherapy

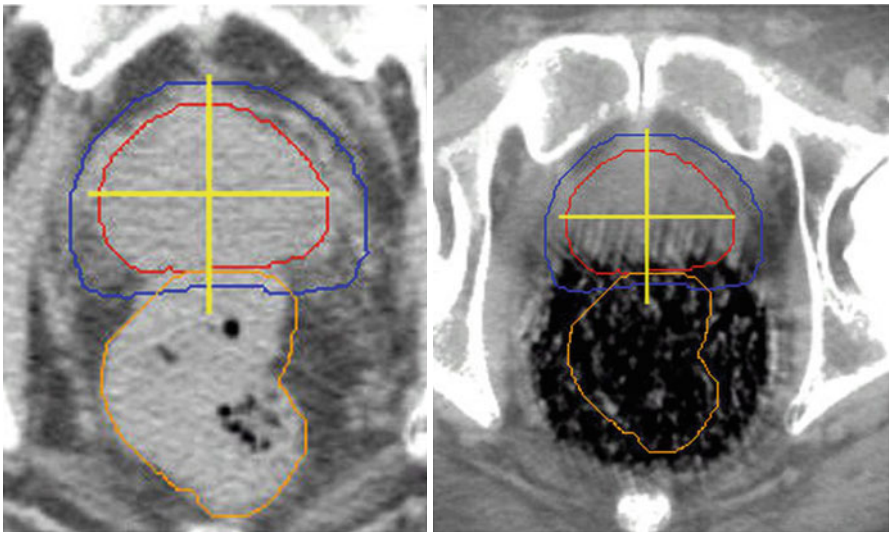

Fig. 11.10 Cone beam CT image guidance: The *left panel* illustrates the patient's planning CT image, with prostate (*red*), PTV (*blue*) and rectal (*orange*) contours superimposed. The *right panel* is a daily cone beam CT image of the same patient, illustrating significant anterior prostate motion and prostate compression, due to excessive fecal contents. In contradistinction to fiducial-based or Calypso-based tracking solutions, cone beam CT imaging gives a more comprehensive evaluation of all regional anatomy during each fraction, allowing a more complete evaluation potential sources of daily target deformation and also potentially revealing target volume changes (e.g. —shrinkage) over time. On the other hand, CT-based imaging is also more subjective than fiducial-based imaging, with surrounding tissue volume averaging obscuring prostate borders to variable degree, and so is perhaps best used as a compliment to fiducial-based SBRT tracking, rather than as a replacement for it

against localized low-to intermediate-risk lesions, the applicability of this prostate SBRT certainly does not stop there. Prostate SBRT is also a potentially valuable modality used as a prostate dose escalation boost for more advanced cases, and as a salvage method for locally relapsed or limited metastatic ("oligometastatic") cases.

If the alpha-beta ratio of prostate cancer really does prove to be 1.5 Gy or lower, the future direction of prostate SBRT could actually include studies to evaluate "de-escalation" of the prescribed dose, to further decrease toxicity rates and possibly further improve potency preservation rates. If this is done, accurate treatment planning and target tracking accuracy will become even more paramount, as the potential for "marginal" relapse would almost certainly increase, due to a very rapid loss of radiobiological power beyond the immediate PTV. The San Diego Virtual HDR prostate protocol in fact does now contain a "dose de-escalation" arm of 34 Gy/5 fractions for selected low and low-intermediate-risk patients (while maintaining "HDR-like" isodose morphology), though follow-up with this lower dose regimen is currently too limited to make any specific efficacy statement.

Even further along the de-escalation continuum, contingent upon continued improvement in prostate imaging techniques, including multiparametric MRI and/

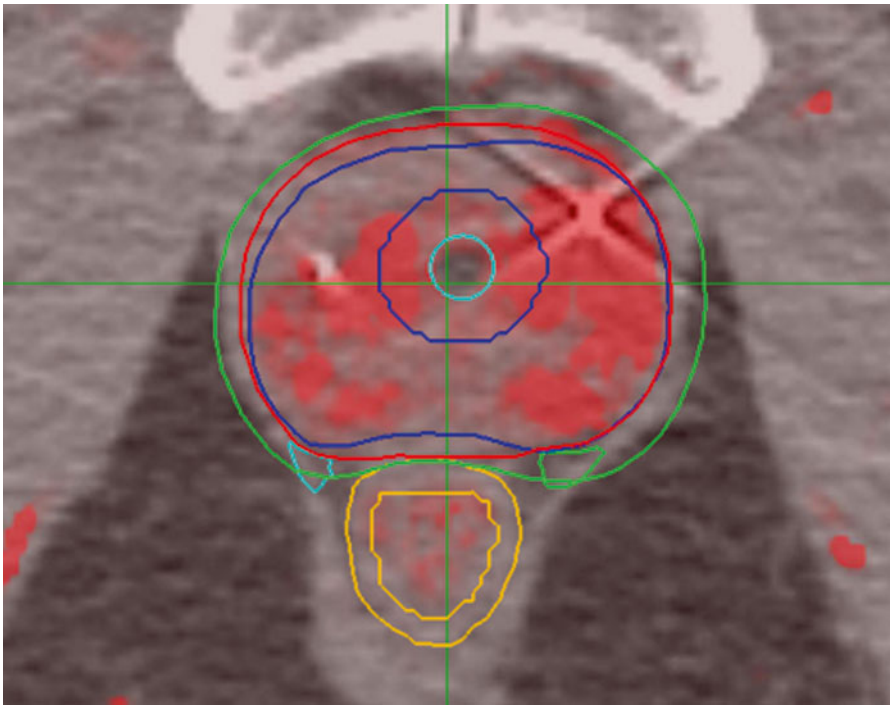

Fig. 11.11 Example of a Dynamic Contrast Enhanced (DCE) MRI image (semi-transparent red) overlying a standard SBRT simulation image. Theoretically, an image of this type (or other prostate dedicated imaging methods) could be used to direct "focal" prostate SBRT approaches. Unfortunately, the sensitivity and specificity of prostate imaging is not high enough to correctly recommend such an approach, outside of a properly designed clinical trial

or emerging PET/CT imaging techniques, SBRT methodology also seems potentially well suited to "focal" treatment, targeting of less than the entire prostate. This strategy is potentially applied in selected "very low-risk" or recurrent cases of prostate cancer. Currently, the primary limitation of focal prostate treatment is more tied to an inadequate capability to accurately map every voxel of prostate cancer involvement within the gland due to imaging limitations, rather than any specific SBRT limitation.

Finally, for more advanced cases, greater work needs to be done to define which, if any, prostate cancer patients *need* combined modality therapy as opposed to optimally powered SBRT monotherapy. Although logistically challenging, in ideal study in this regard could potentially include a "2 × 2 design" for "high-risk, clinically localized" cases—testing SBRT monotherapy versus SBRT boost + wide field "conventional" treatment along one axis, and testing each approach ± a course of neoadjuvant/adjuvant androgen deprivation therapy along the other axis (Table 11.4).

Although the RTOG 94–13 trial was already designed in this same basic format, in retrospect, none of the arms of this trial were likely sufficiently radiobiologically powered to optimize central tumor control, leaving the efficacy of optimally powered "prostate alone" radiotherapy arms still scientifically undefined for "high-risk" cases [60].

Table 11.4 Potential design of a clinical trial for advanced disease

Simple trial matrix for advanced disease study		
	SBRT monotherapy	SBRT boost + whole pelvis IMRT
(+) Androgen suppression		
(−) Androgen suppression		

In conclusion, other than confirming that prostate SBRT works well as monotherapy for most low- and intermediate-risk cases, we have barely scratched the surface of defining the optimal use of this obviously potent treatment modality against the larger spectrum of prostate cancer cases. Much, much investigative work remains to be done.

References

1. Zelefsky MJ, Daly ME, Valicenti RK. Perez and Brady's Principles and Practice of Radiation Oncology: Chapter 65. In: Low-Risk Prostate Cancer, 6 ed. LWW Oncology and Walters Kluwer; 2008. p. 1441.
2. Greene FL, Page DR, Fleming ID, eds. American Joint Committee on Cancer: Prostate Cancer. Springer; 2003. p. 309–16.
3. Muir CS, Nectoux J, Straszewski J. The epidemiology of prostate cancer: geographical distribution and time trends. Acta Oncol. 1991;30:133–40.
4. Narod SA, Dupont A, Cusan L, Diamond P, Gomez JL, Suburu R, Labrie F. The impact of family history on early detection of prostate cancer. Nat Med. 1995;1(2):99–101.
5. Brenner DJ, Hall EJ. Fractionation and protraction for radiotherapy of prostate carcinoma. Int J Radiat Oncol Biol Phys. 1999;43(5):1095–101.
6. Leborgne F, Fowler J, Leborgne JH, Mezzera J. Later outcomes and alpha/beta estimate from hypofractionated conformal three-dimensional radiotherapy versus standard fractionation for localized prostate cancer. Int J Radiat Oncol Biol Phys. 2012;82(3):1200–7.
7. Miralbell R, Roberts SA, Zubizarreta E, Hendry JH. Dose-fractionation sensitivity of prostate cancer deduced from radiotherapy outcomes of 5,969 patients in seven international institutional datasets: $\alpha/\beta = 1.4$ (0.9–2.2) Gy. Int J Radiat Oncol Biol Phys. 2012; 82(1):e17–24.
8. Proust-Lima C, Taylor JM, Sécher S, Sandler H, Kestin L, Pickles T, Bae K, Allison R, Williams S. Confirmation of a low α/β ratio for prostate cancer treated by external beam radiation therapy alone using a post-treatment repeated-measures model for PSA dynamics. Int J Radiat Oncol Biol Phys. 2011;79(1):195–201.
9. Kavanaugh BD. Tracing the earliest medical uses of high dose per fraction external beam radiation. J Radiosurg SBRT. 2011;1:5–11.
10. Marzi S, Saracino B, Petrongari MG, Arcangeli S, Gomellini S, Arcangeli G, Benassi M, Landoni V. Modeling of alpha/beta for late rectal toxicity from a randomized phase II study: conventional versus hypofractionated scheme for localized prostate cancer. J Exp Clin Cancer Res. 2009;28:117.
11. Williams SG, Taylor JM, Liu N, Tra Y, Duchesne GM, Kestin LL, Martinez A, Pratt GR, Sandler H. Use of individual fraction size data from 3756 patients to directly determine the alpha/beta ratio of prostate cancer. Int J Radiat Oncol Biol Phys. 2007;68(1):24–33.
12. Shaffer R, Pickles T, Lee R, Moiseenko V. Deriving prostate alpha-beta ratio using carefully matched groups, long follow-up and the phoenix definition of biochemical failure. Int J Radiat Oncol Biol Phys. 2011;79(4):1029–36.

13. Bentzen SM, Ritter MA. The alpha/beta ratio for prostate cancer: what is it, really? Radiother Oncol. 2005;76(1):1–3.
14. King CR, Lehmann J, Adler JR, Hai J. CyberKnife radiotherapy for localized prostate cancer: rationale and technical feasibility. Technol Cancer Res Treat. 2003;2(1):25–30.
15. Xie Y, Djajaputra D, King CR, Hossain S, Ma L, Xing L. Intrafractional motion of the prostate during hypofractionated radiotherapy. Int J Radiat Oncol Biol Phys. 2008;72(1):236–46.
16. Quon H, Loblaw DA, Cheung PC, Holden L, Tang C, Pang G, Morton G, Mamedov A, Deabreu A. Intra-fraction motion during extreme hypofractionated radiotherapy of the prostate using pre- and post-treatment imaging. Clin Oncol (R Coll Radiol). 2012;24(9):640–5.
17. Curtis W, Khan M, Magnelli A, Stephans K, Tendulkar R, Xia P. Relationship of imaging frequency and planning margin to account for intrafraction prostate motion: analysis based on real-time monitoring data. Int J Radiat Oncol Biol Phys. 2013;85(3):700–6.
18. Wilbert J, Baier K, Hermann C, Flentje M, Guckenberger M. Accuracy of real-time couch tracking during 3-dimensional conformal radiation therapy, intensity modulated radiation therapy, and volumetric modulated Arc therapy for prostate cancer. Int J Radiat Oncol Biol Phys. 2013;85(1):237–42.
19. Ng JA, Booth JT, Poulsen PR, Fledelius W, Worm ES, Eade T, Hegi F, Kneebone A, Kuncic Z, Keall PJ. Kilovoltage intrafraction monitoring for prostate intensity modulated Arc therapy: first clinical results. Int J Radiat Oncol Biol Phys. 2013;84(5):e655–61. doi:10.1016/j.ijrobp.2012.07.2367. pii: S0360–3016(12)03312–3.
20. Shi C, Tazi A, Fang DX, Iannuzzi C. Study of ExacTrac X-ray 6D IGRT setup uncertainty for marker-based prostate IMRT treatment. J Appl Clin Med Phys. 2012;13(3):3757.
21. Wu J, Ruan D, Cho B, Sawant A, Petersen J, Newell LJ, Cattell H, Keall PJ. Electromagnetic detection and real-time DMLC adaptation to target rotation during radiotherapy. Int J Radiat Oncol Biol Phys. 2012;82(3):e545–53. Epub 2011 Oct 17.
22. Grills IS, Martinez AA, Hollander M, Huang R, Goldman K, Chen PY, Gustafson GS. High dose rate brachytherapy as prostate cancer monotherapy reduces toxicity compared to low dose rate palladium seeds. J Urol. 2004;171(3):1098–104.
23. Ghadjar P, Keller T, Rentsch CA, Isaak B, Behrensmeier F, Stroux A, Thalmann GN, Aebersold DM. Toxicity and early treatment outcomes in low- and intermediate-risk prostate cancer managed by high-dose-rate brachytherapy as a monotherapy. Brachytherapy. 2009;8(1):45–51.
24. Yoshioka Y, Konishi K, Sumida I, Takahashi Y, Isohashi F, Ogata T, Koizumi M, Yamazaki H, Nonomura N, Okuyama A, Inoue T. Monotherapeutic high-dose-rate brachytherapy for prostate cancer: five-year results of an extreme hypofractionation regimen with 54 Gy in nine fractions. Int J Radiat Oncol Biol Phys. 2011;80(2):469–75.
25. Demanes DJ, Martinez AA, Ghilezan M, Hill DR, Schour L, Brandt D, Gustafson G. High-dose-rate monotherapy: safe and effective brachytherapy for patients with localized prostate cancer. Int J Radiat Oncol Biol Phys. 2011;81(5):1286–92.
26. Aluwini S, van Rooij PH, Kirkels WJ, Jansen PP, Praag JO, Bangma CH, Kolkman-Deurloo IK. High-dose-rate brachytherapy and external-beam radiotherapy for hormone-naïve low- and intermediate-risk prostate cancer: a 7-year experience. Int J Radiat Oncol Biol Phys. 2012;83(5):1480–5.
27. Martinez AA, Gonzalez J, Ye H, Ghilezan M, Shetty S, Kernen K, Gustafson G, Krauss D, Vicini F, Kestin L. Dose escalation improves cancer-related events at 10 years for intermediate- and high-risk prostate cancer patients treated with hypofractionated high-dose-rate boost and external beam radiotherapy. Int J Radiat Oncol Biol Phys. 2011;79(2):363–70.
28. Hoskin PJ, Rojas AM, Bownes PJ, Lowe GJ, Ostler PJ, Bryant L. Randomised trial of external beam radiotherapy alone or combined with high-dose-rate brachytherapy boost for localised prostate cancer. Radiother Oncol. 2012;103(2):217–22.
29. Deutsch I, Zelefsky MJ, Zhang Z, Mo Q, Zaider M, Cohen G, Cahlon O, Yamada Y. Comparison of PSA relapse-free survival in patients treated with ultra-high-dose IMRT versus combination HDR brachytherapy and IMRT. Brachytherapy. 2010;9(4):313–8.

30. Fuller DB, Naitoh J, Lee C, Hardy S, Jin H. Virtual HDR CyberKnife treatment for localized prostatic carcinoma: dosimetry comparison with HDR brachytherapy and preliminary clinical observations. Int J Radiat Oncol Biol Phys. 2008;70(5):1588–97.
31. Jabbari S, Weinberg VK, Kaprealian T, Hsu IC, Ma L, Chuang C, Descovich M, Shiao S, Shinohara K, Roach 3rd M, Gottschalk AR. Stereotactic body radiotherapy as monotherapy or post-external beam radiotherapy boost for prostate cancer: technique, early toxicity, and PSA response. Int J Radiat Oncol Biol Phys. 2012;82(1):228–34.
32. Fuller, DB, Naitoh, J, Mardirossian G. Virtual HDR CyberKnife radiosurgery for localized prostatic carcinoma: a phase II study. 2006; amended 2012. http://www.clinicaltrials.gov/ct2/show/NCT01045148?term=virtual+hdr+cyberknife&rank=1.
33. King CR, Brooks JD, Gill H, Presti Jr JC. Long-term outcomes from a prospective trial of stereotactic body radiotherapy for low-risk prostate cancer. Int J Radiat Oncol Biol Phys. 2012;82(2):877–82.
34. Freeman DE, King CR. Stereotactic body radiotherapy for low-risk prostate cancer: five-year outcomes. Radiat Oncol. 2011;6:3.
35. Katz AJ, Santoro M, Ashley R, Diblasio F. Stereotactic body radiation therapy for low- and low-intermediate-risk prostate cancer: is there a dose effect? Front Oncol. 2011;1:49.
36. Puech P, Potiron E, Lemaitre L, Leroy X, Haber GP, Crouzet S, Kamoi K, Villers A. Dynamic contrast-enhanced-magnetic resonance imaging evaluation of intraprostatic prostate cancer: correlation with radical prostatectomy specimens. Urology. 2009;74(5):1094–9.
37. Sciarra A, Barentsz J, Bjartell A, Eastham J, Hricak H, Panebianco V, Witjes JA. Advances in magnetic resonance imaging: how they are changing the management of prostate cancer. Eur Urol. 2011;59(6):962–77.
38. Sauvain JL, Palascak P, Gomez W, Nader N, Bremon JM, Bloqueau P, Jung L, Maniere P, Papavero R, Rhomer P. MRI and prostatic cancer: measurements of kinetic perfusion parameters of gadolinium with a computerized-aided diagnostic tool (CAD). Prog Urol. 2010;20(2):121–9.
39. Jackson AS, Reinsberg SA, Sohaib SA, Charles-Edwards EM, Jhavar S, Christmas TJ, Thompson AC, Bailey MJ, Corbishley CM, Fisher C, Leach MO, Dearnaley DP. Dynamic contrast-enhanced MRI for prostate cancer localization. Br J Radiol. 2009;82(974):148–56.
40. Fuller DB, Shirazi R, Naitoh J, Mardirossian G. Virtual HDR SBRT for prostate carcinoma: efficacy and quality of life assessment; ASCO GU symposium, poster presentation, San Francisco; Feb 1 2012.
41. McNeal JE, Redwine EA, Freiha FS, Stamey TA. Zonal distribution of prostatic adenocarcinoma. Correlation with histologic pattern and direction of spread. Am J Surg Pathol. 1988;12(12):897–906.
42. Fuller DB, Mardirossian G, Wong D, et al. Prospective evaluation of SBRT for low and intermediate risk prostate cancer: emulating HDR brachytherapy dose distribution. Int J Radiat Oncol Biol Phys. 2012;84(3 Suppl):S149.
43. Madsen BL, Hsi RA, Pham HT, Fowler JF, Esagui L, Corman J. Stereotactic hypofractionated accurate radiotherapy of the prostate (SHARP), 33.5 Gy in five fractions for localized disease: first clinical trial results. Int J Radiat Oncol Biol Phys. 2007;67(4):1099–105.
44. Pham HT, Song G, Badiozamani K, Yao M, et al. Five-year outcome of stereotactic hypofractionated accurate radiotherapy of the prostate (SHARP) for patients with low-risk prostate cancer abstract. Int J Radiat Oncol Biol Phys. 2010;78(3 Suppl):S58.
45. Boike TP, Lotan Y, Cho LC, Brindle J, DeRose P, Xie XJ, Yan J, Foster R, Pistenmaa D, Perkins A, Cooley S, Timmerman R. Phase I dose-escalation study of stereotactic body radiation therapy for low- and intermediate-risk prostate cancer. J Clin Oncol. 2011;29(15):2020–6.
46. Mantz CA, Fernandez E, Zucker I, Harrison S. A phase II trial of real-time target tracking SBRT for low-risk prostate cancer utilizing the calypso 4D localization system: patient reported health-related quality of life and toxicity outcomes. Abstract. Int J Radiat Oncol Biol Phys. 2010;78(3 Suppl):S57–8.

47. Stephenson AJ, Scardino PT, Bianco Jr FJ, DiBlasio CJ, Fearn PA, Eastham JA. Morbidity and functional outcomes of salvage radical prostatectomy for locally recurrent prostate cancer after radiation therapy. J Urol. 2004;172(6 Pt 1):2239–43.
48. Finley DS, Belldegrun AS. Salvage cryotherapy for radiation-recurrent prostate cancer: outcomes and complications. Curr Urol Rep. 2011;12(3):209–15.
49. Burri RJ, Stone NN, Unger P, Stock RG. Long-term outcome and toxicity of salvage brachytherapy for local failure after initial radiotherapy for prostate cancer. Int J Radiat Oncol Biol Phys. 2010;77(5):1338–44.
50. Aaronson DS, Yamasaki I, Gottschalk A, Speight J, Hsu IC, Pickett B, Roach 3rd M, Shinohara K. Salvage permanent perineal radioactive-seed implantation for treating recurrence of localized prostate adenocarcinoma after external beam radiotherapy. BJU Int. 2009;104(5):600–4.
51. Beyer DC. Salvage brachytherapy after external-beam irradiation for prostate cancer. Oncology (Williston Park). 2004;18(2):151–8.
52. Grado GL. Benefits of brachytherapy as salvage treatment for radiorecurrent localized prostate cancer. Urology. 1999;54(2):204–7.
53. Lee B, Shinohara K, Weinberg V, Gottschalk AR, Pouliot J, Roach 3rd M, Hsu IC. Feasibility of high-dose-rate brachytherapy salvage for local prostate cancer recurrence after radiotherapy: the University of California-San Francisco experience. Int J Radiat Oncol Biol Phys. 2007;67(4):1106–12.
54. Tharp M, Hardacre M, Bennett R, Jones WT, Stuhldreher D, Vaught J. Prostate high-dose-rate brachytherapy as salvage treatment of local failure after previous external or permanent seed irradiation for prostate cancer. Brachytherapy. 2008;7(3):231–6.
55. Fuller DB, et al. Virtual HDR CyberKnife radiosurgery for locally recurrent prostatic carcinoma: a phase II study. ClinicalTrials.gov Identifier: NCT00851916.
56. Fuller DB, Wurzer J, Mardirossian G. Virtual HDR SBRT for post-radiotherapy locally recurrent prostatic carcinoma: evaluation of toxicity, PSA response and disease-free survival. ARO Conference, poster presentation, Dallas, 29 Nov 2012.
57. Jereczek-Fossa BA, Beltramo G, Fariselli L, Fodor C, Santoro L, Vavassori A, Zerini D, Gherardi F, Ascione C, Bossi-Zanetti I, Mauro R, Bregantin A, Bianchi LC, De Cobelli O, Orecchia R. Robotic image-guided stereotactic radiotherapy, for isolated recurrent primary, lymph node or metastatic prostate cancer. Int J Radiat Oncol Biol Phys. 2012;82(2):889–97.
58. Berkovic P, De Meerleer G, Delrue L, Lambert B, Fonteyne V, Lumen N, Decaestecker K, Villeirs G, Vuye P, Ost P. Salvage stereotactic body radiotherapy for patients with limited prostate cancer metastases: deferring androgen deprivation therapy. Clin Genitourin Cancer. 2013;11(1):27–32. pii: S1558–7673.
59. Partin AW, Mangold LA, Lamm DM, Walsh PC, Epstein JI, Pearson JD. Contemporary update of prostate cancer staging nomograms (Partin Tables) for the new millennium. Urology. 2001;58(6):843–8.
60. Lawton CA, DeSilvio M, Roach 3rd M, Uhl V, Kirsch R, Seider M, Rotman M, Jones C, Asbell S, Valicenti R, Hahn S, Thomas Jr CR. An update of the phase III trial comparing whole pelvic to prostate only radiotherapy and neoadjuvant to adjuvant total androgen suppression (TAS): updated analysis of RTOG 94-13, with emphasis on unexpected hormone/radiation interactions. Int J Radiat Oncol Biol Phys. 2007;69(3):646–55.

Chapter 12
Stereotactic Body Radiotherapy for Renal Cancer

Irving D. Kaplan, Anand Mahadevan, and Andrew A. Wagner

Abstract Surgery is the primary treatment for renal cancer. However, with inadequate renal function or in patients with solitary kidneys, it may not be a safe function preserving option. When surgery is not desirable other ablative therapies such as radiofrequency ablation or SBRT have been used. Conventional external beam radiation has limited value and can be toxic to the remaining kidney or the surrounding organs. Highly conformal stereotactic body radiotherapy (SBRT) can be an effective and safe nonsurgical option for selected renal cancers.

Keywords Renal cancer • Ablation • Nephrectomy • Stereotactic body radiotherapy

12.1 Introduction

The American Cancer Society estimates that over 65,150 new cases of renal cancer were diagnosed in the United States in 2013 with more than 13,650 patients dying of this disease [1]. Approximately 90 % of these cases are renal cell carcinoma with the majority clear cell tumors. While surgery is currently the standard treatment for primary renal cell carcinoma, not all patients are suitable for surgery. In addition nephrectomy is associated with increased long-term risk of chronic renal failure. Current alternative treatments—cryotherapy and radiofrequency ablation—have shown tumor control efficacy but are invasive procedures. Renal cell carcinoma is historically considered a "radioresistant" tumor because conventionally fractionated radiation treatments have not been shown to be effective. The development of radiosurgery—allowing an accurate delivery of high doses of radiation to a tumor while maximally sparing surrounding normal organs—may allow the

I.D. Kaplan, MD (✉) • A. Mahadevan, MD, FRCS, FRCR
Department of Radiation Oncology, Beth Israel Deaconess Medical Center, Harvard Medical School, Boston, MA, USA
e-mail: ikaplan@bidmc.harvard.edu

A.A. Wagner, MD
Department of Urology, Beth Israel Deaconess Medical Center, Harvard Medical School, Boston, MA, USA

A. Gaya, A. Mahadevan (eds.), *Stereotactic Body Radiotherapy: A Practical Guide*,
DOI 10.1007/978-0-85729-597-2_12

radioresistance of renal cell cancers to be overcome. Clinical experience using radiosurgery to treat metastatic sites of renal cell carcinoma as well as early experience using radiosurgery for primary renal cell tumors, appear promising and justify further study of this treatment approach.

12.2 Background and Rationale

12.2.1 Rationale for Nephron Sparing Approaches

The current standard treatment for clinically localized disease is surgery. Although radical nephrectomy is the gold-standard surgical approach, nephron-sparing surgery with partial nephrectomy has become increasingly popular as an alternative, especially for small renal masses. The American Urologic Association recommends nephron sparing partial nephrectomy when possible. The rationale for nephron-sparing surgery is to preserve as much renal function as possible, without sacrificing cancer control compared to radical nephrectomy. Partial nephrectomy has been shown to have no statistically significant difference in cancer specific survival in patients with small localized renal cell carcinoma in multiple retrospective studies (Table 12.1) [2–4, 6]. In selected patients, local recurrence after partial nephrectomy is less than 8 % with cancer-specific survival rates 97–100 %.

Nephron-sparing approaches have also shown potential to reduce the post surgical progression to significant chronic kidney disease requiring dialysis [5]. Huang et al., conducted a retrospective study of 662 patients with a normal serum creatinine undergoing elective partial or radical nephrectomy for small solitary renal

Table 12.1 Outcomes after nephron sparing approaches for renal cancer

Authors	Treatment	Mean tumor size (cm)	Follow up (months)	No of patients	Cancer specific survival (%)	Local failure rate (%)
Lane et al. (2007) [6]	Partial nephrectomy	2.9	68	58	100	2.70
Barbalias et al. (1999) [3]	Partial nephrectomy	3.5	68	41	97.50	7.30
	Radical nephrectomy	3.8	68	48	98.40	0
Butler et al. (1995) [2]	Partial nephrectomy	2.5	68	46	100	2.10
	Radical nephrectomy	2.8	68	42	97	2.30
Liebovich et al. (2004) [4]	Partial nephrectomy	4.9	68	91	98	?
	Radical nephrectomy	5.4	68	841	86	?

tumors. Using estimated GFR and defining chronic kidney disease as a GFR <60 they found that the 3 year probability of CKD was 20 % in the partial nephrectomy group and 65 % in the radical nephrectomy group ($p < 0.0001$). A similar study conducted by La Rochelle et al., followed 84 patients undergoing partial nephrectomy and found the estimated 5 year end stage renal disease free survival in patients without local recurrence was 97 % at 5 years [7]. Hence, nephron-sparing approaches can preserve renal function without compromising local control or survival. Laparoscopic partial nephrectomy (LPN) offers patients the same advantages over OPN as LRN but it is technically challenging surgery, which requires advanced laparoscopic skills [8]. In expert hands, LPN appears to offer excellent outcome for tumors <4 cm.

12.2.2 Non-surgical Nephron Sparing Approaches

Not all patients with renal cell carcinoma are suitable surgical candidates, and many patients due to medical comorbidities or body habitus are unable to undergo a nephrectomy. For these patients, other treatments have been used including cryoablation and radiofrequency ablation. These modalities have shown good cancer control outcomes in multiple published series. A meta-analysis of 47 studies in which patients underwent either RFA (775 cases) or cryoablation (600 cases) has recently been published [9]. There was no significant difference in mean patient age, tumor size or duration of follow-up. However, a greater number of the cryoablation patients underwent pretreatment biopsy and surgery via the laparoscopic route. The main findings were a local progression rate that was significantly higher after RFA than cryoablation (12.9 % vs. 5.2 %), and a greater need for repeat ablation with RFA than cryoablation (8.5 % vs. 1.3 %). Although metastasis was seen more commonly after RFA, the difference did not reach statistical significance in this meta-analysis. Lucas et al., retrospectively evaluated 242 patients undergoing radiofrequency ablation, partial nephrectomy or radical nephrectomy for unilateral renal masses smaller than 4 cm [10]. They reported the 3-year freedom from stage III chronic kidney disease for radio frequency ablation, partial nephrectomy and radical nephrectomy was 95.2, 70.7 and 39.9 %, respectively ($p < 0.001$)[1]. These results reaffirm that partial nephrectomy may better preserve renal function compared to radical nephrectomy, and also show that ablative therapies (which treat the tumor without removing the entire kidney) may also be effective for preserving renal function.

12.3 Radiation Therapy for Renal Cell Carcinoma

Conventional radiation therapy, used for almost all cancers, has not been routinely used for primary renal cell carcinoma as there has been no consistent survival benefit shown for either preoperative or postoperative radiation [11–14]. Juusela et al.

randomized 88 patients to preoperative radiation therapy with 33 Gy over 3 weeks or immediate nephrectomy. Five year actuarial survival was 47 % in the radiation group and 63 % in the nephrectomy only group with no statistically significant difference [11]. Kjaer et al. conducted a prospective randomized trial comparing post nephrectomy radiation with 50 Gy in 20 fractions to observation and reported no significant difference in relapse rate or overall survival between the two groups [12]. Of the patients receiving radiation therapy in the later study 44 % reported serious GI side effects. As a result of these studies renal cell carcinoma has typically been thought of as "radioresistant" as it does not respond to conventional external beam radiation at the maximal dose that can be safely delivered.

A retrospective study by Wersall et al., looked at radiosurgical outcomes from 58 patients with extra cranial metastatic renal cell carcinoma or inoperable primary renal cancers. They were able to demonstrate radiologic regression in 30 % of patients, but more importantly a 90 % local control rate [13]. Based on these promising retrospective findings Svedman et al., conducted a prospective phase II trial treating a total of 82 extracranial renal cell carcinoma lesions (primary or metastatic). They were able to obtain local control, defined as radiologically stable disease or partial/complete response in 98 % of treated lesions [15]. These studies showed very encouraging results for the use of stereotactic radiosurgery to treat renal cell carcinoma.

12.4 Stereotactic Body Radiotherapy for Renal Cell Carcinoma

Preclinical and early clinical experience using radiosurgery to treat primary renal cancers appear promising as well: Ponsky et al., from the Cleveland Clinic have treated kidneys in ten female swine all with approximately 2 cm sized lesions with single fractions of 24–40 Gy using the CyberKnife [16]. Sixteen kidneys were harvested at 4, 6, or 8 weeks after treatment and pathologically examined. After 8 weeks, the kidney tumors were completely ablated with fibrosis with a zone of adjacent partial fibrosis. The renal parenchyma surrounding the area of partial fibrosis was histologically normal. Beitler et al. [17], from Staten Island University Hospital treated nine patients who refused surgery for clinically and radiographically non-metastatic renal cell carcinoma with 40 Gy in 5 fractions using conformal external radiation. At 2 years follow up none of the patients had recurred in the radiated area. Four of the nine patients were still alive with minimum follow up of 48 months.

Ponsky et al. [18], from the Cleveland Clinic treated three patients with radiologic evidence of renal tumor less than 4 cm with a total of 16 Gy in 4 fractions over 2 days using the CyberKnife as the first level of a dose escalation study. Patients then underwent partial or total nephrectomy 8 weeks after completion of radiosurgery and surgical specimens were reviewed histologically. All three patients' tumors remained stable or reduced in size and one patient's tumor was completely ablated. In these initial patients, no acute toxicities, no change in renal function and no change in clinical performance status were noted.

Hong et al., 2008 from Harvard Medical School presented initial data from their prospective trial treating patients with primary renal cell carcinoma with CyberKnife radiosurgery [19]. Patients were treated with 21 Gy in 3 fractions. Fourteen patients were treated and there was no tumor progression or increases in creatinine at 1-year follow up. They also reported a mean decrease in tumor volume of 44 % at 12 months follow up with no RTOG Stage II toxicities. The authors in collaboration with Baylor Medical Center have recently completed a Phase I dose escalation study treating primary renal cell carcinoma tumors up to 5 cm. The dose was increased from 7 Gy ×3 fractions (total 21 Gy) to 16 Gy ×3 fractions (total 48 Gy). In 15 patients treated on this trial, no patient experienced Grade 2+ toxicity. Further dose escalation beyond 16 Gy ×3 fractions was deemed medically unnecessary as this dose was felt to be adequate for renal cell carcinoma; therefore, this dose has been selected for the current Phase II study. While not the primary outcome of the Phase I study, tumors treated responded with minimal shrinkage in size, but demonstrated reduction in enhancement (on CT on MRI) suggesting tumor necrosis and fibrosis. This response is consistent with prior studies. Progression has been seen one patient treated at 7 Gy ×3 and one at 9 Gy ×3 dose levels.

12.4.1 Patient Selection

Patients with histological or radiologically confirmed renal cell cancers with no contraindications for nephron sparing ablative therapies are candidates for SBRT. Patients with difficult anatomy, particularly with solitary kidneys are at a high risk for biopsy and pathognomonic radiological findings may have to be relied on. These include Ultrasound, bi-phasic spiral CT and contrast enhanced MRI. The accuracy of up-to-date imaging in detecting and staging renal cancers is over 90 %.

Many SBRT systems utilize fiducial markers for respiratory and motion tracking (e.g. Cyberknife). Inability to place fiducials, due to patient anatomy or bleeding diathesis, may prove to be contraindications for the procedure. While perivascular and other central lesions not suitable for other kidney directed local therapies are ideally suited for SBRT, large central tumors, in solitary kidneys with limited function may be relative contraindications. Inability to obtain imaging to identify target and prior abdominal radiation threatening nephron preservation may be other relative contraindications.

12.4.2 Treatment Planning and Delivery

Simulation is often done in a supine position with reproducible immobilization; usually in a comfortable vac-loc. IV contrast is beneficial in accurate visualization if the target and images obtained in nephrogram phase (100–120 s) for optimal characterization of the mass. Optional sequences based on the system used

are, arms up and down, inspiration-expiration and 4D CT. Respiratory dampening and respiratory gating to account for motion management may need special procedures. Available MRI and PET are often summoned for fusion in the planning system.

Once the image set with fusion is available, the next step is to delineate the target volume. The GTV (Gross Tumor Volume), CTV (Clinical Target Volume—based on predicted microscopic extension of the tumor) are defined. The expansion for PTV (Planning target volume) is often described differently with different systems. With fiducial based continuous live motion tracking (e.g. Cyberknife) the GTV is often considered the PTV. While this approach has the benefit of maximal nephron sparing, there is a risk of missing microscopic disease. On the other hand with gating and respiratory dampening increasing margins are required to achieve target coverage with the prescribed dose- typically 3–5 mm.

Organs at risk are identified—typically reminder of the kidney, the contralateral kidney, liver spinal cord and bowel. Typically when treating in 3 fractions, the recommended dose constraints for organs at risk are as follows:

- Spinal cord: Limited to 6 Gy per fraction, maximum total point dose to spinal cord of 18 Gy;
- Stomach: Limited to 10 Gy per fraction (allow up to 3 cc of stomach to receive this dose) and a maximum point dose of 30 Gy.
- Liver: At least 700 cc of liver receiving less than 7 Gy total dose.
- Small and Large Bowel: Limited to 8 Gy ×3 (to 1 cc) and a maximum point dose of 10 Gy ×3.
- Opposite Kidney: Every effort will be made to limit dose to opposite kidney to less than 2 Gy per fraction with an absolute limit of 50 % of kidney receiving less than 15 Gy

Based on current available data, the authors usually prescribe 16 Gy × 3 = 48 Gy for smaller tumors (<5 cm) and 12 Gy × 4 = 48 GY for larger tumors. The prescription dose will be to the percentage isodose volume that encompasses the PTV; typically 95 % of the PTV receives the prescribed dose. The plan will be constructed so that the chosen prescription percentage isodose volume is left to the discretion of the treating physician but is expected to fall generally in the range of 60–80 %. Treatments may be delivered in 3 consecutive or alternate days.

A representative treatment plan is shown in Fig. 12.1.

12.4.3 Toxicity

Patients will need to be monitored during the treatment course with documentation of acute toxicity. No treatment related toxicities where observed in the Phase I dose escalation study in the authors' institution other than mild fatigue. Nausea has been reported and is managed conservatively with prophylactic or therapeutic antiemetics.

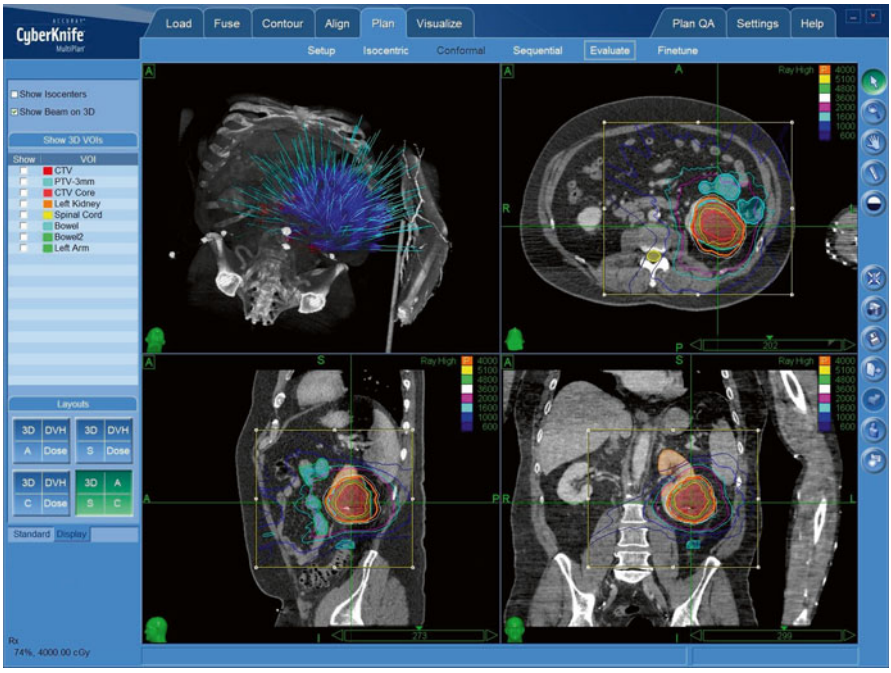

Fig. 12.1 Representative image of non-isocentric SBRT Treatment plan for a renal tumor using the Cyberknife™ system

12.4.4 Post Treatment Care

While clinical examinations re mandatory for monitoring toxicity and quality of life, laboratory assessment of renal function is absolutely essential. Detailed and periodic imaging using modalities outlined above is required for assessment of tumor control. This can often be challenging as post contrast CT and MRI may not be feasible due to their poor renal function. Periodic clinical and radiological follow up is warranted based on institutional protocol. Adverse events and radiological assessments need to be carefully monitored and recorded.

12.5 Future Directions

The role of SBRT for renal cancers is evolving. Phase I/II studies have established the feasibility and safety of SBRT for nephron sparing ablative treatment of renal cancer. Larger Phase II efficacy studies with careful radiological follow-up and toxicity assessment are underway in many institutions including the authors. This would set the stage for future Phase III studies comparing the value of SBRT in relation to other surgical and non-surgical nephron sparing approaches.

References

1. Siegel R, Naishadham D, Jemal A. Cancer statistics, 2013. CA Cancer J Clin. 2013; 63(1):11–30.
2. Butler BP, Novick AC, Miller DP, Campbell SA, Licht MR. Management of small unilateral renal cell carcinomas: radical versus nephron-sparing surgery. Urology. 1995;45(1):34–40; discussion 40–41.
3. Barbalias GA, Liatsikos EN, Tsintavis A, Nikiforidis G. Adenocarcinoma of the kidney: nephron-sparing surgical approach vs. radical nephrectomy. J Surg Oncol. 1999;72(3): 156–61.
4. Leibovich BC, Blute ML, Cheville JC, Lohse CM, Weaver AL, Zincke H. Nephron sparing surgery for appropriately selected renal cell carcinoma between 4 and 7 cm results in outcome similar to radical nephrectomy. J Urol. 2004;171(3):1066–70.
5. Adkins KL, Chang SS, Cookson MS, Smith JA. Partial nephrectomy safely preserves renal function in patients with a solitary kidney. J Urol. 2003;169(1):79–81.
6. Lane BR, Gill IS. 5-Year outcomes of laparoscopic partial nephrectomy. J Urol. 2007;177(1): 70–4; discussion 74.
7. Huang WC, Levey AS, Serio AM, Snyder M, Vickers AJ, Raj GV, et al. Chronic kidney disease after nephrectomy in patients with renal cortical tumours: a retrospective cohort study. Lancet Oncol. 2006;7(9):735–40.
8. Lane BR, Novick AC, Babineau D, Fergany AF, Kaouk JH, Gill IS. Comparison of laparoscopic and open partial nephrectomy for tumor in a solitary kidney. J Urol. 2008;179(3): 847–51; discussion 852.
9. Kunkle DA, Uzzo RG. Cryoablation or radiofrequency ablation of the small renal mass: a meta-analysis. Cancer. 2008;113(10):2671–80.
10. Lucas SM, Stern JM, Adibi M, Zeltser IS, Cadeddu JA, Raj GV. Renal function outcomes in patients treated for renal masses smaller than 4 cm by ablative and extirpative techniques. J Urol. 2008;179(1):75–9; discussion 79–80.
11. Juusela H, Malmio K, Alfthan O, Oravisto KJ. Preoperative irradiation in the treatment of renal adenocarcinoma. Scand J Urol Nephrol. 1977;11(3):277–81.
12. Kjaer M, Iversen P, Hvidt V, Bruun E, Skaarup P, Bech Hansen J, et al. A randomized trial of postoperative radiotherapy versus observation in stage II and III renal adenocarcinoma. A study by the Copenhagen Renal Cancer Study Group. Scand J Urol Nephrol. 1987; 21(4):285–9.
13. Wersall PJ, Blomgren H, Lax I, Kalkner K-M, Linder C, Lundell G, et al. Extracranial stereotactic radiotherapy for primary and metastatic renal cell carcinoma. Radiother Oncol. 2005;77(1):88–95.
14. Finney R. The value of radiotherapy in the treatment of hypernephroma—a clinical trial. Br J Urol. 1973;45(3):258–69.
15. Svedman C, Sandström P, Pisa P, Blomgren H, Lax I, Kälkner K-M, et al. A prospective Phase II trial of using extracranial stereotactic radiotherapy in primary and metastatic renal cell carcinoma. Acta Oncol. 2006;45(7):870–5.
16. Ponsky LE, Crownover RL, Rosen MJ, Rodebaugh RF, Castilla EA, Brainard J, et al. Initial evaluation of Cyberknife technology for extracorporeal renal tissue ablation. Urology. 2003;61(3):498–501.
17. Beitler JJ, Makara D, Silverman P, Lederman G. Definitive, high-dose-per-fraction, conformal, stereotactic external radiation for renal cell carcinoma. Am J Clin Oncol. 2004;27(6):646–8.
18. Ponsky LE, Mahadevan A, Gill IS, Djemil T, Novick AC. Renal radiosurgery: initial clinical experience with histological evaluation. Surg Innov. 2007;14(4):265–9.
19. Hong Y. Cyberknife radiosurgical ablation of primary renal tumors. J Endourol. 2008;22(S1):A1–310.

Chapter 13
Stereotactic Body Radiotherapy for Oligometastasis

Nergiz R. Dagoglu and Anand Mahadevan

Abstract With tremendous strides in loco regional and systemic therapy many cancer patients present with limited metastatic disease. Just like the precedence of surgical metatstatectomy providing significant numbers of long term survivors, other evolving locoregional therapies can potentially achieve similar results, particularly when surgery is not an option or undesirable. Stereotactic Body Radiotherapy (SBRT) is becoming an increasingly valuable tool in the armamentarium against oligometastatic cancer. Future clinical trials are needed to solidify its role in the setting of systemic, targeted, immune and biological therapies.

Keywords Oligometastasis • Systemic therapy • Stereotactic Body Radiotherapy

13.1 Introduction

In spite of the advances in detection and treatment of some malignancies, metastases remain common and account for approximately 80–90 % of cancer deaths. The standard treatment for metastatic disease in most adult cancers is systemic cytotoxic chemotherapy and hormonal deprivation. With the notable exceptions of subsets of leukemias, lymphomas, and germ cell malignancies [1–3], systemic therapies for cancer are not curative. Targeted therapies have shown some promise, but only some, like imatinib for the treatment of chronic myeloid leukemia (CML), has demonstrated curative potential [4]. Response rates to currently available targeted therapies are low and are of limited curative potential in most solid tumors. Therefore, there is a vital need for the development of new therapies, including ablative therapies, for the treatment of patients with metastatic cancer.

N.R. Dagoglu, MD
Department of Radiation Oncology, Istanbul Medical Faculty, Istanbul, Turkey

A. Mahadevan, MD, FRCS, FRCR (✉)
Department of Radiation Oncology, Beth Israel Deaconess Medical Center, Harvard Medical School, Boston, MA, USA
e-mail: amahadev@bidmc.harvard.edu

A. Gaya, A. Mahadevan (eds.), *Stereotactic Body Radiotherapy: A Practical Guide*,
DOI 10.1007/978-0-85729-597-2_13

13.2 Oligometastasis

Based on the natural history of breast cancer [5], lung cancer [6] and other metastatic disease states like melanoma [7]- a clinically significant disease state of oligometastases has been postulated [8]. In this paradigm, a disease state between locoregionally confined and curative treatable disease and widely metastatic cancer may exist where tumors early in their clinical presentation of metastatic progression produce metastases limited in number and location. Such limited metastases could be considered de novo oligometastases [9]. In patients who present with widespread metastases, a state of induced oligometastases may be generated when effective systemic therapy eradicates the majority of metastatic deposits. Residual tumor foci in such patients are attributable to the presence of cells that are resistant to cytotoxic agents, hormonal deprivation and/or targeted agents. In either oligometastatic state, and in the setting of active/potential treatment for occult disease, a window of opportunity may exist where focal therapy to known sites of gross disease may be beneficial. In addition to de novo and induced oligometastasis, other two states have been postulated. In one, oligo recurrence describes the state of limited metastasis in the setting of controlled primary disease, as opposed to oligo metastasis, which occurs alongside an active primary disease site [10].

The utility of local therapy for metastases limited in number and location is supported by the long-term survival of some patients who undergo complete excision of pulmonary, hepatic, and brain metastases [11–13]. Furthermore, patients who develop metachronous and synchronous pulmonary and hepatic metastases have also been shown to have favorable outcomes following resection [14, 15]. Surgical resection for limited metastasis from melanoma has led to long-term survivors [16, 17]. Therefore, identifying patients with oligometastatic disease and delivering an appropriate therapy may be one of the novel approaches needed for the treatment of metastases [18, 19].

13.3 Natural History

While the natural history of cancer suggests that the oligometastatic state may exist, analyzing the patterns of presentation in patients with metastases tests the hypothesis that metastases can be limited in number and location and not associated with widespread disease. Potentially, oligometastasis may reflect an early stage of metastatic growth whereby tumors acquire the ability to only grow in one or two organs and to only form limited metastatic colonies. This conforms to the de novo oligometastasis theory following the “soil and seed” hypothesis first proposed by Sir James Paget. Furthermore, analyzing patterns of progression of metastatic patients after cytotoxic chemotherapy tests the hypothesis that effective chemotherapy could reduce the number and location of metastatic tumors to a limited number of locations that may benefit from local therapy allude to above as the induced oligometatstaic state Taken together, these data suggest that metastases are not always associated with widespread disease and that following chemotherapy, local therapy

to all known sites of disease could potentially benefit a subset of patients. Those patients in whom metastases were not widespread or progressed only in initially involved sites could theoretically benefit from metastasis directed treatment.

13.4 Surgical Precedence

More information is available regarding the surgical removal of metastases than for any other therapy. Literature describing the surgical removal of metastases, or metastectomy, have the largest patient numbers and longest follow-up periods of any modality of treatment. This lends serious credibility to the beneficial role of ablative therapy for localized metastasis. As such, there are undoubtedly differences with regard to patient selection, as well as variabilities in treatment technique and extent of follow-up that confound decisive interpretation. Nonetheless, this experience has taught clinicians much about typical outcomes, selection of patients, improved techniques, and follow-up strategies in addition to confirming that patients can be helped or even cured with ablative local therapy.

13.5 SBRT Rationale

While situations causing bowel obstruction, mass effect and diagnostic uncertainties often warrant surgery, other noninvasive approaches may be preferable in patients not suitable or not keen on surgery, or systemic therapy induced states (e.g. pancytopenia, Anti VEGF therapy) that precludes surgery.

Radiotherapy, similar to surgery, is anatomically targeted therapy. Computed tomography scans dedicated for radiotherapy planning are routinely used in combination with other diagnostic and metabolic imaging to generate three-dimensional tumor volumes. These tumor volumes are then used to design optimal beam arrangements and intensities. An advantage of radiotherapy over other local therapies is the ability to add margins for subclinical disease extent or, on the other hand be extremely conformal to avoid normal tissue toxicity. Recent technological advancements in imaging, patient immobilization, as well as radiotherapy planning and delivery have led to the development of stereotactic body radiotherapy as a useful treatment modality in patients with oligometastasis. Based on the principles of intracranial radiosurgery, this technique was developed in Sweden where, along with Japan, much of the early work with this technique was performed [20–22]. SBRT targets tumors with minimal margins, delivering six to ten times the standard daily amount of radiotherapy (5–22 Gy) in each dose while significantly shortening a course of radiotherapy from 7 weeks of daily treatments to 3–10 treatments over 1–3 weeks. Rigorous and reproducible methods to track target and patient motion including respiratory motion with varying degrees of combination of patient immobilization and tracking is required to ensure delivery of dose to the tumor while avoiding delivery of radiation to nearby critical normal structures.

13.6 SBRT Literature Review

While SBRT has been tested in the phase I and II setting for primary lung cancer [23–28] the data for SBRT to the lung specifically for metastatic disease is evolving. In series reporting both primary and metastatic lung tumors treated with SBRT using either single dose treatment, significantly hypofractionated treatments (3–5 fractions), or mildly hypofractionated treatments, local control rates have been impressive, ranging from 70 to 90 % [28–30]. Furthermore, toxicity has been mild, most commonly limited to radiographic lung changes. A phase I dose-escalation trial was performed for patients with lung metastases from various primary sites. SBRT dose was successfully escalated to 60 Gy in three fractions with minimal toxicity and excellent local control has been reported [31, 32]. Stereotactic radiosurgery (SRS), similar to SBRT but delivered in a single high-dose fraction, has also successfully been performed with respiratory gating or fiducial based continuous tracking for lung metastases [29, 33] with excellent local control with minimal morbidity. Additionally, investigators from Japan reported treating 1–2 pulmonary metastases in 34 patients with various primary tumors using 12 Gy fractions to doses of 48 or 60 Gy. At 2 years, 90 % of patients were free of local failure. Progression free survival was 34.8 % at 2 years [22, 34]. Little toxicity has been reported when SBRT is used to treat peripheral lung tumors, with pneumonitis rates varying from 0 to 10 % [35, 36]. However, when treating primary lung tumors within 2 cm of the proximal bronchial tree to 60–66 Gy in three fractions, investigators from Indiana University noted a 46 % rate of grade 3–5 toxicity compared to 17 % when treating peripheral lesions [25]. Due to high rates of toxicity seen when treating central lesions, alternative fractionation schemes are under investigation. However, for many patients with limited lung metastases, this technique seems promising with limited toxicity.

SBRT for the treatment of liver metastases has been delivered successfully with limited toxicity. In a pilot study of 31 patients with a variety of primary tumors, 17 liver metastases in 14 patients were treated with doses of 7.7–45 Gy in 1–4 fractions. Of 13 lesions treated with greater than 20 Gy, only one lesion progressed with a mean follow-up of almost 10 months [37]. One patient in this series who had a single liver metastasis from ovarian cancer survived disease-free for at least 26 months after irradiation with 40 Gy in two fractions. A Heidelberg University dose escalation study of single fraction body radiosurgery to the liver escalated dose from 14 to 26 Gy with good patient tolerance and 67 % local control at 18 months [38]. However, the majority of these patients failed systemically. A phase I multi-institutional trial sequentially escalated doses up to 60 Gy in three fractions. It was reported that the maximum tolerated dose (MTD) was not reached and a single patient out of 36 patients failed in-field at a median follow-up of 19 months [39]. Subsequent Phase II studies from this group confirmed these results [40]. A Phase I study from Princess Margeret Hospital in Toronto used individualized SBRT dose schemes respecting the normal tissue complication probability. They reported a 1 year local control rate of 71 % with a median overall survival of 17.6 months [41].

Using mildly hypofractionated SBRT (2–6 Gy/dose), the University of Rochester reported 57 % 20-month local control of 174 metastatic tumors [42]. Actuarial long-term survival despite disease progression was achieved at 37 months in nearly 30 % of the 20 patients with colorectal cancer metastases. Pooled analysis from these institutions and systematic reviews have validated the usefulness of SBRT for limited liver metastasis [43, 44].

The outcomes of patients treated with SBRT for multiple organ metastases have also been reported [45, 46]. The University of Rochester recently reported an analysis on patients with 1–5 metastases treated on two consecutive protocols. The first protocol treated breast cancer patients with limited metastases, in which no brain lesions were treated. The second protocol included patients with cancer from any primary site and limited metastases including a brain primary. After treatment with ten fractions of 5 Gy over 2 weeks, metastatic lesions were controlled 77 % of the time at 2 years. However, 75 % of patients developed further metastatic disease at 4 years consistent with an overall survival rate of 28 % at 4 years. A multivariate analysis revealed that total tumor volume, non-breast cancer primary, and the presence of adrenal metastases predicted for worse overall survival [47].

Appropriate SBRT doses when treating multiple metastases in multiple organs is not clear, due to involvement of multiple adjacent dose limiting normal tissues. Additionally, treating a large number of sites in the body can result in a high integral radiation dose. While the University of Rochester reported their results using 50 Gy in 10 fractions, other radiation delivery schemes using fewer fractions at higher doses per fraction have been used. However, based on studies analyzing dose volume histogram parameters on individual sites, allows limitations for thresholds for normal tissue toxicity. To determine the maximal tolerated dose of SBRT delivered in three fractions for patients with oligometastatic disease, a dose escalation study is currently ongoing at the University of Chicago. Early results were presented after 22 metastatic lesions were treated in 11 patients [48]. With a median follow-up of 5.6 months (range 4–10), abdominal and lung sites were safely escalated to 30 Gy. Eight of ten patients had progressive disease outside of the treated sites, but most treated lesions achieved freedom from local progression (83 % of abdominal lesions, 73 % of lung, 50 % of liver lesions, and 1/1 bone lesion). Dose response relationships have also been reported in the treatment of lung and liver metastasis [49, 50].

These early results demonstrate that SBRT for metastatic disease is tolerable at high doses and can result in local control of targeted lesions in the liver, lungs and multiple sites. In the limited series reported, patients have favorable survival compared to those treated with chemotherapy alone. SBRT for metastases limited to the liver or lung has been demonstrated to result in high rates of locoregional control with minimal toxicity. While more data are needed detailing the outcomes of SBRT for multiple organ metastases, the available data suggest that SBRT may be able to deliver locoregional control and survival outcomes similar to that seen with surgery for limited metastatic disease [18, 19].

Published Clinical outcomes for SBRT for metastasis is further tabulated in Tables 13.1, 13.2, 13.3, 13.4, and 13.5 [31, 32, 34, 37–42, 46, 47, 51–81].

Table 13.1 Outcomes of stereotactic body radiation therapy for lung metastases from selected trials

Study	*n* of patients	Median dose/*n* of fraction	Median (range) follow-up, months	Local control rate	Overall survival	Toxicity
Onimaru et al. [51]	45	48 Gy/8; 60 Gy/8	18 (2–44)	3-years, 69.6 % for 48 Gy, 100 % for 60 Gy	2-years, 47.1 %	Grade 5, 1 (2.2 %)
Wulf et al. [52]	27	30 Gy/3; 36 Gy/3	13–17	2-years, 71 %	1-year, 48 % 2-years, 21 %	Grade 3, 1 (3.7 %) Grade 5, 1 (3.7 %)
Yoon et al. [53]	53	30 Gy/3; 40 Gy/4; 48 Gy/4	14 (4–56)	70 % for 30 Gy, 77 % for 40 Gy, 100 % for 48 Gy	1-year, 89 %; 2-years, 51 %	Grade >2, 0 %
Okunieff et al. [31]	50	50 Gy/10; 48 Gy/6; 57 Gy/3	18.7 (3.7–60.9)	3-years, 91 %	2-years, 50 %	Grade 2, 6.1 % Grade 3, 2 %
Norihisa et al. [34]	34	48 Gy/4; 60 Gy/5	27 (10–80)	2-years, 90 %	2-years, 84 %	Grade 2, 4 (12 %) Grade 3, 1 (3 %)
Brown et al. [54]	35	5 Gy/1–60 Gy/4	18 (2–41)	Crude, 77 %	2-years, 72.5 %	Grade 3–4, 1 (2.8 %)
Rusthoven et al. [32]	38	60 Gy/3	15.4 (6–48)	2-years, 96 %	2-years, 39 %	No grade 4 Grade 3, 3 (8 %)
Ricardi et al. [55]	61	45 Gy/3; 26 Gy/1	20.4 (3–77)	2-years, 89 %	2-years, 66.5 %	Grade 3, 1 (1.6 %)

Table 13.2 Summary of recent prospective trials with stereotactic body radiation therapy for liver metastases

Study	*n* of patients	Dose/*n* of fraction	Median (range) follow-up, months	Local control rate	Overall survival	Toxicity
Blomgren et al. [37]	14	Mean dose to PTV 8–63 Gy/1–4	1.5–13	Crude, 70 %	–	Grade >3 toxic effects, 0 %
Blomgren et al. [56]	17	20–45 Gy/2–4	9.6 (mean) (1.5–24)	Crude, 95 %	–	Grade >3 toxic effects, 0 %
Herfarth et al. [38]	33	14–26 Gy/1, prescribed to 80 %	18	Crude, 78 % 6-months, 75 % 12-months, 71 % 18-months,67 %	1-year, 72 %	Radiation-induced liver disease: 0 %
Hoyer et al. [57]	44	45 Gy/3, prescribed to 95 %	4.3 years	86 %	24-months, 38 %	–
Kavanagh et al. [58]	36	60 Gy/3	19	18-months, 93 %	–	–
Lee et al. [41]	70	27.7–60.0 Gy/6, prescribed to isodose line covering PTV (median, 41.4 Gy)	10.8 for 68 assessable patients	1-year, 71 %	18-months, 47 %	Late grade 4 and 5 toxic effects, 2.9 % and 1.5 %, respectively
Méndez Romero et al. [59]	14	37.5 Gy/3, prescribed to 65 %	12.9	Crude, 94 % 1-year, 100 % 2-years, 86 %	1-year, 85 %; 2-years, 62 %	Grade >4 toxic effects, 0 %
Rusthoven et al. [40]	47	12–20 Gy/3, prescribed to isodose line covering PTV	16	1-year, 95 % 2-years, 92 %	2-years, 30 %	Grade 4 toxic effects, 0 %
Goodman et al. [60]	26	18–30 Gy/1, prescribed to 80 %	17.3	1-year, 61.8 %; 2-years, 49.4 %	1-year, 61.8 %; 2-years, 49.4 %	Late grade 2 gastrointestinal toxic effects, 2 of 26 patients

(continued)

Table 13.2 (continued)

Study	*n* of patients	Dose/*n* of fraction	Median (range) follow-up, months	Local control rate	Overall survival	Toxicity
Rule et al. [61]	27	30–60 Gy/5	20	2-years, 56, 89, and 100 % for the 30-, 50-, and 60-Gy cohorts, respectively	–	Grade >3 toxic effects, 0 %
Schefter et al. [39]	18	36–60 Gy/3	7.1	–	–	Grade >3 toxic effects, 0 %
Katz et al. [42]	69	30–55 Gy/7–20 (mean 11), prescribed to 80 %	14.5	10 month, 76 % 20 month, 57 %	Median, 14.5 months	Grade >3, 0 %

Abbreviation: *PTV* planning target volume

Table 13.3 Summary of published trials of stereotactic body radiation therapy for lymph node metastases

Study	Primary	Treated site(s)	*n* of patients	Median dose/*n* of fraction	Median (range) follow-up, months	Local control rate	Overall survival	Toxicity
Choi et al. [62]	Cervix	Paraaortic nodes	30	33–45 Gy/3 (*n* = 24); 4 patients also received 27–45 Gy external beam radiotherapy	15 (2–65)	4-years, 67.4 %	4-years, 50.1 month	Late grade 3 or 4 toxicity, 3 %
Jereczek-Fossa et al. [63]	urological, gastrointestinal, gynecologic, malignancies	Abdominal lymph nodes	69	24 Gy/3	20	3-years, 64.3 %	3-years, 49.9 %	Acute grade 3 toxicity in 2; Grade 4 toxicity in 1
Kim et al. [64]	Stomach	Paraaortic nodes	7	45–51 Gy (median, 48 Gy)/3	26 (19–33)	–	3-years, 43 %	Late grade 3 or 4 toxicity, 0 %
Kim et al. [65]	Colorectum	Pelvic/presacral lymph nodes	7	36–51 Gy/3	26 (15–70)	86 %	3-years, 71.4 %	Late grade 4 toxicity, 14 %
Bignardi et al. [66]	Miscellanous	Abdominal lymph nodes	19	45 Gy/6	12	12-months, 77.8 %	–	Late grade 3 or 4 toxicity, 0 %
Casamassima et al. [67]	Prostate	Pelvic, paraaortic or mediastinal lymph nodes	25	30 Gy/3	29 (14.4–48)	3-years, 90 %	3-years, 92 %	Late grade >2 toxicity, 0 %

Table 13.4 Summary of published trials of stereotactic body radiation therapy for adrenal metastases

Study	*n* of patients	Median dose/*n* of fraction	Median (range) follow-up, months	Local control rate	Overall survival	Toxicity
Casamassima et al. [68]	48	36 Gy/3	16.2 (3–63)	1–2 years, 90 %	1-year, 39.7 %; 2-years, 14.5 %	1 case of grade 2 adrenal insufficiency
Chawla et al. [69]	30	40 Gy/10	9.8 (3.2–28.3)	1-year, 55 %	1-year, 44 % 2-years, 25 %	Mild grade 1 fatigue and nausea, "common"
Oshiro et al. [70]	19	45 Gy/10	11.5 (5.4–87.8)	Objective response rate, 68 %	1-year, 56 %; 2-years, 33 %; 3-years, 22 %	1 grade 2 duodenal ulcer
Holy et al. [71]	18	20 Gy/5; 40 Gy/8	21	Objective response rate, 77 %	Median, 23 months	–
Torok et al. [72]	7	16 Gy/1; 27 Gy/3	14 (1–60)	1-year, 63 %	Median, 8 months	–
Scorsetti et al. [73]	34	32 Gy/4	41 (12–75)	1-year, 66 % 2-years, 33 %	Median, 22 months	No grade 3 or 4 toxicity, 6 % grade 2 nausea

Table 13.5 Summary of published trials of stereotactic body radiation therapy for mixed oligometastatic sites

Study	*n* of patients (*n* of treated targets)	Dose/*n* of fraction	Primary site	Treated site(s)	Treated metastasis control	Toxicity
Milano et al. [47]	121 (293)	Various; median 50 Gy/10	All (mostly breast and colorectal)	Lung, liver, bone, lymph node, 7 CNS	2-year LLC, 77 % 4-year LLC, 74 %	Grade 3 in 1 patient (1 %)
Salama et al. [74]	61 (113)	Increasing from 24 Gy/3 to 48 Gy/3	All (26 % NSCLC)	Lung, liver, lymph node, bone	2-year LLC 66.7 %; 88 % if dose ≥30 Gy in 3 fractions	Acute grade 3 in 2 (3 %), 6 possible late grade 3 (10 %)
Kang et al. [75]	59 (78)	42 Gy/3	Colorectal	Lung, liver, lymph node, other	3-year local control 66 % (note 69 % of patients had PD after chemotherapy)	No grade 3, 3 % grade 4 (gastrointestinal perforation/obstruction)
Inoue et al. [46]	44 (60)	48 Gy/8 (adrenal), 35–60 Gy/4–8	Mostly lung	Lung, adrenal, brain	3-year local control, 80 %	9 % grade 2; no grade 3 or higher
Stinauer et al. [76]	30 (53)	40–50 Gy/5 or 42–60 Gy/3	Renal-cell and melanoma	Lung, liver, bone	18-months local control, 88 %	One grade 3 hypoxia (3 %)
Bae et al. [77]	41 (50)	Median 48 Gy/3	Colorectal	Lymph node, lung, liver	3-year local control, 64 %	No acute grade 3, 7 % late grade 3
Jereczek-Fossa et al. [63]	34 (38)	30 Gy/5 to 36 Gy/3	Prostate	Lymph node, bone, prostate recurrence	88 % local control	6 % grade 3 urinary, 3 % grade 3 rectal (all prostate recurrence patients), 6 % grade 3 late urinary
Hoyer et al. [57]	64 (141)	45 Gy/3	Colorectal	Liver, lung, nodes, other	2-year local control, 63 % (86 % LLC)	30 % grade 3: pain, nausea, skin reaction; 9 % grade 4

(continued)

Table 13.5 (continued)

Study	*n* of patients (*n* of treated targets)	Dose/*n* of fraction	Primary site	Treated site(s)	Treated metastasis control	Toxicity
Wersall et al. [78]	58 (162)	Various: 30–40 Gy/3 was most common dose	Renal cell carcinoma	Lung (majority), renal bed, lymph node, adrenal	Local control 90 % or higher	40 % had grade 1 or higher toxicity, with a high proportion of grade 3 events (some perhaps in the same patient); one death (gastric haemorrhage)
Svedman et al. [79]	30 (82)	Various: 40 Gy/4 was most common dose	Renal cell carcinoma	Lung (majority), renal bed, adrenal	Only 2 % documented progression at median follow-up 52 months	4 % of side-effects were grade 3
Nuyttens et al. [80]	14 (15)	Median 7 Gy/1, median 6 fr	Mixed	Mixed	100 % local control at median follow-up 18 months	No grade 3
Greco et al. [81]	103 (126)	18–24 Gy /1	Protate, renal, colorectal	Majority bone, lymph node, soft tissue	2-year local control, 64 % (82 % if >22 Gy, 25 % for 18–20 Gy)	<4 % grade 3 late (stricture, neuritis)

13.7 SBRT and Systemic Therapy

As the majority of patients treated with SBRT for limited metastatic disease progress distantly, further studies integrating SBRT and systemic agents are needed. It is unclear if sequential, concurrent, or adjuvant therapy is preferential for patients treated with SBRT. Additionally, it is currently unknown if "targeted agents" or traditional systemic agents will be better tolerated when combined with SBRT. The RTOG and SWOG are currently developing such trials for breast cancer patients with limited metastases. A phase II study using SBRT with or without sorafenib (RTOG 1112- www.rtog.org) is underway.

13.8 Pre-SBRT Evaluation

Patients treated with SBRT should have a limited number of demarcated tumors that, if ablated would provide meaningful benefits in progression free and overall survival or symptoms and improve quality of life. From this perspective, SBRT for consolidation of oligometastases should follow the same general treatment philosophy relating to indications for surgical metastectomy. If improvement in survival is the goal, the treatment would likely be most beneficial in patients with controlled primary tumors, limited metastatic disease, metachronous appearance of primary and metastatic disease, younger age, and higher performance status. It is for this reason consideration must be given to performing SBRT for oligo metastasis only in combination with systemic therapy [50]. If systemic therapy is considered the standard of care for metastasic disease, then it is conceivable that SBRT adds to local control and as a corollary decreases the need for and side effects from continuing systemic therapy. In general, all macroscopically viable metastatic disease should be treated if survival improvements are to be realized. For palliative intent, treatment is performed to improve quality of life. The judgment should be that the targeted tumor is indeed the culprit in degrading the patient's quality of life, and that shrinking and controlling this tumor will likely improve the quality of life. Furthermore, the side effects of the treatment should not be severe so as to avoid a further decrease in quality of life. Extremely frail patients or patients with widespread metastatic disease rarely benefit from SBRT.

Prior to undergoing SBRT for lung metastasis, patients should have a clinical pulmonary function assessment, although this is more applicable for primary lung tumors. SBRT does not appreciably affect blood counts, liver enzymes, or kidney function, and therefore routine baseline laboratory testing is not generally necessary. Patients under consideration for SBRT for lung metastases actually have few medical contraindications. However, patients with tumors near the central mediastinal and hilar areas should either not be treated out of concern for toxicity or should be treated on a clinical trial because to our knowledge no safe dose of SBRT has been determined to date for tumors in such locations. Patient selection for SBRT based on disease characteristics should be similar to what was discussed earlier in the sections regarding surgical metastectomy.

13.9 SBRT Technical Issues

The term "stereotactic" simply relates to the correlation of the tumor target position with reliable fiducials with a readily known position. Fiducials define a coordinate system that can be used to target the tumor, orient the treatment planning process, and ultimately guide the therapy toward the intended location in the body. Fiducials help track patient and tumor motion and with good ability to do this dose can be prescribed conformally to the tumor without large expansions for motion, thereby limiting toxicity from irradiating excessive normal tissue. For soft tissue, retroperitoneal and pelvic metastasis fiducial based targeting and tracking are generally used. With good immobilization and specialized tracking software (XSight™ in Cyberknife™) spime metastasis are often treatable without external implantable fiducials.

Dampening, active breathing control (breath hold techniques), gating and tracking (e.g. Synchrony™ with Cyberknife ™) are often basic requirements for treating liver and lung metastasis to account for respiratory motion control. The administration of SBRT for lung metastases is very similar to that for liver metastases . In addition, careful consideration must be made for the proper accounting of lung tissue density correction for lung SBRT. Large errors in dose prescriptions of up to 20–40 %, particularly from using older generation algorithms such as the pencil beam and Clarkson method, have been observed when using sophisticated Monte Carlo methods [82, 83].

13.10 SBRT Complications: Liver Metastases

One of the most serious complications after liver irradiation is radiation-induced liver disease (RILD), a clinical syndrome of anicteric hepatomegaly, ascites, and elevated liver enzymes occurring within 3 months after the completion of therapy. RILD has been observed after whole-liver irradiation, but thankfully, RILD is very rare after SBRT for liver metastases, but has been reported occasionally [37, 57]. To keep the risk of liver toxicity low, a substantial volume of liver must be spared from irradiation, and re-irradiation is generally not recommended. This can be done by keeping the dose to 700 cc of uninvolved liver to less than 15 Gy delivered in 3 fractions 13 or ensuring that no more than 50 % of the liver receives 15 Gy in 3 fractions (or 7 Gy in 1 fraction), and no more than 30 % of the liver receives 21 Gy in 3 fractions (or 12 Gy in 1 fraction). Other potential hepatic toxicities, including a transient increase in liver enzymes, reactivation of hepatitis B, and a general decline in liver function, have been reported after SBRT for hepatocellular carcinoma but are believed to be uncommon after SBRT for liver metastases unless there is underlying liver disease or prior liver irradiation has been delivered [37, 59].

13.11 SBRT Complications: Lung Metastases

The hilar and central mediastinal structures in the chest appear to be very sensitive to the negative effects of SBRT. The majority of toxicity reports regarding SBRT in the lung describe patients with medically inoperable, early-stage primary lung cancer. Primary lung cancer patients tend to present with considerably poorer baseline pulmonary function (due to chronic tobacco abuse) compared to patients with lung metastases from other primary tumor sites. The risk of hypoxia, atelectasis, pneumonitis, decline in pulmonary function, and hemoptysis is greatest for tumors located in the central chest, in which most primary lung cancers occur. As metastases are more typically peripheral in location, treatment is generally better tolerated. Radiation pneumonitis, a common problem encountered with conventional pulmonary radiotherapy, is less likely to occur with SBRT. While the volume of lung receiving high and intermediate doses is limited in commonly used SBRT techniques, large areas are often bathed with low doses due to use of multiple beams or arcs. Instead, there is a risk of decreasing pulmonary reserve, which may not manifest as a toxicity until many years later, particularly if the patient continues smoking. Chest wall complications including pleural effusions, chest wall pain, and rib fracture may occur with pleural-based lesions.

13.12 Conclusions

Local treatment of oligometastases is an important area of progress in improving the survival and quality of life in a clinically significant proportion of cancer patients. As systemic therapies, targeted agents and biological and immune therapies become more and more effective local ablative therapy may play a crucial additional supportive role in the curative treatment for metastatic cancer. Trials should be designed to integrate and optimize systemic and targeted therapies and to demonstrate the benefit of local treatment of oligometastases. SBRT is proving to be an effective and safe local treatment approach for oligometastasis.

References

1. Kaspers GJL, Zwaan CM. Pediatric acute myeloid leukemia: towards high-quality cure of all patients. Haematologica. 2007;92(11):1519–32.
2. Press OW, Unger JM, Braziel RM, Maloney DG, Miller TP, Leblanc M, et al. Phase II trial of CHOP chemotherapy followed by tositumomab/iodine I-131 tositumomab for previously untreated follicular non-Hodgkin's lymphoma: five-year follow-up of Southwest Oncology Group Protocol S9911. J Clin Oncol. 2006;24(25):4143–9.
3. Saxman SB, Finch D, Gonin R, Einhorn LH. Long-term follow-up of a phase III study of three versus four cycles of bleomycin, etoposide, and cisplatin in favorable-prognosis germ-cell tumors: the Indian University experience. J Clin Oncol. 1998;16(2):702–6.

4. O'Brien SG, Guilhot F, Larson RA, Gathmann I, Baccarani M, Cervantes F, et al. Imatinib compared with interferon and low-dose cytarabine for newly diagnosed chronic-phase chronic myeloid leukemia. N Engl J Med. 2003;348(11):994–1004.
5. Hellman S. Karnofsky memorial lecture. Natural history of small breast cancers. J Clin Oncol. 1994;12(10):2229–34.
6. Mehta N, Mauer AM, Hellman S, Haraf DJ, Cohen EEW, Vokes EE, et al. Analysis of further disease progression in metastatic non-small cell lung cancer: implications for locoregional treatment. Int J Oncol. 2004;25(6):1677–83.
7. McLoughlin JM, Zager JS, Sondak VK, Berk LB. Treatment options for limited or symptomatic metastatic melanoma. Cancer Control [Internet]. 2008 [cited 16 Oct 2013];15(3). Available from: http://moffitt.prod.bridgelinedigital.net/File%20Library/Main%20Nav/Research%20and%20Clinical%20Trials/Cancer%20Control%20Journal/v15n3/239.pdf.
8. Hellman S, Weichselbaum RR. Oligometastases. J Clin Oncol. 1995;13(1):8–10.
9. Macdermed DM, Weichselbaum RR, Salama JK. A rationale for the targeted treatment of oligometastases with radiotherapy. J Surg Oncol. 2008;98(3):202–6.
10. Niibe Y, Hayakawa K. Oligometastases and oligo-recurrence: the new era of cancer therapy. Jpn J Clin Oncol. 2010;40(2):107–11.
11. Long-term results of lung metastasectomy: prognostic analyses based on 5206 cases. The International Registry of Lung Metastases. J Thorac Cardiovasc Surg. 1997;113(1):37–49.
12. Simmonds PC, Primrose JN, Colquitt JL, Garden OJ, Poston GJ, Rees M. Surgical resection of hepatic metastases from colorectal cancer: a systematic review of published studies. Br J Cancer. 2006;94(7):982–99.
13. Patchell RA, Tibbs PA, Regine WF, Dempsey RJ, Mohiuddin M, Kryscio RJ, et al. Postoperative radiotherapy in the treatment of single metastases to the brain: a randomized trial. JAMA. 1998;280(17):1485–9.
14. Miller G, Biernacki P, Kemeny NE, Gonen M, Downey R, Jarnagin WR, et al. Outcomes after resection of synchronous or metachronous hepatic and pulmonary colorectal metastases. J Am Coll Surg. 2007;205(2):231–8.
15. Kondo H, Okumura T, Ohde Y, Nakagawa K. Surgical treatment for metastatic malignancies. Pulmonary metastasis: indications and outcomes. Int J Clin Oncol. 2004;10(2):81–5.
16. Martinez SR, Young SE. A rational surgical approach to the treatment of distant melanoma metastases. Cancer Treat Rev. 2008;34(7):614–20.
17. Allen PJ. The surgical management of metastatic melanoma. Ann Surg Oncol. 2002;9(8):762–70.
18. Timmerman RD, Bizekis CS, Pass HI, Fong Y, Dupuy DE, Dawson LA, et al. Local surgical, ablative, and radiation treatment of metastases. CA Cancer J Clin. 2009;59(3):145–70.
19. Kavanagh BD, McGarry RC, Timmerman RD. Extracranial radiosurgery (stereotactic body radiation therapy) for oligometastases. Semin Radiat Oncol. 2006;16(2):77–84.
20. Lax I, Blomgren H, Näslund I, Svanström R. Stereotactic radiotherapy of malignancies in the abdomen. Methodological aspects. Acta Oncol. 1994;33(6):677–83.
21. Shirato H, Shimizu S, Shimizu T, Nishioka T, Miyasaka K. Real-time tumour-tracking radiotherapy. Lancet. 1999;353(9161):1331–2.
22. Uematsu M, Shioda A, Tahara K, Fukui T, Yamamoto F, Tsumatori G, et al. Focal, high dose, and fractionated modified stereotactic radiation therapy for lung carcinoma patients: a preliminary experience. Cancer. 1998;82(6):1062–70.
23. Koto M, Takai Y, Ogawa Y, Matsushita H, Takeda K, Takahashi C, et al. A phase II study on stereotactic body radiotherapy for stage I non-small cell lung cancer. Radiother Oncol. 2007;85(3):429–34.
24. Le Q-T, Loo BW, Ho A, Cotrutz C, Koong AC, Wakelee H, et al. Results of a phase I dose-escalation study using single-fraction stereotactic radiotherapy for lung tumors. J Thorac Oncol. 2006;1(8):802–9.
25. Timmerman R, McGarry R, Yiannoutsos C, Papiez L, Tudor K, DeLuca J, et al. Excessive toxicity when treating central tumors in a phase II study of stereotactic body radiation therapy for medically inoperable early-stage lung cancer. J Clin Oncol. 2006;24(30):4833–9.

26. Fakiris AJ, McGarry RC, Yiannoutsos CT, Papiez L, Williams M, Henderson MA, et al. Stereotactic body radiation therapy for early-stage non-small-cell lung carcinoma: four-year results of a prospective phase II study. Int J Radiat Oncol Biol Phys. 2009;75(3):677–82.
27. McGarry RC, Papiez L, Williams M, Whitford T, Timmerman RD. Stereotactic body radiation therapy of early-stage non-small-cell lung carcinoma: phase I study. Int J Radiat Oncol Biol Phys. 2005;63(4):1010–5.
28. Nagata Y, Takayama K, Matsuo Y, Norihisa Y, Mizowaki T, Sakamoto T, et al. Clinical outcomes of a phase I/II study of 48 Gy of stereotactic body radiotherapy in 4 fractions for primary lung cancer using a stereotactic body frame. Int J Radiat Oncol Biol Phys. 2005;63(5):1427–31.
29. Hara R, Itami J, Kondo T, Aruga T, Abe Y, Ito M, et al. Stereotactic single high dose irradiation of lung tumors under respiratory gating. Radiother Oncol. 2002;63(2):159–63.
30. Onishi H, Araki T, Shirato H, Nagata Y, Hiraoka M, Gomi K, et al. Stereotactic hypofractionated high-dose irradiation for stage I nonsmall cell lung carcinoma: clinical outcomes in 245 subjects in a Japanese multiinstitutional study. Cancer. 2004;101(7):1623–31.
31. Okunieff P, Petersen AL, Philip A, Milano MT, Katz AW, Boros L, et al. Stereotactic body radiation therapy (SBRT) for lung metastases. Acta Oncol. 2006;45(7):808–17.
32. Rusthoven KE, Kavanagh BD, Burri SH, Chen C, Cardenes H, Chidel MA, et al. Multiinstitutional phase I/II trial of stereotactic body radiation therapy for lung metastases. J Clin Oncol. 2009;27(10):1579–84.
33. Meijneke TR, Petit SF, Wentzler D, Hoogeman M, Nuyttens JJ. Reirradiation and stereotactic radiotherapy for tumors in the lung: dose summation and toxicity. Radiother Oncol. 2013;107(3):423–7.
34. Norihisa Y, Nagata Y, Takayama K, Matsuo Y, Sakamoto T, Sakamoto M, et al. Stereotactic body radiotherapy for oligometastatic lung tumors. Int J Radiat Oncol Biol Phys. 2008;72(2):398–403.
35. Guckenberger M, Heilman K, Wulf J, Mueller G, Beckmann G, Flentje M. Pulmonary injury and tumor response after stereotactic body radiotherapy (SBRT): results of a serial follow-up CT study. Radiother Oncol. 2007;85(3):435–42.
36. Song DY, Benedict SH, Cardinale RM, Chung TD, Chang MG, Schmidt-Ullrich RK. Stereotactic body radiation therapy of lung tumors: preliminary experience using normal tissue complication probability-based dose limits. Am J Clin Oncol. 2005;28(6):591–6.
37. Blomgren H, Lax I, Näslund I, Svanström R. Stereotactic high dose fraction radiation therapy of extracranial tumors using an accelerator. Acta Oncol. 1995;34(6):861–70.
38. Herfarth KK, Debus J, Lohr F, Bahner ML, Rhein B, Fritz P, et al. Stereotactic single-dose radiation therapy of liver tumors: results of a phase I/II trial. J Clin Oncol. 2001;19(1):164–70.
39. Schefter TE, Kavanagh BD, Timmerman RD, Cardenes HR, Baron A, Gaspar LE. A phase I trial of stereotactic body radiation therapy (SBRT) for liver metastases. Int J Radiat Oncol Biol Phys. 2005;62(5):1371–8.
40. Rusthoven KE, Kavanagh BD, Cardenes H, Stieber VW, Burri SH, Feigenberg SJ, et al. Multiinstitutional phase I/II trial of stereotactic body radiation therapy for liver metastases. J Clin Oncol. 2009;27(10):1572–8.
41. Lee MT, Kim JJ, Dinniwell R, Brierley J, Lockwood G, Wong R, et al. Phase I study of individualized stereotactic body radiotherapy of liver metastases. J Clin Oncol. 2009;27(10):1585–91.
42. Katz AW, Carey-Sampson M, Muhs AG, Milano MT, Schell MC, Okunieff P. Hypofractionated stereotactic body radiation therapy (SBRT) for limited hepatic metastases. Int J Radiat Oncol Biol Phys. 2007;67(3):793–8.
43. Chang DT, Swaminath A, Kozak M, Weintraub J, Koong AC, Kim J, et al. Stereotactic body radiotherapy for colorectal liver metastases: a pooled analysis. Cancer. 2011;117(17):4060–9.
44. Biasco G, Derenzini E, Grazi G, Ercolani G, Ravaioli M, Pantaleo MA, et al. Treatment of hepatic metastases from colorectal cancer: many doubts, some certainties. Cancer Treat Rev. 2006;32(3):214–28.
45. Almaghrabi MY, Supiot S, Paris F, Mahé M-A, Rio E. Stereotactic body radiation therapy for abdominal oligometastases: a biological and clinical review. Radiat Oncol [Internet]. 2012

[cited 16 Oct 2013];7(1). Available from: http://www.biomedcentral.com/content/pdf/1748–717X-7–126.pdf.
46. Inoue T, Katoh N, Aoyama H, Onimaru R, Taguchi H, Onodera S, et al. Clinical outcomes of stereotactic brain and/or body radiotherapy for patients with oligometastatic lesions. Jpn J Clin Oncol. 2010;40(8):788–94.
47. Milano MT, Zhang H, Metcalfe SK, Muhs AG, Okunieff P. Oligometastatic breast cancer treated with curative-intent stereotactic body radiation therapy. Breast Cancer Res Treat. 2009;115(3):601–8.
48. Weichselbaum R. Phase I, dose escalation of hypofractionated radiation therapy for patients with oligometastasis. Int J Radiat Oncol Biol Phys. 2006;66:S523.
49. McCammon R, Schefter TE, Gaspar LE, Zaemisch R, Gravdahl D, Kavanagh B. Observation of a dose–control relationship for lung and liver tumors after stereotactic body radiation therapy. Int J Radiat Oncol Biol Phys. 2009;73(1):112–8.
50. Carey Sampson M, Katz A, Constine LS. Stereotactic body radiation therapy for extracranial oligometastases: does the sword have a double edge? Semin Radiat Oncol. 2006;16(2):67–76.
51. Onimaru R, Shirato H, Shimizu S, Kitamura K, Xu B, Fukumoto S, et al. Tolerance of organs at risk in small-volume, hypofractionated, image-guided radiotherapy for primary and metastatic lung cancers. Int J Radiat Oncol Biol Phys. 2003;56(1):126–35.
52. Wulf J, Hädinger U, Oppitz U, Thiele W, Ness-Dourdoumas R, Flentje M. Stereotactic radiotherapy of targets in the lung and liver. Strahlenther Onkol. 2001;177(12):645–55.
53. Yoon SM, Choi EK, Lee S-W, Yi BY, Ahn SD, Shin SS, et al. Clinical results of stereotactic body frame based fractionated radiation therapy for primary or metastatic thoracic tumors. Acta Oncol. 2006;45(8):1108–14.
54. Brown WT, Wu X, Fowler JF, García S, Fayad F, Amendola BE, et al. Lung metastases treated by CyberKnife image-guided robotic stereotactic radiosurgery at 41 months. South Med J. 2008;101(4):376–82.
55. Ricardi U, Filippi AR, Guarneri A, Ragona R, Mantovani C, Giglioli F, et al. Stereotactic body radiation therapy for lung metastases. Lung Cancer. 2012;75(1):77–81.
56. Blomgren H, Lax I, Göranson H, Kraepelien T, Nilsson B, Näslund I, et al. Radiosurgery for tumors in the body: clinical experience using a new method. J Radiosurgery. 1998;1(1):63–74.
57. Hoyer M, Roed H, Traberg Hansen A, Ohlhuis L, Petersen J, Nellemann H, et al. Phase II study on stereotactic body radiotherapy of colorectal metastases. Acta Oncol. 2006;45(7):823–30.
58. Kavanagh BD, Schefter TE, Cardenes HR, Stieber VW, Raben D, Timmerman RD, et al. Interim analysis of a prospective phase I/II trial of SBRT for liver metastases. Acta Oncol. 2006;45(7):848–55.
59. Méndez Romero A, Wunderink W, Hussain SM, De Pooter JA, Heijmen BJM, Nowak PCJM, et al. Stereotactic body radiation therapy for primary and metastatic liver tumors: a single institution phase i-ii study. Acta Oncol. 2006;45(7):831–7.
60. Goodman KA, Wiegner EA, Maturen KE, Zhang Z, Mo Q, Yang G, et al. Dose-escalation study of single-fraction stereotactic body radiotherapy for liver malignancies. Int J Radiat Oncol Biol Phys. 2010;78(2):486–93.
61. Rule W, Timmerman R, Tong L, Abdulrahman R, Meyer J, Boike T, et al. Phase I dose-escalation study of stereotactic body radiotherapy in patients with hepatic metastases. Ann Surg Oncol. 2011;18(4):1081–7.
62. Choi CW, Cho CK, Yoo SY, Kim MS, Yang KM, Yoo HJ, et al. Image-guided stereotactic body radiation therapy in patients with isolated para-aortic lymph node metastases from uterine cervical and corpus cancer. Int J Radiat Oncol Biol Phys. 2009;74(1):147–53.
63. Jereczek-Fossa BA, Piperno G, Ronchi S, Catalano G, Fodor C, Cambria R, et al. Linac-based stereotactic body radiotherapy for oligometastatic patients with single abdominal lymph node recurrent cancer. Am J Clin Oncol. 2014;37(3):227–33.
64. Kim M-S, Yoo SY, Cho CK, Yoo HJ, Yang KM, Kang JK, et al. Stereotactic body radiotherapy for isolated para-aortic lymph node recurrence after curative resection in gastric cancer. J Korean Med Sci. 2009;24(3):488–92.

65. Kim M-S, Cho CK, Yang KM, Lee DH, Moon SM, Shin YJ. Stereotactic body radiotherapy for isolated paraaortic lymph node recurrence from colorectal cancer. World J Gastroenterol. 2009;15(48):6091–5.
66. Bignardi M, Navarria P, Mancosu P, Cozzi L, Fogliata A, Tozzi A, et al. Clinical outcome of hypofractionated stereotactic radiotherapy for abdominal lymph node metastases. Int J Radiat Oncol Biol Phys. 2011;81(3):831–8.
67. Casamassima F, Masi L, Menichelli C, Bonucci I, Casamassima E, Lazzeri M, et al. Efficacy of eradicative radiotherapy for limited nodal metastases detected with choline PET scan in prostate cancer patients. Tumori. 2011;97(1):49–55.
68. Casamassima F, Livi L, Masciullo S, Menichelli C, Masi L, Meattini I, et al. Stereotactic radiotherapy for adrenal gland metastases: University of Florence experience. Int J Radiat Oncol Biol Phys. 2012;82(2):919–23.
69. Chawla S, Chen Y, Katz AW, Muhs AG, Philip A, Okunieff P, et al. Stereotactic body radiotherapy for treatment of adrenal metastases. Int J Radiat Oncol Biol Phys. 2009;75(1):71–5.
70. Oshiro Y, Takeda Y, Hirano S, Ito H, Aruga T. Role of radiotherapy for local control of asymptomatic adrenal metastasis from lung cancer. Am J Clin Oncol. 2011;34(3):249–53.
71. Holy R, Piroth M, Pinkawa M, Eble MJ. Stereotactic body radiation therapy (SBRT) for treatment of adrenal gland metastases from non-small cell lung cancer. Strahlenther Onkol. 2011;187(4):245–51.
72. Torok J, Wegner RE, Burton SA, Heron DE. Stereotactic body radiation therapy for adrenal metastases: a retrospective review of a noninvasive therapeutic strategy. Future Oncol. 2011;7(1):145–51.
73. Scorsetti M, Alongi F, Filippi AR, Pentimalli S, Navarria P, Clerici E, et al. Long-term local control achieved after hypofractionated stereotactic body radiotherapy for adrenal gland metastases: a retrospective analysis of 34 patients. Acta Oncol. 2012;51(5):618–23.
74. Salama JK, Saba N, Quon H, Garg MK, Lawson J, McDonald MW, et al. ACR appropriateness criteria® adjuvant therapy for resected squamous cell carcinoma of the head and neck. Oral Oncol. 2011;47(7):554–9.
75. Kang J-K, Kim M-S, Kim JH, Yoo SY, Cho CK, Yang KM, et al. Oligometastases confined one organ from colorectal cancer treated by SBRT. Clin Exp Metastasis. 2010;27(4):273–8.
76. Stinauer MA, Kavanagh BD, Schefter TE, Gonzalez R, Flaig T, Lewis K, et al. Stereotactic body radiation therapy for melanoma and renal cell carcinoma: impact of single fraction equivalent dose on local control. Radiat Oncol. 2011;6:34.
77. Bae SH, Kim M-S, Cho CK, Kang J-K, Kang HJ, Kim YH, et al. High dose stereotactic body radiotherapy using three fractions for colorectal oligometastases. J Surg Oncol. 2012;106(2):138–43.
78. Wersäll PJ, Blomgren H, Lax I, Kälkner K-M, Linder C, Lundell G, et al. Extracranial stereotactic radiotherapy for primary and metastatic renal cell carcinoma. Radiother Oncol. 2005;77(1):88–95.
79. Svedman C, Sandström P, Pisa P, Blomgren H, Lax I, Kälkner K-M, et al. A prospective Phase II trial of using extracranial stereotactic radiotherapy in primary and metastatic renal cell carcinoma. Acta Oncol. 2006;45(7):870–5.
80. Nuyttens JJ, Prevost J-B, Van der Voort van Zijp NC, Hoogeman M, Levendag PC. Curative stereotactic robotic radiotherapy treatment for extracranial, extrapulmonary, extrahepatic, and extraspinal tumors: technique, early results, and toxicity. Technol Cancer Res Treat. 2007; 6(6):605–10.
81. Greco C, Zelefsky MJ, Lovelock M, Fuks Z, Hunt M, Rosenzweig K, et al. Predictors of local control after single-dose stereotactic image-guided intensity-modulated radiotherapy for extracranial metastases. Int J Radiat Oncol Biol Phys. 2011;79(4):1151–7.
82. Chetty IJ, Devpura S, Liu D, Chen D, Li H, Wen NW, et al. Correlation of dose computed using different algorithms with local control following stereotactic ablative radiotherapy (SABR)-based treatment of non-small-cell lung cancer. Radiother Oncol. 2013;109(3):498–504.
83. Altunbas C, Kavanagh B, Dzingle W, Stuhr K, Gaspar L, Miften M. Dosimetric errors during treatment of centrally located lung tumors with stereotactic body radiation therapy: Monte Carlo evaluation of tissue inhomogeneity corrections. Med Dosim. 2013;38(4):436–41.

Chapter 14
Stereotactic Body Radiotherapy in Head and Neck Cancer

David N. Teguh, Peter C. Levendag, Abrahim Al-Mamgani, and Anand Mahadevan

Abstract There is limited data regarding stereotactic radiotherapy (SRT) or stereotactic body radiotherapy (SBRT) for primary head and neck cancers, although it is feasible using SRT for primary HNC and its potential benefit in LC and organ preservation. The dose conformality by using SBRT and reduced CTV to PTV margins do seem to have a substantial effect on the dose received by the swallowing muscles and parotid glands as opposed to those treated with an IMRT or 3DCRT boost. Hypofractionated SRT may have the potential for curative or palliative treatment and could have a shorter duration of treatment, and a highly conformal dose distribution. However, severe late adverse reactions are anticipated with re-irradiation than with initial RT, partly because of the large doses per fraction used in most series. Compared with stereotactic radiosurgery using single fraction of high-dose irradiation, fractionated stereotactic radiotherapy may be superior in terms of tumor control and protection of normal tissues and organs surrounding the target.

This chapter discusses the role of SBRT in head and neck cancers.

Keywords Stereotactic body radiotherapy • Radiosurgery • Head and neck cancer • Toxicity • Dysphagia

14.1 Introduction

Head and Neck cancer (HNC) is the sixth most common type of cancer worldwide, representing approximately 6 % of all malignancies and accounting for an estimated 650,000 new cancer cases and 350,000 cancer deaths, worldwide, annually [1].

D.N. Teguh, MD, PhD (✉) • P.C. Levendag, MD, PhD • A. Al-Mamgani, MD, PhD
Department of Radiation Oncology, Erasmus MC – Daniel den Hoed Cancer Center, Rotterdam, The Netherlands
e-mail: dteguh@erasmusmc.nl

A. Mahadevan, MD, FRCS, FRCR
Department of Radiation Oncology, Beth Israel Deaconess Medical Center, Harvard Medical School, Boston, MA, USA
e-mail: amahadev@bidmc.harvard.edu

A. Gaya, A. Mahadevan (eds.), *Stereotactic Body Radiotherapy: A Practical Guide*,
DOI 10.1007/978-0-85729-597-2_14

Patients with Head & Neck cancer (HNC) can have a variety of malignancies that originate from, for example the paranasal sinuses, nasal cavity, oral cavity, oro-, naso- or hypopharynx, larynx, thyroid gland or from the major- or minor salivary glands. The great majority of these cancers are of squamous cell type origin. Distant metastases at initial presentation is uncommon, arising in about 10 % of the patients [2]. Second primary tumors develop at a rate of 3–5 % every year [3]. An increase in cancers of the base of tongue, and tonsillar fossa and/or soft palate has been noted, especially in young adults in the USA and in some European countries [4]. The overall incidence varies between countries, e.g. in France (oral cavity cancers), in Mediterranean countries (cancer of the nasopharynx), and in countries like India (oral cavity tumors), and far east asia (China, Hong Kong, Indonesia; cancer of the nasopharynx) because of the high incidence of risk factors in these areas. Specifically nasopharyngeal cancer is the most common cause of death in young men this region [5]. Chronic exposure of the upper aerodigestive tract to alcohol and tobacco is the most common risk factor for head and neck cancer. In non-smokers, substantial alcohol consumption (3 drinks per day) has been associated with increased risk of developing HNC [6]. Recently evidence is accumulating pointing to a viral origin for some head and neck cancers. Human papillomavirus (HPV) type 16 and to a lesser extent type 18 are the main types associated with HNC. The association between HPV and HNC is strongest for cancers of the tonsil, intermediate for the rest of the oropharynx, and weakest for the oral cavity and larynx [7]. HPV positivity is a favorable prognostic factor in HNC [8, 9], these patients respond better to radiotherapy (RT), chemotherapy (CHT) or both. Different studies showed superior LC, DFS, and OS rates in HPV-positive oropharyngeal patients compared to those with HPV-negative tumors [8].

The median age of patients with HNC is early 60's, with a male predominance, especially in laryngeal cancer. More than 50 % of the new cases have locally advanced disease, and require an aggressive combined modality treatment approach. Many improvements in the treatment of head and neck cancer have been made although tumor recurrence remains a significant problem. The 5-year survival rate (on the basis of SEER data) for all stages is about 60 %, but for locally advanced disease still below 40 %, despite the multi-modality treatment approaches [10].

The optimal management of squamous cell cancers of the tonsillar fossa (TF) and/or soft palate (SP) varies from surgery (S) only, radiation therapy (RT) alone, to S for the primary cancer and/or neck dissection (ND) combined with postoperative radiation therapy (PORT). For RT, there is still considerable debate regarding issues such as the optimal boost technique (external- vs. interstitial irradiation radiation therapy), planned neck dissection (ND) after previous external beam radiotherapy (EBRT), Resection primary tumor and neck nodes followed by postoperative radiation therapy (PORT) and/or the use of (neo)adjuvant vs. concomitant chemotherapy. A classic problem is the number of lymph node levels to be dissected in a particular PORT case. In the Erasmus MC—Daniel den Hoed Cancer Center, the treatment philosophy over the years has been to aim for organ function preservation: that is, patients are treated by EBRT preferably followed by a boost by means of an implant. Tumors not amenable to brachytherapy (BT) are treated by Surgery (combined

resection) followed by PORT or stereotactic body radiotherapy (SBRT). In recent years, there has been an increasing interest in reporting side effects; functional outcome scores and other health related quality of life (QoL) aspects, as well as costs. We analyzed our results for Tonsillar and/or soft palate tumors and primary- and secondary endpoints have been published in detail [11]. Good tumor control rates were obtained with radiation therapy but accompanied by some adverse effects. Dysphagia and xerostomia are both side-effects which should not be underestimated [12–14]. It has also been argued that the degree of xerostomia correlates with dysphagia experienced by the patient [15, 16]. In order to further decrease the frequency and severity of the side effects, Stereotactic body radiotherapy (SBRT) might therefore have a role in radiotherapy of head and neck cancer.

In the era of organ (function) preservation, radiotherapy has even replaced surgery with regard to long-term tumor control, cosmesis and quality of life in some of the head & neck tumor sites (e.g. the oropharynx). This is undoubtedly due to the routine implementation of normal tissue sparing techniques, such as IMRT; they play a crucial role in the improvement of dose distributions (with sparing capabilities) and ability to dose-escalate; this is undoubtedly the result of recent technological innovations. In recent years noteworthy strategies such as altered fractionation and integration of concomitant CHT with RT schedules have emerged [17, 18]. Nowadays 4D treatment plans can be generated, enabling dedicated linear accelerators and robotics to deliver with sub-millimeter accuracy highly focused doses of radiation to a moving target. When applying radiation therapy in clinic, it is also of relevance to exploit the well-conceived radiobiological principles of radiation therapy. Also the introduction of biological treatment planning is of great interest for the near future.

This chapter focuses on the role for SBRT in head and neck cancer treatment.

14.2 Stereotactic Body Radiotherapy

Potter and colleagues [19] presented practical guidelines for stereotactic body radiation therapy. The use of multiple fixed beams delivered by a linear accelerator, and a particle beam treatment unit share some common features. For a typical treatment, beams converge on a single point in space, the isocenter. Stereotactic localization of the lesion using an appropriate imaging modality, such as computed tomography (CT) or magnetic resonance imaging (MRI), allows accurate placement of one or more isocenters associated with the tumor. Unlike conventional radiation therapy, special stereotactic equipment is employed for more accurate tumor localization, planning, and actual treatment. The stereotactic equipment can be either frame based or frameless. Appropriate accounting of internal organ movement may be required. Imaging, planning, and treatment may occur on the same day for single fraction treatments, or the treatment could be fractionated into several sessions with larger daily doses of radiation than commonly used during conventionally fractionated radiation therapy. Strict protocols for quality assurance must be followed. Quality assurance measures

are required for the extracranial treatments given inherent organ motion, larger field apertures, and often considerably higher doses delivered. In conclusion Potters and colleagues state that SBRT requires the coordination of a large and diverse team of professionals including the radiation oncologist, medical physicist, and radiologist.

While there are many devices available to perform SBRT as described earlier in the textbook, the authors have particular experience with the Cyberknife and its use has been described in great detail previously [20]. All systems primarily aim to deliver a high biological dose to the tumor and a minimal dose to the surrounding normal tissue because of the rapid dose fall-off outside the target volume. Most fiducial based image-guided radiotherapy systems correct for both patient and tumor motion during treatment and allows delivery of nonisocentric beams. The possibility of direct tracking of the position of a radiopaque (skeletal) target by treating head-and-neck cancers (HNC), is a great advantage for these patients [21]. Tumors located under the hyoid require the insertion of fiducial markers to allow accurate localization of the tumor. These markers are placed under general anesthesia by an ENT surgeon or an experienced radiation oncologist. Because of these treatment characteristics of the frameless stereotactic body radiotherapy system, one might achieve a dose distribution comparable to that achieved with brachytherapy planning. This could be of particular relevance for those patients for whatever reason not suitable to undergo a standard brachytherapy boost.

14.3 Diagnostic Investigations

Current CT scanning techniques permit detailed examination of the dimensions and infiltration of primary cancers of the head and Neck. However, compared to CT, MRI has better soft tissue resolution [22]. In nasopharyngeal cancer (NPC), MRI provides an more accurate definition of early invasion beyond the nasopharynx, an improved differentiation of the (retropharyngeal) nodes from the primary tumor, a more precise assessment of the parapharyngeal space and a by far superior accuracy in the assessment of the tumor invasion of the sinus complex. The use of MRI in staging of cancer of the NP, for example, is mandatory. In our institution, after 46 Gy of IMRT, fine/thin (1.25 mm) CT slices were obtained in a standard manner from the top of the skull to the thoracic inlet.

14.4 Treatment Volume Definition for SBRT

Accurate target volume definition is of extreme importance for SBRT. The International Commission on Radiation Units and Measurements (ICRU) has addressed the issue of consistent volume and dose specifications in radiation therapy in the ICRU Report 50, published in 1993 [23]. The gross target volume (GTV) is defined as the gross extent of the tumor determined by clinical examination and imaging studies. As

elective nodal irradiation is not defined with stereotactic radiotherapy, the GTV will not encompass any nodes. The clinical target volume (CTV) is the tissue volume that contains the GTV and the subclinical microscopic disease. The CTV = GTV in SBRT. The Planning Target Volume (PTV) = CTV + 2–3 mm and covers residual positioning inaccuracies. The radiation oncologist should determine the extent of microscopic extension based on the scientific literature knowledge of spread of that particular disease and site (including the lymph nodes), and perineural extension. Although maximum effort must be put into adequate patient positioning and fixation, the planning target volume (PTV) is defined by specifying the margins that must be added around the CTV to compensate for the effects of organ, tumor and patient movements and inaccuracies in beam and patient setup. Boundaries of gross tumor volume (GTV) are based on published atlases, clinical target volume (CTV) and planning target volume (PTV) of neck levels I-VII and boundaries of potential critical normal tissues [24]. Boundaries of the Neck levels I—VII, partly based on the detailed description of the anatomy of the human lymphatic system by Rouviere and on the surgical anatomical landmarks as published by Robbins et al. [25, 26]. The landmarks were translated unto radiographs [27] and CT-slices [24, 28, 29] for neck levels.

14.5 Organs at Risk (OAR)

The sum of the dose delivered to the OAR during the initial treatment and during re-irradiation should not exceed the dose constraints given in equivalent dose in 2 Gy fractions (EQD2) listed in Table 14.1.

14.6 Erasmus MC Brachytherapy Experience—Basis for SBRT Boost

Patients series from 1991 to 2007 treated with brachytherapy (high tumor doses in relatively small volumes) were compared with the non-brachytherapy treated patients. The standard radiotherapy schedule for oropharyngeal cancer (OPC) at the Erasmus MC–Daniel den Hoed Cancer Center consists of 46 Gy of intensity-modulated radiotherapy (IMRT) with or without concomitant chemotherapy when indicated, followed by a pulsed-dose-rate or high-dose-rate brachytherapy boost (BTB; 20–22 Gy). Between 1991 and 2005, a total of 336 patients with primary OPC were treated with this protocol at the Erasmus MC–Daniel den Hoed Cancer Center, with excellent results. The actuarial 5-year LC, DFS and OS rates were significantly better for the BT boost, compared with the non-BT boost (LC 84 % vs. 60 %, $p < 0.001$, DFS 59 % vs. 43 %, $p = 0.0004$, and OS 64 % vs. 39 %, $p < 0.001$) [14].

Responses were are also assessed with validated QoL questionnaires (Table 14.2). In short, best QoL was observed for patients treated with maximal conformality, in

Table 14.1 Overview normal tissue tolerance values

Organ	Dose	Dose (EQD2)	Author(s)
Brachial Plexus	Dmax	60 Gy	Emami B, Lyman J, Brown A, et al. (1991)
	Dmax	66 Gy	Truong MT, Nadgir RN, Hirsch AE, et al. (2010)
Brain		<55/52	Hasselt (1999), Serre (2007)
	Dmax	45 Gy	Emami B, Lyman J, Brown A, et al. (1991)
	Dmax	55 Gy	Armstrong CL, Hunter JV, Ledakis GE, et al. (2002)
	Dmax	72 Gy	Lawrence YR, Li XA, el Naqa I, et al. (2010)
Brain Stem		54	Kam (2003)
	Dmax	54 Gy	Emami B, Lyman J, Brown A, et al. (1991)
	V60	<1 ml	Debus J, Hug EB, Liebsch NJ, et al. (1999)
Chiasm		54/55	Kam (2003), Serre (2007)
Cochlea		45/55	Bhide (2006), Bhandare (2000)
	Dmean	40 Gy	Fleury B, Lapeyre M (2010)
	Dmean	45 Gy	Bhandare N, Jackson A, Eisbruch A. et al. (2010)
Constrictor M	Dmean	55 Gy	Levendag PC, Teguh DN, Voet P, et al. (2007) [14]
	NTCP 25	56 Gy	Eisbruch A, Kim HM, Feng FY, et al. (2011)
	NTCP 50	63 Gy	Eisbruch A, Kim HM, Feng FY, et al. (2011)
Cornea	Dmax	40 Gy	Marchand V, Dendale R (2010)
Frontal lobe		<60	Serre (2007)
Pituitary		<55	Serre (2007)
Lacrimal gland		30	Durkin (2007), Weber (2006)
	Dmax	35 Gy	Durkin SR, Roos D, Higgs B, et al. (2007)
	Dmax	40 Gy	Parsons JT, Bova FJ, Mendenhall WM, et al. (1996)
Larynx	Dmax	64 Gy	Debelleix C, Pointreau Y, Lafond C, et al. (2010)
	Dmean	40 Gy	Debelleix C, Pointreau Y, Lafond C, et al. (2010)
Lens		8–10/12	Serre (2007), Hein (2005)
	Dmax	10 Gy	Marchand V, Dendale R (2010)
Mandibular bone	Dmax	60–70 Gy	Sargos P, Mamou N, Dejean C, et al. (2010)
Mucosa		65–77	Small (2006)
Muscle		70	Small (2006)
Optic Chiasma	Dmax	50 Gy	Emami B, Lyman J, Brown A, et al. (1991)
	Dmax	52 Gy	Hoppe BS, Nelson CJ, Gomez DR, et al. (2008)
Optic nerve		54	Hoppe (2008)
Oral cavity	Dmean	50 Gy	Little M, Schipper M, Feng FY et al. (2011)
Parietal lobe		<60	Serre (2007)

(continued)

Table 14.1 (continued)

Organ	Dose	Dose (EQD2)	Author(s)
Parotid		26	Eisbruch (2003)
	Dmean	26 Gy	Murdoch-Kinch CA, Kim HM, Vineberg KA, et al. (2008)
	NTCP 17–26	25–30 Gy	Dijkema T, Raaijmakers CP, Ten Haken RK, et al. (2010)
	NTCP 50	39.9 Gy	Dijkema T, Raaijmakers CP, Ten Haken RK, et al. (2010)
Peripheral nerves		65–77	Small (2006)
	Dmax	60 Gy	Henriques de Figueiredo B, Huchet A, et al. (2010)
Pituitary gland	Dmax	30–40 Gy	Bhandare N, Kennedy L, Malyapa RS, et al. (2008)
Retina		50/55	Monroe 2005, Serre (2007)
	Dmax	45 Gy	Emami B, Lyman J, Brown A, et al. (1991)
	Dmax	50 Gy	Monroe AT, Bhandare N, Morris CG et al. (2005)
Spinal cord		50	Hasselt (1999)
	Dmax	50 Gy	R.B. Marcus, R.R. Million (1990)
Submandibular gland	Dmean	39	Murdoch (2008)
Temporal lobe		<60	Kam (2003)
Temporomandibular joints		60	Serre (2007)
	Dmax	60 Gy	Emami B, Lyman J, Brown A, et al. (1991)

sequential treatments using boost techniques such as brachytherapy, and stereotactic radiation. Chart review revealed that roughly 31 % of patients experienced moderate to severe dysphagia (RTOG grade 3 and 4). When grouped by the boost technique BT vs. non-BT, severe dysphagia (problem score of QoL H&N35 with swallowing item ≥50) was observed in patients with TF and/or SP tumors in 19 % and for BOT tumors in 22 %. For the non-BT group, severe dysphagia was found in 30 % of the TF/SP tumors and in 47 % for the BOT tumors. A further breakdown of the non-BT group with respect to the booster technique used, showed severe dysphagia in 42 % for P-O, 25 % for 3DCRT, and 25 % for IMRT. Because of the reported dose-effect relationships in HNC, the balance between local control and late side-effects deserves specific attention. We published before a dose-effect relationships for normal tissues for swallowing problems (Fig. 14.1) [14, 31].

14.7 Toxicity Outcomes

Swallowing is a complex action requiring coordination between sensory input and motor function of the swallowing apparatus [32]. Intensification of therapy for head and neck cancer in general, either by altered fractionation RT schemes and/or by the

Table 14.2 Mean quality of life scores for patient with cancers in the oropharynx treated by RT, using different RT boost techniques

Boost	First series (46/2 Gy)	QLQ-C30 global health status[a]	H&N35 swallowing[b]	H&N35 sticky saliva[b]	H&N35 dry mouth[b]	H&N35 pain[b]
IMRT/3DCRT	IMRT/3CRT	72	32	59	67	27
	Par-Opp	33	50	100	100	25
BT	IMRT/3DCRT	74	13	25	38	13
	Par-Opp	74	26	46	61	18
SRT(+CBK)	IMRT/3DCRT	71	15	47	58	26
Par-Opp	Par-Opp	59	46	71	77	33

From Levendag et al. [30]; used with permission
[a]QLQ-C30 function scale: high scores = good functions
[b]H&N35 problem scales: high score = more problems

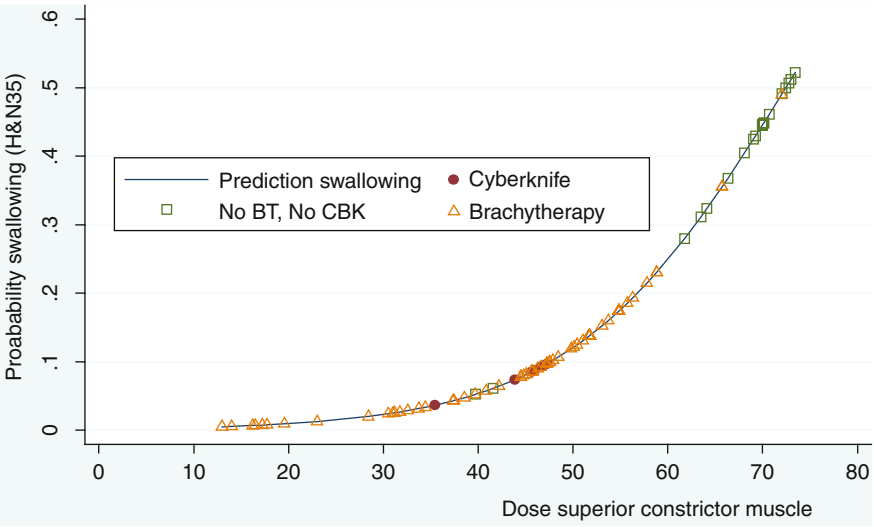

Fig. 14.1 Significant dose-effect relationship for the dysphagia complaint category EORTC H&N35 item and dose in superior constrictor muscle. Patients can be subdivided in those treated by a brachytherapy boost and those treated by 3DCRT boost or by IMRT boost. *BT* brachytherapy, *CBK* cyberknife

addition of concomitant chemotherapy, results in improved locoregional tumor control [33–35], and increase of late sequelae, such as dysphagia. In general, the prevalence of dysphagia is probably being underreported because of its (sometimes) clinically silent nature, but can be as high as 50 % [35–38].

Levendag and colleagues explored the relationships between the mean total dose received by the five swallowing muscles to the responses of the three—dysphagia related—QoL questionnaires (mean QoL scores; H&N35, PSS, & MDADI), per tumor site (i.e. the TF and/or SP or BOT), and per treatment technique (BT vs.

non-BT) [14]. One hundred and fifty five of the 336 patients fulfilled the criteria and were disease free with a minimum follow-up of 1 year. Mean Primary treatment sites were Tonsillar Fossa and/or Soft Palate (TF/SP) (n = 108), or Base of Tongue (BOT) (n = 47). 119/155 (77 %) of patients were BT, 48 boosted by non-BT techniques, boosted stage III&IV.107 patients. More complaints were reported with higher doses, in particular with regard to the superior- and medial constrictor muscles. Figure 14.4 shows an example of the dose-effect relationship computed by logistic regression. The steepness of the curve from 60 Gy, can be expressed by 20 % increase per 10 Gy. We speculate this increase in dysphagia (high dose, no BT, bilateral neck irradiation, no ND) has to do with the increase in irradiated volume and radiation dose. Xerostomia and dysphagia are also strongly correlated [31]. The treatment regime EBRT (or currently IMRT) combined with a BT boost has been applied in our institute preferentially over a great number of years for a variety of reasons: with regard to tumor control, HDR/PDR fractionation is given in an accelerated fashion with intrinsic dose escalation. A high degree of conformality is obtained (accurate CTV delineation, no PTV margin) with rapid dose fall-off. When grouped by boost technique (Table 14.2), severe dysphagia was observed less when BT was used as a boost technique. It is conceivable that such toxicity benefits from more conformal therapy could be achieved similarly with SBRT.

14.8 Erasmus MC SBRT Experience

Given the limitations of the organ preservation protocol (adverse late side effects and costs), improvements of the therapeutic ratio by changing (parts of) the techniques and/or modalities was anticipated. In 2005, an SBRT system (Cyberknife) was installed at our institution In the revised organ preservation protocol (Fig. 14.2), the following basic premises were taken into consideration:

- Since only 6 recurrences (4 %) were observed in the 149 electively treated CL necks, and no relapses were seen in the 29 non-treated CL necks, we suggest not to treat the contralateral neck, unless either the tumor extends beyond the midline of the soft palate (uvula) and/or invades a significant part of the ipsilateral base of tongue
- With the currently available CT-based neck level definitions, more conformal contours, that is tighter boundaries, around the CTV can be designed [24]. This way critical structures can be avoided more easily.
- Because of a number of conditions, some patients are non-eligible for BT, e.g.:
  - Patients with extensive, bulky tumors at the time of the implant
  - Tumors encroaching upon the ascending ramus of the mandible
  - Difficult to implant cavities (tonsillar fossae) after a recently performed tonsillectomy
  - Tumors with parapharyngeal extension
  - Patients non-eligible for surgery [i.e. anaesthesia] per se,
  - Patients refusing surgery.

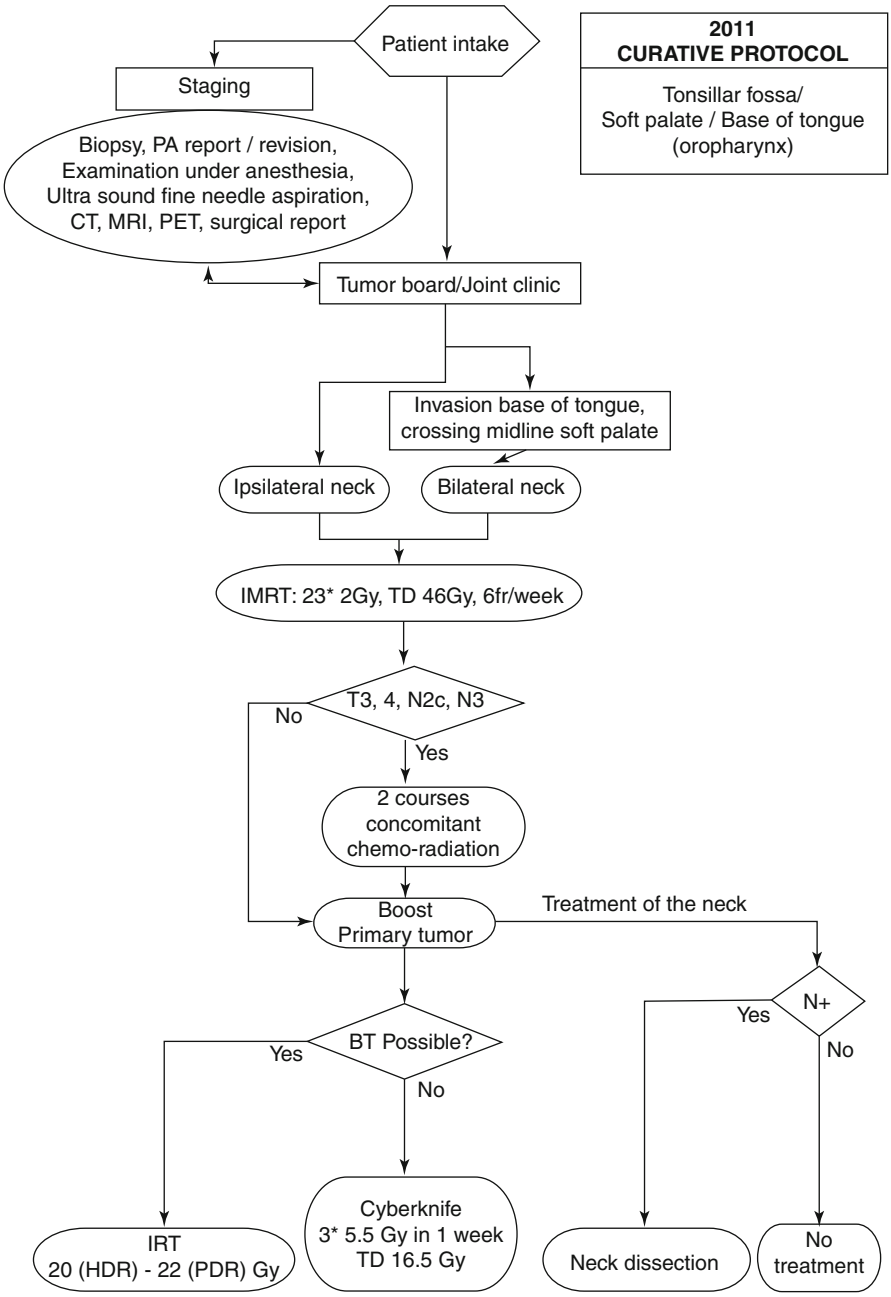

Fig. 14.2 Flow chart of oropharyngeal cancer treatment at the Erasmus MC–Daniel den Hoed Cancer Center. *BT* brachytherapy, *CT* computed tomography, *HDR* high-dose rate, *IMRT* intensity-modulated radiotherapy, *IRT* interstitial radiation therapy, *MRI* magnetic resonance imaging, *PET* positron emission tomography, *PDR* pulsed-dose rate, *TD* total dose, *PA* pathology

Some of the patients not eligible for brachytherapy or surgery can be dealt with in principle by using the Cyberknife.

14.9 Overview of SBRT for Primary Head and Neck Cancers

Kodani and colleagues [39] evaluated the efficacy and safety of stereotactic body radiation therapy for patients with head and neck tumors. Included were 34 patients treated with Cyberknife of which 21 of them had prior RT. Treatment sites were orbit [7], cervical lymph nodes [6], nasopharynx [5], oropharynx [4] and others [12]. The prescribed dose ranged from 20 to 42 Gy (median, 30 Gy) in 3–8 fractions for consecutive days. The target volume ranged from 1 to 78 cm [3] (median, 11.6 cm [3]) and the median follow-up was 16 months. The authors reported that treatment was well tolerated without significant acute complications in any cases. Complete response rate and partial response rate were 32 and 39 %, respectively. The overall survival (OS) rates were 71 and 58 % at 12 and 24 months, respectively. The OS was better in patients without prior radiotherapy within the previous 24 months or in case of smaller target volume. Six patients suffered severe late complications which all had prior radiotherapy, and two of them developed massive hemorrhage in the pharynx and both died of this complication five and 28 months, respectively, after SBRT. The authors suggest that SBRT is an effective treatment modality for head and neck tumors, however, re-irradiation has significant risk of severe and even fatal late complications in the form of necrosis and hemorrhage in re-irradiated areas. Hara and colleagues [40] determined long-term outcomes in 82 patients receiving SBRT as a boost following external beam radiotherapy for locally advanced nasopharyngeal carcinoma between September 1992 and July 2006. Nine patients had T1, 30 had T2, 12 had T3, and 31 had T4 tumors. Patients received 66 Gy of EBRT followed by a single-fraction SBRT boost of 7–15 Gy, delivered 2–6 weeks after EBRT. Seventy patients also received cisplatin-based CHT delivered concurrently with and adjuvant to RT. Only 1 local failure in a patient with a T4 tumor at a median follow-up of 40 months was described. At 5 years, the freedom from local relapse rate was 98 %, freedom from nodal relapse 83 %, freedom from distant metastasis 68 %, freedom from any relapse 67 %, and overall survival 69 %. Late toxicity included radiation-related retinopathy [3], carotid aneurysm [1], and radiographic temporal lobe necrosis (10 patients), of whom 2 patients were symptomatic with seizures. Of 10 patients with temporal lobe necrosis, 9 had T4 tumors. The authors concluded that SBRT boost after EBRT provides excellent local control for patients with nasopharyngeal cancer although better systemic therapies for distant control are needed.

Kawaguchi and colleagues [41] published on the effect of SRT on local control and organ preservation in cases of primary squamous cell head and neck cancer. In this retrospective study, 14 patients with a mean age of 73 years were treated between March 2006 and September 2007 with SRT. The staging consisted of T2 [5], T3 [3], T4 [6], N0 [13], and N1 [1]. Marginal doses were 35–42 Gy in 3 or 5

fractions. Significant tumor reduction was noted at the third month of follow-up with 5 complete responses and 9 partial responses. At a mean follow-up of 36 months the LC and OS rates were 71 % (10/14) and 79 % (11/14), respectively. The authors concluded that it is feasible to use SBRT for primary HNC and its potential benefit in LC and organ preservation.

Al-Mamgani and colleagues prospectively assessed the outcome and toxicity of frameless stereotactic radiotherapy (SRT) as a treatment option for boosting primary oropharyngeal cancers in 51 patients (stage T1–T4N0–N + oropharynx) who were not suitable for brachytherapy boost [42]. In 29 patients technically not suitable for implantation (56 %), 9 patients (18 %) were medically unfit to undergo the procedure of BT because of major comorbidity, in 4 patients (8 %) BT was done because of logistical problems, and in 9 patients (18 %) because of a combination of the above-mentioned factors. They received SBRT boosts (3 fractions of 5.5 Gy), prescribed to the 80 % isodose-line enclosing 100 % of the CTV and at least 95 % of the PTV, after an accelerated scheme of 46 Gy IMRT to the primary tumor and neck (when indicated) in 2 Gy fractions daily. The planning treatment volume (PTV) included a margin of 3 mm beyond the CTV to account for different targeting uncertainties. The boost to the primary tumor consisted of 3 fractions given within 1 week on each consecutive day, for instance, directly after completion of the first part of the treatment with 46 Gy of IMRT within a median overall treatment time of 32 days. Treatment duration varied between 45 and 60 min, depending on the number of beams used and the patient's compliance in finishing the treatment without interruption. The RT was combined with concomitant chemotherapy in patients with T3/T4 and/or 2c/N3 tumors (Fig. 14.2). The median age of the investigated group was 60 years with oropharyngeal cancer situated in the tonsillar fossa in 49 %, with T2 tumors in 53 %, and node-negative in 65 % of the patients. After a median follow-up of 18 months, the 2-year actuarial rates of LC, DFS, and OS were 86, 80, and 82 %, respectively, and the 3-year rates were 70, 66, and 54 %, respectively (Fig. 14.3). The overall 2-year cumulative incidence of grade ≥2 late toxicity was 28 %. Of the patients with 2 years with no evidence of disease (n = 20), only 1 patient was still feeding tube dependent and 2 patients had grade 3 xerostomia. Complete response was achieved in 49 patients (96 %) and partial response in 2 patients (4 %). Both patients with partial response had T3 and T4 disease, but could not receive chemotherapy in combination with radiotherapy because of comorbidities, and have developed a local recurrence after 5 and 6 months. Among all patients, 7 events (5 local recurrences, 1 regional recurrence, and 1 distant metastasis) were reported. Two patients were salvaged successfully with surgery (one local and one regional recurrence) and, at the time of writing, are still alive with no evidence of disease progression. Four patients with local recurrences and the patient with distant metastasis eventually died of their disease. Three other patients died of intercurrent disease or second malignancy without any evidence of relapse. Patients with T1/T2 disease had better LC than patients with T3/T4 (1 vs. 4 local recurrences, respectively; p = 0.08). The most serious acute toxicities were grade 3 dysphagia (feeding tube dependent) in 45 %, grade 3 mucosal toxicity (confluent mucositis) in 25 %, and grade 3 skin toxicity (moist desquamation) in 16 % of the

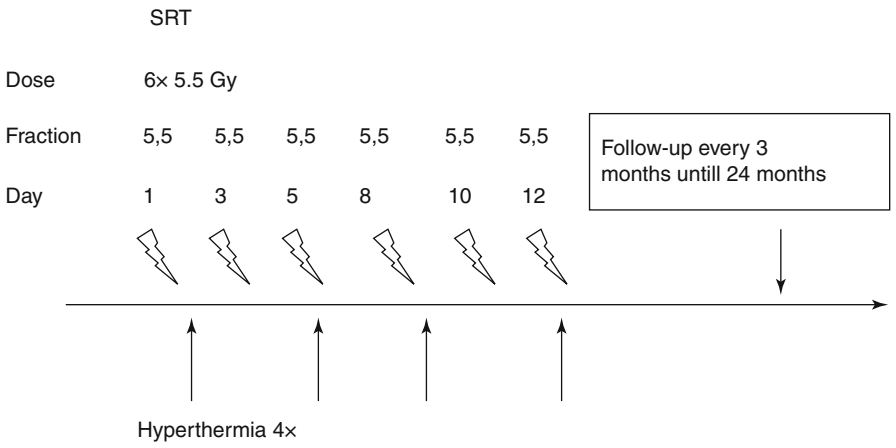

Fig. 14.3 Treatment schedule SRT + HT

patients (Table 14.3). Seven patients (14 %) required hospitalization (5 days (range, 2–16 days)) during treatment because of severe mucositis, dysphagia, and weight loss [5], neutropenic fever [1], or intercurrent infection [1]. Tumor stage, tumor involving the base of tongue, the use of chemotherapy, and bilateral neck irradiation were significant predictors for the need of tube feeding at univariate analysis (Table 14.4). At multivariate regression analysis, only chemotherapy and bilateral neck irradiation remain significant within the multivariate model; the corresponding odds ratios were 12.5 and 9.6, respectively. No grade 4 or 5 late toxicity was seen in the 50 patients with a minimum event-free follow-up of 6 months and in 32 patients with a minimum event-free follow-up of 12 months. The 2-year cumulative incidence of grade ≥2 late toxicity was 28 %. At 6 months, 2 patients reported grade 3 xerostomia and dysphagia; 1 of these patients had the feeding tube in place 2 years post treatment (Table 14.5). The 2-year cumulative incidence of grade ≥2 dysphagia and xerostomia was 15 and 28 %, respectively. No cases of trismus, bone, or soft-tissue necrosis were reported. Al-Mamgani and colleagues concluded that patients with oropharyngeal cancer who are not suitable for BT boost could safely, and effectively receive boosts by SBRT. Given the high fraction size (5.5 Gy) and the shorter overall treatment time in patients treated with SBRT (median overall treatment time, 32 days), compared with those treated with an IMRT boost at Erasmus MC with an accelerated schedule of 6 fractions per week (median overall treatment time, 42 days), the total biologically equivalent doses in 2 Gy/fx of the schedule used in the study (46 Gy of IMRT followed by 16.5 Gy with SBRT) would be 73 Gy. The treatment outcomes are fairly comparable to those in oropharyngeal cancer patients who received boosts by BT at our institution (87, 74, and 80 %, respectively) but compare favorably to those in oropharyngeal cancer patients treated with IMRT or 3DCRT boost (64, 52, and 60 %) [43, 44]. Teguh and colleagues reported grade 3 and 4 dysphagia from chart review in 24/132 (18 % of the patients treated with IMRT or 3DCRT [19], compared to the 2-year cumulative

Table 14.3 Acute radiation toxicity Erasmus SBRT Boost experience, scored according to Common Terminology Criteria for Adverse Events version 3.0 (CTCAE) (N = 51)

Acute side effects	No. of patients (%)
Dermatitis	
Grade 2	30 (59 %)
Grade 3	8 (16 %)
Mucositis	
Grade 2	31 (61 %)
Grade 3	13 (25 %)
Salivary gland changes	
Grade 2	10 (19 %)
Grade 3	0
Dysphagia	
Grade 2	20 (39 %)
Grade 3	23 (45 %)
Pain	
Grade 2	16 (31 %)
Grade 3	0
Taste alteration	
Grade 2	15 (29 %)
Grade 3	0
Nausea	
Grade 2	5 (10 %)
Grade 3	0

Table 14.4 Results of logistic regression analysis for the correlation between different patients' characteristics and the incidence of acute grade 3 dysphagia (feeding tube dependent)—erasmus SBRT boost experience

	Univariate analysis		Multivariate analysis	
Patient characteristics	OR	p	OR	p
Age	1.09	0.87		
Sex	2	0.28		
Tumor stage	3.9	**0.02**		0.7
Involvement of BOT	3.2	**0.05**		0.9
Chemotherapy	20.7	**0.006**	12.5	**0.02**
Bilateral neck irradiation	16.5	**0.01**	9.6	**0.04**

Abbreviations: *BOT* base of tongue, *OR* odds ratio
Significant *p* values are indicated in boldface type

incidence of grade ≥2 dysphagia and xerostomia of 15 and 28 %, respectively in Al-Mamgani's study. The dose conformality afforded by the use of SBRT and reduced CTV)/PTV margins (from 5 mm for IMRT planning to 3 mm for Cyberknife planning) do seem to have a substantial effect on the dose received by the swallowing muscles and parotid glands, which could explain the reduced late toxicity in patients treated with SBRT, as opposed to those treated with an IMRT or 3DCRT boost [19]. In patients treated with SBRT, the mean dose to the swallowing muscles

Table 14.5 Late radiation toxicity, scored according to common terminology criteria for adverse events version 3.0 (CTCAE), in patients with a minimum event-free follow-up of 6 and 12 months—erasmus SBRT boost experience

	6 months ($n=50$)	12 months ($n=32$)
Late side effects	No. of patients (%)	No. of patients (%)
Dysphagia		
Grade 2	7 (14 %)	4 (12 %)
Grade 3	2 (4 %)	1 (3 %)
Xerostomia		
Grade 2	10 (20 %)	7 (22 %)
Grade 3	2 (4 %)	2 (6 %)
Mucosal ulceration		
Grade 2	4 (8 %)	1 (3 %)
Grade 3	0	0
Skin and subcutaneous tissue		
Grade 2	9 (18 %)	6 (19 %)
Grade 3	0	0

was reduced on average by 20–25 % and the mean dose to the contralateral parotid gland by 15 %. The lower incidence of dysphagia in Al-Mamgani's group of patients might also be partly attributed to the reduced incidence of xerostomia in patients who received boosts with SBRT, as dysphagia-related complaints have been shown to increase significantly in patients with reduced production of saliva after chemo (radiation) [19, 22]. Uno and colleagues published a retrospective study of initial results of a Cyberknife boost for tumors in the head and neck area with ten patients [45]. A variety from 9 to 16 Gy in 3–4 fractions was given. They found in three patients local progression when 50 Gy + 15 Gy (4 fraction), 50 Gy + 14 Gy (4 fraction), and 40 Gy + 16 Gy (4 fraction) was used. All progressions were within the CTV of SBRT boost. Dose escalation and/or change in the fractionation schedule in the SBRT boost component is proposed. They reported no grade 3 or worse toxicity directly attributable to the SBRT boost.

14.10 Recurrent Head and Neck Cancer

For patients with recurrent head and neck cancer, treatment of choice is salvage surgery with or without postoperative (chemo-) re-irradiation [46, 47]. However, for the majority of patients surgery is not feasible because of tumor location and extent, medical contra-indications, patient refusal, comorbidity, and extensive disease located near critical structures. Janot and colleagues compared salvage surgery and wait and see groups for toxicity. At 24 months after randomization, 39 % with grade 3 or 4 late toxicity was found in the salvage surgery with chemo-radiation arm, compared to 10 % in the wait and see arm (surgery alone) ($p=0.06$). The main grade

3 and 4 late toxicities were sclerosis, trismus, and osteoradionecrosis [46]. Disease-free survival (DFS) was significantly improved in the RT arm, with a hazard ratio of 1.68 ($p=0.01$), but overall survival was not statistically different. Janot and colleagues concluded that full-dose re-irradiation combined with chemotherapy after salvage surgery significantly improved DFS, but had no significant impact on OS, and an increase in both acute and late toxicity was observed. Because of the poor results of conventional external re-irradiation, other techniques of re-irradiation have been employed for locally recurrent NPC, such as stereotactic radiosurgery. In this section an overview of literature will be given regarding BT and SBRT in recurrent head and neck cancer as limiting the re-irradiated volume by using SBRT may reduce treatment related toxicity.

To date for recurrent head and neck cancer, depending on the location and extent of the tumor, there are several treatment options: Brachytherapy is a treatment of choice due to the rapid dose fall off outside the treatment volume and the typically short treatment time [31]. However some patient groups are not eligible for BT (e.g. patients medically unfit, patient refusal, T4 tumors and//or extensive parapharyngeal extension). Also BT has to be performed in skilful, well-trained hands as BT remains an extremely gratifying technique for applying high doses of radiation for small-volume disease with highly conformal and accelerated properties. Hammerlid and colleagues [48] reported a prospective QoL study of patients with oral and pharyngeal carcinoma treated with external beam irradiation with or without BT. Most symptoms were at their peak 2 or 3 months after the start of treatment. Nutrition and pain were found to be the major problems, and as many as 19–40 % reported psychiatric distress. Patients who received additional BT did not report any increase in QoL problems except for pain compared with those who had external radiation only. QoL does not seem to be affected by the increased local radiation dose given when BT is included in the treatment regimen. Although brachytherapy has a potential to cure oral, oropharyngeal, nasopharyngeal, and lymph node recurrences [47], only superficial small tumors can be treated, and the number of experienced institutions is limited.

Similar to brachytherapy, hypofractionated stereotactic body radiotherapy (SBRT) may have the potential for curative or palliative treatment due to its precision and conformality. However, more severe late adverse reactions are anticipated with re-irradiation than with initial RT. External radiotherapy with or without concomitant chemotherapy is the one of the few potentially curative options left for patients with recurrent HNC disease who are inoperable and unsuitable for BT. The first multi-institutional RTOG 9610-trial of re-irradiation and chemotherapy for unresectable recurrent squamous cell carcinoma of the head and neck was reported by Spencer and colleagues [49]. Four weekly cycles of 5-fluorouracil 300 mg/m^2 IV bolus and hydroxyurea 1.5 g by mouth were used with 60 Gy at 1.5 Gy twice-daily fractions. The 2- and 5-year survival rates were 15, and 4 %, respectively. Langer and colleagues reported the RTOG 99–11 multi-institutional trial with the same radiation course but combined it with a daily bolus of cisplatin (15 mg/m^2), daily paclitaxel infusion (20 mg/m^2) and growth factor support during the rest week of the treatment cycle [50]. The overall survival improved to 50 % at 1 year

and 26 % at 2 years. While these results are promising for a subset of patients, the rate of fatal toxicity ranged from 1 to 12 %. IMRT or SBRT may be promising as more conformal doses can be delivered to target volumes. Lee and colleagues [51] used IMRT combined with concomitant chemo-radiotherapy to treat various recurrent H&N tumors 74 out of 105 patients. On multivariate analysis, non-nasopharynx and non-IMRT were associated with an increased risk of loco-regional (LR) failure.

Stereotactic radiotherapy can precisely target and deliver radiation with reduced margins surrounding the tumor volume. The first HNC cancer patients treated using SBRT were patients with recurrent nasopharyngeal carcinoma and base of skull tumors. Treatment consisted of a single fraction of 7–15 Gy [43, 52]. Risk of late tissue damage increases with an increase of fraction size, so fractionated schedules are used to minimize the risk of complications [52]. Severe toxicity complications commonly reported after stereotactic radiosurgery for recurrent H&N cancer include massive epistaxis, nasopharyngeal necrosis, cranial nerve palsies, temporal lobe necrosis, carotid aneurysm, retinopathy, and osteoradionecrosis of the skull base. Although outcomes of SBRT studies are hard to interpret due to the small study sizes, local control varied from 26 % at 2 years to 58 % at 3 years [53] and a OS of 22 % at 2-years to 31 % at 5-years. Roh and colleagues [52] reported a 43 % complete response rate after 18–40 (median, 30) Gy in 3–5 fractions in 36 patients with recurrent HNC (nasopharynx [8], maxillary sinus [8], neck lymph nodes [8], skull base [7], nasal cavity [4], retropharyngeal lymph nodes [3], orbit [2], and others [4]) who underwent re-irradiation with Cyberknife. Thirteen sites (37 %) achieved a partial response, 3 (9 %) sites maintained stable disease, and four sites (11 %) showed tumor progression. One- and 2-year local recurrence free survival rates were 61 and 52 %, respectively. One- and 2-year OS rates were 52 and 31 %, respectively. After a median follow-up of 17.3 months, grade 3 acute toxicity was reported in 13 patients and late toxicity (bone necrosis, soft issue necrosis) in 3 patients. Le and colleagues [54] reported 100 % LC and 71 % DFS at 3 years in patients with nasopharyngeal cancers who received boosts with SRT after 66 Gy of conventional RT. Chua and colleagues [55] reported a 5-year overall survival rate of 47 % in 48 patients treated by stereotactic radiosurgery with a median dose of 12.5 Gy to the target periphery. Neuro-endocrine complications occurred in 27 % of patients but there were no treatment-related deaths. The time interval from primary RT, rT stage, prior local failures and tumor volume were significant predictive factors for LC and/or survival, and with these a radiosurgery prognostic scoring system was designed. Five-year local failure-free probabilities in patients with good, intermediate and poor prognostic scores were 100, 43, and 10 %, respectively. The corresponding 5-year overall survival rates were 100, 51, and 0 % [55].

Combining stereotactic radiosurgery with high-dose-rate brachytherapy might improve survival because the single large dose of radiosurgery may increase tumor cell kill overcoming the inherent radioresistance of cells according to Suarez and colleagues [56]. Low and colleagues [57] treated 36 patients with local recurrent nasopharyngeal cancer in stage rT1–T2 with a schedule of 18 Gy followed by two separate fractions of 6 Gy each by intracavitary BT. The actuarial 5-year DFS and

OS were 57 % (78 % for rT1, and 39 % for rT2) and 62 % (80 % for rT1, and 48 % for rT2), respectively. However, 44 % of patients had late complications, including cranial nerve palsies (20 %), temporal lobe necrosis (8 %), and osteoradionecrosis of the skull base (17 %). A matched cohort study to select patients with similar characteristics treated by stereotactic radiosurgery (median dose 12.5 Gy) or intracavitary irradiation (total dose of 60 Gy) was published by Chua and colleagues [58] in 74 patients with local nasopharyngeal cancer failure. The 3-year local failure free rate was 78 % for the radio-active gold grain implantation group compared with 68 % for the stereotactic radiosurgery group, whereas the OS rate was better in the stereotactic radiosurgery group (3-year survival rate of 77 vs. 66 %), but not statistically significant. Also, when the impact of tumor volume on treatment outcome was adjusted, no difference in tumor control was observed between the two groups, suggesting that both salvage treatments have comparable efficacy. The incidence of complications was also similar but complications in the stereotactic radiosurgery group were more severe (22 % of neuro-endocrine complications, 13 % of brain necrosis, 5 % of cranial neuropathy, 5 % of pituitary insufficiency, and severe hemorrhage from a carotid artery aneurysm in one patient vs. 30 % of headaches, 16 % of palatal fistula, and 13 % of neuro-endocrine complications in the brachytherapy group) [58]. Pai and colleagues used stereotactic radiosurgery as a boost after re-irradiation with external beam for recurrent nasopharyngeal cancer and published an overall 5-year survival rate of 31 % [53]. The relatively high risk of severe late complications indicates that careful patient selection and treatment planning are required. Kocher and colleagues [59], treated eight patients with recurrent NPC by stereotactic radiosurgery where three patients died of carotid or cerebral hemorrhage after stereotactic radiosurgery using a dose of 15–24 Gy, two patients developed cerebral edema in temporal lobes, and one developed cranial neuropathy. Tumors involving Rosenmueller's fossa and invading deeply to the foramen lacerum are the most important predisposing factor in fatal hemorrhage according to Xiao and colleagues [43]. In their group a fatal carotid artery hemorrhage was the cause of death in 33 % of patients with recurrent NPC treated with fractionated stereotactic radiotherapy. According to Lee and colleagues, the large doses per fraction used in most series on stereotactic radiosurgery may cause the relatively high rates of late complications [51]. Compared with stereotactic radiosurgery using single fractions of high-dose irradiation, fractionated stereotactic radiotherapy may be superior in terms of tumor control and protection of normal tissues and organs surrounding the target [56]. Based on these principles, 56 patients with recurrent NPC in the series of Wu and colleagues received fractionated SRT with a median dose of 48 Gy in 6 fractions [60]. Three-year local failure-free survival, DFS, and progression-free survival rates were 75, 46, and 43 %, respectively. Multivariate analysis showed that recurrent disease and large tumor volume were independent factors that predicted poorer disease-specific survival. Seventeen patients developed late complications, including two with fatal hemorrhage. Severe late complications occurred in 25 % of patients, and 4 % of patients with recurrent disease developed massive hemorrhage in the nasopharynx after fractionated stereotactic radiotherapy and died of this complication, and 6 %

developed brain stem necrosis [60]. Chua and colleagues [55] reported on 125 NPC patients who received salvage SRT comparing single or multiple fractions. The median dose was 12.5 Gy in a single fraction by stereotactic radiosurgery, and 34 Gy in 2–6 fractions by fractionated stereotactic radiotherapy. Local control rate was better in the fractionated group although OS rates were similar (3-year overall survival rates of 66 and 61 %, respectively). Incidence of severe late complications was 33 % in the stereotactic radiosurgery group vs. 21 % in the fractionated stereotactic radiotherapy group, including brain necrosis (16 vs. 12 %) and hemorrhage (5 vs. 2 %) [61]. Vargo and colleagues [61] report the efficacy of SBRT in recurrent, nonsquamous cell cancers of the head and neck in 34 patients. The patients were irradiated to a median dose of 40 Gy in 5 fractions. The 6-month/1-year local control rate was 77/59 %, with a 6-month/1-year OS of 76/59 %. Local control was significantly improved for tumors <25 mL ($p = .030$). Acute/late grade 3 toxicity was 15/6 %, with no grade 4–5 toxicity.

Heron and colleagues [62] from the same group published results of a phase I dose-escalation clinical trial. Twenty-five patients were treated in five dose tiers with up to 44 Gy, given in 5 fractions in 2 weeks. Four patients had grade 1 or 2 acute toxicities. The median time to disease progression was 4 months, and the median survival was 6 months. Patient reported quality of life was not significantly affected by treatment. Fluorodeoxyglucose PET was a more sensitive early measure of response to treatment than CT volume changes. The authors concluded that re-irradiation with up to 44 Gy using SBRT was well tolerated with no grade 4 or 5 treatment-related toxicities in the acute setting. Unger and colleagues [63] reported 65 patients who received SBRT to the oropharynx [13], hypopharynx [8], nasopharynx [7], paranasal sinus [7], neck [7], and other sites [23]. Thirty-eight patients were treated definitively and 27 patients with metastatic disease and/or untreated local disease were treated palliatively. Nine patients underwent complete macroscopic resection before SBRT, and 33 patients received concurrent chemoradiation. The median initial radiation dose was 67 Gy, and the median re-irradiation SBRT dose was 30 Gy (21–35 Gy) in 2–5 fractions. 30 (54 %) had complete, 15 (27 %) had partial, and 11 (20 %) had no response. Median OS for all patients was 12 months. For definitively treated patients, the 2-year OS and locoregional control rates were 41 and 30 %, respectively. Multivariate analysis showed that higher total dose, surgical resection, and nasopharynx site were significantly associated with improved LRC; surgical resection and non-squamous histology were associated with improved OS. Seven patients (11 %) experienced severe re-irradiation related toxicity, including one treatment-attributed death. Yu and colleagues [64] reported 275 patients with isolated local failure. Salvage treatment was given to 200 patients (73 %) with isolated local failure. One hundred fifty-nine patients (80 %) received re-irradiation (108 EBRT, 44 brachytherapy, and 7 EBRT plus BT), 22 patients (11 %) underwent surgery with or without postoperative RT, and 19 patients (9 %) were treated with chemotherapy alone. Four patients died of RT complications, and one died of chemotherapy toxicity in the absence of active NPC. The 3-year actuarial OS for patients with isolated local failure was 74 %. On multivariate analysis, advanced initial T classification (hazard ratio [HR], 1.44; $p = 0.0006$) and the use of

salvage treatment (HR, 0.54; p = 0.0038) were independent prognostic factors. Patients who had early initial T classification had a more favorable prognosis. Subgroup analysis suggests that salvage treatment only prolongs survival in patients with T1 to T2 recurrent disease. Seo and colleagues [65] retrospectively reviewed 35 patients with locally recurrent NPC treated using Cyberknife. Gross tumor volumes ranged from 3 to 64 ml (median, 8 ml). The prescribed dose of fractionated SRT ranged from 24 to 45 Gy (median, 33 Gy) in 3 or 5 fractions. The OS rate, local failure-free survival (LFFS) rate, and disease progression-free survival (DPFS) rate at 5 years were 60, 79, and 74 %, respectively. Twenty-three patients achieved complete response after treatment. Only T stage at recurrence was an independent prognostic factor for OS and DPFS. Five patients had severe late toxicity (grade 4 or 5). Cengiz and colleagues reported 15 % incidence of lethal bleeding after hypofractionated SRT for carotid rupture syndrome [66]. Siddiqui and colleagues treated 21 recurrent tumor patients with SRT. Radiation doses were either single fractions of 13–18 Gy or 36–48 Gy in 5–8 fractions [67]. The tumor control rate at 1 year was 61 % and the median survival time was 7 months. Rwigema and colleagues [68] reviewed 85 patients who received SRT for recurrent squamous cell HNC. The mean SRT dose was 35 Gy (range: 15–44 Gy). The mean total dose of prior radiation to the primary site was 74 Gy (range: 32–170 Gy). Those patients who received SRT <35 Gy had significantly lower local control than those with ≥35 Gy at 6 months, median follow-up time (p = 0.014). Thirty four percent showed complete response, 34 % partial response, 20 % stable disease, and 12 % progressive disease. The 1-year and 2-year LC and OS survival rates for all patients were 51 and 31 %, and 49 and 16 %, respectively. Overall, the median survival for all patients was 12 months (range: 3–51). Treatment was well-tolerated with no grade 4 or 5 treatment-related toxicities. Wang and colleagues [69] reported in 1993 excellent salvage outcomes with re-irradiation in recurrent laryngeal cancer. Single or a few lymph node recurrences can also be treated by re-irradiation using SBRT [51].

Although there is a high rate of severe complications following re-irradiation, the number and severity of complications following surgery, as well as mortality, is lower. The potentially lethal side effects should be kept in mind when re-irradiation by hypofractionated SRT is considered for treatment. The risk of severe late complications reported earlier are between 20 and 40 % and is related to prior radiotherapy dose, primary site, retreatment radiotherapy dose, treatment volume, and technique. Questionable or unclear resection margins would opt for necessary use of postoperative radiotherapy in patients treated surgically; however this may increase morbidity and adversely affect the quality of life. Yamazaki and colleagues [44] reported in their review of literature that re-irradiation is a feasible option for patients who do not otherwise have treatment options available. Evidently, brachytherapy [70] and stereotactic radiosurgery are attractive options for small-volume disease. A practical advantage of hypofractionated SBRT is the shorter duration of treatment. The lack of hematological or systemic toxicity permits the inclusion of patients in poor general condition. Acute mucositis is temporary and can be managed with supportive medication.

14.10.1 Tretament Planning and Prescription

For the delivery of IMRT with a conventional linear accelerator, a margin of 5 mm is suggested. With current developments in image guided radiotherapy (IGRT), modern linear accelerators are equipped with kV imaging devices and cone-beam CT (CBCT). With CBCT not only bony anatomy but also soft tissues are visible for matching. When comparing IMRT, SBRT and brachytherapy, in principle all three modalities can be considered as highly accurate techniques to boost a primary tumor. In the case of a tonsillar fossa tumor, if IMRT is performed, 100 % of the dose is prescribed to the PTV, using a margin of 5 mm to CTV and 5 mm to PTV (Fig. 14.4). If the boost is to be given by SBRT, the dose is generally prescribed to 3 mm (PTV) from the GTV2 (=residual GTV1 after 46 Gy IMRT), in fact, a much smaller volume. One could conclude that because of the smaller margins, in practice one ends up with smaller irradiated tumor volumes (Figs. 14.5 and 14.6). For a similar tonsillar fossa tumor, because of the different techniques available and the way the doses are prescribed, the use of IMRT, SBRT and brachytherapy will eventually lead to different dose distributions, with BT and SBRT being somewhat more conformal than IMRT [31] (Figs. 14.5 and 14.6).

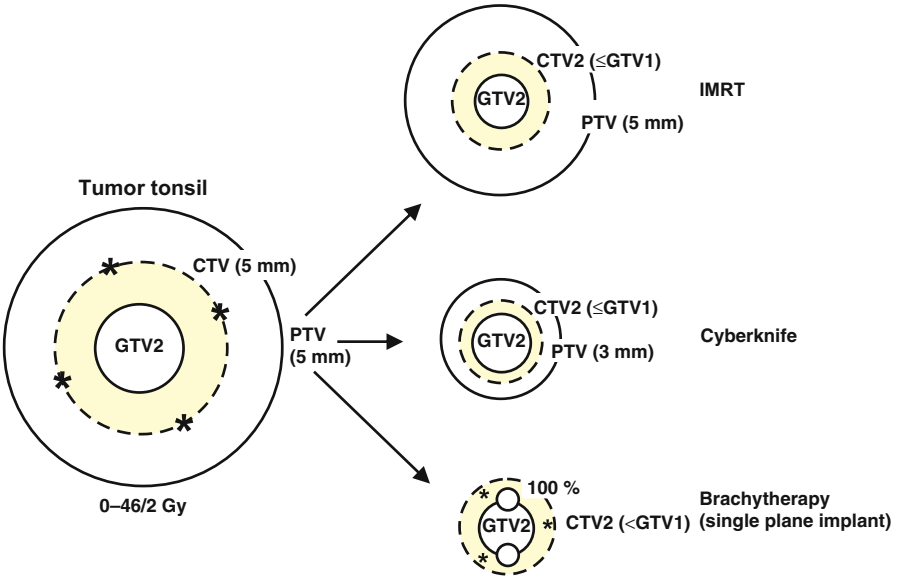

Fig. 14.4 Schematic diagram illustrating guidelines delineation of gross target volume (*GTV*), clinical target volume (*CTV*) and planning target volume (*PTV*), for a tumor radiated with a boost using either IMRT, Cyberknife or HDR brachytherapy. In Erasmus MC, in case of IMRT, the margin of the CTV is 5 mm around the GTV2. The margin for the PTV is 5 mm around the CTV2. For Cyberknife the PTV margin is 3 mm around the GTV2, for Brachytherapy (since the sources are moving with the tumor) 100 % of the dose is prescribed to the CTV (no PTV). *GTV1* gross tumor volume at the start of treatment, *GTV2* gross tumor volume after a dose of 46 Gy; has been applied; *CTV2* clinical target volume after a dose of 46 Gy;

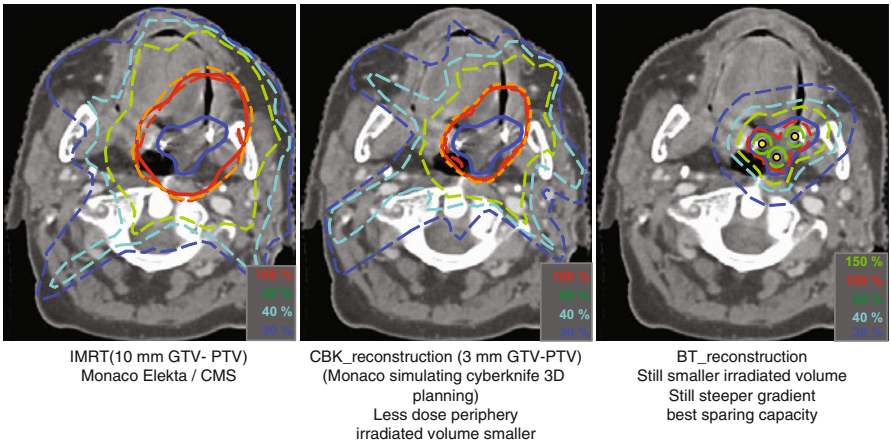

Fig. 14.5 Differences in dose distributions and treated volumes as a consequence of the different dose prescriptions, when using IMRT, Cyberknife or brachytherapy (left pane, middle pane and right pane respectively)

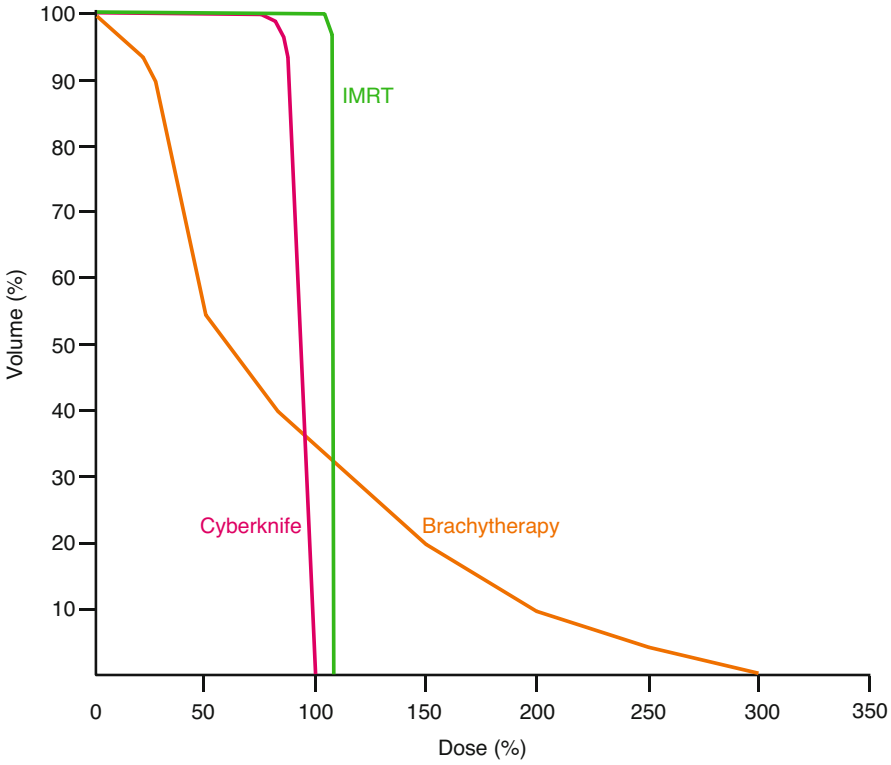

Fig. 14.6 Dose volume histograms (dvh) for a tonsillar fossa tumor as described in Fig. 14.5 when using imrt, cyberknife or brachytherapy

The physical advantage of stereotactic radiation arises from the ability to achieve a highly conformal dose distribution and deliver the treatment with high accuracy. Several limitations should be considered in such advanced limited field radiotherapy. Contour delineation is a problem to be resolved, especially in multi-institution trials. There is a wide range of deviation in GTV, CTV, and PTV delineation methods and the prescribed methods, depending largely on the physician's decision, all of which become more important if a limited small field is treated. The BED formula is a useful model for biological comparison of different fractionations, particularly for adverse reactions.

Optimal Dose fractionation is also an evolving field in Head and Neck SBRT. An overview of published stereotactic studies is shown in Table 14.6, many studies need longer follow-up and frequently SBRT has been used as a boost for external re-irradiation. In the (near) future hyperthermia and protons might have a high potential to increase the therapeutic ratio in locally recurrent head and neck cancer with improved local control and/or less toxicity (see Sect. 14.11).

14.11 Future Directions

In Erasmus MC—Daniel den Hoed Cancer Center an ongoing research trial is running using stereotactic radiotherapy in combination with hyperthermia. Study protocol for SBRT is 6×5.5 Gy, which achieves a biological equivalent dose (BED) to the tumor as close as possible to that of the re-irradiation schedule historically used at the Erasmus MC. Also the BED for normal tissue is comparably low to that of our historical schedule. In total 33 Gy is given using 6 fractions of 5.5 Gy and will be delivered in 3 weeks. The fractions are given on day 1, 3, 5, 8, 10 and 12, and a maximum of 3 fractions are given in 1 week (Fig. 14.3). The dose is prescribed to the isodose line covering 95 % of the target volume. Typically this is the 80 % isodose line. The maximum dose to the target volume is defined by 100 %. Minimum dose is 95 % of the target volume which must receive at least the prescribed dose.

Hyperthermia (HT) is known to enhance the therapeutic ratio of treatment resistant recurrences of various tumors including head and neck lymph nodes [71]. Therefore, a higher local tumor control rate without significant increased toxicity is expected by combining SBRT and HT. The primary endpoint of the study will be toxicity and the secondary endpoint will be local tumor control. Hyperthermia is commonly applied using electromagnetic fields, whereby the energy is focused to the tumor. The tumor absorbs this energy and consequently tumor temperatures increase to as high as 44 °C. The efficiency of this process is normally expressed by the specific absorption rate (SAR). Hyperthermia enhances the effect of radiation by several mechanisms including radiosensitization and direct cytotoxicity [72]. Another important enhancing mechanism of hyperthermia is the increase in blood flow. Hyperthermia increases blood flow to the tumor area, improves oxygenation and nutrient supply to the tumor cells thus making them more sensitive to radiotherapy. As many HNC recurrences are radio- and chemotherapy resistant and

Table 14.6 Overview stereotactic (re)-irradiation studies

Author	n	Dose schedule (Gy)/fx	Boost/ Re-irradiation	Acute toxicity (grade 3/4) (%)	Late toxicity (grade 3/4) (%)	BED 10 (a/b = 10)	BED 3 (a/b = 3)	LC (%)	OS (%)
Hara et al. (2008) [40]	82	7–15/1	Boost	–	17	12–38	23–90	100 at 1-year 98 at 2-years	95 at 1-year 86 % at 2-years
Rwigema et al. (2010) [68]	85	35 (15–50)/1–5	Re-irradiation	5, grade 3 No grade 4	3, grade 3	28–100	47–217	31 at 2-years	59 at 1-year 28 at 2-years
Kodani et al. (2011) [39]	21	30 (20–42)/5 (3–8)	Re-irradiation		29	38–79	62–90		71 at 1-year 58 at 2-years
Vargo et al. (2012) [61]	34	40 (17–50)/1–5	Re-irradiation	15 No grade 4	6 No grade 4	28–100	47–217	77 at 6-months 59 at 1-year	76 at 6-months 59 at 1-year
Roh et al. (2009) [52]	36	30 (18–40)/3–5	Re-irradiation	13 No grade 4	8	29–72	54–147	–	52 at 1-year 31 at 2-years
Cengiz et al. (2011) [66]	46	30 (18–35)/1–5	Re-irradiation	7	13	38–60	117–130	27	46 at 1-year
Voynov et al. (2006) [21]	22	24/1–8	Re-irradiation	2 No grade 4	0	28–48	47–180	26 at 2-years	22 at 2-years
Uno et al. (2010) [45]	10	9–16/3–4	Boost	0, short FU	0, short FU	12–22	18–37	–	–
Al-Mamgani et al. (2012) [42]	51	16.5/3	Boost	45 No grade 4	28, (grade ≥2) No grade 4	26	47	86 at 2-years 70 at 3-years	82 at 2-years 54 at 3-years

toxicity is substantial after concomitant chemoradiation, SBRT and HT could well reduce toxicity while achieving an equal or improved local tumor control rate compared with other non-standard treatment such as concomitant chemoradiation. These combined treatment modalities may offer patients with recurrent H&N tumors a chance of long term survival with less toxicity than the concomitant chemoradiation treatment regimens currently used in phase II trials. Technical advances in hyperthermia may make it conducive for such an approach [73, 74].

Acknowledgements The authors appreciate the contributions in some parts of this chapter by Maarten Paulides, PhD, Gerda M. van de Velde-Verduijn, MD, Noëlle C. van der Voort van Zyp, MD, PhD.

References

1. Jemal A, Bray F, Center MM, Ferlay J, Ward E, Forman D. Global cancer statistics. CA Cancer J Clin. 2011;61(2):69–90.
2. Siegel R, Ma J, Zou Z, Jemal A. Cancer statistics, 2014. CA Cancer J Clin. 2014;64(1):9–29.
3. Khuri FR, Lee JJ, Lippman SM, Kim ES, Cooper JS, Benner SE, et al. Randomized phase III trial of low-dose isotretinoin for prevention of second primary tumors in stage I and II head and neck cancer patients. J Natl Cancer Inst. 2006;98(7):441–50.
4. Gloeckler Ries LA, Reichman ME, Lewis DR, Hankey BF, Edwards BK. Cancer survival and incidence from the Surveillance, Epidemiology, and End Results (SEER) program. Oncologist. 2003;8(6):541–52.
5. Titcomb Jr CP. High incidence of nasopharyngeal carcinoma in Asia. J Insur Med. 2001;33(3):235–8.
6. Hashibe M, Boffetta P, Zaridze D, Shangina O, Szeszenia-Dabrowska N, Mates D, et al. Evidence for an important role of alcohol- and aldehyde-metabolizing genes in cancers of the upper aerodigestive tract. Cancer Epidemiol Biomarkers Prev. 2006;15(4):696–703.
7. Hobbs CGL, Sterne JAC, Bailey M, Heyderman RS, Birchall MA, Thomas SJ. Human papillomavirus and head and neck cancer: a systematic review and meta-analysis. Clin Otolaryngol. 2006;31(4):259–66.
8. Ang KK, Harris J, Wheeler R, Weber R, Rosenthal DI, Nguyen-Tan PF, et al. Human papillomavirus and survival of patients with oropharyngeal cancer. N Engl J Med. 2010;363(1):24–35.
9. Licitra L, Perrone F, Bossi P, Suardi S, Mariani L, Artusi R, et al. High-risk human papillomavirus affects prognosis in patients with surgically treated oropharyngeal squamous cell carcinoma. J Clin Oncol. 2006;24(36):5630–6.
10. Argiris A, Eng C. Epidemiology, staging, and screening of head and neck cancer. Cancer Treat Res. 2003;114:15–60.
11. Levendag P, Nijdam W, Noever I, Schmitz P, van de Pol M, Sipkema D, et al. Brachytherapy versus surgery in carcinoma of tonsillar fossa and/or soft palate: late adverse sequelae and performance status: can we be more selective and obtain better tissue sparing? Int J Radiat Oncol Biol Phys. 2004;59(3):713–24.
12. Feng FY, Kim HM, Lyden TH, Haxer MJ, Feng M, Worden FP, et al. Intensity-modulated radiotherapy of head and neck cancer aiming to reduce dysphagia: early dose-effect relationships for the swallowing structures. Int J Radiat Oncol Biol Phys. 2007;68(5):1289–98.
13. Jensen K, Lambertsen K, Grau C. Late swallowing dysfunction and dysphagia after radiotherapy for pharynx cancer: frequency, intensity and correlation with dose and volume parameters. Radiother Oncol. 2007;85(1):74–82.

14. Levendag PC, Teguh DN, Voet P, van der Est H, Noever I, de Kruijf WJM, et al. Dysphagia disorders in patients with cancer of the oropharynx are significantly affected by the radiation therapy dose to the superior and middle constrictor muscle: a dose-effect relationship. Radiother Oncol. 2007;85(1):64–73.
15. Logemann JA, Pauloski BR, Rademaker AW, Lazarus CL, Mittal B, Gaziano J, et al. Xerostomia: 12-month changes in saliva production and its relationship to perception and performance of swallow function, oral intake, and diet after chemoradiation. Head Neck. 2003;25(6):432–7.
16. Logemann JA, Smith CH, Pauloski BR, Rademaker AW, Lazarus CL, Colangelo LA, et al. Effects of xerostomia on perception and performance of swallow function. Head Neck. 2001;23(4):317–21.
17. Bourhis J, Overgaard J, Audry H, Ang KK, Saunders M, Bernier J, et al. Hyperfractionated or accelerated radiotherapy in head and neck cancer: a meta-analysis. Lancet. 2006;368(9538):843–54.
18. Pignon JP, Bourhis J, Domenge C, Designe L. Chemotherapy added to locoregional treatment for head and neck squamous-cell carcinoma: three meta-analyses of updated individual data. MACH-NC Collaborative Group. Meta-Analysis of Chemotherapy on Head and Neck Cancer. Lancet. 2000;355(9208):949–55.
19. Potters L, Steinberg M, Rose C, Timmerman R, Ryu S, Hevezi JM, et al. American Society for Therapeutic Radiology and Oncology and American College of Radiology practice guideline for the performance of stereotactic body radiation therapy. Int J Radiat Oncol Biol Phys. 2004;60(4):1026–32.
20. Nuyttens JJ, Prevost J-B, Van der Voort van Zijp NC, Hoogeman M, Levendag PC. Curative stereotactic robotic radiotherapy treatment for extracranial, extrapulmonary, extrahepatic, and extraspinal tumors: technique, early results, and toxicity. Technol Cancer Res Treat. 2007;6(6):605–10.
21. Voynov G, Heron DE, Burton S, Grandis J, Quinn A, Ferris R, et al. Frameless stereotactic radiosurgery for recurrent head and neck carcinoma. Technol Cancer Res Treat. 2006;5(5):529–35.
22. Liang SB, Sun Y, Liu LZ, Chen Y, Chen L, Mao YP, et al. Extension of local disease in nasopharyngeal carcinoma detected by magnetic resonance imaging: improvement of clinical target volume delineation. Int J Radiat Oncol Biol Phys. 2009;75(3):742–50.
23. Chavaudra J. Last ICRU recommendations for the prescription, recording and reporting of external bean therapy]. Cancer Radiother. 1998;2(5):607–14.
24. Levendag P, Braaksma M, Coche E, van Der Est H, Hamoir M, Muller K, et al. Rotterdam and Brussels CT-based neck nodal delineation compared with the surgical levels as defined by the American Academy of Otolaryngology-Head and Neck Surgery. Int J Radiat Oncol Biol Phys. 2004;58(1):113–23.
25. Robbins KT, Clayman G, Levine PA, Medina J, Sessions R, Shaha A, et al. Neck dissection classification update: revisions proposed by the American Head and Neck Society and the American Academy of Otolaryngology-Head and Neck Surgery. Arch Otolaryngol Head Neck Surg. 2002;128(7):751–8.
26. Robbins KT, Shaha AR, Medina JE, Califano JA, Wolf GT, Ferlito A, et al. Consensus statement on the classification and terminology of neck dissection. Arch Otolaryngol Head Neck Surg. 2008;134(5):536–8.
27. Gregoire V, Coche E, Cosnard G, Hamoir M, Reychler H. Selection and delineation of lymph node target volumes in head and neck conformal radiotherapy. Proposal for standardizing terminology and procedure based on the surgical experience. Radiother Oncol. 2000;56(2):135–50.
28. Gregoire V, Levendag P, Ang KK, Bernier J, Braaksma M, Budach V, et al. CT-based delineation of lymph node levels and related CTVs in the node-negative neck: DAHANCA, EORTC, GORTEC, NCIC, RTOG consensus guidelines. Radiother Oncol. 2003;69(3):227–36.
29. Wijers OB, Levendag PC, Tan T, van Dieren EB, van Sornsen de Koste J, van der Est H, et al. A simplified CT-based definition of the lymph node levels in the node negative neck. Radiother Oncol. 1999;52(1):35–42.

30. Levendag PC, et al. Dysphagia related quality of life of patients with cancer in the oropharynx: an advantage for brachytherapy? In: Harari PM, Connor NP, Grau C, editors. Function preservation and quality of life in head and neck radiotherapy. Berlin: Springer; 2012.
31. Teguh DN, Levendag PC, Noever I, van Rooij P, Voet P, van der Est H, et al. Treatment techniques and site considerations regarding dysphagia-related quality of life in cancer of the oropharynx and nasopharynx. Int J Radiat Oncol Biol Phys. 2008;72(4):1119–27.
32. Rosenthal DI, Lewin JS, Eisbruch A. Prevention and treatment of dysphagia and aspiration after chemoradiation for head and neck cancer. J Clin Oncol. 2006;24(17):2636–43.
33. Franzmann EJ, Lundy DS, Abitbol AA, Goodwin WJ. Complete hypopharyngeal obstruction by mucosal adhesions: a complication of intensive chemoradiation for advanced head and neck cancer. Head Neck. 2006;28(8):663–70.
34. Lee WT, Akst LM, Adelstein DJ, Saxton JP, Wood BG, Strome M, et al. Risk factors for hypopharyngeal/upper esophageal stricture formation after concurrent chemoradiation. Head Neck. 2006;28(9):808–12.
35. Eisbruch A, Lyden T, Bradford CR, Dawson LA, Haxer MJ, Miller AE, et al. Objective assessment of swallowing dysfunction and aspiration after radiation concurrent with chemotherapy for head-and-neck cancer. Int J Radiat Oncol Biol Phys. 2002;53(1):23–8.
36. Mittal BB, Pauloski BR, Haraf DJ, Pelzer HJ, Argiris A, Vokes EE, et al. Swallowing dysfunction—preventative and rehabilitation strategies in patients with head-and-neck cancers treated with surgery, radiotherapy, and chemotherapy: a critical review. Int J Radiat Oncol Biol Phys. 2003;57(5):1219–30.
37. Nguyen NP, Frank C, Moltz CC, Vos P, Smith HJ, Bhamidipati PV, et al. Aspiration rate following chemoradiation for head and neck cancer: an underreported occurrence. Radiother Oncol. 2006;80(3):302–6.
38. Trotti A. Toxicity in head and neck cancer: a review of trends and issues. Int J Radiat Oncol Biol Phys. 2000;47(1):1–12.
39. Kodani N, Yamazaki H, Tsubokura T, Shiomi H, Kobayashi K, Nishimura T, et al. Stereotactic body radiation therapy for head and neck tumor: disease control and morbidity outcomes. J Radiat Res. 2011;52(1):24–31.
40. Hara W, Loo BW, Goffinet DR, Chang SD, Adler JR, Pinto HA, et al. Excellent local control with stereotactic radiotherapy boost after external beam radiotherapy in patients with nasopharyngeal carcinoma. Int J Radiat Oncol Biol Phys. 2008;71(2):393–400.
41. Kawaguchi K, Sato K, Yamada H, Horie A, Nomura T, Iketani S, et al. Stereotactic radiosurgery in combination with chemotherapy as primary treatment for head and neck cancer. J Oral Maxillofac Surg. 2012;70(2):461–72.
42. Al-Mamgani A, Tans L, Teguh DN, van Rooij P, Zwijnenburg EM, Levendag PC. Stereotactic body radiotherapy: a promising treatment option for the boost of oropharyngeal cancers not suitable for brachytherapy: a single-institutional experience. Int J Radiat Oncol Biol Phys. 2012;82(4):1494–500.
43. Xiao J, Xu G, Miao Y. Fractionated stereotactic radiosurgery for 50 patients with recurrent or residual nasopharyngeal carcinoma. Int J Radiat Oncol Biol Phys. 2001;51(1):164–70.
44. Yamazaki H, Kodani N, Ogita M, Sato K, Himei K. Reirradiation of head and neck cancer focusing on hypofractionated stereotactic body radiation therapy. Radiat Oncol. 2011;6:98.
45. Uno T, Isobe K, Ueno N, Fukuda A, Sudo S, Shirotori H, et al. Fractionated stereotactic radiotherapy as a boost treatment for tumors in the head and neck region. J Radiat Res. 2010;51(4):449–54.
46. Janot F, de Raucourt D, Benhamou E, Ferron C, Dolivet G, Bensadoun RJ, et al. Randomized trial of postoperative reirradiation combined with chemotherapy after salvage surgery compared with salvage surgery alone in head and neck carcinoma. J Clin Oncol. 2008;26(34):5518–23.
47. Sulman EP, Schwartz DL, Le TT, Ang KK, Morrison WH, Rosenthal DI, et al. IMRT reirradiation of head and neck cancer-disease control and morbidity outcomes. Int J Radiat Oncol Biol Phys. 2009;73(2):399–409.
48. Hammerlid E, Mercke C, Sullivan M, Westin T. A prospective quality of life study of patients with oral or pharyngeal carcinoma treated with external beam irradiation with or without brachytherapy. Oral Oncol. 1997;33(3):189–96.

49. Spencer SA, Harris J, Wheeler RH, Machtay M, Schultz C, Spanos W, et al. Final report of RTOG 9610, a multi-institutional trial of reirradiation and chemotherapy for unresectable recurrent squamous cell carcinoma of the head and neck. Head Neck. 2008;30(3):281–8.
50. Langer CJ, Harris J, Horwitz EM, Nicolaou N, Kies M, Curran W, et al. Phase II study of low-dose paclitaxel and cisplatin in combination with split-course concomitant twice-daily reirradiation in recurrent squamous cell carcinoma of the head and neck: results of Radiation Therapy Oncology Group Protocol 9911. J Clin Oncol. 2007;25(30):4800–5.
51. Lee N, Chan K, Bekelman JE, Zhung J, Mechalakos J, Narayana A, et al. Salvage re-irradiation for recurrent head and neck cancer. Int J Radiat Oncol Biol Phys. 2007;68(3):731–40.
52. Roh KW, Jang JS, Kim MS, Sun DI, Kim BS, Jung SL, et al. Fractionated stereotactic radiotherapy as reirradiation for locally recurrent head and neck cancer. Int J Radiat Oncol Biol Phys. 2009;74(5):1348–55.
53. Pai PC, Chuang CC, Wei KC, Tsang NM, Tseng CK, Chang CN. Stereotactic radiosurgery for locally recurrent nasopharyngeal carcinoma. Head Neck. 2002;24(8):748–53.
54. Le QT, Tate D, Koong A, Gibbs IC, Chang SD, Adler JR, et al. Improved local control with stereotactic radiosurgical boost in patients with nasopharyngeal carcinoma. Int J Radiat Oncol Biol Phys. 2003;56(4):1046–54.
55. Chua DTT, Wu S-X, Lee V, Tsang J. Comparison of single versus fractionated dose of stereotactic radiotherapy for salvaging local failures of nasopharyngeal carcinoma: a matched-cohort analysis. Head Neck Oncol. 2009;1:13.
56. Suarez C, Rodrigo JP, Rinaldo A, Langendijk JA, Shaha AR, Ferlito A. Current treatment options for recurrent nasopharyngeal cancer. Eur Arch Otorhinolaryngol. 2010;267(12):1811–24.
57. Low JSH, Chua E-T, Gao F, Wee JTS. Stereotactic radiosurgery plus intracavitary irradiation in the salvage of nasopharyngeal carcinoma. Head Neck. 2006;28(4):321–9.
58. Chua DT, Wei WI, Sham JS, Hung KN, Au GK. Stereotactic radiosurgery versus gold grain implantation in salvaging local failures of nasopharyngeal carcinoma. Int J Radiat Oncol Biol Phys. 2007;69(2):469–74.
59. Kocher M, Voges J, Staar S, Treuer H, Sturm V, Mueller RP. Linear accelerator radiosurgery for recurrent malignant tumors of the skull base. Am J Clin Oncol. 1998;21(1):18–22.
60. Wu SX, Chua DT, Deng ML, Zhao C, Li FY, Sham JS, et al. Outcome of fractionated stereotactic radiotherapy for 90 patients with locally persistent and recurrent nasopharyngeal carcinoma. Int J Radiat Oncol Biol Phys. 2007;69(3):761–9.
61. Vargo JA, Wegner RE, Heron DE, Ferris RL, Rwigema J-CM, Quinn A, et al. Stereotactic body radiation therapy for locally recurrent, previously irradiated nonsquamous cell cancers of the head and neck. Head Neck. 2012;34(8):1153–61.
62. Heron DE, Ferris RL, Karamouzis M, Andrade RS, Deeb EL, Burton S, et al. Stereotactic body radiotherapy for recurrent squamous cell carcinoma of the head and neck: results of a phase I dose-escalation trial. Int J Radiat Oncol Biol Phys. 2009;75(5):1493–500.
63. Unger KR, Lominska CE, Deeken JF, Davidson BJ, Newkirk KA, Gagnon GJ, et al. Fractionated stereotactic radiosurgery for reirradiation of head-and-neck cancer. Int J Radiat Oncol Biol Phys. 2010;77(5):1411–9.
64. Yu KH, Leung SF, Tung SY, Zee B, Chua DTT, Sze WM, et al. Survival outcome of patients with nasopharyngeal carcinoma with first local failure: a study by the Hong Kong Nasopharyngeal Carcinoma Study Group. Head Neck. 2005;27(5):397–405.
65. Seo Y, Yoo H, Yoo S, Cho C, Yang K, Kim M-S, et al. Robotic system-based fractionated stereotactic radiotherapy in locally recurrent nasopharyngeal carcinoma. Radiother Oncol. 2009;93(3):570–4.
66. Cengiz M, Ozyigit G, Yazici G, Dogan A, Yildiz F, Zorlu F, et al. Salvage reirradiaton with stereotactic body radiotherapy for locally recurrent head-and-neck tumors. Int J Radiat Oncol Biol Phys. 2011;81(1):104–9.
67. Siddiqui F, Patel M, Khan M, McLean S, Dragovic J, Jin J-Y, et al. Stereotactic body radiation therapy for primary, recurrent, and metastatic tumors in the head-and-neck region. Int J Radiat Oncol Biol Phys. 2009;74(4):1047–53.

68. Rwigema J-C, Heron DE, Ferris RL, Gibson M, Quinn A, Yang Y, et al. Fractionated stereotactic body radiation therapy in the treatment of previously-irradiated recurrent head and neck carcinoma: updated report of the University of Pittsburgh experience. Am J Clin Oncol. 2010;33(3):286–93.
69. Wang CC, McIntyre J. Re-irradiation of laryngeal carcinoma—techniques and results. Int J Radiat Oncol Biol Phys. 1993;26(5):783–5.
70. Mendenhall WM, Mendenhall CM, Malyapa RS, Palta JR, Mendenhall NP. Re-irradiation of head and neck carcinoma. Am J Clin Oncol. 2008;31(4):393–8.
71. Van der Zee J. Heating the patient: a promising approach? Ann Oncol. 2002;13(8):1173–84.
72. Overgaard J. The current and potential role of hyperthermia in radiotherapy. Int J Radiat Oncol Biol Phys. 1989;16(3):535–49.
73. Paulides MM, Wielheesen DHM, Van der Zee J, Van Rhoon GC. Assessment of the local SAR distortion by major anatomical structures in a cylindrical neck phantom. Int J Hyperthermia. 2005;21(2):125–40.
74. Paulides MM, Bakker JF, Neufeld E, van der Zee J, Jansen PP, Levendag PC, et al. Winner of the "New Investigator Award" at the European Society of Hyperthermia Oncology Meeting 2007. The HYPERcollar: a novel applicator for hyperthermia in the head and neck. Int J Hyperthermia. 2007;23(7):567–76.

Chapter 15
Radiosurgery for Uveal Melanoma

Alexander Muacevic, Kirsten H. Eibl-Lindner, Christoph Fürweger, Martin M. Nentwich, Paul Foerster, Berndt Wowra, and Ulrich C. Schaller

Abstract Uveal melanomas are the most common primary intraocular malignancy. In patients with localized disease eye preservation is often sought if feasible. Radiation therapy has been used as a local organ preserving treatment for decades. Conventional radiation therapy techniques includes plaque brachy therapy and proton beam radiation. While these are effective, they can be invasive or expensive with limited availability. Stereotactic radiosurgery (SRS) and radiotherapy is an evolving modality to deliver conformal radiation with the intent towards eye preservation.

This Chapter outlines the role SRS in the treatment of uveal melanomas in the setting of a large single institution experience with a practical guide on patient selection, treatment planning and outcomes assessment.

Objective: To analyze the local efficacy and eye retention rate after frameless, image-guided robotic radiosurgery against uveal melanoma.

Methods: 200 patients with mainly medium sized and large unilateral uveal melanomas (3 % small, 62 % medium, 35 % large) were treated with a frameless robotic radiosurgery system. Median age was 61 years (range 32–78 years). All patients underwent a single-session procedure beginning with retrobulbar anaesthesia, followed by magnetic resonance imaging (MRI) and computerized tomography (CT) scanning that was used for generation of the treatment plan. The tumor dose was between 18 and 22 Gy (mean: 21 Gy) prescribed to the 70 % isodose line. Three-dimensional treatment planning was aimed at securing the optical lens and the optic disc as much as possible. Follow-up occurred at 3, 6, 12, 18 months and yearly thereafter with clinical, ultrasound and MRI studies.

Results: The median follow up time was 18 months. All patients could be treated in the frameless setup within 3 h. The local control after 1, 2 and 4 years was 97.7,

A. Muacevic, MD (✉) • C. Fürweger, Dr. tchn. • B. Wowra, MD
European CyberKnife Center Munich, Munich, Germany
e-mail: Alexander.Muacevic@cyber-knife.net

K.H. Eibl-Lindner, MD • M.M. Nentwich, MD • P. Foerster, MD
Department of Ophthalmology, Ludwig-Maximilians-University of Munich, Munich, Germany

U.C. Schaller, MD
Herzog Carl-Theodor Eye Clinic, Munich, Germany

A. Gaya, A. Mahadevan (eds.), *Stereotactic Body Radiotherapy: A Practical Guide*,
DOI 10.1007/978-0-85729-597-2_15

92.4 and 77.7 %, respectively. Nineteen of the 200 patients (9.9 %) underwent enucleation because of tumor growth and/or complications (glaucoma, tumor bleeding) during the follow up period.

Conclusion: Frameless, single-session, image-guided robotic radiosurgery is an effective and straight forward treatment option for patients with medium sized and large uveal melanoma which are otherwise difficult to treat.

Keywords Uveal Melanoma • Cyberknife • Radiosurgery • Frameless

15.1 Introduction

Uveal melanomas comprise of 70 % of all primary intraocular malignancies [1]. The incidence is 6–7 in one million (98.7 % white) population with an overall risk for metastasis of 50 % depending on patient age, tumor size and incidence of subretinal fluid, hemorrhage, and extraocular extension [2]. Patients with metastastasis are living longer due to the benefit of various treatment approaches like partial hepatectomy; radiofrequency ablation; ipilumumab immunotherapy; selective internal radiotherapy; intra-hepatic chemotherapy, possibly with isolated liver perfusion; and systemic chemotherapy. The 5-year survival rate is 80 % after surgery or radiotherapy.

The most common manifestation of uveal melanoma is in the choroid (85 %) followed by the ciliary body (10 %) and the iris (5 %). Although genetic factors like loss of heterozygosity (LOH) of chromosome 3 are known to increase the risk of metastasis significantly, there is no familial clustering [3]. Therefore, uveal melanoma is not regarded as an inherited disease and displays an equal sex distribution. In most cases, only one eye is affected in patients older than 50 years of age. It affects in 97.8 % the white population.

Different forms of radiation therapy are now used against uveal melanoma, replacing enucleation as the treatment of choice. Surgery is still used for tumors of large size (prominence over 10 mm) Fractionated proton radiation therapy, radioactive eye plaques, conventional LINAC radiotherapy and frame-based radiosurgical techniques have been described and shown to be effective for local tumor control [4–27].

For small and medium-sized uveal melanoma, ophthalmic plaque radiotherapy is a safe and effective treatment using ruthenium 106 (most cases; beta irradiation), iodine 125 (photon emission) or palladium 103 (photon emission) as radioactive isotopes for therapy. However, for precise placement of the plaque, eye muscles often have to be detached temporarily and the patient needs to stay isolated in the hospital for several days depending on the duration of brachytherapy. Alternative treatment methods include transpupillary thermotherapy and photodynamic therapy which can be considered for small-size melanoma located at the posterior pole close to the optic nerve or the macula. However, longterm results have not been convincing for TTT or PDT as a single treatment approach, but in combination with plaque brachytherapy they might be promising [28].

Single-session radiosurgery using frame-based Gamma Knife® (Elekta AB, Stockholm, Sweden) technology has been used during the last decade to treat middle- to large-size tumors as an alternative to complete removal of the eye [22–24, 29, 30]. Different methods of eye-tracking and diverse fixation techniques, along with the stereotactic head frame application have been described to keep the eye immobile for the duration of treatment [30]. These difficult, and for the patient, highly bothersome techniques challenge somewhat the definition of "minimally invasive treatment".

Today, with the availability of frameless robotic radiosurgery technology, we are able to apply a treatment modality without any eye fixation or frame application. Using local retrobulbar anaesthesia and an image-guided robotic radiosurgery system, a minimally invasive radiosurgical treatment can be delivered [31, 32].

15.2 Indications for SBRT Treatment (I.E Case Selection and Exclusions)

SRS or SBRT is used predominantly for tumors of medium and large size not suitable for brachytherapy (tumor height >6 mm, tumor base >19 mm). Recently also smaller tumors underwent SRS in our centre for patients not willing to undergo brachytherapy which requires surgical intervention with implantation and explantation of the radioactive plaque.

15.3 Radiosurgery Treatment Process

Radiosurgery is an alternative method when the size and location of the tumor is not amenable for brachytherapy or because of the patients' wish to avoid primary enucleation. Table 15.1 shows the main treatment techniques for uveal melanoma. In selected cases patients may undergo radiosurgery after prior unsuccessful brachytherapy to the target lesion.

All patients need to be evaluated by an ophthalmologist and a specialized radiation oncologist for eligibility of treatment. The following standard outpatient procedure we developed in our centre is recommended:

Table 15.1 Treatment options uveal melanoma

Small melanoma (<6 mm)	Medium/large melanoma (≥6 mm)
Brachytherapy 106 Ru	Eye enucleation
Transpupillary thermotherapy	Cyberknife radiosurgery
Proton beam therapy	Gamma Knife radiosurgery
	Brachytherapy 125 iodine
	Proton beam, helium ions therapy

Patients are positioned on the computed tomography (CT) couch and standard retrobulbar anesthesia with goal of complete akinesia of the globe within the orbit is applied. The volume of anesthesia is dependent on the volume of the orbit and is typically between 10 and 15 ml. Suturing of the rectus muscles as described seems not to be needed anymore. A contrast-enhanced CT of the head with 1-mm slice thickness and a 1 mm T2 MRI of the orbit is performed after retrobulbar anesthesia.

Based on the fused CT and MRI sequences, the target volume is defined by the ophthalmologist and the radiosurgeon, and the treatment plan is generated. In all cases, the tumor is covered completely by the 70 % isodose line. We add a 1 mm margin to the target volume to all directions and 2 mm to the posterior tumor border (Fig. dose plan uvea). This is done to compensate for possible posterior movement of the eye bulb after retrobulbar anesthesia. After the planning procedure, the treatment plan is loaded for treatment delivery. Single-session radiosurgery follows immediately after the plan generation is finalized. Radiation is delivered in a single fraction for all cases using 18–22 Gy to the prescription isodose (70 % in the case of Cyberknife) depending on the size and location of the tumor. After radiosurgery the patient is discharged. Typically there are no significant acute toxicities to be expected. Depending on the size and location of the tumor late side effects can develop several weeks or months after treatment with rubeosis, glaucoma or cataract. A secondary glaucoma is the late toxicity most often encountered. About 25 % of patients will develop a secondary glaucoma 3–60 months (mean 21 months after SRS). These side effects are highly individual and also depend on the individual radiation sensitivity of the patient.

Clinical and imaging follow-up will be performed 3, 6, 12 and 18 months after the treatment using standardized A- and B-scan ultrasound and a 1 mm T2 MRI for evaluation of local control. Tumor control is defined as either continuous regression of the tumor or no further progression.

15.4 Results

We used this method to treat 200 patients with uveal melanoma. The mean follow-up for these patients was 18 months. All patients were treated in one treatment session comprising of retrobulbar anaesthesia, CT and MRI imaging, treatment planning and treatment application within 3 h after start of the anaesthesia. The local control after 1, 2 and 4 years was 97.7, 92.4 and 77.7 %, respectively. Treatment parameters as well as dose to the lens of the affected and contralateral eye and point dose to the optic disc of our first 20 Cyberknife patients are shown in Table 15.2.

The median maximum apical tumor height according to standardized A-scan ultrasound before treatment was 8 mm (mean 7.9 mm ±2.6 mm) compared to 5 mm (mean 5.4 ±2.1 mm) at the last follow-up examination ($p < 0.1$) (Figs. 15.1 and 15.2). The visual acuity decreased in most patients over time, typically between 6

Table 15.2 Dose parameters first 20 patients of the Munich series

Patient nr.	Dose	Isodose	Dmax lens affected eye (Gy)	Dmax lens contralateral eye (Gy)	Point dose optic disk affected eye (Gy)
1	20	75	4.8	0	19.7
2	18	70	20.9	1.2	3.5
3	20	70	1.7	0.2	27.3
4	20	75	24.3	0	18.3
5	18	65	20.3	0	4.7
6	22	70	1.7	1.7	10
7	19	70	20.3	0	6
8	21	70	1.2	0.3	13.1
9	18	60	13.8	0	17.2
10	17	70	20.3	0.2	8.1
11	19	70	4.5	0.3	23.2
12	18	70	1.6	0.8	14.9
13	18	70	2.5	0.6	12.3
14	18	70	9.1	1.2	22.6
15	20	70	Blind	0.3	Blind
16	20	70	24.5	0.4	3.3
17	19	70	7.8	0.4	3.7
18	18	70	1.9	0.6	23.4
19	18	70	11.3	0.2	4.3
20	20	70	10.1	0.6	23.6

and 24 months after radiosurgery. The median reflectivity significantly increased during the follow-up period from 42 to 71 % ($p<0.01$). Nineteen patients needed enucleation due to tumor re-growth after radiosurgery (9.5 %). Two patients where successfully retreated by radiosurgery.

15.5 Discussion

Different kinds of therapeutic options exist today for the treatment of uveal melanoma. However, enucleation has remained the gold standard therapy for the condition for many years [19]. Eye conservation is achieved by several techniques, with proton or other heavy charged particle therapies, and episcleral radionuclide plaque therapy being among the most commonly used [7–11]. Adams et al., for example, found no statistically significant survival difference in 223 patients treated with brachytherapy compared to 416 patients who underwent enucleation [4]. Useful vision is usually preserved mainly in cases in which tumors are located in a relatively favorable location with respect to the optic disc or macula. Stereotactic radiosurgery (SRS) and fractionated stereotactic radiotherapy (FSRT) are gaining wider acceptance in the medical community as the clinical data mature, and published evidence

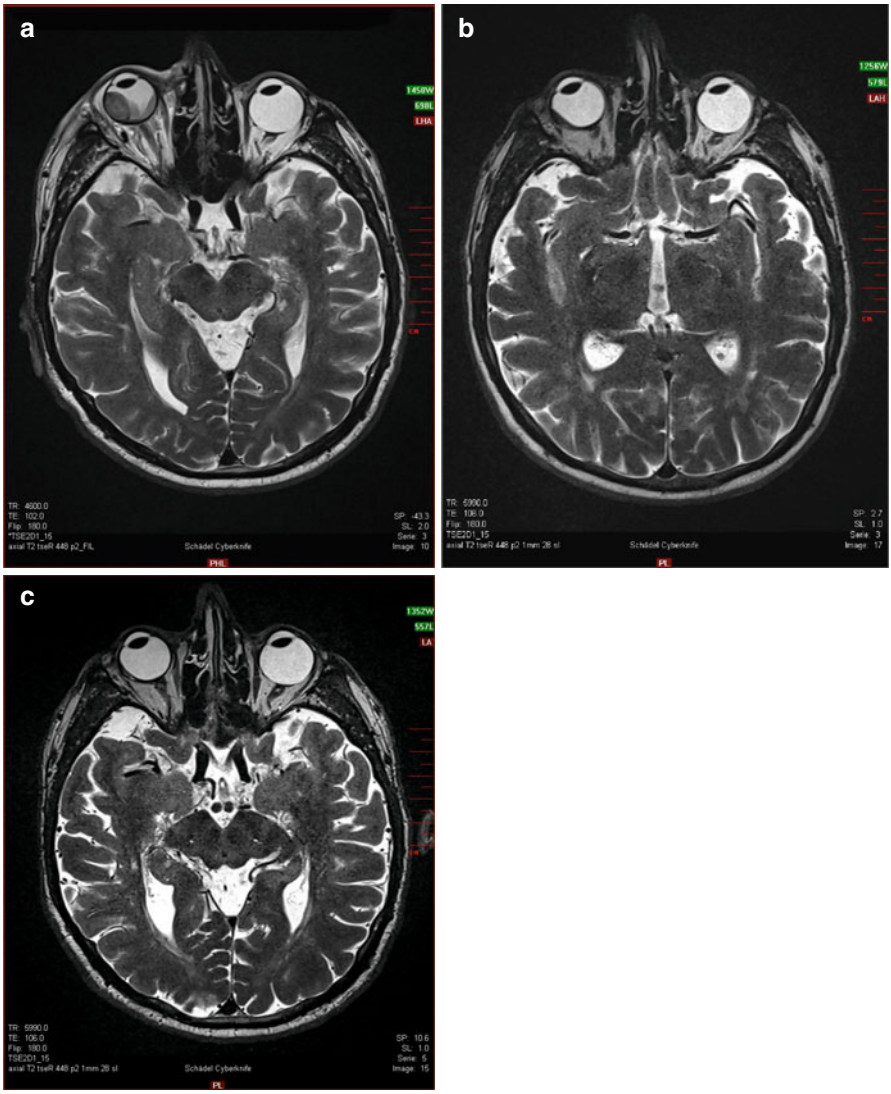

Fig. 15.1 (**a**) T2 MRI sequence showing large Uveal Melanoma on the temporal right eye with associated retinal detachment. (**b**) Follow up after 9 months shows significant tumor volume reduction and reversible retinal detachment. (**c**) Follow up after 18 months displays complete regression of the melanoma

shows this non-invasive treatment option to be reasonably safe and effective [1, 12–19] SRS requires immobilization of the eye in order to accurately plan and deliver the high-dose treatment. Most centers use a stereotactic frame (frame-based stereotactic radiosurgery), retrobulbar anesthesia and suturing of 2-4 rectus muscles. Others have described suction fixation devices for radiosurgical ocular treatments [29].

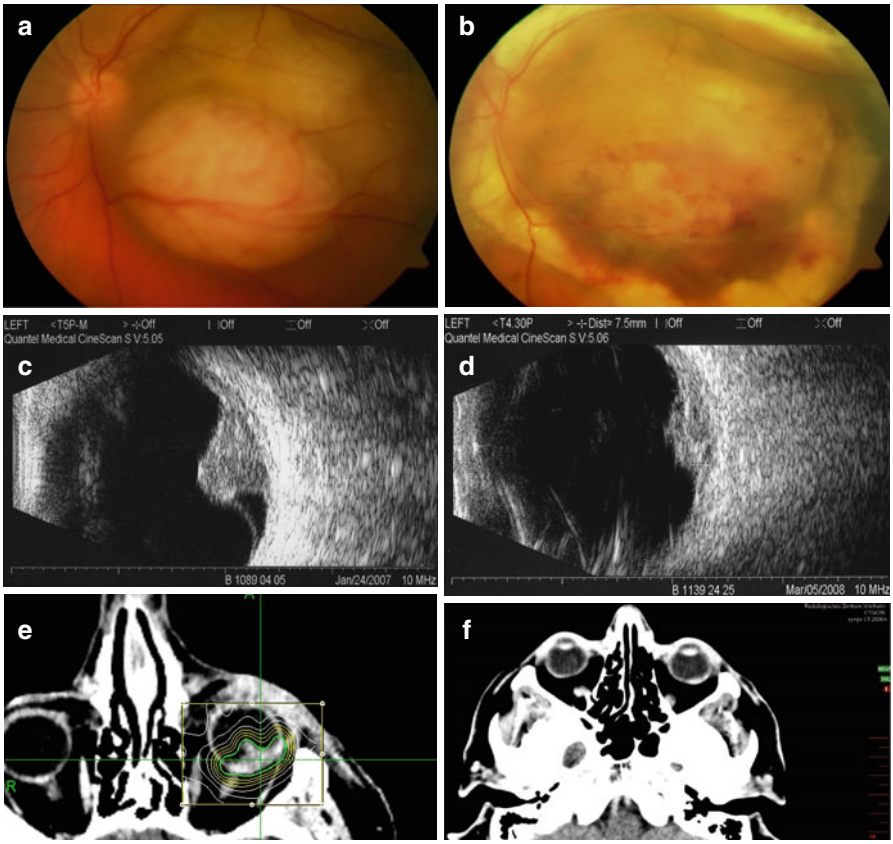

Fig. 15.2 (**a**, **b**) Fundoscopy image before (**a**) and after (**b**) Cyberknife radiosurgery. (**c**, **d**) Ultrasound scan before (**c**) and after (**d**) Cyberknife radisurgery. (**e**) Conformal plan with a steep dose gradient for a typical left-sided uveal melanoma. The isodoses from 10 to 70 % (prescribed isodose, *thick line*) are shown. The tumor was treated with single-session robotic radiosurgery procedure using a dose of 19 Gy. (**f**) Treatment result after 18 months. The tumor was significantly reduced in size

In our previous studies, akinesia of the eye after retrobulbar anesthesia and the induced proptosis lasted for at least 3 h in all of more than 200 treated cases, as shown by MRI studies before and immediately after the radiosurgical procedure [23, 24]. There was no significant soft tissue volume change during this time frame. Therefore, we concluded that retrobulbar anesthesia alone was sufficient for a time frame of at least 3 h and that no other additional eye-bulb immobilization devices were needed. This finding opened the possibility of carrying out the radiosurgical procedure without the highly invasive step of eye-immobilization and led us to develop the sequence of procedures described in this chapter.

We describe here a novel and minimally invasive treatment paradigm using frameless robotic SRS to treat uveal melanoma of the eye. We demonstrated that this treatment option was feasible for treating mid-size and large uveal melanomas

[31]. Compared with our previous series using frame-based SRS, it is far more non-invasive, safe, appears equally effective, and is considerably more comfortable for the patient. The only slightly invasive procedure left in the sequence is the administration of local anesthesia into the retrobulbar space, which is a safe and straightforward procedure routinely performed by experienced ophthalmologists [31]. Given the high tracking precision that retrobulbar anesthesia enables, we do not think that eye ball tracking techniques should replace this minimal invasive procedure with an inherent risk of greater inaccuracies during treatment.

In our earlier series, in which we treated medium- to large-size uveal melanomas, although the treatment proved effective, we did encounter certain adverse effects such as exudative retinal detachment in 20 % of the cases, and subsequently worse visual acuity [23, 24]. Generally, major treatment-related toxicities included neovascular glaucoma, radiation retinopathy or optic neuropathy, which were seen especially in the earlier series of Gamma Knife-based SRS, largely due to higher doses, larger tumor sizes and tumor locations [26, 27]. Larger basal diameter (>10 mm), ciliary body melanomas and doses over 35 Gy appeared to be associated with increased complication rates [17, 18]. Compared with eye-plaque therapy, Stereotactic radiosurgery comes with the advantage of not involving invasive surgery for plaque implantation and removal as well as hospitalization for several days required for radiation protection during brachytherapy. Fractionated proton therapy was not indicated for our patient cohort as proton centers are scarce and proton treatment costs are considerably higher than brachytherapy or radiosurgical treatment options.

Recently, there has been a trend towards dose de-escalation in this application. Several series showed equivalent local control but reduced toxicity rates with lower doses [22, 23, 26]. The dose level applied in the current study was lower than the earlier series. The treatment regimen was developed based on our previous experience and our ability to deliver dose plans with steeper gradients and better tumor coverage compared to the earlier, frame-based techniques we used.

The probability of visual preservation and eye retention with either technique are strongly dependent on tumor size and location. The dose to the lens and the optical disc is determined by the location of the tumor. However, for tumors of the lateral and posterior-lateral parts of the bulb, the dose to the lens and the optical disc could be kept to a minimum due to the steep dose gradient achieved using an inverse planning algorithm. Hirasawa et al. identified the anterior segment of the eye and the optic disc as structures of great risk for neovascular glaucoma based on a multivariate analysis, and recommended irradiation techniques that would spare these structures as much as possible when treating uveal melanoma [17]. The high flexibility of the robotic technology used in the current study is capable of achieving this goal [20]. Robotic radiosurgery has the ability to adjust the dose to the tumor as much as possible by maximally sparing the dose to sensitive structures of the eye.

Accurate treatment planning and delivery requires a stringent setup with an experienced interdisciplinary team comprised of ophthalmologists, radiation oncologists and imaging experts. Under optimal conditions, the described radiosurgical treatment paradigm seems to be safe, effective and comfortable for the patient.

15.6 Conclusions

Robotic radiosurgery is a safe and effective treatment approach for definitive treatment of medium sized and large uveal melanomas. MRI and CT image fusion for treatment planning enhance the exact tumor delineation. In experienced hands, retrobulbar anaesthesia, imaging, treatment planning and treatment application can be performed sequentially in one treatment session within a time frame of less than 3 h.

References

1. Henderson MA, Shirazi H, Lo SS, Mendonca MS, Fakiris AJ, Witt TC, Worth RM, Timmerman RD. Stereotactic radiosurgery and fractionated stereotactic radiotherapy in the treatment of uveal melanoma. Technol Cancer Res Treat. 2006;5:411–9.
2. Shields CL, Kaliki S, Furuta M, Fulco E, Alarcon C, Shields JA. American Joint Committee on Cancer Classification of posterior uveal melanoma (tumor size category) predicts prognosis in 7731 patients. Ophthalmology. 2013;120(10):2066–71.
3. Lake SL, Coupland SE, Taktak AF, Damato BE. Whole-genome microarray detects deletions and loss of heterozygosity of chromosome 3 occurring exclusively in metastasizing uveal melanoma. Invest Ophthalmol. 2010;51:4884–91.
4. Adams KS, Abramson DH, Ellsworth RM, Haik BG, Bedford M, Packer S, Seddon J, Albert D, Polivogianis L. Cobalt plaque versus enucleation for uveal melanoma: comparison of survival rates. Br J Ophthalmol. 1988;72:494–7.
5. Adler Jr JR, Chang SD, Murphy MJ, Doty J, Geis P, Hancock SL. The Cyberknife: a frameless robotic system for radiosurgery. Stereotact Funct Neurosurg. 1997;69:124–8.
6. Adler Jr JR, Murphy MJ, Chang SD, Hancock SL. Image-guided robotic radiosurgery. Neurosurgery. 1999;44:1299–306; discussion 1306–1297.
7. Augsburger JJ, Gamel JW, Lauritzen K, Brady LW. Cobalt-60 plaque radiotherapy vs enucleation for posterior uveal melanoma. Am J Ophthalmol. 1990;109:585–92.
8. Boyd SR, Gittos A, Richter M, Hungerford JL, Errington RD, Cree IA. Proton beam therapy and iris neovascularisation in uveal melanoma. Eye (Lond). 2006;20:832–6.
9. Char DH, Bove R, Phillips TL. Laser and proton radiation to reduce uveal melanoma-associated exudative retinal detachments. Am J Ophthalmol. 2003;136:180–2.
10. Char DH, Phillips T, Daftari I. Proton teletherapy of uveal melanoma. Int Ophthalmol Clin. 2006;46:41–9.
11. Dendale R, Lumbroso-Le Rouic L, Noel G, Feuvret L, Levy C, Delacroix S, Meyer A, Nauraye C, Mazal A, Mammar H, Garcia P, D'Hermies F, Frau E, Plancher C, Asselain B, Schlienger P, Mazeron JJ, Desjardins L. Proton beam radiotherapy for uveal melanoma: results of Curie Institut-Orsay proton therapy center (ICPO). Int J Radiat Oncol Biol Phys. 2006;65:780–7.
12. Dieckmann K, Bogner J, Georg D, Zehetmayer M, Kren G, Potter R. A linac-based stereotactic irradiation technique of uveal melanoma. Radiother Oncol. 2001;61:49–56.
13. Dieckmann K, Georg D, Zehetmayer M, Bogner J, Georgopoulos M, Potter R. LINAC based stereotactic radiotherapy of uveal melanoma: 4 years clinical experience. Radiother Oncol. 2003;67:199–206.
14. Dieckmann K, Georg D, Zehetmayer M, Rottenfusser A, Potter R. Stereotactic photon beam irradiation of uveal melanoma: indications and experience at the University of Vienna since 1997. Strahlenther Onkol. 2007;183 Spec No 2:11–3.

15. Fakiris AJ, Lo SS, Henderson MA, Witt TC, Worth RM, Danis RP, Des Rosiers PM, Timmerman RD. Gamma-knife-based stereotactic radiosurgery for uveal melanoma. Stereotact Funct Neurosurg. 2007;85:106–12.
16. Georgopoulos M, Zehetmayer M, Ruhswurm I, Toma-Bstaendig S, Segur-Eltz N, Sacu S, Menapace R. Tumour regression of uveal melanoma after ruthenium-106 brachytherapy or stereotactic radiotherapy with gamma knife or linear accelerator. Ophthalmologica. 2003;217:315–9.
17. Hirasawa N, Tsuji H, Ishikawa H, Koyama-Ito H, Kamada T, Mizoe JE, Ito Y, Naganawa S, Ohnishi Y, Tsujii H. Risk factors for neovascular glaucoma after carbon ion radiotherapy of choroidal melanoma using dose-volume histogram analysis. Int J Radiat Oncol Biol Phys. 2007;67:538–43.
18. Langmann G, Pendl G, Klaus M, Papaefthymiou G, Guss H. Gamma knife radiosurgery for uveal melanomas: an 8-year experience. J Neurosurg. 2000;93 Suppl 3:184–8.
19. Manschot WA, Lee WR, van Strik R. Uveal melanoma: updated considerations on current management modalities. Int Ophthalmol. 1995;19:203–9.
20. Marchini G, Gerosa M, Piovan E, Pasoli A, Babighian S, Rigotti M, Rossato M, Bonomi L. Gamma Knife stereotactic radiosurgery for uveal melanoma: clinical results after 2 years. Stereotact Funct Neurosurg. 1996;66 Suppl 1:208–13.
21. Muacevic A, Nentwich M, Wowra B, Staerk S, Kampik A, Schaller U. Development of a streamlined, non-invasive robotic radiosurgery method for treatment of uveal melanoma. Technol Cancer Res Treat. 2008;7:369–74.
22. Mueller AJ, Schaller U, Talies S, Horstmann GA, Wowra B, Kampik A. Stereotactic radiosurgery using the gamma knife for large uveal melanomas. Ophthalmologe. 2003;100:122–8.
23. Mueller AJ, Talies S, Schaller UC, Horstmann G, Wowra B, Kampik A. Stereotactic radiosurgery of large uveal melanomas with the gamma-knife. Ophthalmology. 2000;107:1381–7.
24. Rennie I, Forster D, Kemeny A, Walton L, Kunkler I. The use of single fraction Leksell stereotactic radiosurgery in the treatment of uveal melanoma. Acta Ophthalmol Scand. 1996;74:558–62.
25. Shields CL, Shields JA, Gunduz K, Freire JE, Mercado G. Radiation therapy for uveal malignant melanoma. Ophthalmic Surg Lasers. 1998;29:397–409.
26. Simonova G, Novotny Jr J, Liscak R, Pilbauer J. Leksell gamma knife treatment of uveal melanoma. J Neurosurg. 2002;97:635–9.
27. Zehetmayer M, Kitz K, Menapace R, Ertl A, Heinzl H, Ruhswurm I, Georgopoulos M, Dieckmann K, Potter R. Local tumor control and morbidity after one to three fractions of stereotactic external beam irradiation for uveal melanoma. Radiother Oncol. 2000;55:135–44.
28. Pe'er J. Ruthenium brachytherapy. Dev Ophthalmol. 2012;49:27–40.
29. Zehetmayer M, Menapace R, Kitz K, Ertl A. Experience with a suction fixation system for stereotactic radiosurgery of intraocular malignancies. Stereotact Funct Neurosurg. 1995;64 Suppl 1:80–6.
30. Zehetmayer M, Menapace R, Kitz K, Ertl A, Strenn K, Ruhswurm I. Stereotactic irradiation of uveal melanoma with the Leksell gamma unit. Front Radiat Ther Oncol. 1997;30:47–55.
31. Muacevic A, Staehler M, Drexler C, Wowra B, Reiser M, Tonn JC. Technical description, phantom accuracy, and clinical feasibility for fiducial-free frameless real-time image-guided spinal radiosurgery. J Neurosurg Spine. 2006;5:303–12.
32. Zorlu F, Selek U, Kiratli H. Initial results of fractionated CyberKnife radiosurgery for uveal melanoma. J Neurooncol. 2009;94:111–7.

Chapter 16
Stereotactic Body Radiotherapy: A Practical Guide for the Delivery of Accelerated Partial Breast Irradiation

Sandra S. Vermeulen, Huan B. Giap, Cristian Cotrutz, Robert M. Douglas, and Astrid Morris

Abstract Post-operative whole-breast irradiation (WBI) has been used in the last several decades to offer early-stage breast cancer patients options to preserve their breasts. The standard traditional external beam radiation treats the whole breast over a 6–7 week course; however, it is inconvenient and does have potential toxicity to heart, lung, bone, and soft tissues. Over the last decade, accelerated partial breast irradiation (APBI) allows the majority of these patients an attractive alternative to traditional radiation by treating part of the breast over 1–2 weeks. There are more than a dozen APBI techniques emerging over the last decade using various modalities of radiation including superficial X-ray, high-energy photon, proton beam, high-dose rate and low dose-rate brachytherapy. Of these, stereotactic body radiation therapy (SBRT) is an attractive option and is the focus of this chapter. SBRT offers patients the delivery ease of external beam radiotherapy (reproducibility factor) without the protracted time commitment seen with WBI (convenience factor). In addition, SBRT offers increased accuracy of irradiation delivery (target precision factor) without the inherent invasiveness (quality-of-life factor) of a brachytherapy implant. These SBRT abilities will likely increase the number of candidates for

S.S. Vermeulen, MD (✉)
Swedish Radiosurgery Department, Swedish Medical Center, Swedish Radiosurgery Center, Seattle, WA, USA
e-mail: sandra.vermeulen@swedish.org

H.B. Giap, MD, PhD
Clinical Research, GI, Lung, and Breast Services, University of California of San Diego, Scripps Proton Therapy Center, San Diego, CA, USA

C. Cotrutz, PhD
Department of Radiation Oncology, Swedish Cancer Institute, Radiosurgery Center, Seattle, WA, USA

R.M. Douglas, MD
Department of Radiation Oncology, Valley Medical Center, Renton, WA, USA

A. Morris, MD
Department of Radiation Oncology, Tumor Institute Radiation Onc., Seattle, WA, USA

A. Gaya, A. Mahadevan (eds.), *Stereotactic Body Radiotherapy: A Practical Guide*,
DOI 10.1007/978-0-85729-597-2_16

APBI, particularly those patients with difficult to treat anatomy (large/pendulous breasts), busy working women, elderly or disabled patients and those who live far from a radiation therapy clinic. This chapter describes one technique of SBRT for APBI using the CyberKnife system and preliminary data on a small group of patients demonstrates the feasibility and minimal side effects. More clinical studies need to be conducted to explore this new technique with end points of in-breast tumor recurrence, cost effectiveness, and quality of life endpoints including cosmesis, side effects and perceived convenience.

Keywords Accelerated Partial Breast Irradiation (APBI) • Alpha-beta ratio • Brachytherapy • Breast • Breast carcinoma • Breast conserving therapy (BCT) • Clinical target volume (CTV) Conformality • Cosmetic outcome • Cosmesis • CyberKnife • Fiducials • High-dose-rate (HDR) brachytherapy • Intensity-modulated radiotherapy (IMRT) • Isodose • Low-dose-rate (LDR) brachytherapy • Lumpectomy • Margin • Motion • Outcomes • Planning target volume (PTV) • Quality of life • Stereotactic Body Radiotherapy (SBRT) • Three-dimensional conformal radiotherapy (3D-CRT) • Treatment time • Treatment Planning • Whole breast irradiation (WBI)

16.1 Introduction

Breast conserving therapy (BCT) is the preferred treatment modality for many patients with early stage breast carcinoma [1]. Several randomized controlled studies [2–8] including the National Surgical Adjuvant Breast and Bowel Project (NSABP) B-06 have demonstrated equivalent overall survival for patients receiving breast conserving surgery and whole breast irradiation (WBI) compared with patients treated by mastectomy. The major advantages of BCT are superior cosmetic outcome and the reduced emotional and psychological impact from this procedure compared with mastectomy. However, the principal disadvantage of breast conservation as traditionally performed is the prolonged treatment duration of external beam radiation therapy, approximately 6–7 weeks, which may pose substantial problems for some patients such as the elderly, busy working professionals, or those who live far from a radiotherapy facility. Furthermore, traditional BCT irradiates the whole breast, which for patients with large or pendulous breasts could cause significant skin, soft tissue, lung, ribs, and heart (for treatments of the left breast) morbidities. Despite multiple prospective randomized studies showing compatibility of BCT and mastectomy, BCT remains under-utilized [9]. According to the National Cancer Institute, about 40 % of patients who are eligible for BCT have mastectomies instead of BCT, and 10–20 % of patients who undergo breast conservation surgery do not receive radiation following surgery [9]. Many of these patients cite the inconvenience of receiving radiation therapy (i.e., extended period of daily treatments, time-off from work, etc.) and the impact on quality of life due to

concerns of additional side effects from the radiation. Fortunately, in the past decade there has been an explosion of new options for post-op adjuvant radiation therapy as an alternative to conventional WBI.

Mature Phase I and II studies, and some preliminary Phase III studies, have investigated the replacement of WBl with an accelerated course of radiation therapy restricted to the region around the tumor bed. This approach, known as accelerated partial breast irradiation (APBI), builds upon knowledge that following a lumpectomy with clear margins (≥2 mm), 90 % of recurrences in women who present with early disease (stage 0, I, II) are hypothesized to occur within 10 mm of the resection cavity [10–12]. Most of the early experience with APBI has been with interstitial brachytherapy, which shows high local control rates along with acceptable morbidity. However, because of the invasiveness of these procedures, their steep learning curve and risks of infection, lumpectomy cavity coverage with three-dimensional conformal radiotherapy (3D-CRT) and intensity-modulated radiotherapy (IMRT) has grown in popularity. More recently, the use of stereotactic body radiation therapy (SBRT) for delivery of APBI has been examined [13, 14]. In this chapter we provide a brief history of APBI followed by a practical guide to the delivery of APBI with SBRT.

16.2 The Role of Radiotherapy

Attempts to avoid the addition of radiotherapy following breast conserving surgery generally result in unacceptably high rates of local recurrence [15], except possibly for elderly patients with favorable tumors [16]. Indeed, several randomized controlled studies have shown that adjuvant whole breast radiotherapy reduces the risk of local failure by a factor of about two-thirds [2, 10, 15, 17–20]. For instance, NSABP B-06 showed that patients with negative lumpectomy margins, adjuvant whole breast radiotherapy reduced the rate of in-breast recurrence at 20 years from 39.2 % in the lumpectomy alone arm to 14.3 % in the lumpectomy and whole breast irradiation arm [2]. In spite of this very large reduction of in-breast recurrence, the impact of adjuvant radiotherapy on overall survival is small [21].

Whole breast irradiation after wide excision has been postulated to reduce the breast recurrence rate through the elimination of residual foci of cancer remaining both around the excision site as well as occult cancer in remote areas of the breast. It was originally thought that occult multicentricity occurred frequently [22, 23], but the pattern of local recurrences after breast-conserving therapy both with and without adjuvant radiotherapy suggest that these remote areas of occult carcinoma are either encountered less frequently or are of limited clinical significance when patients are more carefully selected to rule out multicentric disease. Sixty-five to 100 % of breast recurrences reported after conservative surgery and whole breast radiation therapy have been found in the same quadrant as the initial tumor, with histology similar to the primary tumor, indicating that these probably represent residual viable cancer around the original site not controlled by radiation therapy

[24–27]. Even without adjuvant radiation therapy, the pattern of recurrence is overwhelmingly around the tumor bed [2, 15–17, 20]. To examine this the serial section mastectomy series by Holland, that originally suggested high rates of multicentricity, was re-analyzed with only those cases with complete mammographic data and excluding those with evidence of microcalcifications or tumor density beyond the main tumor mass and unfavorable characteristics such as any lobular histology, primary tumors larger than 2 cm, and any cancer in the region 1–2 cm beyond the main tumor mass. This re-analysis found that only 4 of 72 cases had any residual carcinoma more than 1 cm beyond the dominant mass (the area that would be treated with APBI) [28]. Furthermore, breast recurrences distant from the primary site tend to occur later than those near the lumpectomy bed, and may well represent second primaries rather than true recurrences [25] and would not be expected to be prevented by whole breast radiotherapy.

From these data, one can infer that in appropriate cases, the main effect of radiation therapy following conservative surgery is the reduction of breast cancer recurrence at or very near the primary site. If radiation therapy is directed only to the tissue surrounding the excision cavity, then the entire course of radiation therapy can be accelerated markedly, reducing treatment time. Furthermore, normal tissues such as the remainder of the breast, underlying muscle, ribs, lung, and heart generally will receive a lower radiation dose with APBI than with whole breast radiotherapy, potentially avoiding toxicity. This may be particularly important for patients with large pendulous breasts who often experience significant acute toxicity from whole breast radiotherapy.

16.3 Accelerated Partial Breast Irradiation

There currently is a large body of mature Phase I and II data along with some preliminary Phase III findings studying the replacement of WBl with an accelerated course of radiation therapy restricted to the region around the tumor bed using a variety of techniques. For appropriately selected patients treated with appropriate techniques, the results are very encouraging and the techniques have been shown to be safe, tolerable, and highly reproducible with outcomes similar to WBI (Table 16.1) [11, 29–42]. For inappropriately selected patients or those treated with suboptimal techniques, the rates of in-breast recurrence are not acceptable, although even then there is no suggestion of an adverse impact on overall survival.

Most experience with APBI has been with interstitial brachytherapy, with most of that experience until recently being with the multi-catheter type (Table 16.1). The primary disadvantages of conventional multi-catheter brachytherapy are the complexity and invasiveness of the procedure. Conventional breast brachytherapy requires the use of up to 20 catheters or needles placed around the excision site (Fig. 16.1).

There are several ways of placing these catheters, or needles, into the breast, and the procedure can be done either under local anesthesia with conscious sedation

Table 16.1 Summary of accelerated partial breast irradiation (APBI) studies using high dose rate (HDR) brachytherapy, low dose rate (LDR) brachytherapy, external beam radiation therapy and intra-operative radiotherapy

Institution	Number of cases	Median follow-up (months)	Fractionation scheme (cGy)	Total dose (cGy)	Percent local recurrence	Good/excellent cosmetic results
HDR brachytherapy						
Ochsner Clinic [29]	26	75	400×8	3,200	2[a]	75[a]
National Institute of Budapest, Hungary Phase II Trial [30]	45	60	520×7	3,640	4.4	97
			433×7	3,030		
National Institute of Oncology, Budapest, Hungary Phase III [30]	221	30	520×7 (HDR)	3,640	0	NS
			200×25[b] (EBRT)	5,000	<1	NS
London Regional Cancer Center London, Ontario [31]	39	20	372×10	3,720	2.6[a]	NS
William Beaumont Hospital [11, 32]	79	52	400×8	3,200	1	100
Radiation Therapy Oncology Group [33]	66	78	340×10	3,400	3	–
MammoSite® (FDA approval trial) [34]	43	8	340×10	3,400	0	97
Tufts-New England Medical Center [35]	32	33	340×10	3,400	3	88
Medical College of Virginia/VCU [36]	44	42			0	80
LDR brachytherapy series						
Ochsner Clinic [29]	26	75	>40 cGy/h	4,500	2[a]	75[a]
Guy's Hospital [37]	27	72	40 cGy/h	5,500	37	83
William Beaumont Hospital [11, 32]	120	82	52 cGy/h	4,992	1	91
Radiation Therapy Oncology Group [33]	33	85	–	4,500	12	NS
Massachusetts General Hospital [38]	48	23	50 cGy/h	5,000–6,000	0	92
External beam radiotherapy series						
William Beaumont Hospital [39]	22	20	340–385×10	3,400–3,850	0	100
New York University [40]	47	18	600×5	3,000	0	All late toxicity ≤Grade 1

Table 16.1 (continued)

Institution	Number of cases	Median follow-up (months)	Fractionation scheme (cGy)	Total dose (cGy)	Percent local recurrence	Good/excellent cosmetic results
Intra-operative radiotherapy series						
European Institute of Oncology, Milan Italy [41]	84	8	1,700–2,100 × 1	1,700–2,100		
University College of London [42]	3	24	500–750 × 1	500–750	0	

Abbreviations: *HDR* high dose rate brachytherapy, *LDR* low dose rate brachytherapy
[a]LDR/HDR patients combined
[b]Whole breast irradiation

after surgery or under general anesthesia at the time of lumpectomy. These needles are inserted through the breast, and flexible catheters are threaded through the needles to cover the target area around the breast cavity. Interstitial brachytherapy has the advantages of high dose conformity to the target volume, independent of organ motion or respiration; delivery of additional simultaneous boost to the inner core of the target (the high risk area); and the ability to adapt to various patients' anatomy and target shape (convexity). The interstitial brachytherapy experience provides the earliest clinical experience and has the longest follow-up clinical data for APBI. Nevertheless, this technique has not gained widespread popularity because of the relative complexity associated with performing an interstitial implant and the lack of significant patient interest in an additional invasive procedure with risk of infection, pain, and bleeding (Fig. 16.1b). As a consequence, multi-catheter APBI has been limited to only a handful of institutions.

The oldest brachytherapy APBI series comes from the Oschner Clinic [29] and the largest series from William Beaumont Hospital [11, 32]. At the Oschner Clinic, 51 women with 52 tumors were treated [29]. Eligibility criteria included intraductal or invasive carcinomas less than or equal to 4 cm in size, 0–3 positive axillary lymph nodes, and negative inked microscopic margins. Multiple plane interstitial implant was placed under direct visualization of the excision cavity or with ultra-sound guidance, and the catheters extended 2 cm beyond the cavity in all peripheral dimensions. Patients were assigned to low-dose-rate (LDR) and high-dose-rate (HDR) brachytherapy alternating in blocks of 10. LDR patients received 45 Gy in 3.5–6 days, while HDR patients received 32 Gy in 8 fractions over 4 days. At a median follow-up of 75 months, there were three grade 3 complications (5.8 % overall, 3.8 % LDR, 7.7 % HDR). Two HDR patients experienced severe fat necrosis, one requiring a mastectomy and the other a quandrantectomy with flap coverage. One LDR patient developed an abscess from an infected seroma at 4 months which was incised and drained. The rate of good/excellent cosmesis was 78 % in LDR and 67 % in HDR ($p = 0.39$). There has been only one local recurrence, located near the surgical scar occurring 78 months after radiotherapy.

In the William Beaumont Hospital Experience with multi-catheter brachytherapy APBI, 199 consecutive women with invasive early-stage breast cancer were treated from 1993 to 2001 [11, 32]. One hundred twenty patients were treated as in-patients with LDR, receiving 50 Gy over approximately 96 h. Seventy-nine were treated as out-patients with HDR, receiving either 32 Gy in 8 fractions of 4 Gy each or 34 Gy in 10 fractions of 3.4 Gy each, twice a day, with at least 6 h between fractions. One hundred fifty-eight patients met the strict eligibility criteria which included infiltrating ductal carcinomas <3 cm, surgical margins clear by at least 2 mm, age >40, no extensive intraductal component (EIC-), and no clinically significant lobular carcinoma in situ. Initially patients with 1–3 involved axillary lymph nodes were allowed. The protocol was modified after the first 50 patients, and the subsequent 149 patients were required to be node negative. At a median follow-up of 65 months (range, 12–115 months), a total of five ipsilateral recurrences were observed; two were located near the original primary site and three were located elsewhere in the breast. The mean time to local failure was 5 years (range, 1.5–7.6 years).

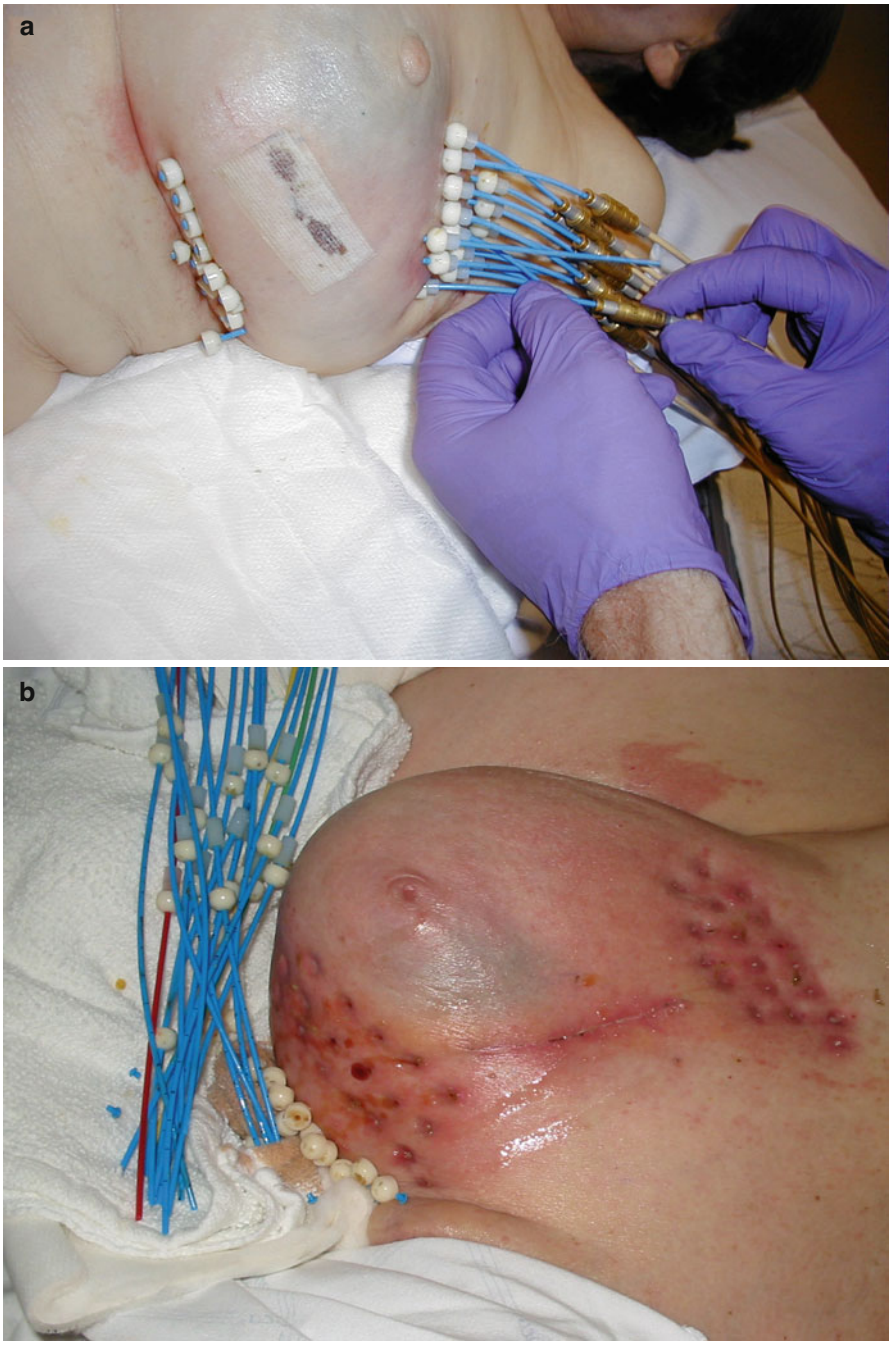
a
b

In recent years, the development of the MammoSite® (Proxima Therapeutics, Inc., Alpharetta, GA) balloon brachytherapy technique has increased interest in APBI.

This brachytherapy applicator was developed as a more "user friendly" technique in which a single balloon is placed in the excision cavity [34]. While nursing care for the single catheter is less and patients may be more comfortable there remain several drawbacks. This technique requires a second surgical procedure to place the catheter and wound care for 1–2 weeks. Some patients are candidates for APBI, but they are not candidates for Mammosite due to geometric factors such as small breast size, too much air/gas in the cavity, or the cavity is too close to the chest wall or skin. The applicator is not suitable for lesions close to the skin surface or for irregularly shaped cavities to which the balloon does not conform. The Mammosite has to be inflated for the entire 7–14 day treatment duration, which can be uncomfortable, and the catheter entry point can serve as a source of infection. Typically, patients with an inserted device are placed on prophylactic antibiotics. All being said, a recent publication from the American Society of Breast Surgeons Mammosite Breast Brachytherapy Registry Trial reported a 91 % good to excellent cosmetic result at a mean follow-up of 54 months (range, 0–86 months) in a treated population of 1,449 women with early breast cancer [43].

Three-dimensional (3D) conformal external beam radiation therapy has also been pursued as a technique to treat patients with APBI using a similar, shortened treatment schedule. This 3D technology is readily available in the majority of radiation facilities allowing many more radiation oncologist groups that do not perform brachytherapy to deliver APBI. Perhaps the greatest advantage of this method of APBI is the fact that no additional invasive procedure is required. However, conventional radiation equipment cannot pinpoint radiation delivery as accurately as brachytherapy. Therefore, a large margin is required to account for the set-up uncertainty and for respiratory motion during treatment. This margin leads to a larger treatment volume and more irradiation of the normal structures (lung, chest wall, skin, heart). Indeed, there are now published concerns of toxicities with unacceptable cosmesis seen in populations of women who elected for APBI using 3-D conformal external beam approach [44, 45].

Fig. 16.1 Example of accelerated partial breast irradiation delivered using intersititial brachytherapy with multiple catheters. (**a**) The flexible hollow catheters are inserted around the lumpectomy cavity during breast conserving surgery. After CT-based treatment planning, these catheters are connected to a High-Dose Rate (HDR) remote after loading machine for delivery of the 10 treatments over 1 week. Immediately following completion of the tenth treatment the catheters are removed. (**b**) Shown is the trauma to the breast (and associated discomfort) along with the possible risk of infection and bleeding associated with interstitial brachytherapy APBI

The NSABP B39/RTOG 0413 trial randomizes select patients with stage 0, I and II breast cancer after lumpectomy to either WBI or APBI with the goal of documenting the long-term equivalence of APBI to WBI. Patients randomized to the APBI arm are treated with either interstitial brachytherapy with catheters/needles; intracavitary brachytherapy with the Mammosite balloon catheter; or 3D conformal external beam radiation therapy. A recent publication by Patel et al. [46] reported the 5-year follow-up for 273 patients treated with brachytherapy using either multicatheter interstitial brachytherapy (n = 247) or Mammosite (n = 26). The patients received 32–34 Gy in 8–10 twice daily fractions using high-dose-rate 192Ir brachytherapy. All patients met the initial inclusion criteria for the trial and were separated into either a high- or low-risk group. The high-risk patients (n = 90), who represent the cohort that remained eligible for the intergroup trial, satisfied one or more of the "high-risk" criteria: age <50, estrogen receptor negative, and/or positive lymph nodes. The low-risk patients comprised the remainder of the cohort (n = 183). At a median 48.5 months follow-up for the entire cohort, no significant difference was found in outcomes at 5 years between the low- and high-risk groups with a local control rate of 97.8 % vs 93.6 %, crude local recurrence rate of 2.2 % (n = 4) vs 4.4 % (n = 4), and overall survival rate of 92.1 % vs 89.5 %, respectively.

A Phase II Electron Intraoperative radiotherapy (ELIOT) trial is underway in Europe. Patients over 55 years of age with tumors ≤2.5 cm are randomized to WBI (50 + 10 Gy boost) versus 21 Gy single fraction electron intra-operative radiotherapy (IORT). The accrual goal for the study is 800 patients. To perform IORT, a mobile linear accelerator with a robotic arm is used to deliver a single-fraction electron dose to the involved quadrant of the breast after quadrantectomy. An aluminum/lead disc is placed between the breast and pectoralis muscle to shield the chest wall and lungs. Initial experience was as an "up-front" boost to anticipate WBI with dose escalation from 10 to 15 Gy. This was well tolerated, and the approach changed to sole treatment with APBI using a single fraction of IORT. Dose was escalated from 17 to 21 Gy without unexpected acute toxicity. It is estimated that 21 Gy in a single fraction is radiobiologically equivalent to 60 Gy in 30 fractions of 2 Gy/fraction over 6 weeks [41].

The advantages of this technique are convenience to patient, minimal risk of radiation to surrounding normal structures (lung, heart and breast), lower cost, and no delay to adjuvant chemotherapy when needed. The critics of this technique cite potential under-coverage of the target volume (due to unknown final margin status and the directional nature and energy of the electron beam), additional use of operating time and patient time under general anesthesia, as well as cost of purchasing the IORT machine.

16.4 Stereotactic Body Radiotherapy Delivery Of APBI

Stereotactic body radiotherapy (SBRT) offers the potential of combining the benefits of the precisely targeted dose delivery of an interstitial brachytherapy APBI with the non-invasiveness of external beam radiation therapy. SBRT delivers a highly

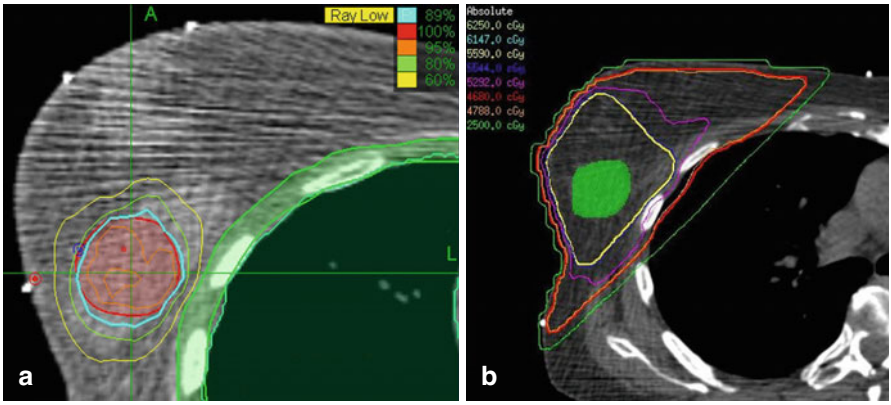

Fig. 16.2 Comparison of (**a**) an SBRT APBI treatment plan to that of (**b**) a conventional radiation treatment plan. Note the high conformality of the SBRT APBI treatment plan's isodoses

conformal dose that mimics the dosimetry of a breast interstitial brachytherapy implant. In order to accomplish this SBRT must employ image-guided delivery, typically via tracking of fiducial markers which in the case of APBI are implanted during tumor resection keeping the subsequent SBRT non-invasive. The CyberKnife (Accuray Incorporated, Sunnyvale, CA) is a frameless robotic stereotactic radiosurgery system that provides image-guidance for continuous tracking of target motion with respiration and patient movement [47]. Recently, the CyberKnife has been explored for SBRT delivery of APBI due to its image-guidance capability which allows continuous tracking of the target's motion with respiration and patient movement. This allows the margins to be reduced to a minimum, thus sparing surrounding critical structures from undue radiation exposure. Researchers at the University of Texas Southwestern Medical recently compared CyberKnife SBRT APBI and 3D-CRT treatment plans. They found that the SBRT APBI treatment plans achieved highly conformal target coverage and reduced the dose to nearby organs at risk relative to 3D-CRT plans [14]. Similarly, a treatment planning comparison from Fox Chase Cancer Institute concluded that the CyberKnife's more conformal dose could result in reduced toxicity by a reduction in dose to surrounding breast tissue [13]. Figure 16.2 presents an SBRT APBI treatment plan in comparison with conventional radiation treatment plans highlighting the dose conformality of the SBRT APBI treatment plan.

At our institution, we have treated 21 patients with CyberKnife delivered SBRT. As experience and knowledge of SBRT APBI delivery grows, this treatment paradigm will evolve. The following presents a guide to how we currently perform SBRT APBI. While our experience has focused on the use of the CyberKnife for delivery of SBRT APBI we have attempted, as much as possible, to ensure this guide is informative for delivery of SBRT APBI with other devices. However, it is imperative that caution be employed to ensure that suitable motion tracking occurs to ensure the accuracy of dose delivery to the target while sparing nearby critical structures.

16.5 SBRT APBI Patient Eligibility

Our patient selection criterion incorporates patients considered "suitable" or "cautionary" candidates as outlined in the ASTRO consensus statement for APBI [48].

- greater than 45 years of age
- stage T1, T2 or Tis without metastases
- histologically confirmed invasive non-l**o**bular carcinoma or ductal carcinoma *in situ* (DCIS) of the breast
- lesion size must be less than 3 cm and treated with wide excision.
- patients with invasive tumors undergo an axillary sentinel node procedure or axillary dissection.
- negative (>2 mm) microscopically assessed surgical margins for both invasive carcinoma and DCIS with no known unresected residual carcinoma or diffuse suspicious microcalcifications. If there is an extensive intraductal component (EIC +), the total size of the EIC and primary invasive tumor should be less than 3 cm, and the post-operative mammogram must show no evidence of suspicious residual abnormality. If the cancer presented with malignancy-associated microcalcifications then they must have a negative post-operative mammogram or specimen radiograph demonstrating removal of all microcalcifications.

16.6 Exclusion Criteria

- pregnancy
- collagen vascular disease
- prosthetic augmentation implants
- prior radiation therapy to the treated breast
- invasive lobular or multicentric carcinoma
- histologically confirmed positive axillary lymph nodes
- tumors that involve the skin, that invade the chest wall/muscle, or that have diffuse suspicious microcalcifications on mammography
- patients must initiate SBRT treatment within 9 weeks of their last breast cancer surgery.

Potential side effects and toxicity of APBI treatment are discussed with patients during informed consent procedure. Table 16.2 lists the adverse reactions patients may expect.

16.7 SBRT APBI Treatment Planning

The high dose delivered during SBRT APBI requires motion tracking of the target during radiation delivery to compensate for respiratory motion. In the case of CyberKnife SBRT this is accomplished by real-time x-ray based tracking of

Table 16.2 Potential acute and long-term reactions to APBI, to be discussed during informed consent

Reactions *during* radiation therapy	Long term reactions
Common:	Common:
Skin reddening, darkening and irritation near the treatment site	Occasional discomfort and sensitivity at the treatment site
Fatigue	Mild increased firmness of the breast at the treatment site
Mild pain at the treatment site	Mild swelling of the treated breast
Swelling at the treatment site	Minor shrinkage of the treated breast
	Skin color change near the treatment site
	Scarring of a small amount of lung just under the chest wall near the treatment site (this rarely causes symptoms)
Uncommon (1–5 % of people):	Rare (less than 1 % of people):
Extensive skin blistering or peeling near the treatment site	Rib fractures near the treatment site
Significant pain at the treatment site	Loss or impairment of nerve function near the treatment site
Significant increase in firmness of the breast at the treatment site	Significant shrinkage of the treated breast
	Lung inflammation
	Skin ulceration near the treatment site
	Inflammation of the lining of the heart (only if left breast treated)
	Cancer in the treated area caused by radiation

From consent form prepared by the Hartford Hospital (http://www.harthosp.org/Portals/1/Images/56/572132.pdf, accessed June 28, 2013)

fiducials. Implantation of the fiducials during lumpectomy prevents an additional invasive procedure and ensures the fiducials are located within the resection cavity. We implant 4–5 bio-compatible 2-mm gold fiducial markers (manufacturer NMPE: product number MT-NW-887–864). The high density of these fiducials allows for good contrast on imaging as compared to the titanium clips more commonly used for other types of SBRT.

Treatment planning begins about 1 month after resection with the aim of performing SBRT 4–5 weeks post-surgery. This corresponds with published series showing this time period has the least amount of volume change in the seroma identifying the lumpectomy cavity [49]. The first step of treatment planning is acquisition of non-contrast computed tomographic (CT) scans (1.0-mm slice thickness). The CT images start at the mandible and extend several centimeters below the inframammary fold. In addition, a non-contrast MRI of the ipsilateral breast is obtained in cases where the lumpectomy cavity is ill-defined on CT. For all pre-treatment imaging and treatment delivery, the patient is positioned head first with their arms at their side. Care must be taken to avoid breast/cavity deformation from the position of the ipsilateral arm or the MRI breast coils. A multi-pronged approach is employed to ensure this. First, a support bra without metal clasps or wires is worn throughout the process of planning and treatment. Second, the MRI breast coils are

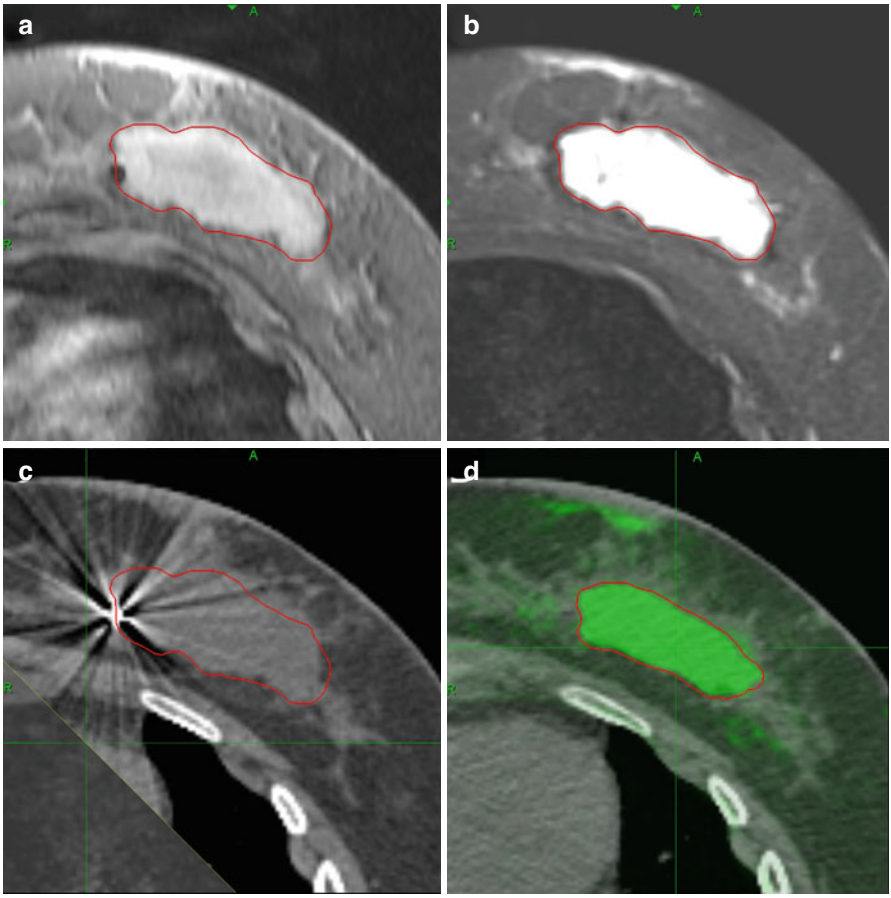

Fig. 16.3 Illustration of MRI and CY image fusion utility. The red outline indicates the delineation of the lumpectomy cavity. If the lumpectomy cavity is not well delineated on the simulation non-contrast CT, an MRI in treatment position is obtained. (**a**) The fiducials can be visualized with the T2*Gradient Echo/2dT2 (STAR) axial sequence which aids in fusing the images to the CT. (**b**) Enhancement of the seroma allows the cavity to be precisely identified on the T2Axial 2 mm/STIR images for targeting. (**c**) CT image showing the artifact from the fiducial which makes delineation of the cavity wall difficult. (**d**) The combined MRI/CT image results in a well delineated lumpectomy cavity for treatment planning

suspended above the breast using styrofoam supports to avoid deformation of the breast/cavity. Lastly, we found that a 3–5 cm thick alpha cradle best immobilizes the patients during treatment by elevating the patient's body while allowing their arms to drop at their side below the level of the chest.

For treatment planning, the CT scans and MRI images are fused. Typically, when an MRI is used, the lumpectomy cavity is best delineated on the T2 axial or STIR MRI images. The fiducials are seen on the 2dT2 (STAR) sequence and used to verify the correctness of the fusion with the CT. We have found that often the cavity cannot be outlined for target identification on the CT alone due to the adjacent

Table 16.3 Dose limitations for normal tissue based on the NSABP/RTOG protocol [50] and for patients treated at our institute with cyberknife APBI to a dose of 34 Gy delivered in 10 fractions (N = 12)

NSABP/RTOG structure	Constraint (3D-CRT)	CyberKnife treatment (mean, range)
Ipslateral breast	V34 <35 %	Volume: 13 %, 8–17 %
	V >17 <60 %	Volume: 28 %, 21–39 %
Contralateral breast	Dmax <1 Gy	Max dose: 1 Gy, 1–8 Gy
Ipslateral lung	V10 <15 %	Volume: 3 %, 0–12 %
Contralateral lung	V1.7 <15 %	Volume: 3 %, 0–19 %
Heart (RT breast)	V1.7 <5 %	Volume: 5 %, 0–19 %
Heart (LT breast)	V1.7 <40 %	Volume: 33 %, 0–42 %
Thyroid	Dmax <1 Gy	Max dose: <1 Gy, 0–0.6 Gy
Skin	Dmax <49.3 Gy	Max dose: 38 Gy, 27–46 Gy
Chest wall	Dmax <40.8 Gy	Max dose: 38 Gy, 29–41 Gy

breast tissue density or artifact scatter from the fiducials. In such cases, both of these issues are overcome with the MRI imaging capabilities (Fig. 16.3).

Next, dose-volume histogram analyses are conducted to ensure dose constraints are met. The dose constraints we employ are based upon the NSABP/RTOG protocol. However, in our case the contralateral breast dose does not reflect a volume, rather it is a maximum radiosurgery point dose. Thus we use the NSABP/RTOG constraints as guidelines adapted to the specifics of radiosurgery APBI; the NSABP/RTOG constraints, and our constraints, are listed in Table 16.3 [50]. Depending on the location of the lumpectomy site, particularly for very medial inner quadrant or lower inner quadrant lesions, acceptance for a high contra-lateral breast dose point is allowed as well as for higher volumes of heart or lung receiving the suggested dose as outlined in the national study.

Using the encouraging data published from Sylvia Formenti at New York University [51] and by applying an alpha-beta ratio of 4.6 Gy [52, 53] for breast cancer tumor control, we initially selected an SBRT dose of 6 Gy delivered in 5 fractions for a total dose of 30 Gy. Unfortunately, limited reimbursement for stereotactic APBI defined by 5 fractions or less resulted in a slow accrual. Since no single gold standard exists for APBI, a decision was made to match the dose fractionation scheme in the single-catheter brachytherapy arm of the NSABP/RTOG study, which gives 34 Gy in 10 fractions to the planning target volume (PTV) as defined by the lumpectomy cavity plus a 10-mm margin. This resulted in extremely small volumes for the ipsilateral breast receiving 100 and 50 % of the prescribed dose with no toxicity documented in our first 2 patients treated. As a result, we now treat with an enlarged PTV which matches the multi-catheter brachytherapy arm of the national study. The clinical target volume (CTV) is defined on a treatment planning non-contrast CT as the lumpectomy cavity plus 15 mm. Based upon this, we define our PTV as the CTV plus a 2-mm margin with a 5-mm sparing distance from the skin and chest wall. The 2-mm CTV margin is added to accommodate for possible tracking error of the fiducials. No additional volumes are considered necessary to account

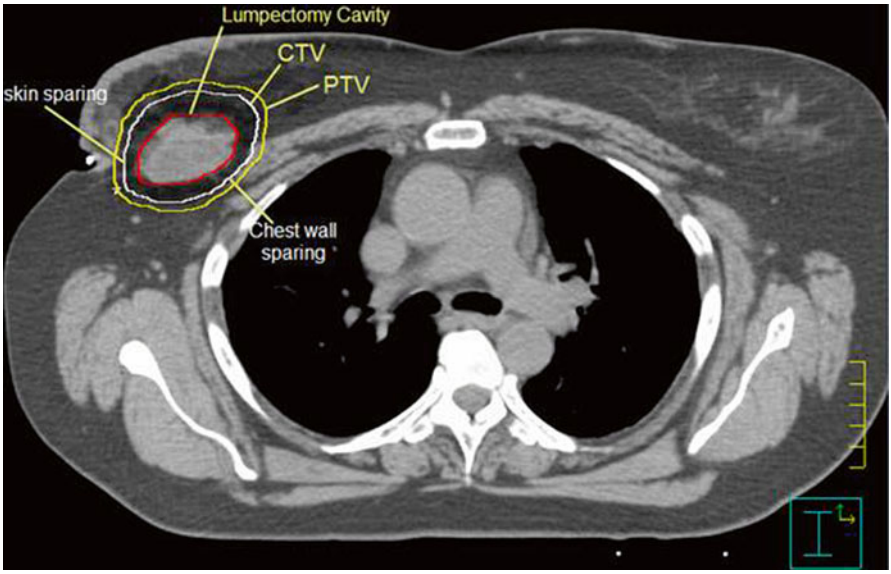

Fig. 16.4 Schematic of the SBRT clinical target volume (*CTV*), planning target volume (*PTV*) and lumpectomy cavity. The CTV is defined as the lumpectomy cavity plus a 15 mm margin, and the PTV is defined as CTV plus a 2 mm margin with a 5 mm sparing distance from the skin and chest wall

for variability in day-to-day set-up or patient mobility. Figure 16.4 provides a schematic of the lumpectomy cavity, CTV and PTV. Our dose prescription is 34 Gy in 10 fractions delivered to the planning target volume (PTV) which is prescribed to greater than the 65 % isodose. Also, we created a field within a field to force the dose maximum into the lumpectomy cavity which is devoid of breast tissue, minimizing potential tissue toxicity. We strive for a dose at the cavity wall of 38.5 Gy. Treatment is performed daily or twice daily per patient convenience and completed over 1–2 weeks with an average treatment time of 60 min or less. The CyberKnife Synchrony Tracking System is used to correct for target and patient motion. Prior to and during the treatment delivery, the fiducial markers in the ipsilateral breast are used for treatment set-up and verification (Fig. 16.5). Lastly, the use of chemohormonal therapy is at the discretion of treating physicians. When used, chemotherapy is not started until at least 2 weeks post-radiation therapy. Tamoxifen or other hormonal therapy may be started at once.

16.8 SBRT APBI Preliminary Outcomes

Since June 2009 we treated 21 patients with early breast cancers. Two patients received our initial dose prescription of 30 Gy in 5 fractions and the remaining 19 received a total dose of 34 Gy in 10 fractions as described above. All patients are followed every 6 months for the first 3 years with alternating mammograms and breast MRI's and annually thereafter. No patients have been lost to follow-up. At a

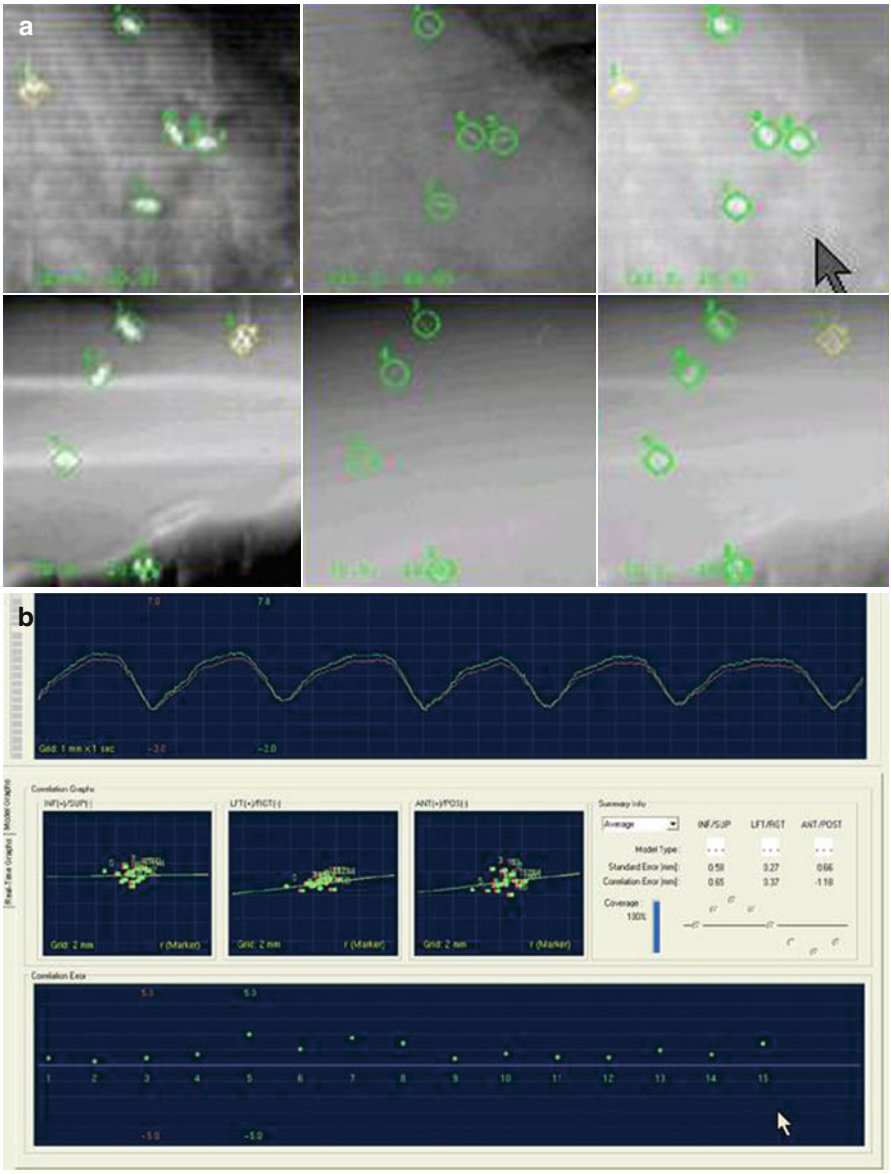

Fig. 16.5 Multiple fiducial markers are used in the breast for patient setup prior to each treatment and during the delivery of CyberKnife APBI. The fiducial markers are tracked continuously during treatment unlike in other APBI external beam techniques. (Panel **a**) The *top and bottom rows* of images show the radiographs from 2 kV imagers. The first column of images shows the fiducial marker generated digitally reconstructed radiograph (DRR) obtained via CT simulation, the second column shows the radiographs of the fiducial markers from the kilovolt x-ray imagers at the time of treatment, and the third column shows the overlaying of fiducial markers from the DRR and kilovolt imagers. The sub-millimeter matching of at least three fiducial markers is required for treatment delivery. (Panel **b**) The *top row* represents the patient's respiratory pattern obtained using LED marker placed on the patient's chest. The *middle row* shows the average movement of the target in the three translational directions. The *bottom row* shows the vector sum of the target movement as a function of time

median follow-up of 31 months (range: 6–57 months), no breast cancer recurrence has been identified. Acute toxicities were minimal, with erythema involving a small portion of the breast reported by two patients and mild fatigue observed by half of the patients. The size, shape and texture of the treated breast was compared to the breast's original appearance after surgery and from pictures taken at the time of simulation. Cosmetic outcome was assessed using the four-point cosmetic rating scale of the NSABP/RTOG protocol [50] whereby an excellent outcome was defined as "minimal or no difference"; a good cosmesis was defined as "a slight difference"; and a fair or poor cosmesis was defined as "obvious differences . . . involving a quarter or less of the breast" or "as marked change. . . . involving more than a quarter of the breast tissue". Using these definitions, all 14 treated patients had excellent or good cosmesis with no patients having a fair or poor cosmesis. Based on these preliminary results we are optimistic that with stereotactic tracking ability and a low prescription isodose, issues involving patient motion, set-up reproducibility and toxicity are of less concern with SBRT APBI than for patients receiving 3D-CRT. Indeed, the PTV in our patient series is similar to that seen in patients treated with multi-catheter or balloon catheter brachytherapy. The mean ipsilateral breast volumes receiving 100 and 50 % of the prescribed dose were less than half that allowable in the NSABP/RTOG study. With mild and limited side effects and excellent/good cosmetic outcomes in our patient population, our preliminary results suggest that CyberKnife delivered SBRT APBI is a suitable non-invasive approach for delivering accelerated partial breast irradiation which meets the normal tissue constraints outlined in national protocols.

16.9 Discussion

Evolving data from the brachytherapy APBI experience indicate early breast cancer local and regional recurrences are rare outside the PTV [29]. Unfortunately, brachytherapy is difficult to perform, uncomfortable for the patient and carries an infection risk. Proponents of brachytherapy argue, however, that 3D-CRT and IMRT require larger treatment volumes for adequate coverage of the PTV. The CyberKnife could bridge a compromise between both techniques, offering a dose profile which mimics brachytherapy without the large PTV requirement of 3D-CRT and IMRT.

The increased PTV volumes in the NSABP trials are a growing concern for its effect on breast cosmesis [50]. The study from the University of Michigan reported unacceptable outcomes when the IMRT V50 and V100 were greater than 46 and 23 %, respectively [45]. Both Jagsi et al. and Hepel et al., from the Tufts University, concluded that the NSABP/RTOG trial's normal dose limitation led to a larger than acceptable number of patients developing subcutaneous fibrosis [44, 45]. A stricter dose volume limit was suggested by both authors for a more acceptable outcome. Our mean target volume for patients receiving 6 Gy in 5 fractions or 34 Gy in 10 fractions was 100 and 105 cm^3, respectively. These volumes were well below the accepted volume in the study by Jagsi et al. of 185.8 cm^3.

In the NSAPB/RTOG trial, the PTV evaluation for patients receiving 3D-CRT is 25 mm or more when considering coverage of the penumbra to adequately cover the 15-mm risk zone for microscopic tumor. Unlike the 3D-CRT coverage in the national trial, the CyberKnife does not require the additional 10 mm to compensate for patient breathing motion or treatment set up variability. In addition, the low prescription isodose (mean and range 70 %) and large number of beams (mean 157, range 112–182) used in CyberKnife APBI at our center resulted in a smaller volume of normal tissue receiving a significant dose. Specifically, the mean ipsilateral breast volume receiving 100 and 50 % of the prescribed dose (V100, V50) in our study was less than half of the allowable volume in the NSABP/RTOG protocol: 13 % versus <35 % and 28 % versus <60 %. Patel et al. [54] compared the V50 and V100 of APBI with 3DCRT versus interstitial brachytherapy. Both were reported to be significantly larger for their patients receiving 3D-CRT than for the implant: 26 % versus 12 % and 52 % versus 24 %, respectively. Similar to brachytherapy, CyberKnife APBI delivers a relatively steep dose gradient within and outside the target volume when the dose maximum is placed inside the seroma of the lumpectomy cavity. Our hypothesis is that the small treatment volumes coupled with the steep dose gradient using CyberKnife APBI will result in low toxicity including acceptable cosmetic outcomes.

16.10 Conclusions

There is now a plethora of APBI techniques for women with early breast cancer to consider. APBI delivered by SBRT is currently under investigation at many centers including a dose escalation Phase I trial at the University of Texas Southwestern Medical Center [30]. SBRT offers patients the delivery ease of external beam radiotherapy (reproducibility factor) without the protracted time commitment seen with WBI (convenience factor). In addition, SBRT offers increased accuracy of irradiation delivery (target precision factor) without the inherent invasiveness (quality-of-life factor) of a brachytherapy implant. These SBRT abilities will likely increase the number of BCT candidates for APBI, particularly those patients with difficult to treat anatomy (large/pendulous breasts), busy working women, elderly or disabled patients and those who live far from a radiation therapy clinics. Needless to say, in-breast tumor recurrence is the primary endpoint of APBI studies with quality of life endpoints including cosmesis, breast-related symptoms, fatigue and perceived convenience of care having equal importance. Continued follow-up is needed to confirm, regardless of the techniques used, that these APBI goals and objectives are met. For now, it is advised that all patients considering ABPI techniques submit to national or Investigational Review Board (IRB) approved institutional studies. Off-study patients should be advised of the ASTRO eligibility guidelines published in 2009 for women considering ABPI [48]. Hopefully, this new modality can increase the number of patients seeking BCT while improve the quality of life in those receiving post-operative radiation as part of their BCT.

References

1. National Institutes of Health, NIH Consensus Statement, Treatment of early stage breast cancer. 1990; 8:1–19.
2. Fisher B, Anderson S, Bryant J, Margolese RG, Deutsch M, Fisher ER, et al. Twenty-year follow-up of a randomized trial comparing total mastectomy, lumpectomy, and lumpectomy plus irradiation for the treatment of invasive breast cancer. N Engl J Med. 2002;347:1233–41.
3. Jacobson JA, Danforth DN, Cowan KH, d'Angelo T, Steinberg SM, Pierce L, et al. Ten-year results of a comparison of conservation with mastectomy in the treatment of stage I and II breast cancer. N Engl J Med. 1995;332:907–11.
4. van Dongen JA, Voogd AC, Fentiman IS, Legrand C, Sylvester RJ, Tong D, et al. Long-term results of a randomized trial comparing breast-conserving therapy with mastectomy: European Organization for Research and Treatment of Cancer 10801 trial. J Natl Cancer Inst. 2000;92:1143–50.
5. Blichert-Toft M, Rose C, Andersen JA, Overgaard M, Axelsson CK, Andersen KW, et al. Danish randomized trial comparing breast conservation therapy with mastectomy: six years of life-table analysis. Danish Breast Cancer Cooperative Group. J Natl Cancer Inst Monogr. 1992:19–25. http://www.ncbi.nlm.nih.gov/pubmed/1627427.
6. Veronesi U, Cascinelli N, Mariani L, Greco M, Saccozzi R, Luini A, et al. Twenty-year follow-up of a randomized study comparing breast-conserving surgery with radical mastectomy for early breast cancer. N Engl J Med. 2002;347:1227–32.
7. Sarrazin D, Le MG, Arriagada R, Contesso G, Fontaine F, Spielmann M, et al. Ten-year results of a randomized trial comparing a conservative treatment to mastectomy in early breast cancer. Radiother Oncol. 1989;14:177–84.
8. Effects of radiotherapy and surgery in early breast cancer. An overview of the randomized trials. Early Breast Cancer Trialists' Collaborative Group. N Engl J Med. 1995;333:1444–55.
9. National Cancer Institute. Cancer trends progress report—2005 update. Bethesda: NIH, DHHS; 2005.
10. Clark RM, McCulloch PB, Levine MN, Lipa M, Wilkinson RH, Mahoney LJ, et al. Randomized clinical trial to assess the effectiveness of breast irradiation following lumpectomy and axillary dissection for node-negative breast cancer. J Natl Cancer Inst. 1992;84:683–9.
11. Vicini FA, Kestin L, Chen P, Benitez P, Goldstein NS, Martinez A. Limited-field radiation therapy in the management of early-stage breast cancer. J Natl Cancer Inst. 2003;95:1205–10.
12. Vicini FA, Kestin LL, Goldstein NS. Defining the clinical target volume for patients with early-stage breast cancer treated with lumpectomy and accelerated partial breast irradiation: a pathologic analysis. Int J Radiat Oncol Biol Phys. 2004;60:722–30.
13. Fan J, Hayes S, Freedman G, Anderson P, Li J, Wang L, et al. Planning the breast boost: dosimetric comparison of CyberKnife, photo mini tangents, IMRT, and electron techniques. Int J Radiat Oncol Biol Phys. 2010;78:S3306.
14. Heinzerling JH, Ding C, Ramirez E, Chang K, Anderson JF, Edwards CM, et al. Comparative dose-volume analsysis for CyberKnife and 3D conformal partial breast irradiation treatment of early stage breast cancer. Int J Radiat Oncol Biol Phys. 2010;78:S3390.
15. Fisher B, Bryant J, Dignam JJ, Wickerham DL, Mamounas EP, Fisher ER, et al. Tamoxifen, radiation therapy, or both for prevention of ipsilateral breast tumor recurrence after lumpectomy in women with invasive breast cancers of one centimeter or less. J Clin Oncol. 2002;20:4141–9.
16. Hughes KS, Schnaper LA, Berry D, Cirrincione C, McCormick B, Shank B, et al. Lumpectomy plus tamoxifen with or without irradiation in women 70 years of age or older with early breast cancer. N Engl J Med. 2004;351:971–7.
17. Veronesi U, Luini A, Del Vecchio M, Greco M, Galimberti V, Merson M, et al. Radiotherapy after breast-preserving surgery in women with localized cancer of the breast. N Engl J Med. 1993;328:1587–91.
18. Forrest AP, Stewart HJ, Everington D, Prescott RJ, McArdle CS, Harnett AN, et al. Randomised controlled trial of conservation therapy for breast cancer: 6-year analysis of the Scottish trial. Scottish Cancer Trials Breast Group. Lancet. 1996;348:708–13.

19. Favourable and unfavourable effects on long-term survival of radiotherapy for early breast cancer: an overview of the randomised trials. Early Breast Cancer Trialists' Collaborative Group. Lancet. 2000;355:1757–70.
20. Uppsala Breast Cancer Study Group. Sector resection with or without postoperative radiotherapy for stage I breast cancer: a randomized trial. J Natl Cancer Inst. 1990;82:277–82.
21. Clarke M, Collins R, Darby S, Davies C, Elphinstone P, Evans E, et al. Effects of radiotherapy and of differences in the extent of surgery for early breast cancer on local recurrence and 15-year survival: an overview of the randomised trials. Lancet. 2005;366:2087–106.
22. Rosen PP, Fracchia AA, Urban JA, Schottenfeld D, Robbins GF. "Residual" mammary carcinoma following simulated partial mastectomy. Cancer. 1975;35:739–47.
23. Holland R, Connolly JL, Gelman R, Mravunac M, Hendriks JH, Verbeek AL, et al. The presence of an extensive intraductal component following a limited excision correlates with prominent residual disease in the remainder of the breast. J Clin Oncol. 1990;8:113–8.
24. Liljegren G, Holmberg L, Adami HO, Westman G, Graffman S, Bergh J. Sector resection with or without postoperative radiotherapy for stage I breast cancer: five-year results of a randomized trial. Uppsala-Orebro Breast Cancer Study Group. J Natl Cancer Inst. 1994;86:717–22.
25. Fisher ER, Sass R, Fisher B, Gregorio R, Brown R, Wickerham L. Pathologic findings from the National Surgical Adjuvant Breast Project (protocol 6). II. Relation of local breast recurrence to multicentricity. Cancer. 1986;57:1717–24.
26. Fowble B, Solin LJ, Schultz DJ, Rubenstein J, Goodman RL. Breast recurrence following conservative surgery and radiation: patterns of failure, prognosis, and pathologic findings from mastectomy specimens with implications for treatment. Int J Radiat Oncol Biol Phys. 1990;19:833–42.
27. Veronesi U, Salvadori B, Luini A, Banfi A, Zucali R, Del Vecchio M, et al. Conservative treatment of early breast cancer. Long-term results of 1232 cases treated with quadrantectomy, axillary dissection, and radiotherapy. Ann Surg. 1990;211:250–9.
28. Faverly DR, Hendriks JH, Holland R. Breast carcinomas of limited extent: frequency, radiologic-pathologic characteristics, and surgical margin requirements. Cancer. 2001;91:647–59.
29. King TA, Bolton JS, Kuske RR, Fuhrman GM, Scroggins TG, Jiang XZ. Long-term results of wide-field brachytherapy as the sole method of radiation therapy after segmental mastectomy for T(is,1,2) breast cancer. Am J Surg. 2000;180:299–304.
30. Polgar C, Sulyok Z, Fodor J, Orosz Z, Major T, Takacsi-Nagy Z, et al. Sole brachytherapy of the tumor bed after conservative surgery for T1 breast cancer: five-year results of a phase I-II study and initial findings of a randomized phase III trial. J Surg Oncol. 2002;80(3):121–8; discussion 9.
31. Perera F, Engel J, Holliday R, Scott L, Girotti M, Girvan D, et al. Local resection and brachytherapy confined to the lumpectomy site for early breast cancer: a pilot study. J Surg Oncol. 1997;65(4):263–7; discussion 7–8.
32. Vicini FA, Baglan KL, Kestin LL, Mitchell C, Chen PY, Frazier RC, et al. Accelerated treatment of breast cancer. J Clin Oncol. 2001;19:1993–2001.
33. Arthur DW, Winter K, Kuske RR, Bolton J, Rabinovitch R, White J, et al. A Phase II trial of brachytherapy alone after lumpectomy for select breast cancer: tumor control and survival outcomes of RTOG 95–17. Int J Radiat Oncol Biol Phys. 2008;72(2):467–73.
34. Keisch M, Vicini F, Kuske RR, Hebert M, White J, Quiet C, et al. Initial clinical experience with the MammoSite breast brachytherapy applicator in women with early-stage breast cancer treated with breast-conserving therapy. Int J Radiat Oncol Biol Phys. 2003;55:289–93.
35. Wazer DE, Berle L, Graham R, Chung M, Rothschild J, Graves T, et al. Preliminary results of a phase I/II study of HDR brachytherapy alone for T1/T2 breast cancer. Int J Radiat Oncol Biol Phys. 2002;53(4):889–97.
36. Arthur DW, Koo D, Zwicker RD, Tong S, Bear HD, Kaplan BJ, et al. Partial breast brachytherapy after lumpectomy: low-dose-rate and high-dose-rate experience. Int J Radiat Oncol Biol Phys. 2003;56(3):681–9.
37. Fentiman IS, Poole C, Tong D, Winter PJ, Gregory WM, Mayles HM, et al. Inadequacy of iridium implant as sole radiation treatment for operable breast cancer. Eur J Cancer. 1996;32A(4):608–11.

38. Lawenda BD, Taghian AG, Kachnic LA, Hamdi H, Smith BL, Gadd MA, et al. Dose-volume analysis of radiotherapy for T1N0 invasive breast cancer treated by local excision and partial breast irradiation by low-dose-rate interstitial implant. Int J Radiat Oncol Biol Phys. 2003;56(3):671–80.
39. Baglan KL, Sharpe MB, Jaffray D, Frazier RC, Fayad J, Kestin LL, et al. Accelerated partial breast irradiation using 3D conformal radiation therapy (3D-CRT). Int J Radiat Oncol Biol Phys. 2003;55(2):302–11.
40. Formenti SC, Truong MT, Goldberg JD, Mukhi V, Rosenstein B, Roses D, et al. Prone accelerated partial breast irradiation after breast-conserving surgery: preliminary clinical results and dose-volume histogram analysis. Int J Radiat Oncol Biol Phys. 2004;60(2):493–504.
41. Veronesi U, Orecchia R, Luini A, Gatti G, Intra M, Zurrida S, et al. A preliminary report of intraoperative radiotherapy (IORT) in limited-stage breast cancers that are conservatively treated. Eur J Cancer. 2001;37:2178–83.
42. Vaidya JS, Tobias JS, Baum M, Wenz F, Kraus-Tiefenbacher U, D'Souza D, et al. TARGeted Intraoperative radiotherapy (TARGIT): an innovative approach to partial-breast irradiation. Semin Radiat Oncol. 2005;15(2):84–91.
43. Vicini F, Beitsch P, Quiet C, Gittleman M, Zannis V, Fine R, et al. Five-year analysis of treatment efficacy and cosmesis by the American Society of Breast Surgeons MammoSite Breast Brachytherapy Registry Trial in patients treated with accelerated partial breast irradiation. Int J Radiat Oncol Biol Phys. 2011;79:808–17.
44. Hepel JT, Tokita M, MacAusland SG, Evans SB, Hiatt JR, Price LL, et al. Toxicity of three-dimensional conformal radiotherapy for accelerated partial breast irradiation. Int J Radiat Oncol Biol Phys. 2009;75:1290–6.
45. Jagsi R, Ben-David MA, Moran JM, Marsh RB, Griffith KA, Hayman JA, et al. Unacceptable cosmesis in a protocol investigating intensity-modulated radiotherapy with active breathing control for accelerated partial-breast irradiation. Int J Radiat Oncol Biol Phys. 2010;76:71–8.
46. Patel RR, Christensen ME, Hodge CW, Adkison JB, Das RK. Clinical outcome analysis in "high-risk" versus "low-risk" patients eligible for national surgical adjuvant breast and bowel B-39/radiation therapy oncology group 0413 trial: five-year results. Int J Radiat Oncol Biol Phys. 2008;70:970–3.
47. Kilby W, Dooley JR, Kuduvalli G, Sayeh S, Maurer Jr CR. The CyberKnife robotic radiosurgery system in 2010. Technol Cancer Res Treat. 2010;9:433–52.
48. Smith BD, Arthur DW, Buchholz TA, Haffty BG, Hahn CA, Hardenbergh PH, et al. Accelerated partial breast irradiation consensus statement from the American Society for Radiation Oncology (ASTRO). Int J Radiat Oncol Biol Phys. 2009;74:987–1001.
49. Weed DW, Yan D, Martinez AA, Vicini FA, Wilkinson TJ, Wong J. The validity of surgical clips as a radiographic surrogate for the lumpectomy cavity in image-guided accelerated partial breast irradiation. Int J Radiat Oncol Biol Phys. 2004;60:484–92.
50. NSABP B-39, RTOG 0413: A Randomized Phase III Study of conventional whole breast irradiation versus partial breast irradiation for women with stage 0, I, or II breast cancer. Clin Adv Hematol Oncol. 2006;4(10):719–21.
51. Formenti SC. External-beam partial-breast irradiation. Semin Radiat Oncol. 2005;15:92–9.
52. Bentzen SM, Agrawal RK, Aird EG, Barrett JM, Barrett-Lee PJ, Bliss JM, et al. The UK Standardisation of Breast Radiotherapy (START) Trial A of radiotherapy hypofractionation for treatment of early breast cancer: a randomised trial. Lancet Oncol. 2008;9:331–41.
53. Bentzen SM, Agrawal RK, Aird EG, Barrett JM, Barrett-Lee PJ, Bliss JM, et al. The UK Standardisation of Breast Radiotherapy (START) Trial B of radiotherapy hypofractionation for treatment of early breast cancer: a randomised trial. Lancet. 2008;371:1098–107.
54. Patel RR, Becker SJ, Das RK, Mackie TR. A dosimetric comparison of accelerated partial breast irradiation techniques: multicatheter interstitial brachytherapy, three-dimensional conformal radiotherapy, and supine versus prone helical tomotherapy. Int J Radiat Oncol Biol Phys. 2007;68:935–42.

Chapter 17
Stereotactic Body Radiotherapy for Bone and Soft Tissue Sarcoma

Mary Ann Stevenson, Anand Mahadevan, Megan E. Anderson, and Anna Cassoni

Abstract Sarcomas are considered radioresitant and surgery has remained the primary treatment. Adjuvant radiation in the pre and post-operative setting has been shown to improve local control. When adjacent normal tissues limit radiation dose, particularly in the recurrent and metastatic setting, conformal radiation techniques like Stereotactic Body Radiotherapy (SBRT), could be a useful treatment modality. This Chapter discusses the role of SBRT in the treatment of soft tissue sarcomas.

Keywords Soft tissue Sarcoma • Radioresistant • Stereotactic body radiotherapy

17.1 Introduction

The American Cancer Society estimates that over 11,300 new cases of soft tissue sarcoma (STS) will be diagnosed in the United States in 2012 with more than 3,900 patients dying of this disease [1]. In addition another 2,900 will be afflicted with cancers of the bone and joints with 1,400 of them dying from it. Surgery with or without adjuvant radiation remains the cornerstone of therapy and with systemic therapy largely being reserved for metastatic disease. Bone and soft tissue sarcoma is historically considered a "radioresistant" tumor because conventionally fractionated radiation treatments have not been shown to be effective as primary treatment for this disease. Moreover, they may arise in virtually any anatomical site, are uncommon tumors and large studies are largely absent and numbers relating to any

M.A. Stevenson, MD, PhD • A. Mahadevan, MD, FRCS, FRCR (✉)
Department of Radiation Oncology, Beth Israel Deaconess Medical Center, Harvard Medical School, Boston, MA, USA
e-mail: amahadev@bidmc.harvard.edu

M.E. Anderson, MD
Department of Orthopedic Surgery, Beth Israel Deaconess Medical Center, Harvard Medical School, Boston, MA, USA

A. Cassoni, FRCR
Department of Clinical Oncology, University College London Hospitals, London, UK

A. Gaya, A. Mahadevan (eds.), *Stereotactic Body Radiotherapy: A Practical Guide*,
DOI 10.1007/978-0-85729-597-2_17

particular site or type, very small or anecdotal. Delivery of high doses of radiation has been limited by the tolerance of normal tissue surrounding the tumor. The development of radiosurgery—allowing an accurate delivery of high doses of radiation to a tumor while maximally sparing surrounding normal organs—may allow the radioresistance of sarcomas to be overcome. This may be particularly true for localized unresectable disease, recurrent disease, as a boost to adjuvant radiation and for limited metastatic disease. This chapter will give a background to these aspects of the disease, whereas data on dose fractionation and outcomes for radiosurgery is limited, extrapolation from other radiation treatment techniques will be presented. Limited clinical experience using radiosurgery to treat metastatic sites of sarcoma as well as early experience using radiosurgery for primary unresectable sarcomas appear promising and justify further study of this treatment approach.

17.2 Background and Rationale

There are many different subtypes, which, for the purposes of discussion can be divided, broadly, into primaries in bone and those arising in soft tissues. They can present at any age, but the age range and site within the body on presentation vary with the histological type, as do the natural history and sensitivity to chemotherapy and radiotherapy. The majority of primaries are in the limbs although there are substantial subgroups within the abdomen and pelvis, base of skull, spine and head and neck.

Types such as osteosarcoma, Ewing's, and rhabdomyosarcoma in the young have a high risk of metastatic disease at presentation, with clear benefit for the use of intensive chemotherapy regimens. In contrast, the natural course of chondrosarcoma and chordoma is dominated by local regional failure and dissemination tends to be a late manifestation and chemotherapy, at present, has no prominent role in these two types. Soft tissue sarcoma of adult type is somewhat intermediate, with 30–70 % eventually manifesting metastases and an intermediate chemosensitivity.

17.3 Radiation Therapy for Sarcoma

The primary treatment of STS patients is surgery. The wider the local excision, the lower the probability of local failure and amputations are seldom necessary. Adjuvant RT is offered in addition to limb-sparing surgery to optimize local control. Two prospective randomized trials have shown significant improvement in local control by the addition of adjuvant RT to limb-sparing surgery [2, 3]. One study used external beam RT (EBRT), randomizing 141 patients (91 with high-grade tumors, 50 with low-grade tumors) to receive or not receive postoperative RT. Patients with high-grade tumors also received chemotherapy. The actuarial local failure rate at 10 years in the high-grade tumors was 0 % for the RT group and 22 % for the no RT group (P = .0001). Benefit was also seen in the low-grade tumors (P = .003) [2].

A second study evaluated postoperative brachytherapy (BRT), randomizing 164 patients to BRT or no additional treatment. The actuarial estimate of freedom from local recurrence at 60 months was 82 and 69 % for the BRT and no BRT groups, respectively (P = .04) [3]. A third trial addressed the influence of preoperative vs. postoperative EBRT comparing 50 Gy in 25 fractions preoperatively and 66 Gy in 33 fractions postoperatively [4]. While improved treatment compliance resulted in slightly better overall survival, there were more wound related complications associated with preopertaive RT. Subsequent analysis revealed no difference in overall survival between pre and postoperative cohorts, however, late radiation morbidity was more significant in patients who received postoperative RT [5].

Evidence from systematic reviews [6, 7] strong strongly suggest that adjuvant RT improves local control combined with conservative surgery in the treatment of ESTS and trunk sarcomas in patients with negative, marginal, or minimally microscopically positive surgical margins. Furthermore, an analysis of 6,960 patients in the Surveillance, Epidemiology, and End Results database has demonstrated a survival benefit for the addition of RT to surgery in ESTSs, especially for large, high-grade sarcomas [8].

Interstitial BRT has been demonstrated to be an effective method of delivering adjuvant RT, within a considerably shorter treatment time than EBRT, and with potentially smaller treatment volumes. However, it is a complex and labor-intensive technique, hence, its relatively limited use. A report by Alektiar et al. demonstrated a 5-year local control rate of 83 %, which seemed lower than the rates achieved in EBRT series [9].

High-dose photon irradiation (50–70 Gy) can be used in combination with aggressive chemotherapy when tumors are located in surgically inaccessible sites such as the pelvic bone, vertebral column, and base of the skull. Chondrosarcomas and chordomas, considered relatively more radiotherapy resistant among sarcomas, are particularly amenable for such radiation techniques. Local control rates of 85–100 % with mixed photon/proton or proton-only protocols (doses up to 79 cobalt Gray equivalents) have been reported [10–12].

Radiotherapy can be considered after incomplete resection, aiming at maximal local control (curative) and in situations where resection is not feasible or would cause unacceptable morbidity (palliative). These are also sites where radiotherapy, even in conventional doses may not be possible. Margin negative surgery is a major factor in local control, survival and the adverse effect of a positive margin, while improved by radiotherapy is not eliminated [13]. For curative intentions, doses >60 Gy or equivalent are required to achieve local control.

There is some data on dose/response for unresected soft tissue sarcoma with conventional external beam radiotherapy. Doses of greater than 63 Gy were associate with local control rate of 60 % compared with 22 % at lower doses [14]. Proton therapy to doses of 69 CGy are reported to produce 74 % 4 year local control [15]. The relationship of control to residual volume is clear from many of the larger series. The largest such series suggest that local control rate overall may be 50 % in tumor not more than 5 cm, falling lower in larger tumors [14]. In patients with chordoma and chondrosarcoma treated with doses of 65 Gy by IMRT resulting in

an overall 5 years local control rate of 83 %, a GTV (Gross Tumor Volume) of not more than 30 cc was predictive of higher control [10]. Whilst calculation based on the linear quadratic equation may not be reliable at low fraction numbers these data may inform the dose selection for stereotactic radiotherapy. Robust dose/volume response relationship for stereotactic radiotherapy and radiosurgery is not yet available from the literature, but volume treated clearly needs to be considered in patient selection and interpretation of results.

17.4 Stereotactic Body Radiotherapy (SBRT) for Sarcoma

Specific data on soft tissue sarcoma treated by stereotactic techniques is limited with reports being anecdotal at particularly difficult sites or with lesions reported as part of larger series. Such tumors have usually been treated on institutional protocols with no evidence, to date, of a different effectiveness in local control although the value of that clearly varies with the natural history and of the tumor type and patient selection [16, 17].

SBRT not only allows the delivery of high Biologically Equivalent Dose (BED) in excess of 65 Gy to paraspinal, spinal and other unresectable sarcomas, and also allows the dose to be hypofractionated. This may potentially be an advantage if the assumption of a low α/β ratio for sarcomas is true. When normal tissue toxicity limits the dose of conventional radiation, which can be delivered, SBRT provides an attractive option.

There has been stereotactic radiosurgery (SRS) experience in skull base and spinal chondrosarcomas in the last two decades. Single fraction SRS with marginal doses of 14–18 Gy achieving 50–80 % 5–10 year control rates have been reported for primary and recurrent chordomas and chondrosarcomas [18–21]. More limited short term outcomes with fractionated SBRT in spinal sarcomas have also been recently reported [22, 23]. SBRT has also proved to be useful anecdotally in unusual sarcomas in critical locations [24–26].

17.4.1 Metastatic Sarcoma

The most common primary site for metastatic disease is the lung, with bone less common; intracranial, liver and other soft tissue deposits are uncommon and are rarely isolated. The mean survival after development of secondary disease is 18 months but with a fairly wide range. Overall a longer disease free interval predicts for a longer survival after development of secondary metastases.

The best evidence base for local treatment is for lung metastases where there is an extensive surgical literature suggesting survival at 5 years of 25–50 % for soft tissue sarcoma and 34–50 % in osteosarcoma in selected patients [27] who underwent metastatectomy. The consistent factor suggestive of a better outcome are:—disease free interval from initial presentation to development of metastases

(12–18 months), with other prognostic factors reported as number of metastases (not more than 5) and, possibly, size of largest metastasis [27–29]. More limited literature suggests an equivalent outcome for RFA with 1 and 2 years PFS of the order of 50–55 and 20–35 % respectively [30]. Stereotactic radiotherapy for pulmonary sarcoma metastases has been reported by a number of authors, has been is associated with a local control rate of 90 % at 2 years and 85 % at 3 year with marginal doses of 50–60 Gy in 4–6 fractions and a survival comparable to surgical series of 75 and 63 % at 2 and 3 years respectively [31]. The development of bone metastases in sarcoma is usually associated with a limited prognosis (median 6 months) and the usual aim of local therapy is palliation. The evidence for radiosurgery in such tumors, within larger series of spinal metastases suggests an equivalent control to other tumor types [32].

17.4.2 Cerebral Metastases

These are relatively uncommon in sarcoma. There is a small literature on radiosurgery in their management. Most suggests equivalent local control to that in other tumor types. One study of 21 patients with intracerebral deposits treated with single fraction radiotherapy—a mean volume of 6.2 cm, and median marginal dose of 16Gy reported 88 % local control with 1 year survival of 61 % but high incidence of subsequent other intracerebral lesions with or without whole brain radiotherapy [33]. However in another study, patients with sarcoma (median volume 1.6 cm, median marginal dose 18Gy)-did significantly worse than other relatively resistant types, possibly because of the high incidence of further lesions [34].

17.5 Patient Selection

Patients with histological or radiologically confirmed sarcoma which are unresectable, recurrent or oligometastatic are candidates for SBRT. Lesions in difficult locations precluding excisional surgery & high dose conventionally fractionated radiation are particularly good candidates.

In summary stereotactic radiotherapy may have a role in the following circumstances:

- inoperable tumors in critical sites;
- small tumors following surgery with gross or microscopic residual disease where adjuvant radiotherapy is limited by normal tissue toxicity of critical structures;
- recurrent sarcoma— at primary site;
- metastatic;
- and especially in tumor types particularly resistant to radiotherapy—chordoma, chondrosarcoma, osteosarcoma—exploiting the higher biological dose that can be given by these techniques.

Many SBRT systems utilize fiducial markers for respiratory and motion tracking (e.g. Cyberknife). Inability to place fiducials, due to patient anatomy or bleeding diathesis, may prove to be relative contraindications for the procedure, unless other image guided techniques or immobilization is implemented. Large central abdominal tumors, with limited renal function may be relative contraindications.

17.6 Treatment Planning and Delivery

The decision between single fraction radiosurgery and more fractionated stereotactic dose/fractionation will depend on tumor size and proximity to sensitive structures, such as spinal cord or previously irradiated tissue (especially neural or mediastinal). Whilst base of skull and spinal and paraspinal lesions may be localized with image guided tracking, soft tissue deposits will require fiducial placement as for other tumors at these sites. Poor respiratory reserve, bleeding diathesis and other significant co-morbidities may prelude treatment. Particular sites, such as those in or adjacent to heart and pulmonary vessels may be amenable to coordination with the cardiac cycle.

Simulation is usually in a supine position with reproducible immobilization, usually in a comfortable vacuum device. IV contrast is beneficial in accurate visualization of the target and organs at risk. Optional sequences based on the system used are, arms up and down, inspiration-expiration and 4D CT. Respiratory dampening and respiratory gating to account for motion management may need special procedures. Fusion of the planning CT scan with recent MRI, or PET images may assist target definition. Performance of these diagnostic images in the treatment position and on a therapy couch will facilitate fusion and minimize error in co-registration. Where target is close to or into the spinal canal CT myelogram may add to localization of the spinal cord.

Once the image set with fusion is available, the next step is to delineate the target volume. The GTV (Gross Tumor Volume), CTV (Clinical Target Volume—based on predicted microscopic extension of the tumor) are defined. Though the main tumor mass = often appears well defined/encompassed by a pseudocapsule, tumor cells have been found at some distance from the main tumor mass within "peritumoral edema" as defined by the high T2 weighted signal changes surrounding the primary soft tissue sarcoma [35]. Thus PTV should include both the primary mass as well as surrounding area of increased T2signal intensity. Data on secondaries are limited but it would appear that metastases are well defined with minimal infiltration into adjacent parenchyma. The expansion for PTV (Planning target volume) is often described differently with different systems. With fiducial based continuous live motion tracking (e.g. Cyberknife) the GTV may be considered the PTV, but generally a few mm may be added. The pixel size of the CT scan should be taken into account when growing margin On the other hand with gating and respiratory dampening increasing margins are required to achieve target coverage with the prescribed dose- typically 3–5 mm.

Organs at risk are identified–Typically when treating in 3 fractions, the recommended dose constraints for organs at risk are as follows: Spinal cord: Limited to 6 Gy per fraction, maximum total point dose to spinal cord of 18 Gy; Stomach: Limited to 8 Gy per fraction (allow up to 3 cc of stomach to receive this dose) and a maximum point dose of 30 Gy; Liver: At least 700 cc of liver receiving less than 7 Gy total dose with V15 and V21 <50 % and 30 % respectively; Small and Large Bowel: Limited to 8 Gy × 3 (to 1 cc) and a maximum point dose of 10 Gy × 3; <30 % of one kidney receiving 15 Gy.

Typical prescription doses range from 15–16 Gy × 3 = 45–48 Gy for smaller tumors (<5 cm) and 12 Gy × 4 = 48 Gy for larger tumors. Dose fractionation is often modified to meet normal tissue constraints; varying from 5–6 Gy × 5 to 16–18 Gy × 3. The prescription dose will be to the percentage isodose volume that encompasses the PTV; typically 95 % of the PTV receives the prescribed dose. The plan will be constructed so that the chosen prescription percentage isodose volume is left to the discretion of the treating physician but is expected to fall generally in the range of 60–80 %. Treatments may be delivered in 3 consecutive or alternate days.

A representative treatment plan is shown in Fig. 17.1.

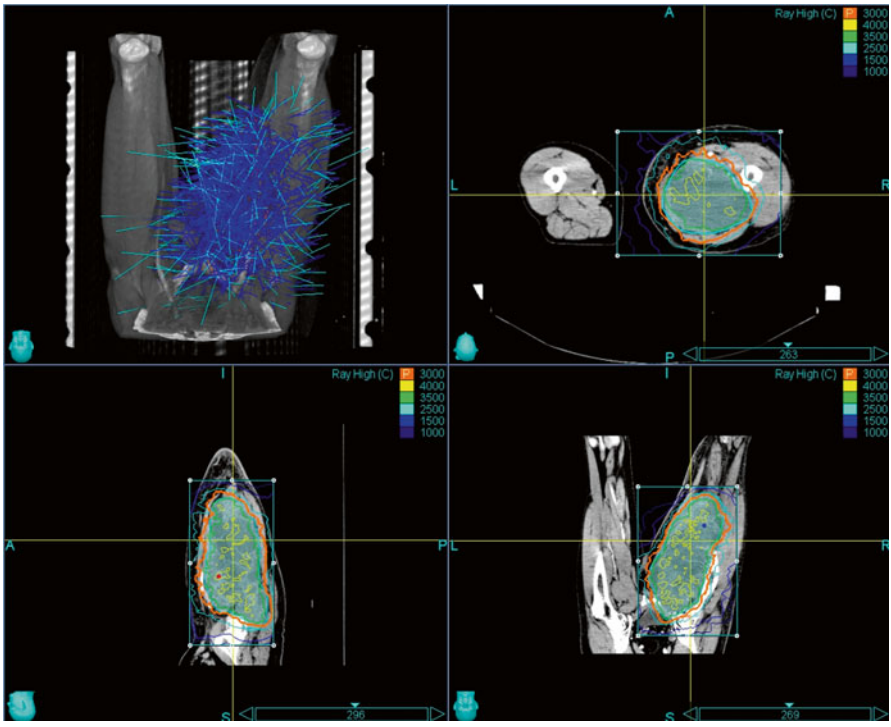

Fig. 17.1 Representative treatment plan of recurrent soft tisuue sarcoma SBRT reirradiation using the Cyberknife™ technique

17.7 Toxicity

Patients will need to be monitored during the treatment course with documentation of acute toxicity. No treatment related toxicities are usually seen other than mild fatigue. Brisk skin reaction can be anticipated with extremity superficial sarcomas. Fibrosis and lymphedema are long term concerns. Nausea has been reported in abdominal sarcomas and is managed conservatively with prophylactic or therapeutic antiemetics.

17.8 Post Treatment Care

Periodic clinical and radiological follow up is warranted based on institutional protocol. A 1 month baseline toxicity and response assessment clinical follow up and MRI, followed by 3–6 month assessment in the first couple of years and less often thereafter is advised. Adverse events and radiological assessments need to be carefully monitored and recorded.

17.9 Future Directions

The role of SBRT for sarcomas is evolving. Systematic study on prospective studies are warranted to assess comparative effectiveness, toxicity, cost benefit and quality of life benefits, Better understanding of dose fractionation and radiobiology will help define definitive role for SBRT for sarcomas.

References

1. Siegel R, Naishadham D, Jemal A. Cancer statistics, 2012. CA Cancer J Clin. 2012;62(1):10–29.
2. Yang JC, Chang AE, Baker AR, Sindelar WF, Danforth DN, Topalian SL, et al. Randomized prospective study of the benefit of adjuvant radiation therapy in the treatment of soft tissue sarcomas of the extremity. J Clin Oncol. 1998;16(1):197–203.
3. Pisters PW, Harrison LB, Leung DH, Woodruff JM, Casper ES, Brennan MF. Long-term results of a prospective randomized trial of adjuvant brachytherapy in soft tissue sarcoma. J Clin Oncol. 1996;14(3):859–68.
4. O'Sullivan B, Davis AM, Turcotte R, Bell R, Catton C, Chabot P, et al. Preoperative versus postoperative radiotherapy in soft-tissue sarcoma of the limbs: a randomised trial. Lancet. 2002;359(9325):2235–41.
5. Davis AM, O'Sullivan B, Turcotte R, Bell R, Catton C, Chabot P, et al. Late radiation morbidity following randomization to preoperative versus postoperative radiotherapy in extremity soft tissue sarcoma. Radiother Oncol. 2005;75(1):48–53.
6. Strander H, Turesson I, Cavallin-Ståhl E. A systematic overview of radiation therapy effects in soft tissue sarcomas. Acta Oncol. 2003;42(5–6):516–31.

7. Haas RLM, DeLaney TF, O'Sullivan B, Keus RB, Le Pechoux C, Olmi P, et al. Radiotherapy for management of extremity soft tissue sarcomas: why, when, and where? Int J Radiat Oncol Biol Phys. 2012;84(3):572–80.
8. Koshy M, Rich SE, Mohiuddin MM. Improved survival with radiation therapy in high-grade soft tissue sarcomas of the extremities: a SEER analysis. Int J Radiat Oncol Biol Phys. 2010;77(1):203–9.
9. Alektiar KM, Velasco J, Zelefsky MJ, Woodruff JM, Lewis JJ, Brennan MF. Adjuvant radiotherapy for margin-positive high-grade soft tissue sarcoma of the extremity. Int J Radiat Oncol Biol Phys. 2000;48(4):1051–8.
10. Potluri S, Jefferies SJ, Jena R, Harris F, Burton KE, Prevost AT, et al. Residual postoperative tumour volume predicts outcome after high-dose radiotherapy for chordoma and chondrosarcoma of the skull base and spine. Clin Oncol (R Coll Radiol). 2011;23(3):199–208.
11. Strike SA, McCarthy EF. Chondrosarcoma of the spine: a series of 16 cases and a review of the literature. Iowa Orthop J. 2011;31:154–9.
12. Chen Y-L, Liebsch N, Kobayashi W, Goldberg S, Kirsch D, Calkins G, et al. Definitive high-dose photon/proton radiotherapy for unresected mobile spine and sacral chordomas. Spine. 2013;38(15):E930–6.
13. Novais EN, Demiralp B, Alderete J, Larson MC, Rose PS, Sim FH. Do surgical margin and local recurrence influence survival in soft tissue sarcomas? Clin Orthop. 2010;468(11):3003–11.
14. Kepka L, DeLaney TF, Suit HD, Goldberg SI. Results of radiation therapy for unresected soft-tissue sarcomas. Int J Radiat Oncol Biol Phys. 2005;63(3):852–9.
15. Weber DC, Rutz HP, Bolsi A, Pedroni E, Coray A, Jermann M, et al. Spot scanning proton therapy in the curative treatment of adult patients with sarcoma: the Paul Scherrer institute experience. Int J Radiat Oncol Biol Phys. 2007;69(3):865–71.
16. Jereczek-Fossa BA, Bossi-Zanetti I, Mauro R, Beltramo G, Fariselli L, Bianchi LC, et al. CyberKnife robotic image-guided stereotactic radiotherapy for oligometastic cancer: a prospective evaluation of 95 patients/118 lesions. Strahlenther Onkol. 2013;189(6):448–55.
17. Siva S, MacManus M, Ball D. Stereotactic radiotherapy for pulmonary oligometastases: a systematic review. J Thorac Oncol. 2010;5(7):1091–9.
18. Martin JJ, Niranjan A, Kondziolka D, Flickinger JC, Lozanne KA, Lunsford LD. Radiosurgery for chordomas and chondrosarcomas of the skull base. J Neurosurg. 2007;107(4):758–64.
19. Hasegawa T, Ishii D, Kida Y, Yoshimoto M, Koike J, Iizuka H. Gamma Knife surgery for skull base chordomas and chondrosarcomas. J Neurosurg. 2007;107(4):752–7.
20. Koga T, Shin M, Saito N. Treatment with high marginal dose is mandatory to achieve long-term control of skull base chordomas and chondrosarcomas by means of stereotactic radiosurgery. J Neurooncol. 2010;98(2):233–8.
21. Iyer A, Kano H, Kondziolka D, Liu X, Niranjan A, Flickinger JC, et al. Stereotactic radiosurgery for intracranial chondrosarcoma. J Neurooncol. 2012;108(3):535–42.
22. Chang UK, Cho WI, Lee DH, Kim MS, Cho CK, Lee SY, et al. Stereotactic radiosurgery for primary and metastatic sarcomas involving the spine. J Neurooncol. 2012;107(3):551–7.
23. Castelli J, Thariat J, Benezery K, Courdi A, Chanalet S, Paquis P, et al. Spinals and paraspinals tumors treated by CyberKnife: feasibility and efficacy. Cancer Radiothér. 2010;14(1):5–10.
24. Soltys SG, Kalani MYS, Cheshier SH, Szabo KA, Lo A, Chang SD. Stereotactic radiosurgery for a cardiac sarcoma: a case report. Technol Cancer Res Treat. 2008;7(5):363–8.
25. Scheithauer BW, Silva AI, Kattner K, Seibly J, Oliveira AM, Kovacs K. Synovial sarcoma of the sellar region. Neuro Oncol. 2007;9(4):454–9.
26. Cummings M, Chowdhry V, Shah H, Back J, Kennedy GA. Recurrent meningeal sarcoma successfully treated with stereotactic radiosurgery. J Neurosurg Pediatr. 2012;10(5):434–8.
27. Treasure T, Fiorentino F, Scarci M, Møller H, Utley M. Pulmonary metastasectomy for sarcoma: a systematic review of reported outcomes in the context of Thames Cancer Registry data. BMJ Open. 2012;2(5). http://www.ncbi.nlm.nih.gov/pubmed/23048062.
28. Bedi M, King DM, Charlson J, Whitfield R, Hackbarth DA, Zambrano EV, et al. Multimodality management of metastatic patients with soft tissue sarcomas may prolong survival. Am J Clin Oncol. 2014;37(3):272–7.

29. Pfannschmidt J, Egerer G, Bischof M, Thomas M, Dienemann H. Surgical intervention for pulmonary metastases. Dtsch Ärztebl Int. 2012;109(40):645–51.
30. Koelblinger C, Strauss S, Gillams A. Outcome after radiofrequency ablation of sarcoma lung metastases. Cardiovasc Intervent Radiol. 2014;37(1):147–53.
31. Dhakal S, Corbin KS, Milano MT, Philip A, Sahasrabudhe D, Jones C, et al. Stereotactic body radiotherapy for pulmonary metastases from soft-tissue sarcomas: excellent local lesion control and improved patient survival. Int J Radiat Oncol Biol Phys. 2012;82(2):940–5.
32. Levine AM, Coleman C, Horasek S. Stereotactic radiosurgery for the treatment of primary sarcomas and sarcoma metastases of the spine. Neurosurgery. 2009;64(2 Suppl):A54–9.
33. Flannery T, Kano H, Niranjan A, Monaco 3rd EA, Flickinger JC, Kofler J, et al. Gamma knife radiosurgery as a therapeutic strategy for intracranial sarcomatous metastases. Int J Radiat Oncol Biol Phys. 2010;76(2):513–9.
34. Chang EL, Selek U, Hassenbusch 3rd SJ, Maor MH, Allen PK, Mahajan A, et al. Outcome variation among "radioresistant" brain metastases treated with stereotactic radiosurgery. Neurosurgery. 2005;56(5):936–45; discussion 936–945.
35. White IM, Wunder JS, Bell RS, et al. Histological assessment of peritumoral edema in soft tissue sarcoma. Int J Radiat Oncol Biol Phys. 2005;61(5):1439–45.

Index

A

Accelerated partial breast irradiation (APBI)
- acute and long-term reaction, 304, 305
- BCT (*see* Breast conserving therapy (BCT))
- clinical target volume, 307, 308
- CT scans and MRI images, 305, 306
- CyberKnife, 303, 308–310
- EBRT, 296–298
- ELIOT, 302
- HDR, 296–299
- IMRT, 295, 310
- interstitial brachytherapy, 299, 300, 302
- intra-operative radiotherapy, 296–298
- LDR, 296–299
- lumpectomy, 295, 299, 302, 308
- patient outcome, 308, 310
- patient selection, 304
- quality of life, 294, 311
- respiratory motion, 301
- 3D-CRT, 295, 302, 310
- treatment planning
  - clinical target volume, 307, 308
  - CT scans and MRI images, 305, 306
  - fiducial, 305–307
  - NSABP/RTOG study, 307
  - PTV, 307, 308

Active breathing control (ABC), 24, 165
American Cancer Society, 225
American Urologic Association, 226
Anisotropic analytic algorithm (AAA), 91
Arteriovenous malformations (AVMs), 116–117

B

Biologically effective dose (BED)
- biological impact, 71
- 'ceiling' dose, 71
- conventional treatment, 72
- linear radiosensitivity coefficient, 71
- LRNT, 73
- Nd, 71–72
- prediction model, 72
- reference value, 72
- single-fraction treatment, 72

Biologically equivalent dose (BED), 318
Breast conserving therapy (BCT)
- advantage, 294
- compatibility of, 294
- disadvantage, 294
- radiotherapy role, 295–296

Breath-hold methods, 133, 135

C

Chronic myeloid leukemia (CML), 233
CI. *See* Conformality index (CI)
Cleveland Clinic, 228
Clinical target volume (CTV), 75, 129, 198–199, 257, 273, 307, 308, 320
Clinical tumor volume (CTV), 99
- lung tumors, 129
- spinal radiosurgery, 118, 119

Conformality index (CI), 89
Cosmesis, 299, 301, 310, 311
CyberKnife planning, 88
CyberKnife Robotic Radiosurgery system, 187
CyberKnife Synchrony software, 23
CyberKnife® system, 37, 38

A. Gaya, A. Mahadevan (eds.), *Stereotactic Body Radiotherapy: A Practical Guide*,
DOI 10.1007/978-0-85729-597-2

D
Data acquisition
  Cyberknife systems, 48
  detector choice, 48–50
  gantry angle tilt, 48, 52
  mMLC type system, 48
  non-scanned data, 50
  output factors, 48, 50
  scanned data, 47–48
  scanning arm tilt, 48, 51
  standard farmer type chamber, 48
Deep inspiration breath-hold technique (DIBH), 133
Delivery quality assurance (DQA) method
  end-to-end QA method, 102
  trigeminal neuralgia, 103, 104
  typical SRS plan, 102, 103
Disease-free survival (DFS), 268
Dosimetry
  intra-fraction imaging, 102
  patient-specific measurements, 102–103
  reference, 101
  relative dosimetry, 101–102
  scatter and leakage dose, 102
DQA. *See* Delivery quality assurance (DQA) method

E
Electronic portal imaging (EPID), 29
Electron Intraoperative radiotherapy (ELIOT), 302
Elekta Axesse™, 36
Erasmus MC—Daniel den Hoed Cancer Center, 254
ExacTrac® Robotic 6D Couch, 36
External beam radiation therapy (EBRT), 296–298, 316, 317

F
Four-dimensional (4D) respiration-correlated CT, 31
Frame-based Gamma Knife® technology, 285

G
Gross target volume (GTV), 198, 256, 273
Gross tumor volume (GTV), 129, 130, 167–168, 230, 257, 320
GyroKnife system, 39, 40

H
HCC. *See* Hepatocellular carcinoma (HCC)
Head and neck cancer (HNC)
  acute radiation toxicity, 265, 266
  alcohol and tobacco, 254
  clinical target volume, 257
  Cyberknife, 256, 263
  diagnostic investigations, 256
  dysphagia and xerostomia, 255
  efficacy and safety, 263
  Erasmus MC
    OPC, 257, 259, 260, 262
    organ preservation protocol, 261–263
  gross target volume, 256–257
  HPV, 254
  hyperthermia, 275
  image-guided radiotherapy systems, 256
  late radiation toxicity, 265, 267
  multivariate regression analysis, 265, 266
  organs at risk (OAR), 257–259
  overall survival (OS) rates, 263
  overview of, 263–264
  PORT, 254–255
  prevalence, 253–254
  recurrent (*see* Recurrent head and neck cancer)
  squamous cell type origin, 254
  SRT + HT treatment schedule, 264, 265
  toxicity outcomes, 259–262
  treatment sites, 263
Hepatocellular carcinoma (HCC)
  dose-volume effect, 151
  evidence, 151–154
  high-precision radiotherapy, 151
  percutaneous ablation, 150
  RFA, 150
  RILD, 150, 151
  staging systems, 150, 151
  surgical resection, 150
  survival outcomes, 150
  systemic chemotherapy, 150
  TACE, 150
High dose fractions. *See* Linear-quadratic (LQ) model
HNC. *See* Head and neck cancer (HNC)
Human papillomavirus (HPV), 254
Hyperthermia (HT), 275
Hypoxic cell sensitising drugs (HCS), 80

I
Image-guided radiation therapy (IGRT), 55

Intensity modulated radiation therapy (IMRT), 87, 257, 295, 310, 317–318
Internal gross tumor volume (ITV), 129, 132–133
International Commission on Radiation Units and Measurements (ICRU), 256
Intra-hepatic cholangiocarcinoma (IHC), 149–151
ITV. *See* Internal gross tumor volume (ITV)

L
Laparoscopic partial nephrectomy (LPN), 227
Late-responding normal tissues (LRNTs), 71
Linear energy transfer (LET), 81
Linear-quadratic (LQ) model
  α/β ratios, 68
  'avalanche' effect, 68
  BED, 71–72
  clinical factors
    co-morbidity, 81
    high linear energy transfer, 81
    RBE issues, 81–82
  downward curvature effect, 68
  fractional cell survival, 68–70
  hot-spots tissue, 75–76
  implications, 82–84
  linear scale and logarithmic scale, 70
  LQ-type formulations, 70
  quantitative evaluation, 70
  radiobiological factors
    cell cycle re-assortment, 80
    extended fraction times, 79–80
    normal tissue volume effects, 80–81
    re-oxygenation, 80
    repair, 78–79
    tumour repopulation, 77–78
    tumour volume effects, 81
  straightening-out effect, 73–75
Liver
  acute toxicity, 175
  CBCT, 174
  CRC metastases
    autopsy study, 154
    chemotherapy, 154
    Child-Pugh score, 161
    clinical assessment, 162
    exclusion criteria, 162
    local control rates, 155
    patient selection criteria, 161
    prospective studies, 155, 158–160
    retrospective studies, 155–157
    site, 155
    surgical data, 154–155
    survival rates, 155
    thermal destruction, 154
  follow up, 176
  fractionation, 169, 172–174
  HCC
    dose-volume effect, 151
    evidence, 151–154
    high-precision radiotherapy, 151
    RFA, 150
    RILD, 150, 151
    staging systems, 150, 151
    surgical resection and percutaneous ablation, 150
    survival outcomes, 150
    systemic chemotherapy, 150
    TACE, 150
  IHC, 149–151
  late toxicity, 175–176
  radiotherapy (*see* Radiotherapy treatment planning)
  treatment planning
    CT scan, 167
    GTV, 167–168
    MRI, 167
    OAR, 168–169
    target volume, 169–174
  treatment response, 176
Liver metastases
  abdominal compression, 8
  active breathing control, 8
  conventional radiotherapy technique, 7
  Elekta stereotactic body frame, 7
  radiofrequency ablation, 7
Lung tumors
  breath-hold methods, 133, 135
  central tumors
    high and low dose fractions, 139–140
    local control rate, 140
    OAR injury, 139
    pericardium/mediastinal structures, 140
    risk-adapted treatment, 141
  clinical outcome, 141–142
  3D CRT, 128
  dose constraints and prescription, 136, 137
  dose distribution, 128
  forced shallow breathing, 133–135
  GTV and CTV, 129
  ITV, 128–129, 132–133
  NSCLC, 128

Lung tumors (*cont.*)
peripheral tumors
BED, 139
cardiovascular and pulmonary diseases, 139, 140
local control, 139
single fraction, 137
T1 *vs.* T2 tumors, 138
real-time tumor tracking
correlation model, 131–132
CT scan, 131
CyberKnife, 130, 132
LEDs, 130
X-ray imaging, 130
respiratory gating methods, 135–136
simulation, 136
toxicity
central lesions, 143
peripheral lesions, 142–143
quality of life, 143–144
treatment planning, 136

M
Micro multi-leaf collimators (mMLC), 47, 48

N
National Surgical Adjuvant Breast and Bowel Project (NSABP), 294
Nephron-sparing surgery, 226–227
Non-small cell lung cancer (NSCLC)
Cyberknife, 6
RTOG, 6
safe and effective treatmen, 6
survival rate, 5
Non-surgical nephron sparing surgery, 227

O
OAR. *See* Organ at risk (OAR)
Oligometastasis
adrenal metastases, 237, 242
de novo oligometastases, 234
fiducials, 246
liver metastases
clinical outcomes, 237, 239–240
RILD, 246
local recurrence/progression, 6–7
lung metastases
clinical outcomes, 237, 238
complications, 247
lymph node metastases, 237, 241
mixed oligometastatic sites, 237, 243–244
natural history, 234–235
patient outcomes, 237
pre-SBRT evaluation, 245
radiotherapy, 235
surgical precedence, 235
systemic therapy, 245
toxicity, 236
Organ at risk (OAR), 89, 168–169
Organ preservation protocol, 261–263
Oropharyngeal cancer (OPC), 257, 259, 260, 262

P
Pancreatic cancer
clinical outcomes, 188, 190
dose prescription, 185–187
incidence, 183
indication, 191
patient selection, 184
patients survival rate, 184
patient work-up, 184–185
systemic chemotherapy, 187–188
toxicity, 188–190
treatment delivery, 187
treatment planning, 185
tumor control, 189, 190
Planning organ at risk (PRV), 99
Planning target volume (PTV), 185, 307, 308, 310, 311, 320
spinal radiosurgery, 118–119
treatment planning, 89, 90
Postoperative radiation therapy (PORT), 254–255
Primary liver tumours, 8
Prostate cancer
flexprone position, 11
hypofractionation
α/β [alpha/beta] ratio, 196, 197
biologic potency, 198
concept of, 196
CyberKnife device, 197
high dose rate (HDR) brachytherapy, 197
patient history, 198–201
incidence, 196
monotherapy
biochemical disease-free survival rate, 204
crude biochemical disease-free survival rate, 201–202
CyberKnife delivered SBRT, 201, 202
gantry-based prostate SBRT, 203, 205
HDR brachytherapy, 202–203
Phoenix definition, 204
planning target volume, 201

neoadjuvant/adjuvant androgen deprivation therapy, 220, 221
"non-escalated" approaches, 208
phase II clinical trial, 11
planning method, 11
prevalence, 196
radiobiology potency considerations
intraprostatic dose, 205, 206
periprostatic dose, 205–207
relapsed and/or metastatic cases
"curative intent" salvage strategies, 209
IRB-approved clinical trial, 209
post-RT prostate recurrence, 210
stereotactic radiotherapy, 210
treatment techniques and strategies
biologic factors, 215–216
CT-based *vs*. MRI, 211–212
image-guidance methodology, 212–215
monotherapy *vs.* combined modality therapy, 210–211
technical factors, 216–218
Prostate CyberKnife SBRT, 198, 199
PTV. *See* Planning target volume (PTV)

Q
Quality assurance (QA), 35–36
CT-based IGRT systems, 55
dosimetric QA
beam stability test, 57
end-to-end test, 57–58
patient specific measurement, 58
validation measurement *vs.* treatment planning output, 56–57
IGRT system accuracy, 56
on-line imaging systems, 53–55
residual correction error method, 55
target localization accuracy, 53
"Winston-Lutz" test, 53

R
Radiation induced liver disease (RILD), 68, 246
Radiation myelopathy, 121
Radiation therapy oncology group (RTOG), 307
Radiofrequency ablation (RFA), 150
Radiotherapy treatment planning
axial, sagittal and coronal sections, 169, 170
delineation
CT scan, 167
CTV, 167–168
GTV, 167
immobilisation, 166–167
MRI, 167
OAR, 168–169
patient positioning, 166–167
PTV, 167–168
fiducial placement, 164
motion tracking, 166
patient positioning, 164, 166–167
pre-treatment imaging, 165
respiratory motion, 166
vs. SBRT delivery systems, 162, 163
tumour motion
ABC technique, 165
abdominal compression, 165
managing respiratory motion, 166
passive respiratory gating, 166
real time tracking, 166
VMAT, 169–174
Real-time Position Management™ (RPM) system, 31
Recurrent head and neck cancer
acute mucositis, 272
brachytherapy, 268
complications, 268–270
DFS, 268
IMRT, 273–274
multivariate analysis, 271
optimal dose fractionation, 275
phase I dose-escalation clinical trial, 271
re-irradiation, 272
salvage surgery, 267
stereotactic radiosurgery, 270–271
Reference dosimetry method, 101
Relative biological effect (RBE), 81–82
Renal cancer
CyberKnife, 228–229
nephron-sparing surgery, 226–227
non-surgical nephron sparing surgery, 227
patient selection, 229
post treatment care, 231
prevalence, 225
radiation therapy, 227–228
"radioresistant" tumor, 225
radiosurgery, 225–226
toxicity, 230
treatment planning and delivery
Cyberknife™ system, 230, 231
GTV and CTV, 230
organ at risk, 230
reproducible immobilization, 229
Renal cell carcinoma (RCC), 10. *See also* Renal cancer
Respiratory gating methods, 135–136

S
Sexual Health Inventory Matrix (SHIM) score, 198
Siemens Primatom™, 36
Soft tissue sarcomas (STS)
  BED, 318
  cerebral metastases, 319
  clinical assessment, 322
  EBRT, 316, 317
  high-dose photon irradiation, 317
  IMRT, 317–318
  local control rate, 317
  metastatic sarcoma, 318–319
  patient selection, 319–320
  radioresistant, 315
  role of, 322
  toxicity, 322
  treatment planning, 320–321
Spinal radiosurgery
  benign intracranial tumors, 113
  CTV, 118, 119
  CyberKnife, 115, 116, 120
  diagnostic images, 117
  dose fractionation, 120, 121
  dose-volume constraints, 119, 120
  epidural spinal cord compression, 113
  follow up, 115, 122
  GTV, 118, 119
  metastatic melanoma, 110, 111
  patient history, 109–110
  patient selection
    ASTRO guidelines, 115, 117
    contraindications, 116, 117
    indications, 116
  peripheral nerve sheath tumor, 110, 112
  PTV, 118–119
  series selection, 113, 114
  simulation, 118
  TomoTherapy, 115, 116
  toxicity, 121–122
  treatment planning, 119–120
  vertebral level, 118, 119
Stereotactic body radiotherapy (SBRT)
  abdominal compression, 21
  APBI (*see* Accelerated partial breast irradiation (APBI))
  characteristics, 20
  clinical evolution, 22–24
  commercially available systems
    CyberKnife® system, 37, 38
    Elekta Axesse™, 36
    ExacTrac® Robotic 6D Couch, 36
    GyroKnife system, 39, 40
    Siemens Primatom™, 36
    tomotherapy, 37, 38
    Varian's TrueBeam STx system, 36–37
    Vero SBRT system, 36, 39
    ViewRay, 39–40
  commissioning system
    beam data, 47
    Cyberknife systems, 48
    detector choice, 48–50
    gantry angle tilt, 48, 52
    mMLC type system, 48
    non-scanned data, 50
    output factors, 48, 50
    scanned data, 47–48
    scanning arm tilt, 48, 51
    standard farmer type chamber, 48
    TPS, 52
  CT/MRI simulator, 23
  Cyberknife, 4
  evaluation, 19
  features, 27
  fractionation and radiobiology, 3
  Gamma Knife treatments, 20
  history, 2–3
  HNC (*see* Head and neck cancer (HNC))
  indications
    kidney, 10
    liver metastases, 7–8
    lung oligometastases, 6–7
    NSCLC, 5–6
    pancreas, 8–9
    primary liver tumours, 8
    primary spinal tumors, 12–13
    prostate, 10–11
    vertebral metastases, 11–12
  locations, 24
  LQ model (*see* Linear-quadratic (LQ) model)
  micro-multi leaf collimator, 4
  Novalis TX, 4
  oligometastasis (*see* Oligometastasis)
  pancreatic cancer (*see* Pancreatic cancer)
  prostate cancer (*see* Prostate cancer)
  QA (*see* Quality assurance (QA))
  radiobiological rationale, 24–25
  Renal cancer (*see* Renal cancer)
  respiratory motion, 4–5
  STS (*see* Soft tissue sarcomas (STS))
  system components and requirements
    beam characteristics, 33–34
    CT, 29, 32
    4D CT, 31
    2D radiography and CT localization systems, 29
    dual/multiple KV image systems, 29

EPID, 29
^{18}F-fluorodeocyglucose (^{18}FDG), 32
gating techniques, 31
MRI, 30, 32
optical systems, 31
patient immobilization, 28–29
QA process, 35–36
radiofrequency-based tracking system, 30
treatment planning, 34–35
ultrasound devices, 30
TomoTherapy System, 4
TPS (*see* Treatment planning system (TPS))
treatment delivery, 23
treatment planning
AVM, 92
conventional IMRT, 87–88
CT scan, 91–92
dose calculation algorithms and heterogeneities, 90–91
DQA method, 102–104
Gamma Knife treatment, 88
high CI, 89
high MU-to-dose ratio, 88
homogeneous *vs.* heterogeneous, 88
impact of planning errors, 103–104
liver, 166–174
lung, 91
metallic stents, 92
non-isocentric techniques, 89
OAR sparing, 89
peripheral dose, 93
PTV, 89, 90
respiratory motion and deformation
respiratory motion and deformation: imaging, 98–99
respiratory motion and deformation: margin determination, 99–100
respiratory motion and deformation: relative motion, 99
RTOG, 92
skin dose, 92–93
TACE, 92
treatment delivery time, 89–90
tumor dose and OAR constraints
brain, 95
liver, 97, 98
lung, 96
pancreas, 97
prostate, 97–98
spine, 95–96
Stereotactic hypofractionated accurate radiotherapy of the prostate (SHARP), 203, 204, 216
Stereotactic radiosurgery (SRS)
brain, 95
CARO recommendations, 96
commercially available systems, 36
dose gradients, 102, 103
image-guided delivery, 89
patient selection, 115
planning, 88–89
quality assurance, 52–55
spine (*see* Spinal radiosurgery)
treatments, 90
Synchrony™ Respiratory Tracking system, 31

T
Tamoxifen, 308
Three-dimensional conformal radiotherapy (3D-CRT), 295
TomoTherapy system, 4, 37, 38
Treatment planning system (TPS)
AAPM Task Group 101 Report, 61, 63
anatomical/clinical patient set up, 59
commissioning, 52
conformality index, 61, 62
3-D coordinate system, 59
dose heterogeneity, 60, 61
motion management, 59, 60
prescription normalization, 60, 62
simulation, 59
target delineation, 59

U
Uveal melanoma
Cyberknife patients, 286, 287
dose de-escalation, 290
fundoscopy image, 286, 289
indications, 285
ophthalmic plaque radiotherapy, 284
prevalence, 284
radiation therapy, 284
radiosurgery treatment process, 285–286
retrobulbar anesthesia, 288, 290
robotic radiosurgery, 290
single-session radiosurgery, 285
T2 MRI sequence, 286, 288
visual preservation and eye retention, 290

V
Varian's TrueBeam STx system, 36–37
Vero SBRT system, 36, 39
Vertebral compression fracture (VCF), 121–122
ViewRay, 39–40
"Virtual HDR®", 202–203
VMAT. *See* Volume modulated arc therapy (VMAT)
Volume modulated arc therapy (VMAT), 89

W
Whole breast irradiation (WBI), 294
"Winston-Lutz" test, 53